Robust stability and performance of nonlinear moving horizon estimation

Julian D. Schiller

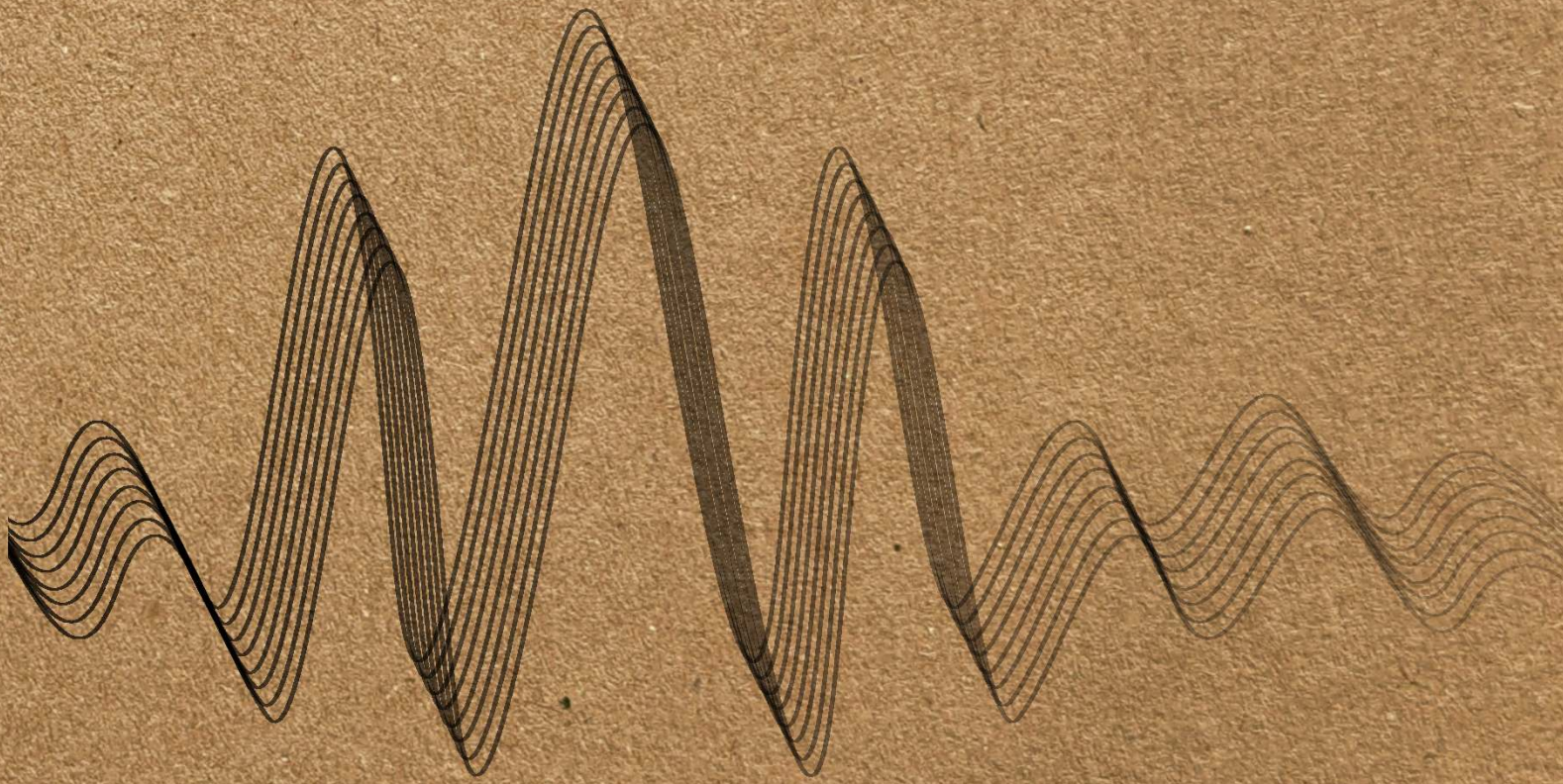

λογος

Julian D. Schiller

Robust stability and performance of nonlinear moving horizon estimation

Logos Verlag Berlin

This work was approved in 2025 by the Faculty of Electrical Engineering and Computer Science at Gottfried Wilhelm Leibniz Universität Hannover as a dissertation for the academic degree Doktor-Ingenieur (Dr.-Ing.).

Bibliographic information published by the Deutsche Nationalbibliothek
The Deutsche Nationalbibliothek lists this publication in the Deutsche Nationalbibliografie; detailed bibliographic data are available on the Internet at http://dnb.d-nb.de .

ORCID: 0000-0002-7091-0849

This publication received financial support from the publication fund NiedersachsenOPEN, funded by zukunft.niedersachsen.

Funded as part of the Excellence Initiative 2025 of Logos Verlag Berlin.

Logos Verlag Berlin GmbH 2025
ISBN 978-3-8325-5963-2
DOI 10.30819/5963

Produced as Logos-Ecobook.
https://www.logos-verlag.de/ecobook

Logos Verlag Berlin GmbH
Georg-Knorr-Str. 4, Geb. 10, 12681 Berlin, Germany

Tel.: +49 (0)30 / 42 85 10 90
Fax: +49 (0)30 / 42 85 10 92

https://www.logos-verlag.com

Acknowledgments

This work is the result of my five-year doctoral studies at the Institute of Automatic Control (IRT) at Leibniz University Hannover. During this time, I have come into contact with many people who have helped and supported me in many ways, and to whom I would like to express my gratitude here.

First of all, I would like to thank my supervisor Prof. Matthias A. Müller for his excellent support over the last years. I will always be grateful to him for giving me the opportunity to be part of his research group and to experience the beauty of control theory—even though when I applied for this position five years ago, I had little to no knowledge about nonlinear systems whatsoever. Matthias has created a very fruitful research environment at IRT, and it has been a pleasure to build on the excellent foundations provided, learn about various different concepts in the mathematics of control, and contribute to the literature myself. I am very much looking forward to many upcoming research interactions and future collaborations with him.

I would also like to thank all my former and current colleagues at IRT who have made my time here very enjoyable; in particular Dr. Torsten Lilge for his valuable support in all organizational and teaching-related matters, and Philipp Buschermöhle, Isabelle Krauss, Dr. Victor G. Lopez, Marko Nonhoff, Tobias M. Wolff, and Dr. Mingzhou Yin for proofreading the first version of this thesis.

I would also like to thank all the collaborators outside the IRT. Specifically, I want to thank Sven Knüfer for the discussions and support in the first few months, which helped me a lot in understanding the overall topic and writing the first publication in this context. Moreover, I also want to thank Dr. Simon Muntwiler, Dr. Johannes Köhler, and Prof. Melanie N. Zeilinger from ETH for their collaboration, and in particular Simon and Johannes for the many fruitful discussions. I look forward to future scientific exchange and meetings at conferences. Furthermore, I am grateful to Prof. Lars Grüne for the inspiring discussions that contributed to our latest results and for hosting me in Bayreuth. I would also like to thank Prof. Moritz Diehl from the University of Freiburg for his interest in my work and his willingness to be a co-examiner of this thesis.

Finally, I would like to wholeheartedly thank my family for their continuous support, especially my wife for her never-ending love and patience with me, and our two boys, who always make sure that I don't work too much.

Julian D. Schiller
Hannover, Feb. 2025

Abstract

In this thesis, we study moving horizon estimation (MHE) schemes for state estimation of general nonlinear dynamical systems that are subject to unknown disturbances and noise. We establish desired robust stability and performance guarantees under realistic conditions, address the practically important case of MHE for real-time applications, and investigate methods specifically tailored to joint state and parameter estimation.

In more detail, we develop a Lyapunov-based MHE framework for general nonlinear continuous-time systems, thus closing the gap to the current discrete-time literature. The proposed method has the decisive advantage that arbitrary sampling strategies can be employed to define time instants at which the underlying optimization problem is actually solved. Our results are based on a novel detectability condition for nonlinear systems in continuous time and its Lyapunov function characterization. We develop methods to systematically construct such functions in practical applications in order to provide detectability certificates for nonlinear discrete- and continuous-time systems, which is crucial to conclude statements about the stability of MHE that go beyond conceptual nature. Furthermore, we address the practically relevant case of MHE algorithms for real-time applications, where the solver is usually terminated before reaching the global optimum. In this context, we consider two fundamentally different MHE formulations for which we show that robust stability guarantees are maintained regardless of the chosen numerical solver and the number of solver iterations performed. For systems that are additionally subject to parametric uncertainties, we also show under which modifications of the MHE scheme constant or time-varying system parameters can be jointly estimated—despite potentially weak or missing excitation. To this end, we propose an adaptive regularization of the cost function that uses real-time information about the current parameter excitation. Finally, we develop novel accuracy and performance guarantees for MHE. Here, we employ a certain turnpike property which essentially requires that solutions to the MHE optimization problems are most of the time close to the omniscient acausal infinite-horizon solution involving all past and future data. This leads to the surprising observation that MHE problems naturally exhibit a leaving arc, which actually may have a strong negative impact on the estimation accuracy. To counteract this, we propose a delayed MHE scheme, and we show that the resulting performance is approximately optimal and implies bounded dynamic regret with respect to the acausal infinite-horizon solution, with error terms that can be made arbitrarily small by an appropriate choice of the delay. We illustrate our theoretical results with various numerical examples from the literature, which highlight the applicability and practical relevance of the developed theory.

Keywords

Moving horizon estimation, state estimation, nonlinear systems, robust stability, detectability, Lyapunov methods, optimization, parameter estimation

Contents

Notation

The following is a list of important abbreviations, acronyms, and symbols used in this work. Additional notation required in certain parts is defined in the respective sections.

Abbreviations and acronyms

EKF	extended Kalman filter
GAS	global asymptotic stability
GGN	generalized Gauss-Newton
i-iIOSS	incremental integral input/output-to-state stability
i-IOSS	incremental input/output-to-state stability
i-ISS	incremental input-to-state stability
iISS	integral input-to-state stability
IOSS	input/output-to-state stability
ISS	input-to-state stability
LMI	linear matrix inequality
LPV	linear parameter-varying
LTI	linear time-invariant
LTV	linear time-varying
MHE	moving horizon estimation
MPC	model predictive control
NLP	nonlinear program
PE	persistence of excitation
RGAS	robust global asymptotic stability
RGES	robust global exponential stability
s.t.	such that
SDP	semidefinite programming
SOS	sum of squares
SSE	sum of squared errors
UBEBS	uniform bounded-energy bounded-state

Real numbers and sets

$\mathbb{R}$	set of real numbers
$\mathbb{R}_{\geq 0}$ ($\mathbb{R}_{>0}$)	set of non-negative (positive) real numbers
$\lceil x \rceil$	smallest integer greater than or equal to $x \in \mathbb{R}$
$\lfloor x \rfloor$	largest integer smaller than or equal to $x \in \mathbb{R}$
$\mathbb{I}$	set of integers
$\mathbb{I}_{\geq a}$ ($\mathbb{I}^{\mathrm{e}}_{\geq a}$)	set of (even) integers greater than or equal to $a \in \mathbb{I}$
$\mathbb{I}_{[a,b]}$	set of integers in the interval $[a, b] \subset \mathbb{I}$

Linear algebra

I_n	identity matrix of dimension $n \times n$
$0_{n\times m}$ (0)	zero matrix of dimension $n \times m$ (zero matrix with the dimension being clear from the context)
$A^\top$	transpose of a matrix $A \in \mathbb{R}^{n\times m}$
$\mathrm{diag}(v)$	diagonal matrix with the elements of v on the main diagonal
$\lvert x \rvert$	Euclidean norm of a vector $x \in \mathbb{R}^n$
$\lvert x \rvert_A$	weighted Euclidean norm $\lvert x \rvert_A = \sqrt{x^\top A x}$ of a vector $x \in \mathbb{R}^n$ for a symmetric positive definite matrix $A \in \mathbb{R}^{n\times n}$
$\lambda_{\max}(A)$	maximum eigenvalue of a symmetric matrix $A \in \mathbb{R}^{n\times n}$
$\lambda_{\min}(A)$	minimum eigenvalue of a symmetric matrix $A \in \mathbb{R}^{n\times n}$
$\lambda_{\max}(A, B)$	maximum generalized eigenvalue of symmetric matrices $A, B \in \mathbb{R}^{n\times n}$, i.e., largest scalar $\lambda \in \mathbb{R}$ satisfying $\det(A - \lambda B) = 0$
$A \succ (\succeq)\ B$	symmetric matrix $X = A - B$ is positive (semi-)definite for matrices $A, B \in \mathbb{R}^{n\times n}$, i.e., $v^\top X v > (\geq)\ 0$ for all $v \in \mathbb{R}^n$ with $v \neq 0$
$A \prec (\preceq)\ B$	symmetric matrix $X = A - B$ is negative (semi-)definite for matrices $A, B \in \mathbb{R}^{n\times n}$, i.e., $v^\top X v < (\leq)\ 0$ for all $v \in \mathbb{R}^n$ with $v \neq 0$

Signals and sequences

$\lVert x \rVert$	essential supremum norm $\operatorname{ess\,sup}_{t\in\mathbb{R}_{\geq 0}} \lvert x(t) \rvert$ of a measurable, locally essentially bounded function $x : \mathbb{R}_{\geq 0} \to \mathbb{R}^n$ (alternatively, supremum norm $\sup_{t\in\mathbb{I}_{\geq 0}} \lvert x(t) \rvert$ of a sequence $x : \mathbb{I}_{\geq 0} \to \mathbb{R}^n$)
$\lVert x \rVert_{0:T}$	essential supremum norm $\operatorname{ess\,sup}_{t\in[0,T]} \lvert x(t) \rvert$ of a truncated measurable, locally essentially bounded function $x : \mathbb{R}_{\geq 0} \to \mathbb{R}^n$ (alternatively, supremum norm $\sup_{t\in\mathbb{I}_{[0,T]}} \lvert x(t) \rvert$ of a truncated sequence $x : \mathbb{I}_{\geq 0} \to \mathbb{R}^n$)

Comparison functions [Kel14]

$\mathcal{K}$	A function $\alpha : \mathbb{R}_{\geq 0} \to \mathbb{R}_{\geq 0}$ is of class $\mathcal{K}$ ($\alpha \in \mathcal{K}$) if it is continuous, strictly increasing, and satisfies $\alpha(0) = 0$.
$\mathcal{K}_\infty$	A function $\alpha : \mathbb{R}_{\geq 0} \to \mathbb{R}_{\geq 0}$ is of class $\mathcal{K}_\infty$ ($\alpha \in \mathcal{K}_\infty$) if $\alpha \in \mathcal{K}$ and additionally $\lim_{s\to\infty} \alpha(s) = \infty$.
$\mathcal{L}$	A function $\theta : \mathbb{R}_{\geq 0} \to \mathbb{R}_{\geq 0}$ is of class $\mathcal{L}$ ($\theta \in \mathcal{L}$) if it is continuous, non-increasing, and $\lim_{t\to\infty} \theta(t) = 0$.
$\mathcal{KL}$	A function $\beta : \mathbb{R}_{\geq 0} \times \mathbb{R}_{\geq 0} \to \mathbb{R}_{\geq 0}$ is of class $\mathcal{KL}$ ($\beta \in \mathcal{KL}$) if $\beta(\cdot, t) \in \mathcal{K}$ and $\beta(s, \cdot) \in \mathcal{L}$ for any fixed $t \in \mathbb{R}_{\geq 0}$ and $s \in \mathbb{R}_{\geq 0}$.

1. Introduction

1.1. Motivation

The knowledge of the internal state of a dynamical system is of crucial importance for many control applications, for example when stabilizing the system via state feedback, when monitoring compliance with safety-critical conditions or when detecting errors and external attacks. In most practical cases, however, the state cannot be completely measured for various (possibly physical or economic) reasons and therefore must be reconstructed using the available input-output signals. This is generally a challenging problem, especially in the presence of nonlinear systems and when robustness to model errors and measurement noise must be ensured.

Moving horizon estimation (MHE) [RMD20] is a modern optimization-based state estimation strategy that is naturally suitable for this purpose. Here, the current state estimate is obtained by solving an optimization problem involving a fixed number of past measurements, extracting the last state of the optimal estimated sequence, and repeating the online optimization in the next sampling time in a receding horizon fashion. It can be interpreted as an approximation to full information estimation (FIE), which optimizes over all available historical data. However, FIE is usually only of theoretical interest (particularly as a benchmark for MHE), since the complexity of the underlying optimization problem continuously grows with time and thus quickly becomes computationally intractable in practical applications.

MHE has several advantages over other state estimation methods: it is naturally applicable to nonlinear systems, provides the ability to include additional information such as constraints, is intuitive to tune, and yields optimal estimation results. Moreover, it is fairly easy to implement using high-level software packages (such as acados [Ver+21] and CasADi [And+18]), merely requiring knowledge of the model equations and corresponding computing resources. This is in strong contrast to most nonlinear observers; they require less computing power when applied, but the corresponding design is usually based on the search for a global transformation into a suitable observer normal form or the solution of a partial differential equation [BAA22], which is generally non-trivial and requires a deeper understanding of the underlying theory, representing a relatively large hurdle for use in practice. For these reasons, and not least because of the steadily growing availability of computing capacities and the development of highly efficient optimization algorithms, MHE is increasingly applied in various different fields, ranging from chemical and process engineering [HCE18; Els+21], mobile robotics and localization [Liu+17; Bre19], offshore engineering and freight transportation [CLH22], to medical applications [Kle+23].

However, the corresponding theory developed rather slowly, with little ability to provide practical tuning guidelines. Only recently, substantial progress has been made by deriving robustness properties of MHE under a relatively mild detectability condition, compare [RMD20]. Nevertheless, many problems and open questions remain that prevent the current MHE theory from providing any value beyond conceptual nature. Specifically, the following problems can be identified.

1. Practical relevance: The recently developed robustness guarantees for MHE require the knowledge of a particular detectability property for the design of the cost function, for which there is no systematic method for verification. Moreover, the results are mostly overly conservative, yielding unrealistic and practically irrelevant design guidelines and estimates on the horizon length.
2. Restrictive design: The most recent results in the field of nonlinear MHE focus on discrete-time systems and do not have a direct continuous-time counterpart. In this context, there is also a lack of fundamental theory on suitable continuous-time notions of detectability and robust stability. However, investigating corresponding MHE schemes is important, as the original physical system to be estimated usually corresponds to a continuous-time model. Having to discretize it first significantly complicates the system representation, restricts flexibility, can lead to additional discretization errors, and requires fixing a particular discretization scheme and sampling period beforehand.
3. Real-time capability: The computing power available in practice is often severely limited, and computing the global optimum at each time step is usually not possible within a fixed time interval. Instead, the solver is usually terminated with a suboptimal solution, which renders the theoretical guarantees invalid (as they usually depend on this criterion).
4. Parametric model uncertainties: In practical applications, the derived system model requires system identification and usually suffers from parametric uncertainties, as only noisy measurement data is available. This, however, may invalidate the available robustness guarantees, which crucially rely on an exact model of the system, or even cause the estimation error to become unstable. Adapting the parameters online to obtain a precise model is not directly possible, as it is yet unclear how to deal with potential lack of excitation (which often occurs frequently or unpredictably in practical applications).
5. Estimation performance: There is no general performance analysis of MHE available. It is therefore unclear how an MHE scheme must be designed in order to ultimately achieve a similar estimation performance to the (desired but impractical) FIE counterpart or a comparable benchmark.

This thesis aims at developing a deepened system-theoretic understanding of MHE and establishing desired robust stability and performance guarantees under realistic and practically relevant conditions, contributing to the greater goal of supplementing the great success of MHE in practical applications with a well-founded theory. In the following two sections, we provide an overview on the related literature and summarize the main contributions of this thesis.

1.2. Literature overview

In this section, we provide a brief overview over the literature related to the research topic. This of course covers works on nonlinear MHE, but also on system-theoretic properties such as detectability and robust stability, methods for combined state and parameter estimation in general, as well as performance and turnpike analysis in the context of optimal control.

1.2.1. Nonlinear detectability

While it is well understood how observability and detectability can be characterized and verified for linear systems (see, for example, Chapters 5 and 6 in [Son90]), this is not the case for general nonlinear systems. Here, one might transfer conceptually similar approaches and generally argue about the indistinguishability of different initial conditions based on the respective output signals or try to analyze the observation space of the system using Lie derivatives along the vector field (see, e.g., [Bes07, Ch. 1]). However, explicit verification of such rather abstract properties in practical applications is generally a complex and difficult problem.

A system-theoretic approach to characterize detectability for nonlinear systems is given by the concept of incremental input/output-to-state stability (i-IOSS). This property requires that the difference between any two trajectories of a dynamical system is upper bounded by the difference in their respective initial conditions, their inputs, and their outputs. Loosely speaking, if the differences between their respective inputs and outputs are small, then the difference between the states must also become small, which hence directly entails an indistinguishability property that is a natural characteristic of detectability in general.

The concept of i-IOSS was originally proposed in [SW97] to extend the notion of (non-incremental) input/output-to-state stability (IOSS)—which compares a system trajectory with the zero-trajectory and can thus only be regarded as "zero-detectability"—to a pair of arbitrary system trajectories. Introduced in an L^∞-to-L^∞ sense, it has been shown that a continuous-time system must necessarily satisfy the i-IOSS property to admit a robustly stable full-order state observer, and its discrete-time analogue has become the standard in the field of optimization-based state estimation, compare, for example, [RJ12; Ji+16; Mül17; RMD20; AR21; KM23; Sch+23; Hu24; Ale25].

The characterization of system properties via Lyapunov functions has turned out to be very useful for system analysis and the design of controllers and observers. Here, it is important to establish the equivalence between the Lyapunov function characterization and its corresponding original notion by means of converse theorems, in order to ensure that considering the Lyapunov function, which is usually easier when designing controllers and observers, is indeed without loss of generality. Such results are available (mostly in both continuous and discrete time) for, e.g., global asymptotic stability (GAS) in [LSW96] and [JW01], input-to-state stability (ISS) in [SW95] and [JW01], (non-incremental) IOSS in [KSW01] and [CT08], and integral

IOSS in [Ing01a; Ing01b]. Stronger, incremental notions are considered in [Ang02] and [TRK16], which address incremental GAS and incremental ISS (i-ISS), albeit under the condition that inputs and external signals (such as, e.g., time-varying parameters or disturbances) of the system take values in compact sets. The condition of compactness could be weakened by using a dissipation inequality in integral form along with relaxing the requirement of smoothness of the Lyapunov function to mere continuity, which is done in [Ang02] and [Ang09] considering the incremental L^2-to-L^∞ (i.e., integral) versions of GAS and ISS for continuous-time systems, respectively.

More recently, time-discounted variants of i-IOSS were proposed in [KM20; ART21] for discrete-time systems, where it was shown that discounting past disturbances appears very natural and even without loss of generality. A corresponding converse Lyapunov result is provided in [ART21], which is structurally easier and more intuitive to establish with such a discount factor than without, as is the case in, e.g., [LSW96; KSW01; Ang02; Ang09]. Moreover, i-IOSS with time-discounting and its associated Lyapunov function are crucial for recent results in the field of optimization-based state estimation for discrete-time systems, compare [KM23; AR21; Sch+23].

1.2.2. Robust stability of MHE

One of the main concerns in MHE theory (and observer design in general) is to ensure, under appropriate conditions, that the corresponding estimation error is bounded and converges to zero in the ideal, unperturbed case, so that the unknown true trajectory can be recovered (at least asymptotically). To this end, an MHE scheme for continuous-time systems was proposed and analyzed in [MM95]. Since a cost function without a prior weighting was used (which can be seen as a regularization term), the system must satisfy an observability condition to ensure exponential convergence of the estimation error. Using such a cost function, however, requires long estimation horizons to ensure satisfactory performance in practice, compare [RMD20, Sec. 4.3.1]. Since the application of MHE inevitably requires some sort of sampling strategy (i.e., discrete time points at which the optimization is performed), schemes for discrete-time systems have recently been the main focus in the literature. Early results in the context of nonlinear systems employed certain uniform observability properties, compare, for example, [MR95; RRM03; ABB08].

In recent years, the notion of i-IOSS has proven to be a very useful concept for nonlinear detectability, enabling significant advances in MHE theory. In particular, in [RJ12], the authors established robust stability of FIE for i-IOSS systems, considering the special case of convergent (i.e., vanishing) disturbances. Robust stability of MHE in the more general and practically relevant case of persistent bounded disturbances was established in [Ji+16], albeit requiring a cost function that does not allow for standard least squares objectives. This was addressed in [Mül17] and generalized in [AR19b], however, yielding theoretical guarantees that—counter-intuitively—deteriorate with an increasing estimation horizon. The Lyapunov-based

approach proposed in [AR21] is able to avoid this drawback, but on the other hand requires an additional stabilizability condition. Alternative approaches rely on an additional pre-estimating observer from which robust stability properties could be inherited [Liu13; GBE21].

In contrast, another line of research considers a cost function that includes explicit time discounting, which in the MHE context originates from the work [KM18]. This establishes a more direct link to the i-IOSS property and allows the derivation of strong robustness guarantees under less restrictive conditions, see, for example, [KM23; Hu24; Ale25]. In particular, the guarantees improve as the horizon length increases and do not require additional assumptions such as stabilizability or pre-estimating observers. The Lyapunov framework proposed in [Sch+23], which essentially relies on the same underlying principles, further simplifies the tuning and provides less conservative conditions on the horizon length sufficient for guaranteed robustly stable state estimation.

1.2.3. MHE for real-time applications

MHE requires solving a usually non-convex optimization problem at each time step, and is hence computationally demanding. Moreover, since the computing power available in practice is often severely limited, solving the optimization problem to global optimality at each time step is usually not possible within a fixed time interval.

In order to improve the real-time applicability of MHE, methods employing an additional *auxiliary observer* were developed to structurally simplify the optimization problem and thus save computing capacity. For example, in [SJF10], an MHE scheme for linear systems was proposed that utilized an additional Luenberger observer to replace the state equation as a dynamical constraint. As this allows to compensate for model uncertainties without computing an optimal disturbance sequence, the optimization variables could be reduced to one, namely the initial state at the beginning of the horizon. In [Suw+14], this idea was transferred to a class of nonlinear systems, and a major speed improvement compared to standard MHE could be shown. However, this results in a loss of degrees of freedom, since there is no possibility to tune the cost function with respect to model disturbances and measurement noise. In [Liu13], an observer was employed to construct a confidence region for the actual system state. Nevertheless, introducing this region as an additional constraint in the optimization problem can be quite restrictive and therefore may not allow significant improvements of MHE compared to the auxiliary observer. In [GBE21], a proximity-MHE scheme was proposed for a general class of nonlinear systems, where an additional observer is used to construct a stabilizing a priori estimate yielding a proper warm start for the low-level optimization algorithm, and nominal stability could be shown by Lyapunov arguments.

Nevertheless, all the above methods require optimal solutions to the (simplified, but still non-convex) MHE problem, and their complete computation within fixed time intervals is difficult (if not impossible) to guarantee. A more intuitive approach is to simply terminate the underlying optimization algorithm after a fixed number of

iterations, which on the one hand provides only suboptimal estimates, but on the other hand ensures fixed computation times. However, since most results from the nonlinear MHE literature are crucially based on optimality [RMD20; Mül17; AR21; Hu24; KM23], stability of suboptimal MHE cannot be straightforwardly deduced. For practical (real-time) applications, it is therefore essential to develop suboptimal schemes that guarantee robust stability without requiring optimal solutions.

To this end, fast MHE methods were developed in [Küh+11; WVD14; AG17], performing only a predetermined number of iterations of a certain optimization algorithm (e.g., gradient- or Newton-based). However, the corresponding results rely on a strong uniform observability condition and (local) contraction properties of the specific algorithms, requiring both a proper initial guess and at least one iteration to ensure (local) stability, compare [WVD14; AG17]. In [WK17], the combination of a fast MHE scheme and pre-estimation using a nonlinear Luenberger observer was considered, combining the advantages of both approaches. A suboptimal proximity-MHE scheme for linear systems was proposed in [GGE22], where nominal stability guarantees could be given without performing any optimization by using a pre-stabilizing observer and contraction properties of a specific gradient-based optimization algorithm. This approach has recently been extended to nonlinear systems in [GGE21], thus providing nominal stability guarantees for a suboptimal nonlinear proximity-MHE scheme using local properties of the optimization algorithm involved. Whereas these algorithms require the computation of first-order sensitivities to perform the iterations, zero-order MHE methods were developed that completely avoid the online evaluation of sensitivities [BZD19] or use fixed approximations [Bau+21]. The resulting MHE schemes are suitable for real-time estimation of large-scale processes (arising, for example, from a discretization of partial differential equations), but their theoretical properties are of qualitative and local nature, and the respective conditions are hard to verify.

1.2.4. Joint state and parameter estimation

MHE is a model-based state estimation technique and hence requires knowledge of a suitable dynamical model of the system to be estimated. However, even if the general structure of the system is known, the model parameters are often uncertain and/or fluctuate during operation, e.g., due to heat production, mechanical wear, temperature changes or other external influences. This may invalidate the robustness guarantees, as they usually rely on an exact model of the real system and are therefore not necessarily valid in the case of parametric model uncertainties. In the worst case, this could even lead to the estimation error becoming unstable, compare, for example, [Fit71; SS71].

To address this problem, a min-max MHE scheme was proposed in [ABB12], where at each time step a least squares cost function is minimized for the worst case of the model uncertainties. However, such a min-max approach becomes computationally intensive for general nonlinear systems, and the worst-case consideration may be too conservative and affect estimation performance. In [MKZ23a], a regularization term

was employed that depends on a given *a priori* estimate of the (constant) uncertain parameters, avoiding a nested min-max optimization scheme and ultimately yielding state estimates that are robust to changes in the true unknown parameter. Here, practical stability of the state estimation error with respect to the *a priori* parameter error could be established.

Yet it is often advantageous to not only ensure robustness against model errors, but also to obtain an estimate of the uncertain parameters, since a precise model is crucially required for, e.g., high-performance control, system monitoring, or fault detection. This demands suitable techniques for online parameter adaptation. In this context, an MHE scheme was proposed in [SJ11] by treating the unknown constant parameters as additional states with constant dynamics. The corresponding stability analysis is based on the transformation of the extended system into an observable and an unobservable but exponentially stable subsystem, where the temporary loss of observability (due to lack of excitation) is handled by suitable regularization and adaptive weights. However, the robustness properties have not been analyzed, and the imposed conditions for guaranteed state and parameter convergence are not trivial to verify in practice. In [FS23], MHE under a non-uniform observability condition is considered, which is potentially also suitable to be used for joint state and parameter estimation. The results, however, rely on persistently exciting inputs and, in particular, no fallback strategy is provided in case a lack of excitation occurs in practice during estimation. The work [BRD22] investigates MHE for joint state and parameter estimation from the perspective of numerical optimization. Here, the lack of excitation is addressed by using additional pseudo-measurements in case the variances of the estimates do not sufficiently decrease over the estimation horizon. This ensures that the corresponding covariance matrix remains bounded and the arrival cost is properly regularized; however, this approach lacks (global) stability guarantees.

An alternative approach to joint state and parameter estimation is provided by *adaptive observers*, which compute state estimates and simultaneously update internal model parameters. This concept originates from the work [Kre77] and has been extensively studied in the literature, see, e.g., [IS12] for an introduction to this topic. Theoretical guarantees usually consider the case of constant parameters and involve a detectability or observability condition on the system states and a persistence of excitation (PE) condition to establish parameter convergence. Different system classes (usually neglecting disturbances) have been considered, e.g., linear time-varying (LTV) systems [ŢB16], Lipschitz nonlinear systems under a linear parameterization [CR97], nonlinearly parameterized systems [Far+09; Tyu+13], or systems in a certain nonlinear adaptive observer canonical form, compare, e.g., [BG88; MST01]. An adaptive sliding mode observer was proposed in [EEZ16], which was generalized to a more general class of systems in [Fra+20], albeit under conditions that imply certain structural restrictions. Adaptive observers usually can also be applied to track (slowly) time-varying parameters if a forgetting factor is used in the design, see, e.g., [ŢB16]. Time-varying parameters are explicitly considered and analyzed in, e.g., [BG88] and [MST01], requiring that the parameter and its time-derivative are globally bounded for all times. Alternative approaches for systems

in canonical forms can be found in, e.g., [BM21], where more general identifiers are used to estimate the dynamics.

The vast part of the literature on state and parameter estimation considers PE conditions to be uniform in time, which usually is restrictive and cannot be guaranteed *a priori* (except, e.g., for linear systems and suitable input trajectories). To ensure practical applicability, it is essential to investigate weaker, especially non-uniform, excitation conditions. In this context, for example, a regularized adaptive Kalman filter (for LTV systems) was proposed in [Mar+22] and an adaptive observer (for systems in a nonlinear adaptive observer canonical form) in [TM23]. In both works it could be shown that the state and parameter estimation errors are bounded without excitation and exponentially stable in the presence of PE. Relaxed excitation conditions have recently received much attention in the context of (pure) parameter estimation of regression models. In [EBO19], however, it was shown that weaker conditions than PE generally only allow for non-uniform asymptotic stability guarantees, which is also consistent with earlier works, e.g., [PLT01]. Using the *dynamic regressor extension and mixing* idea, exponential convergence could be established for linear regression models (and certain classes of nonlinear ones), merely assuming interval excitation (which is strictly weaker than uniform PE), compare, e.g., [Kor+22; ORA22].

1.2.5. Performance guarantees for state estimation

Current research in the field of MHE is primarily concerned with stability and robustness guarantees, see, for example, [RMD20, Ch. 4] and [ABB08; Ale+10; AR21; KM23; Sch+23; Hu24; Ale25]. These works essentially show that under suitable detectability conditions, the estimation error of MHE (i.e., the deviation between the estimated and the real system state) converges to a neighborhood of the origin, the size of which depends on the true unknown disturbance. However, results on the actual performance of nonlinear MHE methods, and in particular on the approximation accuracy and performance loss compared to a particular (challenging) benchmark, are lacking.

In general, a useful metric for quantifying the cumulative performance gap of a certain (estimation or control) algorithm with respect to a given benchmark is provided by the notion of dynamic regret. This is in fact a standard measure for analyzing related methods in the field of reinforcement learning [JOA10; ACJ21]. For the control of linear dynamical systems, regret-optimal controllers are designed in, e.g., [Sab+21; DSZ22; Mar+24b; Mar+24a]. Moreover, a regret analysis is performed for, e.g., online optimal control algorithms [Aga+19; LCL19; NM22], and the relation between bounded dynamic regret and asymptotic stability of the resulting closed loop is formally analyzed in [NM23].

In the context of state estimation for linear systems, regret-optimal filters are designed in [GH23; SH22], which essentially minimize the regret with respect to a clairvoyant (acausal) filter having access to future measurements. This approach is extended in [BDF23], where an exact solution to the minimal-regret observer is pro-

vided utilizing the system level synthesis framework. In [GGE22], an MHE scheme is proposed that provides regret guarantees with respect to an arbitrary comparative (e.g., the clairvoyant) observer. This approach is extended to nonlinear systems in [GGE21], but requires a restrictive convexity condition on the problem and disturbance- and noise-free data.

Whereas performance guarantees for state estimators are generally rather rare and usually restricted to linear systems, they often play an important role in nonlinear optimal control, especially when the overall goal is an economic one. Corresponding results usually employ a *turnpike* property of the underlying nonlinear optimal control problem, compare [McK86; CHL91]. This property essentially implies that optimal trajectories most of the time stay close to an optimal equilibrium (or in general an optimal time-varying reference), which is regarded as the *turnpike*. Turnpike-related arguments are an important tool for assessing the closed-loop performance of nonlinear model predictive controllers with general economic costs on finite and infinite horizons, see, for example, [Grü16; FGM18; GP19; FG22]. Necessary and sufficient conditions for the presence of the turnpike phenomenon in optimal control are discussed in, e.g., [Dam+14; GM16; Fau+22; Tré23], and are usually based on dissipativity, controllability, and suitable optimality conditions.

1.3. Contributions and outline of this thesis

The main contribution of this thesis is the development of MHE methods for general nonlinear systems in the presence of process disturbances and measurement noise, for which desired (and in particular not too conservative) robust stability and performance guarantees can be given under realistic and verifiable conditions. In the following, we outline the structure of this thesis and clarify the contributions in detail.

Chapter 2: Nonlinear detectability

In this chapter, we focus on i-IOSS as a characterization of detectability for general nonlinear systems. We start by introducing different notions of i-IOSS in discrete time in Section 2.1, encompassing the traditional asymptotic-gain formulation and modern, time-discounted versions. Then, in Section 2.2, we concentrate on continuous-time systems and propose a particular L^2-to-L^∞ variant of i-IOSS, namely time-discounted incremental integral IOSS (i-iIOSS). We introduce a corresponding Lyapunov function characterization of i-iIOSS relying on a dissipation inequality in integral form, where we show that an exponential decay can be considered without loss of generality. We establish equivalence between the existence of an i-iIOSS Lyapunov function and i-iIOSS by means of a converse Lyapunov theorem. Our proofs use similar tools as in previous works on incremental integral ISS [Ang09] and i-IOSS in the discrete-time setting [ART21]; however, we point out that the presented results do not straightforwardly follow from them. In particular, continuity of the Lyapunov function candidate is shown by replacing the standard

local Lipschitz assumption on the vector field of the system by a global property involving the Osgood condition [Osg98]. As a byproduct, based on this assumption, we formally prove global existence and uniqueness of system trajectories by adapting the results from [Lip00; Bih56] to the generic class of measurable, locally essentially bounded functions.

Furthermore, we propose a time-discounted integral L^2-to-L^∞ variant of robust global asymptotic stability (RGAS) and show necessity of i-iIOSS for a system to admit a general observer mapping satisfying this property. Asking such a stability property from an observer is advantageous for several reasons: first, it can be seen as accounting for the disturbance energy under fading memory and thus allows for a physical interpretation; second, it directly implies an L^∞ error bound and thus combines the advantages of classical ISS and integral ISS properties. Overall, we provide a general framework for a Lyapunov-based robust stability analysis of observers in continuous time. This will be an essential tool in the context of moving horizon estimation in Chapter 3.

Chapter 3: Robust stability

In this chapter, we focus on robust stability guarantees for MHE and in particular concentrate on a recent Lyapunov-based MHE approach. We first provide a mathematical background on MHE by introducing a basic discrete-time MHE scheme in Section 3.1, where we discuss fundamental properties and characteristics. Then, we briefly introduce the Lyapunov-based MHE framework proposed in [Sch+23, Sec. III], which forms a basis for many of the results in this thesis (but is not itself a contribution[1] of it).

In Section 3.2, we propose a Lyapunov-based MHE scheme for general nonlinear continuous-time systems. We employ a least squares objective with fading memory and establish robust global exponential stability of the estimation error in a time-discounted L^2-to-L^∞ sense. Here, we heavily rely on the concepts of i-iIOSS and RGAS introduced in Chapter 2 to characterize the required detectability and robust stability properties. Our derivation builds on our ideas for the discrete-time case from [Sch+23, Sec. III]; however, the results do not trivially follow from this. Instead, the presented results are more general, require a different proof technique, and offer key advantages over purely discrete-time schemes, especially when the physical system to be estimated actually corresponds to a continuous-time one (which is often the case in practice). First, we note that arbitrary sampling strategies can be employed to define time instants at which the underlying optimization problem is actually solved, which can even be modified online at runtime. This provides a

[1] Julian D. Schiller (the author of this thesis) and Simon Muntwiler are joint first authors of the article [Sch+23]; Simon Muntwiler provided the theoretical analysis of discrete-time Lyapunov-based MHE (Sections III-B and III-C in [Sch+23]), which is part of the contributions of the PhD thesis [Mun24]; Julian D. Schiller contributed the comparison with existing results from the MHE literature (Section III-D), methods to verify the underlying detectability condition (Section IV), and the numerical examples (Section V), which are included in this thesis. A detailed description of the contributions of each author of [Sch+23] is given in Appendix A.

huge additional degree of freedom, and even allows the proposed MHE scheme to be used in an event-triggered fashion, that is, by choosing the sampling instants online depending on a suitable triggering rule. Consequently, the proposed MHE scheme can be better tailored to the problem at hand, which can yield more accurate results with less computational effort compared to standard equidistant sampling. Furthermore, it may be advantageous in practice to characterize the detectability of a continuous-time system instead of its discretized representation, as the corresponding analysis is structurally easier and particularly does not require specifying a certain discretization scheme and a sampling period beforehand, compare also Section 7.1. Moreover, the derived robustness guarantees are valid for MHE applied to the real physical continuous-time system, and not to an approximately discretized model (which may suffer from additional discretization errors).

In Section 3.3, we provide a detailed discussion of Lyapunov-based approaches in nonlinear MHE (covering both discrete- and continuous-time frameworks), highlighting its advantageous properties arising from the fact that we argue entirely in Lyapunov coordinates. Specifically, tuning the MHE cost function in order to achieve valid theoretical guarantees becomes more easy and intuitive, and the derivation generally allows for significantly less conservative (i.e., smaller) estimates of the minimum required horizon length compared to the literature.

We illustrate the applicability of Lyapunov-based MHE for both discrete- and continuous-time systems in Section 3.4, using a nonlinear chemical reaction and a quadrotor model from the literature. Here, we certify detectability by computing i-IOSS and i-iIOSS Lyapunov functions using our methods from Section 7.1 and apply the Lyapunov-based MHE schemes from [Sch+23, Sec. III] and Section 3.2. Overall, our examples show that the combination of the considered Lyapunov-based MHE schemes with our verification methods from Section 7.1 allow for guaranteed robust stability (specifically, RGAS) of MHE under practical conditions, for both discrete- and continuous-time systems.

Chapter 4: Suboptimality guarantees for real-time applications

In this chapter, we present several suboptimal MHE schemes for general perturbed nonlinear discrete-time systems and provide robustness guarantees that particularly do not require optimality of the solutions. This is crucial in order to ensure real-time applicability of MHE in cases where the optimization problem cannot be solved to optimality within one fixed sampling interval. To this end, we establish the "feasibility-implies-stability/robustness" paradigm from model predictive control (MPC) in the context of nonlinear MHE. Indeed, it is well known that if the suboptimal solution to a given MPC problem can be guaranteed to improve the cost of a suitably chosen warm start, then robust stability of the controller can be directly inferred [SMR99; PRW11]. Transferring this concept to state estimation, we prove robust stability of suboptimal MHE by simply requiring that a suboptimal solution improves the cost of a feasible *candidate solution*. Here, we employ an *a priori* known, robustly stable auxiliary observer, from which the robust stability properties can be

inherited. We specify our setup concerning the system and the auxiliary observer in Section 4.1.

In Section 4.2, we consider a classical MHE formulation which optimizes over system trajectories, allowing for suboptimal MHE using a standard least squares cost function, which is typically chosen in practical applications. We propose two different candidate solutions for the MHE problem, where the first one essentially corresponds to a nominal system trajectory initialized with an estimate of the auxiliary observer, and the second one employs the trajectory of the auxiliary observer restricted to the current estimation horizon. While the former is applicable to general nonlinear systems, the latter requires a certain structure of the system and the observer, but provides qualitatively better theoretical guarantees (in particular, disturbance gains that do not deteriorate with increasing estimation horizons). For both candidate solutions, we show that the i-IOSS Lyapunov function characterizing the detectability of the underlying nonlinear system directly serves as Lyapunov function for suboptimal MHE, from which robust stability can be directly inferred. Here, the derived robustness guarantees are valid independent of (i) the horizon length; (ii) the chosen optimization algorithm; (iii) the number of solver iterations performed at each time step (including zero). This represents a major generalization compared to the literature, as theoretical guarantees for real-time capable MHE schemes usually rely on local convergence properties of a particular optimization algorithm.

We additionally extend our results to the practically relevant case where the auxiliary observer may leave the known physical domain of the system (e.g., due to transient dynamics or perturbations), but where such additional knowledge is to be leveraged in the MHE problem through an additional state constraint. To this end, we propose suitable adaptions to the candidate solutions to ensure their feasibility and thus guarantee constraint satisfaction of suboptimal MHE for all times.

We illustrate the applicability of the proposed suboptimal MHE scheme with a chemical reaction example, where we first formally verify the sufficient conditions for robust stability of suboptimal MHE. We observe that performing only a single iteration of the optimizer each time step is sufficient to significantly improve the estimation results from the auxiliary observer and achieve an overall estimation performance close to that obtained with standard (optimal) MHE, while significantly reducing the required computation times. Moreover, this illustrates that the proposed re-initialization strategy used in the construction of the candidate solutions can be very effective, especially in the case of poor transient behavior of the auxiliary observer.

In Section 4.3, we consider a modified MHE formulation where we optimize over trajectories of the auxiliary observer, similar to the idea proposed in [SJF10; SJ14; Suw+14; WK17]. This leads to an estimation scheme that is easier to implement and provides improved theoretical guarantees. Since the corresponding suboptimal MHE scheme is even stronger connected to the auxiliary observer, the theoretical analysis is more direct, ultimately leading to tighter error bounds. Provided that the auxiliary observer admits an i-ISS Lyapunov function, we show that this function directly serves as Lyapunov function for suboptimal MHE under a suitable choice of

the horizon length. In contrast to [Suw+14; WK17; GGE21], the derived guarantees are independent of the optimization algorithm, hold for an arbitrary number of solver iterations, improve as the horizon length increases, and asymptotically approach those from the auxiliary observer (which is the best possible bound given that we derive guarantees for an arbitrary number of iterations, including zero).

The simulation example shows that performing already one iteration is sufficient to significantly improve the estimation results of the auxiliary observer. Moreover, we find that the modified suboptimal MHE scheme can outperform comparable suboptimal/fast MHE schemes from the literature that optimize over system trajectories, especially in case the auxiliary observer is rather aggressive.

Chapter 5: Joint state and parameter estimation

In this chapter, we provide MHE schemes for joint state and parameter estimation for general nonlinear discrete-time systems subject to process disturbances and measurement noise. This is generally a challenging problem, as in practice insufficient excitation may occur frequently or unpredictably, potentially rendering classical approaches based on uniform excitation properties ineffective or invalid. It is therefore essential to deal with concepts of non-uniform PE in order to cover such scenarios and to ensure that the estimation methods are robust in this respect.

We first consider the case of constant parameters in Section 5.2. Here, we propose an MHE scheme that avoids a uniform PE condition and instead uses online information about the current excitation of the parameters to suitably adjust the regularization term in the cost function. We establish a bound on the state and parameter estimation error that is valid for all times—even if the parameters are never or only rarely excited—and which improves the more often sufficient excitation is present. The bound specializes to a robust global exponential stability property under an additional uniform condition on the maximum duration of insufficient excitation. We furthermore discuss the (restrictive) case of uniform PE, where we show that this is equivalent to the existence of a joint i-IOSS Lyapunov function for the augmented state vector consisting of the states and the system parameters, rendering standard MHE methods for state estimation applicable.

In Section 5.3, we extend the MHE scheme and corresponding theoretical results to the more general case of time-varying parameters. The analysis involves an additional weak incremental bounded-energy bounded-state property of the parameter dynamics. Such a condition is naturally required to ensure that arbitrary parameter drifts cannot cause the estimation error to become unstable in case the parameter is insufficiently excited and hence unobservable. This allows us to develop robustness guarantees for the overall (state and parameter) estimation error that are valid independent of the parameter excitation, and which improve the more often the parameters are detected to be sufficiently excited during operation.

The numerical examples illustrate that the proposed MHE schemes in combination with the PE monitoring techniques from Section 7.2 are able to efficiently compensate for phases of weak excitation. Specifically, we obtain reliable estimation results

for all times, which are accurate if sufficient excitation is present and which do not deteriorate arbitrarily in phases without excitation.

Chapter 6: Turnpike analysis and performance guarantees

In this chapter, we take a different perspective on MHE and investigate the underlying optimal state estimation problem through the lens of optimal control. This motivates us to study the turnpike phenomenon in the context of optimal state estimation, which consequently leads to novel performance and regret guarantees for optimization-based state estimators, in particular MHE.

In Section 6.1, we formalize the general optimal state estimation problem that considers a finite data set of available input-output measurements collected from a general nonlinear dynamical system. Then, we specify the benchmark against which we want to compare the corresponding solution: the omniscient optimal state estimator with infinite horizon that has perfect memory and access to future measurements.

In Section 6.2, we discuss and analyze the turnpike phenomenon appearing in finite-horizon optimal estimation problems, which are at the core of all MHE and FIE methods. In particular, we show that the benchmark estimator, i.e., the solution of the (acausal) infinite-horizon optimal state estimation problem, serves as turnpike for finite-horizon problems involving only a subset of the data. We consider different mathematical characterizations of this phenomenon and provide sufficient conditions that involve strict dissipativity and decaying sensitivity of the optimal estimation problem. Furthermore, we perform a detailed turnpike analysis for the special case of linear systems and quadratic cost functions, where we essentially show that decaying sensitivity is naturally present under controllability and observability using standard arguments from optimal control and Riccati theory. We discuss the considered turnpike characterizations with regard to their properties and limitations and introduce a general turnpike definition that combines their advantages. Overall, our turnpike analysis leads to the surprising observation that MHE problems naturally exhibit both an approaching and a leaving arc, which may have a strong negative impact on the estimation accuracy.

In Section 6.3, we propose a slightly modified variant of classical MHE that involves an additional delay to effectively counteract the influence of the leaving arc. We show that the performance of the delayed MHE scheme is approximately optimal and achieves bounded dynamic regret with respect to the infinite-horizon benchmark estimator, with error terms that can be made arbitrarily small by an appropriate choice of the delay. As a result, MHE (with delay) is able to *track the accuracy and performance of the omniscient infinite-horizon benchmark estimator*. Moreover, we propose a novel turnpike prior for MHE formulations with prior weighting, which—in contrast to the classical filtering or smoothing prior—can be shown to converge to a neighborhood around the infinite-horizon benchmark estimator that can be made arbitrarily small by design. Furthermore, we consider the special case of MHE for offline estimation and show that good performance of a state estimator directly implies small estimation errors with respect to the true unknown system state.

In Section 6.4, we illustrate our theoretical results in terms of various numerical examples from the literature, which show that the proposed modifications can significantly improve the estimation results in practice. In particular, we apply the developed theory to a continuously stirred tank reactor and a highly nonlinear quadrotor model with 12 states. Here, we can observe that the turnpike phenomenon is present in MHE. Moreover, we find that even a delay of very few steps in the MHE scheme improves the overall estimation error by 20-25 % compared to standard MHE (without delay). For offline estimation of linear systems, we show that the proposed delayed MHE scheme provides a useful alternative to established iterative methods such as the Kalman filter and related smoothing algorithms, significantly outperforming them especially in the presence of non-normally distributed noise.

Chapter 7: Verification methods

In this chapter, we present various tools to numerically verify important system-theoretic properties of general nonlinear systems in practice, such as detectability (in terms of i-IOSS) and PE. In particular, we employ different tools to reformulate the corresponding mathematical conditions in the form of linear matrix inequalities (LMIs) that can be efficiently verified using semidefinite programming (SDP) and sum-of-squares (SOS) optimization, linear parameter-varying (LPV) embeddings, or gridding techniques.

In Section 7.1, we focus on the computation of i-IOSS and i-iIOSS Lyapunov functions for discrete- and continuous-time systems, which directly certify exponential i-IOSS and i-iIOSS, respectively. Note that the lack of such a method in the literature was generally considered a major problem in [AR21], since i-IOSS became a standard detectability assumption in the recent nonlinear MHE literature [Mül17; AR19b; RMD20; Hu24; KM23; AR21; Ale25]. Here, we address this problem and provide practical tools to actually verify this crucial property in practice.

In Section 7.2, we consider verification methods for PE of trajectory pairs, suitable to monitor non-uniform excitation properties of unknown system parameters. We first consider the case of constant parameters, where we derive a general condition involving a particular observability metric that is constructed using certain matrix recursions, which can be interpreted as the filtered linearized regressor information that is visible at the output. Our method is applicable to general nonlinear systems, requiring the two system trajectories under consideration to be sufficiently close to each other. We show how these results can be strengthened to arbitrary system trajectories by restricting the class of systems to a certain linearly parameterized adaptive observer normal form. We extend our results to the case of time-varying parameters, which under certain conditions can also be used to verify (non-uniform) observability of system states.

The numerical experiments conducted in Chapters 3–6 illustrate the applicability of the proposed verification methods to practical examples from the literature.

Chapter 8: Conclusions

In this chapter, we provide a concluding overview, summarize the most important contributions of this thesis, and explain interesting topics and extensions for future research.

Author statement on previously published works

This thesis presents the outcome of several years of research on MHE theory. Significant parts have therefore already been published in scientific journals and presented at conferences (or have been submitted there for review). These publications are adopted here (in some cases verbatim), further developed, and placed in a broader context. In particular, the Chapters 2–7 are based on the following publications:

- Chapter 2: [SM23c] and [SM24b, Sec. 2]
- Chapter 3: [SM24b] and [Sch+23, Sec. III-D, Sec. V]
- Chapter 4: [SM23d; SWM23; SKM21]
- Chapter 5: [SM23b; SM24a]
- Chapter 6: [SGM24; SGM25]
- Chapter 7: [Sch+23, Sec. IV], [SM24b, Sec. 4], [SM23b, Sec. 5], [SM23a, Sec. 4]

A detailed list of the publications, including a description of the contributions of the individual authors, can be found in Appendix A.

2. Nonlinear detectability

In this chapter, we focus on i-IOSS as a characterization of nonlinear detectability. We start by introducing different notions of i-IOSS in Section 2.1, encompassing the traditional "asymptotic-gain" formulation and time-discounted variants. In contrast to discrete-time systems, where they are fully equivalent to each other, this is generally not the case for continuous-time systems. In Section 2.2, we hence focus on the strongest one, which is given by time-discounted incremental integral IOSS (i-iIOSS). In particular, we provide an equivalent Lyapunov function characterization and establish necessity of i-iIOSS for the existence of state estimators satisfying a robust stability property in a time-discounted L^2-to-L^∞ sense.

The theoretical results in this chapter form the general basis for the MHE schemes presented in Chapter 3 (especially for the continuous-time MHE scheme in Section 3.2). They are complemented with suitable verification methods in Section 7.1, where we provide constructive conditions (in terms of LMIs) to obtain i-IOSS and i-iIOSS Lyapunov functions.

Disclosure: The following chapter is based upon and in parts literally taken from our previous publications [SM23c] and Section 2 in [SM24b]. A detailed description of the contributions of each author is given in Appendix A.

2.1. On different variants of i-IOSS

There are actually multiple ways to define i-IOSS, as we will show in the following. To this end, let us consider the discrete-time system

$$x(t+1) = f(x(t), u(t), d(t)), \quad x(0) = \chi, \tag{2.1a}$$

$$y(t) = h(x(t), u(t)) \tag{2.1b}$$

with discrete time $t \in \mathbb{I}_{\geq 0}$, states $x(t) \in \mathbb{R}^n$, outputs $y(t) \in \mathbb{R}^p$, time-varying parameters $u(t) \in \mathbb{R}^m$, and inputs $d(t) \in \mathbb{R}^q$. Given some initial state $\chi \in \mathbb{R}^n$ and the sequences $u = \{u(j)\}_{j=0}^{\infty}$ and $d = \{d(j)\}_{j=0}^{\infty}$, we denote the corresponding states and outputs of the system (2.1) at time $t \in \mathbb{I}_{\geq 0}$ by $x(t) = x(t, \chi, u, d)$ and $y(t) = y(t, \chi, u, d) = h(x(t, \chi, u, d), u(t))$.

Remark 2.1 (Roles of the inputs)**.** *Note that the naming and roles of the variables u and d is not standard in the ISS-related literature. Nevertheless, this is done to be consistent with the notation used in this thesis (and generally in the literature related to state estimation), where u refers to* known *inputs (e.g., control inputs), and d to* unknown *inputs affecting the dynamics such as process disturbances.*

The notion of i-IOSS characterizes the distance between two state trajectories $x_1 = \{x(t, \chi_1, u, d_1)\}_{t=0}^{\infty}$ and $x_2 = \{x(t, \chi_2, u, d_2)\}_{t=0}^{\infty}$ of the system (2.1) that result from the same parameter sequence u but different initial states χ_1 and χ_2 and different input sequences d_1 and d_2. Defining the corresponding outputs $y_i = \{y(t, \chi_i, u, d_i)\}_{t=0}^{\infty}$, $i = 1, 2$, we can give the traditional i-IOSS definition as introduced in [SW97, Def. 22] (transferred to the discrete-time setting) in terms of a max-based bound using a function $\beta \in \mathcal{KL}$ and asymptotic disturbance gains $\gamma_d, \gamma_y \in \mathcal{K}$:

$$|x_1(t) - x_2(t)| \leq \max\{\beta(|\chi_1 - \chi_2|, t), \gamma_d(\|d_1 - d_2\|_{0:t}), \gamma_y(\|y_1 - y_2\|_{0:t})\} \tag{2.2}$$

for all $t \in \mathbb{I}_{\geq 0}$. This notion essentially implies that the difference between two state trajectories of the system (2.1) is upper bounded by the difference in their respective initial conditions, their inputs, and their corresponding outputs. Here, it is important to note that the influence of the difference in the initial states decays over time due to the fact that $\beta \in \mathcal{KL}$, while the disturbance and output terms persist. Hence, if two system trajectories have small differences in their inputs and outputs, then eventually their states must converge to each other. Consequently, (2.2) entails an asymptotic version of the classical indistinguishability condition and thus represents a detectability property. Moreover, it is not a restrictive condition in the context of robustly stable state observers (which are the focus of this work), since i-IOSS is in fact necessary for the existence of such, compare [SW97, Prop. 23].

Due to the asymptotic gains in (2.2), however, it has turned out that this formulation is difficult to work with and usually only leads to unsatisfactorily conservative stability guarantees in the context of MHE, compare the discussion in Section 3.3 below. A more elegant variant of i-IOSS with additional time-discounting was proposed in [KM20; ART21] (for discrete-time systems), where it was shown that the discounting of past disturbances appears very natural and even without loss of generality. The corresponding property can be characterized as

$$\begin{aligned} |x_1(t) - x_2(t)| \leq \max\Big\{ &\beta(|\chi_1 - \chi_2|, t), \max_{j \in \mathbb{I}_{[0,t-1]}} \beta_d(|d_1(j) - d_2(j)|, t - j - 1), \\ &\max_{j \in \mathbb{I}_{[0,t-1]}} \beta_y(|y_1(j) - y_2(j)|, t - j - 1) \Big\} \end{aligned} \tag{2.3}$$

for all $t \in \mathbb{I}_{\geq 0}$, where $\beta, \beta_d, \beta_y \in \mathcal{KL}$.

Another different formulation is obtained if in (2.3) we replace maximization by summation and apply a certain coordinate transformation in which the asymptotic decay specializes to an exponential one:

$$\begin{aligned} \alpha(|x_1(t) - x_2(t)|) \leq \alpha_x(|\chi_1 - \chi_2|)\eta^t \\ + \sum_{j=0}^{t-1} \eta^{t-j-1} \Big(\alpha_d(|d_1(j) - d_2(j)|) + \alpha_y(|y_1(j) - y_2(j)|) \Big) \end{aligned} \tag{2.4}$$

for all $t \in \mathbb{I}_{\geq 0}$, where $\alpha, \alpha_x, \alpha_d, \alpha_y \in \mathcal{K}_\infty$ and $\eta \in (0, 1)$. This formulation is particularly beneficial since it has an equivalent Lyapunov function[1] characterization,

[1] Whereas in [ART21] there is no formal distinction between the notions from (2.3) and (2.4), the first step in the proof of the converse Lyapunov result [ART21, Th. 3.2] corresponding to the property (2.3) is to transfer (2.3) into (2.4) using Sontag's $\mathcal{KL}$-Lemma [Son98, Prop. 7] and replacing maximization with summation.

see [ART21, Th. 3.2].

A key advantage of considering discrete-time systems as in (2.1) is that all i-IOSS formulations from (2.2)–(2.4) were in fact shown to be fully equivalent, see [ART21], [KM20], and the technical report [ART20]. As a consequence, the Lyapunov function characterization of (2.4) is generally also valid for the properties (2.2) and (2.3), and has therefore proven to be very useful in the context of optimization-based state estimation, compare [AR21; Sch+23].

For continuous-time systems, only the asymptotic notion of i-IOSS (2.2) exists in the literature [SW97, Def. 22]. Transferring (2.3)–(2.4) to continuous time by replacing the maximum operation by the essential supremum norm and summation by integration, we observe that (2.2)–(2.4) turn out to be actually very different properties (without further restricting the class of inputs or the system to evolve on compact sets), and we carefully have to distinguish between them. Note that this is to be expected, because ISS and integral ISS are known to be very different properties in the presence of general continuous-time systems, each suitable for a different class of input functions; for more details, we refer to the book [Mir23]. However, due to the exponential discounting, it is immediately clear that the continuous-time versions of (2.2)–(2.4) satisfy the implications (2.4) $\Rightarrow$ (2.3) $\Rightarrow$ (2.2), compare Proposition 2.4 below. In the following, we focus on the strongest property given by (2.4), which, as we show, is closely connected to a strong robust stability property for state estimators—the main topic of this thesis.

2.2. Incremental integral input/output-to-state stability

In this section, we formalize the time-discounted i-IOSS notion from (2.4) in the context of continuous-time systems—namely, i-iIOSS. To this end, we first specify the general setting and classes of input functions in Section 2.2.1. Then, we define i-iIOSS using nominal and disturbed outputs in Section 2.2.2, propose equivalent Lyapunov function characterizations in Section 2.2.3, and establish necessity of i-iIOSS for the existence of state estimators satisfying a robust stability property in a time-discounted L^2-to-L^∞ sense in Section 2.2.4.

2.2.1. Setup and Preliminaries

We consider continuous-time systems of the form

$$\dot{x}(t) = f(x(t), u(t), d(t)), \quad x(0) = \chi, \tag{2.5a}$$
$$y(t) = h(x(t), u(t), v(t)) \tag{2.5b}$$

with internal states $x(t) \in \mathcal{X} \subseteq \mathbb{R}^n$ $(0 \in \mathcal{X})$, initial condition $\chi \in \mathcal{X}$, outputs $y(t) \in \mathcal{Y} \subseteq \mathbb{R}^p$ $(0 \in \mathcal{Y})$, and time $t \geq 0$. The time-varying parameter $u : \mathbb{R}_{\geq 0} \to \mathcal{U} \subseteq \mathbb{R}^m$

and the inputs[2] $d : \mathbb{R}_{\geq 0} \to \mathcal{D} \subseteq \mathbb{R}^q$ and $v : \mathbb{R}_{\geq 0} \to \mathcal{V} \subseteq \mathbb{R}^o$ are measurable, locally essentially bounded functions[3] (with $0 \in \mathcal{U}, \mathcal{D}, \mathcal{V}$), and we denote the set of such functions as $\mathcal{M}_\mathcal{U}$, $\mathcal{M}_\mathcal{D}$, and $\mathcal{M}_\mathcal{V}$, respectively. For the sake of conciseness, for two input functions $d \in \mathcal{M}_\mathcal{D}$ and $v \in \mathcal{M}_\mathcal{V}$ we sometimes use w to denote the combined input function $w = (d, v) \in \mathcal{M}_\mathcal{D} \times \mathcal{M}_\mathcal{V}$.

The solution of the differential equation (2.5a) at $t \geq 0$ for some initial state $\chi \in \mathcal{X}$ and input signals $u \in \mathcal{M}_\mathcal{U}$ and $d \in \mathcal{M}_\mathcal{D}$ is denoted by $x(t, \chi, u, d)$. Here, we consider solutions in the extended sense, that is, $x(t) = x(t, \chi, u, d)$ is an absolutely continuous function solving the integral equation $x(t) = \chi + \int_0^t f(x(\tau), u(\tau), d(\tau))d\tau$, which satisfies (2.5a) almost everywhere (i.e., for all $t \geq 0$, except on a set of measure zero), see, e.g., [CL55, Sec. 2.1] for further technical details. The corresponding output according to (2.5b) is denoted by $y(t, \chi, u, w) := h(x(t, \chi, u, d), u(t), v(t))$ for any input signal $v \in \mathcal{M}_\mathcal{V}$. We sometimes consider the nominal output of the system (2.5) where $v \equiv 0$, which we denote by $y_\mathrm{n}(t, \chi, u, d) := h(x(t, \chi, u, d), u(t), 0)$.

We impose the following assumption on the vector field f.

Assumption 2.1. *The function $f : \mathcal{X} \times \mathcal{U} \times \mathcal{D} \to \mathbb{R}^n$ satisfies $f(0, 0, 0) = 0$ and*

$$|f(x_1, u_1, d_1) - f(x_2, u_2, d_2)| \leq \kappa_1 \left(|(x_1, u_1, d_1) - (x_2, u_2, d_2)|\right) \tag{2.6}$$

for all $x_1, x_2 \in \mathcal{X}$, all $u_1, u_2 \in \mathcal{U}$, and all $d_1, d_2 \in \mathcal{D}$, where $\kappa_1 : \mathbb{R}_{\geq 0} \to \mathbb{R}_{\geq 0}$ is continuous, non-decreasing, $\kappa_1(0) = 0$, $\kappa_1(s) > 0$ for all $s > 0$, and

$$\int_0^1 \frac{ds}{\kappa_1(3s)} = \infty, \qquad \int_1^\infty \frac{ds}{\kappa_1(3s)} = \infty. \tag{2.7}$$

Assumption 2.1 implies a global uniform continuity property of f along with a maximum growth condition. It is essential for proving the converse Lyapunov theorem for i-iIOSS in Section 2.2.3, where we note that the factor 3 in (2.7) is required for technical reasons and without loss of generality. It replaces the usual assumption of f being locally Lipschitz (which is not suitable in our case, compare Remark 2.7 below) and ensures global existence and uniqueness of solutions of (2.5). Inequality (2.6) together with the first equation in (2.7) is similar to the so-called Osgood condition, which was originally proposed in [Osg98] to establish local uniqueness of solutions of ordinary differential equations without employing a Lipschitz property. The second equation in (2.7) ensures that these solutions exist globally in time. Note that a similar condition is in fact necessary for the global existence of solutions to the scalar differential equation $\dot{\xi} = \kappa_1(\xi)$, compare [Con95]. Valid functions κ_1 that satisfy Assumption 2.1 are, e.g., $s \mapsto s$, $s \mapsto s \ln(s + 1)$, $s \mapsto (s + 1) \ln(s + 1)$, compare also [Con95; Lip00; Osg98]. While especially the second condition in (2.7) may

[2] Again, it should be noted that the naming and roles of the variables u, d, and v are such that they are consistent with the notation used in this thesis, where u usually refers to *known* inputs (e.g., control inputs), and d and v to *unknown* inputs affecting the dynamics (e.g., process disturbances) and the observed output (e.g., measurement noise), respectively, compare Remark 2.1.

[3] See [Son90, Appendix C.1] for definitions and further details on standard technical terms related to Lebesque measure theory.

be a limitation in practice, we point out that global existence of solutions is often assumed in the literature and significantly facilitates the exposition of our results.

The main properties of solutions of (2.5a) under Assumption 2.1 are summarized in the following proposition, which is a straightforward extension of the results from [Lip00; Bih56] by addressing the generic class of inputs considered here.

Proposition 2.1. *Suppose that Assumption 2.1 is satisfied. Then, the ordinary differential equation in* (2.5a) *admits a unique solution defined globally on* $\mathbb{R}_{\geq 0}$ *for all* $\chi \in \mathcal{X}$*, all* $u \in \mathcal{M}_{\mathcal{U}}$*, and all* $d \in \mathcal{M}_{\mathcal{D}}$*.*

To prove Proposition 2.1, we first derive a bound on the difference between trajectories over a fixed time interval by adapting the results from [Lip00] and [Bih56]. This can also be interpreted as a continuity property of the flow of the vector field f in (2.5a).

Lemma 2.1. *Let Assumption 2.1 hold. Then, there exists some* $\rho \in \mathcal{K}_\infty$ *such that for each* $\chi_1, \chi_2 \in \mathcal{X}$*,* $u_1, u_2 \in \mathcal{M}_{\mathcal{U}}$*, and* $d_1, d_2 \in \mathcal{M}_{\mathcal{D}}$*, there exists* $T > 0$ *such that*

$$|x(t, \chi_1, u_1, d_1) - x(t, \chi_2, u_2, d_2)| \leq \ \rho^{-1}(\rho(c)e^t) \tag{2.8}$$

for all $t \in [0, T)$ *with*

$$c := |\chi_1 - \chi_2| + T\kappa_1(3\|u_1 - u_2\|_{0:T}) + T\kappa_1(3\|d_1 - d_2\|_{0:T}). \tag{2.9}$$

Proof. Consider arbitrary $\chi_1, \chi_2 \in \mathcal{X}$, $u_1, u_2 \in \mathcal{M}_{\mathcal{U}}$, $d_1, d_2 \in \mathcal{M}_{\mathcal{D}}$. The existence of the trajectories $x_i(t) = x(t, \chi_i, u_i, d_i)$, $t \in [0, t_i(\chi_i, u_i, d_i))$ is ensured for some $t_i(\chi_i, u_i, d_i) > 0$, $i = 1, 2$ by continuity of f (Assumption 2.1) and Carathéodory's existence theorem (see, for example, [CL55, Th. 1.1, p. 43] and compare also [Mir23, Ch. 1] and [Son90, App. C] for further details). Let $T := \min_{i\in 1,2}\{t_i(\chi_i, u_i, d_i)\}$. Then, for all $t \in [0, T)$, the trajectories x_1 and x_2 satisfy

$$x_1(t) - x_2(t) = \chi_1 - \chi_2 + \int_0^t (f(x_1(\tau), u_1(\tau), d_1(\tau)) - f(x_2(\tau), u_2(\tau), d_2(\tau)))d\tau.$$

Define $\xi(t) = |x_1(t) - x_2(t)|$, $u_\Delta = u_1 - u_2$, and $d_\Delta = d_1 - d_2$. By applying (2.6), the triangle inequality, and the fact that κ_1 is positive definite and non-decreasing, we can deduce that

$$\xi(t) \leq \xi(0) + \int_0^t (\bar{\kappa}_1(\xi(s)) + \bar{\kappa}_1(|u_\Delta(s)|) + \bar{\kappa}_1(|d_\Delta(s)|))ds \tag{2.10}$$

with $\bar{\kappa}_1(s) := \kappa_1(3s)$. Note that

$$\int_0^t (\bar{\kappa}_1(|u_\Delta(s)|) + \bar{\kappa}_1(|d_\Delta(s)|))ds \leq T(\bar{\kappa}_1(\|u_\Delta\|_{0:T}) + \bar{\kappa}_1(\|d_\Delta\|_{0:T})). \tag{2.11}$$

By combining (2.10), (2.11), and the definition of c from (2.9), we obtain

$$\xi(t) \leq c + \int_0^t \bar{\kappa}_1(\xi(s))ds. \tag{2.12}$$

We first assume that $c > 0$. Denote by $U(t)$ the right-hand side of (2.12). Then, $U(0) = c$ and

$$\dot{U}(t) = \bar{\kappa}_1(\xi(t)) \leq \bar{\kappa}_1(U(t)). \tag{2.13}$$

Now consider $G(s) := \int_1^s \frac{dr}{\bar{\kappa}_1(r)}$ for $s > 0$. By Assumption 2.1, $\lim_{s\to 0^+} G(s) = -\infty$ and $\lim_{s\to\infty} G(s) = \infty$. Furthermore, from the Leibniz integral rule, it follows that

$$\frac{d}{dt}G(U(t)) = \frac{d}{dt}\int_1^{U(t)} \frac{dr}{\bar{\kappa}_1(r)} = \frac{\dot{U}(t)}{\bar{\kappa}_1(U(t))}. \tag{2.14}$$

The combination of (2.13) and (2.14) yields $\frac{d}{dt}G(U(t)) \leq 1$. An integration over $[0, t]$ leads to

$$G(U(t)) - G(U(0)) \leq t \qquad \Leftrightarrow \qquad e^{G(U(t))} \leq e^{G(U(0))}e^t. \tag{2.15}$$

Now define $\rho(s) := e^{G(s)}$ for all $s > 0$ and $\rho(0) := 0$. It follows that $\rho \in \mathcal{K}_\infty$ (and thus $\rho^{-1} \in \mathcal{K}_\infty$). Since $\xi(t) \leq U(t)$ for all $t \in [0, T)$ and $U(0) = c$, from (2.15) and the definition of ρ we can conclude that $\xi(t) \leq \rho^{-1}(\rho(c)e^t)$ for all $t \in [0, T)$.

It remains to be shown that (2.8) also applies for $c = 0$. Performing the same steps as before with c replaced by some $\epsilon > 0$ leads to $\xi(t) \leq \rho^{-1}(\rho(\epsilon)e^t)$. Letting $\epsilon \to 0$ recovers (2.8) for $c = 0$ and thus concludes this proof. □

Proof of Proposition 2.1. We note that Proposition 2.1 is an immediate consequence of Lemma 2.1. First, we claim that solutions exist globally in time. Indeed, suppose not. Then, there exist $\chi \in \mathcal{X}$, $u \in \mathcal{M}_\mathcal{U}$, $d \in \mathcal{M}_\mathcal{D}$, and some finite time $T_1 > 0$ such that $\lim_{t\to T_1} |x(t)| = \infty$, where $x(t) = x(t, \chi, u, d)$. Applying Lemma 2.1 with $\chi_1 = \chi$, $u_1 = u$, $d_1 = d$, and $\chi_2 = 0$, $u_2 \equiv 0$, $d_2 \equiv 0$, it follows that (2.8) yields $|x(t)| \leq \rho^{-1}(\rho(|\chi| + T_1(\bar{\kappa}_1(\|u\|_{0:T_1}) + \bar{\kappa}_1(\|d\|_{0:T_1})))e^t)$ for $t \in [0, T_1)$. The right-hand side is bounded for $t \to T_1$, which contradicts finite escape time and hence implies that solutions exist globally on $\mathbb{R}_{\geq 0}$.

It remains to show uniqueness of solutions. To this end, assume that $x_1(t) = x(t, \chi, u, d)$ and $x_2(t) = x(t, \chi, u, d)$ represent two solutions of (2.5a) on the interval $[0, T_2]$ for $T_2 > 0$ with the same initial conditions $\chi \in \mathcal{X}$ and inputs $u \in \mathcal{M}_\mathcal{U}$ and $d \in \mathcal{M}_\mathcal{D}$. It follows that $c = 0$ in (2.9) and $|x_1(t) - x_2(t)| = 0$ for all $t \in [0, T_2]$ by (2.8), which implies uniqueness of solutions on $[0, T_2]$ and hence concludes this proof. □

2.2.2. i-iIOSS for systems with disturbed outputs

For general nonlinear systems in the form of (2.5) where the output equation is subject to an additional nonlinear input v, a natural extension of the i-IOSS formulations from (2.2)–(2.4) (that involve nominal outputs without dependency on v) is to define a similar property with respect to the *disturbed outputs* as previously done in [KM20; KM23]. To this end, we modify the i-IOSS property in (2.4) and transfer it to the general continuous-time setting described in the previous section, which leads to the following definition.

Definition 2.1 (i-iIOSS with disturbed outputs)**.** *The system* (2.5) *is i-iIOSS (with disturbed outputs) if there exist some* $\alpha, \alpha_x, \alpha_w, \alpha_y \in \mathcal{K}_\infty$*, and* $\eta \in (0,1)$ *such that*

$$\begin{aligned}&\alpha(|x_1(t) - x_2(t)|)\\ &\leq \alpha_x(|\chi_1 - \chi_2|)\eta^t + \int_0^t \eta^{t-\tau}\Big(\alpha_w(|w_1(\tau) - w_2(\tau)|) + \alpha_y(|y_1(\tau) - y_2(\tau)|)\Big)d\tau \end{aligned} \tag{2.16}$$

for all $t \geq 0$*, all* $\chi_1, \chi_2 \in \mathcal{X}$*, all* $u \in \mathcal{M}_\mathcal{U}$*, all* $d_1, d_2 \in \mathcal{M}_\mathcal{D}$*, and all* $v_1, v_2 \in \mathcal{M}_\mathcal{V}$*, where* $x_i(t) = x(t, \chi_i, u, d_i)$*,* $y_i(t) = y(t, \chi_i, u, w_i)$*, and* $w_i = (d_i, v_i)$*,* $i = 1, 2$*.*

Due to the fact that we consider the disturbed outputs in (2.16), the bound also needs to explicitly involve the input difference $v_1 - v_2$, which is accomplished by considering the difference in the combined disturbance inputs $w_1 - w_2 = (d_1, v_1) - (d_2, v_2)$.

In the literature concerned with stability notions related to outputs, however, definitions with respect to nominal (undisturbed) outputs $h(x, u, 0)$ predominate, see, e.g., [SW97; ART20] for i-IOSS, [KSW01; CT08] for IOSS, [Ing01a] for integral IOSS, or [Ang+04] for input-to-output stability. In the same way, we can define i-iIOSS with nominal outputs.

Definition 2.2 (i-iIOSS with nominal outputs)**.** *The system* (2.5) *is i-iIOSS (with nominal outputs) if there exist some* $\alpha, \alpha_x, \alpha_d, \alpha_y \in \mathcal{K}_\infty$*, and* $\eta \in (0,1)$ *such that*

$$\begin{aligned}&\alpha(|x_1(t) - x_2(t)|)\\ &\leq \alpha_x(|\chi_1 - \chi_2|)\eta^t + \int_0^t \eta^{t-\tau}\Big(\alpha_d(|d_1(j) - d_2(j)|) + \alpha_y(|y_1(\tau) - y_2(\tau)|)\Big)d\tau \end{aligned} \tag{2.17}$$

for all $t \geq 0$*, all* $\chi_1, \chi_2 \in \mathcal{X}$*, all* $u \in \mathcal{M}_\mathcal{U}$*, and all* $d_1, d_2 \in \mathcal{M}_\mathcal{D}$*, where* $x_i(t) = x(t, \chi_i, u, d_i)$ *and* $y_i(t) = y_\mathrm{n}(t, \chi_i, u, d_i) = h(x_i(t), u_i(t), 0)$*,* $i = 1, 2$*.*

Because we consider the difference between the *nominal* outputs in the bound (2.17), it suffices to consider the difference between the process disturbances $d_1 - d_2$. Detectability properties with respect to nominal outputs become particularly relevant in applications if the true output measurements are corrupted by *additive* measurement noise, compare [ART21; SW97]. In this special case, the above two i-iIOSS notions are equivalent, as we show in the following proposition. However, if the measurement noise v enters nonlinearly in (2.5b), it is beneficial to consider i-iIOSS with respect to the disturbed outputs as this is in fact a stronger[4] detectability property than i-iIOSS with nominal outputs (Definition 2.2). This allows us to construct (optimization-based) state estimators with strong robustness guarantees that explicitly account for this type of measurement noise (compare Section 2.2.4 and Chapter 3), which is not possible under the weaker property of i-iIOSS with nominal outputs.

[4]Note that this is intuitively clear because Definition 2.1 needs to hold for all possible functions v_1, v_2, while Definition 2.2 needs to hold for one specific pair of inputs v_1, v_2 only, namely the special case where $v_1 = v_2 \equiv 0$.

Proposition 2.2. *The i-iIOSS property with disturbed outputs (Definition 2.1) is strictly stronger than i-iIOSS with nominal outputs (Definition 2.2). If the output equation in* (2.5b) *specializes to* $h(x,u,v) = \tilde{h}(x,u) + Ev$ *for some real matrix* E *of appropriate dimension, then Definitions 2.1 and 2.2 are equivalent.*

Proof. The implication (2.16) $\Rightarrow$ (2.17) is trivial by considering the input $v_1 = v_2 \equiv 0$ in (2.16).

We prove (2.17) $\not\Rightarrow$ (2.16) by constructing a simple counterexample that satisfies (2.17) but cannot satisfy (2.16). Consider the scalar system

$$\dot{x}(t) = d(t), \quad x(0) = \chi, \tag{2.18a}$$
$$y(t) = x(t)(1 - v(t)) \tag{2.18b}$$

with $t \geq 0$, initial condition $\chi \in \mathbb{R}$, and inputs $d, v \in \mathcal{M}_{\mathbb{R}}$. The system (2.18) is trivially observable with respect to the nominal output, as $y(t) = x(t)$ for all $t \geq 0$ under $v \equiv 0$. To see that it is also i-iIOSS (Definition 2.2), consider the two solutions $x_i(t) = x(t, \chi_i, d_i)$ producing the nominal outputs $y_i(t) = x_i(t)$, $i = 1, 2$, $t \geq 0$ for some arbitrary initial conditions $\chi_1, \chi_2 \in \mathbb{R}$ and inputs $d_1, d_2 \in \mathcal{M}_{\mathbb{R}}$. Now, define the function $U(x_1, x_2) = |x_1 - x_2|^2$. Computing the derivative of U along the solutions $x_1(t)$ and $x_2(t)$ yields

$$\begin{aligned}\dot{U}(x_1(t), x_2(t)) &= 2(x_1(t) - x_2(t))^\top (\dot{x}_1(t) - \dot{x}_2(t)) \\ &\leq |x_1(t) - x_2(t)|^2 + |d_1(t) - d_2(t)|^2\end{aligned}$$

for almost all $t \geq 0$, where the last inequality followed by applying Young's inequality and the system dynamics (2.18a). To the right-hand side, we add $0 = (1+\kappa)(y_1(t) - y_2(t) - (y_1(t) - y_2(t)))$ for some constant $\kappa > 0$. Recalling that $y_1(t) - y_2(t) = x_1(t) - x_2(t)$ for $v_1 = v_2 \equiv 0$ by (2.18b) and using the definition of U, we obtain

$$\dot{U}(x_1(t), x_2(t)) \leq -\kappa U(x_1(t), x_2(t)) + |d_1(t) - d_2(t)|^2 + (1 + \kappa)|y_1(t) - y_2(t)|^2$$

for almost all $t \geq 0$. By applying the standard comparison principle, we can infer that

$$\begin{aligned}|x_1(t) - x_2(t)|^2 \leq\ & e^{-\kappa t}|\chi_1 - \chi_2|^2 \\ &+ \int_0^t e^{-\kappa(t-\tau)} \left(|d_1(\tau) - d_2(\tau)|^2 + (1 + \kappa)|y_1(\tau) - y_2(\tau)|^2\right) d\tau\end{aligned}$$

for all $t \geq 0$. Hence, the system (2.18) is i-iIOSS with nominal outputs (Definition 2.2) and satisfies (2.17) for all $t \geq 0$ with $\eta = e^{-\kappa} \in (0, 1)$, $\alpha(s) = \alpha_x(s) = \alpha_d(s) = s^2$, and $\alpha_y(s) = (1 + \kappa)s^2$, $s \geq 0$.

However, the system (2.18) cannot be i-iIOSS with disturbed outputs in the sense of Definition 2.1, because the two solutions $x_i(t) = x(t, \chi_i, d_i)$, $i = 1, 2$ with $\chi_1 = 1$ $d_1 \equiv 0$, $v_1 \equiv 1$ and $\chi_2 = 0$ $d_2 \equiv 0$, $v_2 \equiv 1$ produce $x_1(t) - x_2(t) = 1$ for all $t \geq 0$, while $d_1 - d_2 \equiv 0$, $v_1 - v_2 \equiv 0$ and $y_1(t) - y_2(t) = x_1(t)(1 - v_1(t)) - x_2(t)(1 - v_2(t)) = 0$ for all $t \geq 0$. Consequently, there cannot exist $\mathcal{K}_\infty$-functions $\alpha, \alpha_x, \alpha_w, \alpha_y$, and $\eta \in (0, 1)$ such that (2.16) holds for all $t \geq 0$.

Now consider the case where the system is i-iIOSS with nominal outputs (Definition 2.2) and additionally $h(x,u,v) = \tilde{h}(x,u) + Ev$ for some matrix E of appropriate dimension. Then, we can exploit that for any values of $u \in \mathcal{U}$, $x_i \in \mathcal{X}$, $v_i \in \mathcal{V}$, $i = 1,2$, we have

$$\begin{aligned}
&\alpha_y(|h(x_1,u,0) - h(x_2,u,0)|) \\
&= \alpha_y(|h(x_1,u,0) + E(v_1 - v_1) - h(x_2,u,0) + E(v_2 - v_2)|) \\
&\leq \alpha_y(|h(x_1,u,v_1) - h(x_1,u,v_2)| + |E(v_1 - v_2)|) \\
&\leq \alpha_y(2|h(x_1,u,v_1) - h(x_1,u,v_2)|) + \alpha_y\left(2\sqrt{\lambda_{\max}(E^\top E)}|v_1 - v_2|\right),
\end{aligned}$$

where in the last inequality we have used the fact that for any $\mathcal{K}$-function σ, it holds that $\sigma(a+b) \leq \sigma(2a) + \sigma(2b)$ for any $a, b > 0$. Since

$$|v_1 - v_2| = |(0,v_1) - (0,v_2)| \leq |(d_1,v_1) - (d_2,v_2)| \leq |w_1 - w_2|$$

for any $d_i \in \mathcal{D}$ and $w_i = (d_i, v_i)$ for $i = 1,2$, this implies that the system is also i-iIOSS with disturbed outputs in the sense of Definition 2.1 with the $\mathcal{K}_\infty$-function $\alpha_w(s) := 2\max\left\{\alpha_d(s), \alpha_y\left(2\sqrt{\lambda_{\max}(E^\top E)} \cdot s\right)\right\}$, $s \geq 0$, and a simple re-definition of $\alpha_y \in \mathcal{K}$ involving the additional factor 2, which finishes this proof. □

In the proof of Proposition 2.2, we have shown that the system (2.18) is i-iIOSS by constructing an i-iIOSS Lyapunov function (namely, the function U). This characterization is formalized in Section 2.2.3 below. Note also that although Proposition 2.2 and its implications are stated for continuous-time i-iIOSS (Definitions 2.1 and 2.2), they directly carry over to the discrete-time case.

We close this section with the following remarks.

Remark 2.2 (Linear systems and i-iIOSS)**.** *Indeed, for the special case of linear systems, all the different notions of i-iIOSS, i-IOSS, and IOSS coincide*[5] *and, moreover, are equivalent to the standard definition of (linear) detectability, see, for example [SW97] and compare also [KSW01, Example 2.5], [CT08, Sec. 3], and [KM20, Sec. VI].*

Remark 2.3 (Exponential function)**.** *In this thesis, we generally employ functions of the form η^t for some $\eta \in (0,1)$ to characterize an exponential decrease with respect to time $t \geq 0$ (see, e.g., Definitions 2.1 and 2.2). This is in contrast to many other works having a purely continuous-time setting that rather use e^{-kt} for some $k > 0$, since such functions naturally occur in the context of ordinary differential equations, see, e.g., [PW96; Son98]. Obviously, these characterizations are fully equivalent (simply set $\eta = e^{-k}$); however, we use η^t to ensure consistency in the notation between the continuous- and discrete-time MHE formulations discussed in this thesis.*

[5] Definitions 2.1 and 2.2 are equivalent in the presence of linear systems due to Proposition 2.2.

2.2.3. Lyapunov characterizations of i-iIOSS

In the following, we propose two equivalent Lyapunov function characterizations of i-iIOSS. Here, we focus on the stronger notion of i-iIOSS with disturbed outputs (in the sense of Definition 2.1); the converse Lyapunov result (Theorem 2.1 below) is stated for i-iIOSS with nominal outputs (Definition 2.2).

Definition 2.3 (i-iIOSS Lyapunov function)**.** *A function $U : \mathcal{X} \times \mathcal{X} \to \mathbb{R}_{\geq 0}$ is an i-iIOSS Lyapunov function if it is continuous and there exist $\alpha_1, \alpha_2, \sigma_w, \sigma_y \in \mathcal{K}_\infty$ and a constant $\eta \in (0, 1)$ such that*

$$\alpha_1(|\chi_1 - \chi_2|) \leq U(\chi_1, \chi_2) \leq \alpha_2(|\chi_1 - \chi_2|), \tag{2.19a}$$

$$\begin{aligned} &U(x_1(t), x_2(t)) \\ &\leq U(\chi_1, \chi_2)\eta^t + \int_0^t \eta^{t-\tau}\Big(\sigma_w(|w_1(\tau) - w_2(\tau)|) + \sigma_y(|y_1(\tau) - y_2(\tau)|)\Big)d\tau \end{aligned} \tag{2.19b}$$

for all $t \geq 0$, all $\chi_1, \chi_2 \in \mathcal{X}$, all $u \in \mathcal{M}_\mathcal{U}$, all $d_1, d_2 \in \mathcal{M}_\mathcal{D}$, and all $v_1, v_2 \in \mathcal{M}_\mathcal{V}$, where $x_i(t) = x(t, \chi_i, u, d_i)$, $y_i(t) = y(t, \chi_i, u, w_i)$, and $w_i = (d_i, v_i)$, $i = 1, 2$.

The integral form of (2.16) and (2.19b) together with the continuity of U is motivated by [Ang02; Ang09], originally employed to allow for a non-compact input set $\mathcal{D}$, where smooth converse Lyapunov theorems usually fail, compare [Ang02, Rem. 2.4] and [LSW96, Sec. 8]. The exponential decrease in (2.16) and (2.19b) is motivated by recent results in the discrete-time literature, where this is crucial to develop FIE and MHE schemes with suitable stability properties, compare [AR21] and [Sch+23, Sec. III]. In Chapter 3, we show that this carries over to the continuous-time setting. Moreover, in Section 7.1.2, we provide sufficient conditions (in terms of LMIs) for the construction of i-iIOSS Lyapunov functions for special classes of nonlinear systems.

We want to emphasize that considering an exponential decrease in Lyapunov coordinates in Definition 2.3 is actually without loss of generality; in fact, (2.19b) is equivalent to a more standard dissipation inequality as the following proposition shows.

Proposition 2.3. *The system* (2.5) *admits an i-iIOSS Lyapunov function according to Definition 2.3 if and only if there exists a function $W : \mathcal{X} \times \mathcal{X} \to \mathbb{R}_{\geq 0}$ and functions $\bar{\alpha}_1, \bar{\alpha}_2, \bar{\alpha}_2, \bar{\sigma}_w, \bar{\sigma}_y \in \mathcal{K}_\infty$ such that*

$$\bar{\alpha}_1(|\chi_1 - \chi_2|) \leq W(\chi_1, \chi_2) \leq \bar{\alpha}_2(|\chi_1 - \chi_2|), \tag{2.20a}$$

$$\begin{aligned} &W(x_1(t), x_2(t)) - W(\chi_1, \chi_2) \\ &\leq \int_0^t \left(-\bar{\alpha}_3(|x_1(\tau) - x_2(\tau)|) + \bar{\sigma}_w(|w_1(\tau) - w_2(\tau)|) + \bar{\sigma}_y(|y_1(\tau) - y_2(\tau)|)\right) d\tau \end{aligned} \tag{2.20b}$$

for all $t \geq 0$, all $\chi_1, \chi_2 \in \mathcal{X}$, all $u \in \mathcal{M}_\mathcal{U}$, all $d_1, d_2 \in \mathcal{M}_\mathcal{D}$, and all $v_1, v_2 \in \mathcal{M}_\mathcal{V}$, where $x_i(t) = x(t, \chi_i, u, d_i)$, $y_i(t) = y(t, \chi_i, u, w_i)$, and $w_i = (d_i, v_i)$, $i = 1, 2$.

To prove the "only if" part, we exploit the specific structure of the i-iIOSS Lyapunov function—namely, that the right-hand side of (2.19b) is also the solution of a simple scalar initial value problem. To prove the "if" part, we require two additional auxiliary lemmas: a comparison result and its exponential equivalent.

Lemma 2.2. *Suppose there exists a function W as defined in the statement of Proposition 2.3 satisfying* (2.20)*. Consider some $\alpha_3 \in \mathcal{K}_\infty$ such that α_3 is globally Lipschitz and $\alpha_3(s) \leq \bar{\alpha}_3(\bar{\alpha}_2^{-1}(s))$ for all $s \geq 0$. For any $\chi_1, \chi_2 \in \mathcal{X}$, $u \in \mathcal{M}_\mathcal{U}$, $d_1, d_2 \in \mathcal{M}_\mathcal{D}$, and $v_1, v_2 \in \mathcal{M}_\mathcal{V}$, define $x_i(t) = x(t, \chi_i, u, d_i)$, $y_i(t) = y(t, \chi_i, u, w_i)$, $w_i = (d_i, v_i)$, $i = 1, 2$, $t \geq 0$, $w_\Delta := w_1 - w_2$, and $y_\Delta := y_1 - y_2$. Let $\xi : \mathbb{R}_{\geq 0} \to \mathbb{R}_{\geq 0}$ be the solution to the initial value problem*

$$\dot{\xi}(t) = -\alpha_3(\xi(t)) + \bar{\sigma}_w(|w_\Delta(t)|) + \bar{\sigma}_y(|y_\Delta(t)|), \tag{2.21a}$$

$$\xi(0) = W(\chi_1, \chi_2). \tag{2.21b}$$

Then, $W(x_1(t), x_2(t)) \leq \xi(t)$ for all $t \geq 0$.

Proof. We start by noting that any $\mathcal{K}_\infty$-function can be lower bounded by a globally Lipschitz $\mathcal{K}_\infty$-function so that existence of a suitable α_3 is guaranteed, compare [Ang09]. Together with the fact that w_Δ and y_Δ represent measurable, locally essentially bounded functions of time, we can infer that there exists a unique function ξ defined globally on $\mathbb{R}_{\geq 0}$ that solves the initial value problem (2.21) (this follows by a combination of classical existence and uniqueness results in the Carathéodory setting, see, for example, [CL55, Sec. 1.2, Sec. 2.1]) and compare also Proposition 2.1. Now, suppose for contradiction that there exists some $t = t_1 \in (0, \infty)$ such that $W(x_1(t_1), x_2(t_1)) > \xi(t_1)$. Hence, we can define $t_2 = \max\{t \in [0, t_1) : W(x_1(t), x_2(t)) \leq \xi(t)\}$, and since W and ξ are continuous in t, it follows that $W(x_1(t_2), x_2(t_2)) = \xi(t_2)$ and $W(x_1(t), x_2(t)) > \xi(t)$ for $t \in (t_2, t_1]$. By application of (2.20b) and (2.20a) and the definition of α_3, we obtain

$$\begin{aligned}
&W(x_1(t), x_2(t)) - W(x_1(t_2), x_2(t_2)) \\
&\leq \int_{t_2}^{t} (-\alpha_3(W(x_1(\tau), x_2(\tau))) + \bar{\sigma}_w(|w_\Delta(\tau)|) + \bar{\sigma}_y(|y_\Delta(\tau)|))\, d\tau \\
&< \int_{t_2}^{t} (-\alpha_3(\xi(\tau)) + \bar{\sigma}_w(|w_\Delta(\tau)|) + \bar{\sigma}_y(|y_\Delta(\tau)|))\, d\tau \\
&= \xi(t) - \xi(t_2).
\end{aligned}$$

Since $W(x_1(t_2), x_2(t_2)) = \xi(t_2)$, this implies that $W(x_1(t), x_2(t)) < \xi(t)$ for $t \in (t_2, t_1]$, which is a contradiction and hence proves our claim. □

Lemma 2.3. *Consider the initial value problem* (2.21)*. There exist functions $\rho \in \mathcal{K}_\infty$ and $\hat{\sigma}_w, \hat{\sigma}_y \in \mathcal{K}_\infty$ such that $q := \rho(\xi)$ satisfies*

$$\dot{q}(t) \leq -q(t) + \hat{\sigma}_w(|w_\Delta(t)|) + \hat{\sigma}_y(|y_\Delta(t)|) \tag{2.22}$$

for almost all $t \geq 0$.

Proof. The proof utilizes similar arguments as in [SW97, Lem. 10]. Namely, following [PW96, Lem. 11 and 12], there exists a continuously differentiable function $\rho \in \mathcal{K}_\infty$ such that $\rho'(0) = 0$ and $\rho'(s)\alpha_3(s) \geq 2\rho(s)$ for all $s \geq 0$, where $\rho' := d\rho/ds$. Evaluating the time derivative of $q = \rho(\xi)$ with ξ satisfying (2.21) leads to

$$\begin{aligned}\dot{q}(t) &= \frac{d}{dt}\rho(\xi(t)) = \rho'(\xi(t))\dot{\xi}(t) \\ &= \rho'(\xi(t))(-\alpha_3(\xi(t)) + \bar{\sigma}_w(|w_\Delta(t)|) + \bar{\sigma}_y(|y_\Delta(t)|)) \\ &= -\frac{\rho'(\xi(t))\alpha_3(\xi(t))}{2} + \rho'(\xi(t))\left(-\frac{\alpha_3(\xi(t))}{2} + \bar{\sigma}_w(|w_\Delta(t)|) + \bar{\sigma}_y(|y_\Delta(t)|)\right).\end{aligned} \tag{2.23}$$

We distinguish between the following two cases: 1) When $\xi(t) \geq \alpha_3^{-1}(2\bar{\sigma}_w(|w_\Delta(t)|) + 2\bar{\sigma}_y(|y_\Delta(t)|))$, it follows that

$$\rho'(\xi(t))\left(-\frac{\alpha_3(\xi(t))}{2} + \bar{\sigma}_w(|w_\Delta(t)|) + \bar{\sigma}_y(|y_\Delta(t)|)\right) \leq 0;$$

2) if instead $\xi(t) < \alpha_3^{-1}(2\bar{\sigma}_w(|w_\Delta(t)|) + 2\bar{\sigma}_y(|y_\Delta(t)|))$, we obtain

$$\rho'(\xi(t))\left(-\frac{\alpha_3(\xi(t))}{2} + \bar{\sigma}_w(|w_\Delta(t)|) + \bar{\sigma}_y(|y_\Delta(t)|)\right) \leq \hat{\sigma}_w(|w_\Delta(t)|) + \hat{\sigma}_y(|y_\Delta(t)|)$$

for some $\hat{\sigma}_w, \hat{\sigma}_y \in \mathcal{K}_\infty$. (To see this, first note that $-\alpha_3(\xi(t))/2 \leq 0$ for all $t \geq 0$. Second, since ρ' is continuous, $\rho'(s) > 0$ for all $s > 0$, and $\rho'(0) = 0$ (compare [PW96, Lem. 11]), there exists $\bar{\rho} \in \mathcal{K}_\infty$ such that $\bar{\rho}(s) \geq \rho'(s)$ for all $s \geq 0$. Suitable $\mathcal{K}_\infty$-functions $\hat{\sigma}_w, \hat{\sigma}_y$ can then be constructed by exploiting standard $\mathcal{K}$-function properties.) From (2.23), the combination of both cases, and the definition of q, we can conclude that (2.22) holds for almost all $t \geq 0$, which finishes this proof. □

We are now in a position to prove Proposition 2.3.

Proof of Proposition 2.3. We start by showing (2.20) ⇒ (2.19). Define $U(\cdot) := \rho(W(\cdot))$ with ρ as in Lemma 2.3. From Lemma 2.2 and Lemma 2.3, it follows that

$$U(x_1(t), x_2(t)) = \rho(W(x_1(t), x_2(t))) \leq \rho(\xi(t)) = q(t) \tag{2.24}$$

for all $t \geq 0$. Let $\omega : \mathbb{R}_{\geq 0} \to \mathbb{R}_{\geq 0}$ be the solution to the initial value problem

$$\dot{\omega}(t) = -\omega(t) + \hat{\sigma}_w(|w_\Delta(t)|) + \hat{\sigma}_y(|y_\Delta(t)|),\ \omega(0) = q(0).$$

From the standard comparison principle, we know that $q(t) \leq \omega(t)$ for all $t \geq 0$, where $\omega(t)$ is given by

$$\omega(t) = \omega(0)e^{-t} + \int_0^t e^{-(t-\tau)}\Big(\hat{\sigma}_w(|w_\Delta(\tau)|) + \hat{\sigma}_y(|y_\Delta(\tau)|)\Big)d\tau \tag{2.25}$$

for all $t \geq 0$. However, since

$$\omega(0) = q(0) = \rho(\xi(0)) = \rho(W(\chi_1, \chi_2)) = U(\chi_1, \chi_2),$$

from (2.24) and (2.25), it follows that

$$U(x_1(t), x_2(t)) \leq U(\chi_1, \chi_2)e^{-t} + \int_0^t e^{-(t-\tau)}\Big(\hat{\sigma}_w(|w_\Delta(\tau)|) + \hat{\sigma}_y(|y_\Delta(\tau)|)\Big)d\tau.$$

Hence, U satisfies (2.19b) with $\eta = e^{-1}$, $\sigma_w = \hat{\sigma}_w$, $\sigma_y = \hat{\sigma}_y$ and (2.19a) with $\alpha_1 = \rho \circ \bar{\alpha}_1 \in \mathcal{K}_\infty$ and $\alpha_2 = \rho \circ \bar{\alpha}_2 \in \mathcal{K}_\infty$, where "$\circ$" means function composition.

It remains to show that (2.19) $\Rightarrow$ (2.20). Define $k := -\ln \eta$ (i.e., such that $e^{-k} = \eta$) and note that for all $t \geq 0$, the right-hand side of (2.19b) is the solution to the initial value problem

$$\dot{z}(t) = -kz(t) + \sigma_w(|w_\Delta(t)|) + \sigma_y(|y_\Delta(t)|),\ z(0) = U(\chi_1, \chi_2).$$

Consequently, $U(x_1(t), x_2(t)) \leq z(t)$ for all $t \geq 0$. However, by the fundamental theorem of calculus, it follows that

$$\begin{aligned} &U(x_1(t), x_2(t)) - U(\chi_1, \chi_2) \leq z(t) - z(0) = \int_0^t \frac{dz}{d\tau}(\tau)d\tau \\ &= \int_0^t \left(-kz(\tau) + \sigma_w(|w_\Delta(\tau)|) + \sigma_y(|y_\Delta(\tau)|)\right) d\tau \\ &\leq \int_0^t \left(-kU(x_1(\tau), x_2(\tau)) + \sigma_w(|w_\Delta(\tau)|) + \sigma_y(|y_\Delta(\tau)|)\right) d\tau. \end{aligned}$$

Therefore, $W(x_1, x_2) = U(x_1, x_2)$ satisfies (2.20) with $\bar{\alpha}_1 = \alpha_1$, $\bar{\alpha}_2 = \alpha_2$, $\bar{\alpha}_3(s) = k\alpha_1(s)$, $\bar{\sigma}_w = \sigma_w$, and $\bar{\sigma}_y = \sigma_y$, which finishes this proof. □

Remark 2.4 (Relation between discounted and non-discounted notions)**.** *A key advantage of the discrete-time i-IOSS counterpart is that discounted summation and discounted maximization are in some sense equivalent, compare [KM20; ART21]. This, however, does not carry over to the continuous-time setting (the discounted integral in* (2.16) *could indeed be transferred to a discounted L^∞-norm bound, but not vice versa, unless strong regularity assumptions on the input d are enforced). As a result, the proposed notion from Definition 2.1 implies i-IOSS in an L^∞-to-L^∞ sense with time-discounting (similar to* (2.3) *and [ART21, Def. 2.4]) and without discounting as in* (2.2) *and defined in [SW97, Def. 22], compare also Section 2.2.4. Investigating some converse implications may be subject of future research, see also Chapter 8 for further details.*

We now show equivalence between i-iIOSS and its Lyapunov characterization. To establish that the Lyapunov function is necessarily continuous, however, we need to restrict ourselves to output equations $h_{\mathrm{n}}(x, u) = h(x, u, 0)$ and hence consider i-iIOSS with nominal outputs (Definition 2.2). Note that this setup is standard in the literature in the context of stability notions involving outputs and corresponding converse Lyapunov results, see, e.g., [SW97; ART20; KSW01; CT08; Ing01a; Ang+04] and refer to the discussion in Section 2.2.2. Furthermore, we require an additional uniform continuity condition.

Assumption 2.2. *The function $h_{\mathrm{n}}(x, u) = h(x, u, 0)$ satisfies*

$$|h_{\mathrm{n}}(x_1, u) - h_{\mathrm{n}}(x_2, u)| \leq \kappa_2(|x_1 - x_2|) \tag{2.26}$$

for some $\kappa_2 \in \mathcal{K}_\infty$ for all $x_1, x_2 \in \mathcal{X}$ uniformly in $u \in \mathcal{U}$.

The following result establishes equivalence of i-iIOSS with nominal outputs (Definition 2.2) and existence of a continuous i-iIOSS Lyapunov function.

Theorem 2.1. *Let Assumptions 2.1 and 2.2 hold. The system* (2.5) *is i-iIOSS with nominal outputs (Definition 2.2) if and only if there exists a function* $U : \mathcal{X} \times \mathcal{X} \to \mathbb{R}_{\geq 0}$ *and functions* $\alpha_1, \alpha_2, \sigma_d, \sigma_y \in \mathcal{K}_\infty$ *and* $\eta \in (0,1)$ *such that*

$$\alpha_1(|\chi_1 - \chi_2|) \leq U(\chi_1, \chi_2) \leq \alpha_2(|\chi_1 - \chi_2|), \tag{2.27a}$$

$$U(x_1(t), x_2(t)) \leq U(\chi_1, \chi_2)\eta^t + \int_0^t \eta^{t-\tau}\Big(\sigma_d(|d_1(\tau) - d_2(\tau)|) + \sigma_y(|y_1(\tau) - y_2(\tau)|)\Big)d\tau \tag{2.27b}$$

for all $t \geq 0$, *all* $\chi_1, \chi_2 \in \mathcal{X}$, *all* $u \in \mathcal{M}_\mathcal{U}$, *and all* $d_1, d_2 \in \mathcal{M}_\mathcal{D}$, *where* $x_i(t) = x(t, \chi_i, u, d_i)$, $i = 1, 2$ *and* $y_i(t) = y_\mathrm{n}(t, \chi_i, u, d_i) = h(x_i(t), u_i(t), 0)$, $i = 1, 2$.

Before proving Theorem 2.1, we want to briefly comment on the case of i-iIOSS with disturbed outputs.

Remark 2.5 (i-iIOSS with disturbed outputs: additive output disturbances)**.** *In case the output equation specializes to* $h(x, u, v) = h_\mathrm{n}(x, u) + Ev$ *for some matrix* E, *the i-iIOSS Lyapunov function candidate defined in the proof of Theorem 2.1 using the nominal output function* $h_\mathrm{n} = h(x, u, 0)$ *turns out to be a valid Lyapunov function for i-iIOSS with disturbed outputs (Definition 2.3). This becomes apparent by applying the same technique used in the second part of the proof of Proposition 2.2 to the decrease condition* (2.27b)*, leading to the decrease condition* (2.19b) *with disturbed outputs. This fact is actually not surprising in view of Proposition 2.2 and, consequently, yields the following Corollary of Theorem 2.1.*

Corollary 2.1. *Let Assumptions 2.1 and 2.2 hold and suppose that* $h(x, u, v) = h_\mathrm{n}(x, u) + Ev$ *for some real matrix* E *of appropriate dimension. Then, the system* (2.5) *is i-iIOSS with disturbed outputs (Definition 2.1) if and only if there exists an i-iIOSS Lyapunov function in the sense of Definition 2.3.*

Proof. Note that Proposition 2.2 and Theorem 2.1 already imply that the system (2.5) is i-iIOSS with disturbed outputs (Definition 2.1) if and only if there exists an i-iIOSS Lyapunov function satisfying (2.27) (with nominal outputs). The fact that the latter implies the existence of an i-iIOSS Lyapunov function in the sense of Definition 2.3 (with disturbed outputs) is a consequence of the arguments outlined in Remark 2.5; the converse direction follows by considering (2.19) for the special case of $v_1 = v_2 \equiv 0$. □

Remark 2.6 (i-iIOSS with disturbed outputs: the general case)**.** *In the general case where the input* v *enters the output equation nonlinearly, it is still possible to tailor (parts of) Theorem 2.1 and its proof to i-iIOSS for disturbed outputs. Specifically, we can establish sufficiency of an i-iIOSS Lyapunov function (Definition 2.3) for i-iIOSS (Definition 2.1). For the necessity part, we can prove that the i-iIOSS*

Lyapunov function candidate satisfies the properties (2.19a) *and* (2.19b)*; however, showing that it is also necessarily continuous is an open problem (due to fact that some arguments used in the proof of Claim 2.1 below do not apply in this case) and constitute an interesting subject of future work.*

We now proceed with the proof of Theorem 2.1.

Proof of Theorem 2.1. Part I (Sufficiency): The sufficiency part is straightforward and follows by applying the bounds (2.27a) to (2.27b), which directly yields (2.17).

Part II (Necessity): The proof uses and combines similar arguments as in previous converse theorems and Lyapunov function constructions, in particular [ART21; Ing01b]; continuity of the Lyapunov function is proven in a different fashion by invoking Assumptions 2.1 and 2.2, see Claim 2.1 below.

For arbitrary $\chi_1, \chi_2 \in \mathcal{X}$, we consider the following Lyapunov function candidate[6]

$$\begin{aligned} U(\chi_1,\chi_2) := \sup_{t\geq 0, u, d_1, d_2} \eta^{-t/2}\Big(&\alpha(|x(t,\chi_1,u,d_1) - x(t,\chi_2,u,d_2)|) \\ &- \int_0^\infty \eta^{t-\tau} 2\alpha_d(|d_1(\tau) - d_2(\tau)|)d\tau \\ &- \int_0^t \eta^{t-\tau}\alpha_y(|y_{\mathrm{n}}(\tau,\chi_1,u,d_1) - y_{\mathrm{n}}(\tau,\chi_2,u,d_2)|)d\tau\Big) \end{aligned} \tag{2.28}$$

and start by establishing the bounds (2.27a). For the term $\alpha(|x(t,\chi_1,u,d_1) - x(t,\chi_2,u,d_2)|)$ in (2.28), we can directly use the i-iIOSS estimate (2.17), which yields

$$U(\chi_1,\chi_2) \leq \sup_{t\geq 0,u,d_1,d_2} \alpha_x(|\chi_1 - \chi_2|)\eta^{t/2} = \alpha_x(|\chi_1 - \chi_2|),$$

that is, the upper bound in (2.27a) with $\alpha_2 = \alpha_x$. The lower bound follows by considering the candidate inputs $d_1 = d_2$ and $t = 0$, leading to $\alpha_1 = \alpha$ in (2.27a).

We make the following claim, which is proven below.

Claim 2.1. *The function U in* (2.28) *is continuous on $\mathcal{X} \times \mathcal{X}$.*

It remains to establish the dissipation inequality (2.27b). To this end, consider $\zeta_1, \zeta_2 \in \mathcal{X}$, $u \in \mathcal{M}_\mathcal{U}, d_1, d_2 \in \mathcal{M}_\mathcal{D}$, yielding the trajectories $z_j(t) := x(t,\zeta_j,u,d_j)$ with $j = 1, 2$ for $t \geq 0$. We obtain

$$\begin{aligned} &U(z_1(t), z_2(t)) \\ &= \sup_{\bar{t}\geq 0,\bar{u},\bar{d}_1,\bar{d}_2} \eta^{-\bar{t}/2}\Big(\alpha(|x(\bar{t},z_1(t),\bar{u},\bar{d}_1) - x(\bar{t},z_2(t),\bar{u},\bar{d}_2)|) \\ &\qquad - \int_0^\infty \eta^{\bar{t}-\tau} 2\alpha_d(|\bar{d}_1(\tau) - \bar{d}_2(\tau)|) \\ &\qquad - \int_0^{\bar{t}} \eta^{\bar{t}-\tau}\alpha_y(|y_{\mathrm{n}}(\tau,z_1(t),\bar{u},\bar{d}_1) - y_{\mathrm{n}}(\tau,z_2(t),\bar{u},\bar{d}_2)|)d\tau\Big). \end{aligned} \tag{2.29}$$

[6] The input functions u and d_1, d_2 in (2.28) are maximized over the sets $\mathcal{M}_\mathcal{U}$ and $\mathcal{M}_\mathcal{D}$, respectively, which is omitted for brevity.

For two functions $\bar{u}, u$ defined on $[0,\infty)$, let $\bar{u}\sharp_t u$ denote their concatenation at some fixed time $t \geq 0$, i.e.,

$$\bar{u}\sharp_t u(\tau) := \begin{cases} u(\tau), & \tau \in [0,t] \\ \bar{u}(\tau - t), & \tau \in (t,\infty). \end{cases}$$

Hence, in (2.29), we can infer that

$$\begin{aligned} &\alpha(|x(\bar{t}, z_1(t), \bar{u}, \bar{d}_1) - x(\bar{t}, z_2(t), \bar{u}, \bar{d}_2)|) \\ &= \alpha(|x(\bar{t}+t, \zeta_1, \bar{u}\sharp_t u, \bar{d}_1\sharp_t d_1) - x(\bar{t}+t, \zeta_2, \bar{u}\sharp_t u, \bar{d}_2\sharp_t d_2)|). \end{aligned} \tag{2.30}$$

Similarly,

$$\begin{aligned} \int_0^\infty \eta^{\bar{t}-\tau} 2\alpha_d(|\bar{d}_1(\tau) - \bar{d}_2(\tau)|)d\tau = &\int_0^\infty \eta^{\bar{t}+t-\tau} 2\alpha_d(|\bar{d}_1\sharp_t d_1(\tau) - \bar{d}_2\sharp_t d_2(\tau)|)d\tau \\ &- \int_0^t \eta^{\bar{t}+t-\tau} 2\alpha_d(|d_1(\tau) - d_2(\tau)|)d\tau \end{aligned} \tag{2.31}$$

and

$$\begin{aligned} &\int_0^{\bar{t}} \eta^{\bar{t}-\tau} \alpha_y(|y_{\mathrm{n}}(\tau, z_1(t), \bar{u}, \bar{d}_1) - y_{\mathrm{n}}(\tau, z_2(t), \bar{u}, \bar{d}_2)|)d\tau \\ &= \int_0^{\bar{t}+t} \eta^{\bar{t}+t-\tau} \alpha_y(|y_{\mathrm{n}}(\bar{t}+t, \zeta_1, \bar{u}\sharp_t u, \bar{d}_1\sharp_t d_1) - y_{\mathrm{n}}(\bar{t}+t, \zeta_2, \bar{u}\sharp_t u, \bar{d}_2\sharp_t d_2)|)d\tau \\ &\quad - \int_0^t \eta^{\bar{t}+t-\tau} \alpha_y(|y_{\mathrm{n}}(\tau, \zeta_1, u, d_1) - y_{\mathrm{n}}(\tau, \zeta_2, u, d_2)|)d\tau. \end{aligned} \tag{2.32}$$

Now define $\hat{t} := \bar{t} + t$. Consequently, $U(z_1(t), z_2(t))$ in (2.29) can be bounded using the substitutions from (2.30)–(2.32) and the fact that $\eta \leq \sqrt{\eta} \in (0,1)$ as

$$\begin{aligned} &U(z_1(t), z_2(t)) \\ &\leq \sup_{\hat{t}\geq 0, \hat{u}, \hat{d}_1, \hat{d}_2} \eta^{(-\hat{t}+t)/2} \Big(\alpha(|x(\hat{t}, \zeta_1, \hat{u}, \hat{d}_1) - x(\hat{t}, \zeta_2, \hat{u}, \hat{d}_2)|) \\ &\qquad\qquad - \int_0^\infty \eta^{\hat{t}-\tau} 2\alpha_d(|\hat{d}_1(\tau) - \hat{d}_2(\tau)|)d\tau \\ &\qquad\qquad - \int_0^{\hat{t}} \eta^{\hat{t}-\tau} \alpha_y(|y_{\mathrm{n}}(\hat{t}, \zeta_1, \hat{u}, \hat{d}_1) - y_{\mathrm{n}}(\hat{t}, \zeta_2, \hat{u}, \hat{d}_2)|)d\tau \Big) \\ &\quad + \int_0^t \eta^{t-\tau} \Big(2\alpha_d(|d_1(\tau) - d_2(\tau)|) + \alpha_y(|y_{\mathrm{n}}(\tau, \zeta_1, u, d_1) - y_{\mathrm{n}}(\tau, \zeta_2, u, d_2)|) \Big) d\tau \\ &\leq \sqrt{\eta}^t U(\zeta_1, \zeta_2) \\ &\quad + \int_0^t \sqrt{\eta}^{t-\tau} \Big(2\alpha_d(|d_1(\tau) - d_2(\tau)|) + \alpha_y(|y_{\mathrm{n}}(\tau, \zeta_1, u, d_1) - y_{\mathrm{n}}(\tau, \zeta_2, u, d_2)|) \Big) d\tau, \end{aligned}$$

which establishes the dissipation inequality (2.27b) by a suitable redefinition of η and hence concludes this proof. □

To prove Claim 2.1 (i.e, continuity of the Lyapunov function candidate (2.28)), we first need an additional lemma.

Lemma 2.4. *Let Assumptions 2.1 and 2.2 hold. For every $T, r_\chi, r_d > 0$, there exist constants $R_x(T, r_\chi, r_d) > 0$ and $R_y(T, r_\chi, r_d) > 0$ such that*

$$|x(t, \chi_1, u, d_1) - x(t, \chi_2, u, d_1)| \leq R_x(T, r_\chi, r_d),$$
$$|y_{\mathrm{n}}(t, \chi_1, u, d_2) - y_{\mathrm{n}}(t, \chi_2, u, d_2)| \leq R_y(T, r_\chi, r_d)$$

for all $t \in [0, T]$, all $\chi_1, \chi_2 \in \mathcal{X}$ satisfying $|\chi_1 - \chi_2| \leq r_\chi$, all $u \in \mathcal{M}_\mathcal{U}$, and all $d_1, d_2 \in \mathcal{M}_\mathcal{D}$ satisfying $\int_0^\infty \mu^{-s}\alpha(|d_1(s) - d_2(s)|)ds \leq r_d$ for some $\alpha \in \mathcal{K}_\infty$ with $\alpha(s) \geq \kappa_1(3s)$ for all $s \geq 0$ and $\mu \in (0, 1)$.

Proof. For $i = 1, 2$, let $x_i(t) = x(t, \chi_i, u, d_i)$ and $y_i(t) = y_{\mathrm{n}}(t, \chi_i, u, d_i)$, $t \geq 0$, where we note that Proposition 2.1 applies due to satisfaction of Assumption 2.1. Define $d_\Delta := d_1 - d_2$. We can invoke the same arguments as in the proof of Lemma 2.1, where (2.11) can be replaced by

$$\int_0^t \kappa_1(3|d_\Delta(s)|)ds \leq \int_0^\infty \mu^{-s}\alpha(|d_\Delta(s)|)ds \leq r_d,$$

exploiting that $\mu^{-s} \geq 1$ for all $s \geq 0$. Consequently, we obtain $c = r_\chi + r_d$ in (2.9), which by (2.8) implies that

$$|x_1(t) - x_2(t)| \leq \rho^{-1}(\rho(r_\chi + r_d)e^T) =: R_x(T, r_\chi, r_d)$$

uniformly for all $t \in [0, T]$. For the second part, the application of (2.5b) in combination with Assumption 2.2 leads to

$$\begin{aligned}|y_1(t) - y_2(t)| &= |h_{\mathrm{n}}(x_1(t), u(t)) - h_{\mathrm{n}}(x_2(t), u(t))| \leq \kappa_2(|x_1(t) - x_2(t)|) \\ &\leq \kappa_2(R_x(T, r_\chi, r_d)) =: R_y(T, r_\chi, r_d)\end{aligned}$$

for all $t \in [0, T]$, which finishes this proof. □

Proof of Claim 2.1. The proof uses mostly similar arguments as in [ART21, Th. 3.5], with variations due to the continuous-time setting and the class of inputs considered (in particular, Lemmas 2.1 and 2.4). It consists of two parts. First, we show that choosing (χ_1, χ_2) in a compact set implies that the right-hand side of (2.28) is the same when restricting t and (d_1, d_2) to suitable sets; then, we use this property to establish continuity of U.

Part I. Define $\mathcal{B}(C) := \{(\chi_1, \chi_2) \in \mathcal{X} \times \mathcal{X} : 1/C \leq |\chi_1 - \chi_2| \leq C\}$ for $C \geq 1$ and consider $(\chi_1, \chi_2) \in \mathcal{B}(C)$. Then, for any $\epsilon > 0$, there exist inputs $u^\epsilon \in \mathcal{M}_\mathcal{U}$ and $d_1^\epsilon, d_2^\epsilon \in \mathcal{M}_\mathcal{D}$ and a time $t^\epsilon \geq 0$ such that

$$\alpha(|\chi_1 - \chi_2|) \leq U(\chi_1, \chi_2) \tag{2.33}$$

$$\begin{aligned}&\leq \epsilon + \eta^{-t^\epsilon/2}\Big(\alpha(|x(t^\epsilon, \chi_1, u^\epsilon, d_1^\epsilon) - x(t^\epsilon, \chi_2, u^\epsilon, d_2^\epsilon)|) \\ &\qquad - \int_0^\infty \eta^{t^\epsilon - \tau} 2\alpha_d(|d_1^\epsilon(\tau) - d_2^\epsilon(\tau)|)d\tau \\ &\qquad - \int_0^{t^\epsilon} \eta^{t^\epsilon - \tau}\alpha_y(|y_{\mathrm{n}}(\tau, \chi_1, u^\epsilon, d_1^\epsilon) - y_{\mathrm{n}}(\tau, \chi_2, u^\epsilon, d_2^\epsilon)|)d\tau\Big) \\ &\leq \epsilon + \eta^{-t^\epsilon/2}\Big(\alpha_x(|\chi_1 - \chi_2|)\eta^{t^\epsilon} - \int_0^\infty \eta^{t^\epsilon - \tau}\alpha_d(|d_1^\epsilon(\tau) - d_2^\epsilon(\tau)|)d\tau\Big),\end{aligned} \tag{2.34}$$

where the last inequality follows from i-iIOSS (2.17). Consequently,

$$\alpha(|\chi_1 - \chi_2|) \leq \epsilon + \eta^{t^\epsilon/2}\alpha_x(|\chi_1 - \chi_2|). \tag{2.35}$$

Choose $\epsilon \leq \bar{\epsilon}(C) := \alpha(1/C)/2$ and recall that $1/C \leq |\chi_1 - \chi_2| \leq C$. Thus, (2.35) yields $\alpha(1/C)/2 \leq \eta^{t^\epsilon/2}\alpha_x(C)$, which leads to

$$t^\epsilon \leq 2\log_\eta\left(\frac{\alpha(1/C)}{2\alpha_x(C)}\right) =: T(C), \tag{2.36}$$

where $0 < \frac{\alpha(1/C)}{2\alpha_x(C)} < 1$. From (2.34) and the fact that $\epsilon \leq \bar{\epsilon}(C)$, we also obtain that

$$\int_0^\infty \eta^{t^\epsilon-\tau}\alpha_d(|d_1^\epsilon(\tau) - d_2^\epsilon(\tau)|)d\tau \leq \alpha_x(C)\eta^{t^\epsilon} - \frac{1}{2}\alpha(1/C)\eta^{t^\epsilon/2} \leq \alpha_x(C).$$

Since $t^\epsilon \in [0, T(C)]$, it follows that $\eta^{t^\epsilon} \geq \eta^{T(C)}$; hence,

$$\int_0^\infty \eta^{-\tau}\alpha_d(|d_1^\epsilon(\tau) - d_2^\epsilon(\tau)|)d\tau \leq \alpha_x(C)\eta^{-T(C)} =: r_d(C).$$

As a result, we can infer that $(d_1^\epsilon, d_2^\epsilon) \in \mathcal{B}_d(C)$, where

$$\mathcal{B}_d(C) := \left\{(d_1, d_2) \in \mathcal{M}_\mathcal{D} \times \mathcal{M}_\mathcal{D} : \int_0^\infty \eta^{-\tau}\alpha_d(|d_1^\epsilon(\tau) - d_2^\epsilon(\tau)|)d\tau \leq r_d(C)\right\}.$$

Part II. Now consider some $\tilde{\chi}_1, \tilde{\chi}_2 \in \mathcal{X}$ with $\tilde{\chi}_1 \neq \tilde{\chi}_2$. Set $C = 2\max\{|\tilde{\chi}_1 - \tilde{\chi}_2|, 1/|\tilde{\chi}_1 - \tilde{\chi}_2|\} \geq 1$. From the first part of this proof, we know that for $(\chi_1, \chi_2) \in \mathcal{B}(C)$, there exist $\epsilon \in (0, \bar{\epsilon}(C)]$, $u^\epsilon \in \mathcal{M}_\mathcal{U}$, $(d_1^\epsilon, d_2^\epsilon) \in \mathcal{B}_d(C)$, and $t^\epsilon \in [0, T(C)]$ such that (2.34) holds. Define

$$\begin{aligned}
x_1(t) &:= x(t, \chi_1, u^\epsilon, d_1^\epsilon), & y_1(t) &:= y_\mathrm{n}(t, \chi_1, u^\epsilon, d_1^\epsilon),\\
x_2(t) &:= x(t, \chi_2, u^\epsilon, d_2^\epsilon), & y_2(t) &:= y_\mathrm{n}(t, \chi_2, u^\epsilon, d_2^\epsilon),\\
\tilde{x}_1(t) &:= x(t, \tilde{\chi}_1, u^\epsilon, d_1^\epsilon), & \tilde{y}_1(t) &:= y_\mathrm{n}(t, \tilde{\chi}_1, u^\epsilon, d_1^\epsilon),\\
\tilde{x}_2(t) &:= x(t, \tilde{\chi}_2, u^\epsilon, d_2^\epsilon), & \tilde{y}_2(t) &:= y_\mathrm{n}(t, \tilde{\chi}_2, u^\epsilon, d_2^\epsilon)
\end{aligned}$$

for all $t \in [0, T(C)]$. The trajectories $\tilde{x}_1(t)$ and $\tilde{x}_2(t)$ satisfy

$$\begin{aligned}
U(\tilde{\chi}_1, \tilde{\chi}_2) \geq \eta^{-t^\epsilon/2}\Big(&\alpha(|\tilde{x}_1(t^\epsilon) - \tilde{x}_2(t^\epsilon)|) - \int_0^\infty \eta^{t^\epsilon-\tau}2\alpha_d(|d_1^\epsilon(\tau) - d_2^\epsilon(\tau)|)d\tau\\
&- \int_0^{t^\epsilon} \eta^{t^\epsilon-\tau}\alpha_y(|\tilde{y}_1(\tau) - \tilde{y}_2(\tau)|)d\tau\Big).
\end{aligned} \tag{2.37}$$

The combination of (2.33) and (2.37) yields

$$\begin{aligned}
&U(\chi_1, \chi_2) - U(\tilde{\chi}_1, \tilde{\chi}_2)\\
&\leq \epsilon + \eta^{-t^\epsilon/2}\Big(\alpha(|x_1(t^\epsilon) - x_2(t^\epsilon)|) - \alpha(|\tilde{x}_1(t^\epsilon) - \tilde{x}_2(t^\epsilon)|)\\
&\qquad + \int_0^{t^\epsilon} \eta^{t^\epsilon-\tau}(\alpha_y(|\tilde{y}_1(\tau) - \tilde{y}_2(\tau)|) - \alpha_y(|y_1(\tau) - y_2(\tau)|))d\tau\Big).
\end{aligned} \tag{2.38}$$

Without loss of generality, we assume that[7] $\alpha_d(s) \geq \kappa_1(3s)$ for all $s \geq 0$. By Lemma 2.4, there exist $R_x, R_y > 0$ such that

$$\begin{aligned}\max\{|x_1(t) - x_2(t)|, |\tilde{x}_1(t) - \tilde{x}_2(t)|\} &\leq R_x(T(C), C, r_d(C)) =: R_x^C,\\ \max\{|y_1(t) - y_2(t)|, |\tilde{y}_1(t) - \tilde{y}_2(t)|\} &\leq R_y(T(C), C, r_d(C)) =: R_y^C\end{aligned}$$

uniformly for all $t \in [0, T(C)]$. Recall that α, α_y in (2.38) are continuous; hence, they are uniformly continuous on the compact sets $[0, R_x^C]$ and $[0, R_y^C]$, respectively. From [All+17, Prop. 20], there exist $\hat{\alpha}, \hat{\alpha}_y \in \mathcal{K}_\infty$ such that

$$|\alpha(s_1) - \alpha(s_2)| \leq \hat{\alpha}(|s_1 - s_2|),\ s_1, s_2 \in [0, R_x^C], \tag{2.39}$$

$$|\alpha_y(s_1) - \alpha_y(s_2)| \leq \hat{\alpha}_y(|s_1 - s_2|),\ s_1, s_2 \in [0, R_y^C]. \tag{2.40}$$

Evaluating the absolute value of the right-hand side of (2.38), using the triangle inequality, applying (2.39) and (2.40) followed by the reverse triangle inequality and then the standard one lead us to

$$\begin{aligned}U(\chi_1, \chi_2) - U(\tilde{\chi}_1, \tilde{\chi}_2) \leq \epsilon + \eta^{-t^\epsilon/2}\Big(&\hat{\alpha}\left(|x_1(t^\epsilon) - \tilde{x}_1(t^\epsilon)| + |x_2(t) - \tilde{x}_2(t^\epsilon)|\right)\\ &+ \int_0^{t^\epsilon} \eta^{t^\epsilon - \tau}\hat{\alpha}_y\left(|y_1(\tau) - \tilde{y}_1(\tau)| + |y_2(\tau) - \tilde{y}_2(\tau)|\right) d\tau\Big).\end{aligned} \tag{2.41}$$

By applying Lemma 2.1 and similar steps as in the proof of Lemma 2.4, it follows that

$$|x_i(t) - \tilde{x}_i(t)| \leq \rho^{-1}(\rho(|\chi_i - \tilde{\chi}_i|)e^{T(C)}), i = 1, 2, \tag{2.42}$$

$$|y_i(t) - \tilde{y}_i(t)| \leq \kappa_2(\rho^{-1}(\rho(|\chi_i - \tilde{\chi}_i|)e^{T(C)})), i = 1, 2 \tag{2.43}$$

for all $t \in [0, T(C)]$. Hence, from (2.41), using that $\alpha(|a + b|) \leq \alpha(2a) + \alpha(2b)$ for any $\alpha \in \mathcal{K}$ and $a, b \geq 0$ in conjunction with the bounds from (2.42) and (2.43) and the facts that $\eta^{-t^\epsilon/2} \leq \eta^{-T(C)/2}$ and $\int_0^{t^\epsilon} \eta^{t^\epsilon - \tau} d\tau \leq -1/\ln\eta$, we can infer that there exist $\gamma_x, \gamma_y \in \mathcal{K}$ satisfying

$$\begin{aligned}&U(\chi_1, \chi_2) - U(\tilde{\chi}_1, \tilde{\chi}_2)\\ &\leq \epsilon + \gamma_x(|\chi_1 - \tilde{\chi}_1|) + \gamma_x(|\chi_2 - \tilde{\chi}_2|) + \gamma_y(|\chi_1 - \tilde{\chi}_1|) + \gamma_y(|\chi_2 - \tilde{\chi}_2|)\\ &\leq \epsilon + \gamma(|\chi_1 - \tilde{\chi}_1|) + \gamma(|\chi_2 - \tilde{\chi}_2|),\end{aligned}$$

where $\gamma(s) := \gamma_x(s) + \gamma_y(s)$ for all $s \geq 0$. Letting $\epsilon \to 0$ and applying a symmetric argument (recall that $(\tilde{\chi}_1, \tilde{\chi}_2) \in \mathcal{B}(C)$ by the definition of C) let us conclude that

$$|U(\chi_1, \chi_2) - U(\tilde{\chi}_1, \tilde{\chi}_2)| \leq \gamma(|\chi_1 - \tilde{\chi}_1|) + \gamma(|\chi_2 - \tilde{\chi}_2|). \tag{2.44}$$

Since $\mathcal{B}(C)$ contains all pairs (x_1, x_2) within a neighborhood of $(\tilde{\chi}_1, \tilde{\chi}_2)$, (2.44) implies that U is continuous at each $(\tilde{\chi}_1, \tilde{\chi}_2) \in \mathcal{X} \times \mathcal{X}$ for $\tilde{\chi}_1 \neq \tilde{\chi}_2$. It remains to show

[7] If this is violated, simply replace α_d in (2.17) by a suitable $\bar{\alpha}_d \in \mathcal{K}_\infty$ that majorizes both α_d and $\kappa_1(3s)$.

that U is also continuous at $(\tilde{\chi}, \tilde{\chi})$. To this end, consider any $(\chi_1, \chi_2) \in \mathcal{X} \times \mathcal{X}$; since $U(\tilde{\chi}, \tilde{\chi}) = 0$, it follows that

$$|U(\chi_1, \chi_2) - U(\tilde{\chi}, \tilde{\chi})| = U(\chi_1, \chi_2) \leq \alpha_x(|\chi_1 - \chi_2|) \leq \alpha_x(|\chi_1 - \tilde{\chi}| + |\tilde{\chi} - \chi_2|) \\ \leq \alpha_x(2|\chi_1 - \tilde{\chi}|) + \alpha_x(2|\chi_2 - \tilde{\chi}|),$$

which implies that U is continuous at $(\tilde{\chi}, \tilde{\chi})$. Hence, U is continuous on $\mathcal{X} \times \mathcal{X}$, which finishes this proof. □

Remark 2.7 (Input functions)**.** *Part I of the proof of Claim 2.1 gives rise to the fact that $(d_1^\epsilon, d_2^\epsilon) \in \mathcal{B}_d(C)$, i.e., the inputs d_1^ϵ and d_2^ϵ are such that the weighted "energy" of its difference is located in a ball of radius r_d centered at the origin. However, this implies no information about the absolute range of d_1 and d_2, which prevents the use of a local Lipschitz property of f to bound the evolution of the difference between state trajectories in the proof of Claim 2.1 below* (2.38) *and in* (2.42)*. In contrast, the global nature of Assumption 2.1 allows the derivation of such a bound, and the conditions in* (2.7) *ensure that it is finite for any finite t.*

2.2.4. Robust observers and i-iIOSS

In this section, we establish necessity of i-iIOSS (Definition 2.1) for the existence of a general observer mapping that satisfies a desirable robust stability property (namely, an ISS-like bound on the estimation error in a time-discounted L^2-to-L^∞ sense). In this context, we let u include all *known* exogenous signals (such as control inputs) and $w = (d, v)$ all *unknown* inputs, with d affecting the evolution of the system in (2.5a) (such as process disturbances) and v the output measurements in (2.5b) (i.e., measurement noise).

Let the set $\mathcal{M}_\mathcal{Y}$ contain all measurable, locally essentially bounded functions defined on $[0, \infty)$ taking values in $\mathcal{Y}$. For a function z defined on $[0, \infty)$ and any fixed $t \geq 0$, we denote by z_t the truncated signal given by $z_t(\tau) := z(\tau), \tau \in [0, t)$ and $z_t(\tau) := 0, \tau \in [t, \infty)$.

We consider the following general definition of a robustly stable state observer.

Definition 2.4 (Robustly stable state observer)**.** *The mapping*

$$O : \mathbb{R}_{\geq 0} \times \mathcal{X} \times \mathcal{M}_\mathcal{U} \times \mathcal{M}_\mathcal{W} \times \mathcal{M}_\mathcal{Y} \to \mathcal{X} \tag{2.45}$$

is a robustly globally asymptotically stable (RGAS) observer for the system (2.5) *if there exist functions $\beta, \beta_x, \beta_w, \beta_y \in \mathcal{K}_\infty$ and a constant $\rho \in (0, 1)$ such that the estimate*

$$\hat{x}(t) = O(t, \bar{\chi}, u_t, \bar{w}_t, \bar{y}_t), \ \hat{x}(0) = \bar{\chi} \tag{2.46}$$

satisfies

$$\beta(|\hat{x}(t) - x(t)|) \leq \beta_x(|\bar{\chi} - \chi|)\rho^t + \int_0^t \rho^{t-\tau}\Big(\beta_w(|\bar{w}(\tau) - w(\tau)|) + \beta_y(|\bar{y}(\tau) - y(\tau)|)\Big)d\tau \tag{2.47}$$

for all $t \geq 0$, all $\bar{\chi}, \chi \in \mathcal{X}$, $u \in \mathcal{M}_{\mathcal{U}}$, $\bar{w}, (d, v) \in \mathcal{M}_{\mathcal{W}} = \mathcal{M}_{\mathcal{D}} \times \mathcal{M}_{\mathcal{V}}$, and all $\bar{y} \in \mathcal{M}_{\mathcal{Y}}$, where $x(\tau) = x(\tau, \chi, u, d)$ and $y(\tau) = y(\tau, \chi, u, w)$ for all $\tau \in [0, t]$. If additionally $\beta(s) \geq C_1 s^r$ and $\beta_x(s) \leq C_2 s^r$ for some $C_1, C_2, r > 0$, then the state observer is robustly globally exponentially stable (RGES).

Definition 2.4 implies that at any time $t \geq 0$, the mapping O causally[8] reconstructs the state of system (2.5) using (the past values of) some nominal disturbance $\bar{w}$, some measured signal $\bar{y}$, the known inputs u, and some initial estimate $\bar{\chi}$. Considering $\bar{y} \neq y$ provides an additional degree of robustness and accounts for the case where the output model h in (2.5b) is not exact, e.g., when the data are first transformed or traverse additional networks not captured by h, see [KM20] for a more detailed discussion. Note that for the classical case with $\bar{w} \equiv 0$ and $\bar{y} = y$, the RGAS estimate (2.47) reduces to

$$\beta(|\hat{x}(t) - x(t)|) \leq \beta_x(|\bar{\chi} - \chi|)\rho^t + \int_0^t \rho^{t-\tau} \beta_w(|w(\tau)|) d\tau, \quad t \geq 0. \tag{2.48}$$

The integral term in (2.48) can be viewed as the energy of the true disturbance signal w under fading memory and thus has a reasonable physical interpretation, compare also [Son98; PW96].

Clearly, Definition 2.4 can be used to characterize stability properties of conventional full-order state observers; however, due to its general nature, it is particularly useful in the context of state observers that do not admit a convenient state-space representation (such as MHE and FIE). This is mainly because the property (2.48) directly implies that $|\hat{x}(t) - x(t)| \to 0$ if $|w(t)| \to 0$ for $t \to \infty$ (i.e., the intuitive and important property that vanishing disturbances lead to a vanishing estimation error), which otherwise would require an extra analysis of the respective estimation scheme as in, e.g., [Mül17], compare also [ART21; KM20] for similar discussions in a discrete-time setting.

Definition 2.4 provides a time-discounted L^2-to-L^∞ bound for the estimation error; however, the discount factor in (2.47) also permits a direct derivation of an L^∞-to-L^∞ error bound as shown in the following.

Proposition 2.4. *Suppose there exists a state estimator for system (2.5) that is RGAS in the sense of Definition 2.4. Then, there exist functions $\psi \in \mathcal{KL}$ and $\gamma_w, \gamma_y \in \mathcal{K}_\infty$ such that*

$$|\hat{x}(t) - x(t)| \leq \max\{\psi(|\bar{\chi} - \chi|, t), \gamma_w(\|\bar{w} - w\|_{0:t}), \gamma_y(\|\bar{y} - y\|_{0:t})\} \tag{2.49}$$

for all $t \geq 0$, all $\bar{\chi}, \chi \in \mathcal{X}$, $u \in \mathcal{M}_{\mathcal{U}}$, $\bar{w}, (d, v) \in \mathcal{M}_{\mathcal{W}} = \mathcal{M}_{\mathcal{D}} \times \mathcal{M}_{\mathcal{V}}$, and all $\bar{y} \in \mathcal{M}_{\mathcal{Y}}$, where $x(\tau) = x(\tau, \chi, u, d)$ and $y(\tau) = y(\tau, \chi, u, w)$ for all $\tau \in [0, t]$ and $w = (d, v)$. If it is RGES, then there exist $C > 0$ and $\rho \in (0, 1)$ such that (2.49) holds with $\psi(s, t)$ replaced by $Cs\rho^t$ and suitable functions $\gamma_w, \gamma_y \in \mathcal{K}_\infty$.

[8] The observer is causal due to the use of the truncated signals in (2.46).

Proof. The proof is straightforward and follows by noting that

$$\begin{aligned}\int_0^t \rho^{t-\tau}\beta_w(|\bar{w}(\tau)-w(\tau)|)d\tau &\leq \int_0^t \rho^{t-\tau}d\tau \cdot \operatorname*{ess\,sup}_{s\in[0,t]}\{\beta_w(|\bar{w}(s)-w(s)|)\}\\ &= \frac{\rho^t-1}{\ln\rho}\beta_w(\|\bar{w}-w\|_{0:t}) \leq -\frac{1}{\ln\rho}\beta_w(\|\bar{w}-w\|_{0:t}),\end{aligned}$$

where $-1/\ln\rho \geq 0$ since $\rho \in (0,1)$. From the same arguments, we also have that

$$\int_0^t \rho^{t-\tau}\beta_y(|\bar{y}(\tau)-y(\tau)|)d\tau \leq -\frac{1}{\ln\rho}\beta_y(\|\bar{y}-y\|_{0:t}).$$

Consequently, using the fact that $a+b+c \leq \max\{3a,3b,3c\}$ for $a,b,c \geq 0$, the RGAS property from (2.47) implies that

$$\begin{aligned}&\beta(|\hat{x}(t)-x(t,\chi,u,w)|)\\ &\leq \max\left\{3\beta_x(|\hat{\chi}-\chi|)\rho^t, -\frac{3}{\ln\rho}\beta_w(\|\bar{w}-w\|_{0:t}), -\frac{3}{\ln\rho}\beta_y(\|\bar{y}-y\|_{0:t})\right\}. \qquad (2.50)\end{aligned}$$

The application of $\psi(s,t) := \beta^{-1}(3\beta_x(s)\rho^t)$, $\gamma_w(s) := \beta^{-1}(-\frac{3}{\ln\rho}\beta_w(s))$, and $\gamma_y(s) := \beta^{-1}(-\frac{3}{\ln\rho}\beta_y(s))$ shows that (2.50) implies (2.49), where we note that $\psi \in \mathcal{KL}$ and $\gamma_w, \gamma_y \in \mathcal{K}_\infty$.

When the state estimator is additionally RGES, we can exploit in (2.50) that $\beta(s) \geq C_1 s^r$ and $\beta_x(s) \leq C_2 s^r$ with C_1, C_2, r from Definition 2.4, which yields $\psi(s,t) \leq \left(3\frac{C_2}{C_1}\right)^{\frac{1}{r}} s\rho^{\frac{t}{r}}$, $\gamma_w(s) \leq \left(-\frac{3}{C_1\ln\rho}\beta_w(s)\right)^{\frac{1}{r}}$, and $\gamma_y(s) \leq \left(-\frac{3}{C_1\ln\rho}\beta_y(s)\right)^{\frac{1}{r}}$ (recall that $s \mapsto s^{\frac{1}{r}}$ is strictly increasing in $s \geq 0$). Consequently, we can choose $C := \left(3\frac{C_2}{C_1}\right)^{\frac{1}{r}}$ and $\tilde{\rho} := \rho^{\frac{1}{r}} \in (0,1)$. A suitable redefinition of ρ, γ_w, and γ_y establishes our claim and hence concludes this proof. □

Consequently, RGAS as characterized in Definition 2.4 combines the advantages of classical and integral ISS properties: it is applicable and ensures a finite estimation error bound for both (unbounded) disturbance signals with finite energy (by (2.47)) and persistent (non-vanishing) bounded disturbances with infinite energy (by application of Proposition 2.4).

Overall, RGAS is a very desirable property of observers, which we refer to in many of our results contained in this thesis (in continuous and discrete time; for a discrete-time analog of Definition 2.4, see [ART21, Def. 2.3] and [KM20, Def. 3]). However, this raises the question of which detectability property the system must actually have in order for such observers to exist. This question is answered (in the context of continuous-time systems) by the following proposition and is in fact our proposed i-iIOSS notion from Definition 2.1.

Proposition 2.5. *The system* (2.5) *admits an RGAS observer in the sense of Definitions 2.4 only if it is i-iIOSS (Definition 2.1).*

The proof follows similar lines as those of [ART21, Prop. 2.6] and [KM20, Prop. 3], which establish necessity of RGAS (in a time-discounted max-based form [ART21, Def. 2.3]) for the system being i-IOSS (as in (2.3)).

Proof of Proposition 2.5. Consider $\chi_1, \chi_2 \in \mathcal{X}$, $u \in \mathcal{M}_\mathcal{U}$, and $d_1, d_2 \in \mathcal{M}_\mathcal{D}$, $v_1, v_2 \in \mathcal{M}_\mathcal{V}$, yielding $x_i(t) = x(t, \chi_i, u, d_i)$ and $y_i(t) = y(t, \chi_i, u, w_i)$, $i = 1, 2$ for all $t \geq 0$ with $w_i = (d_i, v_i)$, $i = 1, 2$. Suppose that the observer O (2.46) is designed to reconstruct the trajectory x_1 using $\bar{\chi} = \chi_1$, $\bar{w} = w_1$, $\bar{y} = y_1$. By application of (2.47), it follows that $\beta(|\hat{x}(t) - x_1(t)|) = 0$ for all $t \geq 0$. Now assume that this certain design of O is used to reconstruct the trajectory x_2. Then, since $\hat{x}(t) = x_1(t)$ for all $t \geq 0$, the estimate (2.47) directly yields (2.16) with $\alpha = \beta$, $\alpha_x = \beta_x$, $\alpha_w = \beta_w$, $\alpha_y = \beta_y$, and because $\chi_1, \chi_2, u, w_1, w_2$ were arbitrary, the system (2.5) is i-iIOSS, which finishes this proof. □

2.3. Summary

In this chapter, we focused on a system-theoretic approach for characterizing detectability of nonlinear systems, namely i-IOSS. We considered the original asymptotic-gain formulation of i-IOSS and discussed two modern variants that employ additional discounting and a max- or sum-based formulation, which became standard detectability concepts in the context of optimization-based state estimation (in particular, MHE) in the recent years. While these properties could be shown to coincide for the case of discrete-time systems, this is generally not the case for continuous-time systems, and we must carefully distinguish between them.

We proposed the notion of i-iIOSS for continuous-time systems, which essentially constitutes a time-discounted integral variant of i-IOSS. Here, we stated two definitions of i-iIOSS involving the nominal and the disturbed outputs of the underlying system. We showed that these definitions are equivalent for the special case of additive measurement noise, and that the latter constitutes a stronger property in the context of general nonlinear systems (with a potentially nonlinear dependence on measurement noise), consequently allowing for stronger robustness guarantees for state estimators (which are the main topic of this thesis). We proposed a Lyapunov function characterization of i-iIOSS and showed that a dissipation inequality with exponential decrease can be considered without loss of generality. Moreover, we provided a converse Lyapunov theorem for the weaker case of i-iIOSS with nominal outputs.

Finally, we proposed a particular notion of RGAS, characterizing robust stability with respect to process disturbances and measurement noise in a time-discounted L^2-to-L^∞ sense. This constitutes a useful stability property for general observers, as it combines the advantages of classical ISS and iISS characteristics: it is applicable for persistent disturbance signals that have a small magnitude but infinite energy, and for those that may have an infinite magnitude at certain points but otherwise finite (small) energy. Indeed, we found that the proposed i-iIOSS notion is necessary for the existence of state estimators that fulfill this robust stability property.

Overall, the results in this chapter reveal that i-iIOSS is useful to characterize detectability of general nonlinear continuous-time systems, particularly in the context of RGAS observers for which it is even necessary. The proposed definitions of i-iIOSS and RGAS form a fundamental basis for our results in Section 3.2, where we consider and analyze a particular MHE scheme for nonlinear continuous-time systems. We close this chapter by noting that constructive conditions (in terms of LMIs) to obtain i-IOSS and i-iIOSS Lyapunov functions for discrete- and continuous-time systems that certify exponential i-(i)IOSS are provided in Sections 7.1.

3. Robust stability

In this chapter, we focus on the stability and robustness properties of MHE in the context of general detectable nonlinear systems under process disturbances and measurement noise. Since the application of MHE inevitably requires some sort of sampling strategy—that is, specifying discrete time points at which the optimization is performed—schemes for discrete-time systems have recently been the main focus in the literature. For this reason, in Section 3.1 we first introduce the basics of MHE in discrete time and discuss general features and characteristics. We also briefly outline the recently developed Lyapunov-based MHE framework from [Sch+23, Sec. III], which is a fundamental basis for many of the results developed in this thesis. In Section 3.2, we then focus on a Lyapunov-based MHE scheme for continuous-time systems in detail, relying on tools that we developed in Chapter 2. In Section 3.3, we discuss general advantages of Lyapunov-based MHE approaches and compare it to recent results in the field of nonlinear MHE. Finally, we illustrate the applicability of Lyapunov-based MHE in Section 3.4 by means of numerical examples from the literature, involving a chemical reactor process and a 12-state quadrotor model. Here, the verification methods proposed in Chapter 7.1 allow us to apply the Lyapunov-based MHE schemes *with valid theoretical guarantees under practical conditions*.

Disclosure: The following chapter is based upon and in parts literally taken from our previous publications [SM24b] and Sections III-D and V in [Sch+23] (we explicitly point out that Sections III-B and III-C in [Sch+23] are *not* part of this thesis, see also Footnote 1 in Section 1.3). A detailed description of the contributions of each author is given in Appendix A.

3.1. Basics of MHE

We consider the discrete-time counterpart of the continuous-time system from (2.5), where for the sake of conciseness we consider the generalized disturbance input w describing both the process disturbance and the measurement noise, compare Chapter 2 for more details. The overall state-space model reads

$$x(t+1) = f(x(t), u(t), w(t)), \quad x(0) = \chi, \tag{3.1a}$$

$$y(t) = h(x(t), u(t), w(t)) \tag{3.1b}$$

with discrete time $t \in \mathbb{I}_{\geq 0}$, state $x(t) \in \mathbb{R}^n$, initial condition $\chi \in \mathbb{R}^n$, control input $u(t) \in \mathbb{R}^m$, disturbance input $w(t) \in \mathbb{R}^q$, and noisy output measurement $y(t) \in \mathbb{R}^p$.

The overall goal of state estimation is to produce an accurate estimate $\hat{x}(t)$ of the true unknown system state $x(t)$ using only the available input-output data (u, y), prior knowledge of the model, and some initial estimate $\hat{\chi}$. In the presence of process disturbances and measurement noise, it is moreover essential to ensure a certain degree of robustness, such as the implication that small disturbances $|w(t)|$, $t \in \mathbb{I}_{\geq 0}$ results in small estimation errors $|\hat{x}(t) - x(t)|$, $t \in \mathbb{I}_{\geq 0}$, compare also Section 2.2.4.

In this respect, MHE has proven to be a powerful tool that provides these desired characteristics. A typical MHE scheme considers past input-output measurements obtained from the system in (3.1) in a window of (fixed) length $N \in \mathbb{I}_{\geq 0}$, which can be conveniently expressed as

$$u_t = \{u_t(j)\}_{j=0}^{N-1},\ u_t(j) = u(t-N+j),\ j \in \mathbb{I}_{[0,N-1]}, \tag{3.2}$$

$$y_t = \{y_t(j)\}_{j=0}^{N-1},\ y_t(j) = y(t-N+j),\ j \in \mathbb{I}_{[0,N-1]} \tag{3.3}$$

for any time $t \in \mathbb{I}_{\geq N}$. Given a suitably defined cost function $J(\cdot)$, the nonlinear program (NLP) underlying classical MHE schemes to be solved at each time $t \in \mathbb{I}_{\geq N}$ can be formulated as follows:

$$\min_{\hat{x}_t, \hat{w}_t} J(\hat{x}_t, \hat{w}_t, \hat{y}_t, t) \tag{3.4a}$$

$$\text{s.t. } \hat{x}_t(j+1) = f(\hat{x}_t(j), u_t(j), \hat{w}_t(j)),\ j \in \mathbb{I}_{[0,N-1]}, \tag{3.4b}$$

$$\hat{y}_t(j) = h(\hat{x}_t(j), u_t(j), \hat{w}_t(j)),\ j \in \mathbb{I}_{[0,N-1]}, \tag{3.4c}$$

$$\hat{x}_t(j) \in \mathcal{X},\ j \in \mathbb{I}_{[0,N]}, \tag{3.4d}$$

$$\hat{w}_t(j) \in \mathcal{W},\ \hat{y}_t(j) \in \mathcal{Y},\ j \in \mathbb{I}_{[0,N-1]}. \tag{3.4e}$$

Here, the decision variables are the sequences $\hat{x}_t = \{\hat{x}_t(j)\}_{j=0}^{N}$ and $\hat{w}_t = \{\hat{w}_t(j)\}_{j=0}^{N-1}$ that contain estimates of the states[1] and the disturbances over the horizon, respectively, estimated at time t. They (uniquely) define a sequence of output estimates $\hat{y}_t = \{\hat{y}_t(j)\}_{j=0}^{N-1}$ under the output equation[2] in (3.4c). The functions f and h in (3.4b) and (3.4c) correspond to the system model in (3.1), which we assume to be perfectly known. The constraints in (3.4d) and (3.4e) can be used to incorporate additional *a priori* knowledge on the domain of the system, which can significantly improve the estimation results, compare [RMD20, Sec. 4.4]. Here, the sets $\mathcal{X} \subseteq \mathbb{R}^n$, $\mathcal{W} \subseteq \mathbb{R}^q$, and $\mathcal{Y} \subseteq \mathbb{R}^p$ typically follow from the physical nature of the system, for example due to non-negativity of certain physical quantities such as partial pressures

[1] The description of the NLP in (3.4) corresponds to a multiple shooting (or non-condensed) formulation, where the decision variables involve the complete state sequence $\hat{x}_t$. Alternatively, one could eliminate all decision variables of the sequence $\hat{x}_t$ except the initial state $\hat{x}_t(0)$ by recursively applying the system dynamics (3.1a), which corresponds to a single shooting (or condensed) approach. In practice, multiple shooting methods are usually preferred to create and exploit sparsity of the NLP, which renders the optimization algorithm more numerically robust, see [WVD14, Sec. II] and [Rib+20], and compare also [RMD20, Sec. 8.5]. While the formulation has no influence on the theoretical analysis, we use multiple shooting here because it allows for a more compact notation.

[2] Note that in this thesis, we do *not* treat the estimated output sequence $\hat{y}_t$ as a decision variable of the NLP (3.4), since it is completely determined by the sequences $\hat{x}_t$, u_t, and $\hat{w}_t$ using (3.4c). This represents a slight abuse of the notation commonly used in numerical optimization, but increases the readability and interpretability of our methods and results.

and absolute temperatures, or mechanically imposed limits on joint angles or measurement devices. The ability to incorporate such information is an advantageous feature of optimization-based state estimation approaches compared to conventional state observers, where this is not easily possible and which therefore may not provide physically plausible estimates (especially in transient phases), compare also the simulation example in Section 3.4.1 and the discussion in Section 4.2.5. If no such sets are known *a priori*, they can simply be chosen as $\mathcal{X} = \mathbb{R}^n$, $\mathcal{W} = \mathbb{R}^q$, and $\mathcal{Y} = \mathbb{R}^p$, in which case the constraints (3.4d) and (3.4e) can simply be omitted from the optimization.

The cost function used in (3.4a) typically takes the general form

$$J(\hat{x}_t, \hat{w}_t, \hat{y}_t, t) = \Gamma_t(\hat{x}_t(0), \bar{x}(t-N)) + \sum_{j=0}^{N-1} L(\hat{w}_t(j), \hat{y}_t(j) - y_t(j)), \tag{3.5}$$

where we recall that y_t is the sequence of output measurements obtained from the system in (3.1) over the current estimation horizon, see (3.3). The cost function in (3.5) consists of two parts: first, the (possibly time-varying) prior weighting $\Gamma_t : \mathbb{R}^n \times \mathbb{R}^n \to \mathbb{R}_{\geq 0}$, which ideally accounts for the neglected data over $\mathbb{I}_{[0,t-N-1]}$ and acts as regularization term using a given prior estimate $\bar{x}(t-N)$; second, the stage cost $L : \mathbb{R}^q \times \mathbb{R}^p \to \mathbb{R}_{\geq 0}$, which penalizes the estimated disturbance $\hat{w}_t(j)$ and the output fitting error $\hat{y}_t(j) - y_t(j)$, $j \in \mathbb{I}_{[t-N,t-1]}$. Usually, one designs Γ_t and L positive definite and radially unbounded in its arguments, which consequently renders the cost function J radially unbounded in the (condensed) decision variables. Under additional continuity assumptions of the functions f and h, this ensures that the estimation problem in (3.4) admits a (not necessarily unique) globally optimal solution at each time $t \in \mathbb{I}_{\geq N}$, compare [RMD20, Sec. 4.2].

Note that the cost function in (3.5) forms the *prediction form* of the estimation problem, since the most recent measurement $y(t)$ is excluded. This is typically done in theoretical works to simplify the analysis and notation, however, can in general easily be extended to the *filtering form* of the estimation problem (taking into account the most recent measurement $y(t)$), see [RMD20, Ch. 4] for a discussion on this topic.

Remark 3.1 (Output estimates)**.** *In the MHE literature, the estimated output* $\hat{y}_t(j)$ *in* (3.4c) *is often restricted to exactly match the measured output of the real system* $y_t(j)$ *by imposing* $\hat{y}_t(j) = y_t(j)$, $j \in \mathbb{I}_{[1,N_t]}$ *as an additional constraint in the problem* (3.4)*, see, e.g., [RMD20; Mül17; AR19b; All20; Hu24]. Under the assumption that the output equation in* (3.1b) *is subject to additive measurement noise* v*, this is a reasonable approach, as the estimated measurement noise* $\hat{v}_t(j) = y_t(j) - h(\hat{x}_t(j), u_t(j), 0)$ *is equal to the fitting error of MHE, and thus directly accounted for within the penalty for the estimated disturbance* $\hat{w}_t(j) = (\hat{d}_t(j), \hat{v}_t(j))$*. However, we are interested in more general systems where the measurement noise can enter the output equation nonlinearly, compare also the discussion in Section 2.2.2. In this case, trying to enforce a hard output constraint could lead to feasibility issues in practice due to potential model inaccuracies. To prevent this, we avoid such a constraint and instead include an additional term in the cost function that penalizes*

the output fitting error $\hat{y}_t(j) - y_t(j)$, compare also [KM23, Rem. 8]. Note that this formulation was recently also adopted in [Ale25].

We denote a minimizer to the optimization problem (3.4) by $(\hat{x}_t^*, \hat{w}_t^*)$, and the corresponding estimated output sequences by $\hat{y}_t^*$. The resulting state estimate $\hat{x}(t)$ at time step t is then given by the endpoint of the estimated state sequence $\hat{x}_t^*$, i.e., $\hat{x}(t) = \hat{x}_t^*(N)$. The optimization problem (3.4) is applied in a receding horizon fashion, i.e., at each time step $t \in \mathbb{I}_{\geq N}$, the current state estimate $\hat{x}(t)$ is obtained by solving (3.4) based on the N most recent output measurements. When $t \in \mathbb{I}_{[0,N-1]}$, we solve the corresponding FIE problem, where N in (3.4) is replaced by t. To simplify the notation, in the following we usually address both cases simultaneously by replacing N in (3.4) with $N_t = \min\{t, N\}$.

Early works concerned with the stability analysis of nonlinear MHE schemes rely on certain observability conditions, compare [MR95; MM95; RRM03; ABB08]. In recent years, however, the notion of i-IOSS has become the standard for characterizing nonlinear detectability in this context (see Chapter 2), enabling significant advances in MHE theory, compare, for example, [RJ12; Ji+16; Mül17; RMD20; AR21; KM23; Hu24; Ale25], and see Section 3.3 for a detailed overview of the historic development.

In [Sch+23, Sec. III], we developed a Lyapunov-based MHE framework, where the i-IOSS Lyapunov function characterizing the detectability of the system directly serves as N-step Lyapunov function for MHE, see [Sch+23, Thm. 1, Cor. 1]. This crucially relies on the following *discounted* cost function being used in (3.4a):

$$J(\hat{x}_t, \hat{w}_t, \hat{y}_t, t) = \eta^N \Gamma(\hat{x}_t(0), \bar{x}(t-N)) + \sum_{j=0}^{N-1} \eta^{N-j-1} L(\hat{w}_t(j), \hat{y}_t(j) - y_t(j)) \tag{3.6}$$

with the discount factor $\eta \in (0, 1)$, quadratic penalties $\Gamma(x, \bar{x}) = |x - \bar{x}|_P^2$ and $L(w, \Delta y) = |w|_Q^2 + |\Delta y|_R^2$ for some positive definite weighting matrices P, Q, R, and the *filtering prior*[3] $\bar{x}(t-N) = \hat{x}(t-N)$. The cost function in (3.6) essentially constitutes a standard least squares objective under additional *fading memory*, i.e., more recent measurements and disturbances are weighted more heavily in the cost function than older ones. This Lyapunov-based MHE approach has many theoretical advantages and ultimately leads to much less restrictive conditions than comparable approaches, see Section 3.3 for a detailed discussion. The key condition to apply [Sch+23, Thm. 1, Cor. 1] and hence ensure robust stability of MHE is, however, that the cost function parameters η, P, Q, R are chosen in accordance with the i-IOSS Lyapunov function. Hence, in order to apply the theoretical results in practice, such an i-IOSS Lyapunov function must first be found, which is generally a non-trivial task and hence drastically limits its applicability.

Here, our methods developed in Chapter 7 become particularly relevant, which enable the systematic computation of i-IOSS Lyapunov functions by numerically solving certain LMI conditions. Consequently, suitable cost function parameters η, P, Q, R that inherently ensure robust stability of MHE can easily be computed. In

[3] Wording according to [RMD20, Sec. 4.3.3]. Alternative choices for selecting the prior estimate are discussed in more detail in Section 6.3.3.

fact, our verification methods from Chapter 7 thus transform the disadvantage of the scheme from [Sch+23, Sec. III] into a strong advantage, since a time-consuming tuning of the cost function can also be avoided, compare also Remark 3.4 below regarding tuning possibilities.

Due to the numerous advantageous properties of the Lyapunov-based MHE framework for discrete-time systems (resulting from the combination of the results from [Sch+23, Sec. III] and Chapter 7), we will now develop and analyze a corresponding approach for continuous-time systems in the following section, heavily relying on our results from Chapter 2. Here, it turns out that the continuous-time Lyapunov-based MHE framework has advantages over the discrete-time one if the original physical system evolves in continuous-time (which is usually the case in practice), especially concerning the sampling scheme and required detectability verification, see Section 3.3 below for a detailed discussion.

3.2. Continuous-time Lyapunov-based MHE

In this section, we focus on MHE for general nonlinear continuous-time systems. Specifically, we propose a Lyapunov-based MHE scheme with a discounted least squares cost function (Section 3.2.2) and establish robust global exponential stability of the estimation error in a time-discounted L^2-to-L^∞ sense (Section 3.2.3). Here, we employ the notion of i-iIOSS as introduced in Chapter 2 to characterize the underlying detectability property.

3.2.1. Setup

We consider the continuous-time system from (2.5), where we for the sake of conciseness consider the generalized disturbance input w that describes both the process disturbance and the measurement noise, see Chapter 2 for more details. The overall state-space model therefore reads

$$\dot{x}(t) = f(x(t), u(t), w(t)), \quad x(0) = \chi, \tag{3.7a}$$
$$y(t) = h(x(t), u(t), w(t)), \tag{3.7b}$$

where we recall that $t \geq 0$ is the time, $x(t) \in \mathcal{X} \subseteq \mathbb{R}^n$ are the states, $\chi \in \mathcal{X}$ is the initial condition, and $y(t) \in \mathcal{Y} \subseteq \mathbb{R}^p$ are the noisy output measurements. The (known) control input u and the (unknown) disturbance input w are measurable, locally essentially bounded functions taking values in $\mathcal{U} \subseteq \mathbb{R}^m$ and $\mathcal{W} \subseteq \mathbb{R}^q$, and we denote the set of such functions as $\mathcal{M}_\mathcal{U}$ and $\mathcal{M}_\mathcal{W}$, respectively. The mappings $f : \mathcal{X} \times \mathcal{U} \times \mathcal{W} \to \mathbb{R}^n$ and $h : \mathcal{X} \times \mathcal{U} \times \mathcal{W} \to \mathcal{Y}$ constitute the system dynamics and output equation. In the following, we assume that f and h are jointly continuous and that $\mathcal{X}$ and $\mathcal{W}$ are closed.

For any initial state $\chi \in \mathcal{X}$, we denote the solution of (3.7a) at a time $t \geq 0$ driven by the control $u \in \mathcal{M}_\mathcal{U}$ and the disturbance $w \in \mathcal{M}_\mathcal{W}$ by $x(t, \chi, u, w)$, and the corresponding output signal by $y(t, \chi, u, w) := h(x(t, \chi, u, w), u(t), w(t))$. In the

following, we assume that solutions of (3.7) are unique, defined globally on $\mathbb{R}_{\geq 0}$, and satisfy $x(t, \chi, u, w) \in \mathcal{X}$ and $y(t, \chi, u, w) \in \mathcal{Y}$ for all $t \geq 0$ for all $\chi \in \mathcal{X}$, $u \in \mathcal{M}_{\mathcal{U}}$, and $w \in \mathcal{M}_{\mathcal{W}}$.

Since we are interested in an optimization-based method for (nonlinear) state estimation, we inevitably have to employ some sort of sampling strategy. To this end, let $\mathcal{T} \subset \mathbb{R}_{\geq 0}$ be a set containing (arbitrary) distinct time instants. Given some *a priori* estimate $\hat{\chi}$ of the unknown initial condition χ, the overall goal is to compute, at each sampling time $t_i \in \mathcal{T}$, the estimate $\hat{x}(t_i)$ of the true system state $x(t_i)$. In the next section, we provide conditions under which the resulting estimation error converges exponentially (compare Remark 2.3) to a neighborhood around the origin by means of the following definition.

Definition 3.1 (RGAS, RGES)**.** *A state estimator for system* (3.7) *is robustly globally asymptotically stable (RGAS) if there exist functions $\beta, \beta_x, \beta_w \in \mathcal{K}_\infty$ and a constant $\rho \in (0, 1)$ such that the estimated state $\hat{x}$ with $\hat{x}(0) = \hat{\chi}$ satisfies*

$$\beta(|\hat{x}(t_i) - x(t_i, \chi, u, w)|) \leq \beta_x(|\hat{\chi} - \chi|)\rho^{t_i} + \int_0^{t_i} \rho^{t_i - \tau} \beta_w(|w(\tau)|) d\tau \tag{3.8}$$

for all $t_i \in \mathcal{T}$, all initial conditions $\hat{\chi}, \chi \in \mathcal{X}$, all controls $u \in \mathcal{M}_{\mathcal{U}}$, and all disturbances $w \in \mathcal{M}_{\mathcal{W}}$. If additionally $\beta(s) \geq C_1 s^r$ and $\beta_x(s) \leq C_2 s^r$ for some $C_1, C_2, r > 0$, then the state estimator is robustly globally exponentially stable (RGES).

Note that Definition 3.1 slightly differs from the property introduced in Definition 2.4, as we consider (3.8) only pointwise for all $t_i \in \mathcal{T}$ (and not for all $t \geq 0$ as in (2.47)). This is natural in an optimization context, since the estimates are produced at certain time instants and not continuously, compare also [MM95]. However, also note that all the beneficial properties implied by RGAS as discussed in Section 2.2.4 still apply.

Remark 3.2 (Pointwise error bound)**.** *Extensions to account for a pure continuous-time stability notion as in Definition 2.4 can be easily deduced by predicting the estimated state between two consecutive samples t_i, e.g., using the nominal system dynamics or an additional auxiliary observer, compare Chapter 4.*

3.2.2. Design of the MHE scheme

The MHE scheme presented below relies on the detectability property of the system in (3.7), where we employ the notion of i-iIOSS from Definition 2.1—more precisely, its Lyapunov function characterization from Definition 2.3, see Chapter 2 for more details on i-iIOSS and its use in the context of nonlinear detectability. Here, we restrict ourselves to the special case of *exponential detectability*, that is, we assume that the functions $\alpha_1, \alpha_2, \sigma_w, \sigma_y$ in (2.19a) and (2.19b) are of quadratic form.

Assumption 3.1 (Exponential detectability)**.** *System* (3.7) *admits a quadratically bounded i-iIOSS Lyapunov function U according to Definition 2.3 satisfying*

$$|\chi_1 - \chi_2|_{\underline{P}}^2 \leq U(\chi_1, \chi_2) \leq |\chi_1 - \chi_2|_{\overline{P}}^2, \tag{3.9a}$$

$$U(x_1(t), x_2(t)) \leq U(\chi_1, \chi_2)\eta^t + \int_0^t \eta^{t-\tau}\Big(|w_1(\tau) - w_2(\tau)|_Q^2 + |y_1(\tau) - y_2(\tau)|_R^2\Big)d\tau \tag{3.9b}$$

with $\underline{P}, \overline{P}, Q, R \succ 0$ for all $t \geq 0$, $\chi_1, \chi_2 \in \mathcal{X}$, $u \in \mathcal{M}_{\mathcal{U}}$, and $w_1, w_2 \in \mathcal{M}_{\mathcal{W}}$.

Note that the requirement of exponential detectability is a standard condition for robust stability of MHE, ensuring a linear contraction of the estimation error over a (finite) horizon, compare, e.g., [RMD20; AR21; Sch+23; KM23; Hu24]. Moreover, assuming additive measurement noise, by using the same reasoning as in the proofs of Theorem 2.1 and Corollary 2.1, one can show that Assumption 3.1 is equivalent to the system (3.7) being exponentially i-iIOSS with disturbed outputs (compare Definition 2.1), which in turn can be shown to be necessary for the existence of RGES observers by suitable adapting the proof of Proposition 2.5. However, it should be noted that in case the measurement noise enters the output equation nonlinearly, there might be a gap between Assumption 3.1 and the system being exponentially i-iIOSS (with disturbed outputs), compare Remark 2.6.

In Section 7.1.2, we provide sufficient conditions (in terms of LMIs) for constructing a quadratic i-iIOSS Lyapunov function U satisfying (3.9). Assumption 3.1 can be relaxed to asymptotic detectability (Definition 2.3) if the FIE problem is considered, compare Remark 3.8 below.

Let the initial estimate $\hat{\chi} \in \mathcal{X}$ be given. At any sampling time $t_i \in \mathcal{T}$, the proposed MHE scheme considers the past input and output trajectories of the system (3.7) within the moving time interval $[t_i - T_{t_i}, t_i]$ of length $T_{t_i} = \min\{t_i, T\}$ for some $T > 0$. Let $u_{t_i} : [0, T_{t_i}) \to \mathcal{U}$ and $y_{t_i} : [0, T_{t_i}) \to \mathcal{Y}$ denote the currently involved segments of the input and output trajectories of system (3.7), which are defined as

$$u_{t_i}(\tau) := u(t_i - T_{t_i} + \tau),\ \tau \in [0, T_{t_i}), \tag{3.10}$$

$$y_{t_i}(\tau) := y(t_i - T_{t_i} + \tau, \chi, u, w),\ \tau \in [0, T_{t_i}). \tag{3.11}$$

Then, the optimal state trajectory on the interval $[t_i - T_{t_i}, t_i]$ is obtained by solving the following optimization problem:

$$\min_{\hat{\chi}_{t_i}, \hat{w}_{t_i}} J(\hat{\chi}_{t_i}, \hat{w}_{t_i}, \hat{y}_{t_i}, t_i) \tag{3.12a}$$

$$\text{s.t. } \hat{x}_{t_i}(\tau) = x(\tau, \hat{\chi}_{t_i}, u_{t_i}, \hat{w}_{t_i}),\ \tau \in [0, T_{t_i}], \tag{3.12b}$$

$$\hat{y}_{t_i}(\tau) = y(\tau, \hat{\chi}_{t_i}, u_{t_i}, \hat{w}_{t_i}),\ \tau \in [0, T_{t_i}), \tag{3.12c}$$

$$\hat{x}_{t_i}(\tau) \in \mathcal{X},\ \tau \in [0, T_{t_i}], \tag{3.12d}$$

$$\hat{w}_{t_i}(\tau) \in \mathcal{W},\ \hat{y}_{t_i}(\tau) \in \mathcal{Y},\ \tau \in [0, T_{t_i}). \tag{3.12e}$$

The decision variables $\hat{\chi}_{t_i}$ and $\hat{w}_{t_i} : [0, T_{t_i}) \to \mathcal{W}$ denote the estimates of the state at the beginning of the horizon and the disturbance signal over the horizon, respectively,

estimated at time t_i (where $\hat{w}_{t_i}$ is minimized over all measurable, locally essentially bounded functions mapping from $[0, T_{t_i})$ to $\mathcal{W}$). Given the input trajectory segment u_{t_i} in (3.10), these decision variables (uniquely) determine the estimated state and output trajectories $\hat{x}_{t_i}$ and $\hat{y}_{t_i}$ via (3.12b) and (3.12c) as functions defined on $[0, T_{t_i}]$ and $[0, T_{t_i})$, respectively. In (3.12a), we consider the discounted objective

$$J(\hat{\chi}_{t_i}, \hat{w}_{t_i}, \hat{y}_{t_i}, t_i) = \eta^{T_{t_i}} \Gamma(\hat{\chi}_{t_i}, \bar{x}(t_i - T_{t_i})) + \int_0^{T_{t_i}} \eta^{T_{t_i}-\tau} L(\hat{w}_{t_i}(\tau), \hat{y}_{t_i}(\tau) - y_{t_i}(\tau)) d\tau \tag{3.13}$$

with quadratic prior weighting $\Gamma(\chi, \bar{x}) = 2|\chi - \bar{x}|^2_{\overline{P}}$ and stage cost $L(w, \Delta y) = 2|w|^2_Q + |\Delta y|^2_R$, compare Section 3.1 and Remark 2.3. Here, $\bar{x}(t_i - T_{t_i})$ is a prior estimate that is specified below and the parameters $\eta, \overline{P}, Q, R$ are from Assumption 3.1.

Remark 3.3 (Discounting)**.** *The use of exponential discounting in* (3.13) *establishes a direct link between the detectability property (Assumption 3.1), the MHE scheme (via the cost function* (3.13)*), and the desired stability property (RGES, see Definition 3.1 and Theorem 3.1 below). It is motivated by recent time-discounted MHE approaches for discrete-time systems, which, compared to their non-discounted counterparts, allow the direct derivation of stronger and less conservative robustness guarantees by leveraging this particular structural connection, compare, e.g., [KM18; KM23; Hu24; Sch+23] and see also the discussion in Section 3.3.*

Remark 3.4 (Tuning)**.** *We point out that fixing the weighting matrices $\overline{P}, Q, R$ in the MHE objective in* (3.13) *to the values from the i-iIOSS Lyapunov function is in fact without loss of generality and therefore does not restrict any tuning possibilities. In particular, the scaled Lyapunov function $\tilde{U}(x_1, x_2) = KU(x_1, x_2)$ with*

$$K := \Big(\max\{\lambda_{\max}(\overline{P}, \tilde{P}), \lambda_{\max}(Q, \tilde{Q}), \lambda_{\max}(R, \tilde{R})\}\Big)^{-1} \tag{3.14}$$

satisfies[4] Assumption 3.1 with $\overline{P}, Q, R$ replaced by arbitrary positive definite matrices $\tilde{P}, \tilde{Q}, \tilde{R}$ and $\underline{P}$ replaced by $K\underline{P}$, compare also [Sch+23, Rem. 1] for a similar discussion in a discrete-time setting. Note that this also allows for choosing the weights in (3.13) *time-varying (e.g., based on nonlinear Kalman filter update recursions) if uniform bounds are either known a priori or imposed online.*

Moreover, we point out that η in (3.13) *can be replaced by any $\bar{\eta} \in [\eta, 1)$, since the dissipation inequality* (3.9b) *for a given i-iIOSS Lyapunov function U is still a valid dissipation inequality for U if η is replaced by $\bar{\eta} \in [\eta, 1)$. Throughout this section, we choose the parameters $\eta, \overline{P}, Q, R$ in* (3.13) *according to those from the i-iIOSS Lyapunov function from Assumption 3.1 to simplify the notation.*

Note that the continuous-time MHE problem in (3.12) and (3.13) is in fact an infinite-dimensional optimization problem (in contrast to MHE formulations in discrete time, compare Section 3.1). A standard approach to address such problems

[4] Generally, note here that $|x|^2_A \leq \lambda_{\max}(A, B)|x|^2_B$ for any real vector x and any $A, B \succ 0$ of appropriate dimensions.

are *direct methods* that essentially transform them into a finite-dimensional optimization problem, which can then be solved using tailored numerical optimization algorithms, see [RMD20, Ch. 8] for further details. In this case, a global solution to the (discretized) MHE problem exists under Assumption 3.1, since Γ and L are positive definite (due to positive definiteness of $\overline{P}, Q, R$) and radially unbounded in the decision variables and the sets $\mathcal{X}$ and $\mathcal{W}$ are closed.

We denote a minimizer to (3.12) and (3.13) by $(\hat{\chi}^*_{t_i}, \hat{w}^*_{t_i})$, and the corresponding optimal state trajectory by $\hat{x}^*_{t_i}(\tau) = x(\tau, \hat{\chi}^*_{t_i}, u_{t_i}, \hat{w}^*_{t_i})$, $\tau \in [0, T_{t_i}]$. The resulting state estimate at sampling instant $t_i \in \mathcal{T}$ is then given by

$$\hat{x}(t_i) := \hat{x}^*_{t_i}(T_{t_i}). \tag{3.15}$$

Furthermore, we define the estimated state trajectory $\hat{x}(t)$, $t \in [0, t_i]$ as the piecewise continuous function resulting from the concatenation of optimal trajectory segments according to

$$\hat{x}(t) := \begin{cases} \hat{x}^*_{k(t)}(t - k(t) + T_{k(t)}), & t \in (0, t_i] \\ \hat{\chi} & t = 0 \end{cases} \tag{3.16}$$

for all $t_i \in \mathcal{T}$, where $k(t)$ is the sampling time associated with t defined by

$$k(t) := \min_{k \in \{k \in \mathcal{T} : k \geq t\}} k. \tag{3.17}$$

We use the estimated state trajectory $x(t)$ in (3.16) to define the prior estimate $\bar{x}(t)$ appearing in the cost function (3.13); more specifically, we select

$$\bar{x}(t_i - T_{t_i}) = \hat{x}(t_i - T_{t_i}), \quad t_i \in \mathcal{T}. \tag{3.18}$$

Note that this choice corresponds to a continuous-time version of the *filtering prior*, compare Section 3.1.

Remark 3.5 (Estimated trajectory)**.** *Computing the piecewise continuous state trajectory* (3.16) *is essential for the prior estimate* $\bar{x}(t_i - T_{t_i})$ *in* (3.18) *to be well-defined for all* $t_i \in \mathcal{T}$*. To ensure that this estimate is available at time* $t_i \in \mathcal{T}$ *(i.e., has already been computed in the past such that the MHE problem in* (3.12) *can actually be solved at sampling time* t_i*), the horizon length* T *must naturally satisfy*

$$T > \bar{\delta} := \sup_{t \geq 0} k(t) - t, \tag{3.19}$$

where $\bar{\delta}$ *can be referred to as the maximum deviation between a time* t *and its associated sampling time* $k(t) \geq t$ *that may occur for all* $t \geq 0$*. For equidistant sampling using a constant sampling period* $\delta > 0$*, i.e., when* $\mathcal{T} = \{t \in \mathbb{R}_{\geq 0} : t = n\delta, n \in \mathbb{I}_{\geq 0}\}$*, it trivially holds that* $\bar{\delta} = \delta$*. Note that computing the full trajectory* (3.16) *(and hence the third step in the algorithm below) could be avoided by designing* $\mathcal{T}$ *such that* $t_i - T_{t_i} \in \mathcal{T}$ *for all* $t_i \in \mathcal{T}$*, compare also Remark 3.7.*

The MHE problem (3.12) is solved in a receding horizon fashion, and the corresponding algorithm can be summarized as follows. Given the sampling time $t_i \in \mathcal{T}$ and its predecessor $t_i^- \in \mathcal{T}$ (if there is none, set $t_i^- = 0$),

1. collect the input and output trajectory segments u_{t_i} and y_{t_i},
2. solve the MHE problem (3.12) with objective (3.13),
3. update the estimated trajectory (3.16) by attaching the most recent optimal trajectory segment $\hat{x}^*_{t_i}(\tau)$, $\tau \in (t_i^-, t_i]$,
4. update $t_i^- = t_i$, pick the next sampling time $t_i = \min_{k \in \{k \in \mathcal{T} : k > t_i\}} k$, and go back to 1.

The stability properties of the proposed continuous-time MHE scheme are established in the next section. In particular, we provide simple conditions for designing a suitable set $\mathcal{T}$ and a horizon length T such that RGES of MHE (in the sense of Definition 3.1) is guaranteed.

3.2.3. Robust stability analysis

In the following, we show how the i-iIOSS Lyapunov function U from Assumption 3.1 can be used to characterize a decrease of the estimation error $\hat{x}(t) - x(t)$ in Lyapunov coordinates over the interval $[t_i - T_{t_i}, t]$ for any $t \geq 0$ and its corresponding sampling time $t_i = k(t)$ (where we define $x(t) := x(t, \chi, u, w)$, $t \geq 0$ for notational brevity). Indeed, this requires invoking the specific choice of the cost function (3.13) involving the optimal trajectories over the interval $[t_i - T_{t_i}, t_i]$ estimated at time t_i. Then, we apply this bound recursively to establish RGES of MHE in the sense of Definition 3.1, see Theorem 3.1 below.

Proposition 3.1. *Let Assumption 3.1 hold. Then, the state estimate $\hat{x}(t)$ in (3.16) satisfies*

$$U(\hat{x}(t), x(t)) \leq \eta^{-(t_i - t)} \Big(4\lambda_{\max}(\overline{P}, \underline{P}) \eta^{T_{t_i}} U(\hat{x}(t_i - T_{t_i}), x(t_i - T_{t_i})) + 4 \int_{t_i - T_{t_i}}^{t_i} \eta^{t_i - \tau} |w(\tau)|_Q^2 d\tau \Big), \tag{3.20}$$

for all $t \geq 0$, $\hat{\chi}, \chi \in \mathcal{X}$, $u \in \mathcal{M}_{\mathcal{U}}$, $w \in \mathcal{M}_{\mathcal{W}}$, where $t_i = k(t)$ with $k(t)$ from (3.17).

The main idea of the proof of Proposition 3.1 is similar to that of [Sch+23, Prop 1], with technical differences due to the continuous-time setup.

Proof. Given any $t \geq 0$ and its corresponding sampling time $t_i = k(t)$, let $l := t - t_i + T_{t_i} \in [0, T_{t_i}]$ and recall that $\hat{x}(t) = \hat{x}^*_{t_i}(l) = x(l, \hat{\chi}^*_{t_i}, u_{t_i}, \hat{w}^*_{t_i})$ by (3.16). Since $\hat{x}^*_{t_i}$ satisfies (3.7) on $[0, T_{t_i}]$ due to the constraints (3.12b)-(3.12e), we can invoke the i-iIOSS Lyapunov function from Assumption 3.1. To this end, we use that $x(t) = x(t, \chi, u, w) = x(l, x(t - T_{t_i}), u_{t_i}, w_{t_i})$, where $w_{t_i} : [0, T_{t_i}) \to \mathcal{W}$ denotes the segment of w in the interval $[t_i - T_{t_i}, t_i)$ defined by $w_{t_i}(l) := w(t_i - T_{t_i} + l)$, $l \in [0, T_{t_i})$. Then, we can evaluate the dissipation inequality (3.9b) with the trajectories $x_1(l) = \hat{x}^*_{t_i}(l) = x(l, \hat{\chi}^*_{t_i}, u_{t_i}, \hat{w}^*_{t_i})$ and $x_2(l) = x(l, x(t_i - T_{t_i}), u_{t_i}, w_{t_i})$ and the corresponding

outputs $y_1(l) = \hat{y}^*_{t_i}(l)$ and $y_2(l) = y_{t_i}(l)$ with y_{t_i} from (3.11), which yields

$$\begin{aligned}
&U(\hat{x}(t), x(t)) = U(\hat{x}^*_{t_i}(l), x(t_i - T_{t_i} + l)) \\
&\leq U(\hat{x}^*_{t_i}(0), x(t_i - T_{t_i}))\eta^l + \int_0^l \eta^{l-\tau}\Big(|\hat{w}^*_{t_i}(\tau) - w_{t_i}(\tau)|^2_Q + |\hat{y}^*_{t_i}(\tau) - y_{t_i}(\tau)|^2_R\Big)d\tau \\
&\leq \eta^{-(t_i-t)}\Big(U(\hat{\chi}^*_{t_i}, x(t_i - T_{t_i}))\eta^{T_{t_i}} \\
&\qquad + \int_0^{T_{t_i}} \eta^{T_{t_i}-\tau}\Big(|\hat{w}^*_{t_i}(\tau) - w_{t_i}(\tau)|^2_Q + |\hat{y}^*_{t_i}(\tau) - y_{t_i}(\tau)|^2_R\Big)d\tau\Big),
\end{aligned} \tag{3.21}$$

where the last inequality follows by exploiting that $l \leq T_{t_i}$, the definition of l, and the fact that $\hat{x}^*_{t_i}(0) = \hat{\chi}^*_{t_i}$. Define

$$\bar{U} := U(\hat{\chi}^*_{t_i}, x(t_i - T_{t_i}))\eta^{T_{t_i}} + \int_0^{T_{t_i}} \eta^{T_{t_i}-\tau}\Big(|\hat{w}^*_{t_i}(\tau) - w_{t_i}(\tau)|^2_Q + |\hat{y}^*_{t_i}(\tau) - y_{t_i}(\tau)|^2_R\Big)d\tau. \tag{3.22}$$

By Cauchy-Schwarz and Young's inequality, we have

$$|\hat{w}^*_{t_i}(\tau) - w_{t_i}(\tau)|^2_Q \leq 2|\hat{w}^*_{t_i}(\tau)|^2_Q + 2|w_{t_i}(\tau)|^2_Q, \ \tau \in [0, T_{t_i}). \tag{3.23}$$

From a similar reasoning and the application of (3.9a), we obtain

$$\begin{aligned}
U(\hat{\chi}^*_{t_i}, x(t_i - T_{t_i})) &\leq |\hat{\chi}^*_{t_i} - x(t_i - T_{t_i})|^2_P \\
&= |\hat{\chi}^*_{t_i} - \bar{x}(t_i - T_{t_i}) + \bar{x}(t_i - T_{t_i}) - x(t_i - T_{t_i})|^2_P \\
&\leq 2|\hat{\chi}^*_{t_i} - \bar{x}(t_i - T_{t_i})|^2_P + 2|\bar{x}(t_i - T_{t_i}) - x(t_i - T_{t_i})|^2_P.
\end{aligned} \tag{3.24}$$

Then, $\bar{U}$ in (3.22) can be bounded using (3.23)-(3.24), which yields

$$\begin{aligned}
\bar{U} &\leq 2\eta^{T_{t_i}}|\bar{x}(t_i - T_{t_i}) - x(t_i - T_{t_i})|^2_P + \int_0^{T_i} \eta^{T_{t_i}-\tau} 2|w_{t_i}(\tau)|^2_Q d\tau \\
&\quad + 2\eta^{T_{t_i}}|\hat{\chi}^*_{t_i} - \bar{x}(t_i - T_{t_i})|^2_P + \int_0^{T_i} \eta^{T_{t_i}-\tau}\Big(2|\hat{w}^*_{t_i}(\tau)|^2_Q + |\hat{y}^*_{t_i}(\tau) - y_{t_i}(\tau)|^2_R\Big)d\tau \\
&= 2\eta^{T_{t_i}}|\bar{x}(t_i - T_{t_i}) - x(t_i - T_{t_i})|^2_P + 2\int_0^{T_i} \eta^{T_{t_i}-\tau}|w_{t_i}(\tau)|^2_Q d\tau + J(\hat{\chi}^*_{t_i}, \hat{w}^*_{t_i}, \hat{y}^*_{t_i}, t_i),
\end{aligned} \tag{3.25}$$

where in the last equality we used the definition of the cost function from (3.13). By optimality, it further follows that

$$\begin{aligned}
J(\hat{\chi}^*_{t_i}, \hat{w}^*_{t_i}, \hat{y}^*_{t_i}, t_i) &\leq J(x(t_i - T_{t_i}), w_{t_i}, y_{t_i}, t_i) \\
&= 2\eta^{T_{t_i}}|x(t_i - T_{t_i}) - \bar{x}(t_i - T_{t_i})|^2_P + 2\int_0^{T_{t_i}} \eta^{T_{t_i}-\tau}|w_{t_i}(\tau)|^2_Q d\tau.
\end{aligned} \tag{3.26}$$

Hence, (3.25), (3.26), and the definition of the prior estimate in (3.18) lead to

$$\begin{aligned}
\bar{U} &\leq 4\eta^{T_{t_i}}|\hat{x}(t_i - T_{t_i}) - x(t_i - T_{t_i})|^2_P + 4\int_0^{T_i} \eta^{T_{t_i}-\tau}|w_{t_i}(\tau)|^2_Q d\tau \\
&= 4\eta^{T_{t_i}}|\hat{x}(t_i - T_{t_i}) - x(t_i - T_{t_i})|^2_P + 4\int_{t_i - T_{t_i}}^{t_i} \eta^{t_i-\tau}|w(\tau)|^2_Q d\tau,
\end{aligned} \tag{3.27}$$

where the last equality followed by a change of coordinates. In combination, from (3.21) with (3.22) and (3.27), we obtain

$$\begin{aligned} &U(\hat{x}(t), x(t)) \leq \eta^{-(t_i-t)}\bar{U} \\ &\leq \eta^{-(t_i-t)}\Big(4\eta^{T_{t_i}}|\hat{x}(t_i - T_{t_i}) - x(t_i - T_{t_i})|_{\overline{P}}^2 + 4\int_{t_i-T_{t_i}}^{t_i} \eta^{t_i-\tau}|w(\tau)|_Q^2 d\tau\Big). \end{aligned} \tag{3.28}$$

Using $|\hat{x}(t_i - T_{t_i}) - x(t_i - T_{t_i})|_{\overline{P}}^2 \leq \lambda_{\max}(\overline{P}, \underline{P})|\hat{x}(t_i - T_{t_i}) - x(t_i - T_{t_i})|_{\underline{P}}^2$ and the first inequality in (3.9a) yields (3.20), which finishes this proof. □

In the following, we consider the case where the estimation horizon T and set of sampling times $\mathcal{T}$ are designed such that

$$4\lambda_{\max}(\overline{P}, \underline{P})\eta^{T-\bar{\delta}} =: \rho^{T-\bar{\delta}} \in (0, 1) \tag{3.29}$$

holds for some $\rho \in (0, 1)$, where $\bar{\delta}$ is defined in (3.19). Provided that an i-iIOSS Lyapunov function as in Assumption 3.1 is known, we point out that for any design of $\mathcal{T}$, condition (3.29) can be easily satisfied by choosing T such that

$$T > -\frac{\ln(4\lambda_{\max}(\overline{P}, \underline{P}))}{\ln(\eta)} + \bar{\delta}, \tag{3.30}$$

leading to

$$\rho = (4\lambda_{\max}(\overline{P}, \underline{P}))^{\frac{1}{T-\bar{\delta}}}\eta. \tag{3.31}$$

Whenever (3.29) is satisfied, Proposition 3.1 directly provides a dissipation inequality in integral form with exponential decrease for the estimation error in Lyapunov coordinates; consequently, the i-iIOSS Lyapunov function U can be viewed as a Lyapunov-like function for MHE on each interval $[k(t) - T_{k(t)}, t]$ for all $t \geq 0$.

In the following, we establish RGES of MHE by applying the bound (3.20) recursively to cover the whole interval $[0, t_i]$ for a given sampling time $t_i \in \mathcal{T}$. However, special care must be taken when concatenating the dissipation inequalities due to the overlap of their domains.

Theorem 3.1. *Let Assumption 3.1 hold. Suppose that the horizon length T is chosen such that* (3.29) *is satisfied for some $\rho \in (0, 1)$. Then, the estimation error satisfies*

$$|\hat{x}(t_i) - x(t_i)|_{\underline{P}}^2 \leq 4\rho^{t_i}|\hat{\chi} - \chi|_{\overline{P}}^2 + 8\int_0^{t_i} \rho^{t_i-\tau}|w(\tau)|_Q^2 d\tau \tag{3.32}$$

for all $t_i \in \mathcal{T}$ and all $\hat{\chi}, \chi \in \mathcal{X}$, $u \in \mathcal{M}_{\mathcal{U}}$, and $w \in \mathcal{M}_{\mathcal{W}}$, i.e., the proposed MHE scheme is RGES in the sense of Definition 3.1.

Proof. We start by noting that condition (3.29) leads to $\eta \leq \rho$ and

$$4\lambda_{\max}(\overline{P}, \underline{P})\eta^T = \rho^{T-\bar{\delta}}\eta^{\bar{\delta}}.$$

This implies the following relation:

$$4\lambda_{\max}(\overline{P}, \underline{P})\eta^{T-(k(t)-t)} = \rho^{T-\bar{\delta}}\eta^{\bar{\delta}-(k(t)-t)} \leq \rho^{T-\bar{\delta}}\rho^{\bar{\delta}-(k(t)-t)} = \rho^{T-(k(t)-t)}, \tag{3.33}$$

which holds for any $t \geq 0$. Assume that an arbitrary sampling time $t_i \in \mathcal{T}$ is given. We define the sequence of sampling times $\{k_j\}, j \in \mathbb{I}_{\geq 0}$ starting at $k_0 = t_i$ using the following recursion:

$$k_{j+1} = \min_{k \in \mathcal{K}_j} k \tag{3.34}$$

with

$$\mathcal{K}_j := \{k \in \mathcal{T} : k_j > k \geq k_j - T\}$$

if the set $\mathcal{K}_j$ is non-empty, and $k_{j+1} = k_j$ otherwise. In the following, we use $c := 4\lambda_{\max}(\overline{P}, \underline{P})$ for notational brevity.

Now assume that for some time $s \geq 0$, $k_j = k(s) \geq T$ is the corresponding sampling instant. From Proposition 3.1, it follows that

$$\begin{aligned} &U(\hat{x}(s), x(s)) \\ &\leq \eta^{-(k_j - s)} \Big(c\eta^T U(\hat{x}(k_j - T), x(k_j - T)) \\ &\quad + 4 \int_s^{k_j} \eta^{k_j - \tau} |w(\tau)|_Q^2 d\tau + 4 \int_{k_{j+1}}^{s} \eta^{k_j - \tau} |w(\tau)|_Q^2 d\tau + 4 \int_{k_j - T}^{k_{j+1}} \eta^{k_j - \tau} |w(\tau)|_Q^2 d\tau \Big). \end{aligned} \tag{3.35}$$

We aim to apply this property recursively. To this end, we have split the integral on the right-hand side involving the interval $[k_j - T, k_j]$ in three parts (noting that $k_j - T \leq k_{j+1} < s \leq k_j$); the first part overlaps with the previous iteration covering the interval $[k_{j-1} - T, k_{j-1}]$ (unless $k_{j-1} - T \in \mathcal{T} \Rightarrow k_j = k_{j-1} - T$), and the third part overlaps with the succeeding iteration covering the interval $[k_{j+1} - T, k_{j+1}]$ (unless $k_j - T \in \mathcal{T} \Rightarrow k_{j+1} = k_j - T$).

We claim that

$$\begin{aligned} U(\hat{x}(k_0), x(k_0)) \leq c\eta^T \rho^{k_0 - k_j} U(\hat{x}(k_j - T), x(k_j - T)) \\ + 8 \int_{k_{j+1}}^{k_0} \rho^{k_0 - \tau} |w(\tau)|_Q^2 d\tau + 4 \int_{k_j - T}^{k_{j+1}} \rho^{k_0 - \tau} |w(\tau)|_Q^2 d\tau \end{aligned} \tag{3.36}$$

holds for any $k_0 \in \mathcal{T}$ and all $j \in \mathbb{I}_{\geq 0}$ for which $k_{j+1} \geq T$ is satisfied, and we give a proof by induction. For the base case, consider (3.35) with $s = k_0$. We obtain

$$\begin{aligned} U(\hat{x}(k_0), x(k_0)) \leq c\eta^T U(\hat{x}(k_0 - T), x(k_0 - T)) \\ + 4 \int_{k_1}^{k_0} \eta^{k_0 - \tau} |w(\tau)|_Q^2 d\tau + 4 \int_{k_0 - T}^{k_1} \eta^{k_0 - \tau} |w(\tau)|_Q^2 d\tau, \end{aligned}$$

for which (3.36) with $j = 0$ serves as an upper bound.

We now prove (3.36) for general integers $j \in \mathbb{I}_{\geq 0}$. To this end, consider (3.35) with $s = k_j - T$. If $j \in \mathbb{I}_{\geq 0}$ is such that $k_{j+1} \geq T$, we can use the fact that

$$\begin{aligned} &U(\hat{x}(k_j - T), x(k_j - T)) \\ &\leq \eta^{-(k_{j+1} - (k_j - T))} \Big(c\eta^T U(\hat{x}(k_{j+1} - T), x(k_{j+1} - T)) + 4 \int_{k_j - T}^{k_{j+1}} \eta^{k_{j+1} - \tau} |w(\tau)|_Q^2 d\tau \\ &\qquad + 4 \int_{k_{j+2}}^{k_j - T} \eta^{k_{j+1} - \tau} |w(\tau)|_Q^2 d\tau + 4 \int_{k_{j+1} - T}^{k_{j+2}} \eta^{k_{j+1} - \tau} |w(\tau)|_Q^2 d\tau \Big). \end{aligned} \tag{3.37}$$

Now assume that (3.36) is true for some integer $j \in \mathbb{I}_{\geq 0}$ for which $k_{j+1} \geq T$. In the following, we show that (3.36) then also holds for $j+1$. The combination of (3.36) and (3.37) yields

$$\begin{aligned} U(\hat{x}(k_0), x(k_0)) \leq\ & c\eta^{T-(k_{j+1}-(k_j-T))}\rho^{k_0-k_j} \\ & \cdot \Big(c\eta^T U(\hat{x}(k_{j+1}-T), x(k_{j+1}-T)) + 4\int_{k_j-T}^{k_{j+1}} \eta^{k_{j+1}-\tau}|w(\tau)|_Q^2 d\tau \\ & + 4\int_{k_{j+2}}^{k_j-T} \eta^{k_{j+1}-\tau}|w(\tau)|_Q^2 d\tau + 4\int_{k_{j+1}-T}^{k_{j+2}} \eta^{k_{j+1}-\tau}|w(\tau)|_Q^2 d\tau \Big) \\ & + 8\int_{k_{j+1}}^{k_0} \rho^{k_0-\tau}|w(\tau)|_Q^2 d\tau + 4\int_{k_j-T}^{k_{j+1}} \rho^{k_0-\tau}|w(\tau)|_Q^2 d\tau. \end{aligned} \tag{3.38}$$

From (3.33) and (3.34), we can infer that

$$c\eta^{T-(k_{j+1}-(k_j-T))}\rho^{k_0-k_j} \leq \rho^{T-(k_{j+1}-(k_j-T))}\rho^{k_0-k_j} = \rho^{k_0-k_{j+1}}. \tag{3.39}$$

Applying (3.39) to (3.38) and using that $\eta \leq \rho$ leads to

$$\begin{aligned} & U(\hat{x}(k_0), x(k_0)) \\ & \leq \rho^{k_0-k_{j+1}} c\eta^T U(\hat{x}(k_{j+1}-T), x(k_{j+1}-T)) \\ & \quad + 4\int_{k_j-T}^{k_{j+1}} \rho^{k_0-\tau}|w(\tau)|_Q^2 d\tau + 4\int_{k_{j+2}}^{k_j-T} \rho^{k_0-\tau}|w(\tau)|_Q^2 d\tau + 4\int_{k_{j+1}-T}^{k_{j+2}} \rho^{k_0-\tau}|w(\tau)|_Q^2 d\tau \\ & \quad + 8\int_{k_{j+1}}^{k_0} \rho^{k_0-\tau}|w(\tau)|_Q^2 d\tau + 4\int_{k_j-T}^{k_{j+1}} \rho^{k_0-\tau}|w(\tau)|_Q^2 d\tau \\ & \leq \rho^{k_0-k_{j+1}} c\eta^T U(\hat{x}(k_{j+1}-T), x(k_{j+1}-T)) \\ & \quad + 8\int_{k_{j+2}}^{k_0} \rho^{k_0-\tau}|w(\tau)|_Q^2 d\tau + 4\int_{k_{j+1}-T}^{k_{j+2}} \rho^{k_0-\tau}|w(\tau)|_Q^2 d\tau. \end{aligned}$$

This proves (3.36) for all $k_0 \in \mathcal{T}$ and all $j \in \mathbb{I}_{\geq 0}$ for which $k_{j+1} \geq T$ is satisfied. In fact, the above argument shows that (3.36) also holds for the smallest $j \in \mathbb{I}_{\geq 0}$ for which $k_{j+1} < T$. Furthermore, when $k_{j+1} < T$, from (3.28) it follows that

$$\begin{aligned} & U(\hat{x}(k_j-T), x(k_j-T)) \\ & \leq \eta^{-(k_{j+1}-(k_j-T))}\Big(4\eta^{k_{j+1}}|\hat{x}(0)-x(0)|_{\overline{P}}^2 \\ & \qquad + 4\int_{k_j-T}^{k_{j+1}} \eta^{k_{j+1}-\tau}|w(\tau)|_Q^2 d\tau + 4\int_{0}^{k_j-T} \eta^{k_{j+1}-\tau}|w(\tau)|_Q^2 d\tau \Big). \end{aligned}$$

The combination with (3.36) leads to

$$\begin{aligned} & U(\hat{x}(k_0), x(k_0)) \\ & \leq c\eta^{T-(k_{j+1}-(k_j-T))}\rho^{k_0-k_j}\Big(4\eta^{k_{j+1}}|\hat{x}(0)-x(0)|_{\overline{P}}^2 + 4\int_{k_j-T}^{k_{j+1}} \eta^{k_{j+1}-\tau}|w(\tau)|_Q^2 d\tau \\ & \qquad + 4\int_{0}^{k_j-T} \eta^{k_{j+1}-\tau}|w(\tau)|_Q^2 d\tau \Big) \\ & \quad + 8\int_{k_{j+1}}^{k_0} \rho^{k_0-\tau}|w(\tau)|_Q^2 d\tau + 4\int_{k_j-T}^{k_{j+1}} \rho^{k_0-\tau}|w(\tau)|_Q^2 d\tau. \end{aligned} \tag{3.40}$$

By using (3.39) and the fact that $\eta \leq \rho$, from (3.40) it follows that

$$\begin{aligned}
&U(\hat{x}(k_0), x(k_0)) \\
&\leq 4\rho^{k_0}|\hat{x}(0) - x(0)|_{\bar{P}}^2 + 4\int_{k_j-T}^{k_{j+1}} \rho^{k_0-\tau}|w(\tau)|_Q^2 d\tau + 4\int_0^{k_j-T} \rho^{k_0-\tau}|w(\tau)|_Q^2 d\tau \\
&\quad + 8\int_{k_{j+1}}^{k_0} \rho^{k_0-\tau}|w(\tau)|_Q^2 d\tau + 4\int_{k_j-T}^{k_{j+1}} \rho^{k_0-\tau}|w(\tau)|_Q^2 d\tau \\
&\leq 4\rho^{k_0}|\hat{x}(0) - x(0)|_{\bar{P}}^2 + 8\int_0^{k_0} \rho^{k_0-\tau}|w(\tau)|_Q^2 d\tau. \qquad (3.41)
\end{aligned}$$

Applying the lower bound in (3.9a) and recalling that $t_i = k_0$ yields (3.32), which finishes this proof. □

Some remarks are in order.

Remark 3.6 (Horizon length and prior weighting)**.** *Another interpretation of the condition in* (3.29) *on the horizon length for guaranteed RGES of MHE is that this ensures that the prior weighting (specifically, the term $\eta^T\Gamma(\chi, \bar{x})$ in* (3.13)*) is not too large compared to the integral over the stage costs. This is a natural requirement in MHE to ensure that the estimation scheme can keep up with the data and does not only follow a (potentially unstable) system trajectory, compare also [Rao00, Example 4.6.1].*

Remark 3.7 (Sampling strategy)**.** *If the set $\mathcal{T}$ is such that $t_i - T_{t_i} \in \mathcal{T}$ for all $t_i \in \mathcal{T}$ (which is the case, e.g., for equidistant sampling with a constant period $\delta > 0$ and T being an integer multiple of δ, compare Remark 3.5), it follows that the interval boundaries of each time horizon considered in the MHE optimization problem* (3.12) *coincide exactly with two sampling times. Consequently, it suffices to evaluate* (3.20) *only at sampling times $t = t_i \in \mathcal{T}$—yielding a more direct Lyapunov-like function for MHE—and simply apply this bound recursively to establish RGES as is the case in discrete-time settings (e.g., [Sch+23, Cor. 1]), in particular without the need to take into account any discrepancy between horizon boundaries and sampling times. These simplifications result in a slightly weaker condition on the horizon length and a slightly improved RGES result; namely, we can take $\bar{\delta} = 0$ in* (3.29) *and replace the factor* 8 *in* (3.32) *by the factor* 4*.*

Remark 3.8 (Full information estimation)**.** *The restriction to an exponential detectability property (Assumption 3.1) can be relaxed to asymptotic detectability (in the sense of Definition 2.3) if FIE is applied, that is, the MHE scheme in* (3.12) *and* (3.13) *with $T_{t_i} = t_i$. In this case, we consider the cost function* (3.13) *with T_{t_i} replaced by t_i, $\Gamma(\chi, \bar{x}) = \alpha_2(2|\chi - \bar{x}|)$ and $L(w, \Delta y) = \sigma_w(2|w|) + \sigma_y(|\Delta y|)$, where $\alpha_2, \sigma_w, \sigma_y \in \mathcal{K}_\infty$ (and $\alpha_1 \in \mathcal{K}_\infty$ appearing below) correspond to the i-iIOSS Lyapunov function parameters from Definition 2.3. By applying the same steps as in the proof of Proposition 3.1, we can infer that the corresponding estimation error satisfies*

$$\alpha_1(|\hat{x}(t_i) - x(t_i)|) \leq 2\eta^{t_i}\alpha_2(2|\hat{\chi} - \chi|) + 2\int_0^{t_i} \eta^{t_i-\tau}\sigma_w(2|w(\tau)|)d\tau$$

for all $t_i \in \mathcal{T}$ and all $\hat{\chi}, \chi \in \mathcal{X}$, $u \in \mathcal{M}_\mathcal{U}$, and $w \in \mathcal{M}_\mathcal{W}$, which implies that FIE is RGAS in the sense of Definition 3.1.

3.3. Discussion

The MHE framework for continuous-time systems proposed and analyzed in Section 3.2 builds on our ideas for the discrete-time case from [Sch+23, Sec. III]. However, we want to emphasize that the results do not trivially follow from this. Instead, Theorem 3.1 is an interesting (and more general) theoretical result on its own requiring a different proof technique, and moreover, offers significant advantages over purely discrete-time schemes, especially when the physical system to be estimated actually corresponds to a continuous-time one (which is often the case in practice). Specifically, the continuous-time MHE scheme from Section 3.2 allows for arbitrary sampling strategies to define the set $\mathcal{T}$, i.e., the sampling instants at which the underlying optimization problem (3.12) is actually solved, which provides a huge additional degree of freedom compared to [Sch+23, Sec. III]. Since the set $\mathcal{T}$ can be modified online, the proposed MHE scheme can even be used in an event-triggered fashion, that is, by choosing the sampling instants during operation, depending on a suitable triggering rule. Consequently, the continuous-time MHE scheme presented in Section 3.2 can be better tailored to the problem at hand, which can yield more accurate results with less computational effort compared to standard equidistant sampling. Furthermore, the consideration of a continuous-time system model simplifies the detectability analysis (i.e., the verification of certain LMIs, compare Chapter 7), which is structurally easier and particularly does not require specifying a certain discretization scheme and a sampling period beforehand. Moreover, assuming that the numerical solution of the continuous-time MHE problem (3.12) is sufficiently accurate (compare the discussion below Remark 3.4), the robustness guarantees provided by Theorem 3.1 are valid for MHE applied to the real physical continuous-time system, and not to an approximately discretized model (which may suffer from additional discretization errors).

In the following, we focus on the role of the discounting in (3.13), which creates a direct link between detectability, MHE, and robust stability (compare Remark 3.3). Since this conceptually originates from our work [Sch+23, Sec. III] (for discrete-time systems), it is appropriate to discuss it in a more holistic context covering both discrete- and continuous-time MHE approaches and their historical development.

MHE: A trade-off between practical designs and theoretical guarantees

Designing MHE schemes for nonlinear systems generally requires balancing practical designs against valid theoretical guarantees. For example, one may choose a very simple scheme involving a zero prior weighting and standard quadratic penalties, that is, the cost function in (3.13) with $\eta = 1$ and $\overline{P} = 0$, compare [MM95]. However, since past data is completely neglected in the design, the system must in general be observable to ensure stability of MHE, and furthermore, large estimation horizons may be required to obtain a performance comparable to FIE, compare [RMD20, Sec. 4.3.1] and see also Chapter 6 (where we analyze the performance of MHE with and without a prior weighting in more detail). Therefore, a non-zero prior weighting seems appropriate, which, on the other hand, requires a certain dependency on the

unknown FIE cost [RRM03] or knowledge of specific parameters of the observability property [ABB08; AA16] to ensure stable estimation, both of which are generally difficult (or even impossible) to verify for general nonlinear systems.

Establishing MHE for general detectable nonlinear systems that follow a practical design, provide good theoretical guarantees, and require conditions that can be easily verified has also emerged as a major problem in the more recent literature, compare, for example, [Mül17; Hu17; AR19b; KM18]. In particular, robust stability of MHE could be established in [Mül17; AR19b] based on i-IOSS using a general cost function that permits standard quadratic penalties, however, the robustness bounds deteriorate with an increasing estimation horizon. Such a behavior is counter-intuitive and undesired since one would naturally expect better estimation results if more information is taken into account. This issue could be avoided using a modified cost: either by adding a max-term that penalizes the largest single disturbance as in [Mül17; Hu17], or by using a specific cost structure satisfying the triangle inequality [KM18]. Hence, a trade-off between a standard quadratic cost function and good performance guarantees for MHE has arisen. This could be resolved in the Lyapunov-based MHE frameworks from Section 3.2 (in continuous time) and [Sch+23, Sec. III] (in discrete time), which allow choosing standard quadratic penalties (with additional time-discounting) while providing theoretical guarantees that improve as the horizon length increases. We point out that comparable results were achieved earlier by using more general time-discounting with $\mathcal{KL}$-functions [KM23], or without discounting using a Lyapunov-like function [AR21; All20]. In the following, we compare these three structurally different approaches and highlight the benefits of Lyapunov-based MHE.

MHE using general time-discounting [KM23]

The requirements of Theorem 3.1 (and [Sch+23, Thm 1]) for guaranteed robust stability of MHE are fundamentally the same as in [KM23], namely, that the detectability property of the system (given by i-IOSS) must be suitably related to the cost function used for MHE by employing additional time-discounting. Consequently, the robustness bounds established in Theorem 3.1 and [Sch+23, Thm. 1, Cor. 1] are qualitatively comparable to those from [KM23, Thm. 14] for the special case of exponential stability. However, we point out that under certain conditions, [KM23, Thm. 14] also implies an asymptotic stability result using a nonlinear contraction. In contrast, in Section 3.2 (and [Sch+23, Sec. III]), exponential detectability (i.e., a quadratically bounded i-iIOSS Lyapunov function, compare Assumption 3.1) is crucially required to achieve a linear contraction over the estimation horizon, which is in line with most of the recent results on nonlinear MHE [Hu24; AR19b; Hu17; Mül17; KM18], compare also [AR19b, Prop. 1] and [Hu24, Lem. 1].

Whereas [KM23; KM18; Hu24; AR19b; Hu17; Mül17; Ale25] build their analysis on properties of certain $\mathcal{K}$- and $\mathcal{KL}$-functions, we employ corresponding Lyapunov function characterizations in Section 3.2 and [Sch+23, Sec. III]. This fundamental difference enables further theoretical insights and practical improvements. First,

verifying the required detectability condition in order to guarantee RGES of MHE becomes rather straightforward, particularly because we provide simple LMI conditions for computing i-IOSS and i-iIOSS Lyapunov functions in Chapter 7. Even though these results directly imply traditional $\mathcal{KL}$-characterizations of i-IOSS and i-iIOSS as mentioned in Remark 7.4 below, we obtain a stronger and more direct relation between the i-(i)IOSS Lyapunov function and the corresponding MHE cost function (which simplifies its tuning, compare Remark 3.4), as the additional (and possibly conservative) step of calculating the respective $\mathcal{KL}$-functions can be avoided. Furthermore, arguing in Lyapunov coordinates generally allows for less restrictive conditions on the horizon length for guaranteed RGES of MHE compared to, e.g., [KM23, Thm. 14], which can be seen in Table 3.1 and the discussion below. An additional useful feature is that even in the case of merely asymptotic (instead of exponential) detectability, we can still use an exponential decrease in the dissipation inequality without loss of generality (consider the i-iIOSS Lyapunov function from Definition 2.3 together with Proposition 2.3). This enables a much simpler and more intuitive tuning of the FIE cost function compared to, e.g., [KM23, Ass. 1] and [Hu24, Ass. 3] using general $\mathcal{KL}$-function inequalities, see also [Sch+23, Sec. III-C] and Remark 3.8.

A Lyapunov-like function framework for MHE [AR21; All20]

We point out that a Lyapunov approach to stability of FIE already appeared in the literature; in particular, a Lyapunov-like function (termed a Q-function) was used in [AR19a] to establish nominal stability of FIE, and the results were extended in [AR21] and [All20, Ch. 5] to RGES and RGAS of FIE[5], respectively. However, the proposed Q-function significantly differs from the Lyapunov function employed in Section 3.2 and [Sch+23, Sec. III], especially in its non-trivial structure utilizing two time arguments. The key ingredient in [AR21], [All20, Ch. 5] is a sequence of augmented infinite-horizon problems, each considering the first t disturbances and zero disturbances thereafter. As a result, each of these infinite-horizon problems has finite disturbance sequences and therefore well-defined solutions. Then, at any time $t \in \mathbb{I}_{\geq 0}$, the respective infinite-horizon cost function is compared to the truncated finite-horizon cost function considering the partial time interval $\mathbb{I}_{[0,j-1]}$ for some $j \in \mathbb{I}_{[0,t]}$. This procedure allows establishing one-step dissipation in j for each $j \in \mathbb{I}_{[0,t]}$. However, since the resulting function is only semidefinite, it needs to be combined with the i-IOSS Lyapunov function to finally create the desired Q-function. Taking into account its different components, ("pessimistic"[6]) Lyapunov-like bounds on the Q-function are established in [AR21, Prop. 3.14] for exponential, and in [All20, Sec. 5.3] for asymptotic stability. In this context, note that the lower bound of the Q-function is given by the lower bound of the i-IOSS Lyapunov function; the

[5]Note that RGES of MHE was shown in [AR21, Thm. 4.2] assuming that the underlying FIE is RGES and provides a linear contraction over the estimation horizon, i.e., without explicitly constructing a Q-function for MHE, compare [All20, Sec. 5.5.3] and [KM23, Sec. 4].

[6]Wording according to the discussion below [AR21, Cor. 3.18]; it is not distinguished between the influences of long past or recent disturbances.

upper bound, however, requires an additional stabilizability assumption of certain structure, compare [AR21, Ass. 3.6] and [All20, Ass. 5.14].

The Lyapunov-based analysis in Section 3.2 (and [Sch+23, Sec. III]), on the other hand, is much simpler in many respects, enabled by an additional discount factor in the cost function. Note that this corresponds to a *fading memory* design, a concept that has been widely used in the literature for decades in many research areas (see, e.g., [BC85; MS00]), and which was previously exploited also in the context of state estimation, e.g., to deal with model errors in Kalman filter applications [SS71]. Within our Lyapunov-based framework, this results in a strong connection between detectability and the MHE cost such that the i-IOSS Lyapunov function directly serves as a Lyapunov function for MHE, see Proposition 3.1. As a result, many (potentially conservative) steps, excessive over-approximations, and additional conditions such as stabilizability could be avoided in the analysis. Interestingly, the conditions on the cost function in terms of compatibility with i-IOSS are fundamentally similar for all the results considered above (except for the time-discounting), see Remark 3.4, [Sch+23, Rem. 1], [AR21, Ass. 3.5], [All20, Ass. 5.13], and [KM23, Ass. 1].

Lyapunov-based MHE allows for shorter horizons

In the following, we compare the discrete-time methods discussed above by means of their respective conditions on the horizon length for guaranteed RGES of MHE, which illustrates the general benefit of arguing in Lyapunov coordinates (we restrict ourselves to the discrete-time case here, as there are no MHE approaches for continuous-time systems in the literature that are comparable with the results from Section 3.2). For a broader overview, we also consider [AR19b, Thm. 1], i.e., MHE based on a $\mathcal{KL}$-function characterization of i-IOSS, but without a time-discounted objective function as in [KM23]. For a fair comparison, we choose the cost functions for [AR21; KM23; AR19b] such that the smallest possible horizon follows in each case: we consider $b(s,t) = \beta(2s,t)$ according to [KM23, Rem. 6] and $V_\mathrm{p}(\chi,\bar{x}) = |\chi - \bar{x}|^2$ in [AR19b, Ass. 3]. Since the analysis is much more involved for [AR21], we consider only an ideal (strict) lower bound on the minimal horizon length which follows from a vanishing prior weighting ($\underline{c}_\mathrm{x} = \overline{c}_\mathrm{x} \to 0$ in [AR21, Ass. 3.4]) and under a perfect stabilizability condition ($c_\mathrm{c} \to 0$ in [AR21, Ass. 3.6]).

Provided that a quadratically bounded i-IOSS Lyapunov function[7] is given, Table 3.1 shows for each case the resulting constants $C > 0$ and $\mu \in (0,1)$ defining the contraction condition $C\mu^N < 1$ that the horizon length N must satisfy for guaranteed RGES of MHE. Solving the conditions for the minimal stabilizing horizon length by $N_\mathrm{min} = \lceil -\ln C / \ln \mu \rceil$ and applying standard properties of the logarithmic function, we arrive at the following conclusions. First, under optimal choices of the cost functions in terms of the horizon length, the contraction conditions from [KM23, Thm. 14] and [AR19b, Thm. 1] are (except for the additional factor 3) very similar

[7] See Definition 7.1 in Chapter 7 and compare Assumption 3.1.

Table 3.1. Requirement for the horizon length N for different results from the literature.

Result	C	μ
[Sch+23, Thm. 1]	$4\lambda_{\max}(\overline{P}, \underline{P})$	η
[AR21, Thm. 4.2]	$> \sqrt{4\frac{\lambda_{\max}(\overline{P})}{\lambda_{\min}(\underline{P})}}$	$> \sqrt[4]{1-(1-\eta)\frac{\lambda_{\min}(\underline{P})}{4\lambda_{\max}(\overline{P})}}$
[KM23, Thm. 14]	$8\frac{\lambda_{\max}(\overline{P})}{\lambda_{\min}(\underline{P})}$	η
[AR19b, Thm. 1]	$3\sqrt{8\frac{\lambda_{\max}(\overline{P})}{\lambda_{\min}(\underline{P})}}$	$\sqrt{\eta}$

Depicted are the respective constants $C, \mu > 0$, which form the contraction condition $C\mu^N < 1$ that the horizon length N must satisfy for guaranteed RGES of MHE.

to each other, despite a structurally different MHE design and proof technique[8]. Second, we can generally conclude that [Sch+23, Thm. 1] provides the least conservative estimate on the minimal horizon length $N_{\min}$ for guaranteed RGES of MHE; to see this, recall that $\lambda_{\max}(\overline{P})/\lambda_{\min}(\underline{P}) \geq \lambda_{\max}(\overline{P}, \underline{P})$ for all $\overline{P} \succeq \underline{P} \succ 0$ and observe that each constant C, μ in Table 3.1 has its minimal value at $\lambda_{\max}(\overline{P})/\lambda_{\min}(\underline{P}) = 1$. This general fact is also observed in the numerical example in Section 3.4 below, where we compute the minimal stabilizing horizon length for each case (compare Table 3.2). As a side remark, we note that a direct consequence of the choices made in the proof of [AR21, Prop. 3.15] is that generally no better contraction rate than $\mu = \sqrt[4]{3/4} \approx 0.93$ and hence no smaller horizon length than $N = 10$ can be obtained using [AR21, Thm. 4.2], even in case of $\eta \to 0$ in (7.2b) (which corresponds to trivial observability, e.g., in case of full state measurements) and under the ideal setup considered above.

Overall, the Lyapunov-based MHE schemes from Section 3.2 and [Sch+23, Sec. III] employ a practical (fading memory) least squares cost function and provide theoretical stability and robustness guarantees that improve as the horizon length increases. This becomes especially powerful when combining it with our results from Chapter 7 below, where we provide simple LMI conditions to compute quadratically bounded i-IOSS and i-iIOSS Lyapunov functions (for discrete- and continuous-time systems, respectively) so that an MHE design with guaranteed robust exponential stability is directly obtained. The simulation examples in the next section show that this particular combination enables guaranteed robust stability of Lyapunov-based MHE under practical conditions, in particular requiring significantly shorter horizons compared to results from the literature.

[8] For both [KM23, Thm. 14] and [AR19b, Thm. 1], note that the factor 8 in the second column of Table 3.1 could be easily replaced by 4 by a straightforward extension of the respective derivation. The additional factor 3 appearing in the last row results from a max-based i-IOSS bound used in [AR19b, Thm. 1] (whereas [KM23, Thm. 14] allows for using a less-restrictive sum-based i-IOSS bound) and could also be avoided by a suitable modification. Nevertheless, the above conclusions also apply to these improved conditions in the practical case where $\lambda_{\max}(\overline{P})/\lambda_{\min}(\underline{P}) > \lambda_{\max}(\overline{P}, \underline{P})$, compare also the simulation example in Section 3.4.

3.4. Numerical examples

We consider two examples from the literature: a chemical reactor process in Section 3.4.1 and a realistic 12-state quadrotor model with flexible rotor blades in Section 3.4.2. As first step, we apply the verification methods proposed in Sections 7.1.1 and 7.1.2 below to verify i-IOSS and i-iIOSS for the corresponding discrete- and continuous-time models, respectively. Here, it is also worth noting that the lack of such methods in the literature was generally considered a major problem in [AR21], as i-IOSS became a standard detectability assumption in the recent literature on nonlinear MHE, compare Section 3.3. Theorems 7.1 and 7.2 provide useful tools to actually verify this crucial property in practice. Based on these results, we apply the Lyapunov-based MHE schemes from [Sch+23, Sec. III] and Section 3.2. Overall, the following examples demonstrate the practicability of Lyapunov-based MHE and the verification methods presented in Sections 7.1.1 and 7.1.2, thus illustrating the ability of MHE to provide valid theoretical guarantees under practical conditions.

The simulations are performed in MATLAB using CasADi [And+18] and the NLP solver IPOPT [WB05]. LMIs are verified using YALMIP [Löf04; Löf09] and the semidefinite programming solver MOSEK [MOS24].

3.4.1. Chemical reaction

We consider the reversible chemical reaction $2A \rightleftharpoons B$ taking place in a constant volume batch reactor, which is taken from [TR02, Sec. 5]. The system state x consists of the partial pressures of A and B and evolves according to

$$\begin{aligned} \dot{x}_1 &= -2k_1 x_1^2 + 2k_2 x_2, \\ \dot{x}_2 &= k_1 x_1^2 - k_2 x_2 \end{aligned} \tag{3.42}$$

with $k_1 = 0.16$ and $k_2 = 0.0064$. An initial quantity of A and B is fed into the reactor, but the exact composition is unknown. A pressure gauge measures the total pressure prevailing in the reactor, yielding the output equation $y = x_1 + x_2$. The true initial state of the system and its a priori estimate are

$$x(0) = \chi = \begin{bmatrix} 3 \\ 1 \end{bmatrix}, \qquad \hat{\chi} = \begin{bmatrix} 0.1 \\ 4.5 \end{bmatrix}. \tag{3.43}$$

This setup poses a challenge for state estimation; in fact, simple estimators such as the standard EKF can fail to provide meaningful results, compare [RMD20, Example 4.38] and see the simulation results in Figure 3.1 below. This example is frequently used in the MHE literature (see, e.g., [RMD20, Example 4.38]), however, i-IOSS has never been certified. In the following, we apply the methods proposed in Sections 7.1.1 and 7.1.2 to verify this crucial property for both the discretized and the original continuous-time model and apply the Lyapunov-based MHE schemes from [Sch+23, Sec. III] and Section 3.2.

Table 3.2. Minimum required horizon length for guaranteed RGES of MHE compared to the different methods from the literature considered in Table 3.1.

[Sch+23, Thm./Cor. 1]	[AR21, Thm. 4.2]	[KM23, Thm. 14]	[AR19b, Thm. 1]
15	$> 8 \cdot 10^6$	119	142

Discrete-time Lyapunov-based MHE framework

To obtain a discrete-time model of the system (3.42), we apply an Euler discretization using the sampling time $t_\Delta = 0.1$, leading to

$$\begin{aligned} x_1^+ &= x_1 + t_\Delta(-2k_1x_1^2 + 2k_2x_2) + w_1, \\ x_2^+ &= x_2 + t_\Delta(k_1x_1^2 - k_2x_2) + w_2, \\ y &= x_1 + x_2 + w_3, \end{aligned}$$

where we consider additional disturbances $w \in \mathbb{R}^3$. In the following, we treat w as a uniformly distributed random variable satisfying $|w_i| \leq 10^{-3}, i = 1, 2$ for the process disturbances and $|w_3| \leq 0.1$ for the measurement noise. We assume that the prior knowledge $\mathcal{X} = [0.1, 4.5] \times [0.1, 4.5]$ is available, which follows from the physical nature of the system under the above conditions (in particular, the initial conditions (3.43) and boundedness of the disturbance w), compare also the simulation results in Figure 3.1 below.

For the considered system, we can apply Corollary 7.1 in combination with SOS optimization to compute a quadratic Lyapunov function $U(x, \tilde{x}) = |x - \tilde{x}|_P^2$ in the sense of Definition 7.1 with

$$P = \begin{bmatrix} 4.539 & 4.171 \\ 4.171 & 3.834 \end{bmatrix}, \qquad Q = \begin{bmatrix} 10^3 & 0 & 0 \\ 0 & 10^4 & 0 \\ 0 & 0 & 10^3 \end{bmatrix}, \qquad R = 10^3,$$

and the decay rate $\eta = 0.91$. We point out that, to the best of the authors' knowledge, this is the first time that i-IOSS has been explicitly verified for this example.

Based on the i-IOSS Lyapunov function above, we can now compute the minimum horizon length $N_{\min}$ sufficient for robust stability of MHE according to [Sch+23, Sec. III], and compare it to corresponding estimates from the recent nonlinear MHE literature, i.e., the Lyapunov-like function framework [AR21], MHE with general time-discounting [KM23], and without time-discounting [AR19b], by resolving the respective conditions in Table 3.1. As can be seen from Table 3.2, the Lyapunov-based MHE approach from [Sch+23, Sec. III] yields a minimum horizon length that is (at least) one order of magnitude better (i.e., smaller) than those obtained from the literature.

For the following simulation, we choose $N = 30 > N_{\min}$ to provide a small estimation error bound. The simulation results are depicted in Figure 3.1, which shows robustly stable estimation as guaranteed by [Sch+23, Thm. 1]. In order to compare the results, we also simulated the EKF. As can be seen in Figure 3.1, however, the

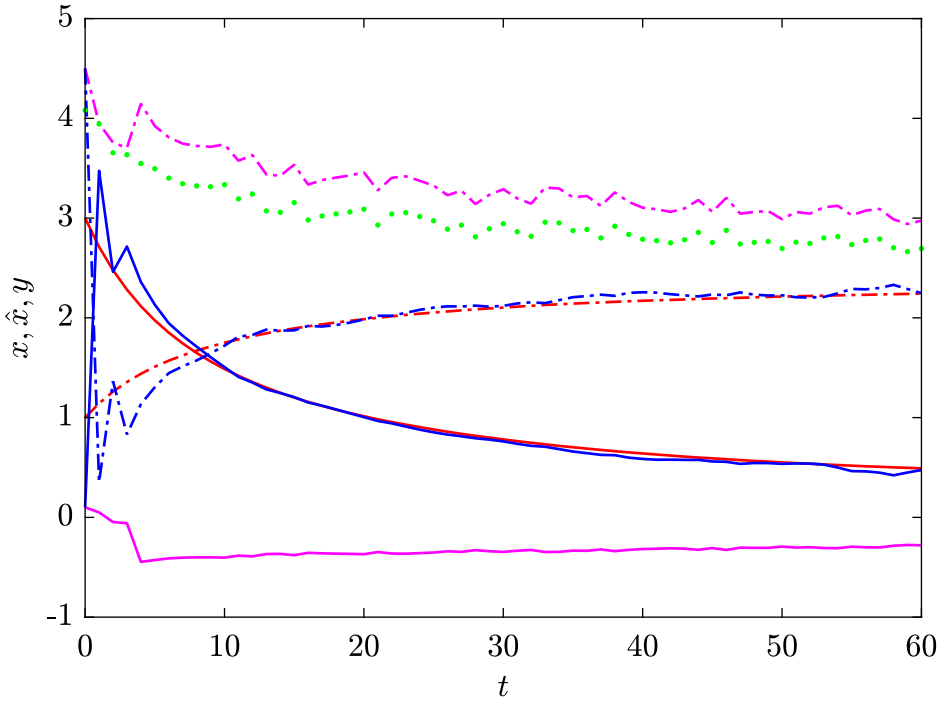

Figure 3.1. Comparison of MHE results (blue), EKF estimates (magenta), real system states (red) and measurements (green circles) for the discretized chemical reaction, where $x_1, \hat{x}_1$ are solid and $x_2, \hat{x}_2$ are dash-dotted. We have used $N = 30$, which guarantees RGES of MHE by [Sch+23, Thm. 1].

corresponding estimates exhibit a serious error compared to MHE, which is partly due to the fact that the physical constraints were not met. In summary, the overall simulation results are similar to [TR02, Sec. 5], [RMD20, Example 4.38], but with valid robustness guarantees for MHE.

Continuous-time Lyapunov-based MHE framework

We consider the system (3.42) with initial condition (3.43) under additional disturbances $w \in \mathbb{R}^3$, which yields

$$\begin{aligned} \dot{x}_1 &= -2k_1 x_1^2 + 2k_2 x_2 + w_1 \\ \dot{x}_2 &= k_1 x_1^2 - k_2 x_2 + w_2 \\ y &= x_1 + x_2 + w_3. \end{aligned} \tag{3.44}$$

We consider the disturbance signal w to be piece-wise constant over intervals of length $t_\Delta = 0.01$ and satisfies $w(t) \in \mathcal{W} = \{w \in \mathbb{R}^3 : |w_i| \leq 0.1,\ i = 1, 2, 3\}$ for all $t \geq 0$, see left plot in Figure 3.2. Here, we consider the simulation length $t_{\text{sim}} = 5$ and additionally assume that the true trajectory x satisfies $x(t) \in \mathcal{X} = \{x \in \mathbb{R}^2 : 0.1 \leq x_i \leq 5, i = 1, 2\}$ for all $0 \leq t \leq t_{\text{sim}}$, which is reasonable under this setup.

We verify the LMI conditions (7.33) on[9] $\mathcal{X} \times \mathcal{W}$, and by application of Theorem 7.2,

[9]Here, we exploit that condition (7.33) is linear in x; for a fixed value of $\eta = 0.4$ and $\kappa = -\ln \eta$, solving (7.33) for the vertices of $\mathcal{X}$ implies that (7.33) holds for all $\mathcal{X} \times \mathcal{W}$ by convexity of $\mathcal{X}$.

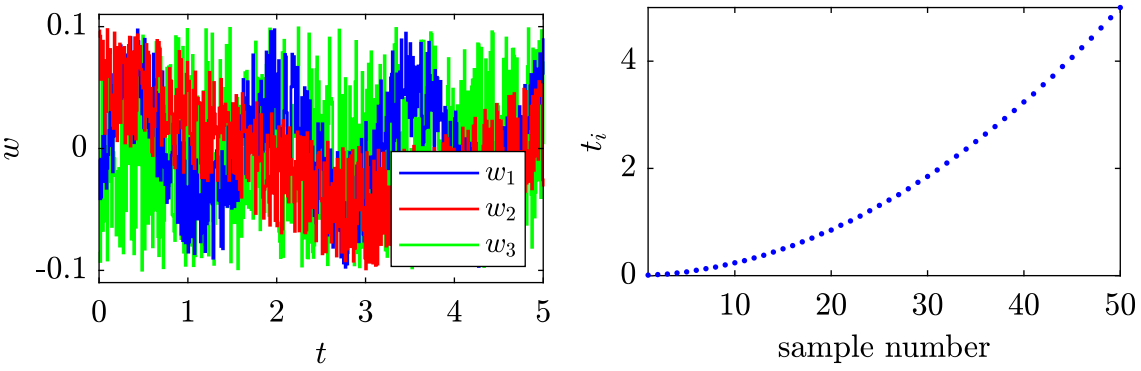

Figure 3.2. Disturbance signal w (left) and sampling times t_i contained in the set $\mathcal{T}$ (right) for the continuous-time MHE scheme applied to the chemical reaction.

the quadratic i-iIOSS Lyapunov function $U(x_1, x_2) = |x_1 - x_2|_P^2$ with

$$P = \begin{bmatrix} 4.009 & 3.768 \\ 3.768 & 3.549 \end{bmatrix}$$

satisfies Assumption 3.1 on $\mathcal{X} \times \mathcal{W}$ with $\eta = 0.4$, $Q = \mathrm{diag}(10^3, 10^3, 10^2)$, and $R = 10^2$.

We use the MHE objective (3.13) with $\Gamma(\chi, \bar{x}) = 2|\chi - \bar{x}|_P^2$ and $L(w, \Delta y) = 2|w|_Q^2 + |\Delta y|_R^2$ and want to perform 50 MHE updates during the simulation (in the interval $[0, t_{\mathrm{sim}}]$). To illustrate the flexibility of the MHE scheme from Section 3.2 allowing for non-equidistant sampling (in particular, in contrast to the discrete-time framework applied in the previous section), we design the set $\mathcal{T}$ such that it contains more samples towards the beginning of the experiment, as can be seen by the blue dots in the right plot in Figure 3.2. This yields $\bar{\delta} = 0.19$ in (3.19). Choosing the horizon length $T = 2$ satisfies (3.29) and guarantees the convergence rate $\rho = 0.86$ in (3.32).

We solve each MHE problem (3.12), where we employ a multiple shooting approach and integrate the system dynamics in (3.44) using the classic Runge-Kutta method (RK4) with step size $t_\Delta = 0.01$. The computations took at most $\tau_{\max} = 19.6\,\mathrm{ms}$ per iterate of the MHE algorithm presented at the end of Section 3.2.2 for all sampling times $t_i \in \mathcal{T}$. The estimation results are depicted in Figure 3.3. This shows fast convergence of the estimation error to a neighborhood around the origin, as guaranteed by Theorem 3.1.

3.4.2. Quadrotor

We adapt the example from [Kai+17] and consider a quadrotor model involving four rotors with flexible blades. Let $\mathcal{I}$ denote the stationary inertial system with its vertical component pointing into the Earth, where position and velocity of the quadrotor are represented by $z = [z_1, z_2, z_3]^\top$ and $s = [s_1, s_2, s_3]^\top$, respectively. By $\mathcal{B}$ we denote the body-fixed frame attached to the quadrotor, with the third component pointing in the opposite direction of thrust generation. The attitude of $\mathcal{B}$ with respect to $\mathcal{I}$ is captured by a rotation matrix R (where we use zyx-convention),

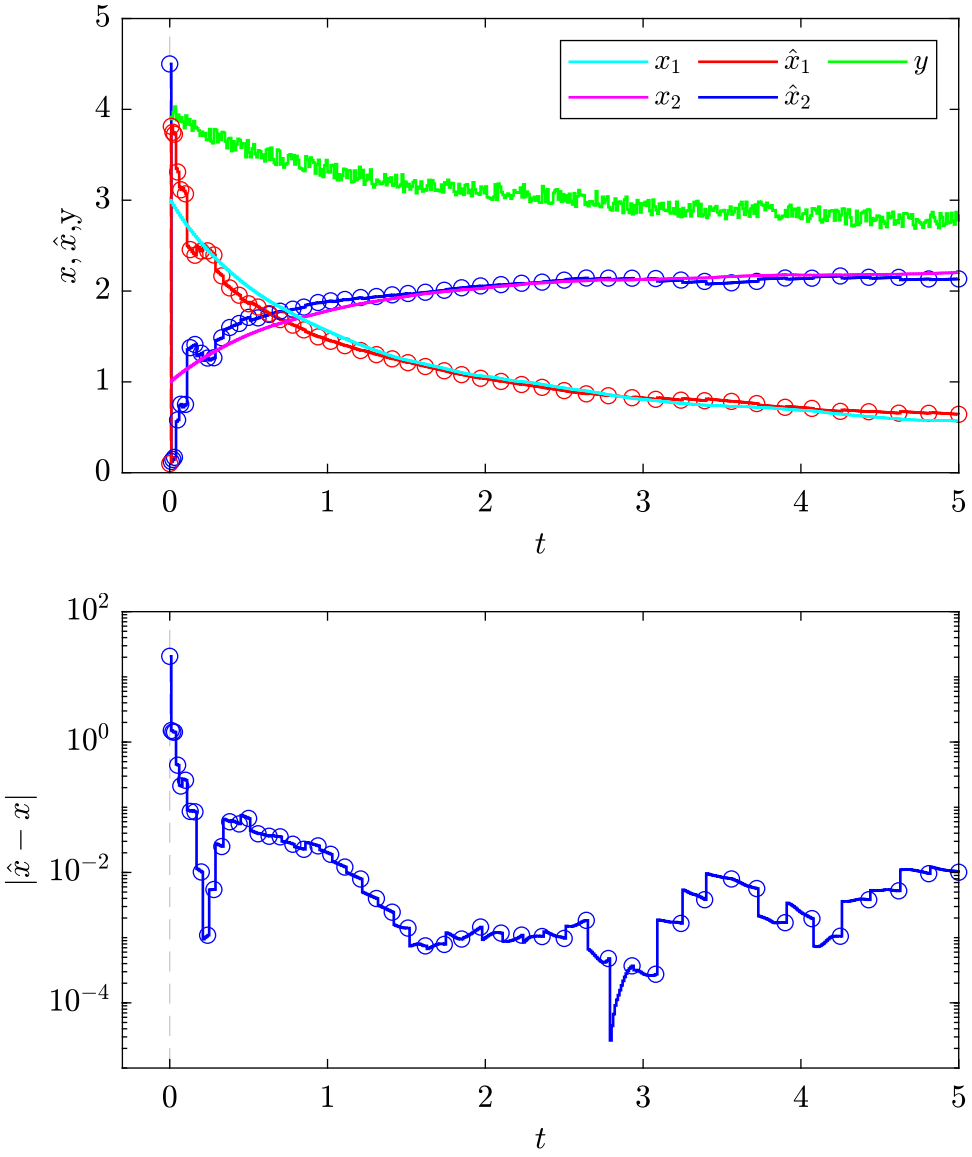

Figure 3.3. Estimation results of the continuous-time Lyapunov-based MHE scheme applied to the chemical reaction. Top: comparison of the estimated trajectory $\hat{x}$ (3.16), the true system trajectory x, and the measurements y; bottom: the corresponding estimation error. The circles correspond to the estimates $\hat{x}(t_i)$ at the sampling times $t_i \in \mathcal{T}$.

which involves the roll, pitch, and yaw angle of the quadrotor represented by $\xi = [\phi, \theta, \psi]^\top$. The angular velocity of the quadrotor in $\mathcal{B}$ with respect to $\mathcal{I}$ is given by $\Omega = [\Omega_1, \Omega_2, \Omega_3]^\top$. Assuming a wind-free environment, the overall dynamics can be described as

$$\begin{aligned} \dot{z} &= s, \\ \dot{\xi} &= \Gamma(\xi)\Omega, \\ m\dot{s} &= mge_3 - TR(\xi)e_3 - R(\xi)B\Omega, \\ J\dot{\Omega} &= -\Omega^\times J\Omega + \tau - D\Omega, \end{aligned} \tag{3.45}$$

where $e_3 = [0, 0, 1]^\top$ and $(\cdot)^\times$ refers to the skew symmetric matrix associated with the cross product such that $u^\times v = u \times v$ for any $u, v \in \mathbb{R}^3$. The thrust $T \in \mathbb{R}$ and the torque $\tau \in \mathbb{R}^3$ are generated by the four rotors by means of their angular velocities ω_i via

$$\begin{bmatrix} T \\ \tau \end{bmatrix} = \begin{bmatrix} c_T & c_T & c_T & c_T \\ 0 & -lc_T & 0 & lc_T \\ lc_T & 0 & -lc_T & 0 \\ -c_Q & c_Q & -c_Q & c_Q \end{bmatrix} \begin{bmatrix} \omega_1^2 \\ \omega_2^2 \\ \omega_3^2 \\ \omega_4^2 \end{bmatrix},$$

and the matrix Γ is defined as

$$\Gamma(\xi) = \begin{bmatrix} 1 & \sin\phi\tan\theta & \cos\phi\tan\theta \\ 0 & \cos\phi & -\sin\phi \\ 0 & \sin\phi\sec\theta & \cos\phi\sec\theta \end{bmatrix}.$$

For further details on the model and its derivation, we refer the interested reader to [Kai+17; NS19]. The parameters are chosen as $m = 1.9$, $J = \mathrm{diag}(5.9, 5.9, 10.7) \cdot 10^{-3}$, $g = 9.8$, $l = 0.25$, $c_T = 10^{-5}$, $c_Q = 10^{-6}$, $B = 1.14 \cdot e_3^\times$, and $D = 0.0297 \cdot e_3 e_3^\top$. In summary, the overall model has the states $x = [z^\top, \xi^\top, s^\top, \Omega^\top]^\top \in \mathbb{R}^{12}$ and the inputs $u = [\omega_1, \omega_2, \omega_3, \omega_4]^\top \in \mathbb{R}^4$. We additionally assume that the dynamics of $\dot{x}_i$ is corrupted by an additive disturbance d_i, $i \in \mathbb{I}_{[1,12]}$, and that only noisy position and orientation measurements $y = [z^\top, \xi^\top]^\top + v$ with noise $v \in \mathbb{R}^6$ are available. In the following, we consider d, v uniformly distributed such that $|d_i| \leq 10^{-3}$, $i = \mathbb{I}_{[1,12]}$, and $|v_i| \leq 0.1$, $i = \mathbb{I}_{[1,6]}$ and define $w = [d^\top, v^\top]^\top \in \mathbb{R}^{18}$. The discrete-time model (3.1) is then obtained via Euler-discretization using the sampling time $t_\Delta = 0.05$.

We assume that some input-output sequences $\{u(t)\}$ and $\{y(t)\}$ have been measured while performing a certain control scenario of the quadrotor that ensures $x(t) \in \mathcal{X} = \{x : |\xi_i| \leq \pi/6, |\Omega_i| \leq 1, i \in \mathbb{I}_{[1,3]}\}$ and $u(t) \in \mathcal{U} = \{u : |u_i| \leq 1500, i \in \mathbb{I}_{[1,4]}\}$ for all $t \in \mathbb{I}_{\geq 0}$; the objective is to reconstruct the corresponding state trajectory using Lyapunov-based MHE. To this end, we verify condition (7.26) on $\mathcal{X} \times \mathcal{U}$ by suitably gridding the state space and thus compute a quadratic i-IOSS Lyapunov function with the decay rate $\eta = 0.87$. Choosing the horizon length $M = 30$ satisfies the conditions [Sch+23, Thm./Cor. 1] such that RGES of MHE is guaranteed.

Figure 3.4 shows the real, measured, and estimated position of the quadrotor (in the frame $\mathcal{I}$) to illustrate the maneuver flown. The overall estimation error in Lyapunov coordinates is depicted in Figure 3.5 and illustrates exponential convergence to a neighborhood around the origin, as guaranteed by [Sch+23, Thm./Cor. 1].

We conclude this section by noting that similar results follow from the application of the continuous-time MHE framework from Section 3.2 (in particular, Theorem 3.1) and the i-iIOSS verification from Section 7.1.2 to the original continuous-time model in (3.45), although we omit a detailed discussion here for reasons of space and redundancy.

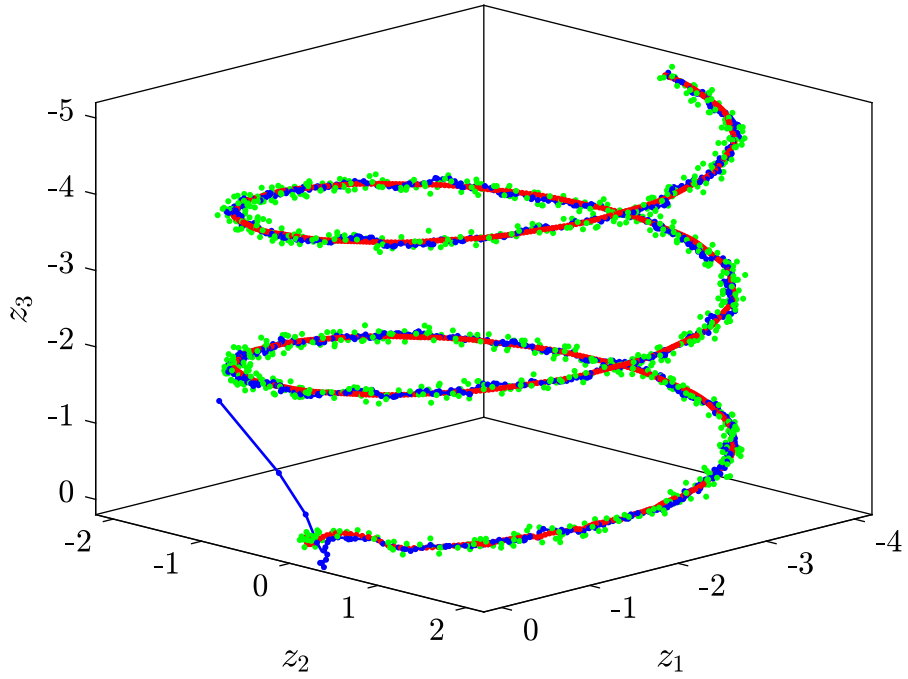

Figure 3.4. Comparison of the estimated (blue), true (red), and measured (green) position of the quadrotor.

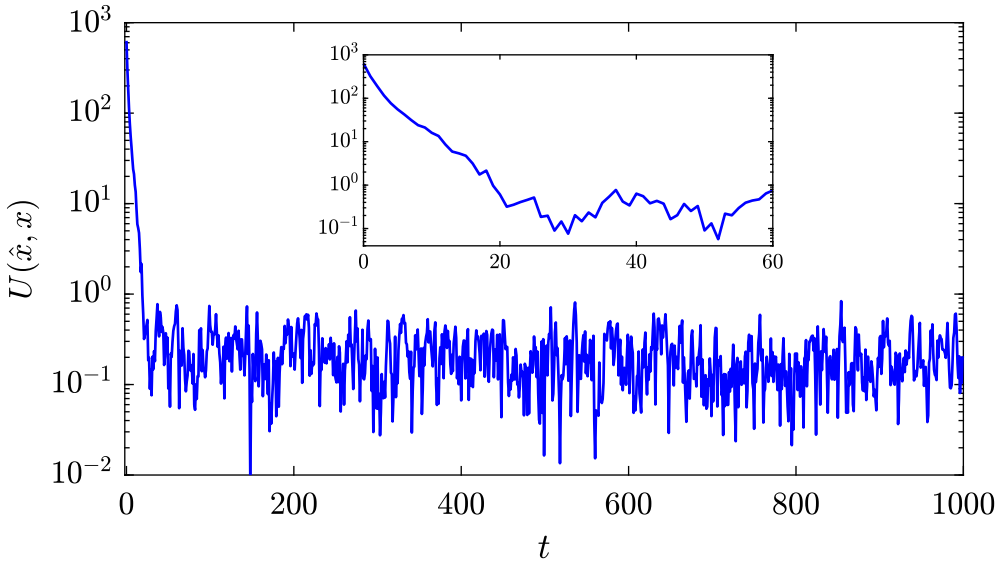

Figure 3.5. Estimation error in Lyapunov coordinates of MHE applied to the discretized quadrotor model.

3.5. Summary

In this chapter, we focused on robust stability guarantees of MHE for detectable nonlinear systems under process disturbances and measurement noise. We discussed a basic MHE scheme in discrete time and discussed the general structure of the underlying optimization problem. We briefly introduced the Lyapunov-based MHE scheme from [Sch+23, Sec. III], which employs a least squares objective under additional discounting and enjoys many beneficial theoretical properties, provided that the cost function is selected in accordance with a known i-IOSS Lyapunov function characterizing the detectability property of the system.

In the second part, we presented a counterpart for continuous-time systems—namely, a Lyapunov-based MHE scheme for general nonlinear perturbed continuous-time systems. Assuming that the system is detectable (i-iIOSS) and admits a corresponding i-iIOSS Lyapunov function, we showed that there exists a sufficiently long estimation horizon that guarantees robust global exponential stability of the estimation error in a time-discounted L^2-to-L^∞ sense. While the overall robust stability analysis is based on similar ideas as in the discrete-time setting in [Sch+23, Sec. III], the continuous-time MHE framework offers some significant advantages in practice. In particular, the sampling times at which the underlying optimization problem is solved can be chosen arbitrarily, which even allows the MHE scheme to be applied in an event-triggered fashion using a suitable triggering rule. Consequently, the proposed MHE scheme can be tailored to the problem at hand, which can yield more accurate results with less computational effort compared to standard equidistant sampling.

We discussed Lyapunov-based MHE (for both discrete- and continuous-time systems) in the context of recent results from the literature, highlighting its advantageous properties arising from the fact that we argue entirely in Lyapunov coordinates. First, tuning the MHE cost function by suitably relating it to i-(i)IOSS in order to achieve valid theoretical guarantees (which typically requires general $\mathcal{KL}$-function inequalities in the literature) becomes easy and intuitive, which even applies for the case of FIE and under merely asymptotic (rather than exponential) detectability. Second, a Lyapunov-based analysis generally allows for significantly less conservative (i.e., smaller) estimates of the minimum required horizon length compared to the literature.

The applicability of Lyapunov-based MHE for discrete- and continuous-time systems was illustrated using a nonlinear chemical reaction and a quadrotor model from the literature. Here, we verified the required detectability condition by computing i-IOSS and i-iIOSS Lyapunov functions using our methods from Sections 7.1.1 and 7.1.2 and successfully applied the Lyapunov-based MHE schemes from [Sch+23, Sec. III] and Section 3.2. For the latter, we used a non-equidistant sampling method, which illustrates the greater degree of flexibility compared to purely discrete-time approaches. Overall, the combination of Lyapunov-based MHE and the verification methods from Sections 7.1.1 and 7.1.2 allow for guaranteed robustly stable state estimation under practical conditions, for both discrete- and continuous-time systems.

4. Suboptimality guarantees for real-time applications

In this chapter, we present several suboptimal MHE schemes for general nonlinear discrete-time systems and provide robustness guarantees with respect to process disturbances and measurement noise that particularly do not require optimality of the solutions. This is crucial in order to ensure the practicability of MHE methods, especially in real-time applications. To this end, we employ an *a priori* known, robustly stable auxiliary observer, from which the robust stability properties can be inherited. In Section 4.1, we specify our setup concerning the system and the auxiliary observer. Then, in Section 4.2, we consider a classical MHE formulation that optimizes over system trajectories and allows the user to choose a standard least squares cost function, as is typical in practical applications. In Section 4.3, we propose a modified MHE formulation where we directly optimize over trajectories of the auxiliary observer, yielding an estimation scheme that is easier to implement, provides improved theoretical guarantees, and can even outperform comparable fast MHE approaches that optimize over system trajectories.

Disclosure: The following chapter is based upon and in parts literally taken from our previous publications [SM23d; SWM23; SKM21]. A detailed description of the contributions of each author is given in Appendix A.

4.1. System description and auxiliary observer

We consider the discrete-time, perturbed nonlinear system

$$x(t+1) = f(x(t), u(t), d(t)), \quad x(0) = \chi, \tag{4.1a}$$

$$y(t) = h(x(t), u(t), v(t)), \tag{4.1b}$$

where $t \in \mathbb{I}_{\geq 0}$ is the discrete time, $x(t) \in \mathbb{R}^n$ is the system state at time t, $\chi \in \mathbb{R}^n$ is the initial condition, $u(t) \in \mathbb{R}^m$ is the (known) control input, $d(t) \in \mathbb{R}^q$ is the (unknown) process disturbance, $v(t) \in \mathbb{R}^r$ is the (unknown) measurement noise, and $y(t) \in \mathbb{R}^p$ is the noisy output measurement. The nonlinear continuous functions $f : \mathbb{R}^n \times \mathbb{R}^m \times \mathbb{R}^q \to \mathbb{R}^n$ and $h : \mathbb{R}^n \times \mathbb{R}^m \times \mathbb{R}^r \to \mathbb{R}^p$ represent the system dynamics and output equation, respectively. We denote the nominal (disturbance-free) system equations as $f_{\mathrm{n}}(x, u) = f(x, u, 0)$ and $h_{\mathrm{n}}(x, u) = h(x, u, 0)$.

Note that in this chapter, the system description (4.1) explicitly distinguishes between process disturbances d (which affect the evolution of the system) and measurement noise v (which affects the output) and hence refrains from employing a

generalized noise input $w = (d, v)$, which is necessary because they require a different treatment here.

In the following, we assume that the unknown true system trajectory satisfies

$$(x(t), u(t), d(t), v(t)) \in \mathcal{X} \times \mathcal{U} \times \mathcal{D} \times \mathcal{V} =: \mathcal{Z},\ t \in \mathbb{I}_{\geq 0}, \tag{4.2}$$

where $\mathcal{Z}$ is forward invariant in the sense that

$$(x, u, d, v) \in \mathcal{Z} \quad \Rightarrow \quad f(x, u, d) \in \mathcal{X},\ h(x, u, v) \in \mathcal{Y}. \tag{4.3}$$

In (4.3), $\mathcal{X} \subseteq \mathbb{R}^n$, $\mathcal{U} \subseteq \mathbb{R}^m$, $\mathcal{D} \subseteq \mathbb{R}^q$, $\mathcal{V} \subseteq \mathbb{R}^r$, $\mathcal{Y} \subseteq \mathbb{R}^p$ are some known closed sets, where we assume that $0 \in \mathcal{D}$ and $0 \in \mathcal{V}$. Such constraints typically arise from the physical nature of the system, e.g., non-negativity of partial pressures, mechanically imposed limits, or parameter ranges. Using this information can significantly improve the estimation results, compare Section 3.1. If no such sets are known *a priori*, they can simply be chosen as $\mathcal{X} = \mathbb{R}^n$, $\mathcal{U} = \mathbb{R}^m$, $\mathcal{D} = \mathbb{R}^q$, $\mathcal{V} = \mathbb{R}^r$, $\mathcal{Y} = \mathbb{R}^p$.

In the following, we require a Lipschitz continuity property of h.

Assumption 4.1 (Lipschitz continuity of h)**.** *The function h in* (4.1b) *is Lipschitz continuous, i.e., there exists a constant $L_{\mathrm{h}} > 0$ such that*

$$|h(x_1, u, v_1) - h(x_2, u, v_2)| \leq L_{\mathrm{h}}(|x_1 - x_2| + |v_1 - v_2|)$$

for all $x_1, x_2 \in \mathcal{X}$ and $v_1, v_2 \in \mathcal{V}$ uniformly for all $u \in \mathcal{U}$.

Given some initial guess $\hat{\chi}$ of the true state χ, the overall goal is, at any time $t \in \mathbb{I}_{\geq 0}$, to provide an estimate $\hat{x}(t)$ of the current state $x(t)$ that satisfies the following stability notion.

Definition 4.1 (RGES)**.** *A state estimator for system* (4.1) *is robustly globally exponentially stable (RGES) if there exist $C_1, C_2, C_3 > 0$ and $\rho \in (0, 1)$ such that the resulting state estimate $\hat{x}(t)$ with $\hat{x}(0) = \hat{\chi}$ satisfies*

$$|\hat{x}(t) - x(t)| \leq \max\left\{C_1\rho^t|\hat{\chi} - \chi|, \max_{j \in \mathbb{I}_{[0,t-1]}} C_2\rho^{t-j-1}|d(j)|, \max_{j \in \mathbb{I}_{[0,t-1]}} C_3\rho^{t-j-1}|v(j)|\right\} \tag{4.4}$$

for all $t \in \mathbb{I}_{\geq 0}$, all initial conditions $\hat{\chi}, \chi \in \mathcal{X}$, and all disturbance and noise sequences $d \in \mathcal{D}^\infty$ and $v \in \mathcal{V}^\infty$.

Definition 4.1 corresponds to a discrete-time (exponential) version of the stability notion from Definition 3.1 and is often used in the recent MHE literature, see, e.g., [RMD20; KM23; AR21; Sch+23], and compare also Section 2.2.4 for more details. Due to the use of exponential discounting in (4.4), we have the following equivalence.

Proposition 4.1. *A state estimator is RGES as characterized in Definition 4.1 if and only if* (4.4) *holds with each maximization operation replaced by summation.*

Proof. The proof is straightforward and follows the lines of the proof of, e.g., [AR21, Prop. 3.13]. □

In the following, we present several MHE schemes with robust stability guarantees that in particular do *not* rely on optimality of the solutions, which is crucial for practical (especially real-time) applications. Instead, stability properties are inherited from an additional (potentially poorly performing) auxiliary observer. To this end, we consider the following standard form given by a mapping $g : \mathcal{O} \times \mathcal{U} \times \mathcal{Y} \to \mathcal{O}$ with $\mathcal{O} \subseteq \mathbb{R}^n$ such that, at any time $t \in \mathbb{I}_{\geq 0}$, the dynamical system

$$z(t+1) = g(z(t), u(t), y(t)), \quad z(0) = \zeta, \tag{4.5}$$

with initial condition $\zeta \in \mathcal{O}$ constitutes an estimate of the state $x(t+1)$ of the system (4.1) using the measured inputs and outputs $(u(t), y(t))$ and the previous internal state $z(t) \in \mathcal{O}$. We assume that some observer in the form of (4.5) is available that satisfies the following property.

Assumption 4.2 (RGES auxiliary observer)**.** *There exists an i-ISS Lyapunov function $V_\mathrm{o} : \mathcal{O} \times \mathcal{X} \to \mathbb{R}_{\geq 0}$ along with matrices $\underline{P}_\mathrm{o}, \overline{P}_\mathrm{o}, Q_\mathrm{o}, R_\mathrm{o} \succ 0$ and a constant $\eta_\mathrm{o} \in (0,1)$ such that*

$$|z - x|^2_{\underline{P}_\mathrm{o}} \leq V_\mathrm{o}(z,x) \leq |z-x|^2_{\overline{P}_\mathrm{o}}, \tag{4.6a}$$

$$V_\mathrm{o}(g(z,u,h(x,u,v)), f(x,u,d)) \leq \eta_\mathrm{o} V_\mathrm{o}(z,x) + |d|^2_{Q_\mathrm{o}} + |v|^2_{R_\mathrm{o}} \tag{4.6b}$$

for all $z \in \mathcal{O}$ and all $(x,u,d,v) \in \mathcal{Z}$.

The i-ISS Lyapunov function V_o provided by Assumption 4.2 implies RGES (Definition 4.1) of the observer in (4.5). Such a characterization was previously used in the context of MHE in [KMA21]. Designing state observers as in (4.5) for perturbed nonlinear systems that admit a corresponding i-ISS Lyapunov function is an active area of research. Assumption 4.2 can be verified with a quadratically bounded i-ISS Lyapunov function V_o satisfying (4.6a) by employing the differential dynamics, compare, e.g., [SP16; YWM22]. Alternatively, we could restrict the design to a quadratic function V_o, where sufficient conditions can be derived based on, e.g., incremental quadratic constraints [Zha+19] or specific Lipschitz properties [GHO92; ZB13]. A quadratic (time-varying) function V_o also arises for Kalman-like observers, compare [RU99; JRB05]. Note that Assumption 4.2 is our key assumption and can restrict the class of systems to which the MHE schemes presented below are applicable.

Remark 4.1 (Observer description)**.** *We want to point out that observers as in* (4.5) *are not in the most general form possible. Instead, we could simply require the observer to be a sequence of maps $\{\Psi_t\}_{t=0}^{\infty}$ rather than a system, such that*

$$z(t+1) = \Psi_t(\zeta, \{(u(j), y(j))\}_{j=0}^{t}), \ t \in \mathbb{I}_{\geq 0}, \tag{4.7}$$

compare [ART21, Def. 2.2] and see also [SW97, Rem. 25]. This general description would also allow for observers that do not admit a classical state-space representation, which we considered in our work [SM23d]. For auxiliary observers in the

context of suboptimal MHE, however, such description is rather of theoretical interest. This is because we are particularly interested in auxiliary observers that can be evaluated fast and with very little computational effort (while they may produce rather poor estimation results). Conventional observers in the form of (4.5) *comply with this condition, as they only require a simple forward simulation of the observer dynamics. More sophisticated estimation methods that can only be described by the general form* (4.7) *(such as MHE or FIE) would potentially provide better estimation results, but would be completely contrary to our goal (i.e., developing fast suboptimal MHE methods for real-time applications).*

In Section 4.2, we consider a rather classical MHE formulation that optimizes over trajectories of the system (4.1), where we use the auxiliary observer in (4.5) to construct a candidate solution for the underlying optimization problem and invoke Assumption 4.2 to infer stability of suboptimal MHE. In Section 4.3, we present a modified MHE problem that optimizes over trajectories of the observer (4.5), where the i-ISS Lyapunov function V_o from Assumption 4.2 directly serves as (multi-step) Lyapunov function for suboptimal MHE.

4.2. Optimizing system trajectories

In this section, we present a suboptimal MHE scheme involving the system dynamics (4.1). We specify the design in Section 4.2.1 and analyze stability in Sections 4.2.2 and 4.2.3 (considering different classes of nonlinear systems). We discuss the theoretical properties resulting from different setups in Section 4.2.4, extend our results to auxiliary observers that may not satisfy the MHE constraints in Section 4.2.5, and provide a numerical example in Section 4.2.6.

To ensure that the unknown true trajectory can actually be recovered from the obtained input-output measurements, we use the following notion of exponential detectability.

Assumption 4.3 (Exponential detectability)**.** *System* (4.1) *admits a quadratically bounded i-IOSS Lyapunov function $U : \mathcal{X} \times \mathcal{X} \to \mathbb{R}_{\geq 0}$, that is, there exist matrices $\underline{P}_\mathrm{s}, \overline{P}_\mathrm{s}, Q_\mathrm{s}, R_\mathrm{s}, G_\mathrm{s} \succ 0$ and a constant $\eta_\mathrm{s} \in (0, 1)$ such that*

$$|x_1 - x_2|^2_{\underline{P}_\mathrm{s}} \leq U(x_1, x_2) \leq |x_1 - x_2|^2_{\overline{P}_\mathrm{s}}, \tag{4.8a}$$

$$\begin{aligned} &U(f(x_1, u, d_1), f(x_2, u, d_2)) \\ &\leq \eta_\mathrm{s} U(x_1, x_2) + |d_1 - d_2|^2_{Q_\mathrm{s}} + |v_1 - v_2|^2_{R_\mathrm{s}} + |h(x_1, u, v_1) - h(x_2, u, v_2)|^2_{G_\mathrm{s}} \end{aligned} \tag{4.8b}$$

for all $(x_1, u, d_1, v_1), (x_2, u, d_2, v_2) \in \mathcal{Z}$.

The i-IOSS Lyapunov function U from Assumption 4.3 is the direct discrete-time counterpart of Definition 2.3 (for continuous-time systems) and corresponds to Assumption 1 in [Sch+23]. It essentially represents an (equivalent) Lyapunov characterization of exponential i-IOSS, which has become standard in recent years as

a notion of nonlinear detectability in the context of MHE, compare, e.g., [RMD20; AR21; Hu24; KM23], and see Chapter 2 for more details on i-IOSS and nonlinear detectability. In Section 7.1, we show how i-IOSS Lyapunov functions can be systematically constructed for general nonlinear systems using the differential dynamics and LMIs.

In the following, we impose a compatibility condition between the i-IOSS Lyapunov function for the system and the i-ISS Lyapunov function for the auxiliary observer.

Assumption 4.4 (Compatibility)**.** *The parameters from Assumptions 4.2 and 4.3 are such that* $\eta_{\mathrm{s}} \leq \eta_{\mathrm{o}}$ *and* $\overline{P}_{\mathrm{s}} \preceq \underline{P}_{\mathrm{o}}$.

Note that Assumption 4.4 is without loss of generality, as the functions U and/or V_{o} can simply be re-scaled to satisfy the compatibility conditions; we only make this assumption for the sake of simplicity. However, we want to point out that considering $\eta_{\mathrm{s}} \leq \eta_{\mathrm{o}}$ is quite natural, since generally no faster convergence of the observer error (captured by η_{o}) can be expected than the slowest decay of the unobservable mode of the system (captured by η_{s}).

4.2.1. Suboptimal MHE design

The general MHE problem considered in this section corresponds to the standard formulation from Section 3.1, with minor technical differences. In particular, at each time $t \in \mathbb{I}_{\geq 0}$, we consider the past input and output data in a moving time window of length $N_t = \min\{t, N\}$ for some fixed $N \in \mathbb{I}_{\geq 0}$. Given the corresponding input and output sequences restricted to the current horizon

$$u_t = \{u_t(j)\}_{j=0}^{N_t-1},\ u_t(j) = u(t - N_t + j),\ j \in \mathbb{I}_{[0,N_t-1]},\ t \in \mathbb{I}_{\geq 0}, \tag{4.9}$$

$$y_t = \{y_t(j)\}_{j=0}^{N_t-1},\ y_t(j) = y(t - N_t + j),\ j \in \mathbb{I}_{[0,N_t-1]},\ t \in \mathbb{I}_{\geq 0}, \tag{4.10}$$

we can state the following NLP:

$$\min_{\hat{x}_t, \hat{d}_t, \hat{v}_t} \ J(\hat{x}_t, \hat{d}_t, \hat{v}_t, \hat{y}_t, t) \tag{4.11a}$$

$$\text{s.t. } \hat{x}_t(j+1) = f(\hat{x}_t(j), u_t(j), \hat{d}_t(j)),\ j \in \mathbb{I}_{[0,N_t-1]}, \tag{4.11b}$$

$$\hat{y}_t(j) = h(\hat{x}_t(j), u(j), \hat{v}_t(j)),\ j \in \mathbb{I}_{[0,N_t-1]}, \tag{4.11c}$$

$$\hat{x}_t(j) \in \mathcal{X},\ j \in \mathbb{I}_{[0,N_t]}, \tag{4.11d}$$

$$\hat{d}_t(j) \in \mathcal{D},\ \hat{v}_t(j) \in \mathcal{V},\ \hat{y}_t(j) \in \mathcal{Y},\ j \in \mathbb{I}_{[0,N_t-1]}. \tag{4.11e}$$

The cost function $J(\cdot)$ is specified below. The decision variables $\hat{x}_t = \{\hat{x}_t(j)\}_{j=0}^{N_t}$, $\hat{d}_t = \{\hat{d}_t(j)\}_{j=0}^{N_t-1}$, and $\hat{v}_t = \{\hat{v}_t(j)\}_{j=0}^{N_t-1}$ are sequences[1] that contain estimates of the state, the process disturbance, and the measurement noise over the estimation

[1] Compared to the problem formulation (3.4) in Section 3.1, the decision variables involve the two sequences d_t and v_t instead of a single (combined) sequence w_t, which is because we explicitly distinguish between process disturbances and measurement noise in the system description in (4.1).

horizon, estimated at time $t \in \mathbb{I}_{\geq 0}$. They uniquely form a sequence of output estimates $\hat{y}_t = \{\hat{y}_t(j)\}_{j=0}^{N_t-1}$ under (4.11c). We consider the following cost function:

$$J(\hat{x}_t, \hat{d}_t, \hat{v}_t, \hat{y}_t, t) := \Gamma(\hat{x}_t(0), \bar{x}(t-N_t)) + \sum_{j=0}^{N_t-1} \bar{\eta}^{N_t-j-1} L(\hat{d}_t(j), \hat{v}_t(j), \hat{y}_t(j) - y_t(j)), \tag{4.12}$$

where $\bar{x}(t-N_t)$ is a prior estimate that is defined below and $\bar{\eta} \geq \eta_{\mathrm{s}}$ is a tuning parameter with η_{s} from Assumption 4.3. The stage cost L and prior weighting Γ are selected as

$$\Gamma(\hat{x}, \bar{x}) = 2|\hat{x} - \bar{x}|^2_{\overline{P}_{\mathrm{s}}}, \tag{4.13}$$

$$L(\hat{d}, \hat{v}, \Delta y) = 2|\hat{d}|^2_{Q_{\mathrm{s}}} + 2|\hat{v}|^2_{R_{\mathrm{s}}} + |\Delta y|^2_{G_{\mathrm{s}}}, \tag{4.14}$$

where the matrices $\overline{P}_{\mathrm{s}}$, Q_{s}, R_{s}, and G_{s} correspond to the i-IOSS Lyapunov function parameters (Assumption 4.3). Note that this does not restrict any tuning possibilities, as the Lyapunov function U can be suitably re-scaled such that (4.8a) and (4.8b) hold for some desired positive definite matrices $\overline{P}_{\mathrm{s}}$, R_{s}, Q_{s}, G_{s}, compare Remark 3.4.

Remark 4.2 (Cost function parameters)**.** *The stage cost L in* (4.13) *and prior weighting Γ in* (4.14) *correspond to the choices we made in Section 3.2 and [Sch+23, Sec. III]. This ensures a compatibility property between MHE and detectability (i-IOSS), similar as in [KM23, Ass. 1], [AR21, Ass. 3.5], [Hu24, Ass. 4], see Section 3.3 for more details. The design parameter $\bar{\eta}$, however, significantly differs from the designs proposed in Section 3.2 and [Sch+23, Sec. III], [KM23] [Hu24], which essentially require $\eta_{\mathrm{s}} \leq \bar{\eta} < 1$ to form a discounted cost function, compare also Remark 3.3. Here, in contrast, we do* not *require a strict upper bound, but merely consider $\eta_{\mathrm{s}} \leq \bar{\eta}$, which hence also covers the practically relevant case of quadratic penalties (without discounting) for $\bar{\eta} = 1$. This is exclusively possible here because we infer RGES of (suboptimal) MHE not from the detectability property of the system, but from the stability property of the auxiliary observer (Assumption 4.2). Note, however, that generally better theoretical guarantees (in terms of tighter error bounds that do not deteriorate with an increasing horizon) emerge using a discounted cost function ($\bar{\eta} < 1$), see also the discussion in Section 4.2.4 below.*

Furthermore, we would like to emphasize that the quadratic penalties in (4.13) *and* (4.14) *could be modified by simply requiring boundedness of Γ and L in terms of general power law functions in the form of Cs^a for arbitrary $C > 0$ and $a \geq 1$, which corresponds to the setup we considered in [SM23d, Ass. 2]. However, this may result in the cost function not being differentiable at certain points, thus requiring the use of non-standard solvers (e.g. derivative-free optimization methods [RS12]) or the introduction of additional auxiliary decision variables, which in turn increases the size of the optimization problem and hence the computational demand. Since quadratic (i.e., least squares) cost functions are also the most relevant in practice, we limit our analysis to these.*

Now, rather than solving (4.11) to optimality at each time $t \in \mathbb{I}_{\geq 0}$, we consider the following suboptimal estimator.

Definition 4.2 (Suboptimal estimator)**.** *Let $t \in \mathbb{I}_{\geq 0}$, $N \in \mathbb{I}_{\geq 1}$, some prior estimate $\bar{x}(t-N_t) \in \mathcal{X}$ and the measured input-output sequences u_t and y_t in* (4.9) *and* (4.10) *be given. Furthermore, let $(\tilde{x}_t, \tilde{d}_t, \tilde{v}_t) \in \mathcal{X}^{N_t+1} \times \mathcal{D}^{N_t} \times \mathcal{V}^{N_t}$ denote a feasible candidate solution to the MHE problem* (4.11) *with the corresponding output sequence $\tilde{y}_t \in \mathcal{Y}^{N_t}$. Then, a suboptimal solution of* (4.11) *is defined as any tuple $(\hat{x}_t, \hat{d}_t, \hat{v}_t) \in \mathcal{X}^{N_t+1} \times \mathcal{D}^{N_t} \times \mathcal{V}^{N_t}$ that satisfies (i) the MHE constraints* (4.11b)–(4.11e) *and (ii) the cost decrease condition*

$$J(\hat{x}_t, \hat{d}_t, \hat{v}_t, \hat{y}_t, t) \leq J(\tilde{x}_t, \tilde{d}_t, \tilde{v}_t, \tilde{y}_t, t). \tag{4.15}$$

The (suboptimal) state estimate at time $t \in \mathbb{I}_{\geq 0}$ is then defined as $\hat{x}(t) = \hat{x}_t(N_t)$.

Remark 4.3 (Decrease Condition)**.** *Note that the condition in* (4.15) *ensures that at a given time $t \in \mathbb{I}_{\geq 0}$, the cost of a suboptimal solution is no larger than the cost of the candidate solution. This property can be achieved by many off-the-shelf numerical solvers if they are applied to the problem* (4.11) *with the candidate solution as a warm start and then terminated after a finite number of iterations (including 0), compare [PRW11]. In particular, one may implement* (4.15) *as an additional constraint and use some algorithm that provides, at every iteration, a feasible estimate, which is the case for, e.g., feasible sequential quadratic programming algorithms [LT01].*

Alternatively, one could explicitly test for satisfaction of the constraints in (4.11b)–(4.11e) *and the condition in* (4.15) *for a given suboptimal solution $(\hat{x}_t, \hat{d}_t, \hat{v}_t)$ (which is obtained, e.g., after terminating the optimization algorithm after a few iterations), and if at least one of these conditions is violated, choose the candidate solution as the current suboptimal solution (which satisfies all constraints by definition). We point out that this does not require warm-starting the optimizer with the candidate solution itself; instead, any warm start could be chosen, e.g., based on the shifted solution from one time step before, extended with a one-step forward prediction using the nominal system dynamics, compare [WVD14; Küh+11]. Taking such an improved warm start into account while having the candidate solution $(\tilde{x}_t, \tilde{d}_t, \tilde{v}_t)$ in hand to ensure condition* (4.15) *and thus guarantee robustly stable state estimation can yield improved performance in practice, compare also the simulation example in Section 4.2.6.*

To establish RGES of the suboptimal estimator from Definition 4.2, we construct the required candidate solution $(\tilde{x}_t, \tilde{d}_t, \tilde{v}_t)$ and the prior weighting $\bar{x}(t-N_t)$ by using the auxiliary observer in (4.5) satisfying Assumption 4.2 (RGES) and Assumption 4.4 (compatibility with i-IOSS). Here, a key element is the following re-initialization procedure. Similar to the receding horizon nature of MHE, we define a second estimation horizon $T_t := \min\{t, T\}$ for some fixed length $T \in \mathbb{I}_{\geq N}$. Then, at each time $t \in \mathbb{I}_{\geq 0}$, we re-initialize the auxiliary observer using

$$\zeta_t := \begin{cases} \hat{x}(t-T), & t \in \mathbb{I}_{\geq T} \\ \hat{\chi}, & t \in \mathbb{I}_{[0,T-1]}, \end{cases} \tag{4.16}$$

where $\hat{x}(t-T)$ is the suboptimal state estimate obtained T steps in the past and $\hat{\chi}$ is the *a priori* guess of the true unknown initial condition χ of the system (4.1).

Next, we perform a forward simulation

$$z_t(j+1) = g(z_t(j), u(t-T_t+j), y(t-T_t+j)), \quad j \in \mathbb{I}_{[0,T_t-1]}, \tag{4.17a}$$
$$z_t(0) = \zeta_t \tag{4.17b}$$

and set the prior estimate according to

$$\bar{x}(t-N_t) = z_t(T_t-N_t), \quad t \in \mathbb{I}_{\geq 0}. \tag{4.18}$$

In Section 4.2.2, we first consider general nonlinear systems as in (4.1) and construct the candidate solution based on a nominal system trajectory initialized with an estimate provided by the auxiliary observer in (4.17). Then, in Section 4.2.3, we consider the special case of systems that are subject to additive disturbances, which allows us to construct the candidate solution from an observer trajectory, leading to tighter error bounds and improved estimation results, compare also the numerical example in Section 4.2.6. To infer stability of suboptimal MHE, the general idea is to consider $T > N$ and exploit the contraction property of the auxiliary observer (provided by Assumption 4.2) from $t-T$ to $t-N$ through the candidate solution $(\tilde{x}_t, \tilde{d}_t, \tilde{v}_t)$. In the following, we show that there always exists some T large enough such that the suboptimal estimator from Definition 4.2 is RGES in the sense of Definition 4.1, even when the optimizer performs zero iterations.

Remark 4.4 (Observer domain)**.** *In Sections 4.2.2 and 4.2.3, we consider the case where the auxiliary observer in* (4.17) *lives in $\mathcal{X}$ to ensure feasibility of the candidate solutions (which corresponds to the requirement $\mathcal{O} = \mathcal{X}$). In practice, however, conventional observers are generally not guaranteed to produce physical plausible state estimates, and if $\mathcal{X} \subset \mathbb{R}^n$, there might be time instants at which the observer state leaves the set $\mathcal{X}$, for example due to transient dynamics or external perturbations. This is addressed in Section 4.2.5, where we consider the case of $\mathcal{O} \supset \mathcal{X}$ and employ additional projections when constructing the candidate solutions to ensure satisfaction of the MHE constraints (in particular,* (4.11d)*).*

To summarize the overall suboptimal MHE algorithm, the steps that need to be performed at each sampling time $t \in \mathbb{I}_{\geq 0}$ to obtain the current suboptimal state estimate $\hat{x}(t)$ are as follows.

1. Collect the current data sequences u_t and y_t and the past suboptimal estimate $\hat{x}(t-T_t)$.
2. Re-initialize[2] the auxiliary observer via (4.16) and perform a forward simulation of (4.17) over T_t steps.
3. Obtain the prior (4.18) and construct the candidate solution $(\tilde{x}_t, \tilde{w}_t, \tilde{v}_t)$.

[2]When implementing the proposed suboptimal MHE scheme, the observer in (4.17) does not need to be re-initialized for $t \in \mathbb{I}_{[0,T-1]}$, as the corresponding observer trajectories coincide in this interval (due to the fact that their initial states are all the same by (4.16)). Consequently, for $t \in \mathbb{I}_{[0,T-1]}$, it suffices to apply a one-step forward prediction of (4.5) initialized with the previous observer state.

4. Approximately solve the MHE problem (4.11).
5. Obtain a new suboptimal estimate $\hat{x}(t) = \hat{x}_t(N_t)$.
6. Set $t = t + 1$ and go back to 1.

4.2.2. Systems subject to nonlinear process disturbances

In this section, we consider the case where the observer in (4.5) satisfies $\mathcal{O} = \mathcal{X}$ (this will be relaxed in Section 4.2.5, compare Remark 4.4). We construct the candidate solution $(\tilde{x}_t, \tilde{d}_t, \tilde{v}_t)$ based on the nominal dynamics f_n initialized with a past estimate obtained from the auxiliary observer in (4.17). Specifically, we define

$$\tilde{x}_t(j+1) = f_\mathrm{n}(\tilde{x}_t(j), u_t(j)),\ j \in \mathbb{I}_{[0,N_t-1]},\ \tilde{x}_t(0) = z_t(T_t - N_t), \tag{4.19a}$$
$$\tilde{d}_t(j) = 0,\ j \in \mathbb{I}_{[0,N_t-1]}, \tag{4.19b}$$
$$\tilde{v}_t(j) = 0,\ j \in \mathbb{I}_{[0,N_t-1]}, \tag{4.19c}$$

which yields the corresponding outputs $\tilde{y}_t(j) = h(\tilde{x}_t(j), u_t(j), \tilde{v}_t(j)),\ j \in \mathbb{I}_{[0,N_t-1]}$ under (4.11c). Note that since $z_t(T_t - N_t) \in \mathcal{X}$ by definition, the forward-invariance property in (4.3) implies that the candidate solution (4.19) is feasible for the MHE problem in (4.11).

To establish RGES of suboptimal MHE, we require an additional Lipschitz continuity assumption on the perturbed dynamics f.

Assumption 4.5 (Lipschitz continuity of f)**.** *The function f is Lipschitz continuous, i.e., there exists some constant $L_\mathrm{f} \geq 1$ such that $|f(x_1, u, d_1) - f(x_2, u, d_2)| \leq L_\mathrm{f}(|x_1 - x_2| + |d_1 - d_2|)$ for all $x_1, x_2 \in \mathcal{X}$ and all $d_1, d_2 \in \mathcal{D}$ uniformly for all $u \in \mathcal{U}$.*

Assumption 4.5 entails a global Lipschitz property of f. Indeed, this can be restrictive in the general case of unbounded sets $\mathcal{X}, \mathcal{U}$, and $\mathcal{D}$; however, it is not restrictive if these sets are compact (which is often the case in practice). Notice also that we impose $L_\mathrm{f} \geq 1$ in Assumption 4.5, which allows for simpler proofs and is indeed without loss of generality. This could also be avoided by merely requiring that $L_\mathrm{f} > 0$ in order to obtain less conservative results; however, a Lipschitz constant $L_\mathrm{f} < 1$ is rather irrelevant in our setting, as this would imply a contracting system behavior, rendering the observer design a trivial task.

We now state a few auxiliary results. The first one provides an upper bound on the estimation error of the observer in (4.17) (in Lyapunov coordinates) in the respective time interval $\mathbb{I}_{[t-T_t,t]}$, which we explicitly state for ease of reference.

Lemma 4.1. *Suppose Assumption 4.2 applies. Let $T \in \mathbb{I}_{\geq 0}$ be arbitrary. The observer in (4.17) satisfies*

$$V_\mathrm{o}(z_t(j), x(t - T_t + j)) \leq V_\mathrm{o}(\zeta_t, x(t - T_t))\eta_\mathrm{o}^j + \sum_{i=0}^{j-1} \eta_\mathrm{o}^{j-i-1} \left(|d(t - T_t + i)|_{Q_\mathrm{o}}^2 + |v(t - T_t + i)|_{R_\mathrm{o}}^2 \right) \tag{4.20}$$

for all $j \in \mathbb{I}_{[0,T_t]}$, all $t \in \mathbb{I}_{\geq 0}$, and all $\zeta_t, \chi \in \mathcal{X}$, $d \in \mathcal{D}^\infty$, and $v \in \mathcal{V}^\infty$.

Proof. The statement follows directly from the application of the dissipation inequality in (4.6b) guaranteed by Assumption 4.2 with respect to the initialization of the observer in (4.16). □

We now establish a bound on the fitting error of the candidate solution.

Lemma 4.2. *Suppose that Assumptions 4.1, 4.2, and 4.5 apply. Let $N \in \mathbb{I}_{\geq 0}$ and $T \in \mathbb{I}_{\geq N}$ be arbitrary. Then, the fitting error of the trajectory defined by the candidate solution in* (4.19) *satisfies*

$$\begin{aligned} &|\tilde{y}_t(j) - y_t(j)|_{G_\mathrm{s}}^2 \\ &\leq \sigma(N_t)(j+1)L_\mathrm{f}^{2j}\left(V_\mathrm{o}(\zeta_t, x(t-T_t))\eta_\mathrm{o}^{T_t} + \sum_{i=t-T_t}^{t-N_t+j} \eta_\mathrm{o}^{t-i-1}\left(|d(i)|_{Q_\mathrm{o}}^2 + |v(i)|_{R_\mathrm{o}}^2\right)\right) \end{aligned} \tag{4.21}$$

for all $j \in \mathbb{I}_{[0,N_t-1]}$ and $t \in \mathbb{I}_{\geq 0}$, where

$$\sigma(s) = 2c_1\lambda_{\max}(G_\mathrm{s})L_\mathrm{h}^2\eta_\mathrm{o}^{-s},\ s \geq 0 \tag{4.22}$$

and $c_1 := \max\{1, \lambda_{\min}(\underline{P}_\mathrm{o})^{-1}, \lambda_{\min}(Q_\mathrm{o})^{-1}, \lambda_{\min}(R_\mathrm{o})^{-1}\}$.

Proof. We start by considering any $t \in \mathbb{I}_{\geq 0}$ and the sequences of the true state, the process disturbance, and the measurement noise, restricted to the current estimation horizon:

$$x_t = \{x_t(j)\}_{j=0}^{N_t},\ x_t(j) = x(t-N_t+j),\ j \in \mathbb{I}_{[0,N_t]}, \tag{4.23}$$

$$d_t = \{d_t(j)\}_{j=0}^{N_t-1},\ d_t(j) = d(t-N_t+j),\ j \in \mathbb{I}_{[0,N_t-1]}, \tag{4.24}$$

$$v_t = \{y_t(j)\}_{j=0}^{N_t-1},\ v_t(j) = v(t-N_t+j),\ j \in \mathbb{I}_{[0,N_t-1]}. \tag{4.25}$$

Since the candidate solution in (4.19) defines a trajectory of system (4.1), we can apply the output equation h in (4.1b). Together with Assumption 4.1 (Lipschitz continuity of h) and Jensen's inequality, the fitting error can be bounded by

$$|\tilde{y}_t(j) - y_t(j)|_{G_\mathrm{s}}^2 \leq 2\lambda_{\max}(G_\mathrm{s})L_\mathrm{h}^2\left(|\tilde{x}_t(j) - x_t(j)|^2 + |v_t(j)|^2\right) \tag{4.26}$$

for all $j \in \mathbb{I}_{[0,N_t-1]}$. Recursive application of the dynamics in (4.1a) (where we recall that $\tilde{d}_t(j) = 0$ for $j \in \mathbb{I}_{[0,N_t-1]}$) together with Assumption 4.5 yields

$$|\tilde{x}_t(j) - x_t(j)| \leq L_\mathrm{f}^j|\tilde{x}_t(0) - x_t(0)| + \sum_{i=1}^{j} L_\mathrm{f}^i|d_t(j-i)|. \tag{4.27}$$

Squaring the result and using Jensen's inequality leads to

$$\begin{aligned} &|\tilde{x}_t(j) - x_t(j)|^2 \\ &\leq (j+1)L_\mathrm{f}^{2j}\left(|\tilde{x}_t(0) - x_t(0)|^2 + \sum_{i=1}^{j}|d_t(j-i)|^2\right) \\ &\leq (j+1)L_\mathrm{f}^{2j}\left(|\tilde{x}_t(0) - x_t(0)|^2 + \lambda_{\min}(Q_\mathrm{o})^{-1}\eta_\mathrm{o}^{-N_t}\sum_{i=t-N_t}^{t-N_t+j-1}\eta_\mathrm{o}^{t-i-1}|d(i)|_{Q_\mathrm{o}}^2\right), \end{aligned} \tag{4.28}$$

where the last step follows by the definition of d_t in (4.24) and the fact that $\eta_{\mathrm{o}}^{-N_t}\eta_{\mathrm{o}}^{i-1} > 1$ for all $i \in \mathbb{I}_{[0,N_t]}$. Since $\tilde{x}_t(0) = z_t(T_t - N_t)$ and $x_t(0) = x(t - N_t)$ due to the definitions of the candidate solution in (4.19) and x_t in (4.23), we can invoke Lemma 4.1, which yields

$$
\begin{aligned}
&|\tilde{x}_t(0) - x_t(0)|^2 = |z_t(T_t - N_t) - x(t - N_t)|^2 \\
&\leq \frac{1}{\lambda_{\min}(\underline{P}_{\mathrm{o}})} V_{\mathrm{o}}(z_t(T_t - N_t), x(t - N_t)) \\
&\leq \frac{\eta_{\mathrm{o}}^{-N_t}}{\lambda_{\min}(\underline{P}_{\mathrm{o}})} \Bigg(V_{\mathrm{o}}(\zeta_t, x(t - T_t))\eta_{\mathrm{o}}^{T_t} \\
&\qquad + \sum_{i=0}^{T_t - N_t - 1} \eta_{\mathrm{o}}^{T_t - i - 1} \left(|d(t - T_t + i)|_{Q_{\mathrm{o}}}^2 + |v(t - T_t + i)|_{R_{\mathrm{o}}}^2 \right) \Bigg) \\
&= \frac{\eta_{\mathrm{o}}^{-N_t}}{\lambda_{\min}(\underline{P}_{\mathrm{o}})} \left(V_{\mathrm{o}}(\zeta_t, x(t - T_t))\eta_{\mathrm{o}}^{T_t} + \sum_{i=t-T_t}^{t-N_t-1} \eta_{\mathrm{o}}^{t-i-1} \left(|d(i)|_{Q_{\mathrm{o}}}^2 + |v(i)|_{R_{\mathrm{o}}}^2 \right) \right). \qquad (4.29)
\end{aligned}
$$

From the combination of (4.28) and (4.29), we obtain

$$
\begin{aligned}
&|\tilde{x}_t(j) - x_t(j)|^2 \\
&\leq (j+1) L_{\mathrm{f}}^{2j} \eta_{\mathrm{o}}^{-N_t} \Bigg(\frac{1}{\lambda_{\min}(\underline{P}_{\mathrm{o}})} \Bigg(V_{\mathrm{o}}(\zeta_t, x(t - T_t))\eta_{\mathrm{o}}^{T_t} \\
&\quad + \sum_{i=t-T_t}^{t-N_t-1} \eta_{\mathrm{o}}^{t-i-1} \left(|d(i)|_{Q_{\mathrm{o}}}^2 + |v(i)|_{R_{\mathrm{o}}}^2 \right) \Bigg) + \frac{1}{\lambda_{\min}(Q_{\mathrm{o}})} \sum_{i=t-N_t}^{t-N_t+j-1} \eta_{\mathrm{o}}^{t-i-1} |d(i)|_{Q_{\mathrm{o}}}^2 \Bigg).
\end{aligned}
$$

Now, considering again (4.26) and using the definition of c_1 as stated in this lemma, we can conclude that

$$
\begin{aligned}
&|\tilde{y}_t(j) - y_t(j)|_{G_{\mathrm{s}}}^2 \\
&\leq 2c_1 \lambda_{\max}(G_{\mathrm{s}}) L_{\mathrm{h}}^2 \eta_{\mathrm{o}}^{-N_t} (j+1) L_{\mathrm{f}}^{2j} \\
&\quad \cdot \left(V_{\mathrm{o}}(\zeta_t, x(t - T_t))\eta_{\mathrm{o}}^{T_t} + \sum_{i=t-T_t}^{t-N_t+j} \eta_{\mathrm{o}}^{t-i-1} \left(|d(i)|_{Q_{\mathrm{o}}}^2 + |v(i)|_{R_{\mathrm{o}}}^2 \right) \right),
\end{aligned}
$$

where we note that the sum now includes the element $i = t - N_t + j$. Defining $\sigma : \mathbb{R}_{\geq 0} \to \mathbb{R}_{\geq 0}$ according to (4.22) leads to (4.21), which finishes this proof. □

We now provide an upper bound on the cost function in (4.12) evaluated at a suboptimal solution as defined in Definition 4.2 using the candidate solution in (4.19).

Lemma 4.3. *Suppose that Assumptions 4.1, 4.2, and 4.5 apply. Let $N \in \mathbb{I}_{\geq 0}$ and $T \in \mathbb{I}_{\geq N}$ be arbitrary. Then, the cost function in* (4.12) *evaluated at any suboptimal solution provided by the estimator from Definition 4.2 using the candidate solution in* (4.19) *satisfies*

$$
\begin{aligned}
&J(\hat{x}_t, \hat{d}_t, \hat{v}_t, \hat{y}_t, t) \\
&\leq \bar{\sigma}(N_t) \left(V_{\mathrm{o}}(\zeta_t, x(t - T_t))\eta_{\mathrm{o}}^{T_t} + \sum_{j=1}^{T_t} \eta_{\mathrm{o}}^{j-1} \left(|d(t-j)|_{Q_{\mathrm{o}}}^2 + |v(t-j)|_{R_{\mathrm{o}}}^2 \right) \right) \qquad (4.30)
\end{aligned}
$$

for all $t \in \mathbb{I}_{\geq 0}$*, where*

$$\bar{\sigma}(s) := s \cdot \sigma(s) \cdot \begin{cases} \frac{\bar{\eta}^s - L_{\mathrm{f}}^{2s}}{\bar{\eta} - L_{\mathrm{f}}^2}, & \bar{\eta} \neq L_{\mathrm{f}}^2 \\ s\bar{\eta}^{s-1}, & \bar{\eta} = L_{\mathrm{f}}^2, \end{cases} \qquad s \geq 0 \tag{4.31}$$

and $\sigma(s)$ *is from* (4.22)*.*

Proof. We start by employing the cost decrease condition in (4.15). By definition of the prior estimate in (4.18) and the candidate solution (in particular, the initial condition in (4.19a) and the zero-disturbances in (4.19b) and (4.19c)), it follows that

$$J(\hat{x}_t, \hat{d}_t, \hat{v}_t, \hat{y}_t, t) \leq J(\tilde{x}_t, \tilde{d}_t, \tilde{v}_t, \tilde{y}_t, t) \leq \sum_{j=0}^{N_t-1} \bar{\eta}^{N_t-j-1} |\tilde{y}_t(j) - y_t(j)|_{G_{\mathrm{s}}}^2$$

for all $t \in \mathbb{I}_{\geq 0}$. Applying Lemma 4.2 for each $j \in \mathbb{I}_{[0,N_t-1]}$ yields

$$\begin{aligned} &J(\hat{x}_t, \hat{d}_t, \hat{v}_t, \hat{y}_t, t) \\ &\leq \sigma(N_t) \sum_{j=0}^{N_t-1} \bar{\eta}^{N_t-j-1}(j+1) L_{\mathrm{f}}^{2j} \Bigg(V_{\mathrm{o}}(\zeta_t, x(t-T_t)) \eta_{\mathrm{o}}^{T_t} \\ &\qquad + \sum_{i=t-T_t}^{t-N_t+j} \eta_{\mathrm{o}}^{t-i-1} \left(|d(i)|_{Q_{\mathrm{o}}}^2 + |v(i)|_{R_{\mathrm{o}}}^2 \right) \Bigg). \end{aligned} \tag{4.32}$$

Here, note that the argument of the inner sum is independent of j; hence, we can simply enlarge the upper bound of summation to its maximum at $j = N_t - 1$ and move the complete term in large brackets in front of the outer sum. The remaining terms can be bounded as

$$\sum_{j=0}^{N_t-1} \bar{\eta}^{N_t-j-1}(j+1) L_{\mathrm{f}}^{2j} \leq N_t \bar{\eta}^{N_t-1} \sum_{j=0}^{N_t-1} (L_{\mathrm{f}}^2/\bar{\eta})^j. \tag{4.33}$$

Considering $\bar{\eta} \neq L_{\mathrm{f}}^2$, by application of the geometric series we further have that

$$\bar{\eta}^{N_t-1} \sum_{j=0}^{N_t-1} (L_{\mathrm{f}}^2/\bar{\eta})^j = \bar{\eta}^{N_t-1} \frac{1 - (L_{\mathrm{f}}^2/\bar{\eta})^{N_t}}{1 - (L_{\mathrm{f}}^2/\bar{\eta})} = \frac{\bar{\eta}^{N_t} - L_{\mathrm{f}}^{2N_t}}{\bar{\eta} - L_{\mathrm{f}}^2}. \tag{4.34}$$

By applying (4.33), (4.34), and the definition of $\bar{\sigma}$ in (4.31) to (4.32), we obtain (4.30) (the remaining case where $\bar{\eta} = L_{\mathrm{f}}^2$ follows by direct computation), which concludes this proof. □

The following proposition provides a multi-step Lyapunov characterization of robust stability for suboptimal MHE.

Proposition 4.2. *Suppose that Assumptions 4.1, 4.2, 4.3, 4.4, and 4.5 apply. Let* $N \in \mathbb{I}_{\geq 0}$ *and* $T \in \mathbb{I}_{\geq N}$ *be arbitrary. Then, the suboptimal estimator from Definition 4.2 using the candidate solution in* (4.19) *satisfies*

$$\begin{aligned} U(\hat{x}(t), x(t)) \leq\ & C(N_t) \eta_{\mathrm{o}}^{T_t} U(\zeta_t, x(t-T_t)) \\ & + \sum_{j=1}^{T_t} \eta_{\mathrm{o}}^{j-1} \left(|d(t-j)|_{Q(N_t)}^2 + |v(t-j)|_{R(N_t)}^2 \right) \end{aligned} \tag{4.35}$$

for all $t \in \mathbb{I}_{\geq 0}$*, where*

$$C(s) := (2 + \bar{\sigma}(s))\lambda_{\max}(\overline{P}_{\mathrm{o}}, \underline{P}_{\mathrm{s}}), \ s \geq 0, \tag{4.36a}$$

$$Q(s) := (2 + \bar{\sigma}(s))Q_{\mathrm{o}} + 2Q_{\mathrm{s}}, \ s \geq 0, \tag{4.36b}$$

$$R(s) := (2 + \bar{\sigma}(s))R_{\mathrm{o}} + 2R_{\mathrm{s}}, \ s \geq 0 \tag{4.36c}$$

with $\bar{\sigma}$ *as defined in* (4.31)*.*

Proof. Consider any $t \in \mathbb{I}_{\geq 0}$ and the true sequences x_t, d_t, and v_t restricted to the estimation horizon as defined in (4.23)–(4.25). Since both the true and the estimated trajectory are trajectories of the system (4.1) evolving in $\mathcal{Z}$, we can describe their difference at any $t \in \mathbb{I}_{\geq 0}$ by evaluating the i-IOSS Lyapunov function from Assumption 4.3. Specifically, applying the dissipation inequality (4.8b) recursively for N_t times yields

$$\begin{aligned} &U(\hat{x}_t(N_t), x_t(N_t)) \\ &\leq \eta_{\mathrm{s}}^{N_t} U(\hat{x}_t(0), x_t(0)) \\ &\quad + \sum_{j=0}^{N_t-1} \eta_{\mathrm{s}}^{N_t-j-1} \Big(|\hat{d}_t(j) - d_t(j)|_{Q_{\mathrm{s}}}^2 + |\hat{v}_t(j) - v_t(j)|_{R_{\mathrm{s}}}^2 + |\hat{y}_t(j) - y_t(j)|_{G_{\mathrm{s}}}^2 \Big) \end{aligned} \tag{4.37}$$

for all $t \in \mathbb{I}_{\geq 0}$. By application of the upper bound in (4.8a) together with Cauchy-Schwarz and Young's inequality, we obtain that

$$\begin{aligned} U(\hat{x}_t(0), x_t(0)) &\leq |\hat{x}_t(0) - x_t(0)|_{\overline{P}_{\mathrm{s}}}^2 \\ &\leq 2|\hat{x}_t(0) - \bar{x}(t - N_t)|_{\overline{P}_{\mathrm{s}}}^2 + 2|\bar{x}(t - N_t) - x_t(0)|_{\overline{P}_{\mathrm{s}}}^2. \end{aligned} \tag{4.38}$$

Similarly, we have that

$$|\hat{d}_t(j) - d_t(j)|_{Q_{\mathrm{s}}}^2 \leq 2|\hat{d}_t(j)|_{Q_{\mathrm{s}}}^2 + 2|d_t(j)|_{Q_{\mathrm{s}}}^2 \tag{4.39}$$

and

$$|\hat{v}_t(j) - v_t(j)|_{R_{\mathrm{s}}}^2 \leq 2|\hat{v}_t(j)|_{R_{\mathrm{s}}}^2 + 2|v_t(j)|_{R_{\mathrm{s}}}^2 \tag{4.40}$$

for all $j \in \mathbb{I}_{[0,N_t-1]}$. Hence, from (4.37) with (4.38)–(4.40) and the definition of the cost function in (4.12), we obtain

$$\begin{aligned} U(\hat{x}_t(N_t), x_t(N_t)) \leq{}& 2\eta_{\mathrm{s}}^{N_t} |\bar{x}(t - N_t) - x_t(0)|_{\overline{P}_{\mathrm{s}}}^2 \\ &+ \sum_{j=0}^{N_t-1} \eta_{\mathrm{s}}^{N_t-j-1} \left(2|d_t(j)|_{Q_{\mathrm{s}}}^2 + 2|v_t(j)|_{R_{\mathrm{s}}}^2 \right) + J(\hat{x}_t, \hat{d}_t, \hat{v}_t, \hat{y}_t, t). \end{aligned} \tag{4.41}$$

By definition of the prior in (4.18) and the compatibility property from Assumption 4.4, the first term of the right-hand side in (4.41) can be bounded by invoking Lemma 4.1, which yields

$$\begin{aligned} &\eta_{\mathrm{s}}^{N_t} |\bar{x}(t - N_t) - x_t(0)|_{\overline{P}_{\mathrm{s}}}^2 \\ &\leq \eta_{\mathrm{s}}^{N_t} |z_t(T_t - N_t) - x(t - N_t)|_{\underline{P}_{\mathrm{o}}}^2 \\ &\leq V_{\mathrm{o}}(\zeta_t, x(t - T_t)) \eta_{\mathrm{o}}^{T_t} + \sum_{j=t-T_t}^{t-N_t-1} \eta_{\mathrm{o}}^{t-j-1} \left(|d(j)|_{Q_{\mathrm{o}}}^2 + |v(j)|_{R_{\mathrm{o}}}^2 \right). \end{aligned} \tag{4.42}$$

Here, we note that

$$V_{\mathrm{o}}(\hat{x},x) \leq |\hat{x}-x|^2_{\overline{P}_{\mathrm{o}}} \leq \lambda_{\max}(\overline{P}_{\mathrm{o}},\underline{P}_{\mathrm{s}})|\hat{x}-x|^2_{\underline{P}_{\mathrm{s}}} \leq \lambda_{\max}(\overline{P}_{\mathrm{o}},\underline{P}_{\mathrm{s}})U(\hat{x},x) \tag{4.43}$$

for all $\hat{x},x \in \mathcal{X}$. Consequently, from (4.41) and (4.42), the application of Lemma 4.3, and (4.43), we obtain (4.35) with C,Q,R as defined in (4.36), which finishes this proof. □

Now, provided that T satisfies

$$\rho^T := C(N)\eta_{\mathrm{o}}^T < 1, \tag{4.44}$$

Proposition 4.2 implies (by the definition of ζ_t in (4.16)) that the i-IOSS Lyapunov function U from Assumption 4.3 is a T-step ISS-like Lyapunov function for suboptimal MHE, satisfying

$$U(\hat{x}(t),x(t)) \leq \rho^T U(\hat{x}(t-T),x(t-T)) + \sum_{j=1}^{T} \eta_{\mathrm{o}}^{j-1}\left(|d(t-j)|^2_{Q(N)} + |v(t-j)|^2_{R(N)}\right)$$

for all $t \in \mathbb{I}_{\geq T}$. Here, we want to emphasize that, for each fixed $N \in \mathbb{I}_{\geq 0}$, there always exists T large enough such that (4.44) is satisfied. Clearly, Proposition 4.2 implies RGES of suboptimal MHE, which we show next.

Theorem 4.1. *Suppose that Assumptions 4.1, 4.2, 4.3, 4.4, and 4.5 apply. Fix some $N \in \mathbb{I}_{\geq 0}$ and let $T \in \mathbb{I}_{\geq N}$ be such that condition* (4.44) *is satisfied. Then, the suboptimal estimator from Definition 4.2 using the candidate solution* (4.19) *is RGES according to Definition 4.1.*

Proof. Define $Q = Q(N)$ and $R = R(N)$. From Proposition 4.2 and the contraction condition (4.44), it follows that

$$\begin{aligned} U(\hat{x}(t+T),x(t+T)) \leq\ & U(\hat{x}(t),x(t))\rho^T \\ & + \sum_{j=1}^{T} \rho^{j-1}(|d(t+T-j)|^2_Q + |v(t+T-j)|^2_R) \end{aligned}$$

for $t \in \mathbb{I}_{\geq 0}$. Recursive application of the previous bound yields

$$\begin{aligned} U(\hat{x}(t+kT),x(t+kT)) \leq\ & U(\hat{x}(t),x(t))\rho^{kT} \\ & + \sum_{j=1}^{kT} \rho^{j-1}\left(|d(t+kT-j)|^2_Q + |v(t+kT-j)|^2_R\right) \end{aligned}$$

for all $t \in \mathbb{I}_{[0,T-1]}$ and all $k \in \mathbb{I}_{\geq 0}$. For $t \in \mathbb{I}_{[0,T-1]}$, by applying the same steps as in the proof of Proposition 4.2 but using only the first inequality in (4.43), it follows that

$$U(\hat{x}(t),x(t)) \leq (2+\bar{\sigma}(N))\rho^t|\hat{\chi}-\chi|^2_{\overline{P}_{\mathrm{o}}} + \sum_{j=1}^{t} \rho^{j-1}\left(|d(t-j)|^2_Q + |v(t-j)|^2_R\right).$$

By combining the previous inequalities and using the lower bound in (4.8a), we hence obtain

$$|\hat{x}(t) - x(t)|^2_{\underline{P}_\mathrm{s}} \leq (2 + \bar{\sigma}(N))\rho^t |\hat{\chi} - \chi|^2_{\overline{P}_\mathrm{o}} + \sum_{j=1}^{t} \rho^{j-1} \left(|d(t-j)|^2_Q + |v(t-j)|^2_R \right) \tag{4.45}$$

for all $t \in \mathbb{I}_{\geq 0}$. By using the fact that $\underline{P}_\mathrm{s}, \overline{P}_\mathrm{o}, Q, R$ are positive definite matrices that can be bounded using their respective eigenvalues, taking the square root, and exploiting subadditivity, it is easy to see that (4.45) corresponds to RGES in a sum-based form. From Proposition 4.1, this is equivalent to RGES in the sense of Definition 4.1 (in a max-based form), which concludes this proof. □

Remark 4.5 (Horizon length)**.** *We want to emphasize that under the conditions of Theorem 4.1, the proposed suboptimal estimator is RGES for* any *choice of $N \in \mathbb{I}_{\geq 0}$; in other words, there is no minimum required horizon length as it is the case in, e.g., [Mül17; KM18; RMD20; AR19b; AR21; KM23; Hu24]. This is due to the fact that we do not require contraction of the estimation error from time $t-N$ to the current time t, but establish stability by exploiting the contracting behavior of the auxiliary observer (Assumption 4.2) from time $t-T$ to $t-N$.*

Remark 4.6 (Re-initializing the auxiliary observer)**.** *Note that the re-initialization and forward simulation of the auxiliary observer as suggested in* (4.16) *and* (4.17) *(i.e., Step 2 in the algorithm outlined below Remark 4.4) is required to compute the prior* (4.18) *and the candidate solution* (4.19)*. To save computation time, however, it is also possible to initialize the auxiliary observer only once at time $t = 0$, thus avoiding its repeated re-initialization. This is a special case of the proposed suboptimal MHE scheme with $T = t$ and was also considered in our work [SKM21]. The corresponding estimation error can be directly bounded using the Lyapunov decrease property in* (4.35)*, which reveals that, not very surprisingly, suboptimal MHE is RGES for $T = t$ and any value of $N \in \mathbb{I}_{\geq 0}$. We point out that the decay rate of the estimation error then takes the theoretically best possible value. In contrast, considering a fixed, sufficiently large constant T in* (4.44) *results in a worse decay rate and a slightly more computationally intensive scheme. In practice, however, much better estimation results are to be expected since improved suboptimal estimates are used to re-initialize the auxiliary observer, thus introducing additional feedback into the suboptimal estimator. This can lead to much faster recovery from a poor initial guess, as also illustrated by the simulation example in Section 4.2.6.*

4.2.3. Systems subject to additive process disturbances

We now construct a second candidate solution based on the entire trajectory of the auxiliary observer within the estimation horizon, which therefore also includes the most recent observer estimates. This more sophisticated approach allows us to avoid many conservative arguments applied in the proof of Lemma 4.2, which, as we will show below and discuss in more detail in Section 4.2.4, leads to improved theoretical

guarantees (especially in combination with a discounted cost function using $\bar{\eta} < 1$). To this end, we have to strengthen the conditions on the considered class of nonlinear systems and auxiliary observer to ensure that the auxiliary observer forms a valid system trajectory. In particular, we impose one-step controllability of the dynamics in (4.1a) with respect to the process disturbance (compare [KMA21, Rem. 2]) and consider an auxiliary observer given in output injection form [KM20; SW97].

Assumption 4.6 (Additive disturbances)**.** *The system dynamics in* (4.1a) *satisfy* $f(x, u, d) = f_{\mathrm{n}}(x, u) + d$.

Assumption 4.7 (Full-order state observer)**.** *The observer dynamics in* (4.5) *satisfy* $g(z, u, y) = f_{\mathrm{n}}(z, u) + k(z, u, h_{\mathrm{n}}(z, u) - y)$ *with the output injection law* $k : \mathbb{R}^n \times \mathbb{R}^m \times \mathbb{R}^p \to \mathbb{R}^n$, *where* $k(\cdot, \cdot, 0) = 0$. *Moreover, there exists some constant* $\kappa > 0$ *such that the injection law can be uniformly linearly bounded by* $|k(z, u, h_{\mathrm{n}}(z, u) - y)| \leq \kappa |h_{\mathrm{n}}(z, u) - y|$ *for all* $z \in \mathcal{O}$, $u \in \mathcal{U}$, $y \in \mathcal{Y}$.

Remark 4.7 (Full-order state observer)**.** *Assumption 4.7 consists of two parts. First, it requires that the auxiliary observer is a full-order state observer in output injection form, compare [KM20; SW97]. Note that this is not restrictive, since from [KM20, Lem. 2] and [SW97, Lem. 21] it follows that any robustly stable full-order state observer must in fact have this form. The second part states a linear bound on the injection law* k *depending on the current fitting error of the observer. Although this linear bound can be restrictive, we note that this is directly satisfied for any observer that utilizes the injection law* $k(z, u, h_{\mathrm{n}}(z, u) - y) = K(z, u) \cdot (h_{\mathrm{n}}(z, u) - y)$, *where* $K : \mathbb{R}^n \times \mathbb{R}^m \to \mathbb{R}^{n \times p}$ *forms a matrix that can be uniformly bounded on* $\mathcal{O} \times \mathcal{U}$. *This is the case for nonlinear Luenberger- or Kalman-like observers (see, for example, [GHO92; GK94; ZB13; BŢ07]) and can also be satisfied for the EKF under uniform observability and boundedness conditions, compare [RU99].*

For ease of notation, in the following we employ the definition

$$k_t(j) := k(z_t(j), u(t - T_t + j), h_{\mathrm{n}}(z_t(j), u(t - T_t + j)) - y(t - T_t + j))$$

for all $j \in \mathbb{I}_{[0, T_t - 1]}$ and $t \in \mathbb{I}_{\geq 0}$. Provided that Assumptions 4.6 and 4.7 hold, the dynamics of the system and the observer share the same structure, which allows us to interpret the terms $f_{\mathrm{n}}(z, u)$ and k of the observer dynamics directly as estimates of the terms $f_{\mathrm{n}}(x, u)$ and d of the system dynamics. We hence choose the candidate solution

$$\tilde{x}_t(j) = z_t(T_t - N_t + j), \ j \in \mathbb{I}_{[0, N_t]}, \tag{4.46a}$$

$$\tilde{d}_t(j) = k_t(T_t - N_t + j), \ j \in \mathbb{I}_{[0, N_t - 1]}, \tag{4.46b}$$

$$\tilde{v}_t(j) = 0, \ j \in \mathbb{I}_{[0, N_t - 1]}, \tag{4.46c}$$

which yields the outputs $\tilde{y}_t(j) = h(\tilde{x}_t(j), u_t(j), \tilde{v}_t(j))$ for all $j \in \mathbb{I}_{[0, N_t - 1]}$ and $t \in \mathbb{I}_{\geq 0}$ under (4.11c). Here, note that in case of $\mathcal{D} \subset \mathbb{R}^n$, we assume that $k_t(T_t - N_t + j) \in \mathcal{D}$ for all $j \in \mathbb{I}_{[0, N_t - 1]}$ and $t \in \mathbb{I}_{\geq 0}$ to ensure feasibility of the candidate solution.

To derive robust stability guarantees for the resulting suboptimal estimator (Definition 4.2), we again start by establishing a bound on the fitting error achieved by the candidate solution in (4.46).

Lemma 4.4. *Suppose that Assumptions 4.1, 4.2, 4.6, and 4.7 apply. Let $N \in \mathbb{I}_{\geq 0}$ and $T \in \mathbb{I}_{\geq N}$ be arbitrary. Then, the fitting error of the trajectory defined by the candidate solution* (4.46) *satisfies*

$$\begin{aligned} &|\tilde{y}_t(j) - y_t(j)|_{G_\mathrm{s}}^2 \\ &\leq c_2 \eta_\mathrm{o}^{-(N_t-j-1)} \left(V_\mathrm{o}(\zeta_t, x(t-T_t))\eta_\mathrm{o}^{T_t} + \sum_{i=t-T_t}^{t-N_t+j} \eta_\mathrm{o}^{t-i-1} \left(|d(i)|_{Q_\mathrm{o}}^2 + |v(i)|_{R_\mathrm{o}}^2 \right) \right) \end{aligned} \tag{4.47}$$

for all $j \in \mathbb{I}_{[0,N_t-1]}$ and $t \in \mathbb{I}_{\geq 0}$, where

$$c_2 = 2\lambda_{\max}(G_\mathrm{s}) L_\mathrm{h}^2 \max\left\{1, \lambda_{\min}(\underline{P}_\mathrm{o})^{-1}, \lambda_{\min}(R_\mathrm{o})^{-1}\right\}. \tag{4.48}$$

Proof. Due to Assumptions 4.6 and 4.7 and the candidate solution in (4.46), it follows that $\tilde{x}_t(j) = z_t(T_t - N_t + j)$ for all $j \in \mathbb{I}_{[0,N_t-1]}$ and $t \in \mathbb{I}_{\geq 0}$. Hence, the application of Assumption 4.1 together with the fact that $\tilde{v}_t(j) = 0$ for $j \in \mathbb{I}_{[0,N_t-1]}$ by (4.46c) and the boundedness property of V_o from (4.6a) yields

$$\begin{aligned} &|\tilde{y}_t(j) - y_t(j)|_{G_\mathrm{s}}^2 \\ &\leq 2\lambda_{\max}(G_\mathrm{s}) L_\mathrm{h}^2 \left(|z_t(T_t - N_t + j) - x(t - N_t + j)|^2 + |v(t - N_t + j)|^2 \right) \\ &\leq \frac{2\lambda_{\max}(G_\mathrm{s}) L_\mathrm{h}^2}{\lambda_{\min}(\underline{P}_\mathrm{o})} V_\mathrm{o}(z_t(T_t - N_t + j), x(t - N_t + j)) + \frac{2\lambda_{\max}(G_\mathrm{s}) L_\mathrm{h}^2}{\lambda_{\min}(R_\mathrm{o})} |v(t - N_t + j)|_{R_\mathrm{o}}^2 \\ &\leq c_2 \left(V_\mathrm{o}(z_t(T_t - N_t + j), x(t - N_t + j)) + |v(t - N_t + j)|_{R_\mathrm{o}}^2 \right), \end{aligned}$$

where in the last inequality we have used the definition of c_2 from (4.48). Since the auxiliary observer is RGES by Assumption 4.2, we can invoke Lemma 4.1, which leads to

$$\begin{aligned} &|\tilde{y}_t(j) - y_t(j)|_{G_\mathrm{s}}^2 \\ &\leq c_2 \Bigg(V_\mathrm{o}(\zeta_t, x(t-T_t))\eta_\mathrm{o}^{T_t - N_t + j} \\ &\qquad + \sum_{i=0}^{T_t - N_t + j - 1} \eta_\mathrm{o}^{T_t - N_t + j - i - 1} \left(|d(t - T_t + i)|_{Q_\mathrm{o}}^2 + |v(t - T_t + i)|_{R_\mathrm{o}}^2 \right) \\ &\qquad + |v(t - N_t + j)|_{R_\mathrm{o}}^2 \Bigg). \end{aligned}$$

By multiplying the sum by $1 = \eta_\mathrm{o}/\eta_\mathrm{o}$ and using the fact that $1/\eta_\mathrm{o} > 1$, we can move

the term $|v(t-N_t+j)|_{R_\mathrm{o}}^2$ into the sum, which yields

$$\begin{aligned}
&|\tilde{y}_t(j)-y_t(j)|_{G_\mathrm{s}}^2 \\
&\leq c_2\eta_\mathrm{o}^{-(N_t-j-1)}\Bigg(V_\mathrm{o}(\zeta_t,x(t-T_t))\eta_\mathrm{o}^{T_t} \\
&\qquad + \sum_{i=0}^{T_t-N_t+j}\eta_\mathrm{o}^{T_t-i-1}\left(|d(t-T_t+i)|_{Q_\mathrm{o}}^2+|v(t-T_t+i)|_{R_\mathrm{o}}^2\right)\Bigg). \quad (4.49)
\end{aligned}$$

A simple change of coordinates shows that (4.49) is equivalent to (4.47), which concludes this proof. □

The following result shows that the i-IOSS Lyapunov function U from Assumption 4.3 is a T-step Lyapunov function for suboptimal MHE, similar to Proposition 4.2.

Proposition 4.3. *Suppose that Assumptions 4.1, 4.2, 4.3, 4.4, 4.6, and 4.7 apply. Let $N \in \mathbb{I}_{\geq 0}$ and $T \in \mathbb{I}_{\geq N}$ be arbitrary. Then, the suboptimal estimator from Definition 4.2 with the candidate solution in* (4.46) *satisfies the property in* (4.35) *for all $t \in \mathbb{I}_{\geq 0}$, where C, Q, R are from* (4.36) *with*

$$\bar{\sigma}(s)=\left(1+\frac{2\lambda_{\max}(Q_\mathrm{s})\kappa^2}{\lambda_{\min}(G_\mathrm{s})}\right)c_2\cdot\begin{cases}\frac{1-\left(\frac{\bar{\eta}}{\eta_\mathrm{o}}\right)^s}{1-\frac{\bar{\eta}}{\eta_\mathrm{o}}}, & \frac{\bar{\eta}}{\eta_\mathrm{o}}\neq 1\\ s, & \frac{\bar{\eta}}{\eta_\mathrm{o}}=1\end{cases},\ s\geq 0. \quad (4.50)$$

Proof. Consider an arbitrary time instant $t \in \mathbb{I}_{\geq 0}$ and the cost decrease condition in (4.15). By applying the candidate solution (4.46), the prior estimate in (4.18), and the definition of the stage cost in (4.14), we obtain

$$J(\hat{x}_t,\hat{d}_t,\hat{v}_t,\hat{y}_t,t)\leq J(\tilde{x}_t,\tilde{d}_t,\tilde{v}_t,\tilde{y}_t,t)\leq\sum_{i=0}^{N_t-1}\bar{\eta}^{N_t-j-1}\left(2|\tilde{d}_t(j)|_{Q_\mathrm{s}}^2+|\tilde{y}_t(j)-y_t(j)|_{G_\mathrm{s}}^2\right). \quad (4.51)$$

Here, from the definition of the candidate solution in (4.46) and Assumption 4.7, it follows that

$$\begin{aligned}
|\tilde{d}_t(j)|_{Q_\mathrm{s}}^2 &\leq \lambda_{\max}(Q_\mathrm{s})|k_t(T_t-N_t+j)|^2\\
&\leq \lambda_{\max}(Q_\mathrm{s})\kappa^2|h_\mathrm{n}(z_t(T_t-N_t+j),u_t(j))-y_t(j)|^2\\
&= \lambda_{\max}(Q_\mathrm{s})\kappa^2|\tilde{y}_t(j)-y_t(j)|^2\\
&\leq \frac{\lambda_{\max}(Q_\mathrm{s})\kappa^2}{\lambda_{\min}(G_\mathrm{s})}|\tilde{y}_t(j)-y_t(j)|_{G_\mathrm{s}}^2.
\end{aligned}$$

Thus, (4.51) leads to

$$J(\hat{x}_t,\hat{d}_t,\hat{v}_t,\hat{y}_t,t)\leq\left(1+\frac{2\lambda_{\max}(Q_\mathrm{s})\kappa^2}{\lambda_{\min}(G_\mathrm{s})}\right)\sum_{j=0}^{N_t-1}\bar{\eta}^{N_t-j-1}|\tilde{y}_t(j)-y_t(j)|_{G_\mathrm{s}}^2. \quad (4.52)$$

By applying Lemma 4.4, we further obtain that

$$\begin{aligned}
&J(\hat{x}_t, \hat{d}_t, \hat{v}_t, \hat{y}_t, t) \\
&\leq \left(1 + \frac{2\lambda_{\max}(Q_{\mathrm{s}})\kappa^2}{\lambda_{\min}(G_{\mathrm{s}})}\right) c_2 \sum_{j=0}^{N_t-1} \left(\frac{\bar{\eta}}{\eta_{\mathrm{o}}}\right)^{N_t-j-1} \\
&\quad \cdot \left(V_{\mathrm{o}}(\zeta_t, x(t-T_t))\eta_{\mathrm{o}}^{T_t} + \sum_{i=t-T_t}^{t-N_t+j} \eta_{\mathrm{o}}^{t-i-1} \left(|d(i)|_{Q_{\mathrm{o}}}^2 + |v(i)|_{R_{\mathrm{o}}}^2\right)\right).
\end{aligned}$$

Now, we enlarge the inner sum by considering $j = N_t - 1$ in the upper bound of summation, which renders the inner sum independent of the outer one. Then, we define $\bar{\sigma}$ as in (4.50), which leads to the upper bound on the suboptimal cost $J(\hat{x}_t, \hat{d}_t, \hat{v}_t, \hat{y}_t, t)$ as defined in (4.30). The remaining part of this proof follows by using exactly the same steps that we applied in the proof of Proposition 4.2 (with $\bar{\sigma}$ from (4.50)). □

Proposition 4.3 provides a T-step ISS-like Lyapunov function for suboptimal MHE (compare the discussion below Proposition 4.2), from which we can directly infer RGES.

Theorem 4.2. *Suppose that Assumptions 4.1, 4.2, 4.3, 4.4, 4.6, and 4.7 apply. Fix some $N \in \mathbb{I}_{\geq 0}$ and let $T \in \mathbb{I}_{\geq N}$ be such that condition* (4.44) *is satisfied. Then, the suboptimal estimator from Definition 4.2 using the candidate solution in* (4.46) *is RGES according to Definition 4.1.*

Proof. Pick some $T \in \mathbb{I}_{\geq N}$ such that the condition in (4.44) is satisfied. The statement follows by applying the same steps as in the proof of Theorem 4.1 (with C, Q, R as defined in (4.36) using $\bar{\sigma}$ from (4.50)). □

Remark 4.8 (Uniform bounds)**.** *If the tuning parameter $\bar{\eta}$ is chosen such that $\bar{\eta} < \eta_{\mathrm{o}}$ (which is always[3] possible), then $\bar{\sigma}(s)$ in* (4.50) *can be uniformly bounded for all $s \geq 0$. In this case, the parameters C, Q, R as defined in Proposition 4.3 also turn out to be uniform in N, which consequently also applies to the disturbance gains C_1, C_2, C_3 determining the bound on the estimation error provided by Theorem 4.2 (i.e., RGES). Therefore, the choice of $\bar{\eta} < \eta_{\mathrm{o}}$ recovers the advantageous property of time-discounted cost function designs (compare, for example, [KM23; Hu24]), providing an error bound that does not deteriorate when increasing the horizon length N, see also the discussion in Section 3.3.*

We note the following corollary from Theorem 4.2, where we consider a suboptimal version of FIE.

Corollary 4.1. *Let the conditions of Theorem 4.2 hold and assume that $\bar{\eta} < \eta_{\mathrm{o}}$. Then, (suboptimal) FIE (i.e., the estimator from Definition 4.2 with $N = t$) using the candidate solution* (4.46) *with $T = N = t$ is RGES.*

[3] This is immediately true if $\eta_{\mathrm{s}} < \eta_{\mathrm{o}}$ (as η_{s} defines the lower bound on the tuning parameter $\bar{\eta}$). In case of $\eta_{\mathrm{s}} = \eta_{\mathrm{o}}$ (which we also allow by Assumption 4.4), one can easily find some $\tilde{\eta}_{\mathrm{o}} \in (\eta_{\mathrm{o}}, 1)$ and replace every η_{o} by $\tilde{\eta}_{\mathrm{o}}$, which again allows for choosing $\bar{\eta}$ such that $\eta_{\mathrm{s}} \leq \bar{\eta} < \tilde{\eta}_{\mathrm{o}}$ is satisfied.

Table 4.1. Summary the different MHE setups considered in Sections 4.2.2 and 4.2.3.

System	Candidate solution	Result	Scaling factor
$f(x,u,d)$	system trajectory (4.19)	Thm. 4.1	$N\eta_{\mathrm{o}}^{-N}\frac{\bar{\eta}^N-L_{\mathrm{f}}^{2N}}{\bar{\eta}-L_{\mathrm{f}}^2},\ \bar{\eta}\neq L_{\mathrm{f}}^2$
$f_{\mathrm{n}}(x,u)+d$	observer trajectory (4.46)	Thm. 4.2	$\frac{1-(\bar{\eta}/\eta_{\mathrm{o}})^N}{1-(\bar{\eta}/\eta_{\mathrm{o}})},\ \bar{\eta}\neq\eta_{\mathrm{o}}$

Proof. The statement directly follows from the fact that suboptimal FIE is a special case of the proposed suboptimal MHE scheme (with $T_t = N_t = t$). Since $\bar{\eta} < \eta_{\mathrm{o}}$ holds by assumption, the parameters C, Q, R in Proposition 4.3 can be rendered uniform in N, see Remark 4.8. Specifically, the property in (4.35) with $T_t = N_t = t$, the matrices C, Q, R from (4.36) with $\bar{\sigma}$ replaced by $\bar{\sigma}_\infty := \lim_{s\to\infty}\bar{\sigma}(s)$ and $\bar{\sigma}(s)$ from (4.50) provides a valid bound on the estimation error of (suboptimal) FIE for all $t \in \mathbb{I}_{\geq 0}$, from which RGES (Definition 4.1) can be directly inferred (see the last part of the proof of Theorem 4.1). □

4.2.4. Discussion

Table 4.1 summarizes the main characteristics of the suboptimal MHE schemes presented in Sections 4.2.2 and 4.2.3. Here, the first column shows the class of systems to which the candidate solution in the second column is applicable, the third column refers to the corresponding result establishing RGES of suboptimal MHE, and the last column shows a scaling factor appearing in the disturbance gains C_1, C_2, C_3 (compare Definition 4.1) to indicate their dependency on the horizon length N and the tuning parameter $\bar{\eta}$.

As can be seen from the first row of Table 4.1, the use of the candidate solution (4.19) allows for considering general nonlinear systems. However, since only a single state estimate of the auxiliary observer is considered for the construction of the candidate solution (to form its initial state) and otherwise the nominal system dynamics are employed, many overly conservative steps had to be applied, especially in the proof of Lemma 4.2. This particularly refers to (i) the recursive application of the Lipschitz property of f (which results in a dependency on L_{f}^N); (ii) the fact that we can exploit the stability property of the observer only once but want to establish RGES with exponentially discounted disturbances (resulting in the factor η_{o}^{-N}); (iii) the fact that we aim for a bound in terms of a sum of squares (instead of a squared sum), which results in the factor N from the application of Jensen's inequality. Here, the improvement obtained by using a discounted cost function design ($\bar{\eta} < 1$) is negligible, as the exponential dependency on N remains.

By strengthening the requirements on the setting (considering additive disturbances in Assumption 4.6 and a full-order state observer involving a linearly bounded output injection law in Assumption 4.7), we can construct a more sophisticated candidate solution in (4.46) based on the entire trajectory of the auxiliary observer within the estimation horizon, see the second row in Table 4.1. Since more recent observer

estimates are thus also taken into account, we can avoid the repeated use of the Lipschitz property of f and Jensen's inequality. This results in disturbance gains that depend on the ratio $\bar{\eta}/\eta_{\mathrm{o}}$, that is, we obtain linear growth in N when $\bar{\eta} = \eta_{\mathrm{o}}$ and exponential growth when $\bar{\eta} > \eta_{\mathrm{o}}$. However, in the case of $\bar{\eta} < \eta_{\mathrm{o}}$, the disturbance gains approach a fixed value for $N \to \infty$, thus applying uniformly for all $N \in \mathbb{I}_{\geq 0}$, see Remark 4.8. Overall, this setup together with the choice of $\bar{\eta} < \eta_{\mathrm{o}}$ provides the potentially least conservative error bound of the suboptimal MHE methods considered here (depending on the constants involved).

4.2.5. Auxiliary observers leaving the domain of the system

Until now, we assumed that the auxiliary observer in (4.5) evolves in $\mathcal{X}$ by imposing that $\mathcal{O} = \mathcal{X}$, which was necessary to ensure that the candidate solutions in (4.19) and (4.46) result in valid system trajectories that satisfy the MHE constraints in (4.11d) and (4.11e). However, it is well-known that state observers in the form of (4.5) do not necessarily provide physically plausible estimates and hence may leave a corresponding set $\mathcal{X}$ due to transient dynamics or external perturbations (consider, for example, the peaking phenomenon in high-gain observers [KP13]). This is a general weakness of conventional observer designs, which may lead to a lack of accuracy, implementation problems, or, in the worst case, to the destabilization of the system in output feedback designs, compare [Ast+21]. Here, a key advantage of optimization-based state estimation methods (such as MHE) becomes apparent, where such constraints can be naturally taken into account. In order to maintain this feature with the previously developed suboptimal MHE methods, we have to suitably adapt the candidate solutions and prior estimate to account for an auxiliary observer that may violate the constraints.

In the following, we therefore consider $\mathcal{O} \supset \mathcal{X}$, where we assume that $\mathcal{X}$ is convex. To render the candidate solutions (4.19) and (4.46) feasible, one could apply the redesign strategy proposed in [Ast+21] to ensure that the modified auxiliary observer satisfies the constraints. However, this severely limits the set of possible observers to a particular method and does not allow for user-defined customization. Instead, we use the projection function $\mathrm{p}_{\mathcal{X}} : \mathbb{R}^n \to \mathcal{X}$ to project the observer state z onto the set $\mathcal{X}$, which can be defined as

$$p_{\mathcal{X}}(z) := \arg\min_{x \in \mathcal{X}} |z - x|. \tag{4.53}$$

Associated with the auxiliary observer (4.17), we furthermore define the *projection error* (that is, the difference between the observer state and its projection):

$$\varepsilon_t(t-j) := z_t(T_t - j) - \mathrm{p}_{\mathcal{X}}(z_t(T_t - j)),\ j \in \mathbb{I}_{[0,T_t]},\ t \in \mathbb{I}_{\geq 0}. \tag{4.54}$$

Here, note that $\varepsilon_t(t-j) = 0$ if $z_t(T_t - j) \in \mathcal{X}$. We aim to show the following property of suboptimal MHE.

Definition 4.3 (ε-RGES)**.** *A (suboptimal) moving horizon estimator for the system in* (4.1) *is ε-RGES if there exist constants $C_1, C_2, C_3, C_\epsilon > 0$ and $\rho \in (0,1)$ such*

that the resulting state estimate $\hat{x}(t)$ *with* $\hat{x}(0) = \hat{\chi}$ *satisfies*

$$|\hat{x}(t) - x(t)| \leq \max\Big\{C_1\rho^t|\hat{\chi} - \chi|, \max_{j\in\mathbb{I}_{[0,t-1]}} C_2\rho^{t-j-1}|d(j)|, \max_{j\in\mathbb{I}_{[0,t-1]}} C_3\rho^{t-j-1}|v(j)|, \max_{j\in\mathbb{I}_{[0,t-1]}} C_\varepsilon\rho^{t-j-1}|\varepsilon_{\tau(j)}(j)|\Big\} \tag{4.55}$$

for all $t \in \mathbb{I}_{\geq 0}$*, all initial conditions* $\hat{\chi}, \chi \in \mathcal{X}$*, and all disturbance sequences* $d \in \mathcal{D}^\infty$ *and* $v \in \mathcal{V}^\infty$*, where* $\tau(j) := t - \lfloor\frac{t-j}{T}\rfloor T$*.*

Remark 4.9 (ε-RGES)**.** *The property in* (4.55) *defines a slightly modified version of the stability notion given in Definition 4.1 that incorporates an additional disturbance term induced by the projection error* ε*. If satisfied, it directly reveals that the influence of the projection error is bounded and decays over time. Note that by Assumption 4.2, the estimation error of the observer converges to a neighborhood of the origin for* $t \to \infty$*. Hence, if the true system state evolves in the interior of* $\mathcal{X}$ *and if the true disturbances* d *and* v *are small enough, there exists some* t^* *such that* $z(t) \in \mathcal{X}$ *for all* $t \in \mathbb{I}_{\geq t^*}$*. Consequently, in this case the influence of the projection error converges to zero for* $t \to \infty$*. Note also that, since we treat the difference between the observer estimate and its projection as an additional disturbance in* (4.55)*, the theoretical bound on the estimation error for suboptimal MHE gets worse when considering* $\mathcal{O} \supset \mathcal{X}$*. In practice, however, better results can be expected [RMD20, Sec. 4.4], especially in combination with the proposed re-initialization strategy of the auxiliary observer, which can also be seen in the example in Section 4.2.6.*

We now adapt both candidate solutions from (4.19) and (4.46) by employing the projection function $\mathrm{p}_\mathcal{X}$ in (4.53). For the first case, we construct a nominal system trajectory initialized with the projected observer state. Specifically, the candidate solution (4.19) is modified to

$$\tilde{x}_t(j+1) = f_\mathrm{n}(\tilde{x}_t(j), u_t(j)),\ j \in \mathbb{I}_{[0,N_t-1]},\ \tilde{x}_t(0) = \mathrm{p}_\mathcal{X}(z_t(T_t - N_t)), \tag{4.56a}$$

$$\tilde{d}_t(j) = 0,\ j \in \mathbb{I}_{[0,N_t-1]}, \tag{4.56b}$$

$$\tilde{v}_t(j) = 0,\ j \in \mathbb{I}_{[0,N_t-1]}. \tag{4.56c}$$

In a similar fashion, we modify the prior estimate in (4.18) according to

$$\bar{x}(t - N_t) = \mathrm{p}_\mathcal{X}(z_t(T_t - N_t)). \tag{4.57}$$

Under these adaptions, we can guarantee ϵ-RGES of suboptimal MHE as shown in the following result.

Theorem 4.3. *Suppose that Assumptions 4.1, 4.2, 4.3, 4.4, and 4.5 apply. Fix some* $N \in \mathbb{I}_{\geq 0}$*. Then, there exists* $T \in \mathbb{I}_{\geq N}$ *such that the suboptimal moving horizon estimator from Definition 4.2 using the candidate solution in* (4.56) *and the prior estimate in* (4.57) *is* ε*-RGES in the sense of Definition 4.3.*

Proof. The proof follows similar lines as the proofs in Section 4.2.2. For ease of comprehension, we have structured it into three parts: first, we derive a bound on the fitting error of the modified candidate solution; second, we derive an upper bound on the suboptimal cost; third, we invoke i-IOSS and conclude RGES.

Part I. We start by following similar arguments that were needed to establish Lemma 4.2, where the first steps to derive (4.27) remain unchanged. Here, due to the modified candidate solution in (4.56) and the definition of the projection error in (4.54), we have that

$$\begin{aligned}
&|\tilde{x}_t(0) - x(t-N_t)|^2 \\
&\leq 2|z_t(T_t-N_t) - x(t-N_t)|^2 + 2|\tilde{x}_t(0) - z_t(T_t-N_t)|^2 \\
&= 2|z_t(T_t-N_t) - x(t-N_t)|^2 + 2|p_{\mathcal{X}}(z_t(T_t-N_t)) - z_t(T_t-N_t)|^2 \\
&= 2|z_t(T_t-N_t) - x(t-N_t)|^2 + 2|\varepsilon_t(t-N_t)|^2.
\end{aligned}$$

Applying similar steps that followed (4.28), observe that (4.21) can be modified to

$$\begin{aligned}
&|\tilde{y}_t(j) - y_t(j)|^2_{G_\mathrm{s}} \\
&\leq 2\sigma(N_t)(j+1)L_\mathrm{f}^{2j}\Bigg(V_\mathrm{o}(\zeta_t, x(t-T_t))\eta_\mathrm{o}^{T_t} + \sum_{i=t-T_t}^{t-N_t+j}\eta_\mathrm{o}^{t-i-1}\left(|d(i)|^2_{Q_\mathrm{o}} + |v(i)|^2_{R_\mathrm{o}}\right) \\
&\qquad\qquad + \eta_\mathrm{o}^{N_t}|\varepsilon_t(t-N_t)|^2\Bigg)
\end{aligned} \tag{4.58}$$

for all $j \in \mathbb{I}_{[0,N_t-1]}$ and $t \in \mathbb{I}_{\geq 0}$.

Part II. Performing similar steps as in the proof of Lemma 4.3 using (4.58), the bound on the suboptimal cost in (4.30) is modified to

$$\begin{aligned}
&J(\hat{x}_t, \hat{d}_t, \hat{v}_t, \hat{y}_t, t) \\
&\leq 2\bar{\sigma}(N_t)\Bigg(V_\mathrm{o}(\zeta_t, x(t-T_t))\eta_\mathrm{o}^{T_t} + \sum_{j=1}^{T_t}\eta_\mathrm{o}^{j-1}\left(|d(t-j)|^2_{Q_\mathrm{o}} + |v(t-j)|^2_{R_\mathrm{o}}\right) \\
&\qquad\qquad + \eta_\mathrm{o}^{N_t}|\varepsilon_t(t-N_t)|^2\Bigg).
\end{aligned} \tag{4.59}$$

Part III. We use similar arguments as in the proof of Proposition 4.2 and first derive (4.41). Here, we additionally note that

$$\begin{aligned}
|\bar{x}(t-N_t) - x_t(0)|^2_{\overline{P}_\mathrm{s}} &\leq |p_{\mathcal{X}}(z_t(T_t-N_t)) - x(t-N_t)|^2_{\overline{P}_\mathrm{s}} \\
&\leq 2|z_t(T_t-N_t) - x(t-N_t)|^2_{\overline{P}_\mathrm{s}} + 2\lambda_{\max}(\overline{P}_\mathrm{s})|\varepsilon_t(t-N_t)|^2 \\
&\leq 2V_\mathrm{o}(z_t(T_t-N_t), x(t-N_t)) + 2\lambda_{\max}(\overline{P}_\mathrm{s})|\varepsilon_t(t-N_t)|^2,
\end{aligned} \tag{4.60}$$

where the latter inequality followed by invoking Assumption 4.4 and boundedness of

V_o from (4.6a). By performing analogous steps as in (4.37)–(4.41), we hence obtain

$$\begin{aligned}
&U(\hat{x}_t(N_t), x_t(N_t)) \\
&\leq 4\eta_\mathrm{s}^{N_t} V_\mathrm{o}(z_t(T_t - N_t), x(t - N_t)) + \sum_{j=1}^{N_t} \eta_\mathrm{s}^{j-1} \left(2|d(t-j)|_{Q_\mathrm{s}}^2 + 2|v(t-j)|_{R_\mathrm{s}}^2\right) \\
&\quad + 4\eta_\mathrm{s}^{N_t} \lambda_{\max}(\overline{P}_\mathrm{s})|\varepsilon_t(t - N_t)|^2 + J(\hat{x}_t, \hat{d}_t, \hat{v}_t, \hat{y}_t, t). \qquad (4.61)
\end{aligned}$$

By applying Lemma 4.1, the upper bound on the suboptimal cost from (4.59), and the fact that $\eta_\mathrm{s} \leq \eta_\mathrm{o}$ (Assumption 4.4), it follows that

$$\begin{aligned}
&U(\hat{x}_t(N_t), x_t(N_t)) \\
&\leq C(N_t)\eta_\mathrm{o}^{T_t} U(\zeta_t, x(t - N_t)) + \sum_{j=1}^{N_t} \eta_\mathrm{s}^{j-1} \left(|d(t-j)|_{Q(N_t)}^2 + |v(t-j)|_{R(N_t)}^2\right) \\
&\quad + \left(4\lambda_{\max}(\overline{P}_\mathrm{s})\eta_\mathrm{s}^{N_t} + 2\bar{\sigma}(N_t)\eta_\mathrm{o}^{N_t}\right)|\varepsilon_t(t - N_t)|^2 \\
&\leq C(N_t)\eta_\mathrm{o}^{T_t} U(\zeta_t, x(t - N_t)) \\
&\quad + \sum_{j=1}^{N_t} \eta_\mathrm{o}^{j-1} \left(|d(t-j)|_{Q(N_t)}^2 + |v(t-j)|_{R(N_t)}^2 + C_\epsilon(N_t)|\varepsilon_t(t-j)|^2\right), \qquad (4.62)
\end{aligned}$$

where[4]

$$C(s) := 2(2 + \bar{\sigma}(s))\lambda_{\max}(\overline{P}_\mathrm{o}, \underline{P}_\mathrm{s}),\ s \geq 0, \qquad (4.63a)$$
$$Q(s) := 2(2 + \bar{\sigma}(s))Q_\mathrm{o} + 2Q_\mathrm{s},\ s \geq 0, \qquad (4.63b)$$
$$R(s) := 2(2 + \bar{\sigma}(s))R_\mathrm{o} + 2R_\mathrm{s},\ s \geq 0, \qquad (4.63c)$$
$$C_\epsilon(s) := 2\eta_\mathrm{o}(2\lambda_{\max}(\overline{P}_\mathrm{s}) + \bar{\sigma}(s)),\ s \geq 0. \qquad (4.63d)$$

Note that the bound in (4.62) implies an ISS-like Lyapunov decrease property for suboptimal MHE, similar to Proposition 4.2. Now, suppose that T satisfies the contraction condition in (4.44) with C from (4.63a). Then, we can apply the same steps as in the proof of Theorem 4.1 to infer that suboptimal MHE is ε-RGES in the sense of Definition 4.3, which hence concludes this proof. □

We now consider the case where the system in (4.1) is subject to additive disturbances (Assumption 4.6) and where the observer in (4.5) specializes to a full-order state observer in output injection form (Assumption 4.7). This allows us to consider (and modify) the candidate solution in (4.46), leading to improved theoretical properties. To this end, we project the whole state trajectory of the observer restricted to the current estimation horizon onto the set $\mathcal{X}$, yielding $\tilde{x}_t(j) = \mathrm{p}_\mathcal{X}(z_t(T_t - N_t + j))$ for all $j \in \mathbb{I}_{[0,N_t]}$ and $t \in \mathbb{I}_{\geq 0}$. To obtain some $\tilde{d}_t(j)$ such that the system dynamics (4.1a) (under Assumption 4.6) are satisfied, we again exploit one-step controllability

[4]Note that the last step applied in (4.62) is indeed conservative and could also be avoided. However, this allows for much simpler and concise proofs, since an inequality similar to (4.62) naturally appears when using the observer-based candidate solution, which is shown in the subsequent theorem.

with respect to the disturbance input d. Overall, we modify the candidate solution (4.46) according to

$$\tilde{x}_t(j) = \mathrm{p}_{\mathcal{X}}(z_t(T_t - N_t + j)),\ j \in \mathbb{I}_{[0,N_t]}, \tag{4.64a}$$
$$\tilde{d}_t(j) = \mathrm{p}_{\mathcal{X}}(z_t(T_t - N_t + j + 1)) - f_{\mathrm{n}}(\mathrm{p}_{\mathcal{X}}(z_t(T_t - N_t + j)), u_t(j)),\ j \in \mathbb{I}_{[0,N_t-1]}, \tag{4.64b}$$
$$\tilde{v}_t(j) = 0,\ j \in \mathbb{I}_{[0,N_t-1]}. \tag{4.64c}$$

Here, in case of $\mathcal{D} \subset \mathbb{R}^q$, we assume that $\tilde{d}_t(j) \in \mathcal{D}$ for all $j \in \mathbb{I}_{[0,N_t-1]}$ and $t \in \mathbb{I}_{\geq 0}$ to ensure feasibility of the candidate solution, compare Section 4.2.3.

Theorem 4.4. *Suppose that Assumptions 4.1, 4.2, 4.3, 4.4, 4.5, 4.6, and 4.7 apply. Fix some $N \in \mathbb{I}_{\geq 0}$. Then, there exists $T \in \mathbb{I}_{\geq N}$ such that the suboptimal moving horizon estimator from Definition 4.2 using the candidate solution* (4.64) *and the prior estimate in* (4.57) *is ε-RGES in the sense of Definition 4.3.*

Proof. The proof follows similar lines as the proofs in Section 4.2.3 and Theorem 4.3. We have again divided it into three parts, where we first derive a bound on the fitting error of the modified candidate solution, then on the suboptimal cost, and finally invoke i-IOSS and conclude RGES.

Part I. We start by applying the same steps as in the proof of Lemma 4.4. Using the candidate solution (4.64), the output equation (4.1b), the triangle inequality, and Assumption 4.1, the fitting error of the candidate solution can be bounded by

$$\begin{aligned}
&|\tilde{y}_t(j) - y_t(j)|_{G_{\mathrm{s}}}^2 \\
&\leq \lambda_{\max}(G_{\mathrm{s}})|\tilde{y}_t(j) - y_t(j)|^2 \\
&\leq \lambda_{\max}(G_{\mathrm{s}})L_{\mathrm{h}}^2(|\tilde{x}_t(j) - x_t(j)| + |v_t(j)|)^2 \\
&\leq \lambda_{\max}(G_{\mathrm{s}})L_{\mathrm{h}}^2(|\tilde{x}_t(j) - z_t(T_t - N_t + j)| + |z_t(T_t - N_t + j) - x_t(j)| + |v_t(j)|)^2
\end{aligned}$$

for all $j \in \mathbb{I}_{[0,N_t-1]}$ and all $t \in \mathbb{I}_{\geq 0}$. Using Jensen's inequality, the definition of the projection error in (4.54), and the lower bound of V_{o} in (4.6a), it follows that

$$\begin{aligned}
|\tilde{y}_t(j) - y_t(j)|_{G_{\mathrm{s}}}^2 \leq 3\lambda_{\max}(G_{\mathrm{s}})L_{\mathrm{h}}^2\Big(&\frac{1}{\lambda_{\min}(\underline{P}_{\mathrm{o}})}V_{\mathrm{o}}(z_t(T_t - N_t + j), x(t - N_t + j)) \\
&+ \frac{1}{\lambda_{\min}(R_{\mathrm{o}})}|v(t - N_t + j)|_{R_{\mathrm{o}}}^2 + |\varepsilon_t(t - N_t + j)|^2\Big).
\end{aligned}$$

The application of Lemma 4.1 then yields a slightly modified version of Lemma 4.4, that is, the bound

$$\begin{aligned}
|\tilde{y}_t(j) - y_t(j)|_{G_{\mathrm{s}}}^2 \leq \frac{3}{2}c_2\eta_{\mathrm{o}}^{-(N_t-j-1)}\Bigg(&V_{\mathrm{o}}(\zeta_t, x(t - T_t))\eta_{\mathrm{o}}^{T_t} \\
&+ \sum_{i=t-T_t}^{t-N_t+j} \eta_{\mathrm{o}}^{t-i-1}\left(|d(i)|_{Q_{\mathrm{o}}}^2 + |v(i)|_{R_{\mathrm{o}}}^2 + |\varepsilon_t(j)|^2\right)\Bigg)
\end{aligned} \tag{4.65}$$

for all $j \in \mathbb{I}_{[0,N_t-1]}$ and all $t \in \mathbb{I}_{\geq 0}$, where c_2 is from (4.48).

Part II. Now, we consider the suboptimal cost $J(\hat{x}_t, \hat{d}_t, \hat{v}_t, \hat{y}_t, t)$ and follow the first part of the proof of Proposition 4.3 to derive (4.51). To establish a bound on the term $|\tilde{d}_t(j)|^2_{Q_\mathrm{s}}$, we first note that for a given $a \in \mathbb{R}^n$, $|\mathrm{p}_{\mathcal{X}}(a) - b| \leq |a - b|$ for any $b \in \mathcal{X}$, since by convexity of $\mathcal{X}$ and optimality of $\mathrm{p}_{\mathcal{X}}$, the angle between $\mathrm{p}_{\mathcal{X}}(a) - a$ and $a - b$ is obtuse [HL93, Thm. 3.1.1, p. 117]. Now, consider the definition of the candidate disturbance $\tilde{d}_t(j)$, $j \in \mathbb{I}_{[0,N_t-1]}$ from (4.64c) and recall that $f_\mathrm{n}(\tilde{x}_t(j), u_t(j)) \in \mathcal{X}$ (due to the invariance property from (4.3) and the fact that $\tilde{x}_t(j) \in \mathcal{X}$ by definition). The application of Assumptions 4.5 and 4.7, the definition of the projection error in (4.54), the triangle inequality, and Assumption 4.1 then lets us infer that

$$
\begin{aligned}
|\tilde{d}_t(j)| &= |\mathrm{p}_{\mathcal{X}}(z_t(T - N_t + j + 1)) - f_\mathrm{n}(\tilde{x}_t(j), u_t(j))| \\
&\leq |z_t(T - N_t + j + 1) - f_\mathrm{n}(\tilde{x}_t(j), u_t(j))| \\
&= |f_\mathrm{n}(z_t(T - N_t + j + 1), u_t(j)) + k_t(T_t - N_t + j) - f_\mathrm{n}(\tilde{x}_t(j), u_t(j))| \\
&\leq L_\mathrm{f}|z_t(T_t - N_t + j) - \tilde{x}_t(j)| + |k_t(T_t - N_t + j)| \\
&\leq L_\mathrm{f}|\varepsilon_t(t - N_t + j)| + \kappa|h_\mathrm{n}(z_t(T_t - N_t + j), u_t(j)) - y_t(j)| \\
&\leq L_\mathrm{f}|\varepsilon_t(t - N_t + j)| + \kappa|h_\mathrm{n}(z_t(T_t - N_t + j), u_t(j)) - h_\mathrm{n}(\tilde{x}_t(j), u_t(j))| \\
&\quad + \kappa|h_\mathrm{n}(\tilde{x}_t(j), u_t(j)) - y_t(j)| \\
&\leq (L_\mathrm{f} + \kappa L_\mathrm{h})|\varepsilon_t(t - N_t + j)| + \kappa|\tilde{y}_t(j) - y_t(j)|
\end{aligned}
$$

for all $j \in \mathbb{I}_{[0,N_t-1]}$ and $t \in \mathbb{I}_{\geq 0}$. Hence, by using Jensen's inequality, we obtain

$$
\begin{aligned}
|\tilde{d}_t(j)|^2_{Q_\mathrm{s}} &\leq \lambda_{\max}(Q_\mathrm{s})|\tilde{d}_t(j)|^2 \\
&\leq 2\lambda_{\max}(Q_\mathrm{s})(L_\mathrm{f} + \kappa L_\mathrm{h})^2|\varepsilon_t(t - N_t + j)|^2 + \frac{2\lambda_{\max}(Q_\mathrm{s})\kappa^2}{\lambda_{\min}(G_\mathrm{s})}|\tilde{y}_t(j) - y_t(j)|^2_{G_\mathrm{s}}
\end{aligned} \tag{4.66}
$$

for all $j \in \mathbb{I}_{[0,N_t-1]}$ and $t \in \mathbb{I}_{\geq 0}$. Combining (4.51) with the bounds in (4.65) and (4.66) leads to

$$
\begin{aligned}
J(\hat{x}_t, \hat{d}_t, \hat{v}_t, \hat{y}_t, t) \leq\ & \left(1 + \frac{4\lambda_{\max}(Q_\mathrm{s})\kappa^2}{\lambda_{\min}(G_\mathrm{s})}\right) \sum_{j=0}^{N_t-1} \bar{\eta}^{N_t-j-1}|\tilde{y}_t(j) - y_t(j)|^2_{G_\mathrm{s}} \\
&+ 4\lambda_{\max}(Q_\mathrm{s})(L_\mathrm{f} + \kappa L_\mathrm{h})^2 \sum_{j=0}^{N_t-1} \bar{\eta}^{N_t-j-1}|\varepsilon_t(t - N_t + j)|^2.
\end{aligned}
$$

Using (4.65), we further obtain that

$$
\begin{aligned}
&J(\hat{x}_t, \hat{d}_t, \hat{v}_t, \hat{y}_t, t) \\
&\leq 2\bar{\sigma}(N_t) \left(V_\mathrm{o}(\zeta_t, x(t - T_t))\eta_\mathrm{o}^{T_t} + \sum_{j=1}^{T_t} \eta_\mathrm{o}^{j-1} \left(|d(t-j)|^2_{Q_\mathrm{o}} + |v(t-j)|^2_{R_\mathrm{o}} \right) \right) \\
&\quad + \sigma_\varepsilon(N_t) \sum_{j=1}^{T_t} \bar{\eta}^{j-1}|\varepsilon_t(t-j)|^2,
\end{aligned} \tag{4.67}
$$

where

$$
\sigma_\varepsilon(s) := \left(2\bar{\sigma}(N_t) + 4\lambda_{\max}(Q_\mathrm{s})(L_\mathrm{f} + \kappa L_\mathrm{h})^2\right) \max\left\{1, (\bar{\eta}/\eta_\mathrm{o})^s\right\} \tag{4.68}
$$

and

$$\bar{\sigma}(s) = \frac{3}{4}\left(1 + \frac{4\lambda_{\max}(Q_{\mathrm{s}})\kappa^2}{\lambda_{\min}(G_{\mathrm{s}})}\right) c_2 \cdot \begin{cases} \frac{1-\left(\frac{\bar{\eta}}{\eta_{\mathrm{o}}}\right)^s}{1-\frac{\bar{\eta}}{\eta_{\mathrm{o}}}}, & \frac{\bar{\eta}}{\eta_{\mathrm{o}}} \neq 1 \\ s, & \frac{\bar{\eta}}{\eta_{\mathrm{o}}} = 1 \end{cases}, \ s \geq 0. \tag{4.69}$$

Note that the factor 2 preceding $\bar{\sigma}$ in (4.67) (and (4.68)) is intentional and canceled by an additional factor 1/2 in (4.69) in order to match the notation to the proof of Theorem 4.3 and thus enable a more direct comparison and concise derivation in the following Part III.

Part III. We proceed similarly to the proof of Theorem 4.3 and first derive (4.61). Using the bound on the suboptimal cost from (4.67), we can establish (4.62), where C, Q, R are as defined in (4.63) using $\bar{\sigma}$ from (4.69) and $C_\varepsilon(s) := 4\eta_{\mathrm{s}}\lambda_{\max}(\overline{P}_{\mathrm{s}}) + \sigma_\varepsilon(s)$. The remaining part follows by applying the same steps in the proof of Theorem 4.3 that were applied after (4.62), which finishes this proof. □

To summarize, by using the modified candidate solutions in (4.56) and (4.64) and the prior estimate in (4.57), we can cover the practically relevant case where the auxiliary observer in (4.5) may leave the set $\mathcal{X}$. Specifically, we could preserve robust stability and constraint satisfaction guarantees of suboptimal MHE without requiring any changes to the design of the auxiliary observer.

4.2.6. Numerical example

We adapt the example from [RMD20, Example 4.39] and consider the set of reversible reactions $A \rightleftharpoons B + C$, $2B \rightleftharpoons C$ taking place in a well-stirred, isothermal, gas-phase batch reactor. The Euler-discretized model describing the evolution of the concentrations of the species A, B, and C over time corresponds to

$$\begin{aligned} x_1^+ &= x_1 + t_\Delta(-p_1 x_1 + p_2 x_2 x_3) + d_1, \\ x_2^+ &= x_2 + t_\Delta(p_1 x_1 - p_2 x_2 x_3 - 2p_3 x_2^2 + 2p_4 x_3) + d_2, \\ x_3^+ &= x_3 + t_\Delta(p_1 x_1 - p_2 x_2 x_3 + p_3 x_2^2 - p_4 x_3) + d_3, \\ y &= x_1 + x_2 + x_3 + v, \end{aligned} \tag{4.70}$$

where $t_\Delta = 0.25$ is the step size and $d \in \mathbb{R}^3$ and $v \in \mathbb{R}$ are additional process disturbances and measurement noise. We consider the parameters $p_1 = 0.2$, $p_2 = 0.05$, $p_3 = 0.2$, and $p_4 = 0.1$ and select the initial conditions $\chi = [0.5, 0.05, 0.1]^\top$ and $\hat{\chi} = [2, 0.5, 0]^\top$. We consider the prior knowledge $\mathcal{X} = \{x \in \mathbb{R}^3 : 0 \leq x_i \leq 3, i = 1, 2, 3\}$, where non-negativity follows from the physical nature of the system (substance concentrations cannot be negative) and the upper bound provides a compact set with respect to realistic initial conditions and disturbances. During the simulations, the disturbances d and v are treated as uniformly distributed random variables that are sampled from the sets $\{d \in \mathbb{R}^3 : |d_i| \leq 10^{-3}, i = 1, 2, 3\}$ and $\{v \in \mathbb{R} : |v| \leq 5 \cdot 10^{-2}\}$. Note that since we consider additive disturbances in (4.70), Assumption 4.6 holds true. Moreover, the functions f and h are Lipschitz on $\mathcal{X}$ with Lipschitz constants $L_{\mathrm{f}} = 1.032$ and $L_{\mathrm{h}} = |[1, 1, 1]| = 1.732$, which renders Assumptions 4.1 and 4.5 valid.

In the following, we verify the remaining technical assumptions used in the previous sections, implement the proposed suboptimal MHE schemes, and compare the respective estimation results with established methods from the literature. The simulations are performed on a standard laptop (Intel Core i7 with 2.6 GHz, 12 MB cache, and 16 GB RAM under Ubuntu Linux 20.04) in MATLAB with CasADi [And+18] and the NLP solver IPOPT [WB05]; LMIs are solved using YALMIP [Löf04] and MOSEK [MOS24].

Observer design and i-IOSS verification

For the system in (4.70), we design a conventional Luenberger observer in the form of

$$z^+ = g(z, y) = f_{\mathrm{n}}(z) + K \cdot (h_{\mathrm{n}}(z) - y). \tag{4.71}$$

Note that this choice immediately validates Assumption 4.7. We compute the constant observer gain $K \in \mathbb{R}^{n \times p}$ based on the differential dynamics, where a sufficient LMI condition analogous to the dual (i.e., control) problem considered in [MS18] can be derived. Here, the domain $\mathcal{O}$ of the observer is chosen as a proper superset of $\mathcal{X}$ by selecting $\mathcal{O} = \{z \in \mathbb{R}^3 : -0.04 \leq z_2 \leq 4, -2 \leq z_3 \leq 4\}$, as the observer is not guaranteed to adhere to the physical constraint of non-negative states (i.e., substance concentrations), see also Figure 4.1 below. By imposing a quadratic Lyapunov function $V_{\mathrm{o}}(z, x) = |z - x|_P^2$ (leading to $\overline{P}_{\mathrm{o}} = \underline{P}_{\mathrm{o}} = P$ in (4.6a)), we can thus verify Assumption 4.2 on $\mathcal{O}$ with $\eta_{\mathrm{o}} = 0.97$ and

$$K = \begin{bmatrix} -0.1 \\ -0.1 \\ -0.5 \end{bmatrix}, \quad P = \begin{bmatrix} 3.100 & 2.170 & 1.674 \\ 2.170 & 4.210 & 2.154 \\ 1.674 & 2.154 & 3.077 \end{bmatrix}, \quad Q_{\mathrm{o}} = \begin{bmatrix} 10^3 & 0 & 0 \\ 0 & 10^3 & 0 \\ 0 & 0 & 10^3 \end{bmatrix}, \quad R_{\mathrm{o}} = 10^3.$$

Now, we compute an i-IOSS Lyapunov function U for the system in (4.70) that satisfies Assumption 4.3. To this end, we adapt Corollary 7.1 in Section 7.1.1 to our current setup (that is, considering distinct process disturbances d and measurement noise v instead of a generalized disturbance input $w = (d, v)$). We verify the corresponding LMI conditions on the set $\mathcal{X}$ while imposing $U(x_1, x_2) = V_{\mathrm{o}}(x_1, x_2)$ to ensure the compatibility condition in Assumption 4.4 and achieve the smallest possible value of $\lambda_{\max}(\overline{P}_{\mathrm{o}}, \underline{P}_{\mathrm{s}}) = 1$ (which is generally beneficial in practice to allow for smaller disturbance gains and observer horizons T). The remaining parameters are $\eta_{\mathrm{s}} = 0.9383$ and

$$Q_{\mathrm{s}} = \begin{bmatrix} 10^2 & 0 & 0 \\ 0 & 10^2 & 0 \\ 0 & 0 & 10^2 \end{bmatrix}, \qquad R_{\mathrm{s}} = 10^2, \qquad G_{\mathrm{s}} = 50.$$

Thus, all technical assumption employed in the theoretical analysis in Sections 4.2.2–4.2.5 are verified.

Table 4.2. Value of $T_{\min}$ for different state constraints and candidate solutions.

Admissible constraint	Candidate solution	Result	$T_{\min}$
$\hat{x}_t(j) \in \mathcal{O}$	System trajectory (4.19)	Theorem 4.1	263
	Observer trajectory (4.46)	Theorem 4.2	247
$\hat{x}_t(j) \in \mathcal{X}$	System trajectory (4.56)	Theorem 4.3	286
	Observer trajectory (4.64)	Theorem 4.4	349

Suboptimal MHE design

In the following, we consider the cost function in (4.12) and select the horizon length $N = 3$, parameterize the prior weighting and stage cost in (4.13) and (4.14) according to the i-IOSS Lyapunov function parameters from above, and choose $\bar{\eta} = \eta_{\mathrm{s}}$. We first compare the theoretical requirements for suboptimal MHE using the candidate solutions in (4.19) and (4.46) (which do not allow the inclusion of prior knowledge about the set $\mathcal{X} \subset \mathcal{O}$ in the MHE problem in (4.11)) and the projected candidate solutions in (4.56) and (4.64) (which allow enforcing the state constraint $\hat{x}_t(j) \in \mathcal{X}$, $j \in \mathbb{I}_{[0,N_t-1]}$ in (4.11d)).

Table 4.2 compares the estimates of the minimum required observer horizons $T_{\min}$ to guarantee robust stability of suboptimal MHE provided by Theorems 4.1–4.4. For the first case ($\hat{x}_t(j) \in \mathcal{O}$), we observe that the observer-based candidate solution (4.46) provides a tighter error bound (and hence yields a smaller estimate of $T_{\min}$) compared to the system-based candidate solution (4.19), which is in line with the main observations in Section 4.2.4. For the second case ($\hat{x}_t(j) \in \mathcal{X}$), the respective error bounds (and thus the estimates of $T_{\min}$) are larger compared to the first case, which is due to additional conservative steps in the respective proofs leading to more conservative disturbance gains, compare the respective formulas in (4.36) and (4.63); this in particular applies to the proof of Theorem 4.4, resulting in slightly more conservative guarantees and hence a larger value of $T_{\min}$ compared to that required by Theorem 4.3. In practice, however, better estimation results can be expected if knowledge about $\mathcal{X}$ is included in the MHE scheme and a corresponding candidate solution is used, compare also the simulation results below.

Generally, we note that the values of $T_{\min}$ in Table 4.2 are rather large. This is on the one hand due to the fact that we guarantee robust stability of suboptimal MHE without any optimization, and on the other hand due to various conservative steps within the respective proofs; hence, the guarantees are rather of conceptual nature, and good simulation results are also obtained for much smaller values of T. However, it should be noted that the estimates of $T_{\min}$ do *not* jeopardize the real-time capability of suboptimal MHE, as this only determines the forward simulation of the observer in (4.71) (which is computationally cheap and has fixed complexity). Moreover, we want to point out that a valid choice is always $T = t$, which would directly lead to RGES of suboptimal MHE for each candidate solution from above and any horizon length N, while only one observer iteration needs to be performed at each time step to construct the current candidate solution, compare Remark 4.6.

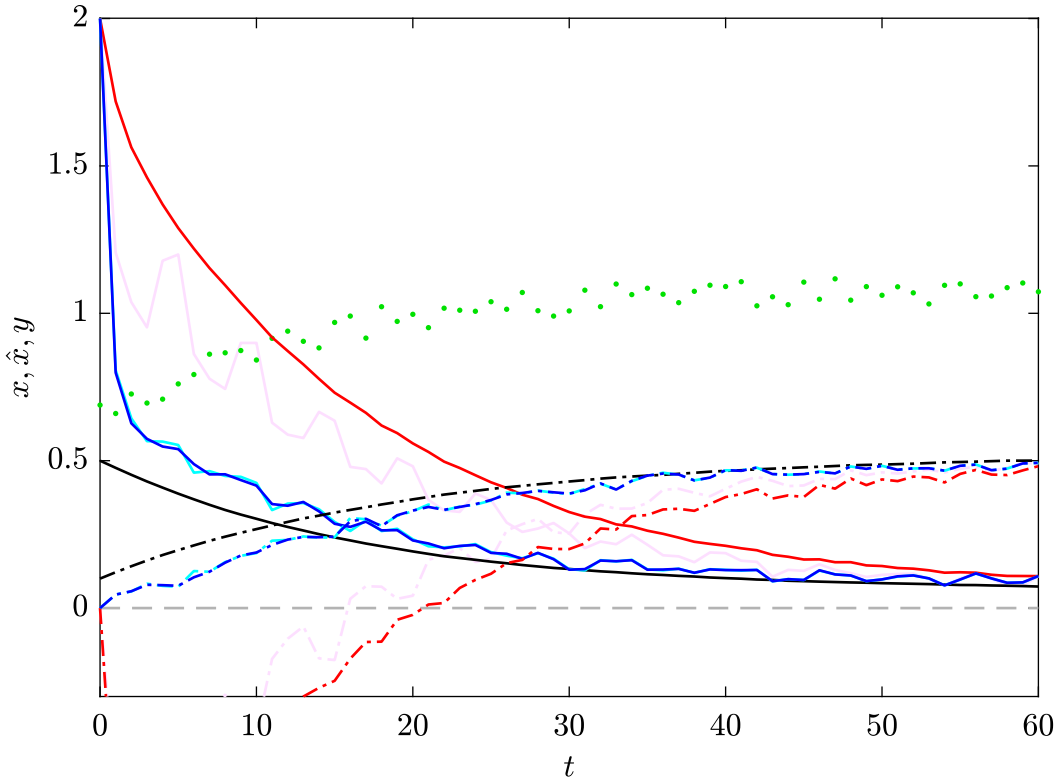

Figure 4.1. Comparison of suboptimal MHE results using the candidate solution in (4.56) (blue) and the candidate solution in (4.64) (cyan) after performing $i = 3$ steps of the optimizer (IPOPT), the Luenberger observer (red), real system states (black), and output measurements y (green dots). The light magenta curves show the estimation results of suboptimal MHE using the unmodified (i.e., non-projected) candidate solution (4.46) and $\hat{x}_t(j) \in \mathcal{O}$, $j \in \mathbb{I}_{[0,N_t]}$ in (4.11d). Solid lines correspond to the first state $x_1, \hat{x}_1, z_1$, dashed-dotted lines to the third state $x_3, \hat{x}_3, z_3$ (where the minimum value of z_3 is $z_3(2) = -1.015$). The gray dashed line represents the lower bound of the set $\mathcal{X}$.

In the following, we focus on suboptimal MHE involving the state constraint $\hat{x}_t(j) \in \mathcal{X}$ in (4.11d) to avoid potentially poor transient behavior caused by the Luenberger observer, compare Figures 4.1 and 4.2 below. Specifically, we implement two suboptimal estimators relying on the projected candidate solutions from (4.56) and (4.64), respectively. To ensure feasibility of the candidate solutions, we consider $\mathcal{D} = \mathbb{R}^n$ and $\mathcal{V} = \mathcal{Y} = \mathbb{R}^p$ in the MHE problem in (4.11e). To illustrate the potential of the proposed re-initialization strategy in practice, we choose $T = 5$ in the following, although we must note that this choice is not theoretically covered.

Simulation results

Figure 4.1 shows the estimation results of the suboptimal estimators after performing $i = 3$ steps of the optimizer (IPOPT) compared to the real system states and the Luenberger observer from (4.71), which we use for constructing the candidate solutions and the warm start for the optimizer. We observe that both suboptimal estimators are capable of improving the estimates of the auxiliary observer (that

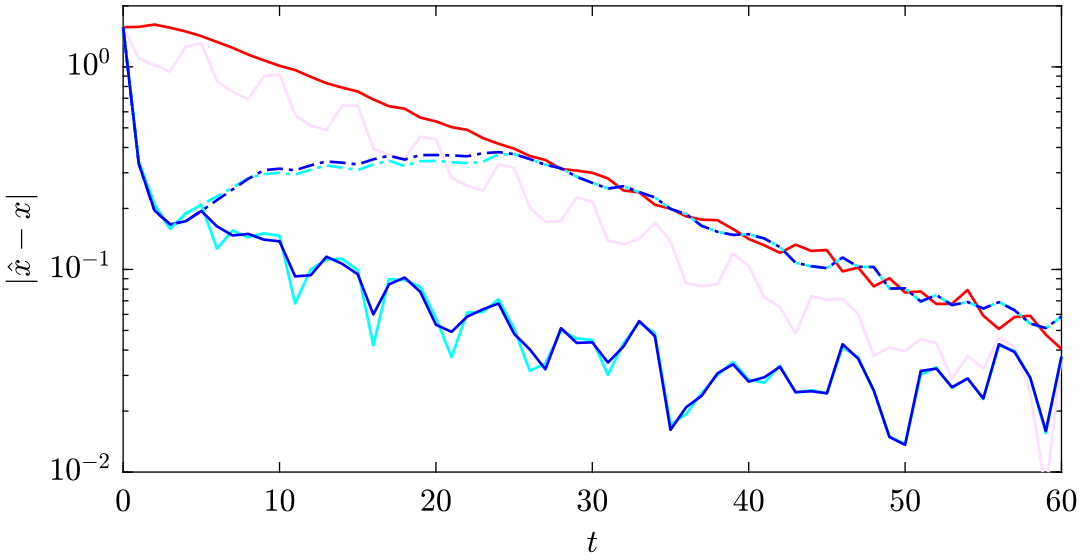

Figure 4.2. Estimation error for the Luenberger observer (red) compared to suboptimal MHE using the system-based candidate solution in (4.56) (blue) and the observer-based candidate solution in (4.64) (cyan) after performing $i = 3$ steps of the optimizer (IPOPT). Solid lines correspond to $T = 5$, dashed-dotted lines to $T = t$ (i.e., without re-initializing the auxiliary observer). The light magenta curve shows the estimation error of suboptimal MHE for the case of $N = 3$, $T = 5$, and $i = 3$ using the unmodified (i.e., non-projected) candidate solution (4.46) and the constraint $\hat{x}_t(j) \in \mathcal{O}$, $j \in \mathbb{I}_{[0,N_t]}$ in (4.11d).

leaves the set $\mathcal{X}$ in its transient phase) while providing physically plausible estimates. The corresponding estimation errors over time are depicted in Figure 4.2 (solid lines), which illustrates robust stability, fast convergence, and overall significantly improved behavior compared to the Luenberger observer. This advantage becomes particularly apparent when comparing the results with suboptimal MHE using the set $\mathcal{O}$ instead of $\mathcal{X}$ as state constraint (this corresponds to the first case in Table 4.2), which yields physically implausible estimates and only slightly improves the results of the auxiliary observer, see the light magenta curves in Figures 4.1 and 4.2.

Figure 4.2 additionally shows the estimation error of suboptimal MHE with $T = t$ (i.e., without re-initializing the auxiliary observer). Here, the suboptimal estimators initially show a significant improvement compared to the Luenberger observer, which is mainly due to the fact that the corresponding estimates satisfy the state constraints $\mathcal{X}$. However, without re-initializing the observer with an improved suboptimal estimate, the prior weighting causes the suboptimal estimates to converge close to its trajectory again. This illustrates the effectiveness of the proposed re-initialization strategy, which provides the ability to quickly recover from a poor transient behavior of the auxiliary observer, see also Remark 4.6.

For a more detailed numerical comparison, we employ two different performance metrics: the sum of squared errors (SSE) defined as $\text{SSE} := \sum_{t=0}^{t_{\text{sim}}} |\hat{x}(t) - x(t)|^2$ and the normalized accumulated cost $J_{\text{acc}} := \frac{1}{N} \sum_{t=0}^{t_{\text{sim}}} J(\hat{x}_t, \hat{d}_t, \hat{v}_t, \hat{y}_t, t)$. To evaluate the computational complexity, we also consider the average computation time per sample τ_{avrg} (considering all $t \in \mathbb{I}_{\geq N}$). Table 4.3 compares the values of the SSE,

Table 4.3. Estimation performance for different configurations of suboptimal MHE.

Configuration			candidate solution (4.56)			candidate solution (4.64)		
N	T	i	SSE	J_{acc}	τ_{avrg}	SSE	J_{acc}	τ_{avrg}
3	5	0	16.09	740.31	1.88	13.06	486.66	1.88
3	5	1	3.00	24.05	2.60	3.19	26.66	2.60
3	5	2	2.58	23.01	3.29	2.61	22.92	3.30
3	5	3	2.68	22.48	4.01	2.68	22.48	4.01
3	5	4	2.81	22.42	4.70	2.81	22.43	4.69
3	5	5	2.90	22.38	5.37	2.91	22.38	5.38
3	5	10	2.97	22.34	6.69	2.97	22.34	6.67
3	5	$*$	2.97	22.36	6.64	2.97	22.36	6.63
10	15	0	25.07	1295.10	2.08	15.16	457.06	2.09
10	15	1	4.55	100.19	2.85	3.67	27.93	2.86
10	15	2	2.49	20.35	3.60	2.55	20.09	3.61
10	15	3	2.56	19.89	4.36	2.62	19.75	4.36
10	15	4	2.70	19.65	5.16	2.72	19.64	5.18
10	15	5	2.76	19.74	5.92	2.78	19.73	5.93
10	15	10	2.84	19.67	7.53	2.84	19.67	7.52
10	15	$*$	2.83	19.72	7.60	2.83	19.72	7.58

Each value represents the average over 100 simulations of length $t_{\text{sim}} = 60$; asterisks represent fully converged optimization problems; the Luenberger observer achieves SSE = 28.65.

J_{acc}, and τ_{avrg} for different configurations of the proposed suboptimal estimator and for different values of i representing the maximum number of iterations allowed solving the respective NLP, averaged over 100 simulations. For suboptimal MHE with $N = 3$ and $T = 5$, we see that performing only one iteration of the optimizer is already sufficient to significantly improve the estimation results of the auxiliary observer (achieving a reduction of the SSE by $\approx 90\,\%$). Moreover, we observe that $i = 3$ iterations are sufficient to provide estimation results that are close to optimal MHE (that is, where we consider optimal solutions of the NLP), while saving $\approx 40\,\%$ of the corresponding computation time. Consequently, the influence of the different candidate solutions (and warm starts) also becomes negligible for $i \geq 3$ iterations.

To investigate the influence of longer estimation horizons, we also consider suboptimal MHE with $N = 10$ and $T = 15$. Here, we can observe qualitatively the same behavior as before; however, the estimation results for $i = 0, 1$ are slightly worse compared to the case where $N = 3$ and $T = 5$. This is due to the fact for $T = 15$, the (initially poorly performing) auxiliary observer is re-initialized later than in the case of $T = 5$, hence yielding a worse warm start trajectory and therefore requiring more iterations to improve. For $i \geq 2$, better performance is then achieved compared to the case where $N = 3$ (in terms of SSE and J_{acc}), however, requiring longer computation times as expected. Overall, this example shows that performing only very few iterations of the optimizer already leads to significantly improved estimation results compared to the auxiliary observer while reducing computation

times compared to optimal MHE, demonstrating the effectiveness of the proposed suboptimal MHE framework.

Comparison with fast MHE schemes from the literature

We compare the proposed suboptimal estimator to the fast MHE schemes from [Küh+11] and [WVD14], which are referred to as f-MHE$_1$ and f-MHE$_2$ in the remainder of this section, respectively. Both schemes rely on the generalized Gauss-Newton (GGN) algorithm and employ a quadratic cost function in filtering form, that is, where the estimation horizon at a given time t includes the most recent measurement $y(t)$. For a meaningful comparison, we implement the proposed suboptimal MHE scheme in a similar fashion, that is, in its filtering form[5] and using the GGN algorithm (with Lagrange relaxation, compare [WVD14]) for approximately solving the optimization problem. We consider the candidate solution based on the nominal system trajectory (4.56) and on the projected observer trajectory (4.64) and denote the resulting estimators as s-MHE$_1$ and s-MHE$_2$, respectively. For each estimator, we choose $N = 3$ (and $T = 5$ for s-MHE$_{1,2}$), parameterize each cost function according to the choices from the previous section based on the i-IOSS Lyapunov function U, construct the respective warm start using the previously obtained (suboptimal) solution (compare Remark 4.3), and incorporate the constraint set $\mathcal{X}$ using a simple active-set method [Jat00].

Table 4.4 compares the estimation results in terms of SSE and computation time τ_{avrg} per sample, averaged over 100 simulations. Here, it can be seen that the estimation results of s-MHE$_{1,2}$ are generally more accurate (in terms of SSE) and also require less computation time compared to the corresponding values in Table 4.3, which results from the fact that we use the filtering (instead of prediction) form of MHE and the GGN algorithm (instead of IPOPT), respectively. Moreover, performing $i \geq 1$ GGN iterations reveals that s-MHE$_1$ and s-MHE$_2$ perform slightly faster than f-MHE$_1$ and slower than f-MHE$_2$, which was to be expected and is mainly due to the respective design of the cost function. Specifically, s-MHE$_{1,2}$ has a prior weighting Γ involving constant parameters only, f-MHE$_1$ has a time-varying prior weighting where the parameters of Γ needs to be updated each time-step using a QR decomposition [Küh+11], and f-MHE$_2$ has no prior weighting and penalizes solely the fitting error [WVD14]. This is also the reason why f-MHE$_2$ performs best (i.e., achieves the lowest SSE) for $i = 1$, as the prior weighting prevents the other estimators from converging as similarly fast. However, for $i \geq 2$, the prior weighting is able to improve the estimation results, which generally yields a lower SSE for s-MHE$_{1,2}$ and f-MHE$_1$ compared to f-MHE$_2$.

Overall, this example shows that the considered suboptimal/fast estimation methods perform very similarly, both in terms of their accuracy (SSE) and their computation times (τ_{avrg}). However, our proposed suboptimal MHE framework is more flexible

[5] Note that the results derived in Sections 4.2.2–4.2.5 for the prediction form of MHE (i.e., without incorporating the current measurement $y(t)$ at time t) can be straightforwardly extended to the filtering form of MHE, compare also [RMD20, Sec. 4], [AR19b, Sec. 3], and the discussion in Section 3.1.

Table 4.4. Comparison of the estimation results of the proposed suboptimal (s-MHE$_{1,2}$) and fast MHE schemes (f-MHE$_{1,2}$) for different numbers of GGN iterations i.

i	s-MHE$_1$		s-MHE$_2$		f-MHE$_1$		f-MHE$_2$	
	SSE	τ_{avrg}	SSE	τ_{avrg}	SSE	τ_{avrg}	SSE	τ_{avrg}
0	17.70	0.07	14.22	0.08	135.12	0.05	135.12	0.01
1	3.02	0.51	2.98	0.51	2.23	0.52	1.63	0.43
2	0.73	0.87	0.73	0.87	0.77	0.92	0.79	0.80
3	0.67	1.27	0.68	1.28	0.41	1.35	0.54	1.20
4	0.28	1.62	0.25	1.63	0.27	1.72	0.42	1.56

Each value represents the average over 100 simulations of length $t_{\text{sim}} = 60$; the average computation time τ_{avrg} is in milliseconds (ms).

than that of [Küh+11; WVD14], as it is applicable to a larger class of nonlinear detectable systems and allows for a completely free choice of optimization algorithm. Moreover, we can provide robust stability guarantees independent of the horizon length and the number of iterations performed; in contrast, fMHE$_{1,2}$ provide either no guarantees at all [Küh+11] or only for observable systems [WVD14], heavily relying on the convergence properties of the GGN algorithm.

4.3. Optimizing observer trajectories

In the previous section, we have considered a classical MHE formulation that optimizes over trajectories of the system (4.1). Now, we consider a modified MHE problem that directly optimizes over trajectories of the observer (4.5), which is specified in Section 4.3.1. This formulation allows for a more direct stability analysis in Section 4.3.2, ultimately leading to tighter error bounds. Moreover, the numerical example in Section 4.3.3 shows that the resulting suboptimal MHE scheme can yield improved convergence behavior in applications if the auxiliary observer is rather aggressive.

4.3.1. Suboptimal MHE design

Given some finite estimation horizon $N \in \mathbb{I}_{\geq 0}$ and a time $t \in \mathbb{I}_{\geq 0}$, we consider the following modified MHE problem:

$$\min_{\hat{x}_t} J(\hat{x}_t, \hat{y}_t, t) \tag{4.72a}$$

$$\text{s.t. } \hat{x}_t(j+1) = g(\hat{x}_t(j), u_t(j), y_t(j)),\ j \in \mathbb{I}_{[0,N_t-1]}, \tag{4.72b}$$

$$\hat{y}_t(j) = h_{\text{n}}(\hat{x}_t(j), u_t(j)),\ j \in \mathbb{I}_{[0,N_t-1]}, \tag{4.72c}$$

$$\hat{x}_t(j) \in \mathcal{O},\ j \in \mathbb{I}_{[0,N_t]}, \tag{4.72d}$$

where $N_t = \min\{t, N\}$, u_t is defined in (4.9) and corresponds to the truncated input sequence applied to the system (4.1), g in (4.72b) corresponds to the dynamics of

the auxiliary observer from (4.5) evolving in the set $\mathcal{O}$, and h_{n} in (4.72c) represents the nominal output equation of the system in (4.1). The decision variables of the optimization problem in (4.72) are the elements of the estimated state sequence $\hat{x}_t = \{\hat{x}_t(j)\}_{j=0}^{N_t}$, which (uniquely) defines a sequence of output estimates $\hat{y}_t = \{\hat{y}_t(j)\}_{j=0}^{N_t-1}$ under (4.72c). The cost function J in (4.72a) is defined as

$$J(\hat{x}_t, \hat{y}_t, t) = 2|\hat{x}_t(0) - \bar{x}(t-N_t)|_W^2 + \frac{\lambda_{\min}(\underline{P}_{\mathrm{o}})}{2L_{\mathrm{h}}^2\lambda_{\max}(G)} \sum_{j=0}^{N_t-1} \eta_{\mathrm{o}}^{N_t-j} |\hat{y}_t(j) - y_t(j)|_G^2, \quad (4.73)$$

where $\bar{x}(t-N_t)$ is the prior estimate defined below, y_t is defined in (4.10) and corresponds to the truncated output sequence obtained from the system (4.1), the parameters η_{o} and $\underline{P}_{\mathrm{o}}$ are from the i-ISS Lyapunov function V_{o} (Assumption 4.2), and L_{h} refers to the Lipschitz property of h (Assumption 4.1). The parameters $G \succeq 0$ and $W \succ 0$ are weighting matrices that can be tuned arbitrarily; their respective influence on the theoretical properties of the resulting estimator is discussed in detail in Remark 4.13 below.

Remark 4.10 (Discounting)**.** *The cost function in* (4.73) *involves a discounted stage cost using η_{o} as discount factor. This could be generalized by replacing η_{o} in* (4.73) *with a tuning parameter $\bar{\eta}$ satisfying $0 < \bar{\eta} < 1$. However, note that in contrast to Section 4.2, we aim to establish a contraction over the estimation horizon from time $t-N$ to time t and hence require a discounted cost with $\bar{\eta} < 1$, compare Remark 4.2 (but without requiring a lower bound on $\bar{\eta}$ apart from zero, as we do not invoke i-IOSS here). Adopting the key ideas from Section 4.2, it is possible to modify the scheme and corresponding analysis to allow for an arbitrary tuning parameter $\bar{\eta} > 0$, see Remark 4.15 below for details. However, we emphasize that choosing $\bar{\eta} \geq 1$ would deteriorate the theoretical guarantees.*

Remark 4.11 (Optimizing observer trajectories)**.** *In contrast to all other MHE formulations considered in this thesis and also to most of the literature on nonlinear MHE for uncertain systems (see, e.g., [RMD20; KM23; AR21; Küh+11; Hu24]), the MHE scheme in* (4.72) *does not optimize over process disturbances $\hat{d}_t(j)$, $j \in \mathbb{I}_{[0,N_t-1]}$ (in contrast to, e.g., the NLP in* (4.11)*). Instead, we optimize over trajectories of the auxiliary observer by employing its dynamics in* (4.72b)*, avoiding the need for an additional disturbance input. This is computationally beneficial as it drastically reduces the number of decision variables, compare the simulation results in Section 4.3.3. Similar MHE formulations were previously considered in [SJF10; SJ14; Suw+14; WK17]. In Section 4.3.2 below, we show that this direct coupling between MHE and the auxiliary observer allows for using the corresponding i-ISS Lyapunov function V_{o} (Assumption 4.2) as N-step Lyapunov function for (suboptimal) MHE.*

A direct consequence of this formulation is that the estimated states $\hat{x}_t(j)$, $j \in \mathbb{I}_{[0,N_t-1]}$ naturally live in the domain of the auxiliary observer (that is, the set $\mathcal{O}$), which we explicitly invoke in (4.72d)*. Now consider the case where the true system state $x(t)$ is known to evolve in some set $\mathcal{X}$ (e.g., due to the physical nature of the system* (4.22)*, see the discussion below* (4.3) *and compare also Section 3.1). As we rely on rather conventional state observers in* (4.5)*, we generally have that $\mathcal{O} \supseteq \mathcal{X}$,*

as there is no guarantee that the observer provides physically plausible state estimates for all times, compare the discussion in Section 4.2.5. To still use the additional knowledge about $\mathcal{X}$ in the MHE formulation to improve its estimation performance, one could suitably re-design the auxiliary observer as suggested in [Ast+21] (to ensure that $\mathcal{O} = \mathcal{X}$) or use additional projections as in Section 4.2.5. However, it should be noted that such projections lead to a worse bound on the corresponding estimation error, compare Definition 4.3.

Instead of solving the NLP in (4.72) to optimality, we consider the following suboptimal estimator.

Definition 4.4 (Suboptimal estimator)**.** *Let $t \in \mathbb{I}_{\geq 0}$, $N \in \mathbb{I}_{\geq 0}$, some prior estimate $\bar{x}(t - N_t)$, and the input-output sequences u_t and y_t in* (4.9) *and* (4.10) *be given. Furthermore, let $\tilde{x}_t \in \mathcal{O}^{N_t+1}$ denote a feasible candidate solution to the MHE problem* (4.72) *with the corresponding output sequence $\tilde{y}_t$. Then, the corresponding suboptimal solution of* (4.72) *is defined as any sequence $\hat{x}_t \in \mathcal{O}^{N_t+1}$ that satisfies (i) the MHE constraints* (4.72b)-(4.72d) *and (ii) the cost decrease condition*

$$J(\hat{x}_t, \hat{y}_t, t) \leq J(\tilde{x}_t, \tilde{y}_t, t). \tag{4.74}$$

The (suboptimal) state estimate at time $t \in \mathbb{I}_{\geq 0}$ is then defined as $\hat{x}(t) = \hat{x}_t(N_t)$.

We consider the following candidate solution $\tilde{x}_t \in \mathcal{O}^{N_t+1}$:

$$\tilde{x}_t(j+1) = g(\tilde{x}_t(j), u_t(j), y_t(j)),\ j \in \mathbb{I}_{[0,N_t-1]}, \tag{4.75a}$$

$$\tilde{x}_t(0) = \begin{cases} \hat{x}(t-N), & t \in \mathbb{I}_{\geq N}, \\ \hat{\chi}, & t \in \mathbb{I}_{[0,N-1]}. \end{cases} \tag{4.75b}$$

where u_t and y_t are defined in (4.9) and (4.10), respectively, and correspond to the input-output sequences obtained from the system (4.1) in the current estimation horizon. The corresponding candidate output sequence is generated from (4.72c) and denoted as $\tilde{y}_t = \{\tilde{y}_t(j)\}_{j=0}^{N_t-1}$.

Note that the candidate solution in (4.75) does *not* restrict the warm start of the particular algorithm used to (approximately) solve the NLP in (4.72), compare also Remark 4.3. Here, a practical choice is, e.g., the observer trajectory generated by (4.5) initialized using the most recent suboptimal solution (specifically, the element $\hat{x}_{t-1}(1)$) and driven by the current input-output sequences u_t and y_t. We also want to emphasize that the candidate solution in (4.75) is much simpler in contrast to the ones we constructed in Section 4.2, where the auxiliary observer needed to be re-initialized, re-simulated, and transformed into a trajectory of the system (4.1).

It remains to define the prior estimate $\bar{x}(t - N_t)$ used in the cost function in (4.73). Here, we choose the standard filtering prior

$$\bar{x}(t - N_t) = \begin{cases} \hat{x}(t-N), & t \in \mathbb{I}_{\geq N} \\ \hat{\chi}, & t \in \mathbb{I}_{[0,N-1]}, \end{cases} \tag{4.76}$$

where $\hat{x}(t-N)$ is the suboptimal estimate obtained N steps in the past and $\hat{\chi}$ corresponds to the *a priori* guess of the unknown initial condition χ of the system (4.1).

In the next section, we derive practical conditions for robust stability of suboptimal MHE, simply by exploiting the direct coupling between the MHE problem in (4.72) and the auxiliary observer in (4.5) satisfying Assumption 4.2.

4.3.2. Stability analysis

We first require an auxiliary result that establishes a bound on the cost of the candidate solution (4.75).

Lemma 4.5. *Let Assumptions 4.1 and 4.2 hold and $\hat{\chi} \in \mathcal{O}$. Let $N \in \mathbb{I}_{\geq 0}$ be arbitrary. Then, the cost function* (4.73) *evaluated at the candidate solution* (4.75) *satisfies*

$$\begin{aligned} J(\tilde{x}_t, \tilde{y}_t, t) \leq\ & N_t \eta_{\mathrm{o}}^{N_t} V_{\mathrm{o}}(\bar{x}(t-N_t), x(t-N_t)) + N_t \sum_{j=1}^{N_t} \eta_{\mathrm{o}}^{j-1} |d(t-j)|_{Q_{\mathrm{o}}}^2 \\ & + \left(\eta_{\mathrm{o}} \frac{\lambda_{\min}(P_1)}{\lambda_{\min}(R_{\mathrm{o}})} + N_t \right) \sum_{j=1}^{N_t} \eta_{\mathrm{o}}^{j-1} |v(t-j)|_{R_{\mathrm{o}}}^2 \end{aligned} \tag{4.77}$$

for all $t \in \mathbb{I}_{\geq 0}$.

Proof. First, note that the candidate solution (4.75) is feasible for the problem in (4.72), which follows from the definition of the observer in (4.5) and the fact that $\hat{\chi} \in \mathcal{O}$. From the cost function (4.73) and using that $\tilde{x}_t(0) = \bar{x}(t-N_t)$ by (4.75b) and the definition of the prior estimate in (4.76), it follows that

$$J(\tilde{x}_t, \tilde{y}_t, t) \leq \frac{\lambda_{\min}(P_1)}{2L_{\mathrm{h}}^2 \lambda_{\max}(G)} \sum_{j=0}^{N_t-1} \eta_{\mathrm{o}}^{N_t-j} |\tilde{y}_t(j) - y_t(j)|_G^2. \tag{4.78}$$

The output equation (4.1b), Assumption 4.1, and the definitions of the true state and measurement sequences x_t and v_t from (4.23) and (4.25) imply that

$$\begin{aligned} |\tilde{y}_t(j) - y_t(j)|_G^2 &\leq \lambda_{\max}(G) |h(\tilde{x}_t(j), u_t(j), 0) - h(x_t(j), u_t(j), v_t(j))|^2 \\ &\leq \lambda_{\max}(G) 2L_{\mathrm{h}}^2 (|\tilde{x}_t(j) - x_t(j)|^2 + |v_t(j)|^2) \\ &\leq 2L_{\mathrm{h}}^2 \left(\frac{\lambda_{\max}(G)}{\lambda_{\min}(P_1)} |\tilde{x}_t(j) - x_t(j)|_{P_1}^2 + \frac{\lambda_{\max}(G)}{\lambda_{\min}(R_{\mathrm{o}})} |v_t(j)|_{R_{\mathrm{o}}}^2 \right). \end{aligned} \tag{4.79}$$

By combining (4.78), (4.79), and the lower bound on V_{o} from (4.6a), we therefore obtain

$$J(\tilde{x}_t, \tilde{y}_t, t) \leq \sum_{j=0}^{N_t-1} \eta_{\mathrm{o}}^{N_t-j} \left(V_{\mathrm{o}}(\tilde{x}_t(j), x_t(j)) + \frac{\lambda_{\min}(P_1)}{\lambda_{\min}(R_{\mathrm{o}})} |v_t(j)|_{R_{\mathrm{o}}}^2 \right). \tag{4.80}$$

Since $\tilde{x}_t$ constitutes a state trajectory of the observer (4.5) via (4.72d), we can invoke Assumption 4.2 and apply the dissipation inequality (4.6b) for each $j \in \mathbb{I}_{[0,N_t-1]}$ for

j times. This leads to

$$\eta_{\mathrm{o}}^{N_t-j} V_{\mathrm{o}}(\tilde{x}_t(j), x_t(j)) \leq \eta_{\mathrm{o}}^{N_t-j} \left(\eta_{\mathrm{o}}^{j} V_o(\tilde{x}_t(0), x_t(0)) + \sum_{i=0}^{j-1} \eta_{\mathrm{o}}^{j-i-1} \left(|d_t(i)|_{Q_{\mathrm{o}}}^2 + |v_t(i)|_{R_{\mathrm{o}}}^2 \right) \right)$$

for each $j \in \mathbb{I}_{[0,N_t-1]}$. Summing up over all $j \in \mathbb{I}_{[0,N_t-1]}$ yields

$$\begin{aligned} \sum_{j=0}^{N_t-1} \eta_{\mathrm{o}}^{N_t-j} V_{\mathrm{o}}(\tilde{x}_t(j), x_t(j)) \leq\ & N_t \eta_{\mathrm{o}}^{N_t} V_{\mathrm{o}}(\tilde{x}_t(0), x_t(0)) \\ & + N_t \sum_{j=0}^{N_t-1} \eta_{\mathrm{o}}^{N_t-j-1} \left(|d_t(j)|_{Q_{\mathrm{o}}}^2 + |v_t(j)|_{R_{\mathrm{o}}}^2 \right), \end{aligned} \tag{4.81}$$

where d_t is from (4.24). Combining (4.80) and (4.81) yields

$$\begin{aligned} J(\tilde{x}_t, \tilde{y}_t, t) \leq\ & N_t \eta_{\mathrm{o}}^{N_t} V_{\mathrm{o}}(\tilde{x}_t(0), x_t(0)) + N_t \sum_{j=1}^{N_t} \eta_{\mathrm{o}}^{N_t-j-1} |d_t(j)|_{Q_{\mathrm{o}}}^2 \\ & + \left(\eta_{\mathrm{o}} \frac{\lambda_{\min}(P_1)}{\lambda_{\min}(R_{\mathrm{o}})} + N_t \right) \sum_{j=0}^{N_t-1} \eta_{\mathrm{o}}^{N_t-j-1} |v_t(j)|_{R_{\mathrm{o}}}^2. \end{aligned} \tag{4.82}$$

By recalling that $\tilde{x}_t(0) = \bar{x}(t - N_t)$ by (4.75b) and (4.76) and the definitions of the sequences x_t, d_t, v_t, we observe that (4.82) is equivalent to (4.77), which hence concludes this proof. □

In the following, we show that V_{o} is an N-step Lyapunov function for suboptimal MHE.

Theorem 4.5. *Let Assumptions 4.1 and 4.2 hold and $\hat{\chi} \in \mathcal{O}$. Let $N \in \mathbb{I}_{\geq 0}$ be arbitrary. Then, the suboptimal state estimate $\hat{x}(t)$ satisfies*

$$\begin{aligned} V_{\mathrm{o}}(\hat{x}(t), x(t)) \leq\ & \gamma_1(N_t) V_{\mathrm{o}}(\bar{x}(t - N_t), x(t - N_t)) \\ & + \sum_{j=1}^{N_t} \eta_{\mathrm{o}}^{j-1} \left(\gamma_2(N_t) |d(t-j)|_{Q_{\mathrm{o}}}^2 + \gamma_3(N_t) |v(t-j)|_{R_{\mathrm{o}}}^2 \right) \end{aligned} \tag{4.83}$$

for all $t \in \mathbb{I}_{\geq 0}$ and any $N \in \mathbb{I}_{\geq 0}$, where

$$\overline{\gamma}_1(k, r, s) := 2\lambda_{\max}(\overline{P}_{\mathrm{o}}, \underline{P}_{\mathrm{o}}) \eta_{\mathrm{o}}^{s} + \lambda_{\max}(\overline{P}_{\mathrm{o}}, W) k \eta_{\mathrm{o}}^{r+s}, \tag{4.84a}$$

$$\overline{\gamma}_2(k, r) := 1 + \lambda_{\max}(\overline{P}_{\mathrm{o}}, W) k \eta_{\mathrm{o}}^{r}, \tag{4.84b}$$

$$\overline{\gamma}_3(k, r) := 1 + \lambda_{\max}(\overline{P}_{\mathrm{o}}, W) \left(\eta_{\mathrm{o}} \frac{\lambda_{\min}(P_1)}{\lambda_{\min}(R_{\mathrm{o}})} + k \right) \eta_{\mathrm{o}}^{r} \tag{4.84c}$$

with[6] *$\gamma_1(r) := \overline{\gamma}_1(r, r, r)$ and $\gamma_i(r) := \overline{\gamma}_i(r, r)$, $i = \{2, 3\}$.*

[6] We define the functions $\overline{\gamma}_i$ in (4.84) as functions of three (two) separate variables, since this will be convenient for various extensions and adaptations discussed in Remark 4.15 and Section 4.3.3.

Proof. At any $t \in \mathbb{I}_{\geq 0}$, the constraint in (4.72b) ensures that the estimated suboptimal trajectory $\hat{x}_t = \{\hat{x}_t(j)\}_{j=0}^{N_t}$ is a trajectory of the observer (4.5), which by Assumption 4.2 admits the i-ISS Lyapunov function V_o. Hence, we can apply the dissipation inequality (4.6b) for N_t times, which leads to

$$\begin{aligned} V_\mathrm{o}(\hat{x}(t), x(t)) &= V_\mathrm{o}(\hat{x}_t(N_t), x_t(N_t)) \\ &\leq \eta_\mathrm{o}^{N_t} V_\mathrm{o}(\hat{x}_t(0), x_t(0)) + \sum_{j=1}^{N_t} \eta_\mathrm{o}^{j-1} \left(|d(t-j)|_{Q_\mathrm{o}}^2 + |v(t-j)|_{R_\mathrm{o}}^2 \right), \end{aligned} \tag{4.85}$$

where x_t corresponds to the truncated state sequence as defined in (4.23). Using (4.6a) with Cauchy-Schwarz and Young's inequality, we further have that

$$\begin{aligned} V_\mathrm{o}(\hat{x}_t(0), x_t(0)) &\leq |\hat{x}_t(0) - \bar{x}(t-N_t)|_{\overline{P}_\mathrm{o}}^2 \\ &\leq 2|\hat{x}_t(0) - \bar{x}(t-N_t)|_{\overline{P}_\mathrm{o}}^2 + 2|\bar{x}(t-N_t) - x_t(0)|_{\overline{P}_\mathrm{o}}^2. \end{aligned} \tag{4.86}$$

The second term of the right-hand side in (4.86) can be bounded by exploiting (4.6a) according to

$$2|\bar{x}(t-N_t) - x_t(0)|_{\overline{P}_\mathrm{o}}^2 \leq 2\lambda_{\max}(\overline{P}_\mathrm{o}, \underline{P}_\mathrm{o}) V_\mathrm{o}(\bar{x}(t-N_t), x_t(0)). \tag{4.87}$$

Using a similar reasoning, the first term of the right-hand side in (4.86) satisfies

$$2|\hat{x}_t(0) - \bar{x}(t-N_t)|_{\overline{P}_\mathrm{o}}^2 \leq \lambda_{\max}(\overline{P}_\mathrm{o}, W) J(\hat{x}_t, \hat{y}_t, t), \tag{4.88}$$

which follows from the definition (and non-negativity) of the cost function (4.73). In combination, from (4.85) with (4.86)–(4.88), we obtain

$$\begin{aligned} V_\mathrm{o}(\hat{x}(t), x(t)) \leq{}& \lambda_{\max}(\overline{P}_\mathrm{o}, W) \eta_\mathrm{o}^{N_t} J(\hat{x}_t, \hat{y}_t, t) + 2\lambda_{\max}(\overline{P}_\mathrm{o}, \underline{P}_\mathrm{o}) \eta_\mathrm{o}^{N_t} V_\mathrm{o}(\bar{x}(t-N_t), x_t(0)) \\ &+ \sum_{j=1}^{N_t} \eta_\mathrm{o}^{j-1} \left(|d(t-j)|_{Q_\mathrm{o}}^2 + |v(t-j)|_{R_\mathrm{o}}^2 \right). \end{aligned} \tag{4.89}$$

Now recall that

$$J(\hat{x}_t, \hat{y}_t, t) \leq J(\tilde{x}_t, \tilde{y}_t, t) \tag{4.90}$$

due to (4.74). Consequently, from (4.89) with (4.90) and Lemma 4.5, we obtain (4.83), which hence concludes this proof. □

Provided that $N \in \mathbb{I}_{\geq 0}$ is chosen such that

$$\rho^N := \gamma_1(N) < 1 \tag{4.91}$$

holds, Theorem 4.5 directly implies that

$$\begin{aligned} V_\mathrm{o}(\hat{x}(t), x(t)) \leq{}& \rho^N V_\mathrm{o}(\hat{x}(t-N), x(t-N)) \\ &+ \sum_{j=1}^{N} \eta_\mathrm{o}^{j-1} \left(\gamma_2(N) |d(t-j)|_{Q_\mathrm{o}}^2 + \gamma_3(N) |v(t-j)|_{R_\mathrm{o}}^2 \right) \end{aligned} \tag{4.92}$$

for $t \in \mathbb{I}_{\geq N}$ (recall the definition of the prior estimate in (4.76)). Consequently, the i-ISS Lyapunov function V_o characterizing robust stability of the auxiliary observer is an N-step ISS-like Lyapunov function for robust stability of suboptimal MHE.

Some remarks are in order.

Remark 4.12 (Condition on the horizon length)**.** *By standard properties of the exponential function, one can easily verify specific properties of* $\gamma_1 : \mathbb{R}_{\geq 0} \to \mathbb{R}_{\geq 0}$ *on the open interval* $[0, \infty)$*—namely, that* γ_1 *is continuous, has one (global) maximum, and* $\lim_{N\to\infty} \gamma_1(N) = 0$*. Consequently, there always exists some* $N_{\min} \in \mathbb{I}_{\geq 0}$ *sufficiently large such that* (4.91) *holds for all* $N \in \mathbb{I}_{\geq N_{\min}}$*. In practice, a suitable value of* N *can be easily obtained by evaluating the condition in* (4.91) *numerically.*

Remark 4.13 (Parameterization of the cost function)**.** *The matrices* W *and* G *in used in the cost function in* (4.73) *are arbitrary tuning parameters (satisfying* $W \succ 0$ *and* $G \succeq 0$*). The choice of* G *has no impact on the theoretical guarantees (note that* G *does not appear in* (4.83)*), since the stage cost is normalized by its largest eigenvalue* $\lambda_{\max}(G)$*. Consequently,* G *can be used to scale the output estimates differently in case* $p > 1$*. In contrast,* W *has a direct influence on all functions* $\gamma_1, \gamma_2, \gamma_3$ *in* (4.84) *via the generalized eigenvalue* $\lambda_{\max}(\overline{P}_{\mathrm{o}}, W)$*. This can be exploited to adjust the degree of confidence in the observer's estimates by specifying how much the estimated trajectory* $\hat{x}_t = \{\hat{x}_t(j)\}_{j=0}^{N_t}$ *may (*$\lambda_{\max}(\overline{P}_{\mathrm{o}}, W) \gg 1$*) or may not (*$\lambda_{\max}(\overline{P}_{\mathrm{o}}, W) \ll 1$*) deviate from the observer trajectory initialized at* $\hat{x}(t - N_t)$ *and driven by the current input-output sequences* u_t *and* y_t *from* (4.9) *and* (4.10)*. For small values of* $\lambda_{\max}(\overline{P}_{\mathrm{o}}, W)$*, the minimum horizon length is dominated by the first summand in* (4.84a)*, and the functions* $\overline{\gamma}_2$ *and* $\overline{\gamma}_3$ *in* (4.84b) *and* (4.84c) *approach unity; consequently, the disturbance gains of suboptimal MHE appearing in* (4.83) *become closer to that of the auxiliary observer given in* (4.6b) *(and converge to them for* $\lambda_{\max}(\overline{P}_{\mathrm{o}}, W) \to 0$*). Conversely, the further one allows to deviate from the stabilizing observer by choosing large values of* $\lambda_{\max}(\overline{P}_{\mathrm{o}}, W)$ *in* (4.84)*, the worse the guarantees become and the larger the horizons must be chosen (which is also intuitive, since our design is mainly aimed at preserving the stability properties of the auxiliary observer). On the other hand, this choice typically leads to good results in practice, since the estimate from the auxiliary observer can (potentially significantly) be improved with only a few iterations, compare also the simulation example in Section 4.3.3.*

Remark 4.14 (Asymptotic behavior for large N)**.** *Similar properties as discussed in Remark 4.12 for the function* γ_1 *also apply to* γ_2 *and* γ_3*. In particular, both of these functions are monotonically decreasing in* N *for* N *large enough, and* $\lim_{N\to\infty} \gamma_2(N) = \lim_{N\to\infty} \gamma_3(N) = 1$*. Together with the fact that* $\lim_{N\to\infty} \gamma_1(N) = 0$ *(see Remark 4.12), this implies the appealing theoretical property that for* $N \to \infty$*, the bound from Theorem 4.5 converges to the bound given by the i-ISS Lyapunov function* V_{o} *in* (4.6)*, regardless of how the cost function* (4.73) *is parameterized. This is generally not the case for the suboptimal MHE schemes presented in Section 4.2, where the guarantees for suboptimal MHE are strictly worse than those from the auxiliary observer.*

Remark 4.15 (Alternative candidate solution)**.** *For* $N \in \mathbb{I}_{\geq 0}$ *arbitrarily fixed, we could also apply the re-initialization strategy that we suggested in Section 4.2 (see* (4.16) *and* (4.17) *above) and derive a* T*-step Lyapunov function for a sufficiently large* $T \in \mathbb{I}_{\geq N}$*, thus ensuring robust stability of suboptimal MHE for an arbitrary horizon length* $N \in \mathbb{I}_{\geq 0}$*. However, the candidate solution becomes more intricate.*

In particular, at each $t \in \mathbb{I}_{\geq 0}$, we need to re-initialize the auxiliary observer $T_t = \min\{t, T\}$ steps in the past using $z_t(0) = \hat{x}(t-T_t)$ and perform a forward simulation for T_t steps to obtain the candidate solution $\tilde{x}_t(j) = z_t(T_t - N_t + j)$, $j \in \mathbb{I}_{[0,N_t]}$; in addition, the prior estimate $\bar{x}(t-N_t)$ needs to be replaced by $z_t(T_t - N_t)$ as in (4.18)*, see Section 4.2 for more details. Then, by suitably modifying the proofs of Lemma 4.5 and Theorem 4.5, we can derive* (4.83)–(4.84) *with functions $\overline{\gamma}_1(N_t, N_t, T_t)$, $\gamma_2(N_t)$, $\gamma_3(N_t)$, where* 1 *is replaced by $2\lambda_{\max}(\overline{P}_{\mathrm{o}}, \underline{P}_{\mathrm{o}})$ in* (4.84b)–(4.84c)*. Condition* (4.91) *(with $\gamma_1(N)$ replaced by $\overline{\gamma}_1(N, N, T)$) can then be easily solved for a sufficiently large value of T. Alternatively, one may also omit the re-initialization step of the auxiliary observer and use $T = t$ instead, which considerably simplifies the construction of the candidate solution. In this case, the property in* (4.83) *directly implies RGES of suboptimal MHE, compare Remark 4.6 and see also the simulation example in Section 4.3.3.*

Remark 4.16 (Filtering form of MHE)**.** *The MHE problem in* (4.72) *neglects the current measurement $y(t)$ and thus corresponds to the prediction form of MHE. However, we want to emphasize that our results can be easily extended to the filtering form of MHE (i.e., such that the cost function in* (4.73) *includes the term $|\hat{y}_t(N_t) - y_t(N_t)|^2_G$), albeit with a (significantly) more cumbersome notation, compare also [RMD20, Sec. 4.2]. In particular, by suitably adapting the proof of Theorem 4.5, we can derive* (4.83) *with the functions $\gamma_1(N_t)$, $\gamma_2(N_t)$, and $\gamma_3(N_t)$ replaced by $\overline{\gamma}_1(N_t+1, N_t, N_t)$, $\overline{\gamma}_2(N_t+1, N_t)$, and $\overline{\gamma}_3(N_t+1, N_t)/\eta_{\mathrm{o}}$, respectively.*

From Theorem 4.5, we can straightforwardly deduce RGES of suboptimal MHE as shown in the following corollary.

Corollary 4.2. *Suppose the conditions of Theorem 4.5 are satisfied. Let $N \in \mathbb{I}_{\geq 0}$ be such that the condition in* (4.91) *holds. Then, the suboptimal moving horizon estimator from Definition 4.4 is RGES.*

Proof. We start by defining $c_1 := \overline{\gamma}_1(N, 0, 0)$, $c_2 := \overline{\gamma}_2(N, 0)$, and $c_3 := \overline{\gamma}_3(N, 0)$ such that $\overline{\gamma}_1(k, r, s) \leq c_1 \eta_{\mathrm{o}}^s$, $\overline{\gamma}_2(k, r) \leq c_2$, $\overline{\gamma}_3(k, r) \leq c_3$ for all $k \in [0, N]$ and all $r, s \geq 0$. Due to definition of the prior in (4.76), Theorem 4.5 implies that

$$V_{\mathrm{o}}(\hat{x}(t), x(t)) \leq c_1 \eta_{\mathrm{o}}^t V_{\mathrm{o}}(\hat{\chi}, \chi) + \sum_{j=1}^{t} \eta_{\mathrm{o}}^{j-1} \left(c_2 |d(t-j)|^2_{Q_{\mathrm{o}}} + c_3 |v(t-j)|^2_{R_{\mathrm{o}}} \right) \tag{4.93}$$

for all $t \in \mathbb{I}_{[0,N-1]}$. For $t \in \mathbb{I}_{\geq N}$, on the other hand, Theorem 4.5 implies (by satisfaction of (4.91)) the Lyapunov decrease property in (4.92), which leads to

$$\begin{aligned} V_{\mathrm{o}}(\hat{x}(t), x(t)) \leq{}& \rho^N V_{\mathrm{o}}(\hat{x}(t-N), x(t-N)) \\ &+ \sum_{j=1}^{N} \eta_{\mathrm{o}}^{j-1} \left(c_2 |d(t-j)|^2_{Q_{\mathrm{o}}} + c_3 |v(t-j)|^2_{R_{\mathrm{o}}} \right). \end{aligned} \tag{4.94}$$

The combination of (4.93) and (4.94) together with the fact that $\eta_{\mathrm{o}} \leq \rho$ (which is a simple consequence of (4.91)) yields

$$V_{\mathrm{o}}(\hat{x}(t), x(t)) \leq c_1 \rho^t V_{\mathrm{o}}(\hat{\chi}, \chi) + \sum_{j=1}^{t} \rho^{j-1} \left(c_2 |d(t-j)|^2_{Q_{\mathrm{o}}} + c_3 |v(t-j)|^2_{R_{\mathrm{o}}} \right) \tag{4.95}$$

for all $t \in \mathbb{I}_{\geq 0}$ (compare the proof of Theorem 4.1). By applying the uniform boundedness condition of V_o from (4.6a) and taking the square root, we can straightforwardly transform (4.95) into a sum-based formulation of RGES. By Proposition 4.1, this is equivalent to RGES in the sense of Definition 4.1, which concludes this proof. □

4.3.3. Numerical example

To illustrate our results, we consider the batch reactor example from Section 3.4.1, which corresponds to the dynamical system

$$x_1^+ = x_1 + t_\Delta(-2k_1x_1^2 + 2k_2x_2) + d_1, \tag{4.96a}$$
$$x_2^+ = x_2 + t_\Delta(k_1x_1^2 - k_2x_2) + d_2, \tag{4.96b}$$
$$y = x_1 + x_2 + v \tag{4.96c}$$

with parameters $k_1 = 0.16$, $k_2 = 0.0064$, and $t_\Delta = 0.1$, see Section 3.4.1 for more details. We consider the initial condition $\chi = [3, 1]^\top$ and the poor *a priori* guess $\hat{\chi}_0 = [0.1, 4.5]^\top$. The disturbances $d \in \mathbb{R}^2$ and $v \in \mathbb{R}$ are modeled as uniformly distributed random variables sampled from $\{d \in \mathbb{R}^2 : |d_i| \leq 2 \cdot 10^{-3}, i = \{1, 2\}\}$ and $\{v \in \mathbb{R} : |v| \leq 10^{-2}\}$ during the simulation.

In the following, we consider the proposed suboptimal MHE scheme from Section 4.3.1, where we first analyze the influence of the weighting matrix W; then, we compare the estimation results to the suboptimal scheme from Section 4.2 (more specifically, Section 4.2.3) and two fast MHE schemes from the literature.

In order to apply suboptimal MHE, we first have to design an auxiliary observer for the system in (4.96). To this end, we consider a simple Luenberger observer in the form of (4.71) and design the constant observer gain K by following the same procedure as in Section 4.2.6. Consequently, Assumption 4.2 can be verified on $\mathcal{O} = \{z \in \mathbb{R}^n : 0.1 \leq z_1 \leq 6\}$ using a quadratic Lyapunov function $V_\mathrm{o}(z, x) = |z-x|_P^2$ and the parameters $\eta_\mathrm{o} = 0.955$,

$$K = \begin{bmatrix} 7.999 \\ -9.997 \end{bmatrix}, \quad P = \begin{bmatrix} 1.537 & 1.380 \\ 1.380 & 1.254 \end{bmatrix}, \quad Q_\mathrm{o} = \begin{bmatrix} 10^3 & 0 \\ 0 & 10^3 \end{bmatrix}, \quad R_\mathrm{o} = 100,$$

leading to $\overline{P}_\mathrm{o} = \underline{P}_\mathrm{o} = P$ in (4.6a).

As additional benchmark for suboptimal MHE, we consider the standard (i.e., fully optimized with respect to the system dynamics) MHE formulation presented in [Sch+23, Sec. III]. This essentially corresponds to the scheme outlined in Section 3.1 using the discounted cost function from (4.12) with $\bar{\eta} = \eta_\mathrm{s}$ and the prior weighting and stage cost from (4.13) and (4.14), respectively. For the validity of the theoretical guarantees from [Sch+23, Thm. 1], the cost function parameters η_s, $\overline{P}_\mathrm{s}$, Q_s, R_s, G_s are to be chosen according to an i-IOSS Lyapunov function U in the sense of Assumption 4.3 (which is also required in the design of the suboptimal MHE scheme from Section 4.2). To this end, we adapt Corollary 7.1 to our current setup (with distinct process disturbances and measurement noise) and verify the

corresponding LMI conditions on $\mathcal{O}$, while imposing $U(x_1, x_2) = V_\mathrm{o}(z, x)$ for the sake of comparability. The remaining parameters are $\eta_\mathrm{s} = 0.9545$ and

$$\overline{P}_\mathrm{s} = P_\mathrm{o}, \quad Q_\mathrm{s} = \begin{bmatrix} 2 \cdot 10^3 & 0 \\ 0 & 2 \cdot 10^3 \end{bmatrix}, \quad R_\mathrm{s} = 2 \cdot 10^3, \quad G_\mathrm{s} = 200.$$

Suboptimal MHE with different prior weightings

In the following, we consider $G = 1$ and $W = a\overline{P}_\mathrm{o}$ in (4.73), where we select $a \in \{10^2, 1, 10^{-3}, 10^{-4}\}$ in order to illustrate the influence of the prior weighting as theoretically analyzed in Remark 4.13. Moreover, we consider the filtering form of MHE (which is generally beneficial in practical applications) and hence employ the modifications from Remark 4.16. The respective minimum required horizon lengths N_min ensuring the contraction condition (4.91) are shown in the upper part of Table 4.5. Here, we can observe that the value of a has a direct influence on the value of N_min, which is clear because the factor $\lambda_\mathrm{max}(\overline{P}_\mathrm{o}, W) = 1/a$ appears in the function $\bar{\gamma}_1$ in (4.84a) and hence in the contraction condition in (4.91), see also Remark 4.13.

We simulate each suboptimal estimator and the benchmark MHE scheme in MATLAB with CasADi [And+18] and the NLP solver IPOPT [WB05], where we select $N = N_\mathrm{min}$ so that valid theoretical guarantees[7] are obtained in each case. Table 4.5 shows the SSE and the average computation time τ_avrg per sampling instant for different numbers of solver iterations i. Here, we observe that small values of a are required to improve the estimates from the Luenberger observer (which corresponds to the case of $i = 0$ in Table 4.5). In line with Remark 4.13, this requires larger horizons in order to satisfy condition (4.91). However, Table 4.5 indicates that the choice of larger horizons only has a relatively small impact on the computation time. This is in line with the simulation results reported in [Suw+14; WK17] and mainly due to the formulation of the MHE problem in (4.72), which in particular avoids the estimation of additional process disturbances (and thus the use of corresponding decision variables) compared to classical MHE schemes, see, e.g., (4.11). Moreover, we find that already $i = 1$ iteration is sufficient to significantly improve the estimates of the auxiliary observer, while preserving its robustness guarantees and reducing the computational complexity in terms of τ_avrg compared to the benchmark MHE scheme by $\approx 66\,\%$. In fact, Table 4.5 also shows that performing one iteration of the optimizer yields estimation results that are close to the fully converged ones. The reason why allowing more iterations sometimes leads to smaller computation times in Table 4.5 can be attributed to the fact that this generally produces very accurate (close to optimal) warm starts for the optimization problems, which accelerates the optimization algorithm accordingly.

[7] Note that using a different (worse conditioned) matrix P allows for choosing a smaller horizon length for the benchmark MHE scheme, compare Section 3.4.1.

Table 4.5. Comparison of the estimation results of suboptimal MHE for different weighting matrices $W = a\overline{P}_\mathrm{o}$ and different numbers of solver iterations i.

i	$a = 10^2$ N_min=16		$a = 1$ N_min=45		$a = 10^{-3}$ N_min=128		$a = 10^{-4}$ N_min=155	
	SSE	τ_avrg	SSE	τ_avrg	SSE	τ_avrg	SSE	τ_avrg
0	42.90	2.30	42.90	2.50	42.90	2.86	42.85	2.97
1	42.83	3.09	42.47	3.34	3.49	3.53	1.11	3.61
2	42.85	3.14	42.48	3.41	3.49	4.13	1.09	3.45
3	42.93	3.14	42.52	3.40	3.46	4.05	1.12	3.36
$*$	42.98	3.14	42.53	3.40	3.50	4.10	1.12	3.40

Each value represents the average over 100 simulations of length $t_\mathrm{sim} = 200$; the average computation time τ_avrg is in milliseconds (ms); asterisks represent fully converged optimization problems; the benchmark MHE yields $N_\mathrm{min} = 30$ and achieves SSE = 0.5 with $\tau_\mathrm{avrg} = 10.86$ ms.

Comparison with fast MHE schemes from the literature

We compare the proposed suboptimal estimator (which we denote in following as s-MHE$_1$) to the suboptimal MHE scheme presented in Section 4.2 (s-MHE$_2$) and to the fast MHE schemes from [Küh+11] (f-MHE$_1$) and [WVD14] (f-MHE$_2$). For comparison reasons, we fix the horizon length to $N = 10$, and thus, consider the modifications from Remark 4.15. Motivated by the findings from Table 4.5, we choose $W = 10^{-4}\overline{P}_\mathrm{o}$ and select $T = t$, which trivially ensures RGES of suboptimal MHE, see Remark 4.15 (here, it turned out that the additional effort of re-initializing the auxiliary observer was not worthwhile for this application example). For s-MHE$_2$, we consider the observer-based candidate solution from (4.46) and use the same cost function as for the benchmark MHE (i.e., the discounted cost function from (4.12)–(4.14) parameterized using the i-IOSS Lyapunov function U from above and with $\bar{\eta} = \eta_\mathrm{s}$). Here, we also select $T = t$ to ensure valid theoretical guarantees, compare Remark 4.6. The cost function for f-MHE$_1$ is parameterized analogously, whereas f-MHE$_2$ does not allow for tuning, see [WVD14] for further details. Since f-MHE$_1$ and f-MHE$_2$ both rely on the GGN algorithm, we implement the suboptimal MHE schemes s-MHE$_1$ and s-MHE$_2$ in a similar fashion, relying on a Lagrange relaxation [WVD14]. To this end, we have to adapt the initial estimate to $\hat{\chi} = [2, 1.8]^\top$, since the GGN algorithm does not converge using the previously chosen initial estimate, illustrating its local nature, compare [WVD14]. As additional comparison, we again consider the benchmark MHE scheme from above, although the corresponding guarantees do not hold anymore since $N = 10 < N_\mathrm{min} = 30$.

Figure 4.3 shows the simulation results for all estimators under study, which reveals an improved transient behavior of s-MHE$_1$ compared to s-MHE$_2$, the fast MHE schemes f-MHE$_1$ and f-MHE$_2$, and the auxiliary observer. This is mainly due to the fact that the auxiliary observer is rather aggressive and converges accordingly fast, albeit being highly sensitive to noise and exhibiting significant oscillations. These oscillations are efficiently reduced by the proposed suboptimal scheme s-MHE$_1$ (as

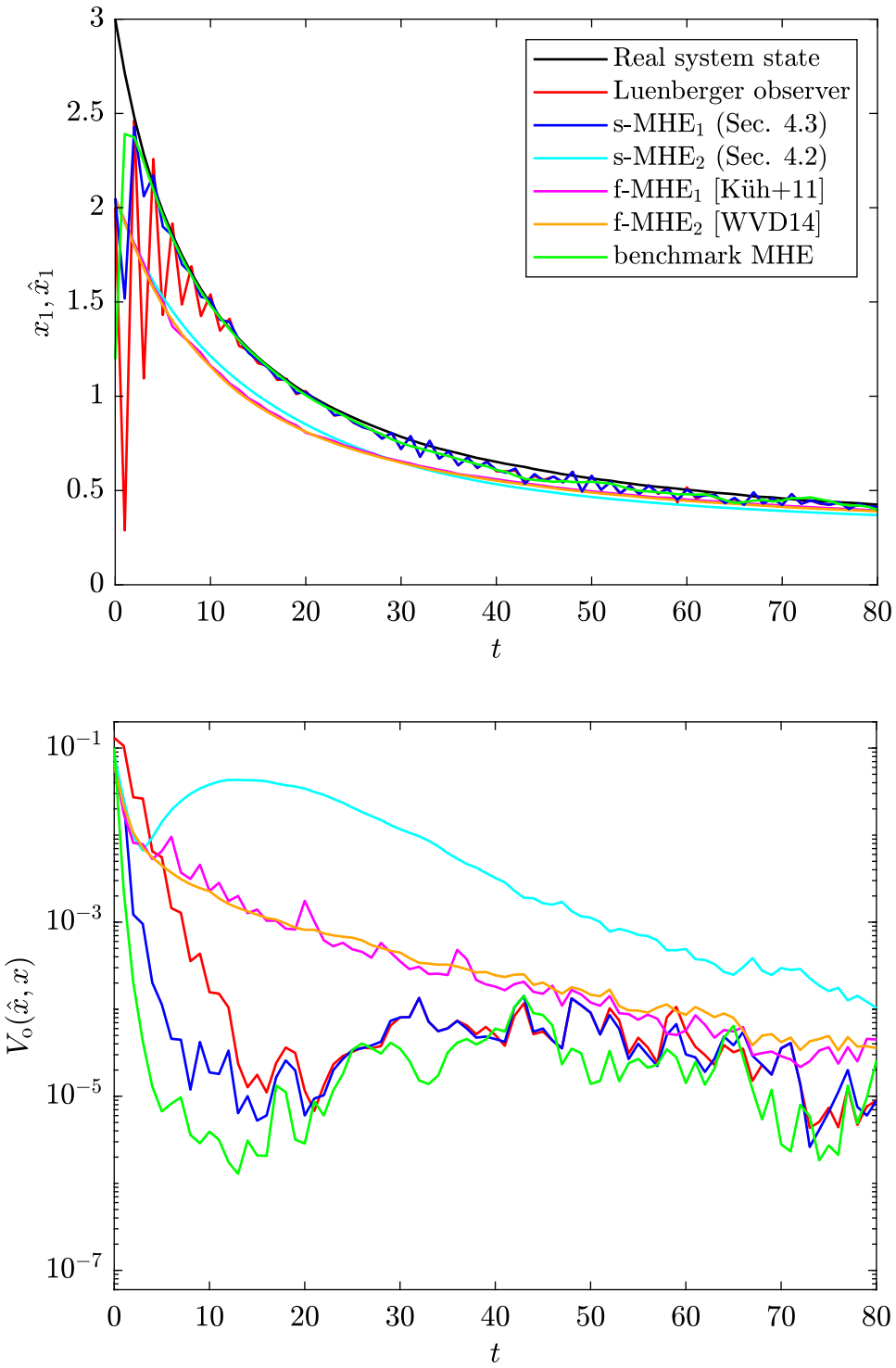

Figure 4.3. Estimation results for the proposed suboptimal MHE scheme under the modifications from Remark 4.15 (s-MHE$_1$), suboptimal MHE from Section 4.2 (s-MHE$_2$), and the fast MHE schemes f-MHE$_1$ [Küh+11] and f-MHE$_2$ [WVD14] after performing $i = 1$ GGN iteration compared to the Luenberger observer and the (fully optimized) benchmark MHE using a fixed estimation horizon $N = 10$. Top: Real system state x_1 and its estimates $\hat{x}_1$ over time; bottom: estimation error in Lyapunov coordinates.

Table 4.6. Average computation time τ_{avrg} per sample in milliseconds (ms) for the proposed suboptimal scheme compared to similar methods from the literature.

s-MHE$_1$	s-MHE$_2$	f-MHE$_1$	f-MHE$_2$	benchmark
0.57	0.69	0.61	0.46	10.55

Each value represents the average over 100 simulations of length $t_{\text{sim}} = 80$.

we use a small weighting matrix W), while its fast convergence property could be preserved. Moreover, the estimates are close to those of the benchmark MHE. In contrast, the suboptimal/fast MHE schemes that optimize over system trajectories converge much slower, which is due to the slower dynamics of the system compared to the auxiliary observer. To achieve a faster convergence and improved transient behavior, one would have to perform more than one GGN iteration per time step, which is consistent with the simulation results obtained in Section 4.2.6. Further simulations have shown that the use of auxiliary observers with significantly slower error dynamics does not necessarily lead to advantages (in terms of the convergence rate) of the proposed suboptimal MHE scheme over the methods from Section 4.2. This is in line with intuition and suggests that the auxiliary observer should be designed rather aggressively in applications to achieve fast convergence of suboptimal MHE.

From the computation times shown in Table 4.6, we observe that s-MHE$_1$ is slightly faster than s-MHE$_2$ and f-MHE$_1$, which is mainly due to the fact that less decision variables are used in the optimization problem (4.72) compared to (4.11). Moreover, s-MHE$_1$ is slightly slower than f-MHE$_2$, as the latter avoids the computation of a prior weighting. Overall, the differences in the computation times are rather small, and all suboptimal/fast MHE schemes under consideration are capable of reducing the computational complexity (measured in terms of τ_{avrg}) compared to the benchmark MHE by $\approx 95\,\%$. However, the proposed suboptimal MHE scheme is generally much more flexible compared to f-MHE$_1$ and f-MHE$_2$ from [Küh+11] and [WVD14] (in particular, since arbitrary optimization algorithms can be used) and has the potential to converge faster than schemes relying on a standard MHE formulation (such as SMHE$_2$ and f-MHE$_{1,2}$), while providing valid theoretical guarantees.

4.4. Summary

In this chapter, we presented several suboptimal MHE schemes that are applicable to general nonlinear systems and established robust stability guarantees with respect to unknown process disturbances and measurement noise. This is crucial in order to ensure real-time applicability of MHE in cases where the optimization problem cannot be solved to optimality within one fixed sampling interval. The suboptimal schemes rely on an *a priori* known, robustly stable auxiliary observer, which is used to construct a suitable candidate solution to the respective MHE problems. By imposing that any suboptimal solution to the MHE problem achieves at most the

same cost, the proposed suboptimal estimators inherit the stability properties of the auxiliary observer while benefiting from the performance of numerical optimizers. Here, we considered two conceptually different MHE formulations: first, a rather classical one that optimizes over trajectories of the system, and second, a modified version that optimizes directly over trajectories of the auxiliary observer.

The first MHE formulation allows for the use of a standard least squares cost function (with or without additional discounting), which is typically chosen in practical applications. In this context, we considered two different candidate solutions; one is applicable to general nonlinear systems, the other requires a certain structure of the system and the observer, but provides qualitatively better theoretical guarantees (in particular, disturbance gains that do not deteriorate with increasing estimation horizons). Moreover, we suitably modified the candidate solutions to account for the practically relevant case where the auxiliary observer may violate the MHE constraints. We showed that the i-IOSS Lyapunov function characterizing the detectability of the underlying nonlinear system is a Lyapunov function for suboptimal MHE, from which robust stability can be directly inferred. In contrast to most of the related literature, the derived robustness guarantees are valid independent of (i) the horizon length; (ii) the chosen optimization algorithm; (iii) the number of solver iterations performed at each time step (including zero).

The second MHE formulation (which directly optimizes over trajectories of the auxiliary observer) can further improve the estimation results, both from a theoretical and a practical point of view. Since the corresponding suboptimal MHE scheme is even stronger connected to the auxiliary observer, the theoretical analysis is more direct, ultimately leading to tighter error bounds. Specifically, we show that the Lyapunov function characterizing robust stability of the auxiliary observer is also a Lyapunov function for suboptimal MHE under a suitable choice of the horizon length. Consequently, the derived guarantees are independent of the optimization algorithm, hold for an arbitrary number of solver iterations (including zero), improve as the horizon length increases, and asymptotically approach those from the auxiliary observer (which is the best possible bound). However, in contrast to classical MHE formulations optimizing over system trajectories, it is not directly possible to consider state constraints in the MHE problem if the auxiliary observer does not naturally comply with them, see Remark 4.11 and compare also Section 4.2.5.

The simulation examples showed that both MHE formulations are very effective, especially in the case of poor transient behavior of the auxiliary observer. Moreover, with only a few iterations of the optimizer, we were able to significantly improve the estimates of the auxiliary observer and achieve an overall estimation performance close to that obtained with standard (optimal) MHE, while significantly reducing the required computation times.

5. Joint state and parameter estimation

In this chapter, we address the case where the dynamical model of a system to be estimated suffers from additional parametric uncertainties. To this end, we propose and analyze MHE schemes for joint state and parameter estimation that are applicable to general nonlinear systems. Here, our main concern is to avoid the restrictive assumption of a uniform PE condition for the parameters (compare the discussion in Section 1.2.4) and instead consider the practically relevant case where insufficient excitation may occur frequently and unpredictably during operation. Here, the basic idea is to use online information about the current excitation of the parameters and to adjust the corresponding regularization term in the cost function accordingly. This allows us to establish theoretical guarantees for the state and parameter estimation error that are valid for all times, even if the parameters are never or only rarely excited.

In Section 5.1, we introduce the general problem setup. In Section 5.2, we present and analyze an MHE scheme for joint state and parameter estimation, where we first restrict ourselves to the special case of constant parameters. This will be relaxed in Section 5.3, where we generalize the proposed MHE framework to time-varying parameters. Our results are complemented by the verification methods developed in Section 7.2, which provide practical tools for online monitoring PE properties of general nonlinear systems.

Disclosure: The following chapter is based upon and in parts literally taken from our previous publications [SM23b] and [SM24a]. A detailed description of the contributions of each author is given in Appendix A.

5.1. Setup

We consider discrete-time systems in the form of (3.1) with additional parametric dependency, that is,

$$x(t+1) = f(x(t), u(t), w(t), p(t)), \quad x(0) = \chi, \tag{5.1a}$$
$$p(t+1) = g(p(t), u(t), w(t)), \quad p(0) = \xi, \tag{5.1b}$$
$$y(t) = h(x(t), u(t), w(t), p(t)), \tag{5.1c}$$

where $t \in \mathbb{I}_{\geq 0}$ is the discrete time, $x(t) \in \mathbb{R}^n$ is the state at time t, $p(t) \in \mathbb{R}^o$ is the unknown (generally time-varying) parameter, $\chi \in \mathbb{R}^n$ and $\xi \in \mathbb{R}^o$ are the corresponding initial conditions, $y(t) \in \mathbb{R}^p$ is the (noisy) output measurement, $u(t) \in \mathbb{R}^m$ is a

known input (e.g., the control input), and $w(t) \in \mathbb{R}^q$ is an unknown generalized disturbance input representing both process disturbances and measurement noise. The nonlinear continuous functions $f : \mathbb{R}^n \times \mathbb{R}^m \times \mathbb{R}^q \times \mathbb{R}^o \to \mathbb{R}^n$, $g : \times \mathbb{R}^o \times \mathbb{R}^m \times \mathbb{R}^q \to \mathbb{R}^o$, and $h : \mathbb{R}^n \times \mathbb{R}^m \times \mathbb{R}^q \times \mathbb{R}^o \to \mathbb{R}^p$ represent the system dynamics, the parameter dynamics, and the output equation, respectively.

The system description (5.1) obviously covers standard setups in the context of parameter estimation:

1. Constant parameters $p(t) = p$, $t \in \mathbb{I}_{\geq 0}$ for some unknown constant vector p, where $g(p, u, w) = p$ in (5.1b). This corresponds to the special case considered in most of the theory on system identification and online parameter estimation, compare, for example, [Lju99; IS12]. This case is addressed in Section 5.2.
2. Time-varying parameters $p(t)$, where $g(p, u, w)$ can be used to model known internal dynamics of p, the variable u can represent the influence of known inputs (e.g. explicit dependence of p on time) and the input w can represent, e.g., an unknown drift. We consider the case of time-varying parameters in Section 5.3. Note that this covers the important special case of

$$g(p, u, w) = p + B_{\mathrm{p}} w \tag{5.2}$$

for some matrix B_{p}, where the term $B_{\mathrm{p}} w$ corresponds to an unknown input.

In the following, we assume that the states $x(t)$ are uniformly detectable (i-IOSS) and the parameters $p(t)$ are non-uniformly observable (in the sense that observability depends on the excitation of the system and may be absent during operation). Here, we want to emphasize that the distinction between states and parameters is rather artificial, as discussed in the following remark.

Remark 5.1 (Distinction between states and parameters)**.** *Note that the separation between* states *and* parameters *in the system description in* (5.1) *is rather for ease of presentation and may not necessarily correspond to the physical understanding of the model. In general, the variable x can represent all time-varying quantities of a (possibly extended) system that are uniformly detectable, and p represents all quantities that are non-uniformly observable. This is particularly relevant for systems in which the observability of certain states depends on the excitation (which can then be described by* (5.1b)*), or for systems in which certain parameters prove to be uniformly detectable (which can then be described by* (5.1a)*).*

In the following, we assume that the unknown true system trajectories satisfy

$$(x(t), u(t), w(t), p(t)) \in \mathcal{Z},\ t \in \mathbb{I}_{\geq 0}, \tag{5.3}$$

where

$$\begin{aligned} \mathcal{Z} := \{(x, u, w, p) \in \mathcal{X} \times \mathcal{U} \times \mathcal{W} \times \mathcal{P} :& \\ f(x, u, w, p) \in \mathcal{X},\ g(p, u, w) \in \mathcal{P},\ h(x, u, w, p) \in \mathcal{Y}\}& \end{aligned}$$

and $\mathcal{X} \subseteq \mathbb{R}^n$, $\mathcal{P} \subseteq \mathbb{R}^o$, $\mathcal{U} \subseteq \mathbb{R}^m$, $\mathcal{W} \subseteq \mathbb{R}^q$, and $\mathcal{Y} \subseteq \mathbb{R}^p$ are some known closed sets. The set $\mathcal{Z}$ can be used to incorporate additional information about the physical

domain of the real system trajectories in the estimation scheme, which can often significantly improve the estimation results, compare [RMD20, Sec. 4.4] and see Section 3.1 for further details. Such constraints typically arise from the physical nature of the system, e.g., non-negativity of partial pressures, mechanically imposed limits, or known parameter ranges. If no such information is available, they can simply be chosen as $\mathcal{X} = \mathbb{R}^n$, $\mathcal{P} = \mathbb{R}^o$, $\mathcal{U} = \mathbb{R}^m$, $\mathcal{W} = \mathbb{R}^q$, $\mathcal{Y} = \mathbb{R}^p$.

The overall goal is to compute at each time $t \in \mathbb{I}_{\geq 0}$ the estimates $\hat{x}(t)$ and $\hat{p}(t)$ of the true unknown state $x(t)$ and parameter $p(t)$ using some given *a priori* estimates $\hat{\chi}$ and $\hat{\xi}$ and the past measured input-output sequence $\{(u(j), y(j))\}_{j=0}^{t-1}$. To ensure robust estimation under disturbances and noise, we require suitable detectability and excitation properties, which we specify in detail below.

Assumption 5.1 (State detectability)**.** *System* (5.1) *admits an i-IOSS Lyapunov function* $U : \mathcal{X} \times \mathcal{X} \to \mathbb{R}_{\geq 0}$*, that is, there exist matrices* $\underline{P}, \overline{P}, S_{\mathrm{x}}, Q_{\mathrm{x}}, R_{\mathrm{x}} \succ 0$ *and a constant* $\eta_{\mathrm{x}} \in (0, 1)$ *such that*

$$|x_1 - x_2|_{\underline{P}}^2 \leq U(x_1, x_2) \leq |x_1 - x_2|_{\overline{P}}^2, \tag{5.4}$$

$$\begin{aligned} &U(f(x_1, u, w_1, p_1), f(x_2, u, w_2, p_2)) \\ &\leq \eta_{\mathrm{x}} U(x_1, x_2) + |p_1 - p_2|_{S_{\mathrm{x}}}^2 + |w_1 - w_2|_{Q_{\mathrm{x}}}^2 + |h(x_1, u, w_1, p_1) - h(x_2, u, w_2, p_2)|_{R_{\mathrm{x}}}^2 \end{aligned} \tag{5.5}$$

for all $(x_1, u, w_1, p_1), (x_2, u, w_2, p_2) \in \mathcal{Z}$.

Assumption 5.1 is equivalent[1] to exponential i-IOSS when interpreting the parameter p as additional (constant) exogenous input in (5.1a). This concept became standard as a description of nonlinear detectability in the context of MHE (for state estimation) in recent years, see, e.g., [RMD20; AR21; KM23; Hu24; Sch+23]. It essentially implies that the difference between any two state trajectories is bounded by the differences of their initial states, their disturbance inputs, their parameters, and their outputs, see Chapter 2 for more details on this topic. We point out that Assumption 5.1 is not restrictive; in fact, by an extension of the results from [ART21; KM23], one can show that this constitutes a necessary and sufficient condition for the existence of robustly stable state estimators if the true parameter is known, and of practically stable state estimators with respect to the parameter error when only an estimate of the true parameter is available. Moreover, Assumption 5.1 can be numerically verified using LMIs and SDP by adapting our results from Section 7.1.1 below.

In the following, we first consider the special case of constant parameters $p(t) = p$ in (5.1b) and propose a suitable MHE scheme for joint state and parameter estimation. To this end, we employ a certain non-uniform PE property to distinguish the cases where the currently involved data segments are informative enough for parameter estimation or not. In Section 5.3, we generalize the overall MHE framework by considering the case of time-varying parameters as described by (5.1b). Here, we adapt our notion of PE and modify the MHE scheme and analysis accordingly.

[1] This follows by a straightforward adaption of the converse Lyapunov theorem from [ART21].

5.2. Constant parameters

In this section, we address MHE for joint state and parameter estimation for the case of constant parameters, that is, where $g(p, u, w) = p$ in (5.1b). We outline the MHE design in Section 5.2.1, provide a detailed technical analysis in Section 5.2.2, discuss the special case of uniform persistent excitation in Section 5.2.3, and illustrate the efficiency of the proposed approach with a numerical example in Section 5.2.4.

We now specify the notion of PE used in this section. In particular, we define the set of persistently excited trajectory pairs, which contains all trajectory pairs that exhibit a T-step distinguishability property with respect to the parameters.

Definition 5.1 (Set of persistently excited trajectory pairs)**.** *Consider some fixed matrices $S_\mathrm{p}, P_\mathrm{p}, Q_\mathrm{p}, R_\mathrm{p} \succ 0$ and a constant $\eta_\mathrm{p} \in (0, 1)$. The set containing all persistently excited trajectory pairs of length $T \in \mathbb{I}_{\geq 0}$ is defined as*

$$\begin{aligned}\mathbb{E}_T := \Bigg\{ & \left(\{(x_1(t), u(t), w_1(t), p_1)\}_{t=0}^{T-1}, \{(x_2(t), u(t), w_2(t), p_2)\}_{t=0}^{T-1}\right) \in \mathcal{Z}^T \times \mathcal{Z}^T : \\ & x_i(t+1) = f(x_i(t), u(t), w_i(t), p_i),\ i = 1, 2,\ t \in \mathbb{I}_{[0,T-1]}, \\ & y_i(t) = h(x_i(t), u(t), w_i(t), p_i),\ i = 1, 2,\ t \in \mathbb{I}_{[0,T-1]}, \\ & |p_1 - p_2|_{S_\mathrm{p}}^2 \leq \eta_\mathrm{p}^T |x_1(0) - x_2(0)|_{P_\mathrm{p}}^2 \\ & \qquad + \sum_{j=0}^{T-1} \eta_\mathrm{p}^{T-j-1} \left(|w_1(j) - w_2(j)|_{Q_\mathrm{p}}^2 + |y_1(j) - y_2(j)|_{R_\mathrm{p}}^2\right) \Bigg\}.\end{aligned}$$

For two trajectories that share the same initial state and the same disturbance inputs, if they form a pair contained in the set $\mathbb{E}_T$, it holds that the sum of their output differences is zero if and only if their parameters are the same. In other words, trajectory pairs contained in $\mathbb{E}_T$ are sufficiently excited—and hence informative enough—for parameter estimation. In Section 5.2.3, we discuss the relation between detectability of the states (Assumption 5.1), excited trajectory pairs (Definition 5.1), uniform PE, and a uniform joint detectability condition for both the states and the parameters.

5.2.1. Design

The MHE scheme we propose below is a modification of the basic discrete-time MHE scheme from Section 3.1, particularly tailored to joint state and parameter estimation. Here, we will mainly focus on the technical description of the scheme; for a more detailed discussion, we refer to Section 3.1.

At each time $t \in \mathbb{I}_{\geq 0}$, the proposed MHE scheme considers measured past input-output sequences of the system (5.1) within a moving horizon of length $N_t = \min\{t, N\}$ for some $N \in \mathbb{I}_{\geq 0}$. For convenience, we denote them by the corresponding

truncated data sequences restricted to the horizon:

$$u_t = \{u_t(j)\}_{j=0}^{N_t-1},\ u_t(j) = u(t-N_t+j),\ j \in \mathbb{I}_{[0,N_t-1]},\ t \in \mathbb{I}_{\geq 0}, \tag{5.6}$$
$$y_t = \{y_t(j)\}_{j=0}^{N_t-1},\ y_t(j) = y(t-N_t+j),\ j \in \mathbb{I}_{[0,N_t-1]},\ t \in \mathbb{I}_{\geq 0}. \tag{5.7}$$

The current state and parameter estimates $\hat{x}(t)$ and $\hat{p}(t)$ at time $t \in \mathbb{I}_{\geq 0}$ are then obtained by solving the following NLP:

$$\min_{\hat{x}_t, \hat{p}_t, \hat{w}_t} \ J(\hat{x}_t, \hat{p}_t, \hat{w}_t, \hat{y}_t, t) \tag{5.8a}$$
$$\text{s.t. } \hat{x}_t(j+1) = f(\hat{x}_t(j), u_t(j), \hat{w}_t(j), \hat{p}_t),\ j \in \mathbb{I}_{[0,N_t-1]}, \tag{5.8b}$$
$$\hat{y}_t(j) = h(\hat{x}_t(j), u(j), \hat{w}_t(j), \hat{p}_t),\ j \in \mathbb{I}_{[0,N_t-1]}, \tag{5.8c}$$
$$(\hat{x}_t(j), u_t(j), \hat{w}_t(j), \hat{p}_t) \in \mathcal{Z},\ j \in \mathbb{I}_{[0,N_t-1]}. \tag{5.8d}$$

The cost function $J(\cdot)$ is specified below. The decision variables $\hat{x}_t := \{\hat{x}_t(j)\}_{j=0}^{N_t} \in \mathcal{X}^{N_t+1}$, $\hat{p}_t \in \mathcal{P}$, and $\hat{w}_t := \{\hat{w}_t(j)\}_{j=0}^{N_t-1} \in \mathcal{W}^{N_t}$ denote the estimated state sequence, parameter, and disturbance sequence over the horizon, respectively, estimated at time t. When implementing the scheme in practice, it may be beneficial to employ a multiple shooting formulation for the parameter as well in order to create sparsity of the NLP, compare also Section 3.1. In this case, the vector $\hat{p}_t$ needs to be replaced by a sequence $\hat{p}_t = \{\hat{p}_t(j)\}_{j=0}^{N_t}$ that is kept constant by adding the artificial constant parameter dynamics $\hat{p}_t(j+1) = \hat{p}_t(j)$, $j \in \mathbb{I}_{[0,N_t-1]}$ as optimization constraint in (5.8). The constraint in (5.8d) enforces prior knowledge about the domain of the system, where we use the set $\mathcal{Z}$ defined in (5.3) to keep the notation concise, compare Section 3.1 for an alternative (variable-wise) formulation. Given the past input sequence u_t in (5.6), the decision variables $\hat{x}_t$, $\hat{p}_t$, and $\hat{w}_t$ uniquely define a sequence of output estimates $\hat{y}_t := \{\hat{y}_t(j)\}_{j=0}^{N_t-1}$ under the output equation in (5.8c).

In (5.8a), we use the discounted quadratic cost function

$$\begin{aligned} J(\hat{x}_t, \hat{p}_t, \hat{w}_t, \hat{y}_t, t) := \gamma(N_t)|\hat{x}_t(0) - \bar{x}(t-N_t)|^2_{W(t-N_t)} + \eta_1^{N_t}|\hat{p}_t - \bar{p}(t-N_t)|^2_{V(t-N_t)} \\ + \sum_{j=0}^{N_t-1} \eta_2^{N_t-j-1}\Big(|\hat{w}_t(j)|^2_{Q(t-N_t+j)} + |\hat{y}_t(j) - y_t(j)|^2_{R(t-N_t+j)}\Big), \end{aligned} \tag{5.9}$$

where the prior state and parameter estimates $\bar{x}(t-N_t)$ and $\bar{p}(t-N_t)$ are specified below. We impose the following conditions on the cost function parameters $\gamma(\cdot)$, η_1, η_2 and the weighting matrices $W(t)$, $V(t)$, $Q(t)$, and $R(t)$.

Assumption 5.2 (Cost function)**.** *The discount parameters γ, η_1, η_2 satisfy*

$$\gamma(s) = \eta_{\mathrm{x}}^s + \lambda_{\max}(P_{\mathrm{p}}, \overline{P})\eta_{\mathrm{p}}^s,\ s \geq 0, \tag{5.10}$$
$$\eta_1 \in (\max\{\eta_{\mathrm{x}}, \eta_{\mathrm{p}}\}, 1), \tag{5.11}$$
$$\eta_2 \in [\max\{\eta_{\mathrm{x}}, \eta_{\mathrm{p}}\}, 1). \tag{5.12}$$

Furthermore, there exist matrices $\overline{W}, \underline{V}, \overline{V}, \overline{Q}, \overline{R} \succ 0$ *such that*

$$2\overline{P} \preceq W(t) \preceq \overline{W}, \tag{5.13}$$
$$2S_{\mathrm{p}} \preceq 2\underline{V} \preceq V(t) \preceq \overline{V}, \tag{5.14}$$
$$2(Q_{\mathrm{x}} + Q_{\mathrm{p}}) \preceq Q(t) \preceq \overline{Q}, \tag{5.15}$$
$$R_{\mathrm{x}} + R_{\mathrm{p}} \preceq R(t) \preceq \overline{R} \tag{5.16}$$

uniformly for all $t \in \mathbb{I}_{\geq 0}$.

Assumption 5.2 ensures large tuning capabilities of the cost function (5.9) while satisfying certain relations to the detectability and excitation properties from Assumption 5.1 and Definition 5.1. This is conceptually similar to the recent MHE literature (for state estimation) and typically permits a less conservative stability analysis due to the structural similarities between the detectability condition, the MHE scheme, and the desired stability property, compare Remark 3.3 and see the discussion in Section 3.3 for more details. Potential time dependency of the weighting matrices in (5.13)–(5.16) can be used to incorporate additional knowledge (e.g., by choosing Kalman filter covariance update laws [QH09; RRM03]), which can be beneficial in practice to improve estimation performance. Assumption 5.2 implies that the cost function (5.9) is radially unbounded in the (condensed) decision variables, which together with continuity of f and h ensures that the estimation problem described by (5.8) and (5.9) admits a (not necessarily unique) globally optimal solution at any time $t \in \mathbb{I}_{\geq 0}$, compare [RMD20, Sec. 4.2]. In the following, we denote a corresponding minimizer by the tuple $(\hat{x}_t^*, \hat{p}_t^*, \hat{w}_t^*)$.

It remains to define suitable update laws for the prior estimates to ensure a proper regularization of the cost function (5.9). To this end, for the state prior we select

$$\bar{x}(t) = \begin{cases} \hat{x}_t^*(N), & t \in \mathbb{I}_{\geq N} \\ \hat{\chi}, & t \in \mathbb{I}_{[0,N-1]}. \end{cases}$$

This choice corresponds to the *filtering prior*, compare [RMD20, Sec. 4.3] and see also Section 3.1. For the parameter prior, we propose the following excitation-dependent update law:

$$\bar{p}(t) = \begin{cases} \hat{p}_t^*, & \text{if } t \in \mathbb{I}_{\geq N} \text{ and } X(t) \in \mathbb{E}_N, \\ \bar{p}(t - N_t), & \text{otherwise,} \end{cases} \tag{5.17}$$

where $\bar{p}(0) = \hat{\xi}$ and

$$X(t) := \left(\{(\hat{x}_t^*(j), u_t(j), \hat{w}_t^*(j), \hat{p}_t^*)\}_{j=0}^{N_t-1}, \{(x(j), u(j), w(j), p)\}_{j=t-N_t}^{t-1} \right)$$

is the pair of the currently optimal and (unknown) true trajectory restricted to the estimation horizon. The update law in (5.17) depends on the excitation of the trajectory pair $X(t)$, where $\mathbb{E}_N$ is from Definition 5.1. In particular, the prior estimate $\bar{p}(t)$ is updated with the currently estimated parameter $\hat{p}_t^*$ only if $\hat{p}_t^*$ was computed using sufficiently informative data. Conversely, if we detect insufficient excitation, we simply select the past prior $\bar{p}(t - N_t)$ as the new prior $\bar{p}(t)$. Overall,

this procedure ensures that the MHE cost function in (5.9) is always regularized with a meaningful prior that was computed using informative data. In Section 7.2, we propose suitable methods to practically check whether the respective PE condition $X(t) \in \mathbb{E}_N$ holds (in particular, without knowledge of the unknown true trajectory).

The resulting state and parameter estimates at time $t \in \mathbb{I}_{\geq 0}$ are then defined $\hat{x}(t) = \hat{x}_t^*(N_t)$ and $\hat{p}(t) = \hat{p}_t^*$ (compare also Remark 5.2 for an alternative definition of the current parameter estimate). This leads to the joint state and parameter estimation error

$$e(t) = \begin{bmatrix} e_{\mathrm{x}}(t) \\ e_{\mathrm{p}}(t) \end{bmatrix} = \begin{bmatrix} \hat{x}(t) - x(t) \\ \hat{p}(t) - p \end{bmatrix}, \ t \in \mathbb{I}_{\geq 1}, \quad e(0) = \begin{bmatrix} \hat{\chi} - \chi \\ \hat{\xi} - p \end{bmatrix}. \tag{5.18}$$

In the following, we show how the horizon length N must be chosen so that the estimation error (5.18) exhibits a certain robust stability property that is valid regardless of the parameter excitation.

5.2.2. Stability analysis

Our theoretical analysis relies on the following two Lyapunov function candidates:

$$\Gamma_1(t, \hat{x}, x, \hat{p}, p) = U(\hat{x}, x) + |\hat{p} - p|^2_{V(t)}, \tag{5.19}$$

$$\Gamma_2(\hat{x}, x, \hat{p}, p) = U(\hat{x}, x) + c|\hat{p} - p|^2_{\overline{V}}, \ c \geq 1, \tag{5.20}$$

where U is the i-IOSS Lyapunov function from Assumption 5.1 and $V(t) \preceq \overline{V}$ is from the cost function (5.9) under Assumption 5.2. The following two auxiliary results establish fundamental properties of Γ_1 and Γ_2 for the two cases where the current level of excitation is too low ($X(t) \notin \mathbb{E}_N$, Lemma 5.1) or sufficiently high ($X(t) \in \mathbb{E}_N$, Lemma 5.2).

Lemma 5.1. *Let Assumption 5.1 hold. Consider the MHE scheme* (5.8) *with the cost function* (5.9) *satisfying Assumption 5.2. Assume that* $t \in \mathbb{I}_{[0,N-1]}$ *or* $t \in \{t \in \mathbb{I}_{\geq N} : X(t) \notin \mathbb{E}_N\}$. *Then, it holds that*

$$\begin{aligned} \Gamma_1(t, \hat{x}(t), x(t), \hat{p}(t), p) \leq\ & \eta_1^{-N} c_1(N_t)(\eta_{\mathrm{x}}^{N_t} + \gamma(N_t))|\bar{x}(t - N_t) - x(t - N_t)|^2_{\overline{W}} \\ & + 2c_1(N_t)\eta_1^{-N}\eta_1^{N_t}|\bar{p}(t - N_t) - p|^2_{\overline{V}} \\ & + 2c_1(N_t)\eta_1^{-N} \sum_{j=1}^{N_t} \eta_2^{j-1}|w(t - j)|^2_{\overline{Q}}, \end{aligned} \tag{5.21}$$

where

$$c_1(s) := \bar{\lambda}(S_{\mathrm{x}}, \underline{V}) \frac{1 - \eta_{\mathrm{x}}^s}{1 - \eta_{\mathrm{x}}} + \lambda_{\max}(\overline{V}, \underline{V}), \ s \geq 0. \tag{5.22}$$

Proof. We start by defining the sequences of the true states and disturbances restricted to the estimation horizon:

$$x_t := \{x_t(j)\}_{j=0}^{N_t}, \ x_t(j) = x(t - N_t + j), \ j \in \mathbb{I}_{[0,N_t]}, \ t \in \mathbb{I}_{\geq 0}, \tag{5.23}$$

$$w_t := \{w_t(j)\}_{j=0}^{N_t-1}, \ w_t(j) = w(t - N_t + j), \ j \in \mathbb{I}_{[0,N_t-1]}. \ t \in \mathbb{I}_{\geq 0}. \tag{5.24}$$

Now, consider the function Γ_1 in (5.19). Since we have that $\hat{x}(t) = \hat{x}_t^*(N_t)$, the boundedness property of $V(t)$ from (5.14) implies

$$\Gamma_1(t, \hat{x}(t), x(t), \hat{p}(t), p) \leq U(\hat{x}_t^*(N_t), x_t(N_t)) + \lambda_{\max}(\overline{V}, \underline{V})|\hat{p}_t^* - p|_{\underline{V}}^2. \tag{5.25}$$

Due to satisfaction of the MHE constraints (5.8b)–(5.8d), we can invoke Assumption 5.1 (in particular, the dissipation inequality (5.5)), which lets us conclude that

$$\begin{aligned} U(\hat{x}_t^*(N_t), x_t(N_t)) \leq \eta_{\mathrm{x}}^{N_t} U(\hat{x}_t^*(0), x_t(0)) + \sum_{j=0}^{N_t-1} \eta_{\mathrm{x}}^{N_t-j-1} |\hat{p}_t^* - p|_{S_{\mathrm{x}}}^2 \\ + \sum_{j=0}^{N_t-1} \eta_{\mathrm{x}}^{N_t-j-1} \left(|\hat{w}_t^*(j) - w_t(j)|_{Q_{\mathrm{x}}}^2 + |\hat{y}_t^*(j) - y_t(j)|_{R_{\mathrm{x}}}^2 \right). \end{aligned} \tag{5.26}$$

Note that $|\hat{p}_t^* - p|_{S_{\mathrm{x}}}^2 \leq \bar{\lambda}(S_{\mathrm{x}}, \underline{V})|\hat{p}_t^* - p|_{\underline{V}}^2$. Furthermore, by applying the geometric series we obtain

$$\sum_{j=0}^{N_t-1} \eta_{\mathrm{x}}^{N_t-j-1} |\hat{p}_t^* - p|_{S_{\mathrm{x}}}^2 \leq \bar{\lambda}(S_{\mathrm{x}}, \underline{V}) \frac{1 - \eta_{\mathrm{x}}^{N_t}}{1 - \eta_{\mathrm{x}}} |\hat{p}_t^* - p|_{\underline{V}}^2. \tag{5.27}$$

From the upper bound in (5.4) and Jensen's inequality, we have

$$\begin{aligned} U(\hat{x}_t^*(0), x_t(0)) &\leq |\hat{x}_t^*(0) - x_t(0)|_{\overline{P}}^2 \\ &\leq 2|\hat{x}_t^*(0) - \bar{x}(t - N_t)|_{\overline{P}}^2 + 2|\bar{x}(t - N_t) - x_t(0)|_{\overline{P}}^2 \end{aligned} \tag{5.28}$$

for all $j \in \mathbb{I}_{[1,N_t]}$. Similarly, we obtain

$$|\hat{p}_t^* - p|_{\underline{V}}^2 \leq 2|\hat{p}_t^* - \bar{p}(t - N_t)|_{\underline{V}}^2 + 2|\bar{p}(t - N_t) - p|_{\underline{V}}^2 \tag{5.29}$$

and

$$|\hat{w}_t^*(j) - w_t(j)|_{Q_{\mathrm{x}}}^2 \leq 2|\hat{w}_t^*(j)|_{Q_{\mathrm{x}}}^2 + 2|w_t(j)|_{Q_{\mathrm{x}}}^2 \tag{5.30}$$

for all $j \in \mathbb{I}_{[1,N_t]}$. Applying (5.26)–(5.30) to (5.25) leads to

$$\begin{aligned} &\Gamma_1(t, \hat{x}(t), x(t), \hat{p}(t), p) \\ &\leq \eta_{\mathrm{x}}^{N_t} \left(2|\hat{x}_t^*(0) - \bar{x}(t - N_t)|_{\overline{P}}^2 + 2|\bar{x}(t - N_t) - x_t(0)|_{\overline{P}}^2 \right) \\ &\quad + c_1(N_t) \left(2|\hat{p}_t^* - \bar{p}(t - N_t)|_{\underline{V}}^2 + 2|\bar{p}(t - N_t) - p|_{\underline{V}}^2 \right) \\ &\quad + \sum_{j=0}^{N_t-1} \eta_{\mathrm{x}}^{N_t-j-1} \left(2|\hat{w}_t^*(j)|_{Q_{\mathrm{x}}}^2 + 2|w_t(j)|_{Q_{\mathrm{x}}}^2 + |\hat{y}_t^*(j) - y_t(j)|_{R_{\mathrm{x}}}^2 \right), \end{aligned}$$

where we have used the definition of $c_1(s)$ from (5.22). Using that $\eta_1^{N_t-N} \geq 1$ and $c_1(N_t) > 1$, we can invoke the cost function (5.9) due to the facts that $\eta_{\mathrm{x}}^s \leq \gamma(s)$ for all $s \geq 0$, $\eta_{\mathrm{x}} \leq \eta_2$, and $2\overline{P} \preceq W(t) \preceq \overline{W}$, $2\underline{V} \preceq V(t) \preceq \overline{V}$, $2Q_{\mathrm{x}} \preceq Q(t) \preceq \overline{Q}$, $R_{\mathrm{x}} \preceq R(t)$ for all $t \in \mathbb{I}_{\geq 0}$ by Assumption 5.2, which yields

$$\begin{aligned} &\Gamma_1(t, \hat{x}(t), x(t), \hat{p}(t), p) \\ &\leq \eta_1^{-N} c_1(N_t) \Big(\eta_{\mathrm{x}}^{N_t} |\bar{x}(t - N_t) - x_t(0)|_{\overline{W}}^2 + \eta_1^{N_t} |\bar{p}(t - N_t) - p|_{\overline{V}}^2 \\ &\qquad + \sum_{j=0}^{N_t-1} \eta_2^{N_t-j-1} |w_t(j)|_{\overline{Q}}^2 + J(\hat{x}_t^*, \hat{p}_t^*, \hat{w}_t^*, \hat{y}_t^*, t) \Big). \end{aligned} \tag{5.31}$$

Using optimality and boundedness of $W(t)$, $V(t)$, and $Q(t)$ leads to

$$\begin{aligned}&J(\hat{x}_t^*, \hat{p}_t^*, \hat{w}_t^*, \hat{y}_t^*, t) \leq J\left(x_t, p, w_t, y_t, t\right)\\ &\leq \gamma(N_t)|x_t(0) - \bar{x}(t-N_t)|_{\overline{W}}^2 + \eta_1^{N_t}|p - \bar{p}(t-N_t)|_{\overline{V}}^2 + \sum_{j=0}^{N_t-1} \eta_2^{N_t-j-1}|w_t(j)|_{\overline{Q}}^2. \quad (5.32)\end{aligned}$$

Combining (5.31) and (5.32) and recalling the definitions in (5.23) and (5.24) yields (5.21), which hence concludes this proof. □

Lemma 5.2. *Let Assumption 5.1 hold. Consider the MHE scheme* (5.8) *with the cost function* (5.9) *satisfying Assumption 5.2. Assume that $X(t) \in \mathbb{E}_N$ for some $t \in \mathbb{I}_{\geq N}$. Then, it holds that*

$$\begin{aligned}\Gamma_2(\hat{x}(t), x(t), \hat{p}(t), p) \leq \mu^N \Gamma_1(t-N, \bar{x}(t-N), x(t-N), \bar{p}(t-N), p)\\ + 2c_2(c,N)\sum_{j=1}^{N} \eta_2^{j-1}|w(t-j)|_{\overline{Q}}^2, \quad (5.33)\end{aligned}$$

for all $c \geq 1$, where

$$\mu := \max\left\{ \sqrt[N]{2\lambda_{\max}(\overline{W}, \underline{P})c_2(c,N)\gamma(N)},\ \sqrt[N]{c_2(c,N)}\eta_1 \right\} \quad (5.34)$$

and, for any $c \geq 1$ and $s \geq 0$,

$$c_2(c,s) := c\lambda_{\max}(\overline{V}, S_{\mathrm{p}}) + \lambda_{\max}(S_{\mathrm{x}}, S_{\mathrm{p}})(1-\eta_{\mathrm{x}}^s)/(1-\eta_{\mathrm{x}}). \quad (5.35)$$

Proof. We start by following the same arguments as in the beginning of the proof of Lemma 5.1 (based on the fact that the optimal estimated trajectory is a trajectory of the i-IOSS system (5.1) by invoking the MHE constraints (5.8b)–(5.8d)). This allows us to exploit (5.26) and (5.27) with $\underline{V}$ replaced by S_{p}, leading to

$$\begin{aligned}\Gamma_2(\hat{x}(t), x(t), \hat{p}(t), p) &= U(\hat{x}_t^*(N), x_t(N)) + c|\hat{p}_t^* - p|_{\overline{V}}^2\\ &\leq \eta_{\mathrm{x}}^N U(\hat{x}_t^*(0), x_t(0)) + c_2(c,N)|\hat{p}_t^* - p|_{S_{\mathrm{p}}}^2\\ &\quad + \sum_{j=0}^{N-1} \eta_{\mathrm{x}}^{N-j-1}\left(|\hat{w}_t^*(j) - w_t(j)|_{Q_{\mathrm{x}}}^2 + |\hat{y}_t^*(j) - y_j(j)|_{R_{\mathrm{x}}}^2\right)\end{aligned}$$

with x_t and w_t as defined in (5.23) and (5.24), respectively, and where we have used the definition of $c_2(c,N)$ from (5.35). In the following, we drop the arguments of c_2 for the sake of brevity. Since $X(t) \in \mathbb{E}_N$ by assumption, it follows that

$$\begin{aligned}|\hat{p}_t^* - p|_{S_{\mathrm{p}}}^2 &\leq \eta_{\mathrm{p}}^N |\hat{x}_t^*(0) - x_t(0)|_{P_{\mathrm{p}}}^2\\ &\quad + \sum_{j=0}^{N-1} \eta_{\mathrm{p}}^{N-j-1}\left(|\hat{w}_t^*(j) - w_t(j)|_{Q_{\mathrm{p}}}^2 + |\hat{y}_t^*(j) - y_t(j)|_{R_{\mathrm{p}}}^2\right).\end{aligned}$$

Using the bound on U together with the definition of $\gamma(s)$ from (5.10) and the fact that $c_2(c,s) \geq 1$ for all $s > 0$ due to $c \geq 1$ and (5.14), we obtain

$$\begin{aligned}&\Gamma_2(\hat{x}(t), x(t), \hat{p}(t), p)\\ &\leq c_2\Big(\gamma(N)|\hat{x}_t^*(0) - x_t(0)|_{\overline{P}}^2 + \sum_{j=0}^{N-1} \tilde{\eta}^{N-j-1}\left(|\hat{w}_t^*(j) - w_t(j)|_{\tilde{Q}}^2 + |\hat{y}_t^*(j) - y_t(j)|_{\tilde{R}}^2\right)\Big),\end{aligned}$$

where $\tilde{\eta} := \max\{\eta_{\mathrm{x}}, \eta_{\mathrm{p}}\}$, $\tilde{Q} = Q_{\mathrm{x}} + Q_{\mathrm{p}}$, and $\tilde{R} := R_{\mathrm{x}} + R_{\mathrm{p}}$. Application of (5.28) and (5.30) with Q_{x} replaced by $\tilde{Q}$ together with the definition of the cost function J from (5.9) and Assumption 5.2 leads to

$$\Gamma_2(\hat{x}(t), x(t), \hat{p}(t), p) \leq c_2\Big(\gamma(N)|\bar{x}(t-N) - x_t(0)|^2_{\overline{W}} + \sum_{j=0}^{N-1} \eta_2^{N-j-1}|w_t(j)|^2_{\overline{Q}} + J(\hat{x}^*_t, \hat{p}^*_t, \hat{w}^*_t, \hat{y}^*_t, t)\Big).$$

By optimality, the first inequality in (5.32) holds, which leads to

$$\Gamma_2(\hat{x}(t), x(t), \hat{p}(t), p) \leq 2c_2\gamma(N)|\bar{x}(t-N) - x_t(0)|^2_{\overline{W}} + c_2\eta_1^N|\bar{p}(t-N) - p|^2_{V(t-N)} + 2c_2\sum_{j=0}^{N-1} \eta_2^{N-j-1}|w_t(j)|^2_{\overline{Q}}.$$

Application of $|\bar{x}(t-N) - x_t(0)|^2_{\overline{W}} \leq \lambda_{\max}(\overline{W}, \underline{P})|\bar{x}(t-N) - x_t(0)|^2_{\underline{P}}$ and recalling the definitions of Γ_1 from (5.19), μ from (5.34), and x_t and w_t from (5.23) and (5.24) yields (5.33), which finishes this proof. □

Now, let

$$\rho := \max\left\{\eta_1^{-N}c_1(N)(\eta_{\mathrm{x}}^N + \gamma(N))\lambda_{\max}(\overline{W}, \underline{P}), \eta_2^N\right\} \tag{5.36}$$

and c be such that

$$c = 2c_1(N)/(1-\rho) + 1 \tag{5.37}$$

with c_1 from (5.22). The robustness guarantees for the proposed MHE scheme require satisfaction of the following conditions on the horizon length N:

$$2\lambda_{\max}(\overline{W}, \underline{P})c_2(c, N)\gamma(N) < 1, \tag{5.38}$$

$$c_2(c, N)\eta_1^N < 1, \tag{5.39}$$

$$\eta_1^{-N}c_1(N)(\eta_{\mathrm{x}}^N + \gamma(N))\lambda_{\max}(\overline{W}, \underline{P}) < 1, \tag{5.40}$$

where $c_1(s)$ and $\gamma(s)$ are from (5.22) and (5.10), respectively. The conditions (5.38) and (5.39) imply that $\mu \in (0, 1)$ in (5.34) and hence ensure contraction of the state and parameter estimation error in case the excitation condition used in (5.17) is met (i.e., $X(t) \in \mathbb{E}_N$). Condition (5.40) implies $\rho \in (0, 1)$ in (5.36) and $c \geq 1$ in (5.37) and hence ensures boundedness of the estimation error in case the excitation condition is not met (i.e., $X(t) \neq \mathbb{E}_N$). Under Assumption 5.2, there always exists a sufficiently large N such that the contraction conditions (5.38)–(5.40) are satisfied. This becomes apparent by noting that the left-hand side of each of these conditions can be bounded by a function that exponentially decays to zero as $N \to \infty$, which follows by invoking (5.10)–(5.12) and uniform boundedness of c_1 and c_2 from (5.22) and (5.35).

At each time $t \in \mathbb{I}_{\geq 0}$, we split the interval $[0, t]$ into sub-intervals of length N and the remainder $l = t - \lfloor t/N \rfloor N$:

$$t = l + \sum_{m=1}^{k}(i_m + 1)N + jN, \tag{5.41}$$

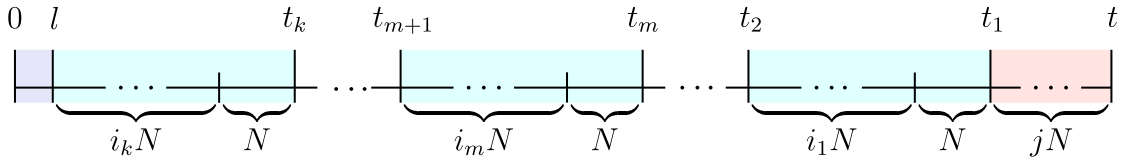

Figure 5.1. Division of the current time interval $\mathbb{I}_{[0,t]}$ corresponding to the sum in (5.41). The times $t_1, t_2, ..., t_k$ refer to PE horizons where $X(t_i) \in \mathbb{E}_N$ for $i \in \mathbb{I}_{[1,k]}$.

where $k \in \mathbb{I}_{\geq 0}$, $i_m \in \mathbb{I}_{[1,k]}$ for $k \in \mathbb{I}_{\geq 1}$, and $j \in \mathbb{I}_{\geq 0}$ are defined as follows. First, let the set

$$\mathcal{T}_t := \left\{ \tau \in \mathbb{I}_{[N,t]} : t - \tau = \left\lfloor \frac{t-\tau}{N} \right\rfloor N,\ X(\tau) \in \mathbb{E}_N \right\}$$

contain all past time instants from the set $\{t, t-N, t-2N, ...\}$ at which the excitation condition used in (5.17) was met (in the following also referred to as *PE horizons* for simplicity). The variable k denotes the total number of PE horizons that occurred until the current time t and is defined as the cardinality of $\mathcal{T}_t$, i.e., $k := |\mathcal{T}_t|$. Suppose that $k \in \mathbb{I}_{\geq 1}$. The sequence $\{t_m\}_{m=1}^k$ contains time instants corresponding to PE horizons, where $t_1 := \max\{\tau \in \mathcal{T}_t\}$ and

$$t_{m+1} = \max\{\tau \in \mathcal{T}_t : \tau < t_m\},\ m \in \mathbb{I}_{[1,k-1]}$$

if $k \in \mathbb{I}_{\geq 2}$. The sequence $\{i_m\}_{m=1}^k$ denotes the numbers of non-PE horizons (i.e., past time instants where the excitation condition (5.17) was not met) between two successive times t_m and t_{m+1} with

$$i_m = \frac{t_m - N - t_{m+1}}{N},\ m \in \mathbb{I}_{[1,k-1]}$$

if $k \in \mathbb{I}_{\geq 2}$, and[2] $i_k = (t_k - N - l)/N$. Finally, j stands for the number of non-PE horizons that occurred between time t and t_1 if $k \geq 1$ (and between time t and l if $k = 0$), i.e.,

$$j := \frac{t - \max\{\tau \in \mathcal{T}_t, l\}}{N}.$$

Overall, the partitioning in (5.41) allows us to theoretically cover occasional occurrence of PE horizons, which of course includes the special cases in which PE horizons never occur ($k = 0$), or in which all horizons are PE ($j = 0$, $i_m = 0$ for all $m = 1, ..., k$). The general partitioning of the interval $\mathbb{I}_{[0,t]}$ is also visualized in Figure 5.1.

We are now in a position to state our main result of this section. Our key argument is that the Lyapunov function Γ_2 in (5.20) decreases from t_m to t_{m+1} (i.e., over the light-cyan colored areas in Figure 5.1) by invoking the contraction conditions (5.38)–(5.40) and Lemmas 5.1 and 5.2, provided that N is sufficiently large.

Theorem 5.1. *Let Assumption 5.1 hold. Consider the MHE scheme* (5.8) *with the cost function* (5.9) *satisfying Assumption 5.2. Suppose that the horizon length N*

[2]Note that $\{t_m\}_{m=1}^k, \{i_m\}_{m=1}^k$ do not have to be formally defined for $k = 0$, as this yields an empty sum in (5.41).

satisfies (5.38)–(5.40). *Then, it holds that*

$$\begin{aligned}
&\frac{1}{C_0}\Gamma_1(t,\hat{x}(t),x(t),\hat{p}(t),p)\\
&\leq \mu^{kN}\left(C_1\tilde{\eta}^l|\hat{\chi}-\chi|_{\overline{W}}^2+C_2\eta_1^l|\hat{\xi}-p|_{\overline{V}}^2\right)\\
&\quad+\mu^{kN}\sum_{r=1}^{l}\eta_2^{r-1}|w(l-r)|_Q^2+\sum_{r=1}^{jN}\rho_N^{r-1}|w(t-r)|_Q^2\\
&\quad+\sum_{m=1}^{k}\mu^{(m-1)N}\sum_{r=1}^{(i_m+1)N}\bar{\mu}^{r-1}|w(t-jN-\sum_{q=1}^{m-1}(i_q+1)N-r)|_Q^2
\end{aligned}\tag{5.42}$$

for all $t\in\mathbb{I}_{\geq 0}$ *and all* $\hat{\chi},\chi\in\mathcal{X}$*, all* $\hat{\xi},p\in\mathcal{P}$*, and all input and disturbance sequences* $u\in\mathcal{U}^\infty$ *and* $w\in\mathcal{W}^\infty$*, respectively, where* $\tilde{\eta}=\max\{\eta_\mathrm{x},\eta_\mathrm{p}\}$*,* $\bar{\mu}=\max\{\mu,\rho_N\}$*,* $\rho_N=\sqrt[N]{\rho}$ *with* ρ *from* (5.36)*, and*

$$C_0 := c\lambda_{\max}(\overline{V},\underline{V}),\tag{5.43}$$
$$C_1 := \eta_1^{-N}c_1(N)(2+\lambda_{\max}(P_\mathrm{p},\overline{P})),\tag{5.44}$$
$$C_2 := (2c_1(N)+\lambda_{\max}(\overline{V},\underline{V})^{-1})\eta_1^{-N},\tag{5.45}$$
$$Q := \max\left\{\eta_1^{-N}c_1(N),c_2(c,N)\right\}2\overline{Q}.\tag{5.46}$$

Before proving Theorem 5.1, we want to highlight some key properties.

1. By the definition of Γ_1 in (5.19) and the lower bound in (5.4), it follows that $\Gamma_1(t,\hat{x}(t),x(t),\hat{p}(t),p)=U(\hat{x}(t),x(t))+|\hat{p}(t)-p|_{V(t)}^2\geq|e_\mathrm{x}(t)|_{\underline{P}}^2+|e_\mathrm{p}(t)|_{\underline{V}}^2\geq\min\{\lambda_{\min}(\underline{P}),\lambda_{\min}(\underline{V})\}|e(t)|^2$, $t\in\mathbb{I}_{\geq 0}$. Hence, Theorem 5.1 provides a bound on the joint state and parameter estimation error (5.18) that is valid regardless of the parameter excitation; it also applies if the excitation condition in (5.17) is never met (which corresponds $k=0$ in (5.42)) and constitutes a bounded-disturbance bounded-estimation-error property.
2. Satisfaction of the excitation condition in (5.17) for some $t\in\mathbb{I}_{\geq N}$ (leading to non-zero values of k in (5.42)) always improves the error bound (5.42) with respect to the initial estimation error.
3. If $k\to\infty$ for $t\to\infty$, then the estimation error converges to a ball centered at the origin with the radius defined by the true disturbances.

Proof of Theorem 5.1. We prove the statement in five parts—namely, by deriving bounds

1) on $\Gamma_1(t,\cdot)$ involving data from $[t-jN,t-1]$,
2) on $\Gamma_2(\cdot)$ involving data from $[t_2,t_1-1]$,
3) on $\Gamma_2(\cdot)$ involving data from $[t_k,t_1-1]$,
4) on $\Gamma_2(\cdot)$ involving data from $[0,l-1]$,
5) on $\Gamma_1(t,\cdot)$ involving all available data from $[0,t-1]$.

Part 1. We define

$$\tilde{\Gamma}_1(t) := \Gamma_1(t, \hat{x}(t), x(t), \hat{p}(t), p) \tag{5.47}$$

for notational brevity and assume that $j \in \mathbb{I}_{\geq 1}$. From Lemma 5.1, the fact that $|\bar{x}(t-N) - x(t-N)|_{\overline{W}}^2 \leq \lambda_{\max}(\overline{W}, \underline{P}) U(\bar{x}(t-N), x(t-N))$ by (5.4), and the contraction condition (5.40), we obtain

$$\tilde{\Gamma}_1(t) \leq \rho U(\bar{x}(t-N), x(t-N)) + c_1' |\bar{p}(t-N) - p|_{\overline{V}}^2 + \sum_{r=1}^{N} \eta_2^{r-1} |w(t-r)|_Q^2, \tag{5.48}$$

where $c_1' = 2c_1(N)$, $2c_1(N)\eta_1^{-N}\overline{Q} \preceq Q$ with Q from (5.46), and ρ satisfies $\rho < 1$. In (5.48), note that $\bar{x}(t-N) = \hat{x}(t-N)$ and $\bar{p}(t-N) = \bar{p}(t-qN) = \bar{p}(t-jN)$ for all $q = 1, ..., j$ due to the update rule (5.17). Since $U(\hat{x}(t-N), x(t-N)) \leq \tilde{\Gamma}_1(t-N)$ by (5.19) and the definition of $\tilde{\Gamma}_1$ from above, we can recursively apply (5.48) for j times, yielding

$$\begin{aligned} \tilde{\Gamma}_1(t) \leq \rho^j U(\hat{x}(t-jN), x(t-jN)) + \sum_{q=1}^{j} \rho^{q-1} c_1' |\bar{p}(t-jN) - p|_{\overline{V}}^2 \\ + \sum_{q=1}^{j} \rho^{q-1} \sum_{r=1}^{N} \eta_2^{r-1} |w(t-(q-1)N-r)|_Q^2. \end{aligned} \tag{5.49}$$

Using $\rho_N := \sqrt[N]{\rho} \geq \eta_2$ (this follows by the definition of ρ in (5.36)), the geometric series, and $c_1'/(1-\rho) = 2c_1(N)/(1-\rho) < c$ by (5.37), we have that

$$\tilde{\Gamma}_1(t) \leq \Gamma_2(\hat{x}(t-jN), x(t-jN), \bar{p}(t-jN), p) + \sum_{r=1}^{jN} \rho_N^{r-1} |w(t-r)|_Q^2. \tag{5.50}$$

Part 2. Assume that $k \in \mathbb{I}_{\geq 1}$. Then, $t - jN = t_1$ corresponds to the most recent PE horizon where $X(t_1) \in \mathbb{E}_N$ and $\bar{p}(t-jN) = \hat{p}(t_1)$ by (5.17). Invoking Lemma 5.2 yields

$$\begin{aligned} &\Gamma_2(\hat{x}(t-jN), x(t-jN), \bar{p}(t-jN), p) = \Gamma_2(\hat{x}(t_1), x(t_1), \hat{p}(t_1), p) \\ &\leq \mu^N \Gamma_1(t_1 - N, \bar{x}(t_1 - N), x(t_1 - N), \bar{p}(t_1 - N), p) + \sum_{r=1}^{N} \eta_2^{r-1} |w(t_1 - r)|_Q^2, \end{aligned} \tag{5.51}$$

where we have used that $2c_2(c, N)\overline{Q} \preceq Q$ with Q from (5.46). By the definition of Γ_1 from (5.19), we obtain

$$\begin{aligned} &\Gamma_1(t_1 - N, \bar{x}(t_1 - N), x(t_1 - N), \bar{p}(t_1 - N), p) \\ &= U(\bar{x}(t_1 - N), x(t_1 - N)) + |\bar{p}(t_1 - N) - p|_{V(t-N)}^2 \\ &\leq \Gamma_1(t_1 - N, \hat{x}(t_1 - N), x(t_1 - N), \hat{p}(t_1 - N), p) + |\bar{p}(t_1 - (i_1 + 1)N) - p|_{\overline{V}}^2, \end{aligned} \tag{5.52}$$

where we have used that $\bar{x}(t_1 - N) = \hat{x}(t_1 - N)$ and $\bar{p}(t_1 - N) = \bar{p}(t_1 - qN) = \bar{p}(t_1 - (i_1 + 1)N)$ for all $q = 1, ..., i_1 + 1$. In the following, consider $k \in \mathbb{I}_{\geq 2}$. Then,

$\bar{p}(t_1-(i_1+1)N) = \hat{p}(t_2)$. Using a similar argument as in (5.49), the geometric series, and the definition of ρ_N, we have that

$$\begin{aligned}&\Gamma_1(t_1 - N, \hat{x}(t_1 - N), x(t_1 - N), \hat{p}(t_1 - N), p)\\ &\leq \rho^{i_1} U(\hat{x}(t_2), x(t_2)) + \frac{c_1'}{1-\rho}|\hat{p}(t_2) - p|_{\overline{V}}^2 + \sum_{r=1}^{i_1 N} \rho_N^{r-1} |w(t_1 - N - r)|_Q^2. \end{aligned} \tag{5.53}$$

Combining (5.51)–(5.53) with the fact that $c = c_1'/(1-\rho) + 1$ and the definition of $\bar{\mu} := \max\{\mu, \rho_N\}$, we obtain

$$\Gamma_2(\hat{x}(t_1), x(t_1), \hat{p}(t_1), p) \leq \mu^N \Gamma_2(\hat{x}(t_2), x(t_2), \hat{p}(t_2), p) + \sum_{r=1}^{(i_1+1)N} \bar{\mu}^{r-1} |w(t_1 - r)|_Q^2. \tag{5.54}$$

Part 3. Suppose that $k \in \mathbb{I}_{\geq 2}$. By applying (5.54) recursively for all $m \in \mathbb{I}_{[1,k-1]}$ and the fact that $t - jN - \sum_{m=1}^{k}(i_m + 1)N = l$ by (5.41), we can infer that

$$\begin{aligned}&\Gamma_2(\hat{x}(t - jN), x(t - jN), \bar{p}(t - jN), p)\\ &\leq \mu^{kN} \Gamma_2(\hat{x}(l), x(l), \bar{p}(l), p)\\ &\quad + \sum_{m=1}^{k} \mu^{(m-1)N} \sum_{r=1}^{(i_m+1)N} \bar{\mu}^{r-1} |w(t - jN - \sum_{q=1}^{m-1}(i_q + 1)N - r)|_Q^2. \end{aligned} \tag{5.55}$$

Part 4. By the definition of Γ_2 from (5.20), it follows that

$$\begin{aligned}\Gamma_2(\hat{x}(l), x(l), \bar{p}(l), p) &= U(\hat{x}(l), x(l)) + c|\bar{p}(l) - p|_{\overline{V}}^2 + c|\hat{p}(l) - p|_{\overline{V}}^2\\ &\leq C_0(\Gamma_1(l, \hat{x}(l), x(l), \hat{p}(l), p) + \lambda_{\max}(\overline{V}, \underline{V})^{-1} |\bar{p}(l) - p|_{\overline{V}}^2)\end{aligned} \tag{5.56}$$

with C_0 from (5.43), and where $\bar{p}(l) = \hat{\xi}$ by (5.17). By using Lemma 5.1 with $\bar{x}(0) = \hat{\chi}$ and $\bar{p}(0) = \hat{\xi}$, we obtain

$$\begin{aligned}&\Gamma_1(l, \hat{x}(l), x(l), \hat{p}(l), p)\\ &\leq c_1(N)\eta_1^{-N}(\eta_{\mathrm{x}}^l + \gamma(l))|\hat{\chi} - \chi|_{\overline{W}}^2 + c_1'\eta_1^{-N}\eta_1^l|\hat{\xi} - p|_{\overline{V}}^2 + \sum_{r=1}^{l} \eta_2^{r-1} |w(l - r)|_Q^2, \end{aligned} \tag{5.57}$$

where we have used the definitions of c' and Q together with the facts that $l < N$ and $c_1(s)$ is monotonically increasing in s. From (5.56) and (5.57) and the definitions of C_1 and C_2 from (5.44) and (5.45), we can infer that

$$\Gamma_2(\hat{x}(l), x(l), \bar{p}(l), p) \leq C_0\Big(C_1\tilde{\eta}^l|\hat{\chi} - \chi|_{\overline{W}}^2 + C_2\eta_1^l|\hat{\xi} - p|_{\overline{V}}^2 + \sum_{r=1}^{l} \eta_2^{r-1} |w(l - r)|_Q^2\Big). \tag{5.58}$$

Part 5. The property in (5.42) finally follows by combining (5.50), (5.55), and (5.58), using that $C_0 > 1$, and noting that the result holds for all $l \in \mathbb{I}_{[0,N-1]}$, $k \in \mathbb{I}_{\geq 0}$, and $j \in \mathbb{I}_{\geq 0}$ (i.e., for all $t \in \mathbb{I}_{\geq 0}$), which finishes this proof. □

Remark 5.2 (Periodicity in the parameter estimates)**.** *The update rule* (5.17) *leads to a certain periodic behavior of the estimation error and its theoretical bounds. In particular, while accurate estimates and error bounds propagate over an integer multiple of N time steps, this has no effect on the estimates and bounds in between. Improving this is an interesting topic for future work; this would require using a different prior parameter estimate $\bar{p}(t-N_t)$ (e.g., the most recent estimate that was computed with sufficiently excited data), demanding the development of different proof techniques. A practical solution to avoid propagation of poor parameter estimates is to just select $\hat{p}(t)$ as the most recent estimate that was computed using PE data, i.e., $\hat{p}(t)=\hat{p}_\tau^*$, $\tau=\max\{\tau\in\mathbb{I}_{[0,t]}, X(\tau)\in\mathbb{E}_{N_t}\}$. We emphasize that in this case, the above developed theoretical guarantees are still valid: the error $e_\mathrm{p}(t)=\hat{p}(t)-p$ is bounded by* (5.42) *at time $t=\tau$ due to the fact that $\lambda_{\min}(\underline{V})|e_\mathrm{p}(\tau)|^2\leq\Gamma_1(\tau,\hat{x}(\tau),x(\tau),\hat{p}(\tau),p)$.*

In the following, we show that if the time between two consecutive PE horizons can be uniformly bounded for all times, Theorem 5.1 specializes to RGES of the estimation error. In practice, this can be the case for processes that are subject to a certain periodicity, such as in industrial robotics or automated logistics, compare, for example, [FTK13; Rom+22].

Corollary 5.1. *Let the conditions of Theorem 5.1 be satisfied. Assume that there exists a constant $\kappa\geq 0$ such that $j\leq\kappa$ and $i_m\leq\kappa$ for all $m\in\mathbb{I}_{[1,k]}$ uniformly for all $t\in\mathbb{I}_{\geq 0}$. Then, the joint estimation error* (5.18) *is RGES, that is, there exist $K_1,K_2\geq 0$ and $\lambda_1,\lambda_2\in(0,1)$ such that*

$$|e(t)|\leq\max\left\{K_1\lambda_1^t|e(0)|, K_2\max_{r\in[1,t]}\lambda_2^{r-1}|w(t-r)|\right\} \tag{5.59}$$

for all $t\in\mathbb{I}_{\geq 0}$ and all $\hat{\chi},\chi\in\mathcal{X}$, all $\hat{\xi},p\in\mathcal{P}$, and all input and disturbance sequences $u\in\mathcal{U}^\infty$ and $w\in\mathcal{W}^\infty$.

Proof. Consider (5.42). Define $\mu_\kappa:=\bar{\mu}^{\frac{1}{\kappa+1}}$ with $\bar{\mu}\geq\max\{\mu,\rho_N\}$ from Theorem (5.1). Since j and i_m are uniformly bounded by κ for all $m\in\mathbb{I}_{[1,k]}$ and $k\in\mathbb{I}_{\geq 1}$, we can write that

$$\mu^{sN}\leq\mu_\kappa^{s(\kappa+1)N}\leq\mu_\kappa^{\sum_{m=1}^{s}(i_m+1)N} \tag{5.60}$$

for all $s\in\mathbb{I}_{[0,k]}$. Since, $1\leq\mu_\kappa^{-\kappa N}\mu_\kappa^{qN}$ for all $q\in\{j,\{i_m\}_{m=1}^k\}$ and $\mu_\kappa\geq\tilde{\eta}$, we can also infer that

$$\mu^{kN}\eta_1^l\leq\mu^{kN}\tilde{\eta}^l\leq\mu_\kappa^{-\kappa N}\mu_\kappa^{jN}\mu^{kN}\mu_\kappa^l\leq\mu_\kappa^{-\kappa N}\mu_\kappa^t, \tag{5.61}$$

where the last inequality followed by (5.60). In addition, we can write that

$$\sum_{m=1}^{k}\mu^{(m-1)N}\sum_{r=1}^{(i_m+1)N}\bar{\mu}^{r-1}|w(t-jN-\sum_{q=1}^{m-1}(i_q+1)N-r)|_Q^2\leq\sum_{r=1}^{t-jN-l}\bar{\mu}^{r-1}|w(t-jN-r)|_Q^2 \tag{5.62}$$

by (5.60) with $s=m-1$ and (5.41). Hence, from Theorem 5.1, the definition of μ_κ, and (5.60)–(5.62), we obtain

$$\frac{\mu_\kappa^{\kappa N}}{C_0}\Gamma_1(t,\hat{x}(t),x(t),\hat{p}(t),p)\leq C_1\mu_\kappa^t|\hat{\chi}-\chi|_W^2+C_2\mu_\kappa^t|\hat{\xi}-p|_V^2+\sum_{r=1}^{t}\mu_\kappa^{r-1}|w(t-r)|_Q^2.$$

Using the definition of Γ_1 from (5.19), the estimation error (5.18) satisfies

$$|e(t)|^2 \leq \tilde{K}_1 \mu_\kappa^t |e(0)|^2 + \tilde{K}_2 \sum_{r=1}^{t} \mu_\kappa^{r-1} |w(t-r)|^2 \tag{5.63}$$

with the constants $\tilde{K}_1 := \tilde{K}_3 \max\{C_1 \lambda_{\max}(\overline{W}), C_2 \lambda_{\max}(\overline{V})\}$ and $\tilde{K}_2 := \tilde{K}_3 \lambda_{\max}(Q)$, where $\tilde{K}_3 := C_0 (\mu_\kappa^{\kappa N} \min\{\lambda_{\min}(\underline{P}), \lambda_{\min}(\underline{V})\})^{-1}$. By the geometric series, we have that

$$\sum_{r=1}^{t} \mu_\kappa^{r-1} |w(t-r)|^2 \leq \frac{1}{1-\sqrt{\mu_\kappa}} \max_{r \in [1,t]} \sqrt{\mu_\kappa}^{r-1} |w(t-r)|^2. \tag{5.64}$$

By taking the square root of (5.63) and using (5.64), we obtain (5.59) with constants $K_1 = \sqrt{2\tilde{K}_1}$, $K_2 = \sqrt{2\tilde{K}_2/(1-\sqrt{\mu_\kappa})}$, $\lambda_1 = \sqrt{\mu_\kappa}$, and $\lambda_2 = \sqrt[4]{\mu_\kappa}$, which finishes this proof. □

5.2.3. Special case: uniform persistent excitation

In the following, we consider the special case in which the excitation condition in (5.17) is always satisfied by the following uniform PE condition.

Assumption 5.3 (Uniform persistent excitation)**.** *There exists $T \in \mathbb{I}_{\geq 0}$ such that*

$$\left(\{(x_1(t), u(t), w_1(t), p_1)\}_{t=0}^{K-1}, \{(x_2(t), u(t), w_2(t), p_2)\}_{t=0}^{K-1} \right) \in \mathbb{E}_K$$

for all $K \in \mathbb{I}_{\geq T}$ and all trajectories $\{(x_i(t), u(t), w_i(t), p_i)\}_{t=0}^{K-1} \in \mathcal{Z}^K$, $i = 1, 2$, satisfying (5.1) *for all $t \in \mathbb{I}_{[0,K-1]}$.*

Assumption 5.3 essentially imposes that *any* two system trajectories of certain length form a persistently excited trajectory pair. Robust stability guarantees for joint state and parameter estimation under Assumptions 5.1 and 5.3 are provided by Corollary 5.1 (with $\kappa = 0$); however, we want to emphasize the following implications.

Proposition 5.1. *Consider the system* (5.1)*. The following statements are equivalent:*

(a) Assumptions 5.1 and 5.3 hold.

(b) There exists a joint i-IOSS Lyapunov function $G : \mathcal{X} \times \mathcal{X} \times \mathcal{P} \times \mathcal{P} \to \mathbb{R}_{\geq 0}$ such that, for some $\underline{G}, \overline{G}, Q, R \succ 0$ and a constant $\eta \in (0, 1)$,

$$\left| \begin{bmatrix} x_1 - x_2 \\ p_1 - p_2 \end{bmatrix} \right|_{\underline{G}}^2 \leq G(x_1, x_2, p_1, p_2) \leq \left| \begin{bmatrix} x_1 - x_2 \\ p_1 - p_2 \end{bmatrix} \right|_{\overline{G}}^2, \tag{5.65}$$

$$\begin{aligned} &G(f(x_1, u, w_1, p_1), f(x_2, u, w_2, p_2), p_1, p_2) \\ &\leq \eta G(x_1, x_2, p_1, p_2) + |w_1 - w_2|_Q^2 + |h(x_1, u, w_1, p_1) - h(x_2, u, w_2, p_2)|_R^2 \end{aligned} \tag{5.66}$$

for all $(x_1, u, w_1, p_1), (x_2, u, w_2, p_2) \in \mathcal{Z}$.

Proposition 5.1 essentially implies that state detectability (Assumptions 5.1) and uniform PE of the parameters (Assumption 5.3) is equivalent to uniform detectability (exponential i-IOSS) of the *augmented state* $x^{\mathrm{a}} = [x^\top, p^\top]^\top$. Consequently, under these assumptions one could simply consider the augmented state x^{a} and apply MHE schemes with corresponding theory for state estimation (e.g., [AR21; KM23; Sch+23]). However, Assumption 5.3 is restrictive, usually not satisfied in practice, and its *a priori* verification is generally impossible. The proposed method from Section 5.2.1, on the other hand, provides a strict relaxation, since it is applicable in the practically relevant case where the parameters are only rarely (or never) excited, which violates Assumption 5.3 and hence implies that the augmented state cannot be uniformly detectable (exponentially i-IOSS) and no joint i-IOSS Lyapunov function satisfying (5.65) and (5.66) can exist.

Proof of Proposition 5.1. Let $K \in \mathbb{I}_{\geq 1}$ and $\{(x_i(t), u(t), w_i(t), p_i)\}_{t=0}^{K-1} \in \mathcal{Z}^K$, $i = 1, 2$ be two sequences that satisfy (5.1) for all $t \in \mathbb{I}_{[0,K-1]}$. Define the corresponding outputs $y_i(t) = h(x_i(t), u(t), w_i(t), p_i)$, $i = 1, 2$, $t \in \mathbb{I}_{[0,K-1]}$. For the sake of conciseness, define $\Delta x(t) := x_1(t) - x_2(t)$ for $t \in \mathbb{I}_{[0,K]}$, $\Delta w(t) := w_1(t) - w_2(t)$ and $\Delta y(t) := y_1(t) - y_2(t)$ for $t \in \mathbb{I}_{[0,K-1]}$, and $\Delta p := p_1 - p_2$.

We start with $(a) \Rightarrow (b)$. Assumption 5.1 implies the following bound (by application of (5.5), (5.4), and the geometric series):

$$\begin{aligned} |\Delta x(t)|_{\underline{P}}^2 + |\Delta p|_{S_{\mathrm{x}}}^2 \leq \eta_{\mathrm{x}}^t |\Delta x(0)|_{\overline{P}}^2 + \left(\frac{1}{1-\eta_{\mathrm{x}}} + 1\right) |\Delta p|_{S_{\mathrm{x}}}^2 \\ + \sum_{j=1}^{t} \eta_{\mathrm{x}}^{j-1} \left(|\Delta w(t-j)|_{Q_{\mathrm{x}}}^2 + |\Delta y(t-j)|_{R_{\mathrm{x}}}^2\right) \end{aligned} \tag{5.67}$$

for all $t \in \mathbb{I}_{[0,K]}$, where we also added $|\Delta p|_{S_{\mathrm{x}}}^2$ to both sides. We make a case distinction and first consider $t \in \mathbb{I}_{[T,K]}$. Application of $|\Delta p|_{S_{\mathrm{x}}}^2 \leq \lambda_{\max}(S_{\mathrm{x}}, S_{\mathrm{p}}) |\Delta p|_{S_{\mathrm{p}}}^2$ and Assumption 5.3 leads to

$$|\Delta x(t)|_{\underline{P}}^2 + |\Delta p|_{S_{\mathrm{x}}}^2 \leq \tilde{\eta}^t |\Delta x(0)|_{\tilde{P}_1}^2 + \sum_{j=1}^{t} \tilde{\eta}^{j-1} \left(|\Delta w(t-j)|_{\tilde{Q}}^2 + |\Delta y(t-j)|_{\tilde{R}}^2\right), \tag{5.68}$$

where we have used the definitions $\tilde{\eta} := \max\{\eta_{\mathrm{x}}, \eta_{\mathrm{p}}\}$, $\tilde{P}_1 := \overline{P} + c_1 P_{\mathrm{p}}$, $\tilde{Q} := Q_{\mathrm{x}} + c_1 Q_{\mathrm{p}}$, and $\tilde{R} := R_{\mathrm{x}} + c_1 R_{\mathrm{p}}$ with $c_1 := \left(\frac{1}{1-\eta_{\mathrm{x}}} + 1\right) \lambda_{\max}(S_{\mathrm{x}}, S_{\mathrm{p}})$. Now, recall that (5.67) also applies for $t \in \mathbb{I}_{[0,T-1]}$. Using the fact that $1 \leq \tilde{\eta}^{1-T} \tilde{\eta}^t$ for all $t \in \mathbb{I}_{[0,T-1]}$, one can verify that

$$\begin{aligned} c_2 \left(|\Delta x(t)|^2 + |\Delta p|^2\right) \leq c_3 \tilde{\eta}^t \left(|\Delta x(0)|^2 + |\Delta p|^2\right) \\ + \sum_{j=1}^{t} \tilde{\eta}^{j-1} \left(|\Delta w(t-j)|_{\tilde{Q}}^2 + |\Delta y(t-j)|_{\tilde{R}}^2\right) \end{aligned} \tag{5.69}$$

for all $t \in \mathbb{I}_{[0,K]}$, where $c_2 := \min\{\lambda_{\min}(\underline{P}), \lambda_{\min}(S_{\mathrm{x}})\}$ and

$$c_3 := \max\left\{\lambda_{\max}(\tilde{P}_1), \lambda_{\max}(S_{\mathrm{x}}) \tilde{\eta}^{1-T} \left(\frac{1}{1-\eta_{\mathrm{x}}} + 1\right)\right\}.$$

Consider the augmented states

$$x_1^{\mathrm{a}}(t) = \begin{bmatrix} x_1(t) \\ p_1 \end{bmatrix}, \quad x_2^{\mathrm{a}}(t) = \begin{bmatrix} x_2(t) \\ p_2 \end{bmatrix},$$

which evolve according to the augmented system dynamics

$$x_i^{\mathrm{a}}(t+1) = f_{\mathrm{a}}(x_i^{\mathrm{a}}(t), u(t), w_i(t)) := \begin{bmatrix} f(x_i(t), u(t), w_i(t), p_i) \\ p_i \end{bmatrix}, \ i = 1, 2, \ t \in \mathbb{I}_{[0,K-1]}. \tag{5.70}$$

By satisfaction of (5.69) and the fact that $|\Delta x(t)|^2 + |\Delta p|^2 = |x_1^{\mathrm{a}}(t) - x_2^{\mathrm{a}}(t)|^2$, we observe that the system (5.70) is exponentially i-IOSS [RMD20, Def. 4.5] with respect to the outputs $y_i^{\mathrm{a}}(t) = h_{\mathrm{a}}(x_i^{\mathrm{a}}(t), u(t), w_i(t)) := h(x_i(t), u(t), w_i(t), p_i)$, $i = 1, 2$, $t \in \mathbb{I}_{[0,K-1]}$. Existence of an i-IOSS Lyapunov function $G(\cdot)$ and suitable matrices $\underline{G}, \overline{G}, Q, R \succ 0$ satisfying (5.65) and (5.66) follows by a straightforward extension of the converse Lyapunov theorem from [ART21].

It remains to show $(b) \Rightarrow (a)$. Application of (5.66) and (5.65) yields

$$\begin{aligned} \lambda_{\min}(\underline{G}) \left(|\Delta x(t)|^2 + |\Delta p|^2 \right) \leq \lambda_{\max}(\overline{G}) \eta^t \left(|\Delta x(0)|^2 + |\Delta p|^2 \right) \\ + \sum_{j=1}^{t} \eta^{j-1} \left(|\Delta w(t-j)|_Q^2 + |\Delta y(t-j)|_R^2 \right) \end{aligned} \tag{5.71}$$

for all $t \in \mathbb{I}_{[0,K]}$. Using that $|\Delta p| \geq 0$, we obtain

$$\begin{aligned} \lambda_{\min}(\underline{G}) |\Delta x(t)|^2 \leq \lambda_{\max}(\overline{G}) \eta^t |\Delta x(0)|^2 \\ + \sum_{j=1}^{t} \eta^{j-1} \left(\lambda_{\max}(\overline{G}) |\Delta p|^2 + |\Delta w(t-j)|_Q^2 + |\Delta y(t-j)|_R^2 \right), \end{aligned}$$

which is an (exponential) i-IOSS bound for the system (5.1) considering p as an additional constant input. Existence of an i-IOSS Lyapunov function $U(x_1, x_2)$ and matrices $\underline{P}, \overline{P}, Q_{\mathrm{x}}, R_{\mathrm{x}} \succ 0$ and $\eta_{\mathrm{x}} \in (0, 1)$ satisfying Assumption 5.1 follows by a straightforward extension of the converse Lyapunov theorem from [ART21]. Now fix $T \in \mathbb{I}_{\geq 1}$ and consider some $K \in \mathbb{I}_{\geq T}$. From (5.71) with $t = K$ and the facts that $\eta^K \leq \eta^T$ and $|\Delta x_K|^2 \geq 0$, we obtain

$$\begin{aligned} (\lambda_{\min}(\underline{G}) - \lambda_{\max}(\overline{G}) \eta^T) |\Delta p|^2 \leq \lambda_{\max}(\overline{G}) \eta^K |\Delta x(0)|^2 \\ + \sum_{j=1}^{K} \eta^{j-1} \left(|\Delta w(K-j)|_Q^2 + |\Delta y(K-j)|_R^2 \right) \end{aligned}$$

for all $K \in \mathbb{I}_{\geq T}$. Since there always exists $T \in \mathbb{I}_{\geq 1}$ such that $(\lambda_{\min}(\underline{G}) - \lambda_{\max}(\overline{G}) \eta^T) > 0$, Assumption 5.3 is satisfied, which finishes this proof. □

5.2.4. Numerical example

To illustrate our results, we consider the following system

$$\begin{aligned} x_1^+ &= x_1 + t_\Delta b_1(x_2 - a_1 x_1 - a_2 x_1^2 - p x_1^3) + w_1, \\ x_2^+ &= x_2 + t_\Delta(x_1 - x_2 + x_3) + w_2, \\ x_3^+ &= x_3 - t_\Delta b_2 x_2 + w_3, \\ y &= x_1 + w_4, \end{aligned}$$

which corresponds to the Euler-discretized modified Chua's circuit system from [YZ15] using the step size $t_\Delta = 0.01$ under additional disturbances $w(t) \in \mathbb{R}^4$ and (noisy) output measurements. The parameters are $b_1 = 12.8$, $b_2 = 19.1$, $a_1 = 0.6$, $a_2 = -1.1$, and $p = 0.45$, which leads to a chaotic behavior of the system. In the following, we treat $w(t)$ as a uniformly distributed random variable with $|w_i(t)| \leq 10^{-3}, i = 1, 2, 3$ for the process disturbance and $|w_4(t)| \leq 0.1$ for the measurement noise for all $t \in \mathbb{I}_{\geq 0}$. We consider the initial condition $x(0) = \chi = [1, 0, -1]^\top$ and assume that $x(t)$ evolves in the (known) set $\mathcal{X} = [-1, 3] \times [-1, 1] \times [-3, 3]$. Furthermore, we consider the case where the exact parameter p is unknown but contained in the set $\mathcal{P} = [0.2, 0.8]$.

From the system equations, we see that the unknown parameter p enters the dynamics through the product px_1^3; hence, the excitation of p crucially depends on the magnitude of x_1. Figure 5.2 shows an exemplary system trajectory for the initial condition χ under random disturbances and measurement noise. Here, we find that there are relatively large time intervals in which the state x_1 is close to zero. This suggests that p is not sufficiently excited in these intervals for proper parameter estimation, demanding for estimation techniques that are robust in this respect.

The objective is now to compute the state and parameter estimates $\hat{x}(t)$ and $\hat{p}(t)$ by applying the MHE scheme proposed in Section 5.2 using the initial estimates $\hat{\chi} = [-1, 0.1, 2]^\top$ and $\hat{\xi} = 0.2$.

To this end, we first construct the i-IOSS Lyapunov function U (Assumption 5.1) and the set $\mathbb{E}_N$ (Definition 5.1) using the verification methods presented in Sections 7.1.1 and 7.2.1, respectively. The computations are carried out in MATLAB using YALMIP [Löf09] and the SDP solver MOSEK [MOS24]. Specifically, we compute a quadratic i-IOSS Lyapunov function $U(x_1, x_2) = |x - \tilde{x}|^2_{P_\mathrm{x}}$ with $P_\mathrm{x} \succ 0$ by adapting Corollary 7.1. Fixing some $\eta_\mathrm{x} \in (0, 1)$, we can reformulate the dissipation condition (5.5) as an infinite set of LMIs using the differential dynamics, which we verify on $\mathcal{X}$ at selected grid points. The conditions are met for, e.g., $\eta_\mathrm{x} = 0.91$,

$$P_\mathrm{x} = \begin{bmatrix} 14.85 & -1.91 & 0.02 \\ -1.91 & 2.18 & -0.18 \\ 0.02 & -0.18 & 0.04 \end{bmatrix}, \tag{5.72}$$

$S_\mathrm{x} = 2 \cdot 10^2$, $Q_\mathrm{x} = \mathrm{diag}(4, 6, 1, 8) \cdot 10^2$, and $R_\mathrm{x} = 8 \cdot 10^2$. The set $\mathbb{E}_N$ is constructed using the methods proposed in Section 7.2.1, where we verify Assumption 7.6 by choosing $L(z_1, z_2)$ such that Φ in (7.40) becomes constant. The LMI (7.41) is satisfied

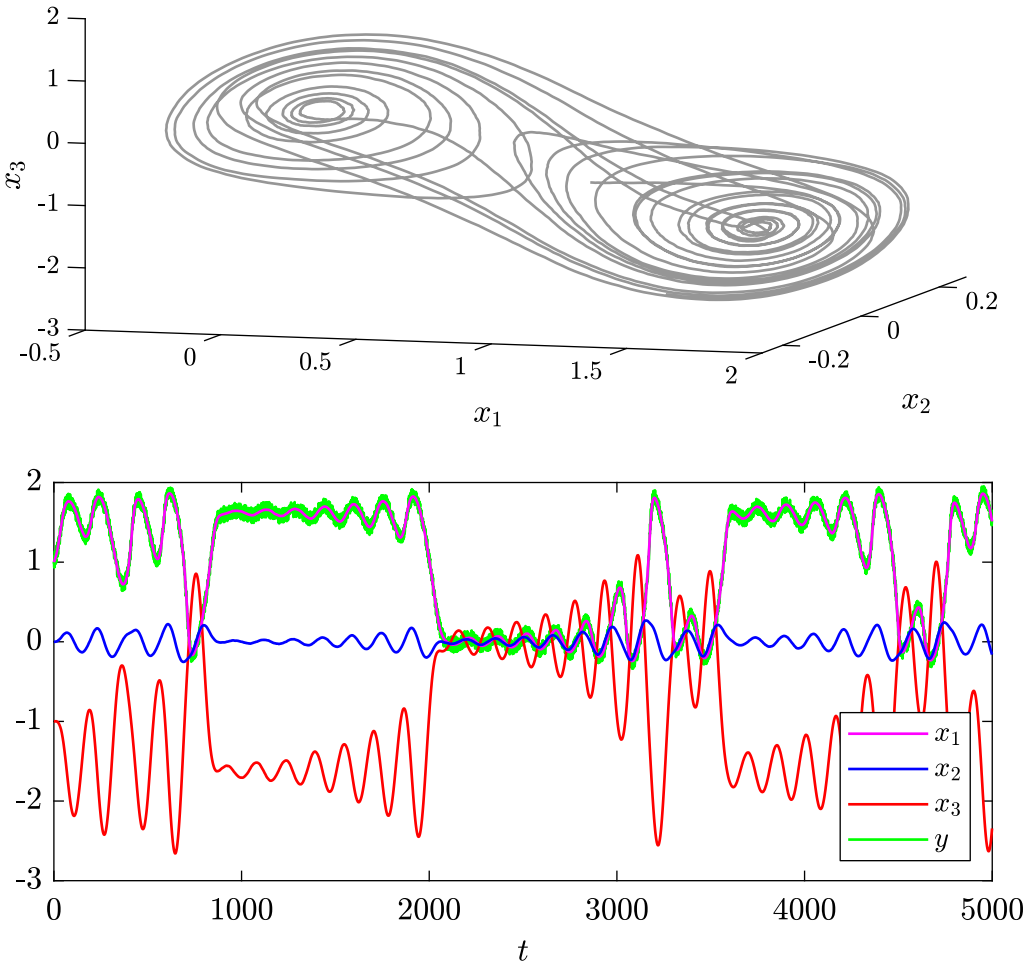

Figure 5.2. Solution of the modified Chua's circuit system under process disturbances and measurement noise in 3D space (top) and over time (bottom).

for, e.g., $\eta = 0.71$ and

$$P = \begin{bmatrix} 8.13 & -3.67 & 0.13 \\ -3.67 & 2.78 & -0.14 \\ 0.13 & -0.14 & 0.01 \end{bmatrix}.$$

Then, we choose $\epsilon = 10^{-2}$ and $\gamma = 10^{-5}$ in the proof of Proposition 7.1 such that $\eta_p = \mu = 0.747$ in (7.55). We compute the matrices $Q_{\mathrm{p}} = \mathrm{diag}(6, 3, 3, 12) \cdot 10^3$ and $R_{\mathrm{p}} = 6{\cdot}10^3$ by verifying (7.56) and (7.57) on $\mathcal{Z} \times \mathcal{Z}$ using SOS programming. Finally, we choose $\alpha = 10^{-3}$ and set $S_{\mathrm{p}} = \alpha\gamma I_o$, which completes the offline verification.

For a simple cost function design, we first re-scale the i-IOSS Lyapunov function U (i.e., the matrices P_{x}, Q_{x}, R_{x}, S_{x}) by the factor $\lambda_{\max}(S_{\mathrm{x}}, S_{\mathrm{p}})$. We select constant weighting matrices $W(t) = 2P_{\mathrm{p}}$, $V(t) = 100S_{\mathrm{p}}$, $Q(t) = 2(Q_{\mathrm{x}} + Q_{\mathrm{p}})$, and $R(t) = R_{\mathrm{x}} + R_{\mathrm{p}}$ for all $t \in \mathbb{I}_{\geq 0}$, the discount factors $\eta_1 = 0.934$, and $\eta_2 = 0.9997$, and the horizon length $N = 150$. These choices satisfy Assumption 5.2 and the contraction conditions (5.38)–(5.40); the minimal horizon length for the selected parameters is $N_{\min} = 137$. We point out that such a relatively large horizon length is on the one hand due to some conservative steps in the proofs, but on the other hand inherently required here since the dynamics of the system under consideration are rather slow

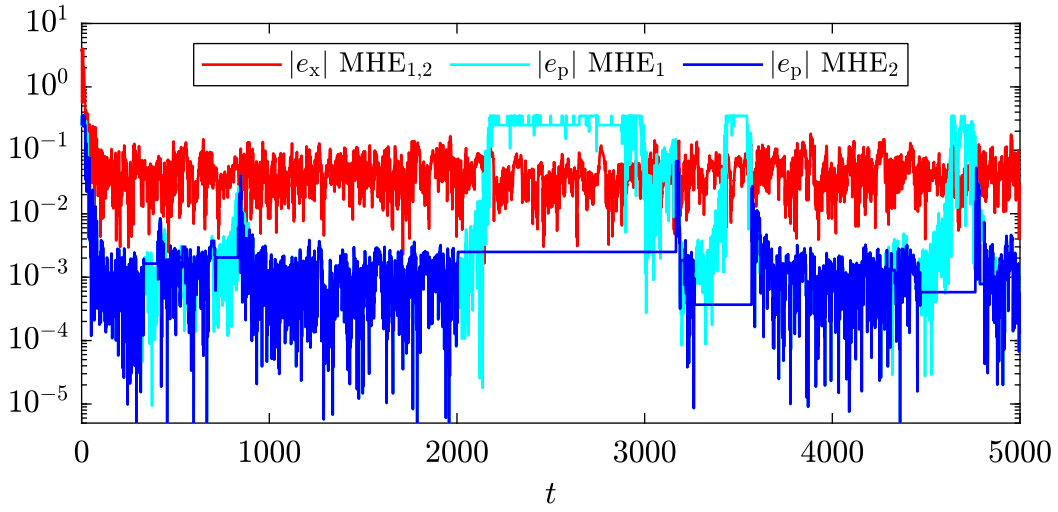

Figure 5.3. State and parameter estimation errors of MHE$_1$ (assuming uniform PE) and MHE$_2$ (using excitation monitoring and adaptive regularization).

compared to the sampling time t_Δ.

We consider the proposed MHE scheme presented in Section 5.2.1 under two different settings: first, without explicit excitation monitoring and naively assuming uniform PE (satisfaction of Assumption 5.3), denoted as MHE$_1$; second, with the proposed excitation-dependent regularization update (5.17) and the estimate $\hat{p}(t)$ in accordance with Remark 5.2, denoted as MHE$_2$. For the latter, we check if $X(t) \in \mathbb{E}_{N_t}$ by evaluating the function $\mathcal{O}_{N_t}(Z_t^*)$ defined in (7.62) in Section 7.2.1 at the currently optimal solution $Z_t^* = \left(\hat{x}_t^*(0), \hat{p}_t^*, \{\hat{w}_t^*(j)\}_{j=0}^{N_t-1}\right)$. If the minimal eigenvalue $\alpha_t := \lambda_{\min}(\mathcal{O}_T(Z_t^*))$ satisfies $\alpha_t \geq \alpha$ for the predefined threshold α used in the design of the set $\mathbb{E}_N$ below (5.72) (compare also (7.62) and (7.44)), we consider that $X(t) \in \mathbb{E}_{N_t}$, and $X(t) \notin \mathbb{E}_{N_t}$ otherwise.

The simulations are carried out in MATLAB over $t_{\text{sim}} = 5000$ time steps. The estimation errors of MHE$_1$ and MHE$_2$ are shown in Figure 5.3, which initially shows a fast convergence of the state and parameter estimation errors for both schemes. This is also evident in Figure 5.4, which illustrates the respective estimated parameters over time. The initially accurate parameter estimation of both methods results from a sufficiently high excitation level at the beginning of the simulation, which can be seen in Figure 5.5.

However, phases of weak excitation occur during the simulation, especially in the time interval $[2000, 3000]$ (α_t is close to zero in Figure 5.5). This renders the parameter unobservable in this interval such that Assumption 5.3 is violated. Consequently, MHE$_1$ provides very poor parameter estimates in this interval (see the cyan-colored curves in the Figures 5.3 and 5.4). MHE$_2$, on the other hand, explicitly takes into account the current excitation level and modifies the cost function and parameter estimates accordingly. This efficiently compensates for the phases of poor excitation and leads to significantly better parameter estimation results (see the blue curves in Figures 5.3 and 5.4). In contrast, we can also observe that the unobservability of the

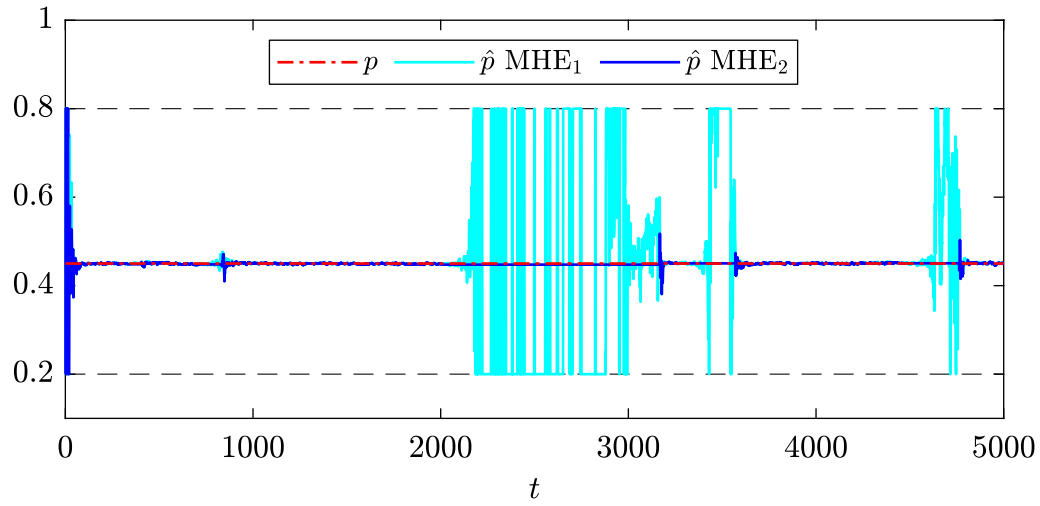

Figure 5.4. Parameter estimation results for MHE_1 and MHE_2. The black-dotted lines correspond to the bounds of the set $\mathcal{P}$.

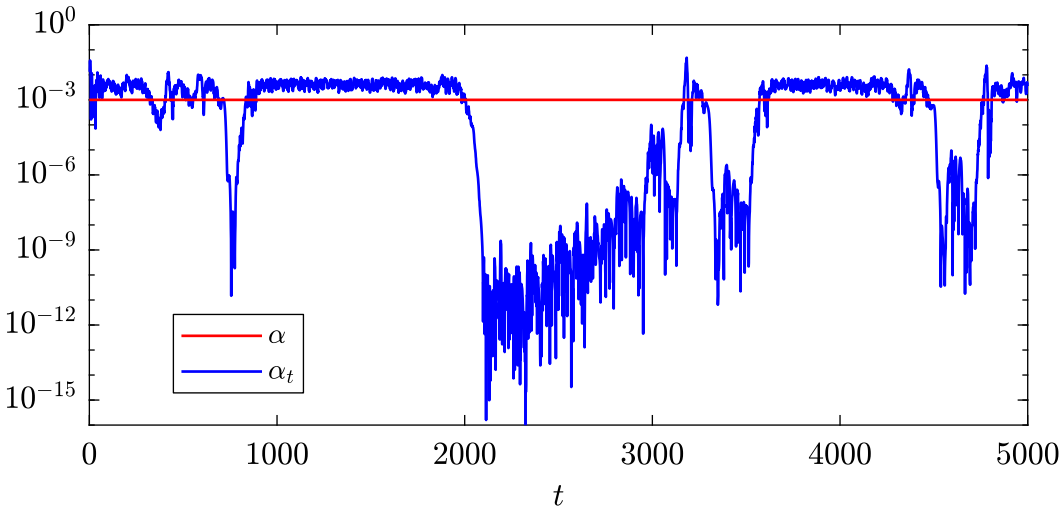

Figure 5.5. Excitation level α_t; values of α_t above the red line indicate sufficient excitation.

parameter has almost no effect on the state estimation results. In fact, the optimal state trajectories produced by MHE_1 and MHE_2 are almost identical (hence only shown as one red curve in Figure 5.3). This can be attributed to the fact that the parameter has a vanishing influence on the cost function when it is unobservable (in particular, the influence is not visible in the output fitting error over the horizon). To quantitatively support our statement, we additionally consider the root mean square error (RMSE) for the state and parameter estimation error. As Table 5.1 shows, the RMSE of the state estimation error are equal for both MHE_1 and MHE_2, whereas the RMSE of the parameter estimation error for MHE_2 is more than six times smaller than MHE_1.

We now compare the average time τ_{avrg} required to solve the nonlinear program (5.8) at each time step (on a standard laptop) for the two schemes MHE_1 and MHE_2. As the last column in Table 5.1 shows, these are very similar, which is due to the fact

Table 5.1. Comparison of RMSE and average computation times τ_{avrg} of MHE_1 and MHE_2.

Scheme	$\text{RMSE}(e_{\text{x}})$	$\text{RMSE}(e_{\text{p}})$	τ_{avrg} [ms]
MHE_1	0.1707	0.1379	50.01
MHE_2	0.1707	0.0209	49.96

$\text{RMSE}(e_i) := \sqrt{\frac{1}{N_{\text{sim}}} \sum_{r=0}^{N_{\text{sim}}} |e_i(t)|^2}$, $i = \{\text{x}, \text{p}\}$

that the additional computation of α_t required in MHE_2 (which mainly consists of matrix operations) saves time in solving the actual optimization problem due to a better conditioning of the cost function compared to MHE_1 (especially due to the parameter prior update in (5.17)).

Overall, this simulation example illustrates the efficiency of the presented MHE scheme for joint state and parameter estimation. In particular, we find that the proposed adaptive regularization formed by the excitation-dependent update in (5.17) together with the online excitation monitoring method from Section 7.2.1 is able to effectively compensate for phases of weak excitation and thus ensure reliable estimation results at all times.

5.3. Time-varying parameters

We now extend the theory developed in the previous sections for constant parameters to the more general case of time-varying parameters. Even if the basic idea remains the same, this modified problem setting requires that some main components of the scheme must be changed, additional tools used, and a different proof technique employed. We clarify the modified setup below, provide the MHE design in Section 5.3.1, analyze its theoretical properties in Section 5.3.2, and illustrate the efficiency of the proposed approach with a numerical example in Section 5.3.3.

Since the parameters $p(t)$ of the model in (5.1) are generally unobservable, we require the following property of the parameter dynamics g in (5.1b) to ensure boundedness of the estimation error.

Assumption 5.4 (Parameter dynamics)**.** *There exists a continuous function* $V : \mathcal{P} \times \mathcal{P} \to \mathbb{R}_{\geq 0}$ *and matrices* $\underline{V}, \overline{V} \succ 0$, $Q_{\text{v}} \succeq 0$ *such that*

$$|p_1 - p_2|_{\underline{V}} \leq V(p_1, p_2) \leq |p_1 - p_2|_{\overline{V}}, \tag{5.73}$$

$$V(g(p_1, u, w_1), g(p_2, u, w_2)) - V(p_1, p_2) \leq |w_1 - w_2|_{Q_{\text{v}}} \tag{5.74}$$

for all $(x_1, u, w_1, p_1), (x_2, u, w_2, p_2) \in \mathcal{Z}$.

Assumption 5.4 essentially constitutes an incremental Lyapunov characterization of a uniform bounded-energy bounded-state (UBEBS) stability property. This concept was originally introduced by [ASW00b] for continuous-time systems and is frequently

employed in the context of integral input-to-state stability, see, e.g., [HM20; Liu+22]. A (non-incremental) Lyapunov version of UBEBS is also termed *zero-output dissipativity* by [ASW00a]. Note that Assumption 5.4 does *not* impose asymptotic stability of $|p_1(t) - p_2(t)|$, which would render our estimator design task trivial. Instead, it merely implies that the difference $|p_1(t) - p_2(t)|$ is bounded at each time $t \in \mathbb{I}_{\geq 0}$ in terms of the initial difference $|p_1(0) - p_2(0)|$ and the sum of the disturbance differences $|w_1(j) - w_2(j)|, j \in \mathbb{I}_{[0,t-1]}$, and particularly does not diverge because of unstable internal dynamics. While this may seem restrictive at first glance, it is actually very intuitive and in fact necessary for providing bounded estimation errors with respect to the disturbance energy for the case when the parameter p is unobservable during operation (which is also covered in our setup). Note that for the common special case where $g(p, u, w) = p + B_{\mathrm{p}} w$, Assumption 5.4 can be satisfied by choosing $V(p_1, p_2) = |p_1 - p_2|$ and $Q_{\mathrm{v}} = B_{\mathrm{p}}^\top B_{\mathrm{p}}$.

In order estimate the unknown parameter $p(t)$, a suitable (non-uniform) observability notion is required. Here, we consider a modified version of Definition 5.1 and define the set $\mathbb{E}_T$ containing all trajectory pairs that are sufficiently excited for parameter estimation.

Definition 5.2 (Set of persistently excited trajectory pairs)**.** *Consider some fixed matrices $S_{\mathrm{p}}, P_{\mathrm{p}}, Q_{\mathrm{p}}, R_{\mathrm{p}} \succ 0$ and a constant $\eta_{\mathrm{p}} \in (0, 1)$. The set containing all persistently excited trajectory pairs of length $T \in \mathbb{I}_{\geq 0}$ is defined as*

$$
\begin{aligned}
\mathbb{E}_T := \Bigg\{ & \left(\{(x_1(t), u(t), w_1(t), p_1(t))\}_{t=0}^{T-1}, \{(x_2(t), u(t), w_2(t), p_2(t))\}_{t=0}^{T-1} \right) \in \mathcal{Z}^T \times \mathcal{Z}^T : \\
& x_i(t+1) = f(x_i(t), u(t), w_i(t), p_i(t)),\ i = 1, 2,\ t \in \mathbb{I}_{[0,T-1]}, \\
& p_i(t+1) = g(p_i(t), u(t), w_i(t)),\ i = 1, 2,\ t \in \mathbb{I}_{[0,T-1]}, \\
& y_i(t) = h(x_i(t), u(t), w_i(t), p_i(t)),\ i = 1, 2,\ t \in \mathbb{I}_{[0,T-1]}, \\
& |p_1(0) - p_2(0)|_{S_{\mathrm{p}}}^2 \leq \eta_{\mathrm{p}}^T |x_1(0) - x_2(0)|_{P_{\mathrm{p}}}^2 \\
& \qquad + \sum_{j=0}^{T-1} |w_1(j) - w_2(j)|_{Q_{\mathrm{p}}}^2 + |y_1(j) - y_2(j)|_{R_{\mathrm{p}}}^2 \Bigg\}. \qquad (5.75)
\end{aligned}
$$

In contrast to Definition 5.1 for the case of constant parameters, the PE property embedded in the set $\mathbb{E}_T$ is defined with respect to the initial parameters $p_i(0)$, $i = 1, 2$ of the respective parameter sequences and without discounting the inputs and outputs. Note that this constitutes a classical observability condition which has often been used in the literature in the context of nonlinear state estimation, see, e.g., [RMD20, Def. 4.28] and [FS23; WVD14; ABB08; RRM03], and compare also [Bes07, Def. 11] and [Bes16]. The additional terms depending on the differences $x_1(0) - x_2(0)$ and $w_1(j) - w_2(j)$, $j \in \mathbb{I}_{[0,T-1]}$ represent a robust generalization and stem from the fact that we consider an unknown initial state ($x_1(0) \neq x_2(0)$) and the presence of unknown disturbances ($w_1(j) \neq w_2(j)$, $j \in \mathbb{I}_{[0,T-1]}$).

5.3.1. Design

The MHE scheme that we present below is a modification of the scheme from Section 5.2.1 (for the case of constant parameters), mainly differing in that we use a non-discounted cost function for structural reasons, compare Remark 5.4 below.

At each time $t \in \mathbb{I}_{\geq 0}$, we consider the measured past input-output sequences u_t and y_t of the system (5.1) as defined in (5.6) and (5.7), respectively, where we recall that $N_t = \min\{t, N\}$ for some fixed horizon length $N \in \mathbb{I}_{\geq 0}$. The current estimates $\hat{x}(t)$ and $\hat{p}(t)$ are then obtained by solving the following NLP:

$$\min_{\hat{x}_t, \hat{p}_t, \hat{w}_t} \; J(\hat{x}_t, \hat{p}_t, \hat{w}_t, \hat{y}_t, t) \tag{5.76a}$$

$$\text{s.t. } \hat{x}_t(j+1) = f(\hat{x}_t(j), u_t(j), \hat{w}_t(j), \hat{p}_t(j)),\ j \in \mathbb{I}_{[0,N_t-1]}, \tag{5.76b}$$

$$\hat{p}_t(j+1) = g(\hat{p}_t(j), u_t(j), \hat{w}_t(j)),\ j \in \mathbb{I}_{[0,N_t-1]}, \tag{5.76c}$$

$$\hat{y}_t(j) = h(\hat{x}_t(j), u_t(j), \hat{w}_t(j), \hat{p}_t(j)),\ j \in \mathbb{I}_{[0,N_t-1]}, \tag{5.76d}$$

$$(\hat{x}_t(j), u_t(j), \hat{w}_t(j), \hat{p}_t(j)) \in \mathcal{Z},\ j \in \mathbb{I}_{[0,N_t-1]}. \tag{5.76e}$$

The decision variables $\hat{x}_t = \{\hat{x}_t(j)\}_{j=0}^{N_t}$, $\hat{p}_t = \{\hat{p}_t(j)\}_{j=0}^{N_t}$, and $\hat{w}_t = \{\hat{w}_t(j)\}_{j=0}^{N_t-1}$ are the estimated state, parameter, and disturbance sequence over the horizon, respectively, estimated at time t, which define a sequence of output estimates $\hat{y}_t = \{\hat{y}_t(j)\}_{j=0}^{N_t-1}$ under (5.76d). We consider the cost function

$$\begin{aligned} J(\hat{x}_t, \hat{p}_t, \hat{w}_t, \hat{y}_t, t) = {} & 2\gamma(N_t)|\hat{x}_t(0) - \bar{x}(t-N_t)|_{\overline{P}}^2 + 2\eta^{N_t}|\hat{p}_t(0) - \bar{p}(t-N_t)|_{\overline{V}}^2 \\ & + \sum_{j=0}^{N_t-1} 2|\hat{w}_t(j)|_Q^2 + |\hat{y}_t(j) - y_t(j)|_R^2, \end{aligned} \tag{5.77}$$

where the prior estimates $\bar{x}(t-N_t)$ and $\bar{p}(t-N_t)$ are defined below. The cost function parameters are chosen depending on the parameters of Assumption 5.1, Assumption 5.4, and Definition 5.2. In particular, we select $Q = Q_\mathrm{x} + Q_\mathrm{v} + Q_\mathrm{p}$, $R = R_\mathrm{x} + R_\mathrm{p}$, and the discount factors

$$\gamma(s) = \eta_\mathrm{x}^s + \lambda_{\max}(P_\mathrm{p}, \overline{P})\eta_\mathrm{p}^s, \tag{5.78}$$

$$\eta \in (\max\{\eta_\mathrm{x}, \eta_\mathrm{p}\}, 1). \tag{5.79}$$

Note that tuning the cost function in practice is possible by re-scaling the functions U and V from Assumptions 5.1 and 5.4, respectively, or the parameters of the set $\mathbb{E}_T$ from Definition 5.2, compare also Remark 3.4. Moreover, note also that we can easily generalize the cost function design to time-varying weighting matrices as in Section 5.2.1 (i.e., Assumption 5.2); however, for the sake of simplicity we restrict ourselves to constant weights in the following. As this choice is in fact a special case of Assumption 5.2, it follows that the optimization problem in (5.76) with (5.77) admits a globally optimal solution at any time $t \in \mathbb{I}_{\geq 0}$ (compare the discussion below Assumption 5.2), which we denote by the tuple $(\hat{x}_t^*, \hat{p}_t^*, \hat{w}_t^*)$.

The prior estimates $\bar{x}(t)$ and $\bar{p}(t)$ are updated similarly to the MHE scheme presented in Section 5.2.1; in particular, for the state prior $\bar{x}(t)$, we select the filtering prior

$$\bar{x}(t) = \begin{cases} \hat{x}_t^*(N), & t \in \mathbb{I}_{\geq N} \\ \hat{\chi}, & t \in \mathbb{I}_{[0,N-1]}, \end{cases}$$

while the parameter prior $\bar{p}(t-N_t)$ is adapted to the level of excitation that is currently present. To this end, at any time $t \in \mathbb{I}_{\geq 0}$, let

$$X(t) := \left(\{(\hat{x}_t^*(j), u_t(j), \hat{w}_t^*(j), \hat{p}_t^*(j))\}_{j=0}^{N_t-1}, \{(x(j), u(j), w(j), p(j))\}_{j=t-N_t}^{t-1}\right)$$

denote the pair of the currently optimal and the true system trajectory restricted to the estimation horizon. Then, we choose the prior estimate $\bar{p}(t)$ (that will be used in the cost function (5.77) in N time steps in the future) according to the following update rule:

$$\bar{p}(t) = \begin{cases} \hat{p}_t^*(N), & \text{if } t \in \mathbb{I}_{\geq N} \text{ and } X(t) \in \mathbb{E}_T, \\ g^{(N_t)}(\bar{p}(t-N_t)), & \text{otherwise} \end{cases} \tag{5.80}$$

for $t \in \mathbb{I}_{\geq 1}$ and $\bar{p}(0) = \hat{\xi}$, where $g^{(N_t)}(\bar{p}(t-N_t))$ is the solution of the system (5.1b) after N_t steps initialized at $\bar{p}(t-N_t)$ and driven by the input sequence u_t from (5.6) and the nominal disturbance $w_{\mathrm{n}}(j) = 0$, $j \in \mathbb{I}_{[0,N_t-1]}$ for all $t \in \mathbb{I}_{\geq 0}$.

The MHE estimates are defined as last element of the optimal state and parameter sequences $\hat{x}_t^*$ and $\hat{p}_t^*$, i.e.,

$$\hat{x}(t) = \hat{x}_t^*(N_t), \qquad \hat{p}(t) = \hat{p}_t^*(N_t), \tag{5.81}$$

and the corresponding estimation error as

$$e(t) = \begin{bmatrix} e_{\mathrm{x}}(t) \\ e_{\mathrm{p}}(t) \end{bmatrix} = \begin{bmatrix} \hat{x}(t) - x(t) \\ \hat{p}(t) - p(t) \end{bmatrix}, \ t \in \mathbb{I}_{\geq 1}, \quad e(0) = \begin{bmatrix} \hat{\chi} - \chi \\ \hat{\xi} - \xi \end{bmatrix}. \tag{5.82}$$

Remark 5.3 (Excitation monitoring)**.** *The proposed MHE scheme requires monitoring whether $X(t) \in \mathbb{E}_T$ currently holds or not. This is, however, non-trivial for general nonlinear systems since the second trajectory contained in the pair $X(t)$ is the true, unknown system trajectory. It can be checked locally by adapting, e.g., the techniques from [SJ11] or [FS23] that are based on the construction of nonlinear observability maps using the mean-value theorem evaluated at the estimated trajectory. For the important special case where $g(p,u,w) = p + B_{\mathrm{p}}w$, in Section 7.2.2 we provide a method to practically check whether the PE condition $X(t) \in \mathbb{E}_N$ holds (in particular, without knowledge of the unknown true trajectory) by evaluating a suitably constructed observability metric.*

Remark 5.4 (Non-discounted cost function)**.** *The main structural difference to the design in Section 5.2.1 is the fact that the cost function in* (5.77) *involves a non-discounted sum of the stage costs. As a consequence, there is a fundamental mismatch between the detectability condition and cost function, compare Remark 3.3 and the discussion in Section 3.3. Therefore, the bound on the estimation error that we establish in Theorem 5.2 below is also conceptually weaker when compared to Theorem 5.1 in the sense that it merely constitutes a bounded-disturbance-energy bounded-estimation-error property (compared to the bounded-disturbance bounded-estimation-error property provided by Theorem 5.1). This is mainly because if the parameter is unobservable during operation, we can only use the Assumption 5.4 to bound the evolution of the parameter estimation error (which in itself is a non-discounted incremental UBEBS property, compare the discussion below Assumption 5.4), which needs to be captured in cost function* (5.77).

5.3.2. Stability analysis

In this section, we establish fundamental stability properties of the estimation error (5.82). The general idea of the proof is similar to the one we used in Section 5.2.2. Technical difficulties due to the fact that the parameter $p(t)$ evolves according to the dynamical system (5.1b) are addressed by invoking Assumption 5.4.

We consider the Lyapunov function candidate

$$\Gamma(c, \hat{x}, x, \hat{p}, p) = U(\hat{x}, x) + cV(\hat{p}, p)^2, \quad c \geq 1. \tag{5.83}$$

The following two auxiliary lemmas establish boundedness properties of Γ depending on the level of excitation.

Lemma 5.3. *Let Assumptions 5.1 and 5.4 be satisfied. Consider the MHE scheme in* (5.76) *with the cost function in* (5.77)*. Assume that* $t \in \mathbb{I}_{[0,N-1]}$ *or* $t \in \{t \in \mathbb{I}_{\geq N} : X(t) \notin \mathbb{E}_N\}$*. Then, the estimates* (5.81) *satisfy*

$$\begin{aligned}
&\Gamma(1, \hat{x}(t), x(t), \hat{p}(t), p(t)) \\
&\leq \eta^{-N} c_1(1, N_t) \Big((2\eta_{\mathrm{x}}^{N_t} + 2\gamma(N_t)) |\bar{x}(t - N_t) - x(t - N_t)|_{\bar{P}}^2 \\
&\qquad + 4\eta^{N_t} |\bar{p}(t - N_t) - p(t - N_t)|_{\bar{V}}^2 + 4 \sum_{j=1}^{N_t} |w(t - j)|_Q^2 \Big)
\end{aligned} \tag{5.84}$$

with

$$c_1(r, s) = \max\{r, \lambda_{\max}(S_{\mathrm{x}}, \underline{V}) \eta_{\mathrm{x}}^{-1}\}(s + 1) \frac{1 - \eta_{\mathrm{x}}^{s+1}}{1 - \eta_{\mathrm{x}}}. \tag{5.85}$$

Proof. We start by defining the sequences of the true states, parameters, and disturbances restricted to the estimation horizon:

$$x_t := \{x_t(j)\}_{j=0}^{N_t}, \ x_t(j) = x(t - N_t + j), \ j \in \mathbb{I}_{[0,N_t]}, \ t \in \mathbb{I}_{\geq 0}, \tag{5.86}$$

$$p_t := \{p_t(j)\}_{j=0}^{N_t}, \ p_t(j) = p(t - N_t + j), \ j \in \mathbb{I}_{[0,N_t]}, \ t \in \mathbb{I}_{\geq 0}, \tag{5.87}$$

$$w_t := \{w_t(j)\}_{j=0}^{N_t - 1}, \ w_t(j) = w(t - N_t + j), \ j \in \mathbb{I}_{[0,N_t-1]}, \ t \in \mathbb{I}_{\geq 0}. \tag{5.88}$$

From (5.83) and the optimal estimates (5.81), we obtain

$$\Gamma(1, \hat{x}(t), x(t), \hat{p}(t), p(t)) = U(\hat{x}_t^*(N_t), x_t(N_t)) + V(\hat{p}_t^*(N_t), p_t(N_t))^2. \tag{5.89}$$

Satisfaction of the MHE constraints (5.76b)–(5.76e) implies that the optimal trajectory satisfies the dynamics (5.1) and $(\hat{x}_t^*(j), u_t(j), w_t^*(j), \hat{p}_t^*(j)) \in \mathcal{Z}$ for all $j \in \mathbb{I}_{[0,N_t-1]}$. Invoking the property (5.5) yields

$$\begin{aligned}
&\Gamma(1, \hat{x}(t), x(t), \hat{p}(t), p(t)) \\
&\leq \eta_{\mathrm{x}}^{N_t} U(\hat{x}_t^*(0), x_t(0)) + \sum_{j=0}^{N_t - 1} \eta_{\mathrm{x}}^{N_t - j - 1} \left(|\hat{w}_t^*(j) - w_t(j)|_{Q_{\mathrm{x}}}^2 + |\hat{y}_t^*(j) - y_t(j)|_{R_{\mathrm{x}}}^2 \right) \\
&\quad + V(\hat{p}_t^*(N_t), p_t(N_t))^2 + \sum_{j=0}^{N_t - 1} \eta_{\mathrm{x}}^{N_t - j - 1} |\hat{p}_t^*(j) - p_t(j)|_{S_{\mathrm{x}}}^2.
\end{aligned}$$

From the bound (5.73) and application of the geometric series, we obtain that

$$V(\hat{p}_t^*(N_t), p_t(N_t))^2 + \sum_{j=0}^{N_t-1} \eta_{\mathrm{x}}^{N_t-j-1} |\hat{p}_t^*(j) - p_t(j)|_{S_{\mathrm{x}}}^2$$
$$\leq \max\{1, \lambda_{\max}(S_{\mathrm{x}}, \underline{V})\eta_{\mathrm{x}}^{-1}\} \sum_{j=0}^{N_t} \eta_{\mathrm{x}}^{N_t-j} V(\hat{p}_t^*(j), p_t(j))^2.$$

From (5.74) and Jensen's inequality, we further have that for each $j \in \mathbb{I}_{[0,N_t]}$,

$$V(\hat{p}_t^*(j), p_t(j))^2 \leq \Big(V(\hat{p}_t^*(0), p_t(0)) + \sum_{i=0}^{N_t-1} |\hat{w}_t^*(i) - w_t(i)|_{Q_{\mathrm{v}}}\Big)^2$$
$$\leq (N_t+1)\Big(V(\hat{p}_t^*(0), p_t(0))^2 + \sum_{i=0}^{N_t-1} |\hat{w}_t^*(i) - w_t(i)|_{Q_{\mathrm{v}}}^2\Big).$$

Combining the previous inequalities and using the geometric series, we obtain that

$$\begin{aligned}
&\Gamma(1, \hat{x}(t), x(t), \hat{p}(t), p(t)) \\
&\leq \eta_{\mathrm{x}}^{N_t} U(\hat{x}_t^*(0), x_t(0)) + \sum_{j=0}^{N_t-1} \eta_{\mathrm{x}}^{N_t-j-1} \left(|\hat{w}_t^*(j) - w_t(j)|_{Q_{\mathrm{x}}}^2 + |\hat{y}_t^*(j) - y_t(j)|_{R_{\mathrm{x}}}^2\right) \\
&\quad + c_1(1, N_t)\Big(V(\hat{p}_t^*(0), p_t(0))^2 + \sum_{j=0}^{N_t-1} |\hat{w}_t^*(j) - w_t(j)|_{Q_{\mathrm{v}}}^2\Big)
\end{aligned}$$

with $c_1(r, s)$ from (5.85). Using the fact that $c_1(1, s) \geq 1$ for all $s \geq 0$, it follows that

$$\begin{aligned}
&\Gamma(1, \hat{x}(t), x(t), \hat{p}(t), p(t)) \\
&\leq c_1(1, N_t)\Big(\eta_{\mathrm{x}}^{N_t} U(\hat{x}_t^*(0), x_t(0)) + V(\hat{p}_t^*(0), p_t(0))^2 \\
&\qquad + \sum_{j=0}^{N_t-1} |\hat{w}_t^*(j) - w_t(j)|_{Q_{\mathrm{x}}+Q_{\mathrm{v}}}^2 + |\hat{y}_t^*(j) - y_t(j)|_{R_{\mathrm{x}}}^2\Big).
\end{aligned} \tag{5.90}$$

By application of the bounds (5.4) and (5.73) together with Jensen's inequality, we obtain

$$U(\hat{x}_t^*(0), x_t(0)) \leq |\hat{x}_t^*(0) - x_t(0)|_{\overline{P}}^2 \leq 2|\hat{x}_t^*(0) - \bar{x}(t-N_t)|_{\overline{P}}^2 + 2|\bar{x}(t-N_t) - x_t(0)_{\overline{P}}^2, \tag{5.91}$$

and

$$V(\hat{p}_t^*(0), p_t(0))^2 \leq |\hat{p}_t^*(0) - p_t(0)|_{\overline{V}}^2 \leq 2|\hat{p}_t^*(0) - \bar{p}(t-N_t)|_{\overline{V}}^2 + 2|\bar{p}(t-N_t) - p_t(0)|_{\overline{V}}^2. \tag{5.92}$$

Similarly, we have that

$$|\hat{w}_t^*(j) - w_t(j)|_{\tilde{Q}}^2 \leq 2|\hat{w}_t^*(j)|_{\tilde{Q}}^2 + 2|w_t(j)|_{\tilde{Q}}^2 \tag{5.93}$$

for all $j \in \mathbb{I}_{[1,N_t]}$ with $\tilde{Q} = Q_\mathrm{x} + Q_\mathrm{v}$. Using (5.90)–(5.93) in (5.89), the facts that $\eta^{N_t-N} \geq 1$ and $c_1(1, N_t) > 1$, and the definition of the cost function (5.77) lets us infer that

$$\begin{aligned}
&\Gamma(1, \hat{x}(t), x(t), \hat{p}(t), p(t)) \\
&\leq \eta^{-N} c_1(1, N_1) \Big(2\eta_\mathrm{x}^{N_t} |\bar{x}(t-N_t) - x_t(0)|_{\overline{P}}^2 + 2\eta^{N_t} |\bar{p}(t-N_t) - p_t(0)|_{\overline{V}}^2 \\
&\qquad + \sum_{j=0}^{N_t-1} 2|w_t(j)|_Q^2 + J(\hat{x}_t^*, \hat{p}_t^*, \hat{w}_t^*, \hat{y}_t^*, t) \Big). \qquad (5.94)
\end{aligned}$$

By optimality, it follows that

$$\begin{aligned}
&J(\hat{x}_t^*, \hat{p}_t^*, \hat{w}_t^*, \hat{y}_t^*, t) \leq J(x_t, p_t, w_t, y_t, t) \\
&\leq 2\gamma(N_t) |x_t(0) - \bar{x}(t-N_t)|_{\overline{P}}^2 + 2\eta^{N_t} |p_t(0) - \bar{p}(t-N_t)|_{\overline{V}}^2 + 2 \sum_{j=0}^{N_t-1} |w_t(j)|_Q^2. \qquad (5.95)
\end{aligned}$$

Combining (5.94) and (5.95) and recalling the definitions in (5.86)–(5.88) yields (5.84), which finishes this proof. □

Lemma 5.4. *Let Assumptions 5.1 and 5.4 be satisfied. Consider the MHE scheme in* (5.76) *with the cost function in* (5.77). *Assume that at some time* $t \in \mathbb{I}_{\geq N}$, $X(t) \in \mathbb{E}_N$. *Then, the corresponding estimates* (5.81) *satisfy*

$$\begin{aligned}
\Gamma(c, \hat{x}(t), x(t), \hat{p}(t), p(t)) &\leq \mu \Gamma(1, \bar{x}(t-N), x(t-N), \bar{p}(t-N), p(t-N)) \\
&\quad + 4c_1(c, N) \max\{1, \lambda_{\max}(\overline{V}, S_\mathrm{p})\} \sum_{j=1}^{N} |w(t-j)|_Q^2 \qquad (5.96)
\end{aligned}$$

with

$$\mu := c_1(c, N) \max\{1, \lambda_{\max}(\overline{V}, S_\mathrm{p})\} \max\left\{4\lambda_{\max}(\overline{P}, \underline{P})\gamma(N), 2\lambda_{\max}(\overline{V}, \underline{V})\eta^N\right\} \qquad (5.97)$$

for all $c \geq 1$.

Proof. We start by using the same arguments as in the beginning of the proof of Lemma 5.3, which leads to

$$\begin{aligned}
&\Gamma(c, \hat{x}(t), x(t), \hat{p}(t), p(t)) = U(\hat{x}_t^*(N), x_t(N)) + cV(\hat{p}_t^*(N), p_t(N))^2 \\
&\leq c_1(c, N) \Big(\eta_\mathrm{x}^N U(\hat{x}_t^*(0), x_t(0)) + V(\hat{p}_t^*(0), p_t(0))^2 \\
&\qquad + \sum_{j=0}^{N-1} |\hat{w}_t^*(j) - w_t(j)|_{Q_\mathrm{x}+Q_\mathrm{v}}^2 + |\hat{y}_t^*(j) - y_t(j)|_{R_\mathrm{x}}^2 \Big)
\end{aligned}$$

with x_t, p_t, and w_t defined in (5.86), (5.87), and (5.88), respectively. Note that $V(\hat{p}_t^*(0), p_t(0))^2 \leq \lambda_{\max}(\overline{V}, S_\mathrm{p}) |\hat{p}_t^*(0) - p_t(0)|_{S_\mathrm{p}}^2$, where

$$|\hat{p}_t^*(0) - p_t(0)|_{S_\mathrm{p}}^2 \leq \eta_\mathrm{p}^N |\hat{x}_t^*(0) - x_t(0)|_{P_\mathrm{p}}^2 + \sum_{j=0}^{N-1} |\hat{w}_t^*(j) - w_t(j)|_{Q_\mathrm{p}}^2 + |\hat{y}_t^*(j) - y_t(j)|_{R_\mathrm{p}}^2$$

due to the fact that $X(t) \in \mathbb{E}_N$. Hence, we obtain

$$\begin{aligned}
&\Gamma(c, \hat{x}(t), x(t), \hat{p}(t), p(t)) \\
&\leq c_1(c, N) \max\{1, \lambda_{\max}(\overline{V}, S_{\mathrm{p}})\} \Big(\eta_{\mathrm{x}}^N U(\hat{x}_t^*(0), x_t(0)) + \eta_{\mathrm{p}}^N |\hat{x}_t^*(0) - x_t(0)|_{P_{\mathrm{p}}}^2 \\
&\qquad + \sum_{j=0}^{N-1} |\hat{w}_t^*(j) - w_t(j)|_Q^2 + |\hat{y}_t^*(j) - y_t(j)|_R^2 \Big),
\end{aligned}$$

where we recall that $Q = Q_{\mathrm{x}} + Q_{\mathrm{v}} + Q_{\mathrm{p}}$ and $R = R_{\mathrm{x}} + R_{\mathrm{p}}$. Using the definition of γ from (5.78), the bounds from (5.91) and (5.93), and the cost function (5.77), we have that

$$\begin{aligned}
&\Gamma(c, \hat{x}(t), x(t), \hat{p}(t), p(t)) \\
&\leq c_1(c, N) \max\{1, \lambda_{\max}(\overline{V}, S_{\mathrm{p}})\} \Big(2\gamma(N) |\bar{x}(t-N) - x_t(0)|_{\overline{P}}^2 \\
&\qquad + 2 \sum_{j=0}^{N-1} |w_t(j)|_Q^2 + J(\hat{x}_t^*, \hat{p}_t^*, \hat{w}_t^*, \hat{y}_t^*, t) \Big).
\end{aligned}$$

Exploiting optimality as in (5.95), using the definition of μ from (5.97), and recalling the definitions in (5.86)–(5.88) yields (5.96), which finishes this proof. □

Now, let

$$\rho := \eta^{-N} c_1(1, N) \left(2\eta_{\mathrm{x}}^N + 2\gamma(N) \right) \lambda_{\max}(\overline{P}, \underline{P}) \tag{5.98}$$

and c be such that

$$c = \frac{8 c_1(1, N) \lambda_{\max}(\overline{V}, \underline{V})}{1 - \rho} + 2 \tag{5.99}$$

with c_1 from (5.85). The robustness guarantees for the MHE require that η, N are chosen such that

$$\max\{\mu, \rho\} < 1. \tag{5.100}$$

Note that this is always possible, since η satisfies condition (5.79) and c_1 is dominated by a factor that exponentially decreases with N.

Now, we divide the time interval $[0, t]$ into sub-intervals (horizons) of length N and the remainder $l = t - \lfloor t/N \rfloor N$, essentially using a similar partitioning as in Section 5.2.1 with (5.41). In comparison, however, the overall notation becomes simpler here, as we do not have to consider any additional time discounting of the disturbances. More specifically, we define the set of time instants at which the corresponding MHE optimization problem was solved involving an excited trajectory pair as

$$\mathcal{T}_t := \left\{ \tau \in \mathbb{I}_{[N,t]} : t - \tau = \left\lfloor \frac{t - \tau}{N} \right\rfloor N,\ X(\tau) \in \mathbb{E}_N \right\}. \tag{5.101}$$

By $k \in \mathbb{I}_{\geq 0}$, we denote the cardinality of $\mathcal{T}_t$, i.e., $k := |\mathcal{T}_t|$. Furthermore, we define the sequence of times $\{t_m\}_{m=1}^{k+1}$ by $t_1 := \max\{\tau \in \mathcal{T}_t\}$,

$$t_{m+1} := \max\{\tau \in \mathcal{T}_t : \tau < t_m\},\ m \in \mathbb{I}_{[1,k-1]},$$

and $t_{k+1} := l$, compare also Figure 5.1 for a visualization.

The following lemma establishes boundedness of the estimation error on $[t_1, t]$ and a decrease in Lyapunov coordinates on each interval $[t_{m+1}, t_m]$ for all $m \in \mathbb{I}_{[1,k]}$.

Lemma 5.5. *Let Assumptions 5.1 and 5.4 be satisfied. Consider the MHE scheme in* (5.76) *with the cost function in* (5.77)*. Suppose that η and N satisfy* (5.100)*. Then, there exist $c_{\mathrm{Q},1}, c_{\mathrm{Q},2} > 0$ such that the estimates* (5.81) *satisfy the following bounds:*

$$\Gamma(1, \hat{x}(t), x(t), \hat{p}(t), p(t)) \leq \Gamma(c, \hat{x}(t_1), x(t_1), \bar{p}(t_1), p(t_1)) + c_{\mathrm{Q},1} \left(\sum_{r=t_1}^{t-1} |w(r)|_Q \right)^2 \tag{5.102}$$

and

$$\begin{aligned} &\Gamma(c, \hat{x}(t_m), x(t_m), \hat{p}(t_m), p(t_m)) \\ &\leq \mu \Gamma(c, \hat{x}(t_{m+1}), x(t_{m+1}), \bar{p}(t_{m+1}), p(t_{m+1})) + c_{\mathrm{Q},2} \left(\sum_{r=t_{m+1}}^{t_m-1} |w(r)|_Q \right)^2 \end{aligned} \tag{5.103}$$

for all $t \in \mathbb{I}_{\geq 0}$, all $m \in \mathbb{I}_{[1,k]}$, all initial states $\hat{\chi}, \chi \in \mathcal{X}$, all initial parameters $\hat{\xi}, \xi \in \mathcal{P}$, and all sequences $u \in \mathcal{U}^\infty$ and $w \in \mathcal{W}^\infty$, where we recall that $t_{k+1} = l$ for any $k \in \mathbb{I}_{\geq 0}$.

Proof. We start with the bound (5.102). Let j denote the number of insufficiently excited horizons that occurred between time t and t_1, i.e., $j := (t - t_1)/N$. First, assume that $j \in \mathbb{I}_{\geq 1}$. From Lemma 5.3, the fact that $|\bar{x}(t-N) - x(t-N)|_{\overline{P}}^2 \leq \lambda_{\max}(\overline{P}, \underline{P}) U(\bar{x}_{t-N}, x_{t-N})$ by (5.4), and the definition of ρ from (5.98), we obtain

$$\begin{aligned} &\Gamma(1, \hat{x}(t), x(t), \hat{p}(t), p(t)) \\ &\leq \rho U(\bar{x}(t-N), x(t-N)) + c_1' |\bar{p}(t-N) - p(t-N)|_{\overline{V}}^2 + c_1' \eta^{-N} \sum_{r=t-N}^{t-1} |w(r)|_Q^2 \end{aligned}$$

with $c_1' = 4c_1(1, N)$, and where ρ satisfies $\rho < 1$ due to satisfaction of (5.100). Note that $\bar{x}(t-N) = \hat{x}(t-N)$ and $\bar{p}(t-N)$ satisfies the update rule (5.80), which implies that $\bar{p}(t - qN) = g^{((j-q)N)}(\bar{p}(t - jN))$ for all $q \in [0, j]$ and $t - jN = t_1$. From Assumption 5.4 and Jensen's inequality, it further follows that

$$V(\bar{p}(t - qN), p(t - qN))^2 \leq 2V(\bar{p}(t_1), p(t_1))^2 + 2 \left(\sum_{r=t_1}^{t-qN-1} |w(r)|_{Q_{\mathrm{v}}} \right)^2. \tag{5.104}$$

Combined, we can write that

$$\begin{aligned} \Gamma(1, \hat{x}(t), x(t), \hat{p}(t), p(t)) \leq{}& \rho U(\bar{x}(t-N), x(t-N)) + 2c_1' \lambda_{\max}(\overline{V}, \underline{V}) V(\bar{p}(t_1), p(t_1))^2 \\ &+ c_1' \max\{2\lambda_{\max}(\overline{V}, \underline{V}), \eta^{-N}\} \left(\sum_{r=t_1}^{t-1} |w(r)|_Q \right)^2. \end{aligned} \tag{5.105}$$

Since

$$U(\hat{x}(t-N),x(t-N)) \leq \Gamma(1,\hat{x}(t-N),x(t-N),\hat{p}(t-N),p(t-N))$$

by (5.83), we can recursively apply (5.105) for j times, which by exploiting the geometric series yields

$$\begin{aligned}\Gamma_1(t,\hat{x}(t),x(t),\hat{p}(t),p(t)) \leq \rho^j U(\hat{x}(t_1),x(t_1)) + \frac{2c_1'\lambda_{\max}(\overline{V},\underline{V})}{1-\rho}V(\bar{p}(t_1),p(t_1))^2 \\ + \frac{c_1'\max\{2\lambda_{\max}(\overline{V},\underline{V}),\eta^{-N}\}}{1-\rho}\left(\sum_{r=t_1}^{t-1}|w(r)|_Q\right)^2.\end{aligned} \tag{5.106}$$

By (5.99), we have that $2c_1'\lambda_{\max}(\overline{V},\underline{V})/(1-\rho) < c$, leading to (5.102) with $c_{\mathrm{Q},1} = c_1'\max\{2\lambda_{\max}(\overline{V},\underline{V}),\eta^{-N}\}/(1-\rho)$, and we note that (5.102) holds for any $j \in \mathbb{I}_{\geq 0}$.

It remains to establish the bound (5.103). Assume that $k \in \mathbb{I}_{\geq 1}$. Then, t_1 corresponds to the most recent horizon where $X(t_1) \in \mathbb{E}_N$. We can invoke Lemma 5.4, which yields

$$\begin{aligned}\Gamma(c,\hat{x}(t_1),x(t_1),\hat{p}(t_1),p(t_1)) \leq \mu\Gamma(1,\bar{x}(t_1-N),x(t_1-N),\bar{p}(t_1-N),p(t_1-N)) \\ + 4c_1(c,N)\max\{1,\lambda_{\max}(\overline{V},S_{\mathrm{p}})\}\sum_{r=t_1-N}^{t_1-1}|w(r)|_Q^2.\end{aligned} \tag{5.107}$$

We further have that

$$\begin{aligned}&\Gamma(1,\bar{x}(t_1-N),x(t_1-N),\bar{p}(t_1-N),p(t_1-N)) \\ &= U(\bar{x}(t_1-N),x(t_1-N)) + V(\bar{p}(t_1-N),z(t_1-N))^2 \\ &\leq \Gamma(1,\hat{x}(t_1-N),x(t_1-N),\hat{p}(t_1-N),p(t_1-N)) + V(\bar{p}(t_1-N),p(t_1-N))^2 \\ &\leq \Gamma(1,\hat{x}(t_1-N),x(t_1-N),\hat{p}(t_1-N),p(t_1-N)) \\ &\quad + 2V(\bar{p}(t_2),p_{t_2})^2 + 2\left(\sum_{r=t_2}^{t_1-N-1}|w(r)|_{Q_{\mathrm{v}}}\right)^2,\end{aligned} \tag{5.108}$$

where in the latter inequality we have used similar arguments that were applied to derive (5.104). Adapting the arguments applied to derive (5.106), we have that

$$\begin{aligned}&\Gamma(1,\hat{x}(t_1-N),x(t_1-N),\hat{p}(t_1-N),p(t_1-N)) \\ &\leq U(\hat{x}(t_2),x(t_2)) + \frac{2c_1'\lambda_{\max}(\overline{V},\underline{V})}{1-\rho}V(\bar{p}(t_2),p(t_2))^2 \\ &\quad + \frac{c_1'\max\{2\lambda_{\max}(\overline{V},\underline{V}),\eta^{-N}\}}{1-\rho}\left(\sum_{r=t_2}^{t_1-N-1}|w(r)|_Q\right)^2,\end{aligned} \tag{5.109}$$

where we have used that $\rho^s \leq 1$ for all $s \in \mathbb{I}_{\geq 0}$. The combination of (5.107)–(5.109) (which also hold with t_1 and t_2 replaced by t_m and t_{m+1} for each $m \in \mathbb{I}_{[1,k]}$) and

using the definition of c from (5.99) leads to (5.103), where

$$c_{\mathrm{Q},2} := \max\left\{\mu\left(\frac{c_1' \max\{2\lambda_{\max}(\overline{V},\underline{V}),\eta^{-N}\}}{1-\rho}+2\right), 4c_1(c,N)\max\{1,\lambda_{\max}(\overline{V},S_{\mathrm{p}})\}\right\},$$

which finishes this proof. □

We now combine the properties provided by Lemma 5.5 and establish a bound on the overall state and parameter estimation error in terms of the initial errors and the past disturbances that occurred in the interval $\mathbb{I}_{[0,t-1]}$.

Theorem 5.2. *Let Assumptions 5.1 and 5.4 be satisfied. Consider the MHE scheme in* (5.76) *with the cost function in* (5.77)*. Suppose that η and N satisfy* (5.100)*. Then, the estimates* (5.81) *satisfy*

$$\begin{aligned}
&C_0|\hat{x}(t)-x(t)|_{\underline{P}} + C_0|\hat{p}(t)-p(t)|_{\underline{V}} \\
&\leq \sqrt{\mu}^k\left(\sqrt{C_1}\sqrt{\tilde{\eta}}^l|\hat{\chi}-\chi|_{\overline{P}} + \sqrt{C_2}\sqrt{\tilde{\eta}}^l|\hat{\xi}-\xi|_{\overline{V}}\right) \\
&\quad + \sqrt{\mu}^k\sum_{r=0}^{l-1}|w(r)|_{Q_3} + \sum_{m=1}^{k}\sqrt{\mu}^{m-1}\sum_{r=t_{m+1}}^{t_m-1}|w(r)|_{Q_3} + \sum_{r=t_1}^{t-1}|w(r)|_{Q_3}
\end{aligned} \tag{5.110}$$

for all $t \in \mathbb{I}_{\geq 0}$, all initial states $\hat{\chi},\chi \in \mathcal{X}$, all initial parameters $\hat{\xi},\xi \in \mathcal{P}$, and all sequences $u \in \mathcal{U}^\infty$ and $w \in \mathcal{W}^\infty$, where $\tilde{\eta} := \max\{\eta_{\mathrm{x}},\eta_{\mathrm{p}}\}$, $C_0 := \sqrt{2}/2$, and

$$C_1 := 2\eta^{-N}c_1(1,N)(2+\lambda_{\max}(P_{\mathrm{p}},\overline{P})), \tag{5.111}$$
$$C_2 := (4c_1(1,N)+2c)\eta^{-N}, \tag{5.112}$$
$$Q_3 := \max\{c_{\mathrm{Q},1}, c_{\mathrm{Q},2}, (4c_1(1,N)\eta^{-N}+2c)\}Q. \tag{5.113}$$

Before proving Theorem 5.2, we want to highlight the key properties of the resulting bound on the estimation errors.

- The bound in (5.110) is valid independent of the parameter excitation, and it improves the more often the excitation condition (5.80) is satisfied during operation.
- If $k \to \infty$ for $t \to \infty$, then the state and parameter estimation error $e(t)$ as defined in (5.82) converges to a ball centered at the origin with the radius defined by the energy of the true disturbance sequence. If additionally $w(t) \to 0$ for $t \to \infty$, then $e(t) \to 0$.
- If $t-t_1$ and $t_{m+1}-t_m$ can be uniformly bounded for all times, then the estimation error converges exponentially, which follows by using similar arguments as in Corollary 5.1.
- In contrast to our results for constant parameters in Section 5.2, the bound in (5.110) involves the (non-discounted) sum of disturbances $w(r)$ over $r \in \mathbb{I}_{[t_1,t]}$, which can be interpreted as the energy of the corresponding disturbance subsequence $\{w(r)\}_{r=t_1}^{t}$. This is due to the fact that for trajectories that are

insufficiently excited in some interval, we use the nominal dynamics of (5.1b) to predict the evolution of $p(t)$ and invoke Assumption 5.4 to bound the current parameter estimation error $|e_{\mathrm{p}}(t)|$. Hence, no qualitatively better error bound can be expected without further assumptions on the dynamics (5.1b), the disturbance w, or satisfaction of the excitation condition (5.80).

Proof of Theorem 5.2. The claim follows by combining the bounds from Lemma 5.5 and invoking Assumption 5.4 for $l \in \mathbb{I}_{[0,N-1]}$. First, suppose that $k \in \mathbb{I}_{\geq 1}$ and note that $\bar{p}(t_m) = \hat{p}(t_m)$ for all $m \in \mathbb{I}_{[1,k]}$. Hence, the recursive application of (5.103) and the fact that $t_{k+1} = l$ yield

$$\begin{aligned}&\Gamma(c, \hat{x}(t_1), x(t_1), \bar{p}(t_1), p(t_1))\\ &\leq \mu^k \Gamma(c, \hat{x}(l), x(l), \bar{p}(l), p(l)) + \sum_{m=1}^{k} \mu^{m-1} \left(c_{Q,2} \sum_{r=t_{m+1}}^{t_m - 1} |w(r)|_Q \right)^2, \end{aligned} \tag{5.114}$$

which is valid for all $k \geq 0$ (in case $k = 0$, we have $t_1 = l$). For $l \in \mathbb{I}_{[0,N-1]}$, it follows that

$$\begin{aligned}\Gamma(c, \hat{x}(l), x(l), \bar{p}(l), p(l)) &= U(\hat{x}(l), x(l)) + cV(\bar{p}(l), p(l))^2\\ &\leq \Gamma(1, \hat{x}(l), x(l), \hat{p}(l), p(l)) + cV(\bar{p}(l), p(l))^2. \end{aligned} \tag{5.115}$$

By using Lemma 5.3 with $\bar{x}(0) = \hat{\chi}$ and $\bar{p}(0) = \hat{\xi}$, we obtain

$$\begin{aligned}\Gamma(1, \hat{x}(l), x(l), \hat{p}(l), p(l)) &\leq c_1(1, N)\eta^{-N}(2\eta_{\mathrm{x}}^l + 2\gamma(l))|\hat{\chi} - \chi|_P^2\\ &\quad + c_1' \eta^{-N} \eta^l |\hat{\xi} - \xi|_V^2 + c_1' \eta^{-N} \sum_{r=0}^{l-1} |w(r)|_Q^2, \end{aligned} \tag{5.116}$$

where we have used the definition $c_1' = 4c_1(1, N)$ together with the facts that $l < N$ and $c_1(1, s) < c_1(1, N)$ for all $s \in [0, N-1]$. By Assumption 5.4, the facts that $\bar{p}_l = g^{(l)}(\bar{p}(0))$ and $\bar{p}(0) = \hat{\xi}$, and Jensen's inequality, it further follows that

$$V(\bar{p}(l), p(l))^2 \leq 2V(\hat{\xi}, \xi)^2 + 2 \left(\sum_{r=0}^{l-1} |w(r)|_{Q_{\mathrm{v}}} \right)^2. \tag{5.117}$$

From (5.115)–(5.117) and the definitions of γ, C_1, and C_2 from (5.78), (5.111), and (5.112), respectively, we can infer that

$$\begin{aligned}\Gamma(c, \hat{x}(l), x(l), \bar{p}(l), p(l)) &\leq C_1 \tilde{\eta}^l |\hat{\chi} - \chi|_P^2 + C_2 \eta^l |\hat{\xi} - \xi|_V^2\\ &\quad + (c_1' \eta^{-N} + 2c) \left(\sum_{r=0}^{l-1} |w(r)|_Q \right)^2. \end{aligned} \tag{5.118}$$

Combining (5.102), (5.114), and (5.118), using the definition of Q_3 from (5.113), applying the square root (which is concave and subadditive on $\mathbb{R}_{\geq 0}$), and Jensen's inequality finally leads to (5.110). Since (5.110) holds for any $l \in \mathbb{I}_{[0,N-1]}$ and $k \in \mathbb{I}_{\geq 0}$, it holds for all $t \in \mathbb{I}_{\geq 0}$, which finishes this proof. □

5.3.3. Numerical example

To illustrate our results, we consider the following system

$$\begin{aligned} x_1^+ &= x_1 + t_\Delta b_1(x_2 - a_1 x_1 - a_2 x_1^2 - p x_1^3) + w_1, \\ x_2^+ &= x_2 + t_\Delta(x_1 - x_2 + x_3) + w_2, \\ x_3^+ &= x_3 - t_\Delta b_2 x_2 + w_3, \\ p^+ &= p + w_4, \\ y &= x_1 + w_5. \end{aligned}$$

This corresponds to the perturbed modified Chua's circuit system from Section 5.2.4, where we additionally assume that the parameter $p(t)$ is time-variant and subject to an unknown disturbance input $w_4(t)$. Note that from the system description it is immediately apparent that the observability of $p(t)$ depends on the magnitude of $x_1(t)$, compare also Figure 5.2 and the respective discussion in Section 5.2.4. The parameters are $b_1 = 12.8$, $b_2 = 19.1$, $a_1 = 0.6$, $a_2 = -1.1$. The disturbances w_i, $i = 1, 2, 3, 5$ are uniformly distributed with $|w_i(t)| \leq 10^{-3}, i = 1, 2, 3$ for the process disturbance, and $|w_5(t)| \leq 5 \cdot 10^{-2}$ for the measurement noise for all $t \in \mathbb{I}_{\geq 0}$. The disturbance w_4 consists of two superimposed square waves such that $w_4(t) \in \{-10^{-4}, 0, 10^{-4}\}$, $t \in \mathbb{I}_{\geq 0}$, compare the red curve in Figure 5.7 below. We consider the initial conditions $\chi = [2, 0, -1]^\top$ and $\xi = 0.45$ and assume that $x(t)$ and $p(t)$ evolve in the (known) sets $\mathcal{X} = [-1, 3] \times [-1, 1] \times [-3, 3]$ and $\mathcal{P} = [0.2, 0.8]$. The objective is to compute the state and parameter estimates $\hat{x}(t)$ and $\hat{p}(t)$ by applying the MHE scheme proposed in Section 5.3.1 using the initial estimates $\hat{\chi} = [-1, 0.1, 2]^\top$ and $\hat{\xi} = 0.6$.

Assumption 5.4 is satisfied with the function $V(p_1, p_2) = |p_1 - p_2|$ and matrix $\mathrm{Q_v} = B_\mathrm{p}^\top B_\mathrm{p}$ using $B_\mathrm{p} = [0, 0, 0, 1, 0]$. We compute a quadratic i-IOSS Lyapunov function $U(x_1, x_2) = |x_1 - x_2|_{P_\mathrm{x}}^2$, $P_\mathrm{x} \succ 0$ by adapting the verification method from Section 7.1.1, compare Section 5.2.4. To monitor the excitation of trajectory pairs, we evaluate at each time $t \in \mathbb{I}_{\geq 0}$ the matrix $\mathcal{O}_T(Z_t^*)$ in (7.93) at the currently optimal solution $Z_t^* = \left(\hat{x}_t^*(0), p_t^*(0), \{\hat{w}_t^*(t)\}_{j=0}^{N_t-1}\right)$, see Section 7.2.2 for more details. Here, we consider a trajectory pair $X(t)$ to be sufficiently excited if $\alpha_t = \lambda_{\min}(\mathcal{O}_{N_t}(Z_t^*)) \geq \alpha = 5 \cdot 10^{-4}$.

Tuning the cost function (5.77) based on the parameters of U, V, and the set $\mathbb{E}_T$ yields a minimum required horizon length $N_{\min} \approx 300$. This is rather conservative due to conservative steps in the proofs (in particular, Lemmas 5.3 and 5.4), and good performance is obtained using a smaller horizon length. To illustrate the potential of the proposed MHE scheme, we choose $N = 200$ and $\eta = 0.9$, $\gamma(s) = \eta^s$, $\overline{P} = I_2$, $\overline{V} = 1$, $Q = 10^7 I_4$, $R = 10^3$, although these invalidate the theoretical guarantees established in Section 5.3.2. Furthermore, we update $\hat{p}(t)$ only if $X(t) \in \mathbb{E}_{N_t}$, compare Remark 5.2.

The simulations are carried out in Matlab over $t_\mathrm{sim} = 4000$ time steps. The estimation error of the proposed scheme is shown in Figure 5.6, which shows fast convergence of the estimation errors. This is also evident in Figure 5.7, which illustrates the respective estimated parameter $\hat{p}(t)$ over time. In phases without sufficiently

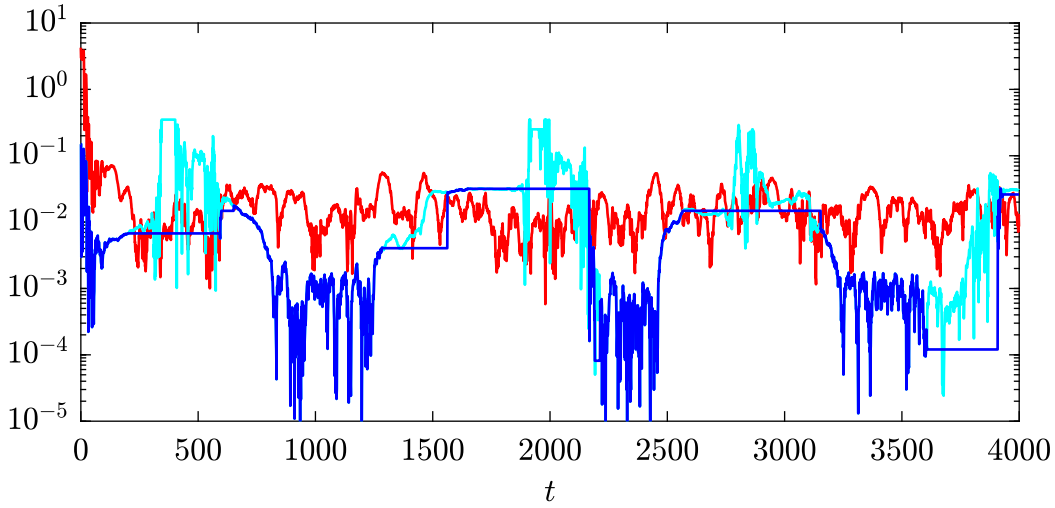

Figure 5.6. Estimation errors $|e_{\mathrm{x}}(t)|$ (red) and $|e_{\mathrm{p}}(t)|$ (blue) for the proposed MHE scheme compared to $|e_{\mathrm{p}}(t)|$ for MHE without excitation monitoring (cyan).

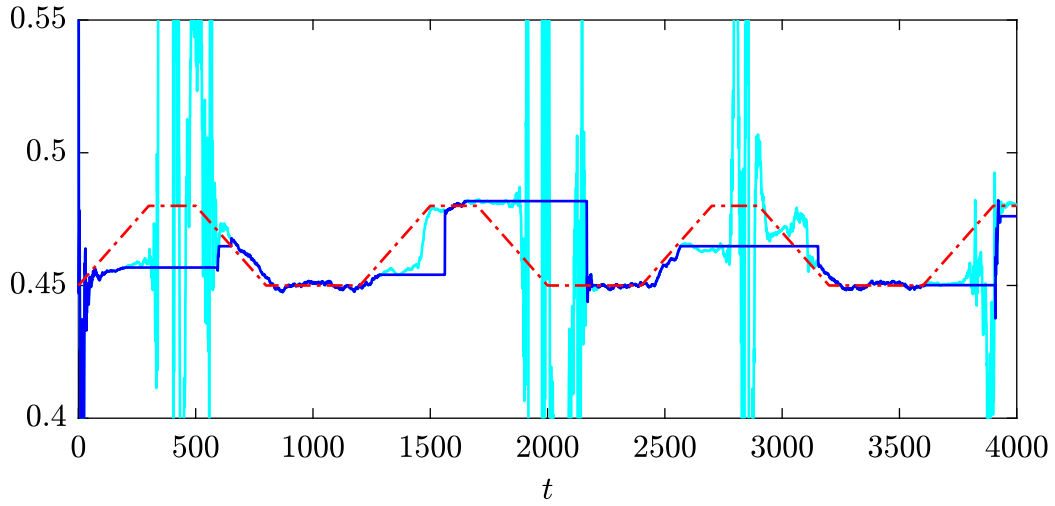

Figure 5.7. Estimates $\hat{p}(t)$ for the proposed MHE scheme (blue) compared to MHE without excitation monitoring (cyan) and the true parameter $p(t)$ (red).

high excitation levels ($\alpha_t \ll \alpha$, see Figure 5.8), the proposed MHE scheme is not able to track the true parameter $p(t)$ (which is clear due to the lack of information). However, it still provides estimates with bounded errors that are much smaller compared to using MHE without excitation monitoring (see the cyan-colored curve in Figures 5.6 and 5.7).

This simulation example illustrates the efficiency of the proposed MHE scheme from Section 5.3. When $p(t)$ is observable from data, it is able to robustly track the true parameter. If it is unobservable, it reacts appropriately to prevent the estimation error from deteriorating arbitrarily.

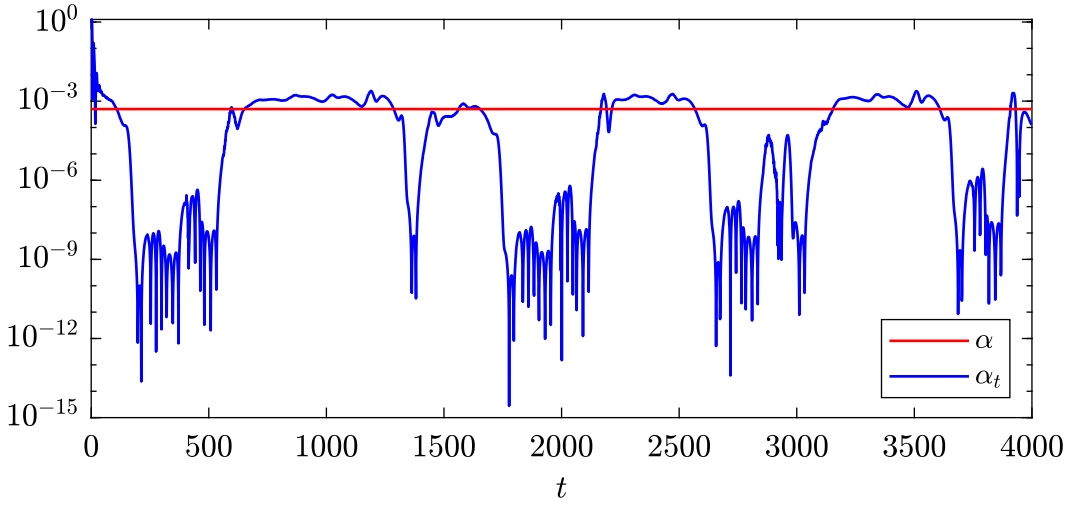

Figure 5.8. Excitation level α_t; values above the red line indicate sufficient excitation.

5.4. Summary

In this chapter, we proposed MHE schemes for joint state and parameter estimation that are applicable to general nonlinear systems, particularly tailored for parameters that may suffer from insufficient excitation. Specifically, the cost function involves an adaptive regularization term that is adjusted according to real-time excitation information, where we rely on the excitation monitoring techniques developed in Section 7.2. We first considered the case of constant parameters and derived a bound for the state and parameter estimation error that is valid regardless of excitation of the parameter, and in particular also applies if the parameter is never or only rarely excited during operation. In the general case without excitation, our result constitutes a bounded-disturbance bounded-estimation-error property, which is qualitatively the best result that can be expected without additional specifications for the excitation or setup. The derived bound improves with respect to the initial estimates the more often the parameter is detected to be sufficiently excited. Moreover, if the time between two PE intervals occurred during online operation can be uniformly bounded, our result specializes to RGES, i.e., it implies exponential convergence of the state and parameter estimation error to a neighborhood around the origin defined by the true disturbances. Note that although this requires some *a priori* knowledge about PE, it is still weaker than the standard uniform PE condition. For the latter case, we showed that uniform PE is equivalent to the existence of a joint i-IOSS Lyapunov function for the augmented state vector consisting of the states and the system parameters. This establishes the intuitive implication that state detectability plus uniform PE of the parameter is equivalent to the augmented system being uniformly detectable, which renders standard MHE methods for state estimation applicable.

We extended our results to the more general case of time-varying parameters, which additionally involved an incremental UBEBS property of the parameter dynamics in order to provide bounded estimation errors. This is naturally required to ensure that

arbitrary parameter drifts cannot cause the estimation error to become unstable in case the parameter is unobservable.

The numerical examples illustrated that the proposed MHE schemes in combination with the PE monitoring techniques from Section 7.2 are able to efficiently compensate for phases of weak excitation. For both constant and time-varying parameters, we obtained reliable estimation results for all times, which in particular were prevented from deteriorating arbitrarily in phases without excitation, while being accurate in phases with sufficient excitation.

6. Turnpike analysis and performance guarantees

In this chapter, we investigate the turnpike phenomenon in optimal state estimation problems using tools from optimal control, and leverage the insights gained to develop novel accuracy, performance, and regret guarantees for MHE.

We start by formalizing the setup in Section 6.1, which includes some structural differences and generalizations to previously considered MHE formulations. We define a particular benchmark for MHE, namely the omniscient infinite-horizon optimal state estimator, which has access to all past and future measurements. In Section 6.2, we discuss and analyze the turnpike behavior of MHE problems with respect to this benchmark in detail, leading to new insights into optimal state estimation. These are exploited in Section 6.3, where we propose a slightly modified variant of MHE involving an additional delay and derive corresponding performance and regret guarantees with respect to the benchmark estimator. In Section 6.4, we illustrate the results in terms of various numerical examples from the literature, which show that the proposed modifications can significantly improve the estimation results in practice.

Disclosure: The following chapter is based upon and in parts literally taken from our previous publications [SGM24] and [SGM25]. A detailed description of the contributions of each author is given in Appendix A.

6.1. Setup

System description

In this chapter, we focus on nonlinear uncertain discrete-time systems of the following form:

$$x(t+1) = f(x(t), u(t), d(t)), \quad x(0) = \chi, \tag{6.1a}$$

$$y(t) = h(x(t), u(t)) + v(t) \tag{6.1b}$$

with discrete time $t \in \mathbb{I}_{\geq 0}$, state $x(t) \in \mathbb{R}^n$, initial condition $\chi \in \mathbb{R}^n$, control input $u(t) \in \mathbb{R}^m$, (unknown) process disturbance $d(t) \in \mathbb{R}^q$, (unknown) measurement noise $v(t) \in \mathbb{R}^p$, and output measurement $y(t) \in \mathbb{R}^p$. The functions $f : \mathbb{R}^n \times \mathbb{R}^m \times \mathbb{R}^q \to \mathbb{R}^n$ and $h : \mathbb{R}^n \times \mathbb{R}^m \to \mathbb{R}^p$ define the system dynamics and output equation, which we assume to be continuous.

Remark 6.1 (System description)**.** *Note that we consider additive measurement noise in* (6.1b)*, which corresponds to a special case of the output equation usually considered throughout this thesis, compare Section 3.1 and see also Section 2.2.2 for a detailed discussion on this topic. Here, this facilitates the analysis as it directly allows us to gain intuition from standard optimal control theory. However, we conjecture that the results presented below can be extended to the more general case of nonlinear measurement noise, and the derivation of the formal proofs is an interesting topic for future work. However, we want to emphasize that the case of additive measurement noise is actually frequently assumed in MHE theory (see, e.g., [ABB08; RMD20; Mül17; AR19b; All20; Hu24] and compare also Remark 3.1) and moreover is usually considered in practice, see, e.g., [HCE18; Els+21; Liu+17; Bre19; CLH22; Kle+23].*

In the following, we assume that trajectories of the system (6.1) satisfy

$$(x(t), u(t), d(t), v(t)) \in \mathcal{X} \times \mathcal{U} \times \mathcal{D} \times \mathcal{V},\ t \in \mathbb{I}_{\geq 0} \tag{6.2}$$

for some known sets $\mathcal{X} \subseteq \mathbb{R}^n$, $\mathcal{U} \subseteq \mathbb{R}^m$, $\mathcal{D} \subseteq \mathbb{R}^q$ (where $0 \in \mathcal{D}$), and $\mathcal{V} \subseteq \mathbb{R}^p$, and furthermore, that

$$(x, u, d) \in \mathcal{X} \times \mathcal{U} \times \mathcal{D} \Rightarrow f(x, u, d) \in \mathcal{X}. \tag{6.3}$$

Such knowledge typically arises from the physical nature of the system (e.g., non-negativity of certain physical quantities such as partial pressure or absolute temperature), the incorporation of which can significantly improve the estimation results, see [RMD20, Sec. 4.4] and compare also Section 3.1 for more details.

The optimal state estimation problem

MHE generally relies on the repeated solution of optimal state estimation problems, compare, for example, Section 3.1. In the following, we study such schemes through the lens of optimization theory, and in particular interpret the optimal estimation problem as a graph-structured NLP that is parameterized by the data provided to the NLP. We now revisit the principles of MHE in this context.

For ease of notation, we define the input-output data (or parameter) tuple $D(t) := (u(t), y(t))$ obtained from the system (6.1) at time $t \in \mathbb{I}_{\geq 0}$. Now, consider a given batch of input-output data $D = \{D(j)\}_{j=0}^{N}$ of length $N+1$ for some $N \in \mathbb{I}_{\geq 0}$. We aim to compute the state sequence $\hat{x} = \{\hat{x}(j)\}_{j=0}^{N}$ along with the disturbance input sequences $\hat{d} = \{\hat{d}(j)\}_{j=0}^{N-1}$ that are optimal in the sense that they minimize a cost function involving the full data set D. In particular, we consider the following

optimal state estimation problem

$$
\begin{aligned}
P_N(D): \qquad & \min_{\hat{x},\hat{d}} \; J_N(\hat{x},\hat{d};D) && \text{(6.4a)}\\
\text{s.t.} \quad & \hat{x}(j+1) = f(\hat{x}(j),u(j),\hat{d}(j)),\ j \in \mathbb{I}_{[0,N-1]}, && \text{(6.4b)}\\
& \hat{x}(j) \in \mathcal{X},\ j \in \mathbb{I}_{[0,N]}, && \text{(6.4c)}\\
& \hat{d}(j) \in \mathcal{D},\ j \in \mathbb{I}_{[0,N-1]}, && \text{(6.4d)}\\
& y(j) - h(\hat{x}(j),u(j)) \in \mathcal{V},\ j \in \mathbb{I}_{[0,N]}. && \text{(6.4e)}
\end{aligned}
$$

For convenience, we define the combined sequence $\hat{z} = \{\hat{z}(j)\}_{j=0}^{N}$ containing both decision variables $\hat{x}$ and $\hat{d}$ as $\hat{z}(j) := (\hat{x}(j), \hat{d}(j))$ for $j \in \mathbb{I}_{[0,N-1]}$ and $\hat{z}(N) := (\hat{x}(N), 0)$. The constraints (6.4b)–(6.4e) enforce the prior knowledge about the system model, the domain of the true trajectories, and the disturbances and noise (note that feasibility is always guaranteed due to our standing assumptions).

In (6.4a), we find it convenient to emphasize the dependency of the cost function J_N used in (6.4a) on the data set D and the horizon length N, which is a slightly different notation than the one we usually employ in this thesis, compare, e.g., (3.4b) in Section 3.1. In particular, we define

$$
J_N(\hat{x},\hat{d};D) := \sum_{j=0}^{N-1} L(\hat{x}(j),\hat{d}(j);D(j)) + L_{\mathrm{tc}}(\hat{x}(N);D(N)) \tag{6.5}
$$

with continuous stage cost $L : \mathcal{X}\times\mathcal{D}\times\mathcal{U}\times\mathbb{R}^p \to \mathbb{R}_{\geq 0}$ and terminal cost $L_{\mathrm{tc}} : \mathcal{X}\times\mathcal{U}\times\mathbb{R}^p \to \mathbb{R}_{\geq 0}$. We point out that this is a generalization of classical designs for state estimation, where L and L_{tc} are positive definite in the disturbance input $\hat{d}$ and the fitting error $y - h(\hat{x},u)$ for all $\hat{x} \in \mathcal{X}$, $\hat{d} \in \mathcal{D}$, $u \in \mathcal{U}$, and $y \in \mathbb{R}^p$, compare [RMD20, Ch. 4] and see also Section 3.1; it particularly includes the practically relevant case of quadratic stage and terminal cost

$$
L(x,d;(u,y)) = |d|_Q^2 + |y - h(x,u)|_R^2 \tag{6.6}
$$

and

$$
L_{\mathrm{tc}}(x;(u,y)) = |y - h(x,u)|_S^2, \tag{6.7}
$$

respectively, where Q, R, S are positive definite weighting matrices. However, our results also hold for more general cost functions L and L_{tc}, which allow the objective (6.5) to be tailored to the specific problem at hand. Note that cost functions with an additional prior weighting in (6.5) (as usual in MHE, compare Section 3.1) are considered in Section 6.3.3.

In the state estimation context, a cost function with terminal cost as in (6.7) is usually referred to as the *filtering form* of the state estimation problem. To simplify the analysis and notation, the most recent works on FIE/MHE theory often consider a cost function with $L_{\mathrm{tc}} = 0$ (i.e., without terminal cost), which corresponds to the *prediction form* of the state estimation problem, compare Section 3.1 and [Sch+23; KM23; AR21; Hu24], and see also [RMD20, Ch. 4] for a discussion on this topic.

The optimization problem P_N in (6.4) is a parametric NLP, the solution of which solely depends on the (input-output) data provided, that is, the sequence D. We characterize solutions to P_N using the generic solution mapping ζ_N:

$$\hat{z}^*(j) := \zeta_N(j, D),\ j \in \mathbb{I}_{[0,N]}, \tag{6.8}$$

which yields the value function $V_N(D) = J_N(\hat{z}^*; D)$ where $\hat{z}^* = \{\hat{z}^*(j)\}_{j=0}^N$. While the function ζ_N returns a pair of optimal state and disturbance input, we use ζ_N^x to refer only to the optimal state of this pair, so that $\hat{x}^*(j) = \zeta_N^x(j, D)$ for all $j \in \mathbb{I}_{[0,N]}$.

Remark 6.2 (Existence of solutions to P_N)**.** *Throughout the following, we assume that whenever we employ the solution mapping ζ_N, the corresponding solution exists. Note that under continuity of f and h in* (6.1)*, this can generally be guaranteed by choosing the stage cost L and terminal cost L_{tc} such that the cost function J_N is radially unbounded in the (condensed) decision variables (which requires positive definiteness of L and L_{tc} and observability[1] of the system with a corresponding horizon length N, compare [RMD20, Sec. 4.3.1]), or under compactness of the sets $\mathcal{X}$ and $\mathcal{D}$, see [RMD20, Prop. A.7].*

Remark 6.3 (Discounting)**.** *We use a non-discounted cost function in* (6.5)*, which is conceptually different from most of the MHE formulations considered in this thesis, compare Section 3.1 and the discussion in Section 3.3. This is because, in this chapter, we are not interested in deriving robust stability of MHE (where discounting plays a crucial role), but in performance estimates and regret bounds with respect to a particular benchmark solution. As this is a novel approach, we consider here the case of non-discounted costs, which simplifies the analysis. Extending our results presented below to cost functions with discounting (i.e, where the sum in* (6.5) *contains an additional term η^{N-j} for some discount factor $\eta \in (0, 1)$) constitutes an interesting topic for future work, which may be addressed by using similar arguments as in the context of discounted economic MPC, compare, for example, [GKW16; Grü+21; ZG22], see Chapter 8 for more details.*

Benchmark solution

We are interested in how the optimal solution defined by (6.8) compares to a certain (challenging) benchmark problem. For this purpose, we interpret the data sequence D as a segment of an infinite data sequence $D_\infty = \{D_\infty(j)\}_{j=-\infty}^{\infty}$ such that $D_\infty(j) = D(j)$, $j \in \mathbb{I}_{[0,N]}$, where D_∞ contains all past and future data that could possibly be generated by the system (6.1) in the interval $\mathbb{I}$. Then, we consider the *omniscient infinite-horizon estimator*, that is, the solution of the (acausal) infinite-horizon optimal state estimation problem

$$P_\infty(D_\infty)\ :\ \min_{\hat{z}} \sum_{j=-\infty}^{\infty} L(\hat{z}(j), \hat{d}(j); D_\infty(j))\ \text{ s.t. }\ (6.4\text{b})\text{–}(6.4\text{e}),\ j \in \mathbb{I}, \tag{6.9}$$

[1] Observability is required here because the cost function J_N does not contain an additional prior weighting as is the case in, e.g., Section 3.1; the case of MHE with prior weighting, which does not require observability, is considered in Section 6.3.3 below.

where $\hat{z}(j) = (\hat{x}(j), \hat{d}(j))$, $j \in \mathbb{I}$. We denote the solution to $P_\infty(D_\infty)$ by the infinite sequence $z^\infty := \{z^\infty(j)\}_{j=-\infty}^{\infty}$ with $z^\infty(j) = (x^\infty(j), d^\infty(j))$, $j \in \mathbb{I}$, where we assume that z^∞ exists and is unique for any possible D_∞, compare Remark 6.2.

Note that in linear settings [SH22; BDF23], a common benchmark for observers estimating the state $x(t)$ at some time $t \in \mathbb{I}_{\geq 0}$ is the clairvoyant acausal observer relying on data from the interval $\mathbb{I}_{[0,\infty)}$, where in particular data from $\mathbb{I}_{[t+1,\infty)}$ is only fictitious (as it depends on future disturbances and noise) and may or may not actually be measured at a future point in time (e.g., if the experiment is terminated). We adopt this approach and take it even further by assuming that our benchmark—the omniscient infinite-horizon estimator—can not only predict the future (knowing data from $\mathbb{I}_{[t+1,\infty)}$), but also has a perfect memory (knowing data from $\mathbb{I}_{(-\infty,-1]}$).

In the following section, we will investigate how the solution $\hat{z}^*$ in (6.8) behaves compared to the benchmark z^∞ on the common domain of existence, i.e., the interval $\mathbb{I}_{[0,N]}$. In particular, we show that solutions of the finite-horizon problem $P_N(D)$ exhibit the turnpike phenomenon with respect to the solution of the infinite-horizon problem $P_\infty(D_\infty)$ (Section 6.2), which we then employ to construct (causal) estimators that provide performance guarantees and bounded regret with respect to this benchmark (Section 6.3).

6.2. Turnpike in optimal state estimation problems

Optimal state estimation problems (such as P_N in (6.4)) can generally be interpreted as optimal control problems using the disturbance $\hat{d}$ as the control input (compare also [RMD20, Sec. 4.2.3] and [All20, Sec. 4]). In particular, a cost function (6.5) that is positive definite in the estimated disturbance and the fitting error (as, e.g., in (6.6) and (6.7)) can be regarded as an economic output tracking cost, penalizing deviations from the ideal reference $(d^{\mathrm{r}}(j), y^{\mathrm{r}}(j)) = (0, y(j))$, $j \in \mathbb{I}_{[0,N]}$. This reference, however, is generally unreachable, as it is usually impossible to attain zero cost $V_N(D) = 0$, except for the special case where $y(j)$, $j \in \mathbb{I}_{[0,N]}$ corresponds to an output sequence of (6.1) under zero disturbances, i.e., $d, v \equiv 0$. For unreachable references, on the other hand, it is known that the corresponding optimal control problem exhibits the turnpike property with respect to the *best reachable reference* [KMA19], which suggests that a similar phenomenon can also be expected in optimal state estimation problems.

In Section 6.2.1, we provide a simple motivating example that supports this intuition. Then, we consider two mathematical characterizations of the turnpike phenomenon and provide corresponding sufficient conditions that rely on strict dissipativity (Section 6.2.2) and decaying sensitivity (Section 6.2.3). For the latter, we show in Section 6.2.4 how this is naturally satisfied in the linear quadratic setting using standard optimal control and Riccati theory. In Section 6.2.5, we discuss the considered turnpike characterizations with regard to their properties and limitations and introduce a general turnpike definition that combines their advantages.

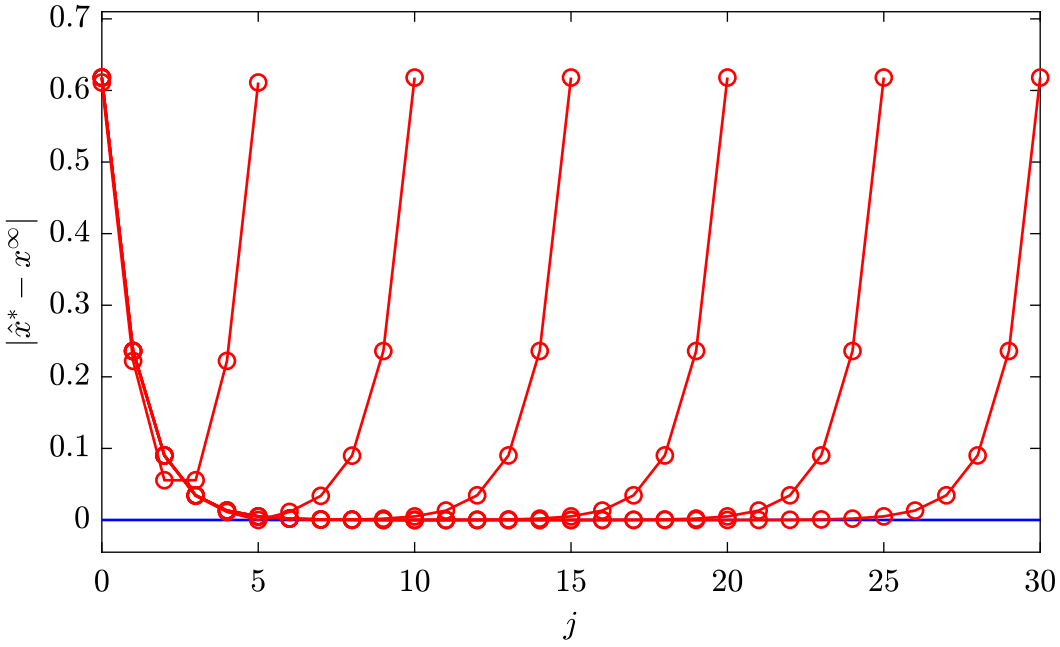

Figure 6.1. Difference between the solution x^∞ of the infinite-horizon problem P_∞ and solutions $\hat{x}^*$ of the finite-horizon problem P_N for different values of N.

6.2.1. Motivating example

Suppose that some output data $y = \{y(j)\}_{j=0}^T$ for $T = 30$ is measured from the system $x(t+1) = x(t)+d(t)$ with $x(0) = 1$ and $y(t) = x(t)+v(t)$, where $d(t) = v(t) = 1$ for all $t \in \mathbb{I}$. We consider the finite-horizon optimal estimation problem $P_N(D)$ with $D = \{D(j)\}_{j=0}^N = \{y(j)\}_{j=0}^N$, the quadratic stage and terminal cost (6.6) and (6.7) using $Q = R = S = 1$, and different values of N. For the benchmark estimator, we also consider the infinite-horizon problem $P_\infty(D_\infty)$, which we approximate by simulating the system and computing the solution on some extended interval $\mathbb{I}_{[-T_e,T+T_e]}$, where we choose T_e such that the solution does not change (up to numerical accuracy) on $\mathbb{I}_{[0,T]}$ if T_e is further increased.

Figure 6.1 shows the difference between the infinite-horizon solution $x^\infty(j)$ and the solution of the finite-horizon problem $\hat{x}^*(j)$ for $j \in \mathbb{I}_{[0,N]}$ and different values of N. One can clearly see that the benchmark x^∞ serves as turnpike for the solution $\hat{x}^*$. In particular, we find that $\hat{x}^*$ is constructed from three pieces: an initial transient where $\hat{x}^*$ converges to the turnpike x^∞, a large phase where $\hat{x}^*$ stays near the turnpike x^∞, and a transient at the end of the horizon where $\hat{x}^*$ diverges from the turnpike x^∞. Figure 6.1 also indicates that these transients[2] are independent of the horizon length N. Note that a similar behavior could also be observed for the disturbance difference $\hat{d}^*(j) - d^\infty(j)$, $j \in \mathbb{I}_{[0,N-1]}$.

In the following sections, we provide and discuss different mathematical characterizations of the turnpike phenomenon observed in this motivating example, relying on strict dissipativity and decaying sensitivity.

[2] In the turnpike-related literature, the left transient is usually referred to as the *approaching arc* (or *entry arc*), and the right transient as the *leaving arc*, compare [FG22].

6.2.2. Turnpike under strict dissipativity

Motivated by the literature on nonlinear optimal control and economic MPC, we first consider a strict dissipativity condition. Here, we focus on the terminal cost $L_{\mathrm{tc}}(x;(u,y)) = 0$ to simplify the analysis.

Assumption 6.1 (Strict dissipativity)**.** *Consider an infinite data sequence D_∞ associated with the system* (6.1) *and the solution z^∞ of the infinite-horizon problem $P_\infty(D_\infty)$ from* (6.9)*. The finite-horizon problem $P_N(D)$ in* (6.4) *for $N \in \mathbb{I}_{\geq 0}$ and the truncated data set $D = \{D(j)\}_{j=0}^N$ with $D(j) = D_\infty(j)$, $j \in \mathbb{I}_{[0,N]}$ is* strictly dissipative *with respect to the supply rate*

$$s(j,x,d) = L(x,d;D(j)) - L(x^\infty(j),d^\infty(j);D(j)),\ j \in \mathbb{I}_{[0,N-1]}, \tag{6.10}$$

i.e., there exists a time-varying storage function $\lambda : \mathbb{I} \times \mathcal{X} \to \mathbb{R}$ and $\alpha \in \mathcal{K}_\infty$ such that

$$\lambda(j+1, f(x,u(j),d)) - \lambda(j,x) \leq -\alpha(|z - z^\infty(j)|) + s(j,x,d) \tag{6.11}$$

for all $j \in \mathbb{I}_{[0,N]}$ and all $z = (x,d) \in \mathcal{X} \times \mathcal{D}$. Moreover, there exists $\alpha_\lambda \in \mathcal{K}_\infty$ such that $|\lambda(j,x)| \leq \alpha_\lambda(|x - x^\infty(j)|)$ uniformly for all $j \in \mathbb{I}_{[0,N]}$.

Strict dissipativity is a standard assumption in the context of (economic) model predictive control, usually employed to establish turnpike behavior of open-loop optimal control problems and obtain stability and performance guarantees of the resulting closed loop, see, e.g., [FGM18; GP19; KMA19]. Here, we define strict dissipativity using a time-varying storage function and supply rate involving the (time-varying) infinite-horizon solution z^∞, compare [GPS18, Def. 6] for a time-varying setup in the context of optimal control and see also the discussion in Section 6.2.5. The upper bound on the storage function λ provides an additional continuity property with respect to the infinite-horizon solution.

The following result shows that under strict dissipativity (in the sense of Assumption 6.1), the solutions of the finite-horizon problems P_N are close to the optimal solution of the infinite-horizon problem P_∞ for most of the time, which hence constitutes the turnpike associated with the optimal estimation problem.

Theorem 6.1. *Let $\mathcal{X}$ be compact and suppose that Assumption 6.1 is satisfied. Consider the infinite-horizon solution z^∞ for some data set D_∞ associated with the system* (6.1)*. Then, there exists $\sigma \in \mathcal{L}$ such that for all $Q \in \mathbb{I}_{[0,N]}$, at least Q points $j \in \mathbb{I}_{[0,N-1]}$ of the solution $\hat{z}^*(j) = \zeta_N(j,D)$ using the truncated data set $D = \{D(j)\}_{j=0}^N$ with $D(j) = D_\infty(j)$, $j \in \mathbb{I}_{[0,N]}$ satisfy*

$$|\hat{z}^*(j) - z^\infty(j)| \leq \sigma(N-Q) \tag{6.12}$$

for all $N \in \mathbb{I}_{\geq 0}$ and all possible data D_∞.

Proof. We consider the rotated stage cost

$$\begin{aligned} L_{\mathrm{rot}}(j,x,d) := L(x,d;D(j)) - L(x^\infty(j),d^\infty(j);D(j)) \\ + \lambda(j,x) - \lambda(j+1, f(x,u(j),d)) \end{aligned}$$

for all $j \in \mathbb{I}_{[0,N-1]}$ and any point $z = (x,d) \in \mathcal{X} \times \mathcal{D}$. From strict dissipativity (Assumption 6.1), we know that

$$L_{\mathrm{rot}}(j,x,d) \geq \alpha(|z - z^\infty(j)|),\ j \in \mathbb{I}_{[0,N-1]}, \tag{6.13}$$

which implies that the rotated stage cost is positive definite with respect to the difference $|z - z^\infty(j)|$ for all $j \in \mathbb{I}_{[0,N-1]}$ and any $z \in \mathcal{X} \times \mathcal{D}$.

Now consider some $N \in \mathbb{I}_{\geq 0}$ and the solution $\hat{z}^*(j) = \zeta_N(j,d)$, $j \in \mathbb{I}_{[0,N]}$. Evaluating the rotated cost function along $\hat{z}^*$ yields

$$\begin{aligned} \sum_{j=0}^{N-1} L_{\mathrm{rot}}(j,\hat{x}^*(j),\hat{d}^*(j)) = \sum_{j=0}^{N-1} L(\hat{x}^*(j),\hat{d}^*(j);D(j)) - L(x^\infty(j),d^\infty(j);D(j)) \\ + \lambda(0,\hat{x}^*(0)) - \lambda(N,\hat{x}^*(N)). \end{aligned}$$

The application of (6.13) then leads to

$$\begin{aligned} &\sum_{j=0}^{N-1} L(\hat{x}^*(j),\hat{d}^*(j);D(j)) - L(x^\infty(j),d^\infty(j);D(j)) \\ &\geq \lambda(N,\hat{x}^*(N)) - \lambda(0,\hat{x}^*(0)) + \sum_{j=0}^{N-1} \alpha(|\hat{z}^*(j) - z^\infty(j)|). \end{aligned} \tag{6.14}$$

Due to the fact that $\mathcal{X}$ is compact and the storage function is bounded (Assumption 6.1), we can define $C_\lambda := \max_{x_1,x_2 \in \mathcal{X}} \alpha_\lambda(|x_1 - x_2|)$ such that $|\lambda(j,x)| \leq C_\lambda$ for all $j \in \mathbb{I}_{[0,N]}$ and all $x \in \mathcal{X}$. We claim that the turnpike property holds with

$$\sigma(r) = \alpha^{-1}\left(\frac{2C_\lambda}{r}\right). \tag{6.15}$$

For the sake of contradiction, suppose not. Then, at least $N-Q+1$ points $j \in \mathbb{I}_{[0,N-1]}$ satisfy $|\hat{z}^*(j) - z^\infty(j)| > \sigma(N-Q)$. Hence, from (6.14) it follows that

$$\begin{aligned} \sum_{j=0}^{N-1} L(\hat{x}^*(j),\hat{d}^*(j);D(j)) - L(x^\infty(j),d^\infty(j);D(j)) &> -2C_\lambda + (N-Q)\alpha(\sigma(N-Q)) \\ &= 0, \end{aligned} \tag{6.16}$$

where the last equality follows from (6.15). However, (6.16) contradicts optimality of $\hat{z}^*$ since it generally must hold that

$$\begin{aligned} \sum_{j=0}^{N-1} L(\hat{x}^*(j),\hat{d}^*(j);D(j)) - L(x^\infty(j),d^\infty(j);D(j)) &= V_N(D) - J_N\left(\{z^\infty(j)\}_{j=0}^N; D\right) \\ &\leq 0, \end{aligned}$$

which proves our claim. □

Remark 6.4 (Relation to the literature)**.** *Theorem 6.1 and its proof follow the lines of classical turnpike results in the context of (receding horizon) optimal control, see, e.g., [GPS18, Th. 1]. However, because the initial state is free in the estimation problem and not fixed as typical in control, we can avoid the need for an additional reachability/controllability property to bound the value function $V_N(D)$, simply by exploiting the fact that the trajectory z^∞ truncated to the interval $\mathbb{I}_{[0,N]}$ is a feasible candidate solution.*

6.2.3. Turnpike under decaying sensitivity

In the previous section, we established turnpike behavior in optimal state estimation problems using strict dissipativity. The property characterized by Theorem 6.1 is, however, rather weak in the sense that we actually do not know which points of the solution $\hat{z}^*$ are close to the turnpike z^∞, and which are not. We can, however, strengthen this result under a decaying sensitivity condition, compare [NA20; SAZ22; SZ21] and see also [Shi+23; GSS20].

To this end, for any $N \in \mathbb{I}_{\geq 0}$, let us consider the auxiliary problem $\bar{P}_N(\bar{D}, x^\mathrm{i}, x^\mathrm{t})$ parameterized by the data $(\bar{D}, x^\mathrm{i}, x^\mathrm{t})$, where $\bar{D} = \{\bar{D}(j)\}_{j=0}^N$ with $\bar{D}(j) = (\bar{u}(j), \bar{y}(j)) \in \mathcal{U} \times \mathbb{R}^p$, $j \in \mathbb{I}_{[0,N]}$, and $x^\mathrm{i}, x^\mathrm{t} \in \mathcal{X}$:

$$\min_{\bar{x},\bar{d}} \sum_{j=0}^{N-1} L(\bar{x}(j), \bar{d}(j); \bar{D}(j)) \tag{6.17a}$$

$$\text{s.t. } \bar{x}(0) = x^\mathrm{i}, \tag{6.17b}$$

$$\bar{x}(N) = x^\mathrm{t}, \tag{6.17c}$$

$$\bar{x}(j+1) = f(\bar{x}(j), \bar{u}(j), \bar{d}(j)),\ j \in \mathbb{I}_{[0,N-1]}, \tag{6.17d}$$

$$\bar{x}(j) \in \mathcal{X},\ j \in \mathbb{I}_{[0,N]}, \tag{6.17e}$$

$$\bar{d}(j) \in \mathcal{D},\ \bar{y}(j) - h(\bar{x}(j), \bar{u}(j)) \in \mathcal{V},\ j \in \mathbb{I}_{[0,N-1]}. \tag{6.17f}$$

For the sequences $\bar{x} = \{\bar{x}(j)\}_{j=0}^N$ and $\bar{d} = \{\bar{d}(j)\}_{j=0}^{N-1}$, let $\bar{z}(j) := (\bar{x}(j), \bar{d}(j))$, $j \in \mathbb{I}_{[0,N-1]}$, and $\bar{z}(N) := (\bar{x}(N), 0)$. The constraints in (6.17b) and (6.17c) specify fixed initial and terminal states of the sequence $\bar{x}$ for some given parameters x^i and x^t. We characterize solutions to the problem (6.17) (assuming that they exist, compare Remark 6.2) using the solution mapping $\bar{\zeta}_N$, i.e., such that $\bar{z}^*(j) = \bar{\zeta}_N(j, \bar{D}, x^\mathrm{i}, x^\mathrm{t})$, $j \in \mathbb{I}_{[0,N]}$ with $\bar{z}^*(j) := (\bar{x}^*(j), \bar{d}^*(j))$, $j \in \mathbb{I}_{[0,N-1]}$, and $\bar{z}^*(N) := (\bar{x}^*(N), 0)$.

We point out the following relation between the infinite-horizon problem P_∞ in (6.9) and the auxiliary problem $\bar{P}_N$ in (6.17).

Lemma 6.1. *Consider an infinite data sequence D_∞ associated with the system* (6.1) *and the causal subsequence $D = \{D(j)\}_{j=0}^N$ such that $D(j) = D_\infty(j)$ for $j \in \mathbb{I}_{[0,N]}$. Any minimizer of $P_\infty(D_\infty)$ is a minimizer of $\bar{P}_N(D, x^\infty(0), x^\infty(N))$ for any $N \in \mathbb{I}_{\geq 0}$.*

Proof. The proof relies on the principle of optimality. First, note that the problem $\bar{P}_N(D, x^\infty(0), x^\infty(N))$ is feasible because the candidate solution $\{z^\infty(j)\}_{j=0}^N$ satisfies

the constraints (6.17b)–(6.17f) with $\bar{D} = D$. Let $\bar{z}^*(j) := \bar{\zeta}_N(j, D, x^\infty(0), x^\infty(N))$. Now, suppose the claim is false. Then,

$$\sum_{j=0}^{N-1} L(z^\infty(j); D(j)) > \sum_{j=0}^{N-1} L(\bar{z}^*(j); D(j)).$$

To both sides of this inequality, we add the cost terms

$$\sum_{j=-\infty}^{-1} L(z^\infty(j); D_\infty(j)) + \sum_{j=N}^{\infty} L(z^\infty(j); D_\infty(j)),$$

which yields

$$V(D_\infty) > \sum_{j=-\infty}^{-1} L(z^\infty(j); D_\infty(j)) + \sum_{j=0}^{N-1} L(\bar{z}^*(j); D(j)) + \sum_{j=N}^{\infty} L(z^\infty(j); D_\infty(j)), \tag{6.18}$$

where $V(D_\infty)$ corresponds to the the value function associated with the infinite-horizon problem $P_\infty(D_\infty)$. Now, consider the infinite sequence $\xi = \{\xi(j)\}_{j=-\infty}^{\infty}$ defined as

$$\xi(j) = (\chi(j), \omega(j)) := \begin{cases} z^\infty(j), & j \in \mathbb{I}_{\leq -1} \\ \bar{z}^*(j), & j \in \mathbb{I}_{[0,N-1]} \\ z^\infty(j), & j \in \mathbb{I}_{\geq N}. \end{cases} \tag{6.19}$$

Then, (6.18) can be re-written as

$$V(D_\infty) > \sum_{j=-\infty}^{\infty} L(\xi(j); D_\infty(j)). \tag{6.20}$$

The sequence ξ satisfies the constraints in (6.9) due to the initial and terminal constraints in (6.17b) and (6.17c), respectively, and hence constitutes a valid candidate solution for the infinite-horizon problem $P_\infty(D_\infty)$. However, the strict inequality in (6.20) contradicts minimality of $V(D_\infty)$, which proves the claim. □

We make the following assumption.

Assumption 6.2 (Decaying sensitivity)**.** *There exists $\beta \in \mathcal{KL}$ such that for any $x_1^{\mathrm{i}}, x_2^{\mathrm{i}} \in \mathcal{X}$ and $x_1^{\mathrm{t}}, x_2^{\mathrm{t}} \in \mathcal{X}$, and any data sequence $D = \{D(j)\}_{j=0}^{N}$ for which the NLP in* (6.17) *is feasible and admits a solution, it holds that*

$$|\bar{\zeta}_N(j, D, x_1^{\mathrm{i}}, x_1^{\mathrm{t}}) - \bar{\zeta}_N(j, D, x_2^{\mathrm{i}}, x_2^{\mathrm{t}})| \leq \beta(|x_1^{\mathrm{i}} - x_2^{\mathrm{i}}|, j) + \beta(|x_1^{\mathrm{t}} - x_2^{\mathrm{t}}|, N - j) \tag{6.21}$$

for all $j \in \mathbb{I}_{[0,N]}$ and all $N \in \mathbb{I}_{\geq 0}$.

Decaying sensitivity is a quite natural property of parametric NLPs that characterizes how much perturbations in the data at one stage influence the solution of the optimization problem at another stage [NA20; SAZ22]. In our case, the property (6.21) refers to two solutions of the optimization problem where the data sets involved only differ in the initial conditions $x_1^{\mathrm{i}}, x_2^{\mathrm{i}}$ and terminal conditions $x_1^{\mathrm{t}}, x_2^{\mathrm{t}}$,

but otherwise contain exactly the same data; consequently, the bound given by the right-hand side in (6.21) involves only those terms. In Section 6.2.4, we show that Assumption 6.2 is naturally satisfied for linear systems under standard observability and controllability conditions.

The following result establishes turnpike behavior in optimal state estimation problems using Assumption 6.2.

Theorem 6.2. *Suppose that Assumption 6.2 is satisfied. Consider the infinite-horizon solution z^∞ of the problem P_∞ in (6.9) for some data set D_∞ associated with the system (6.1). Then, the solution $\hat{z}^*$ of the finite-horizon problem P_N in (6.4) using the truncated data set $D = \{D(j)\}_{j=0}^N$ with $D(j) = D_\infty(j)$, $j \in \mathbb{I}_{[0,N]}$ satisfies*

$$|\hat{z}^*(j) - z^\infty(j)| \leq \beta(|\hat{z}^*(0) - z^\infty(0)|, j) + \beta(|\hat{z}^*(N) - z^\infty(N)|, N - j) \tag{6.22}$$

for all $j \in \mathbb{I}_{[0,N]}$, $N \in \mathbb{I}_{\geq 0}$, and all possible D_∞.

Proof. Theorem 6.2 is a simple consequence of Lemma 6.1 and Assumption 6.2. First, note that the sequence $\hat{z}^*$ is a minimizer of $\bar{P}_N(D, \hat{x}^*(0), \hat{x}^*(N))$, which follows by optimality of $\hat{z}^*$ and the fact that the solution of (6.17) is not changed by adding the terminal cost $L_{\mathrm{tc}}(\hat{x}^*(N); D(N))$ in (6.5) due to the terminal constraint in (6.17c). Moreover, by application of Lemma 6.1, we also know that z^∞ is a minimizer of $\bar{P}_N(D, x^\infty(0), x^\infty(N))$. Hence, we can invoke Assumption 6.2 to compare $\hat{z}^*$ and z^∞ on $\mathbb{I}_{[0,N]}$, which leads to (6.22) and hence finishes this proof. □

6.2.4. Linear systems

In this section, we show how Assumption 6.2 (decaying sensitivity) is naturally satisfied in the standard linear quadratic setting. More specifically, we consider the LTI system

$$x(t+1) = Ax(t) + B_{\mathrm{x}}u(t) + Ed(t) \tag{6.23a}$$
$$y(t) = Cx(t) + B_{\mathrm{y}}u(t) + Fv(t) \tag{6.23b}$$

and the quadratic stage cost

$$L(x, d; (u, y)) = \frac{1}{2}|d|_Q^2 + \frac{1}{2}|y - (Cx + B_{\mathrm{y}}u)|_R^2 \tag{6.24}$$

for some weighting matrices $Q, R \succ 0$.

Now, consider the solution $\bar{z}^*$ of the NLP in (6.17) for some given admissible parameters $(\bar{D}, x^{\mathrm{i}}, x^{\mathrm{t}})$ and $N \in \mathbb{I}_{\geq 1}$. Invoking the first-order necessary conditions for optimality, there exist adjoints (also called costates or dual variables) $\bar{\lambda}^*(j)$, $j \in \mathbb{I}_{[0,N]}$ such that the following equations are satisfied for all $j \in \mathbb{I}_{[0,N-1]}$:

$$\bar{x}^*(j+1) = \frac{\partial \mathcal{H}}{\partial \lambda}(j, \bar{x}^*(j), \bar{d}^*(j), \bar{\lambda}^*(j+1)), \tag{6.25a}$$
$$\bar{\lambda}^*(j) = \frac{\partial \mathcal{H}}{\partial x}(j, \bar{x}^*(j), \bar{d}^*(j), \bar{\lambda}^*(j+1)), \tag{6.25b}$$
$$0 = \frac{\partial \mathcal{H}}{\partial d}(j, \bar{x}^*(j), \bar{d}^*(j), \bar{\lambda}^*(j+1)), \tag{6.25c}$$

where $\mathcal{H}$ is the associated Hamiltonian

$$\mathcal{H}(j, x, d, \lambda) := L(x, d; \bar{D}(j)) + \lambda^\top f(x, \bar{u}(j), d).$$

For more details, we refer to [BH75] and [FG22]. For the linear quadratic setup from above (i.e., the LTI system (6.1) and the quadratic stage cost (6.24)), the equations in (6.25) specialize to

$$\bar{x}^*(j+1) = A\bar{x}^*(j) + B_{\mathrm{x}}\bar{u}(j) + E\bar{d}^*(j), \tag{6.26a}$$
$$\bar{\lambda}^*(j) = A^\top\bar{\lambda}^*(j+1) + C^\top RC\bar{x}^*(j) - C^\top R\bar{y}(j) + C^\top RB_{\mathrm{y}}\bar{u}(j), \tag{6.26b}$$
$$0 = Q\bar{d}^*(j) + E^\top\bar{\lambda}^*(j+1), \tag{6.26c}$$

where the boundary conditions are formed by the initial and terminal constraints in (6.17b) and (6.17c). Solving (6.26c) for the optimal disturbance input yields $\bar{d}^*(j) = -Q^{-1}E^\top\bar{\lambda}^*(j+1)$ (recall that Q is positive definite and hence invertible), which together with (6.26a) and (6.26b) leads to the Hamiltonian system

$$\begin{bmatrix}\bar{x}^*(j+1)\\ \bar{\lambda}^*(j)\end{bmatrix} = \begin{bmatrix}A & -EQ^{-1}E^\top\\ C^\top RC & A^\top\end{bmatrix}\begin{bmatrix}\bar{x}^*(j)\\ \bar{\lambda}^*(j+1)\end{bmatrix} + \begin{bmatrix}B_{\mathrm{x}} & 0\\ C^\top RB_{\mathrm{y}} & -C^\top R\end{bmatrix}\begin{bmatrix}\bar{u}(j)\\ \bar{y}(j)\end{bmatrix} \tag{6.27}$$

with $j \in \mathbb{I}_{[0,N-1]}$. Note that the forced part in (6.27) involving the input-output data $\bar{D}(j) = (\bar{u}(j), \bar{y}(j))$, $j \in \mathbb{I}_{[0,N-1]}$ stems from the nature of the problem (which can be seen as an optimal control problem for output tracking with an additional input reference).

In the following, we consider two optimal solutions $\bar{z}_i^*$, $i = 1, 2$ that differ in their boundary conditions; more precisely, such that $\bar{z}_i^*(j) = \bar{\zeta}_N(j, \bar{D}, x_i^{\mathrm{i}}, x_i^{\mathrm{t}})$ for some feasible $\bar{D}$, x_i^{i}, x_i^{t}, $i = 1, 2$, yielding the corresponding adjoints $\bar{\lambda}_i^*(j)$ for $j \in \mathbb{I}_{[0,N]}$ and $i = 1, 2$. For convenience, we define the differences in the optimal states $\bar{x}_i^*(j)$, adjoints $\bar{\lambda}_i^*(j)$, and disturbances $\bar{d}_i^*(j)$, $i = 1, 2$ as

$$\Delta x(j) = \bar{x}_1^*(j) - \bar{x}_2^*(j), \quad j \in \mathbb{I}_{[0,N]}, \tag{6.28a}$$
$$\Delta\lambda(j) = \bar{\lambda}_1^*(j) - \bar{\lambda}_2^*(j), \quad j \in \mathbb{I}_{[0,N]}, \tag{6.28b}$$
$$\Delta d(j) = \bar{d}_1^*(j) - \bar{d}_2^*(j), \quad j \in \mathbb{I}_{[0,N-1]}. \tag{6.28c}$$

Note that both optimal trajectories evolve according to (6.27); moreover, since they rely on the same data $\bar{D}$, the differences $\Delta x(j)$ and $\Delta\lambda(j)$ in (6.28a) and (6.28b) satisfy the equations of the unforced Hamiltonian system

$$\begin{bmatrix}\Delta x(j+1)\\ \Delta\lambda(j)\end{bmatrix} = \begin{bmatrix}A & -EQ^{-1}E^\top\\ C^\top RC & A^\top\end{bmatrix}\begin{bmatrix}\Delta x(j)\\ \Delta\lambda(j+1)\end{bmatrix}.$$

Assuming that A is non-singular, we can rewrite this into

$$\begin{bmatrix}\Delta x(j+1)\\ \Delta\lambda(j+1)\end{bmatrix} = H\begin{bmatrix}\Delta x(j)\\ \Delta\lambda(j)\end{bmatrix} \tag{6.29}$$

with the Hamiltonian matrix

$$H = \begin{bmatrix} A + \tilde{Q}A^{-\top}\tilde{R} & -\tilde{Q}A^{-\top} \\ -A^{-\top}\tilde{R} & A^{-\top} \end{bmatrix}, \tag{6.30}$$

where $\tilde{Q} := EQ^{-1}E^\top$ and $\tilde{R} := C^\top RC$ are symmetric. The matrix H in (6.30) occurs very frequently in the context of linear quadratic optimal control and associated Riccati theory; in particular, it is well-known that the reciprocals of the eigenvalues of H are also eigenvalues of H, compare, for example, [Vau70] and [Kuč72].

Now, consider the discrete algebraic Riccati equation (DARE)

$$X - A^\top X(I + \tilde{Q}X)^{-1}A - \tilde{R} = 0. \tag{6.31}$$

We impose the following assumption.

Assumption 6.3 (System properties)**.** *The pairs (A, E) and (A, C) are controllable and observable[3], respectively.*

Under Assumption 6.3 and invertibility of the system matrix A, it is well-known that the DARE (6.31) admits a maximal positive definite solution P_+ and a minimal negative definite solution P_- (which correspond to the unique stabilizing and anti-stabilizing solution, respectively), compare, e.g., [KN99; Ion96; Kuč72; WK72], and see also Sections 3.5–3.7 in [IOW99]. Moreover, these properties ensure that the Hamiltonian matrix H in (6.30) has neither eigenvalues on the unit circle nor in the origin, compare [Kuč72, Lem. 1, Lem. 4]. Note that observability and invertibility of A could be relaxed at the expense of a more technically involved analysis, see Remark 6.5 below for further details.

The stabilizing and anti-stabilizing solutions to the DARE lead to the corresponding "closed-loop" matrices

$$A_+ = A - \tilde{Q}A^{-\top}(P_+ - \tilde{R}), \tag{6.32}$$

$$A_- = A - \tilde{Q}A^{-\top}(P_- - \tilde{R}), \tag{6.33}$$

where the eigenvalues of A_+ and A_- are strictly inside and outside the unit circle.

The following proposition builds on the results from [NM05; FN05] and illustrates that all trajectories satisfying the Hamiltonian system (6.29) can be suitably re-parameterized using the solutions to the DARE (6.31).

Proposition 6.1. *Consider the LTI system in* (6.23) *under Assumption 6.3 and let A in* (6.23a) *be non-singular. Furthermore, consider the quadratic stage cost in* (6.24) *and let $Q, R \succ 0$. Then, any solution to the Hamiltonian system* (6.29) *formed by the two sequences $\{\Delta x(j)\}_{j=0}^N$ and $\{\Delta\lambda(j)\}_{j=0}^N$ can be parameterized as*

$$\begin{bmatrix} \Delta x(j) \\ \Delta\lambda(j) \end{bmatrix} = \begin{bmatrix} I \\ P_+ \end{bmatrix} A_+^j p + \begin{bmatrix} I \\ P_- \end{bmatrix} A_-^{-(N-j)} q, \ j \in \mathbb{I}_{[0,N]} \tag{6.34}$$

for suitable $p, q \in \mathbb{R}^n$.

[3]Here, we refer to the usual definitions of controllability and observability in terms of the associated rank conditions with respect to the matrix pair involved, see, e.g., Definition 3.3.1 (p. 90) and Theorem 16 (p. 200) in [Son90].

Proof. The proof essentially follows the lines of the proof of [FN05, Thm. 5]. It can be structured into two parts, where we first show that parameterized trajectories satisfying (6.34) are trajectories of the Hamiltonian system (6.29), and conversely, that all solutions of the Hamiltonian system (6.29) can be expressed in terms of (6.34) for suitable $p, q \in \mathbb{R}^n$.

Part I. In order to show that trajectories of (6.34) also satisfy the dynamics of the Hamiltonian system (6.29), we simply need to verify if the following equality holds true:

$$\begin{bmatrix} I \\ P_+ \end{bmatrix} A_+^{j+1} p + \begin{bmatrix} I \\ P_- \end{bmatrix} A_-^{-(N-j-1)} q = H\left(\begin{bmatrix} I \\ P_+ \end{bmatrix} A_+^{j} p + \begin{bmatrix} I \\ P_- \end{bmatrix} A_-^{-(N-j)} q \right), \ j \in \mathbb{I}_{[0,N]}. \tag{6.35}$$

This can be separated into two parts involving p and q independently of each other. For the terms corresponding to p, by recalling the definition of H from (6.30) and multiplying with A_+^{-j} from the right, we obtain the condition

$$\begin{bmatrix} I \\ P_+ \end{bmatrix} A_+ = \begin{bmatrix} A + \tilde{Q} A^{-\top} \tilde{R} & -\tilde{Q} A^{-\top} \\ -A^{-\top} \tilde{R} & A^{-\top} \end{bmatrix} \begin{bmatrix} I \\ P_+ \end{bmatrix}. \tag{6.36}$$

Here, we note that the first block row directly holds true by definition of A_+ in (6.32). The second block row follows by using the definition of A_+ and replacing the difference $(P_+ - \tilde{R})$ by application of the DARE (6.31):

$$\begin{aligned}
0 &\overset{!}{=} P_+ A_+ + A^{-\top} \tilde{R} - A^{-\top} P_+ \\
&= P_+ A - P_+ \tilde{Q} A^{-\top} (P_+ - \tilde{R}) - A^{-\top} (P_+ - \tilde{R}) \\
&= P_+ A - (I + P_+ \tilde{Q}) A^{-\top} (P_+ - \tilde{R}) \\
&= P_+ A - (I + P_+ \tilde{Q}) A^{-\top} (A^\top P_+ (I + \tilde{Q} P_+)^{-1} A) \\
&= P_+ A - (I + P_+ \tilde{Q}) P_+ (I + \tilde{Q} P_+)^{-1} A \\
&= P_+ A - (P_+ + P_+ \tilde{Q} P_+)(I + \tilde{Q} P_+)^{-1} A \\
&= P_+ A - P_+ (I + \tilde{Q} P_+)(I + \tilde{Q} P_+)^{-1} A \\
&= P_+ A - P_+ A \\
&= 0,
\end{aligned}$$

which hence establishes the desired equality in (6.36). Considering the terms involving q in (6.35), it must hold that

$$\begin{bmatrix} I \\ P_- \end{bmatrix} A_- = \begin{bmatrix} A + \tilde{Q} A^{-\top} \tilde{R} & -\tilde{Q} A^{-\top} \\ -A^{-\top} \tilde{R} & A^{-\top} \end{bmatrix} \begin{bmatrix} I \\ P_- \end{bmatrix}. \tag{6.37}$$

This equality can be verified by using the definition of A_- from (6.33), the DARE in (6.31), and the same arguments that were applied to establish (6.36). Consequently, both (6.36) and (6.37) hold under the stated conditions, which implies that (6.35) is satisfied and hence finishes the first part of this proof.

Part II. We now show that all solutions of the Hamiltonian system (6.29) can be expressed in terms of (6.34) for suitable values of p and q. To this end, we prove

that the parameterized system (6.34) has $2n$ linearly independent trajectories and represents the complete set of solutions of (6.29). Define $V_+ = \begin{bmatrix} I \\ P_+ \end{bmatrix}$ and $V_- = \begin{bmatrix} I \\ P_- \end{bmatrix}$. From the first part of this proof, it follows that

$$HV_+ = V_+ A_+, \quad HV_- = V_- A_-.$$

This essentially implies that $\operatorname{im}(V_+)$ and $\operatorname{im}(V_-)$ constitute H-invariant subspaces, where the eigenvalues of H restricted to $\operatorname{im}(V_+)$ and $\operatorname{im}(V_-)$ correspond to the eigenvalues of A_+ and A_- and hence are all stable and anti-stable, respectively. Hence, it follows that $\operatorname{im}(V_+) \cap \operatorname{im}(V_-) = \{0\}$. Therefore, for a given $p, q \in \mathbb{R}^n$, the two trajectories $V_+ A_+^j p$ and $V_- A_-^{-(N-j)} q$ are linearly independent, and the dimension of the linear space of trajectories of the parameterized system (6.34) is given by the sum of the dimensions n_1 and n_2 of the subspaces of trajectories of (6.34) corresponding to the cases where $p = 0$ and $q = 0$, respectively. Because V_+ and V_- are full column rank and the powers of A_+ and A_- are nonsingular for all $j \in \mathbb{I}_{[0,N]}$, we have that $n_1 = n$ and $n_2 = n$. Consequently, the parameterized system (6.34) has $2n$ linearly independent solutions, which implies that (6.34) parameterizes the complete set of solutions of (6.29) and hence concludes this proof. □

Remark 6.5 (Conditions of Propositions 6.1)**.** *Propositions 6.1 essentially requires that the system matrix A is invertible, that the pairs (A, E) and (A, C) are controllable and observable, and that the weighting matrices Q and R are positive definite. While controllability (with respect to the disturbance input) and positive definiteness of Q and R are not overly restrictive in the estimation context, the invertibility of A and observability may limit the applicability in practice. However, we emphasize that these conditions are only imposed for the sake of clarity, ensuring that the derived results and implications are easier to interpret. Specifically, they can be relaxed by avoiding the derivation of the Hamiltonian system* (6.29) *and instead consider the extended symplectic Hamiltonian system in descriptor form as done in [FN05; FN07]. Similar conclusions may then be derived by adapting [FN05, Th. 5], simply requiring positive semidefiniteness of Q and R, controllability of the pair (A, E), and conditions on the extended symplectic matrix pencil associated with the system, ensuring that it is regular and has no generalized eigenvalues on the unit circle. However, formulating the corresponding results with sufficient technical precision would require many additional tools and concepts, which would distract from the main message.*

Proposition 6.2. *Consider the LTI system in* (6.23) *under Assumption 6.3 and let A in* (6.23a) *be non-singular. Furthermore, consider the quadratic stage cost in* (6.24) *and let $Q, R \succ 0$. Then, the optimal estimation problem in* (6.17) *satisfies the decaying sensitivity condition in Assumption 6.2. More specifically, there exist constants $C > 0$ and $\lambda \in (0, 1)$ such that the differences defined in* (6.28) *satisfy*

$$|\Delta x(j)| + |\Delta d_{\mathrm{e}}(j)| + |\Delta \lambda(j)| \leq C \left(\lambda^j |\Delta x(0)| + \lambda^{N-j} |\Delta x(N)| \right) \tag{6.38}$$

for all $j \in \mathbb{I}_{[0,N]}$ and any $N \in \mathbb{I}_{\geq 1}$, where $\Delta d_{\mathrm{e}}(j) = \Delta d(j)$ for $j \in \mathbb{I}_{[0,N-1]}$ and $\Delta d_{\mathrm{e}}(N) = 0$.

Proof. Consider some $N \in \mathbb{I}_{\geq 1}$, $\bar{D}$, x_i^{i}, x_i^{t}, $i = 1, 2$ such that the optimal estimation problem (6.17) is feasible for both sets of parameters $(\bar{D}, x_i^{\mathrm{i}}, x_i^{\mathrm{t}})$, $i = 1, 2$. Consider the optimal solutions $\bar{z}_i^*(j) = \bar{\zeta}_N(j, \bar{D}, x_i^{\mathrm{i}}, x_i^{\mathrm{t}})$ along with the corresponding adjoints $\bar{\lambda}_i^*(j)$, $j \in \mathbb{I}_{[0,N]}$, $i = 1, 2$. Their differences in the states, adjoints, and disturbance inputs can be characterized by (6.28), which satisfy the Hamiltonian system (6.29) for all $j \in \mathbb{I}_{[0,N-1]}$.

Since the conditions of Proposition 6.1 are satisfied, we can alternatively use the parameterization provided by (6.34) to express the evolution of the differences in (6.28). Here, we note that because A_+ and A_-^{-1} are constant Schur stable matrices where the eigenvalues of A_+ coincide with the eigenvalues of A_-^{-1}, there exists a constant $C_A > 0$ such that

$$\max\left\{\left|\begin{bmatrix} I \\ P_+ \end{bmatrix}\right| \left|A_+^j\right|, \left|\begin{bmatrix} I \\ P_- \end{bmatrix}\right| \left|A_-^{-j}\right|\right\} \leq C_A \lambda^j \tag{6.39}$$

uniformly for all $j \in \mathbb{I}_{[0,N]}$, where $\lambda = \lambda_{\max}(A_+) \in (0, 1)$ (see, for example, [Per01, Thm. 2, p. 56], the proof of which can be straightforwardly adapted to the discrete-time setting considered here). In combination, we thus obtain

$$\left|\begin{bmatrix} \Delta x(j) \\ \Delta\lambda(j) \end{bmatrix}\right| \leq C_A \lambda^j |p| + C_A \lambda^{N-j} |q| \tag{6.40}$$

for $j \in \mathbb{I}_{[0,N]}$.

We now compute suitable p and q depending on the boundary conditions given by the initial and terminal constraints in (6.17b) and (6.17c) in terms of the parameters x_i^{i}, x_i^{t}, $i = 1, 2$—implying that $\Delta x(0) = x_1^{\mathrm{i}} - x_2^{\mathrm{i}}$ and $\Delta x(N) = x_1^{\mathrm{t}} - x_2^{\mathrm{t}}$. In particular, by evaluating (6.34) at $j = 0$ and $j = N$, we obtain the following system of linear equations:

$$\begin{bmatrix} \Delta x(0) \\ \Delta x(N) \end{bmatrix} = \begin{bmatrix} I & A_-^{-N} \\ A_+^N & I \end{bmatrix} \begin{bmatrix} p \\ q \end{bmatrix}.$$

This can be solved for p and q by simple matrix inversion. To this end, let $M := (I - A_+^N A_-^{-N})^{-1}$ (where we note that M is well-defined for any $N \in \mathbb{I}_{\geq 1}$), which leads to

$$\begin{aligned} p &= (I + A_-^{-N} M A_+^N)\Delta x(0) - A_-^{-N} M \Delta x(N), \\ q &= -M A_+^N \Delta x(0) + M \Delta x(N). \end{aligned}$$

Since A_+ and A_-^{-1} are Schur stable, there exists a constant $c > 0$ such that $|M| \leq c$ uniformly for all $N \in \mathbb{I}_{\geq 1}$. In combination with the property in (6.39), there exist constants $C_1, C_2 > 0$ such that

$$|p| \leq C_1 |\Delta x(0)| + C_2 \lambda^N |\Delta x(N)|, \tag{6.41a}$$
$$|q| \leq C_2 \lambda^N |\Delta x(0)| + C_1 |\Delta x(N)|. \tag{6.41b}$$

From (6.40) and (6.41), we hence obtain that

$$\begin{aligned} \left|\begin{bmatrix} \Delta x(j) \\ \Delta\lambda(j) \end{bmatrix}\right| &\leq C_A \left(\lambda^j C_1 + \lambda^{N-j} C_2 \lambda^N\right) |\Delta x(0)| + C_A \left(\lambda^j C_2 \lambda^N + \lambda^{N-j} C_1\right) |\Delta x(N)| \\ &\leq C_A (C_1 + C_2) \left(\lambda^j |\Delta x(0)| + \lambda^{N-j} |\Delta x(N)|\right) \end{aligned} \tag{6.42}$$

uniformly for all $j \in \mathbb{I}_{[0,N]}$. This establishes the desired bound on the state and adjoint differences. It remains to derive a similar bound on the disturbance difference. Using (6.28c), the optimality condition in (6.26c), and the dynamics of the adjoint difference according to (6.29) with (6.30), we have that

$$\begin{aligned} |\Delta d(j)| &\leq |Q^{-1}E^\top \Delta\lambda(j+1)| \\ &\leq |Q^{-1}E^\top A^{-\top}|(|\tilde{R}||\Delta x(j)| + |\Delta\lambda(j)|) \\ &\leq C_\mathrm{d}(|\Delta x(j)| + |\Delta\lambda(j)|) \end{aligned}$$

for $j \in \mathbb{I}_{[0,N-1]}$, where $C_\mathrm{d} := |Q^{-1}E^\top A^{-\top}| \max\{|\tilde{R}|, 1\}$. Define the extended disturbance sequence $\Delta d_\mathrm{e} := \{\Delta d_\mathrm{e}(j)\}_{j=0}^N$ satisfying $\Delta d_\mathrm{e}(j) = \Delta d(j)$, $j \in \mathbb{I}_{[0,N-1]}$ and $\Delta d_\mathrm{e}(N) = 0$. Hence, we obtain

$$\begin{aligned} |\Delta x(j)| + |\Delta d_\mathrm{e}(j)| + |\Delta\lambda(j)| &\leq (1 + C_\mathrm{d})(|\Delta x(j)| + |\Delta\lambda(j)|) \\ &\leq \sqrt{2}(1 + C_\mathrm{d}) \left| \begin{bmatrix} \Delta x(j) \\ \Delta\lambda(j) \end{bmatrix} \right| \end{aligned} \tag{6.43}$$

for all $j \in \mathbb{I}_{[0,N]}$. Using (6.42) in (6.43) and defining $C := \sqrt{2}(1 + C_\mathrm{d})C_A(C_1 + C_2)$ establishes the desired bound in (6.38) for any $N \in \mathbb{I}_{\geq 1}$. For the special case of $N = 0$, the bound in (6.38) trivially holds for the state and disturbance difference $\Delta x(0)$ and $\Delta d_\mathrm{e}(0)$, which implies that Assumption 6.2 holds and hence finishes this proof. □

6.2.5. Discussion

From the previous sections, one can see that there are in fact multiple ways to formalize the turnpike behavior observed in the motivating example in Section 6.2.1. Specifically, in Section 6.2.2 we used a dissipativity condition (Assumption 6.1) of the optimal estimation problem to derive a bound on the number of elements of the sequence $\hat{z}^*$ that lie outside an ϵ-neighborhood of the turnpike, compare [GM16; GPS18]. This definition is particularly suitable for use in the context of economic model predictive control (see, for example, [FGM18]), and also has the decisive advantage that the corresponding sufficient condition (strict dissipativity, see Assumption 6.1) is a global concept. Unfortunately, the resulting turnpike property (Theorem 6.1) is rather weak in the sense that it is not possible to infer *which* elements of the solution $\hat{z}^*$ are actually close to the turnpike z^∞, and which are not. However, this additional information is crucially required in the context of state estimation, as will be clear in Section 6.3.

In contrast, in Section 6.2.3 we used a decaying sensitivity property (Assumption 6.2) of the optimal estimation problem and derived an explicit bound on the difference between the solution $\hat{z}^*$ and the turnpike z^∞, see Theorem 6.2. To infer a global turnpike property, Assumption 6.2 is required to hold globally as well, that is, for any two optimal solutions of the NLP in (6.17) involving arbitrary (admissible) $x_i^\mathrm{i}, x_i^\mathrm{t} \in \mathcal{X}$, $i = 1, 2$. This is naturally satisfied for linear systems under controllability and observability, see Section 6.2.4. However, in the context of general

nonlinear systems, such a global condition is indeed (and unnecessarily) restrictive, and corresponding results are usually stated in a local sense, that is, for two optimal solutions that are sufficiently close to each other. In particular, it is shown in [SAZ22] that (local) exponentially decaying sensitivity is present under standard regularity and optimality conditions of the problem (such as a uniform second-order sufficient condition for optimality and uniform boundedness of the Hessian of the Lagrangian), which are satisfied under certain local observability and controllability assumptions, see [SZ21] and compare also [GSS20]. However, using a local version of Assumption 6.2 would require that the finite-horizon solution $\hat{x}^*$ is already close to the unknown infinite-horizon solution z^∞ in order to apply a local decaying sensitivity property and deduce turnpike behavior, and consequently allow for local results only.

In the context of nonlinear optimal control, global turnpike properties featuring an explicit (exponential or polynomial) time-dependent bound on the difference between optimal solutions and the turnpike are provided in, e.g., [Dam+14; TZ15; Tré23; HZ22]. The corresponding results are usually established by combining assumptions of global nature (such as strict dissipativity) with assumptions of local nature that involve the linearizations of the extremal equations at the turnpike (an optimal equilibrium), compare [Dam+14; Tré23]. For general nonlinear optimal state estimation problems, establishing a global turnpike property in the sense of (6.22), for example by combining global strict dissipativity (Assumption 6.1) with a local version of decaying sensitivity (Assumption 6.2), is an interesting topic for future work.

In the following, we employ a turnpike characterization that essentially reproduces the core property from Theorem 6.2 in a global sense, where we retain general $\mathcal{KL}$-functions to cover arbitrary decay rates.

Definition 6.1 (Turnpike for optimal state estimation)**.** *Consider the infinite-horizon solution z^∞ of the problem $P_\infty(D_\infty)$ in* (6.9) *for some data set D_∞ associated with the system* (6.1)*. The optimal estimation problem $P_N(D)$ using the truncated data set $D = \{D(j)\}_{j=0}^N$ with $D(j) = D_\infty(j)$, $j \in \mathbb{I}_{[0,N]}$ exhibits the turnpike property with respect to z^∞ if there exists $\beta \in \mathcal{KL}$ such that $\hat{z}^*(j) = \zeta_N(j, D)$ satisfies*

$$|\hat{z}^*(j) - z^\infty(j)| \leq \beta(|\hat{z}^*(0) - z^\infty(0)|, j) + \beta(|\hat{z}^*(N) - z^\infty(N)|, N - j) \tag{6.44}$$

for all $j \in \mathbb{I}_{[0,N]}$, $N \in \mathbb{I}_{\geq 0}$, and all possible data D_∞.

In the following section, we use the turnpike property from Definition 6.1 to assess the performance of MHE and its regret with respect to the benchmark z^∞. For practical applications, a reliable indicator for the presence of turnpike behavior in non-convex optimal state estimation problems is to simply run simulations and check whether the turnpike property can be observed, compare also the simulation examples in Section 6.4.

We want to close this section devoted to turnpike in optimal state estimation with the following remark.

Remark 6.6 (Approaching and leaving arcs)**.** *Note that the finite-horizon problem $P_N(D)$ considers a segment of the data set that underlies the infinite-horizon problem $P_\infty(D_\infty)$. Specifically, the neglected information involves the fictitious historical data $\{D_\infty(j)\}_{j=-\infty}^{-1}$ and the future data $\{D_\infty(j)\}_{j=N+1}^{\infty}$, which is why, under the turnpike property from Definition 6.1, finite-horizon solutions exhibit both a left approaching arc and a right leaving arc, see Figure 6.1.*

6.3. Performance analysis

In online state estimation, one is generally interested in obtaining, at each time instant $t \in \mathbb{I}_{\geq 0}$, an accurate estimate of the current true (unknown) state $x(t)$. A natural approach is to simply solve the optimal state estimation problem in (6.4) based on all available (in particular: causal) historical data $D = \{D(j)\}_{j=0}^{t}$ (by setting $N = t$ in (6.4)). This corresponds to the case of FIE, which can be formalized using the solution mapping ζ_N^x defined below (6.8) as follows:

$$\hat{x}^{\mathrm{fie}}(t) = \zeta_t^x\left(t, D\right),\ t \in \mathbb{I}_{\geq 0}. \tag{6.45}$$

However, repeatedly solving $P_t(D)$ for the current FIE solution $\hat{x}^{\mathrm{fie}}(t)$ is generally infeasible in practice since the problem size continuously grows with time. Instead, MHE considers the truncated optimal estimation problem $P_N(D_t)$ using only the most recent data

$$D_t = \{D_t(j)\}_{j=0}^{N} = \{D(j)\}_{j=t-N}^{t},\ t \in \mathbb{I}_{\geq N},$$

where the horizon length $N \in \mathbb{I}_{\geq 0}$ is fixed. More precisely, the MHE estimate at the current time $t \in \mathbb{I}_{\geq 0}$ can be written as

$$\hat{x}^{\mathrm{mhe}}(t) = \begin{cases} \zeta_N^x(N, D_t), & t \in \mathbb{I}_{\geq N} \\ \zeta_t^x(t, D), & t \in \mathbb{I}_{[0,N-1]}. \end{cases} \tag{6.46}$$

Such MHE schemes constitute well-established methods for state estimation, which are increasingly applied in practice, compare Chapter 3. However, assuming that the underlying optimal estimation problem exhibits the turnpike property in the sense of Definition 6.1, we know that both the FIE sequence defined by (6.45) and the MHE sequence defined by (6.46) consist of point estimates of finite-horizon problems that lie on the leaving arc, see Figure 6.2; hence, *MHE and FIE might produce estimates that are actually far away from the turnpike.*

In the following, we employ a novel performance analysis to improve the estimation results of MHE as follows:

- Reduce the influence of the leaving arc by introducing an artificial delay in the estimation (Sections 6.3.1 and 6.3.2).
- Reduce the influence of the approaching arc by using a turnpike-based prior weighting (Section 6.3.3).

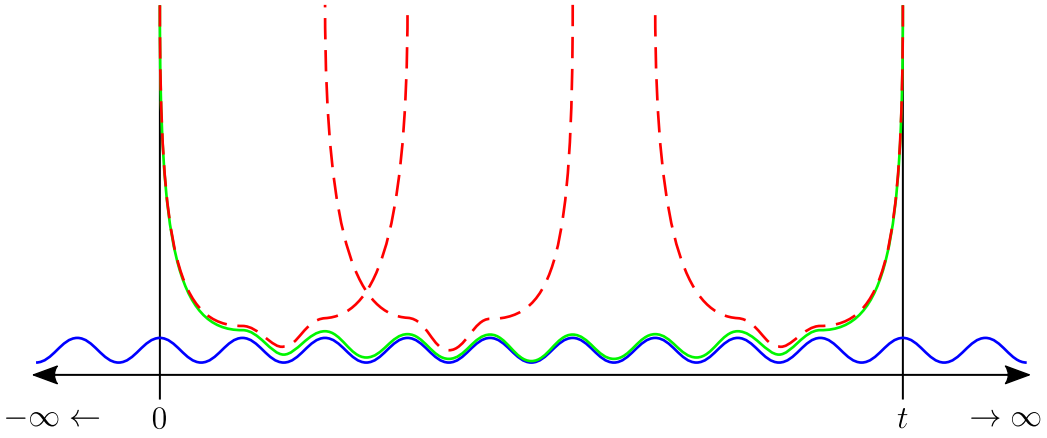

Figure 6.2. Sketch of the infinite-horizon solution x^∞ (blue), the current FIE solution $\zeta_t(t, D)$ (green), and finite-horizon solutions $\zeta_N(j, D_\tau)$, $j \in \mathbb{I}_{[\tau-N,\tau]}$ for different values of $\tau \in \mathbb{I}_{[N,t]}$ (red dashed).

Our results in this section are based on the assumption that the MHE problems exhibit the turnpike behavior from Definition 6.1.

Assumption 6.4 (Turnpike)**.** *The finite-horizon optimal state estimation problem P_N in* (6.4) *exhibits the turnpike property in the sense of Definition 6.1.*

In the following, for the sake of simplicity we restrict ourselves to horizons N being a non-negative even number, the set of which we denote by $\mathbb{I}^{\mathrm{e}}_{\geq 0}$.

6.3.1. A delay improves the estimation results

To avoid the influence of naturally appearing leaving arcs in finite-horizon estimation problems that underlie MHE as in (6.46), it seems meaningful to introduce a delayed MHE scheme (δMHE). Specifically, for a fixed delay $\delta \in \mathbb{I}_{[0,N/2]}$ with $N \in \mathbb{I}^{\mathrm{e}}_{\geq 0}$, we define

$$\hat{x}^{\delta\mathrm{mhe}}(t-\delta) = \begin{cases} \zeta_N^x\left(N-\delta, D_t\right), & t \in \mathbb{I}_{\geq N} \\ \zeta_t^x\left(t-\delta, D\right), & t \in \mathbb{I}_{[\delta,N-1]}. \end{cases} \tag{6.47}$$

Note that for the special case $\delta = 0$, δMHE reduces to standard MHE (6.46). Hence, the parameter δ is an additional degree of freedom that constitutes a trade-off between delaying the estimation results and reducing the influence of the leaving arc.

Remark 6.7 (δFIE)**.** *By replacing N with t and using only the second case in* (6.47)*, we can similarly define a delayed FIE scheme (δFIE). Consequently, all the following results and implications derived for δMHE directly carry over to δFIE. However, as MHE is of greater practical importance, we will limit ourselves to it in the remainder of this chapter.*

Remark 6.8 (Smoothing form of MHE)**.** *Considering a fixed delay in the estimation scheme to improve the estimation results is actually quite common in signal processing and filtering theory and refers to* fixed-lag smoothing algorithms *[CJ11, Ch. 5]. Early results for linear systems can be found in, e.g., [Moo73]; more recent works address, e.g., robustness against model errors [YZ23] or extensions to certain classes of nonlinear systems [RP15]. For linear systems with Gaussian noise, fixed-lag receding horizon smoothers are proposed in [SS13; Kim13; KK22]. In this context, the proposed δMHE scheme can also be interpreted as the (fixed-lag) smoothing form of MHE. Compared to the literature on smoothing algorithms, however, we consider general nonlinear systems under arbitrary process and measurement noise and provide performance and regret guarantees with respect to the infinite-horizon optimal solution using turnpike arguments.*

The following result shows that by a suitable choice of the delay δ, the estimated state sequence (6.47) can be made arbitrarily close to the state sequence of the omniscient infinite-horizon estimator z^∞.

Proposition 6.3. *Let Assumption 6.4 hold and $\mathcal{X}$ be compact. Then, there exists $\sigma \in \mathcal{L}$ such that the estimated state sequence of δMHE in* (6.47) *satisfies*

$$|\hat{x}^{\delta\mathrm{mhe}}(j) - x^\infty(j)| \leq \sigma(\delta),\ j \in \mathbb{I}_{[\delta,t-\delta]} \tag{6.48}$$

for all $t \in \mathbb{I}_{\geq\delta}$, $\delta \in [0, N/2]$, $N \in \mathbb{I}^{\mathrm{e}}_{\geq 0}$, and all possible data D_∞.

Proof. By compactness of $\mathcal{X}$, there exists $C > 0$ such that $|x_1 - x_2| \leq C$ for all $x_1, x_2 \in \mathcal{X}$. The rest of this proof directly follows from the definition of δMHE in (6.47) and Assumption 6.4. Specifically, for all $j \in \mathbb{I}_{[\delta,N-\delta-1]}$, we have that

$$\begin{aligned}
&|\hat{x}^{\delta\mathrm{mhe}}(j) - x^\infty(j)| \\
&\leq |\zeta_{j+\delta}(j, D) - z^\infty(j)| \\
&\leq \beta(|\zeta^x_{j+\delta}(0, D) - x^\infty(0)|, j) + \beta(|\zeta^x_{j+\delta}(j+\delta, D) - x^\infty(j+\delta)|, \delta) \\
&\leq \beta(C, j) + \beta(C, \delta) \\
&\leq 2\beta(C, \delta),
\end{aligned}$$

where $D(j) = D_\infty(j)$, $j \in \mathbb{I}_{[0,j+\delta]}$. For $j \in \mathbb{I}_{[N-\delta,t-\delta]}$, on the other hand, it follows that

$$\begin{aligned}
&|\hat{x}^{\delta\mathrm{mhe}}(j) - x^\infty(j)| \\
&\leq |\zeta_N(N-\delta, D_{j+\delta}) - z^\infty(j)| \\
&\leq \beta(|\zeta^x_N(0, D_{j+\delta}) - x^\infty(j+\delta-N), N-\delta) + \beta(|\zeta^x_N(N, D_{j+\delta}) - x^\infty(j+\delta)|, \delta) \\
&\leq \beta(C, N-\delta) + \beta(C, \delta) \\
&\leq 2\beta(C, \delta),
\end{aligned}$$

where $D_{j+\delta}(i) = D_\infty(i)$, $i \in \mathbb{I}_{[j+\delta-N,j+\delta]}$. Combining both cases for $j \in \mathbb{I}_{[\delta,t-\delta]}$ and defining $\sigma(s) := 2\beta(C, s)$, $s \geq 0$ yields (6.48), which finishes this proof. □

Proposition 6.3 provides an estimate on the accuracy of δMHE in the sense of how close the obtained sequence $\hat{x}^{\delta\mathrm{mhe}}$ is to the benchmark x^∞ on the interval $\mathbb{I}_{[\delta,t-\delta]}$. Since $\sigma \in \mathcal{L}$, this difference can be made arbitrarily small by increasing the delay δ (as well as N if needed). This is in line with intuition, as increasing δ results in the state estimates in (6.47) being closer to the turnpike.

In the following, we establish novel performance guarantees for δMHE and analyze the regret with respect to the infinite-horizon benchmark solution.

6.3.2. Performance estimates for MHE

In this section, we consider the case where the dynamics (6.1a) are subject to additive disturbances:

$$f(x,u,d) = f_\mathrm{a}(x,u) + d \tag{6.49}$$

with $d \in \mathcal{D} = \mathbb{R}^n$. Furthermore, we impose a Lipschitz condition on the nonlinear functions f_a and h on $\mathcal{X}$.

Assumption 6.5 (Lipschitz continuity)**.** *The functions f_a and h are Lipschitz in $x \in \mathcal{X}$ uniformly for all $u \in \mathcal{U}$, i.e., there exist constants $L_\mathrm{f}, L_\mathrm{h} > 0$ such that*

$$|f_\mathrm{a}(x_1,u) - f_\mathrm{a}(x_2,u)| \leq L_\mathrm{f}|x_1 - x_2|, \tag{6.50}$$
$$|h(x_1,u) - h(x_2,u)| \leq L_\mathrm{h}|x_1 - x_2| \tag{6.51}$$

for all $x_1, x_2 \in \mathcal{X}$ uniformly for all $u \in \mathcal{U}$.

Note that Assumption 6.5 is not restrictive in practice under compactness of $\mathcal{X}$ (as considered in Proposition 6.3).

The dynamics (6.49) ensure one-step controllability with respect to the disturbance input d; consequently, the estimates $\hat{x}^{\delta\mathrm{mhe}}(j)$, $j \in \mathbb{I}_{[\delta,t-\delta]}$ form a feasible state trajectory of system (6.1), driven by the disturbance input $\hat{d}^{\delta\mathrm{mhe}}(j) = \hat{x}^{\delta\mathrm{mhe}}(j+1) - f_\mathrm{a}(\hat{x}^{\delta\mathrm{mhe}}(j), u(j))$, $j \in \mathbb{I}_{[\delta,t-\delta-1]}$. For the sake of conciseness, we define the combined sequence $\hat{z}^{\delta\mathrm{mhe}}$ as

$$\hat{z}^{\delta\mathrm{mhe}}(j) := (\hat{x}^{\delta\mathrm{mhe}}(j), \hat{d}^{\delta\mathrm{mhe}}(j)),\ j \in \mathbb{I}_{[\delta,t-\delta-1]}, \quad \hat{z}^{\delta\mathrm{mhe}}(t-\delta) := (\hat{x}^{\delta\mathrm{mhe}}(t-\delta), 0). \tag{6.52}$$

We now specify the performance measure. To this end, we denote with $t_1, t_2 \in \mathbb{I}_{\geq 0}$ the time instants defining some interval of interest $\mathbb{I}_{[t_1,t_2]}$. For a given sequence $\hat{z}$ with $\hat{z}(j) = (\hat{x}(j), \hat{d}(j))$ satisfying the system dynamics $\hat{x}(j+1) = f(\hat{x}(j), u(j), \hat{d}(j))$ for $j \in \mathbb{I}_{[0,t_2]}$, we consider the performance criterion

$$J_{[t_1,t_2]}(\hat{z}) := \sum_{j=t_1}^{t_2-1} L(\hat{z}(j); d(j)) \tag{6.53}$$

with the stage cost L from (6.5). The following result provides a performance estimate for δMHE, and moreover, can be used to quantify the dynamic regret with respect to the omniscient infinite-horizon benchmark solution z^∞.

Theorem 6.3. *Consider the system dynamics* (6.49) *and the quadratic stage cost in* (6.6)*. Let Assumptions 6.4 and 6.5 be satisfied. Then, there exists* $\bar{\sigma} \in \mathcal{L}$ *such that for any choice of* $\epsilon > 0$*, the sequence* $\hat{z}^{\delta\mathrm{mhe}}$ *in* (6.52) *obtained using* δ*MHE for some arbitrary delay* $\delta \in \mathbb{I}_{[0,N/2]}$ *and horizon length* $N \in \mathbb{I}^{\mathrm{e}}_{\geq 0}$ *satisfies the following performance estimate:*

$$J_{[t_1,t_2]}(\hat{z}^{\delta\mathrm{mhe}}) \leq (1+\epsilon) J_{[t_1,t_2]}(z^\infty) + \frac{1+\epsilon}{\epsilon}((t_2-t_1)\bar{\sigma}(\delta)) \tag{6.54}$$

for all $t_1, t_2 \in \mathbb{I}_{[\delta, t-\delta]}$*, all* $t \in \mathbb{I}_{\geq \delta}$*, and all possible data* D_∞*.*

Before proving Theorem 6.3, we want to highlight some key properties of the performance estimate (6.54).

Remark 6.9 (Performance of δMHE)**.**

1. *The performance of* δ*MHE (the sequence* $\hat{z}^{\delta\mathrm{mhe}}$*) is approximately optimal on the interval* $\mathbb{I}_{[t_1,t_2]}$ *with respect to the infinite-horizon solution* z^∞*, with error terms that depend on the choices of* ϵ*,* δ*, and the interval length* $t_2 - t_1$*.*
2. *The performance estimate in* (6.54) *directly yields a bound on the dynamic regret (i.e., the performance loss) of* δ*MHE with respect to the omniscient infinite-horizon benchmark solution* z^∞*; in particular, it follows that*

   $$J_{[t_1,t_2]}(\hat{z}^{\delta\mathrm{mhe}}) - J_{[t_1,t_2]}(z^\infty) \leq \epsilon J_{[t_1,t_2]}(z^\infty) + \frac{1+\epsilon}{\epsilon}((t_2-t_1)\bar{\sigma}(\delta)),$$

   compare also Corollary 6.1 and the corresponding discussion below.
3. *In case of an exponential turnpike property (i.e., Assumption 6.4 holds with* $\beta(s,t) = Ks\lambda^t$ *in Definition 6.1 for some* $K > 0$ *and* $\lambda \in (0,1)$*), the* $\mathcal{L}$*-functions* σ *and* $\bar{\sigma}$ *in Proposition 6.3 and Theorem 6.3 also exhibit exponential decay. In this case, the performance of* δ*MHE converges* exponentially *to the performance of the infinite-horizon estimator as* δ *increases. This behavior is also evident in the numerical example in Section 6.4.*
4. *The performance estimate* (6.54) *grows linearly with the size of the performance interval (i.e., the difference* $t_\Delta = t_2 - t_1$*) and tends to infinity if* t_Δ *approaches infinity. This property is to be expected (due to the fact that the turnpike is never exactly reached) and conceptually similar to (non-averaged) performance results in economic model predictive control, see, for example, [FGM18, Sec. 5] and [Grü16]. To make meaningful performance estimates in case* $t_\Delta \to \infty$*, we analyze the averaged performance in Corollary 6.2 below.*
5. *Theorem 6.3 is stated for the practically relevant case of quadratic stage costs as in* (6.6) *for ease of presentation, but can easily be extended to more general cost functions that fulfill a weak triangle inequality.*

Proof of Theorem 6.3. Using the definitions from (6.5)–(6.7), the performance criterion evaluated for δMHE reads

$$J_{[t_1,t_2]}(\hat{z}^{\delta\mathrm{mhe}}) = \sum_{j=t_1}^{t_2-1} |\hat{d}^{\delta\mathrm{mhe}}(j)|_Q^2 + |y(j) - h(\hat{x}^{\delta\mathrm{mhe}}(j), u(j))|_R^2. \tag{6.55}$$

From the definition of $\hat{x}^{\delta\mathrm{mhe}}(j)$ in (6.47) and the fact that $f_\mathrm{a}(x^\infty(j),u(j))+d^\infty(j)-x^\infty(j+1)=0$ using (6.49), the square root of the input cost satisfies

$$\begin{aligned}
&|\hat{d}^{\delta\mathrm{mhe}}(j)|_Q \\
&= |\hat{x}^{\delta\mathrm{mhe}}(j+1)-x^\infty(j+1)+f_\mathrm{a}(x^\infty(j),u(j))-f_\mathrm{a}(\hat{x}^{\delta\mathrm{mhe}}(j),u(j))+d^\infty(j)|_Q \\
&\leq |\hat{x}^{\delta\mathrm{mhe}}(j+1)-x^\infty(j+1)|_Q+\lambda_{\max}(Q)L_\mathrm{f}|x^\infty(j)-\hat{x}^{\delta\mathrm{mhe}}(j)|+|d^\infty(j)|_Q \quad (6.56)
\end{aligned}$$

for all $j\in\mathbb{I}_{[t_1,t_2-1]}$, where in the last step we have used the triangle inequality and Assumption 6.5. Using Proposition 6.3 and the fact that $t_1,t_2\in\mathbb{I}_{[\delta,t-\delta]}$, it follows that

$$|\hat{x}^{\delta\mathrm{mhe}}(j)-x^\infty(j)|\leq|\hat{z}^{\delta\mathrm{mhe}}(j)-z^\infty(j)|\leq\sigma(\delta),\ j\in\mathbb{I}_{[t_1,t_2]}, \quad (6.57)$$

where $\sigma\in\mathcal{L}$. Hence, from (6.56) we obtain

$$|\hat{d}^{\delta\mathrm{mhe}}(j)|_Q\leq|d^\infty(j)|_Q+(1+L_\mathrm{f})\lambda_{\max}(Q)\sigma(\delta),\ j\in\mathbb{I}_{[t_1,t_2-1]}.$$

Squaring both sides and using the fact that for any $\epsilon>0$, it holds that $(a+b)^2\leq(1+\epsilon)a^2+\frac{1+\epsilon}{\epsilon}b^2$ for all $a,b\geq0$ then lets us conclude that

$$|\hat{d}^{\delta\mathrm{mhe}}(j)|_Q^2\leq(1+\epsilon)|d^\infty(j)|_Q^2+\frac{1+\epsilon}{\epsilon}(1+L_\mathrm{f})^2\lambda_{\max}(Q)^2\sigma(\delta)^2 \quad (6.58)$$

for each $j\in\mathbb{I}_{[t_1,t_2-1]}$. A similar reasoning for the fitting error (where we add $h(x^\infty(j),u(j))-h(x^\infty(j),u(j))=0$, $j\in\mathbb{I}_{[t_1,t_2-1]}$) yields

$$|y(j)-h(\hat{x}^{\delta\mathrm{mhe}}(j),u(j))|_R\leq|y(j)-h(x^\infty(j),u(j))|_R+L_\mathrm{h}\lambda_{\max}(R)\sigma(\delta)$$

for all $j\in\mathbb{I}_{[t_1,t_2-1]}$. By squaring both sides and using the same argument that allowed us to obtain (6.58), we get

$$\begin{aligned}
|y(j)-h(\hat{x}^{\delta\mathrm{mhe}}(j),u(j))|_R^2\leq{}&(1+\epsilon)|y(j)-h(x^\infty(j),u(j))|_R^2 \\
&+\frac{1+\epsilon}{\epsilon}L_\mathrm{h}^2\lambda_{\max}(R)^2\sigma(\delta)^2 \quad (6.59)
\end{aligned}$$

for all $j\in\mathbb{I}_{[t_1,t_2-1]}$. The performance criterion (6.55) together with (6.58), (6.59), and the definition of

$$\bar{\sigma}(s):=\left((1+L_\mathrm{f})^2\lambda_{\max}(Q)^2+L_\mathrm{h}^2\lambda_{\max}(R)^2\right)\sigma(s)^2,s\geq0$$

(where we note that $\bar{\sigma}\in\mathcal{L}$) establishes (6.54) and hence finishes this proof. □

To further derive a linear bound on the dynamic regret and an estimate of the asymptotic averaged performance of δMHE, we first show that $J_{[t_1,t_2]}(z_\infty)$ grows at maximum linearly in the difference t_2-t_1.

Lemma 6.2. *Let $\mathcal{D}$ and $\mathcal{V}$ be compact. There exists $A>0$ such that $J_{[t_1,t_2]}(z_\infty)\leq A(t_2-t_1)$ for any possible data D_∞.*

Proof. Due to $\mathcal{D}$ and $\mathcal{V}$ being compact, there exist constants $C_\mathrm{Q},C_\mathrm{R}>0$ such that $|\hat{d}|_Q^2\leq C_\mathrm{Q}$ and $|y-h(\hat{x},u)|_R^2\leq C_\mathrm{R}$ for all $(\hat{x},\hat{d},u,y)\in\mathcal{X}\times\mathcal{D}\times\mathcal{U}\times\mathbb{R}^p$ such that $y-h(\hat{x},u)\in\mathcal{V}$. Hence, the claim holds with $A=C_\mathrm{Q}+C_\mathrm{R}$. □

The following Corollary from Theorem 6.3 establishes bounded dynamic regret of δMHE with respect to the benchmark z^∞.

Corollary 6.1. *Let the conditions of Theorem 6.3 be satisfied. Assume that $\mathcal{D}$ and $\mathcal{V}$ are compact. Then, the regret of δMHE can be bounded by*

$$J_{[t_1,t_2]}(z^{\delta\mathrm{mhe}}) - J_{[t_1,t_2]}(z^\infty) \leq (t_2 - t_1)\left(\epsilon A + \frac{1+\epsilon}{\epsilon}\bar{\sigma}(\delta)\right) \tag{6.60}$$

for all $t_1, t_2 \in \mathbb{I}_{[\delta,t-\delta]}$, all $t \in \mathbb{I}_{\geq\delta}$, and all possible data D_∞, where $\epsilon > 0$ and $\bar{\sigma} \in \mathcal{L}$ are from Theorem 6.3 and $A > 0$ is from Lemma 6.2.

We emphasize that the regret bound provided by Corollary 6.1 is linear in the interval length $t_2 - t_1$, where the slope $C(\epsilon,\delta) := \left(\epsilon A + \frac{1+\epsilon}{\epsilon}\bar{\sigma}(\delta)\right)$ can be rendered arbitrarily small by suitable choices of ϵ and δ. Again, linear dependency on $(t_2 - t_1)$ is to be expected as the turnpike is never exactly reached, compare Remark 6.9.

The following result establishes an estimate on the averaged performance of δMHE for the asymptotic case when $(t_2 - t_1) \to \infty$.

Corollary 6.2. *Let the conditions of Theorem 6.3 be satisfied. Assume that $\mathcal{D}$ and $\mathcal{V}$ are compact. Then, δMHE satisfies the averaged performance estimate:*

$$\limsup_{t_\Delta\to\infty} \frac{1}{t_\Delta} J_{[t_1,t_2]}(z^{\delta\mathrm{mhe}}) \leq \limsup_{t_\Delta\to\infty} \frac{1}{t_\Delta} J_{[t_1,t_2]}(z^\infty) + \epsilon A + \frac{1+\epsilon}{\epsilon}\bar{\sigma}(\delta)$$

for all possible data D_∞, where $\epsilon > 0$ and $\bar{\sigma} \in \mathcal{L}$ are from Theorem 6.3, $A > 0$ is from Lemma 6.2, and $t_\Delta = t_2 - t_1$.

Corollary 6.2 implies that the averaged performance of δMHE is finite (due to the fact that $J_{[t_1,t_2]}(z^\infty)$ can be bounded as $J_{[t_1,t_2]}(z^\infty)/t_\Delta \leq A$ by Lemma 6.2) and approximately optimal with respect to the infinite-horizon solution z^∞, with error terms that can be made arbitrarily small by suitable choices of ϵ and δ.

As we show in the following, in the limit $\delta \to \infty$ we can even fully recover the benchmark performance. To this end, we need the following auxiliary lemma.

Lemma 6.3. *For any function $\theta \in \mathcal{L}$, there exists a continuous function $\delta : (0,\infty) \to (0,\infty)$, strictly decreasing, satisfying $\lim_{s\to 0}\delta(s) = \infty$ and $\lim_{s\to\infty}\delta(s) = 0$, and such that $\theta(\delta(s)) \leq s^2$ for all $s > 0$.*

Proof. We prove our claim by constructing a suitable function δ. To this end, note that for any $\theta \in \mathcal{L}$, there exists a continuous function $g : (0,\infty) \to (0,\infty)$ satisfying the following properties:

- $g(s)$ is strictly decreasing on $(0,\infty)$,
- $\lim\limits_{s\to 0} g(s) = \infty$ and $\lim\limits_{s\to\infty} g(s) = 0$,
- $g(s) \geq \theta(s)$ for all $s > 0$.

A possible choice is, for example, $g(s) = \theta(s) + \frac{1}{s}$. Since g is strictly decreasing, it is one-to-one; hence, there exists an inverse $g^{-1} : (0, \infty) \to (0, \infty)$. Now, define $\delta(s) = g^{-1}(s^2)$, $s > 0$. It is easy to see that δ is strictly decreasing and satisfies $\lim_{s \to 0} \delta(s) = \infty$, and $\lim_{s \to \infty} \delta(s) = 0$ (as g^{-1} does). Moreover, this particular choice of δ implies

$$\theta(\delta(s)) \leq g(\delta(s)) \leq g(g^{-1}(s^2)) = s^2$$

for all $s > 0$, which yields the desired result and hence finishes this proof. □

This enables the following corollary of Theorem 6.3.

Corollary 6.3. *Let the conditions of Theorem 6.3 be satisfied. Assume that $\mathcal{D}$ and $\mathcal{V}$ are compact. Furthermore, let the delay δ be parameterized in $\epsilon > 0$ with δ having the properties from Lemma 6.3 for $\theta = \bar{\sigma}$, where $\bar{\sigma} \in \mathcal{L}$ is from Theorem 6.3. Then, letting $\epsilon \to 0$, the averaged regret of δMHE satisfies*

$$\limsup_{\substack{t_\Delta \to \infty \\ \epsilon \to 0}} \frac{1}{t_\Delta} \left(J_{[t_1,t_2]}(z^{\delta\mathrm{mhe}}) - J_{[t_1,t_2]}(z^{\infty}) \right) = 0,$$

for all possible data D_∞, where $t_\Delta = t_2 - t_1$.

Proof. Consider the regret bound in (6.60), which applies due to the fact that the assumptions of Corollary 6.3 are satisfied. As $\bar{\sigma} \in \mathcal{L}$, we can choose δ according to Lemma 6.3 such that $\bar{\sigma}(\delta(\epsilon)) \leq \epsilon^2$. Consequently, from (6.60) we obtain

$$\limsup_{t_\Delta \to \infty} \frac{1}{t_\Delta} \left(J_{[t_1,t_2]}(z^{\delta\mathrm{mhe}}) - J_{[t_1,t_2]}(z^{\infty}) \right) \leq \epsilon A + \frac{1+\epsilon}{\epsilon} \epsilon^2 = \epsilon^2 + (1 + A)\epsilon. \tag{6.61}$$

Letting $\epsilon \to 0$ establishes the desired statement and hence finishes this proof. □

The construction of the function $\delta(\epsilon)$ employed in Corollary 6.3 establishes a direct relation between the upper bound on the averaged regret of δMHE and the delay δ; in particular, for the averaged regret approaching zero, we require that $\delta \to \infty$, while for a larger bound smaller values of δ suffice, see (6.61) and recall that $\delta(\epsilon)$ is strictly decreasing in its argument.

Overall, Proposition 6.3, Theorem 6.3, and Corollaries 6.1–6.3 imply that δMHE is able to track the solution and the performance of the omniscient infinite-horizon benchmark estimator. Generally, larger values of δ reduce the influence of the leaving arc and thus improve the performance estimates. Here, the best performance is achieved for $\delta = N/2$, which, on the other hand, introduces a potentially large delay (depending on the choice of N). However, in the practically relevant case of exponential turnpike behavior, already small values of δ are expected to significantly reduce the influence of the leaving arc and hence improve the estimation results compared to standard MHE (without delay), which is also evident in the simulation examples in Section 6.4.2.

We conclude this section by noting that while it is possible in MPC to design suitable terminal ingredients that yield finite non-averaged performance for $t \to \infty$ (see, for

example, [GP15]), this does not seem to be possible here, as it would imply that we have certain information about future data in order to exactly reach and stay on the solution of the acausal infinite-horizon optimal estimation problem.

6.3.3. MHE with prior weighting

It is known that MHE schemes with a cost function as in (6.5) might require relatively large estimation horizons to achieve satisfactory estimation results, compare [RMD20, Sec. 4.3.2]. In order to reduce the required horizon length and enable faster computations, MHE formulations that leverage an additional prior weighting are therefore usually preferred in practice, compare also Chapters 3–5. The prior weighting can generally be seen as additional regularization of the cost function, ensuring that the initial state $\hat{x}(0)$ of an estimated sequence $\hat{x} = \{\hat{x}(j)\}_{j=0}^{N}$ solving the problem (6.4) stays in a meaningful region. In view of our turnpike results, a well-chosen prior weighting hence reduces the influence of the approaching arc and ensures that solutions of truncated finite-horizon problems can reach the turnpike in fewer steps.

The prior weighting is usually parameterized by a given prior estimate $\bar{x} \in \mathcal{X}$ and a (possibly time-varying) function $\Gamma_t(x, \bar{x})$ that is positive definite and uniformly bounded in the difference $|x - \bar{x}|$. As in previous chapters, we use the definition $N_t := \min\{t, N\}$, which is convenient as it avoids additional case distinctions. At a given time $t \in \mathbb{I}_{\geq 0}$, the (time-varying) MHE cost function with prior weighting can then be formulated as

$$J_{N_t}^{\mathrm{p}}(\hat{x}_t, \hat{d}_t; D_t, t) := \Gamma_{t-N_t}(\hat{x}_t(0), \bar{x}(t - N_t)) + J_{N_t}(\hat{x}_t, \hat{d}_t; D_t), \tag{6.62}$$

with the current decision variables $\hat{x}_t = \{\hat{x}_t(j)\}_{j=0}^{N_t}$ and $\hat{d}_t = \{\hat{d}_t(j)\}_{j=0}^{N_t-1}$, the current data sequence $D_t = \{D_t(j)\}_{j=0}^{N_t} = \{D(j)\}_{j=t-N_t}^{t}$, and where J_{N_t} is from (6.5) with N replaced by N_t. At any time $t \in \mathbb{I}_{\geq 0}$, the current MHE problem to solve is given by the optimal estimation problem (6.4) with N replaced by N_t and the cost function $J_{N_t}^{\mathrm{p}}$ from (6.62), which we denote by $P_{N_t}^{\mathrm{p}}(D_t, \bar{x}_{t-N_t}, t)$. The corresponding solution (which exists under mild conditions, see Remark 6.2 and compare also Section 3.1) is described by the sequence $\tilde{z}^* = \{\tilde{z}^*(j)\}_{j=0}^{N}$, where $\tilde{z}^*(j) = (\tilde{x}^*(j), \tilde{d}^*(j))$, $j \in \mathbb{I}_{[0,N_t-1]}$ and $\tilde{z}^*(N_t) = (\tilde{x}^*(t), 0)$. The prior estimate $\bar{x}(t - N_t)$ is typically chosen in terms of a past solution of the problem $P_{N_t}^{\mathrm{p}}$, which introduces a coupling between the MHE problems. For easier reference, it is therefore convenient to introduce an additional index, where, e.g., $\tilde{z}_t^*(j)$, $j \in \mathbb{I}_{[0,N_t]}$ refers to the element $\tilde{z}^*(j)$ of the solution of $P_{N_t}^{\mathrm{p}}(\cdot, t)$ computed at time $t \in \mathbb{I}_{\geq 0}$, compare, e.g., Section 3.1.

We first consider the standard MHE case and set the current state estimate $\hat{x}^{\mathrm{mhe,p}}(t)$ to the last state of the optimal estimated sequence $\tilde{z}_t^*(N_t)$, i.e., $\hat{x}^{\mathrm{mhe,p}}(t) := \tilde{x}_t^*(N_t)$ for all $t \in \mathbb{I}_{\geq 0}$. In Remark 6.11 below, we again consider an additional delay in the MHE scheme to reduce the influence of the naturally appearing leaving arc.

A popular choice for the prior weighting is the quadratic cost

$$\Gamma_t(x, \bar{x}) = |x - \bar{x}|_{W(t)}^2, \tag{6.63}$$

where $W(t)$ is a constant or time-varying positive definite weighting matrix that might be updated using, for example, covariance update laws from nonlinear Kalman filtering, compare [RRM03; QH09; BZD20; Küh+11]. Given some initial guess $\hat{\chi} \in \mathcal{X}$ of the true initial condition χ, there are two common choices for updating the prior estimate $\bar{x}(t - N_t)$: first, the *filtering prior*

$$\bar{x}(t - N_t) = \begin{cases} \tilde{x}^*_{t-N}(N), & t \in \mathbb{I}_{\geq N} \\ \hat{\chi}, & t \in \mathbb{I}_{[0,N-1]}, \end{cases} \tag{6.64}$$

which corresponds to the state estimate computed N steps in the past, i.e., the last element of the solution to the problem $P^{\mathrm{p}}_N(\cdot, t - N)$; second, the *smoothing prior*

$$\bar{x}(t - N_t) = \begin{cases} \tilde{x}^*_{t-1}(1), & t \in \mathbb{I}_{\geq 1} \\ \hat{\chi}, & t = 0, \end{cases} \tag{6.65}$$

which refers to the second element of the solution to $P^{\mathrm{p}}_{N_t}(\cdot, t - 1)$ computed at the previous time step $t - 1$, compare [RMD20, Sec. 4.3.2]. MHE with a smoothing prior can generally recover faster from poor initial estimates, whereas MHE with a filtering prior essentially comprises measurements from two time horizons and may therefore be advantageous in the long term. Notice that we mainly analyze MHE with the filtering prior in this thesis, as this allows us to derive a contraction of the estimation error over the horizon (and thus establish robust stability of MHE, see for example Chapter 3), which is also in line with the most recent literature in this context, compare, e.g., [Mül17; AR21; KM23; Sch+23; Hu24; Ale25]. In contrast, the smoothing prior is used, for example, in [ABB08; AG17], and often serves in practice-oriented works as a linearization point for computing an improved prior estimate based on EKF updates, compare, e.g., [Küh+11; BZD20] and see also the review article [Els+21] for a more detailed discussion on this topic.

However, from our turnpike analysis in Section 6.2, we know that both of these two choices may in fact be unsuitable if we are interested in approximating the infinite-horizon optimal performance; the smoothing prior corresponds to an element of a finite-horizon solution on the approaching arc, and the filtering prior to an element of the solution on the leaving arc. To counteract this, we propose the following *turnpike prior*:

$$\bar{x}(t - N_t) = \begin{cases} \tilde{x}^*_{t-N/2}(N/2), & t \in \mathbb{I}_{\geq N/2} \\ \hat{\chi}, & t \in \mathbb{I}_{[0,N/2-1]}, \end{cases} \tag{6.66}$$

which corresponds to the middle element of the solution of $P_N(\cdot, t - N/2)$ computed at time $t - N/2$. This particular choice avoids the influence of the approaching and leaving arcs (for $t \in \mathbb{I}_{\geq N}$). In fact, we can even show that the prior estimate $\bar{x}(t - N_t)$ converges to a neighborhood of the turnpike x^∞ under the following modified (exponential) turnpike property of the MHE problem $P^{\mathrm{p}}_{N_t}$.

Assumption 6.6 (Exponential turnpike for MHE with prior weighting)**.** *There exist constants $K > 0$ and $\lambda \in (0, 1)$ such that for all $N \in \mathbb{I}_{\geq 0}$, the solutions of the*

finite-horizon problem $P_N^{\mathrm{p}}(D_t, \bar{x}, t)$ *and the infinite-horizon problem* $P_\infty(D_\infty)$ *satisfy*

$$|\tilde{z}_t^*(j) - z^\infty(t-N+j)| \leq K\left(|\tilde{x}_t^*(0) - x^\infty(t-N)|\lambda^j + |\tilde{x}_t^*(N) - x^\infty(t)|\lambda^{N-j}\right) \tag{6.67}$$

for all $j \in \mathbb{I}_{[0,N]}$, $t \in \mathbb{I}_{\geq N}$, $\bar{x} \in \mathcal{X}$, *and all possible data* D_∞, *where* $D_t = \{D_t(j)\}_{j=0}^N = \{D_\infty(j)\}_{j=t-N}^t$.

Assumption 6.6 essentially states that the infinite-horizon solution z^∞ serves as turnpike for MHE problems with prior weighting, compare the discussion in Section 6.2.5. Note that such behavior could be observed in all our numerical examples in Section 6.4.2.

Remark 6.10 (Exponential turnpike)**.** *In contrast to Definition 6.1, we impose an exponential turnpike property in Assumption 6.6, which is crucially required to derive uniform (exponential) convergence of the turnpike prior* $\bar{x}(t-N_t)$ *to the turnpike* x^∞ *in the following proposition. Note that this is conceptually similar to recent stability results for nonlinear MHE, which also require exponential detectability (rather than asymptotic detectability) to establish a linear contraction of the estimation error over the estimation horizon (and thus derive exponential stability), see Chapter 3 for more details and compare also [AR19b; AR21; Sch+23; Hu24].*

Proposition 6.4. *Let Assumption 6.6 hold and the sets* $\mathcal{X}$, $\mathcal{D}$, *and* $\mathcal{V}$ *be compact. Suppose there exist constants* $c_1, c_2 > 0$ *and* $a \geq 1$ *such that*

$$c_1|x - \bar{x}|^a \leq \Gamma_t(x, \bar{x}) \leq c_2|x - \bar{x}|^a \tag{6.68}$$

for all $x, \bar{x} \in \mathcal{X}$ *uniformly for all* $t \in \mathbb{I}_{\geq 0}$. *Furthermore, assume that there exist* $\alpha_1, \alpha_2, \alpha_3 \in \mathcal{K}_\infty$ *such that*

$$L(\hat{x}, \hat{d}; (u, y)) \leq \alpha_1(|\hat{d}|) + \alpha_2(|y - h(\hat{x}, u)|), \tag{6.69}$$

$$L_{\mathrm{tc}}(\hat{x}; (u, y)) \leq \alpha_3(|y - h(\hat{x}, u)|) \tag{6.70}$$

for all $\hat{x} \in \mathcal{X}$, $\hat{d} \in \mathcal{D}$, $(u, y) \in \mathcal{U} \times \mathbb{R}^p$ *satisfying* $y - h(\hat{x}, u) \in \mathcal{V}$. *Then, there exists* $\sigma \in \mathcal{L}$ *such that for any* $\rho \in (0, 1)$, *there exists* $\bar{N} \in \mathbb{I}_{\geq 0}^{\mathrm{e}}$ *such that the turnpike prior* (6.66) *satisfies*

$$|\bar{x}(t - N/2) - x^\infty(t - N/2)| \leq \rho|\bar{x}(t-N) - x^\infty(t-N)| + \sigma(N) \tag{6.71}$$

for all $N \in \mathbb{I}_{\geq \bar{N}}^{\mathrm{e}}$ *and* $t \in \mathbb{I}_{\geq N}$.

Proof. Consider any $t \in \mathbb{I}_{\geq N}$, the data sequence D_∞ associated with the system (6.1), and an arbitrary prior $\bar{x}(t-N) \in \mathcal{X}$. Let $\tilde{z}_t^* = \{\tilde{z}_t^*(j)\}_{j=0}^N$ denote the solution of the problem $P_N^{\mathrm{p}}(D_t, \bar{x}(t-N), t)$ computed at time t, where $D_t(j) = D_\infty(j)$, $j \in \mathbb{I}_{[t-N,t]}$. Furthermore, let $\tilde{x}_t^* = \{\tilde{x}_t(j)\}_{j=0}^N$ and $\tilde{d}_t^* = \{\tilde{d}_t^*(j)\}_{j=0}^{N-1}$ denote the optimal state and disturbance sequences contained in $\tilde{z}_t^*$, and consider the solution z^∞ of the infinite-horizon problem $P_\infty(D_\infty)$. From Assumption 6.6, we obtain

$$|\tilde{z}_t^*(j) - z^\infty(t-N+j)| \leq K|\tilde{x}_t^*(0) - x^\infty(t-N)|\lambda^j + KC\lambda^{N-j} \tag{6.72}$$

for all $j \in \mathbb{I}_{[0,N]}$, where $C > 0$ satisfies $|x_1 - x_2| \leq C$ for all $x_1, x_2 \in \mathcal{X}$ (compactness of $\mathcal{X}$ ensures existence of such C). By the triangle inequality, it follows that

$$|\tilde{x}_t^*(0) - x^\infty(t-N)| \leq |\tilde{x}_t^*(0) - \bar{x}(t-N)| + |\bar{x}(t-N) - x^\infty(t-N)|. \tag{6.73}$$

Using (6.68), the cost function (6.62), and optimality of $\tilde{z}^*$, it holds that

$$\begin{aligned}
&c_1|\tilde{x}_t^*(0) - \bar{x}(t-N)|^a \\
&\leq J_N^{\mathrm{p}}(\tilde{x}_t^*, \tilde{d}_t^*; D_t, t) \\
&\leq J_N^{\mathrm{p}}\left(\{x^\infty(j)\}_{j=t-N}^{t}, \{d^\infty(j)\}_{j=t-N}^{t-1}; D_t, t\right) \\
&\leq c_2|x^\infty(t-N) - \bar{x}(t-N)|^a + J_N\left(\{x^\infty(j)\}_{j=t-N}^{t}, \{d^\infty(j)\}_{j=t-N}^{t-1}; D_t, t\right).
\end{aligned} \tag{6.74}$$

The bounds in (6.69) and (6.70), compactness of $\mathcal{D}$ and $\mathcal{V}$, and similar arguments as in the proof of Lemma 6.2 imply the existence of uniform constants $A, B > 0$ such that $J_N\left(\{x^\infty(j)\}_{j=t-N}^{t}, \{d^\infty(j)\}_{j=t-N}^{t-1}; D_t, t\right) \leq AN + B$. In combination with (6.73) and (6.74), this leads to

$$\begin{aligned}
&|\tilde{x}_t^*(0) - x^\infty(t-N)| \\
&\leq |x^\infty(t-N) - \bar{x}(t-N)| + \left(\frac{c_2}{c_1}|x^\infty(t-N) - \bar{x}(t-N)|^a + \frac{AN+B}{c_1}\right)^{1/a} \\
&\leq \left(1 + \left(\frac{c_2}{c_1}\right)^{1/a}\right)|x^\infty(t-N) - \bar{x}(t-N)| + \left(\frac{AN+B}{c_1}\right)^{1/a},
\end{aligned}$$

where in the last inequality we have used that the function $r \mapsto r^{1/a}$ is subadditive for $r \geq 0$ and $a \geq 1$. Evaluating (6.72) at $j = N/2$, we can infer that

$$\begin{aligned}
|\tilde{z}_t^*(N/2) - z^\infty(t-N/2)| \leq{}& K\left(1 + \left(\frac{c_2}{c_1}\right)^{1/a}\right)|x_{t-N}^\infty - \bar{x}_{t-N}|\lambda^{N/2} \\
&+ K\left(\frac{AN+B}{c_1}\right)^{1/a}\lambda^{N/2} + KC\lambda^{N/2}.
\end{aligned} \tag{6.75}$$

For any $\rho \in (0,1)$, there exists $\bar{N} \in \mathbb{I}_{\geq 0}^{\mathrm{e}}$ such that $K(1 + (c_2/c_1)^{1/a})\lambda^{N/2} \leq \rho$ for all $N \in \mathbb{I}_{\geq \bar{N}}$. Define $\sigma_1(s) := K((As+B)/c_1)^{1/a}\lambda^{s/2}$, $s \geq 0$. Obviously, σ_1 is continuous; moreover, $\sigma_1(s)$ converges to zero for $s \to \infty$, since the exponential term dominates for large enough s. Hence, there exists a function $\bar{\sigma}_1 \in \mathcal{L}$ satisfying $\sigma_1(s) \leq \bar{\sigma}_1(s)$ for all $s \geq 0$. Thus, from (6.75), we can infer that the updated turnpike prior $\bar{x}(t - N/2) = \tilde{x}_t^*(N/2)$ satisfies

$$\begin{aligned}
|\bar{x}(t-N/2) - x^\infty(t-N/2)| &\leq |\tilde{z}_t^*(N/2) - z^\infty(t-N/2)| \\
&\leq \rho|\bar{x}(t-N) - x^\infty(t-N)| + \bar{\sigma}_1(N) + KC\lambda^{N/2}
\end{aligned}$$

for all $t \in \mathbb{I}_{\geq N}$ and $N \in \mathbb{I}_{\geq \bar{N}}^{\mathrm{e}}$. Defining $\sigma(s) = \bar{\sigma}_1(s) + KC\lambda^{s/2}$ for $s \geq 0$ and noting that $\sigma \in \mathcal{L}$ establishes the statement of this proposition and hence concludes this proof. □

The conditions in (6.68)–(6.70) on the prior weighting, stage cost, and terminal cost are standard (compare, e.g., [RMD20, Ass. 4.22]) and obviously satisfied for the practically relevant case of quadratic penalties as in (6.6), (6.7), and (6.63). Provided that the horizon length N is chosen sufficiently large, Proposition 6.4 implies (by a recursive application of the property in (6.71)) that the turnpike prior $\bar{x}(t-N_t)$ defined in (6.66) forms a sequence that exponentially converges to a neighborhood of the turnpike (i.e., the infinite-horizon solution x^∞), which is also evident in the simulation example in Section 6.4.2. Here, we want to emphasize that the size of this neighborhood depends on the horizon length N and can in fact be made arbitrarily small by choosing larger values of N (due to the fact that $\sigma \in \mathcal{L}$).

Overall, a properly selected prior weighting Γ_t according to Proposition 6.4 ensures that the initial state $\tilde{x}_t^*(0)$ of the solution of the MHE problem $P_{N_t}^{\mathrm{p}}(\cdot,t)$ is close to the turnpike, which hence effectively reduces the approaching arc and allows using short horizons. However, the natural occurrence of the leaving arc can still cause the resulting estimate $\hat{x}^{\mathrm{mhe,p}}(t) = \tilde{x}_t^*(N)$ to be again relatively far away from the turnpike, which could again be reduced by introducing an artificial delay in the MHE scheme as suggested in Section 6.3.1.

Remark 6.11 (Performance of δMHE with prior weighting)**.** *For some fixed delay $\delta \in \mathbb{I}_{[0,N/2]}$, we can define δMHE (with prior weighting) as*

$$\hat{x}^{\delta\mathrm{mhe,p}}(t-\delta) = \tilde{x}_t^*(N_t-\delta),\ t \in \mathbb{I}_{\geq\delta}. \tag{6.76}$$

Under Assumption 6.6, it is straightforward to show that $|\hat{x}^{\delta\mathrm{mhe,p}}(j) - x^\infty(j)| \leq \sigma(\delta)$ for all $j \in \mathbb{I}_{[\delta,t-\delta]}$, $t \in \mathbb{I}_{\geq\delta}$, with $\sigma \in \mathcal{L}$ from Proposition 6.3 (which can be easily modified to this case). As a result, the performance estimates from Theorem 6.3 along with the Corollaries 6.1–6.3 directly carry over to δMHE with prior weighting. Consequently, δMHE with prior weighting and a suitably selected delay δ can recover the accuracy and performance of the infinite-horizon estimator, with shorter horizons compared to δMHE without prior weighting. Here, we want to emphasize that this conclusion holds under Assumption 6.6, i.e., for any choice of the prior estimate $\bar{x}(t-N_t)$ from (6.64)–(6.66) *(in contrast to Proposition 6.4, which is an exclusive feature of the proposed turnpike prior* (6.66)*). Our simulation results in Section 6.4.2 show that already (very) small values of δ significantly improve the estimation accuracy.*

6.3.4. Offline state estimation

We now want to briefly discuss the case of offline state estimation, which can be interpreted as a special case of our previous setup. Here, one is interested in matching an *a priori* given data sequence $D = \{D(j)\}_{j=0}^T$ for some $T \in \mathbb{I}_{\geq 0}$ to the system equations (6.1) to obtain an estimate of the true unknown state sequence $\{x(j)\}_{j=0}^T$. To this end, a natural approach is to simply solve the optimal state estimation problem in (6.4) with $N = T$. However, if the data set (in particular, the value of T) or the underlying model is very large or the computations are limited in terms of

time or resources, solving the full problem $P_T(D)$ for the optimal solution is usually difficult (or even impossible) in practice.

Instead, we can construct an approximation of the optimal state sequence corresponding to the solution of the full problem $P_T(D)$ using a sequence of smaller problems P_N of length $N \in \mathbb{I}^{\mathrm{e}}_{\geq 0}$ and our results from Section 6.3. Specifically, we define the *approximate estimator*

$$\hat{x}^{\mathrm{ae}}(j) = \begin{cases} \zeta^x_N(j, D_N), & j \in \mathbb{I}_{[0,N/2]} \\ \zeta^x_N(N/2, D_{j+N/2}), & j \in \mathbb{I}_{[N/2+1,T-N/2-1]} \\ \zeta^x_N(N-T+j, D_T), & j \in \mathbb{I}_{[T-N/2,T]}, \end{cases} \tag{6.77}$$

where ζ^x_N is defined below (6.8) and $D_i = \{D_i(j)\}_{j=0}^N = \{D(j)\}_{j=i-N}^i$ for $i \in \mathbb{I}_{[N,T]}$ are subsets (or partitions) of the full data set D.

Note that for $j \in \mathbb{I}_{[N/2+1,T-N/2-1]}$, the approximate estimator in (6.77) corresponds to the δMHE scheme in (6.47) with $\delta = N/2$. Hence, the accuracy and performance estimates established in Section 6.3 (i.e, Proposition 6.3, Theorem 6.3, and Corollary 6.1) directly apply with respect to the benchmark z^∞ (where the underlying data set D_∞ is a suitable extension of D to the interval $\mathbb{I}$ such that the system dynamics (6.1) and (6.2) are satisfied for all $t \in \mathbb{I}$). Therefore, under Assumption 6.4, the estimates $\hat{x}^{\mathrm{ae}}(j)$ are close to the turnpike $z^\infty(j)$ for all $j \in \mathbb{I}_{[N/2,T-N/2]}$. Notice, however, that the turnpike property imposed in Assumption 6.4 also applies to the full problem $P_T(D)$, which implies that the corresponding solution is also close to z^∞ on the interval $\mathbb{I}_{[N/2,T-N/2]}$, compare Figure 6.2. Hence, Assumption 6.4 ensures that the estimated sequence in (6.77) is approximately optimal on $\mathbb{I}_{[N/2,T-N/2]}$ with respect to the (unknown) desired solution of the full problem $P_T(D)$, compare Remark 6.9.

Moreover, since the individual finite-horizon estimation problems in (6.77) are completely decoupled from each other, computing the approximate estimator (6.77) can be parallelized and hence has the potential to significantly save time and resources. In other words, the construction in (6.77) can be considered as a distributed computation of the optimal solution $P_T(D)$ with negligible error (provided that N is large enough), which can also be seen in the simulation example in Section 6.4.1. This is practically relevant for, e.g., large data assimilation problems that appear in geophysics and environmental sciences [ABN16; Car+18], but also more general in the context of robust optimization for data-driven decision making, compare, e.g., [Moh+18; MK17].

Remark 6.12 (Reduced computations)**.** *We can easily generalize our results by constructing the approximate estimator $\hat{x}^{\mathrm{ae}}$ by concatenating subsequences of the solutions of the truncated problems. Specifically, from each solution $\zeta_N(j, D_i)$, instead of using only the single element at $j = N/2$ as in* (6.77)*, we take all the elements corresponding to $j \in \mathbb{I}_{[N/2-\Delta,N/2+\Delta]}$ for some $\Delta \in \mathbb{I}_{[0,N/2]}$. This construction allows for qualitatively similar performance results as in Theorem 6.3 and Corollary 6.1, albeit with slightly worse bounds depending on the length of the subsequences (i.e., Δ). However, this approach can greatly reduce the number of*

problems to be solved. In particular, assuming that there exists $k \in \mathbb{I}_{\geq 0}$ such that T, N, Δ satisfy $T = N + (k+1)(2\Delta+1)$, our modified construction requires solving $K_\Delta := k + 2 = \frac{T-N}{2\Delta+1} + 1$ truncated problems. For the special case of $\Delta = 0$ (i.e., the approximate estimator (6.77)*), it follows that $K_\Delta = T - N + 1$, which is quite large if T is large. However, increasing the value of Δ significantly reduces the value of K_Δ (as K_Δ is proportional to $1/\Delta$). In fact, our simulation example in Section 6.4.1 shows that it is sufficient to select Δ relatively close to $N/2$ such that only the first (resp. last) few elements on the approaching (resp. leaving) arc of the truncated solutions are discarded, which significantly reduces the number of problems to solve.*

6.3.5. Good performance implies accurate state estimates

So far, we have investigated how close the solutions of finite-horizon state estimation problems are to the infinite-horizon solution. In practice, however, one is usually interested in the accuracy of the estimation results with respect to the real (unknown) system trajectory. In this section, we draw a direct link between the performance of a state estimator (measured by the criterion in (6.53)) and its accuracy (in terms of the estimation error). To this end, a detectability condition is required to ensure that the collected measurement data contains sufficient information about the real unknown state trajectory, where we again consider the notion of i-IOSS.

Assumption 6.7 (Exponential i-IOSS)**.** *The system* (6.1) *is exponentially i-IOSS, i.e., there exists a continuous function $U : \mathcal{X} \times \mathcal{X} \to \mathbb{R}_{\geq 0}$ together with matrices $\underline{P}, \overline{P}, Q, R \succ 0$ and a constant $\eta \in (0,1)$ such that*

$$|x_1 - x_2|_{\underline{P}}^2 \leq U(x_1, x_2) \leq |x_1 - x_2|_{\overline{P}}^2, \tag{6.78a}$$

$$\begin{aligned} &U(f(x_1, u, d_2), f(x_2, u, d_2)) \\ &\leq \eta U(x_1, x_2) + |d_1 - d_2|_Q^2 + |h(x_1, u) - h(x_2, u)|_R^2 \end{aligned} \tag{6.78b}$$

for all $(x_1, u, d_1), (x_2, u, d_2) \in \mathcal{X} \times \mathcal{U} \times \mathcal{D}$.

Assumption (6.7) is a Lyapunov function characterization of exponential i-IOSS, which became a standard detectability condition in the context of MHE in recent years, see, e.g., [RMD20; AR21; KM23; Sch+23; Hu24]. For further details on i-IOSS and its use as a notion of nonlinear detectability, we refer to Chapter 2. We want to emphasize that Assumption 6.7 is not restrictive in the state estimation context; in fact, by adapting the results from [ART21; KM23], it is indeed necessary and sufficient for the existence of robustly (exponentially) stable state estimators. Moreover, Assumption 6.7 can be verified using LMIs, see Section 7.1.

Given a sequence $\hat{x} = \{\hat{x}(j)\}_{j=0}^t$, $t \in \mathbb{I}_{\geq 0}$ produced by some state estimator, the following result establishes a bound with respect to the true state estimates $x(j)$ for $j \in \mathbb{I}_{[0,t]}$ in terms of its performance.

Proposition 6.5. *Suppose Assumption 6.7 holds. Consider the performance measure* (6.5) *for some $t_1, t_2 \in \mathbb{I}_{\geq 0}$ and the quadratic stage cost* (6.6) *for some $Q, R \succ 0$.*

Then, there exist $C_1, C_2, C_3 > 0$ *such that*

$$\begin{aligned}&|\hat{x}(\tau) - x(\tau)|^2\\ &\leq C_1\eta^{\tau-t_1}|\hat{x}(t_1) - x(t_1)|^2 + C_2 \max_{j\in\mathbb{I}_{[t_1,\tau-1]}} \left\{|d(j)|^2, |v(j)|^2\right\} + C_3 J_{[t_1,t_2]}(\hat{z})\end{aligned} \tag{6.79}$$

for all $\tau \in \mathbb{I}_{[t_1,t_2]}$*, all initial conditions* $\chi, \hat{\chi} \in \mathcal{X}$*, and all input and disturbance sequences* $u \in \mathcal{U}^\infty$*,* $d, \hat{d} \in \mathcal{D}^\infty$*, and* $v \in \mathcal{V}^\infty$*, where* $\eta \in (0,1)$ *is from Assumption 6.7 and*

$$\begin{aligned}x(\tau+1) &= f(x(\tau), u(\tau), d(\tau)), & \hat{x}(\tau+1) &= f(\hat{x}(\tau), u(\tau), \hat{d}(\tau)),\\ x(0) &= \chi, & \hat{x}(0) &= \hat{\chi},\\ y(\tau) &= h(x(\tau), u(\tau)) + v(\tau), & \hat{z}(\tau) &= (\hat{x}(\tau), \hat{d}(\tau))\end{aligned}$$

for all $\tau \in \mathbb{I}_{\geq 0}$.

Proof. Without loss of generality, we can assume that the matrices Q and R used in the stage cost (6.6) are the same matrices as those in (6.78b). (In fact, for any positive definite weighting matrices Q and R, the i-IOSS Lyapunov function U from Assumption 6.7 can be suitably scaled such that (6.78b) holds with that choice of Q and R.) As the sequences x and $\hat{x}$ form trajectories of the i-IOSS system (6.1), we can apply Assumption 6.7 to evaluate their difference. Specifically, using the dissipation inequality (6.78b), the fact that $|a-b|_H^2 \leq 2|a|_H^2 + 2|b|_H^2$ for any real vectors a, b and matrix $H \succ 0$ by Cauchy-Schwarz and Young's inequality, and the definition of the performance criterion in (6.53), we can infer that

$$\begin{aligned}&U(\hat{x}(\tau), x(\tau))\\ &\leq \eta^{\tau-t_1}U(\hat{x}(t_1), x(t_1)) + \sum_{j=1}^{\tau-t_1} \eta^{j-1}\Big(|\hat{d}(\tau-j) - d(\tau-j)|_Q^2\\ &\quad + |h(\hat{x}(\tau-j), u(\tau-j)) - h(x(\tau-j), u(\tau-j))|_R^2\Big)\\ &\leq \eta^{\tau-t_1}U(\hat{x}(t_1), x(t_1)) + 2\sum_{j=1}^{\tau-t_1} \eta^{j-1}\left(|d(\tau-j)|_Q^2 + |v(\tau-j)|_R^2\right)\\ &\quad + 2\sum_{j=1}^{\tau-t_1} \eta^{j-1}\left(|\hat{d}(\tau-j)|_Q^2 + |y(\tau-j) - h(\hat{x}(\tau-j), u(\tau-j))|_R^2\right)\\ &\leq \eta^{\tau-t_1}U(\hat{x}(t_1), x(t_1)) + 2\sum_{j=1}^{\tau-t_1} \eta^{j-1}\left(|d(\tau-j)|_Q^2 + |v(\tau-j)|_R^2\right) + 2J_{[t_1,t_2]}(\hat{z}).\end{aligned}$$

The fact that $a + b \leq \max\{2a, 2b\}$ for all $a, b \geq 0$ together with the convergence property of the geometric series leads to

$$\sum_{j=1}^{\tau-t_1} \eta^{j-1}\left(|d(\tau-j)|_Q^2 + |v(\tau-j)|_R^2\right) \leq \frac{2C}{1-\eta} \max_{j\in\mathbb{I}_{[t_1,\tau-1]}} \left\{|d(j)|^2, |v(j)|^2\right\},$$

where $C := \max\{\lambda_{\max}(Q), \lambda_{\max}(R)\}$. Using (6.78a), we obtain (6.79) with $C_1 = \lambda_{\max}(\overline{P})/\lambda_{\min}(\underline{P})$, $C_2 = 4C/(\lambda_{\min}(\underline{P})(1-\eta))$, and $C_3 = 2/\lambda_{\min}(\underline{P})$, which finishes this proof. □

Proposition 6.5 draws a direct link between the performance of an estimator (measured by the criterion in (6.53)) and the corresponding state estimation error. In particular, for large τ, the error is upper bounded by the performance $J_{[t_1,t_2]}$ and the maximum of the disturbances $d(j), v(j),\ j \in \mathbb{I}_{[t_1,\tau-1]}$ that affected the past system behavior and associated measurement data. Hence, if the disturbances are small, we directly have that good performance (small values of $J_{[t_1,t_2]}$) implies accurate estimation results (small errors $|\hat{x}(\tau) - x(\tau)|$). Consequently, it is indeed advisable to design estimators that achieve good performance in the sense of the criterion $J_{[t_1,t_2]}$.

We want to emphasize that Proposition 6.5 and its implications apply for *any* state estimator/observer design. However, as the performance criterion appearing in the estimation error bound in (6.79) constitutes a part of the cost function used in the infinite-horizon problem P_∞, the corresponding solution z^∞ provides a comparatively small bound for the estimation accuracy for all $\tau \in \mathbb{I}_{[t_1,t_2]}$ for *any* $t_1, t_2 \in \mathbb{I}_{\geq 0}$. Under the turnpike condition from Assumption 6.4, we know that δMHE along with a suitably selected delay δ achieves nearly the same performance as the benchmark z^∞ on any interval $\mathbb{I}_{[t_1,t_2]} \subseteq \mathbb{I}_{[\delta,t-\delta]}$ for all $t \in \mathbb{I}_{\geq \delta}$, and is hence expected to be similarly accurate (note that this conclusion also applies to δMHE with prior weighting under Assumption 6.6). This highly useful feature of δMHE can also be seen in all our simulation examples in Section 6.4.

6.4. Numerical examples

We now illustrate our theoretical results presented in Section 6.3. The following simulations were performed on a standard laptop in MATLAB using CasADi [And+18] and the NLP solver IPOPT [WB05].

In Section 6.4.1, we first consider the offline estimation case by means of a nonlinear batch reactor model and a linear system with more than 100 states. Our simulations show that the proposed estimator (6.77) along with the modifications from Remark 6.12 approximates the optimal (full) solution with negligible error, which is particularly important in practice when the desired solution of the full problem cannot be computed due to the size of the problem and common iterative solutions (such as those provided by the Kalman filter and corresponding smoothing algorithms) are not sufficiently accurate.

Then, in Section 6.4.2, we consider the online estimation case and particularly focus on MHE with prior weighting, which we investigate using two realistic examples from the literature: a continuous stirred-tank reactor and a highly nonlinear 12-state quadrotor model. In both examples, we can observe the turnpike behavior being present in MHE problems with prior weighting. Our main observation is that already a small delay in the MHE scheme (one to three steps) reduces the overall estimation error with respect to the true unknown system state by 20–25 %.

6.4.1. Offline estimation

Batch reactor example

We consider the following dynamical system

$$\begin{aligned} x_1^+ &= x_1 + t_\Delta(-2k_1x_1^2 + 2k_2x_2) + u_1 + d_1, \\ x_2^+ &= x_2 + t_\Delta(k_1x_1^2 - k_2x_2) + u_2 + d_2, \\ y &= x_1 + x_2 + v, \end{aligned} \tag{6.80}$$

with parameters $k_1 = 0.16$, $k_2 = 0.0064$, and $t_\Delta = 0.1$. This corresponds to the chemical reaction example from Section 3.4.1 under Euler discretization and with additional controls $u \in \mathbb{R}^2$, process disturbances $d \in \mathbb{R}^2$, and measurement noise $v \in \mathbb{R}$. We consider a given data set $D = \{D(j)\}_{t=0}^T = \{(u(t), y(t))\}_{j=t}^T$ with $T = 400$, where the process started at $x(0) = \chi = [3, 0]^\top$, was subject to uniformly distributed random disturbances and noise satisfying $d(t) \in \{d \in \mathbb{R}^2 : |d_i| \leq 0.05, i = 1, 2\}$ and $v(t) \in \{v \in \mathbb{R} : |v| \leq 0.5\}$, $t \in \mathbb{I}_{[0,T]}$, and where the input $u(t)$ was used to periodically empty and refill the reactor such that $x(t+1) = [3, 0]^\top + d(t)$ for all $t = 50i$ with $i \in \mathbb{I}_{[1,7]}$ and $u(t) = 0$ for all $t \neq 50i$. To reconstruct the unknown state trajectory $\{x(t)\}_{t=0}^T$, we consider the cost function (6.5)–(6.7) and select $Q = I_2$ and $R = S = 1$. In the following, we compare the performance and accuracy of the optimal solution $\hat{x}^*$ of the full problem $P_T(D)$, the proposed approximate estimator (AE) $\hat{x}^{\mathrm{ae}}$ from (6.77), and standard MHE $\hat{x}^{\mathrm{mhe}}$ from (6.46) for different choices of the horizon length N.

From Figure 6.3, for small horizons ($N = 40$) we observe that the AE achieves significantly worse performance compared to the solution of the full problem (and MHE). This can be attributed to the problem length N being too small, leading to the fact that the estimates contained in $\hat{x}^{\mathrm{ae}}$ correspond to solutions of truncated problems that are far away from the turnpike, compare also the motivating example in Section 6.2.1, particularly Figure 6.1 for small values of N. For increasing values of N, the estimates are getting closer to the turnpike, and the performance improves significantly. Specifically, we see *exponential* convergence to the optimal performance. This could be expected since the system is exponentially detectable [Sch+23, Sec. V.A] and controllable with respect to the input d, which suggests that the turnpike property specializes to an exponential one and hence renders the third statement of Remark 6.9 valid. Overall, a problem length of $N = 130$ is sufficient to achieve nearly optimal performance. The MHE sequence $\hat{x}^{\mathrm{mhe}}$, on the other hand, generally yields worse performance than the AE (for $N \geq 70$). This is completely in line with our theory, because $\hat{x}^{\mathrm{mhe}}$ is a concatenation of solutions of truncated problems that are on the right leaving arc and hence may be far from the turnpike, see the discussion below (6.46).

To assess the accuracy of the estimated state sequence with respect to the real unknown system trajectory x, we compare the SSE of the full solution $\hat{x}^*$, the AE $\hat{x}^{\mathrm{ae}}$, and MHE $\hat{x}^{\mathrm{mhe}}$ for different sizes N of the truncated problems, accumulated over the interval $\mathbb{I}_{[0,T]}$. The corresponding results in Table 6.1 show qualitatively the same behavior as in the previous performance analysis. In particular, the full solution

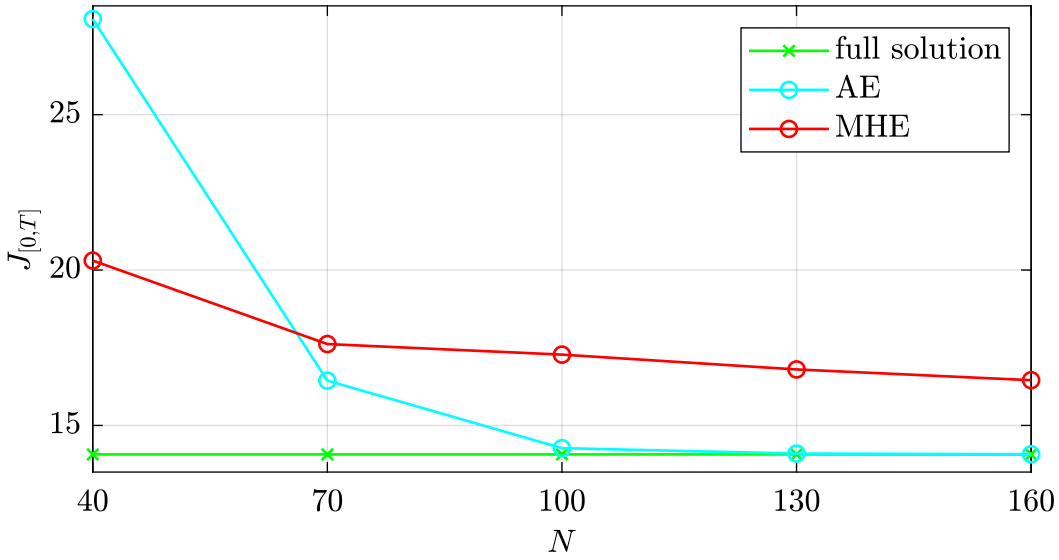

Figure 6.3. Performance $J_{[0,T]}$ of the AE $\hat{x}^{\mathrm{ae}}$ (cyan) and MHE $\hat{x}^{\mathrm{mhe}}$ (red) for different lengths N of the problem P_N compared to the performance of the full solution $\hat{x}^*$ (green).

Table 6.1. SSE for the proposed AE and MHE.

Problem length N	AE	MHE
40	36.598 (+73.5 %)	27.197 (+28.9 %)
70	24.265 (+15.0 %)	24.311 (+15.2 %)
100	21.708 (+2.9 %)	23.986 (+13.7 %)
130	21.320 (+1.0 %)	23.341 (+10.6 %)
160	21.176 (+0.4 %)	23.325 (+10.5 %)

Values in parentheses indicate the relative increase in the SSE compared to the full solution x^* (which achieves SSE = 21.1).

yields the most accurate estimates with the lowest SSE. The proposed AE yields much higher SSE for small horizons (SSE increase of 73.5 % for $N = 40$ compared to the full solution), but improves very fast as N increases, and exponentially converges to the SSE of the full solution. On the other hand, the SSE of MHE improves much slower, and is particularly much worse than that of the full solution and the proposed AE (for $N \geq 70$).

Large estimation problems

We illustrate the potential of the proposed AE for large estimation problems where the computation of the full solution is either time-consuming or simply impossible. To this end, we consider the LTI system

$$\begin{aligned} x(t+1) &= Ax(t) + Bu(t) + d(t), \\ y(t) &= Cx(t) + v(t), \end{aligned}$$

Table 6.2. Simulation results for the full solution (full), the proposed approximate estimator (AE), the fixed-interval smoother (FIS), and the Kalman filter (KF).

n	p	Estimator	$J_{[0,T]}$	SSE	τ [s]
30	10	full	12.91	40.81	9.914
30	10	AE	12.93	40.83	0.828
30	10	FIS	15.62	53.04	0.536
30	10	KF	4513.66	69.02	0.113
60	20	full	16.30	51.91	37.648
60	20	AE	16.31	51.91	2.849
60	20	FIS	19.02	66.80	1.608
60	20	KF	4021.66	94.68	0.354
120	40	AE	21.03	84.52	11.456
120	40	FIS	29.21	148.49	4.756
120	40	KF	18403.92	202.58	0.960

where the matrices A, B, C correspond to a randomly selected stable system (computed using the drss command of MATLAB) with $m = 30$ inputs, $n \in \{30, 60, 120\}$ states and $p \in \{10, 20, 40\}$ outputs. We consider a batch of measured input-output data $D = \{D(t)\}_{t=0}^{T}$ with $T = 4803$, where the system was subject to $x(0) = \chi = 0$, a known sinusoidal input sequence u, and unknown process disturbance d and measurement noise v; here, each element of $d(t)$ was drawn from a uniform distribution over $[-0.01, 0.01]$ superimposed with a deterministic sinusoidal function of time with a magnitude of 0.01 that may represent unmodeled nonlinear dynamics, and each element of $v(t)$ was drawn from a uniform distribution over $[-0.1, 0.1]$. For reconstructing the unknown state sequence x, we consider the quadratic cost function (6.5)–(6.7) and select $Q = I_n$, $R = S = I_p$. In the following, we compare the full solution of the problem $P_T(D)$ with the AE (6.77), where we rely on the modifications from Remark 6.12 and select $k = 32$, $N = 150$, $\Delta = 70$ (this modification reduces the number of truncated problems to be solved from $K_\Delta = 4654$ for $\Delta = 0$ to merely $K_\Delta = 34$, i.e., by more than 99 %). The full and truncated optimal estimation problems can be cast as unconstrained quadratic programs (QPs), which we solve using the quadprog implementation of MATLAB. The truncated QPs for the AE are additionally solved in parallel using the Parallel Computing Toolbox. For comparison reasons, we also consider the Kalman filter (KF) using the covariance matrices Q^{-1} and R^{-1}, where the initial estimate $\hat{x}^{\mathrm{kf}}(0)$ is drawn from an isotropic normal distribution with zero mean and identity covariance matrix I_n, and the initial covariance is chosen as $\hat{P}^{\mathrm{kf}}(0) = I_n$. Moreover, we consider the fixed-interval smoother (FIS) considering the entire batch of measurements, which provides the best possible estimates in the context of KF-related smoothing algorithms, see [CJ11, Ch. 5] for further details and a description of the corresponding algorithm.

Table 6.2 shows the estimation results in terms of the performance index $J_{[0,T]}$, accuracy (SSE), and total computation time τ_{tot} for different system dimensions.

For $n \in \{30, 60\}$, we observe that the performance $J_{[0,T]}$ and the SSE of the full solution and the AE are nearly identical. However, the AE can be computed more than 10 times faster than the full solution (saving more than 90 % of the computation time) due to a (much) smaller problem size and the fact that the truncated problems are solved in parallel. For $n = 120$, it was already impossible to numerically solve the full problem $P_T(D)$ due to the problem size (in contrast to the AE). For all system realizations, the KF is much faster, as expected (because the QPs are replaced by simple matrix computations), however, performs much worse than the AE (both in terms of $J_{[0,T]}$ and SSE), which is mainly due to the fact that only past data is used to compute the corresponding estimates. In contrast, the FIS combines the KF forward recursion with a backward recursion so that each estimate is computed based on the entire batch of data, which requires more computations but provides improved estimates compared to the KF; however, the performance and accuracy are still worse compared to the AE due to the fact that the considered disturbance and noise distributions violate the conditions for the FIS to be optimal.

This example shows that the modifications from Remark 6.12 are very effective for computing the AE in practice. Specifically, to recover the performance and accuracy of the full solution, it suffices to choose Δ close to $N/2$ such that only the first and last few elements of the truncated solutions (which lie on the approaching and leaving arcs) are discarded. Overall, it turns out that the AE approximates the full solution with negligible error, which is particularly important in practice when the full problem $P_T(D)$ cannot be solved due to the size or complexity of the problem and iterative solutions such as the KF and related smoothing algorithms are not sufficiently accurate.

6.4.2. Online estimation

Continuous stirred-tank reactor

We consider the continuous stirred-tank reactor (CSTR) from [RMD20, Example 1.11], where an irreversible, first order reaction $A \to B$ occurs in the liquid phase and the reactor temperature is regulated with external cooling, see also [PR03] for more details. The continuous-time nonlinear state-space model is given by

$$\begin{aligned}
\frac{dc}{dt} &= \frac{F_0(c_0 - c)}{\pi r^2 h} - k_0 \exp\left(\frac{-E}{RT}\right) c, \\
\frac{dT}{dt} &= \frac{F_0(T_0 - T)}{\pi r^2 h} + \frac{-\Delta H}{\rho C_p} k_0 \exp\left(\frac{-E}{RT}\right) c + \frac{2U}{r \rho C_p}(T_c - T), \\
\frac{dh}{dt} &= \frac{F_0 - F}{\pi r^2},
\end{aligned}$$

where the states are c (the molar concentration of species A), T (the reactor temperature), and h (the level of the tank), and the control inputs are T_c (the coolant liquid temperature) and F (the outlet flowrate). The model parameters are taken from [RMD20, Example 1.11]. The open-loop stable steady-state solution is $x^{\mathrm{ss}} =$

$[0.878, 323.5, 0.659]^\top$ associated with the input $u^{\mathrm{ss}} = [300, 0.1]^\top$. By using Runge-Kutta discretization (RK4) with sampling time $t_\Delta = 0.25$, we obtain the discrete-time model

$$\begin{aligned} x(t+1) &= f(x(t), u(t), d(t)) = f_{\mathrm{a}}(x(t), u(t)) + d(t), \\ y(t) &= h(x(t), u(t)) + v(t) = \begin{bmatrix} 0 & 1 & 0 \end{bmatrix} x(t) + v(t), \end{aligned}$$

where we define $x(t) = [c(t), T(t), h(t)]^\top$ and $u(t) = [T_c(t), F(t)]^\top$, assume that only the temperature of the reactor T can be measured, and consider additional process disturbance $d(t) \in \mathbb{R}^3$ and measurement noise $v(t) \in \mathbb{R}$. The real system is initialized with $x(0) = \chi = [0.8, 295, 0.7]^\top$. In the following, we consider the simulation time $T_{\mathrm{s}} = 200$ and apply an open-loop control sequence u with $u_2(t) = u_2^{\mathrm{ss}}$ for $t \in \mathbb{I}_{[0,T_{\mathrm{s}}]}$ and $u_1(t)$ as a trapezoidal input sequence with plateaus at u_1^{ss} and $u_1^{\mathrm{ss}} - 25$. During the simulations, we sample the disturbances $d(t)$ and $v(t)$ from uniform distributions over $\{d \in \mathbb{R}^3 : |d_1| \leq 5 \cdot 10^{-3}, |d_2| \leq 1, |d_3| \leq 5 \cdot 10^{-3}\}$ and $\{v \in \mathbb{R} : |v| \leq 3\}$. Figure 6.4 depicts exemplary state trajectories of the reactor for the given setup under random disturbances and noise.

To estimate the true unknown state $x(t)$ from the measured input-output data online, we design different MHE schemes that rely on the cost function (6.62) with the horizon length $N = 10$ and quadratic costs (6.6) and (6.7), where we select the weighting matrices $Q = \mathrm{diag}(10^3, 1, 10^5)$ and $R = S = 1$. Moreover, we consider the initial guess $\hat{\chi} = [0.97, 268, 0.59]^\top$ and use a quadratic prior weighting (6.63) with time-varying matrix $W(t)$, $t \in \mathbb{I}_{\geq 0}$, initialized with $W(0) = 10^{-2} I_3$ and updated using the well-known covariance formulas of the EKF. In the optimal estimation problems, we also impose the state constraints $\mathcal{X} = [0.5, 1.5] \times [200, 400] \times [0.5, 1.5]$, but we consider the disturbance sets to be unknown and use $\mathcal{D} = \mathbb{R}^3$ and $\mathcal{V} \in \mathbb{R}$. In the following, we compare MHE with filtering prior (6.64), smoothing prior (6.65), and turnpike prior (6.66) and additionally consider the infinite-horizon estimator (IHE), which we approximate by solving the clairvoyant FIE problem using all simulation data $D = \{D(t)\}_{t=0}^{T_{\mathrm{s}}}$.

From Figure 6.5, we can observe that all MHE problems (for all priors) exhibit the turnpike behavior with respect to the infinite-horizon solution, with clear approaching and leaving arcs, which is a strong indicator that Assumption 6.6 holds true. We additionally compare the standard MHE schemes (without delay) with δMHE (6.76) using the turnpike prior, where we consider $\delta = 1$ and $\delta = N/2$. From Figure 6.6, we see that the standard MHE schemes yield very similar estimation results in terms of the difference to the IHE (for all priors), that δMHE with $\delta = 1$ provides estimates that are much closer to the IHE, and that δMHE with $\delta = N/2$ (which corresponds to the turnpike prior (6.66)) converges into a (small) neighborhood of the IHE, which nicely illustrates Proposition 6.4.

We consider 100 different simulations with random disturbances and randomly selected initial estimates $\hat{\chi}$ that are sampled from a uniform distribution over the interval centered at χ with a relative deviation of 25 % for each state. Figure 6.7 indicates that the standard MHE schemes are again very similar in terms of their SSE (for all priors), significantly outperformed by δMHE for $\delta = 1$ (which yields a

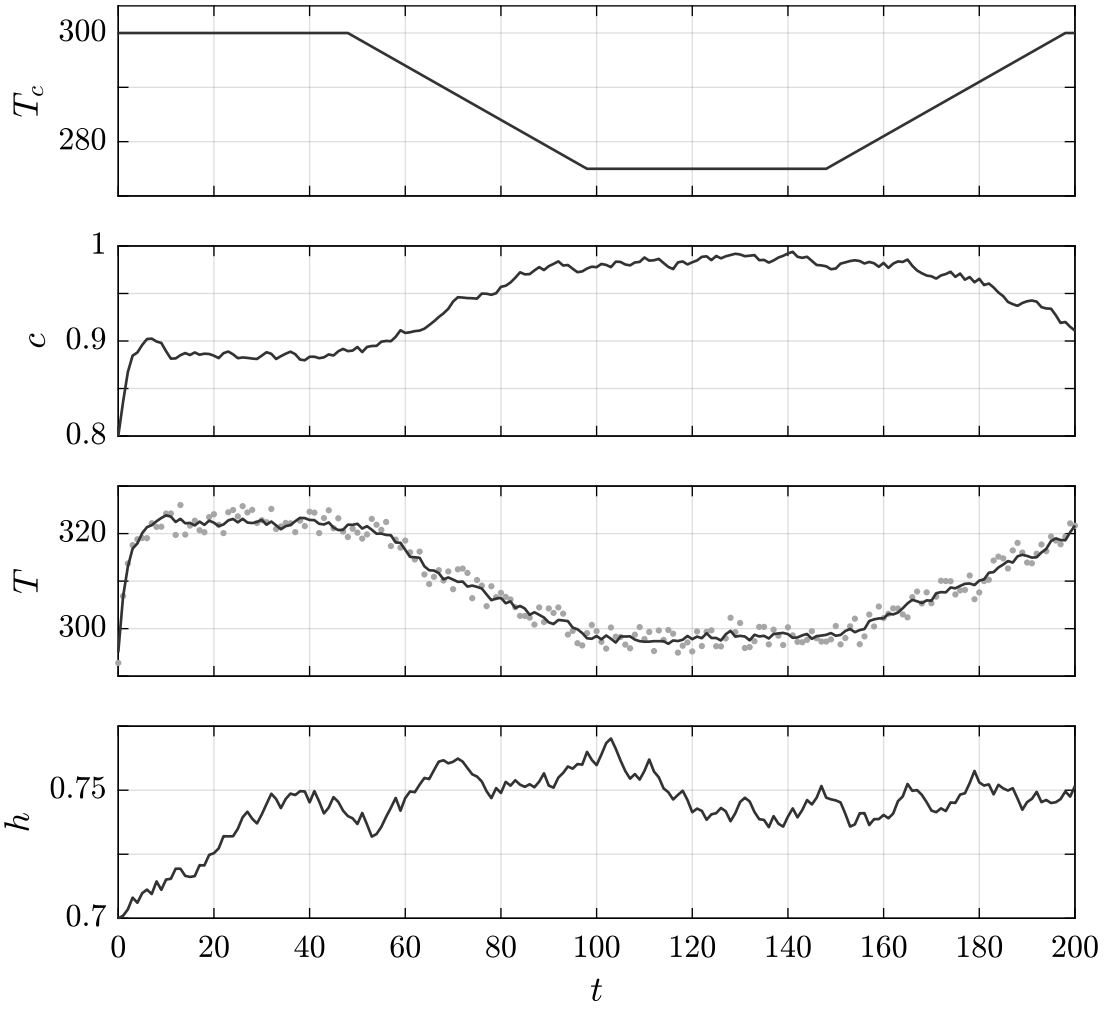

Figure 6.4. CSTR: Exemplary state trajectories under random disturbances and noise for the initial condition χ and the given control profile for the coolant temperature T_c. The gray dots represent noisy measurements of the reactor temperature T.

reduction in the SSE by 20 %). Moreover, we observe that the SSE of δMHE with $\delta = N/2$ is very close to that of the IHE.

Overall, this example nicely illustrates the developed theory. In particular, it shows that MHE problems with prior weighting exhibit the turnpike behavior with respect to the IHE (Assumption 6.6), with a potentially strong leaving arc, compare Figure 6.5. This motivates to incorporate an artificial delay in the estimation scheme in order to reduce the influence of the leaving arc. Surprisingly, already a one-step delay is sufficient to significantly reduce the influence of the leaving arc such that δMHE tracks the performance and accuracy of the IHE with small error, compare Figure 6.6 and Figure 6.7.

Quadrotor

We consider the quadrotor example from Section 3.4.2 and briefly recall the overall model. By $\mathcal{I}$ we denote the stationary inertial system with its vertical component

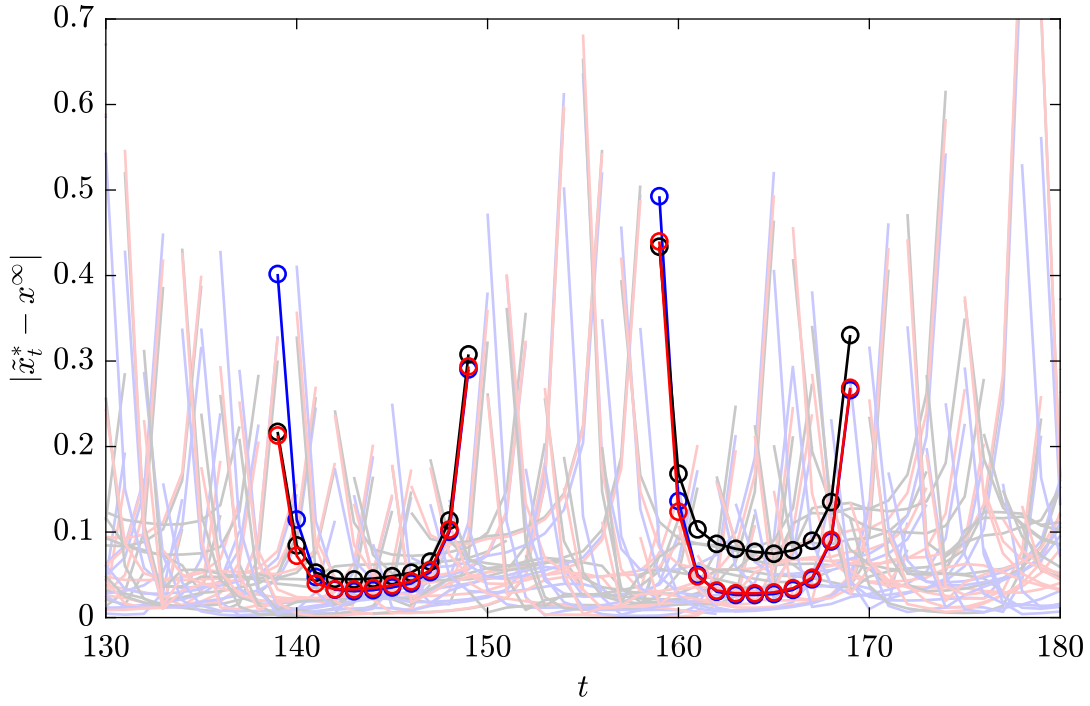

Figure 6.5. CSTR: Finite-horizon solutions $\tilde{x}_t^*(j)$ compared to $x^\infty(t-N+j)$, $j \in \mathbb{I}_{[0,N]}$ for $t \in \mathbb{I}_{[130,180]}$ using the filtering prior (blue), smoothing prior (black), and turnpike prior (red); highlighted are particular solutions obtained at $t = 149$ and $t = 169$.

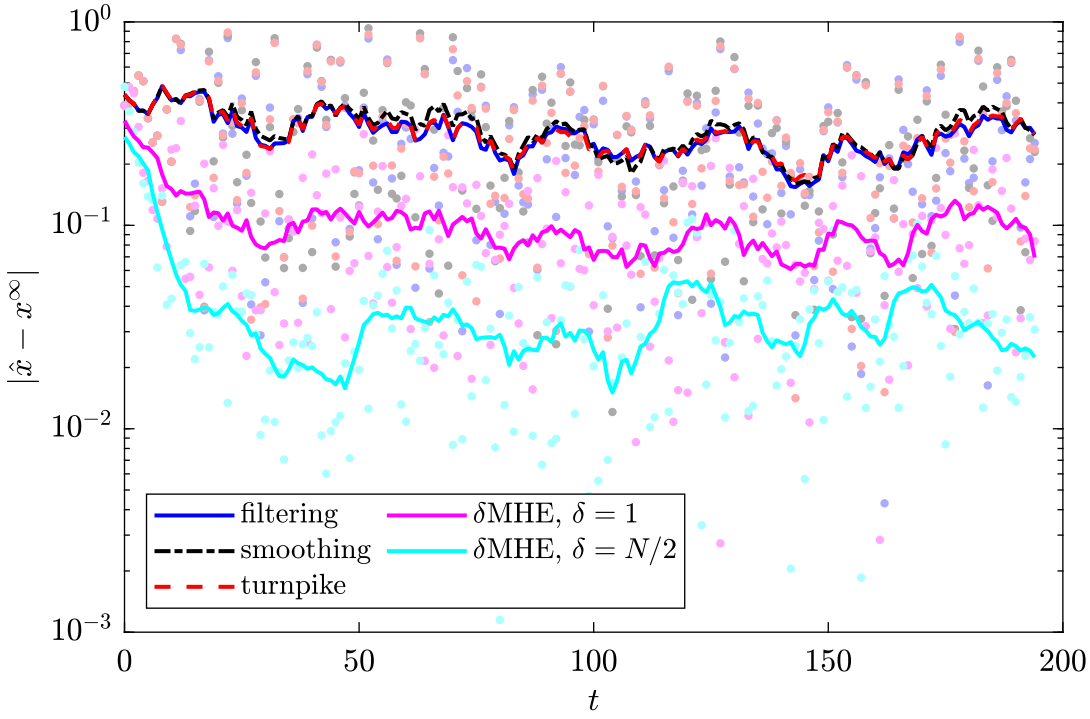

Figure 6.6. CSTR: Distance between state estimates using different MHE schemes and the IHE. Dots indicate values at time t, lines indicate the moving average over a sliding window of size $N + 1$.

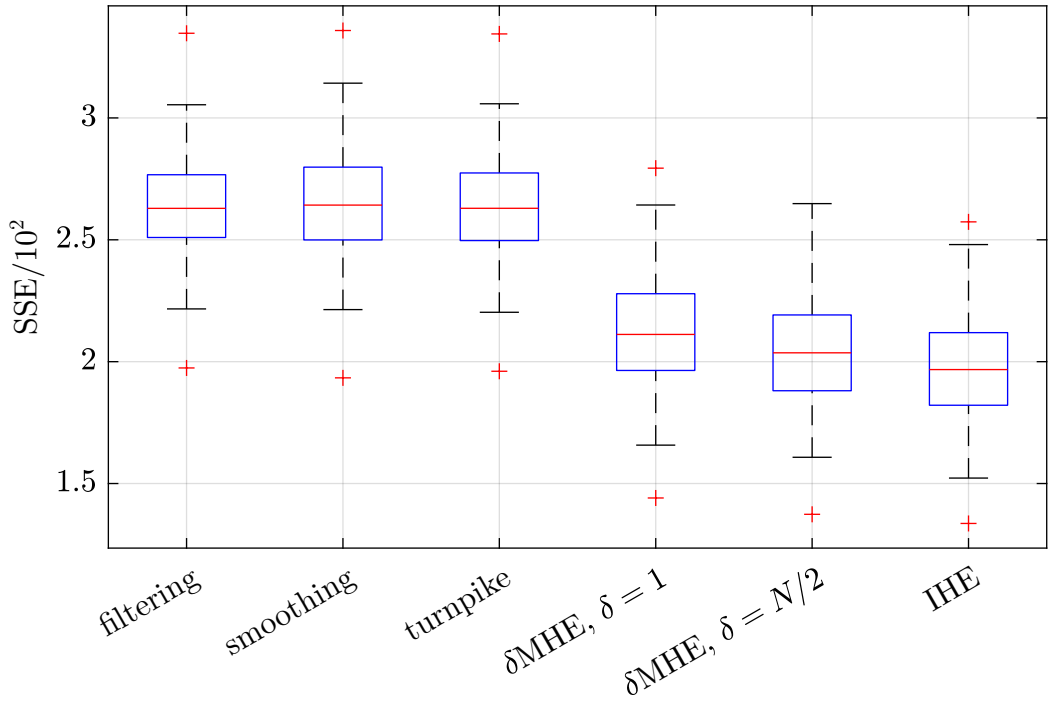

Figure 6.7. CSTR: Boxplot of the SSE for MHE using the filtering prior, the smoothing prior, and the turnpike prior, δMHE using the turnpike prior for $\delta = 1$ and $\delta = N/2 = 5$, and the IHE over 100 different simulations with random disturbance/noise and randomly selected initial priors.

pointing into the Earth, where the position and velocity of the quadrotor are represented by $z = [z_1, z_2, z_3]^\top$ and $s = [s_1, s_2, s_3]^\top$, respectively. By $\mathcal{B}$ we refer to the body-fixed frame attached to the quadrotor, with the third component pointing in the opposite direction of thrust generation. The attitude of $\mathcal{B}$ with respect to $\mathcal{I}$ is described by a rotation matrix R (using zyx-convention), which involves the roll, pitch, and yaw angle of the quadrotor that we denote by $\xi = [\phi, \theta, \psi]^\top$. The angular velocity of the quadrotor in $\mathcal{B}$ with respect to $\mathcal{I}$ is given by $\Omega = [\Omega_1, \Omega_2, \Omega_3]^\top$. Assuming a wind-free environment, the overall dynamics can be described as

$$\begin{aligned} \dot{z} &= s, \\ \dot{\xi} &= \Gamma(\xi)\Omega, \\ m\dot{s} &= mge_3 - TR(\xi)e_3 - R(\xi)B\Omega, \\ J\dot{\Omega} &= -\Omega^\times J\Omega + \tau - D\Omega, \end{aligned}$$

where $e_3 = [0, 0, 1]^\top$ and $(\cdot)^\times$ refers to the skew symmetric matrix associated with the cross product such that $u^\times v = u \times v$ for any $u, v \in \mathbb{R}^3$. The thrust $T \in \mathbb{R}$ and the torque $\tau \in \mathbb{R}^3$ are generated by the velocities ω_i of the four rotors via

$$\begin{bmatrix} T \\ \tau \end{bmatrix} = \begin{bmatrix} c_T & c_T & c_T & c_T \\ 0 & -lc_T & 0 & lc_T \\ lc_T & 0 & -lc_T & 0 \\ -c_Q & c_Q & -c_Q & c_Q \end{bmatrix} \begin{bmatrix} \omega_1^2 \\ \omega_2^2 \\ \omega_3^2 \\ \omega_4^2 \end{bmatrix}$$

and the matrix Γ is defined as

$$\Gamma(\xi) = \begin{bmatrix} 1 & \sin\phi\tan\theta & \cos\phi\tan\theta \\ 0 & \cos\phi & -\sin\phi \\ 0 & \sin\phi\sec\theta & \cos\phi\sec\theta \end{bmatrix},$$

see [Kai+17; NS19] for further details regarding the model and its derivation. The parameters are chosen as $m = 1.9$, $J = \mathrm{diag}(5.9, 5.9, 10.7) \cdot 10^{-3}$, $g = 9.8$, $l = 0.25$, $c_T = 10^{-5}$, $c_Q = 10^{-6}$, $B = 1.14 \cdot e_3^{\times}$, and $D = 0.0297 \cdot e_3 e_3^{\top}$.

The overall model has the states $x = [z^{\top}, \xi^{\top}, s^{\top}, \Omega^{\top}]^{\top} \in \mathbb{R}^{12}$ and the inputs $u = [\omega_1, \omega_2, \omega_3, \omega_4]^{\top} \in \mathbb{R}^4$. Using Euler-discretization and the sampling time $t_\Delta = 0.05$, we obtain the discrete-time model

$$\begin{aligned} x(t+1) &= f(x(t), u(t), d(t)) = f_{\mathrm{a}}(x(t), u(t)) + d(t), \\ y(t) &= h(x(t), u(t)) + v(t) = \begin{bmatrix} I_6 & 0_{6\times 6} \end{bmatrix} x(t) + v(t), \end{aligned}$$

where we consider additional process disturbances $d(t) \in \mathbb{R}^{12}$ and assume that only measurements of the position $z(t)$ and orientation $\xi(t)$ are available, subject to the measurement noise $v(t) \in \mathbb{R}^6$. In the simulations, the disturbance $d(t)$ and noise $v(t)$ are uniformly distributed random variables sampled from the sets $\{d \in \mathbb{R}^{12} : |d_i| \leq 2 \cdot 10^{-2}, i = 1, 2, 3,\ |d_i| \leq 2 \cdot 10^{-5}, i = 4, 5, 6,\ |d_i| \leq 2 \cdot 10^{-3}, i = 7, 8, 9,\ |d_i| \leq 2 \cdot 10^{-6}, i = 10, 11, 12\}$ and $\{v \in \mathbb{R}^6 : |v_i| \leq 2 \cdot 10^{-1}, i = 1, 2, 3,\ |v_i| \leq 5 \cdot 10^{-2}, i = 4, 5, 6\}$. We consider the simulation time $T_{\mathrm{s}} = 1000$ and a given open-loop control input sequence $\{u(t)\}_{t=0}^{T_{\mathrm{s}}}$, which moves the quadrotor spirally upwards, see Figure 6.8 for an exemplary trajectory under a specific disturbance realization.

To estimate the unknown state $x(t)$, we consider the cost function (6.62) with the horizon length $N = 30$ and quadratic costs (6.6) and (6.7), where we select $Q = \mathrm{diag}(10^2 I_3, 10^4 I_3, 10^3 I_3, 10^5 I_3)$ and $R = S = \mathrm{diag}(10^1 I_3, 10^2 I_3)$. Moreover, we use the quadratic prior weighting (6.63), where the weighting matrix $W(t)$ is initialized with $W(0) = 10 I_{12}$ and updated using the EKF covariance formulas for all $t \in \mathbb{I}_{\geq 0}$. We consider the case where no additional information about the domains of the states and disturbances is available and use $\mathcal{X} = \mathbb{R}^{12}$, $\mathcal{D} = \mathbb{R}^{12}$, $\mathcal{V} = \mathbb{R}^6$ in (6.4c)–(6.4e). In the following, we examine 100 different simulations with random disturbances, where we additionally sample the initial estimate $\hat{\chi}$ from a uniform distribution over the set $\mathcal{X}_0 = \{x : |z_i| \leq 1, |\xi_i| \leq \pi/16, i = 1, 2, 3,\ v = 0,\ \Omega = 0\}$. We compare standard MHE with filtering prior (6.64), smoothing prior (6.65), and turnpike prior (6.66), δMHE (6.76) with turnpike-based prior weighting and $\delta = 1$, $\delta = 3$, and $\delta = N/2$, and the IHE (which we approximate by solving the clairvoyant FIE problem using all simulation data $D = \{D(t)\}_{t=0}^{T_{\mathrm{s}}}$).

From Figure 6.9, we observe that the MHE schemes with filtering and turnpike prior perform quite similarly. The fact that MHE with smoothing prior is slightly worse can be attributed to the fact that the movement of the quadrotor is rather slow compared to the sampling time, while the horizon length $N = 30$ is also rather small. In such setting, MHE with filtering or turnpike prior proves beneficial, as this essentially considers measurements from a larger estimation window, compare the discussion below (6.65). For δMHE, we can observe a reduction of the SSE of

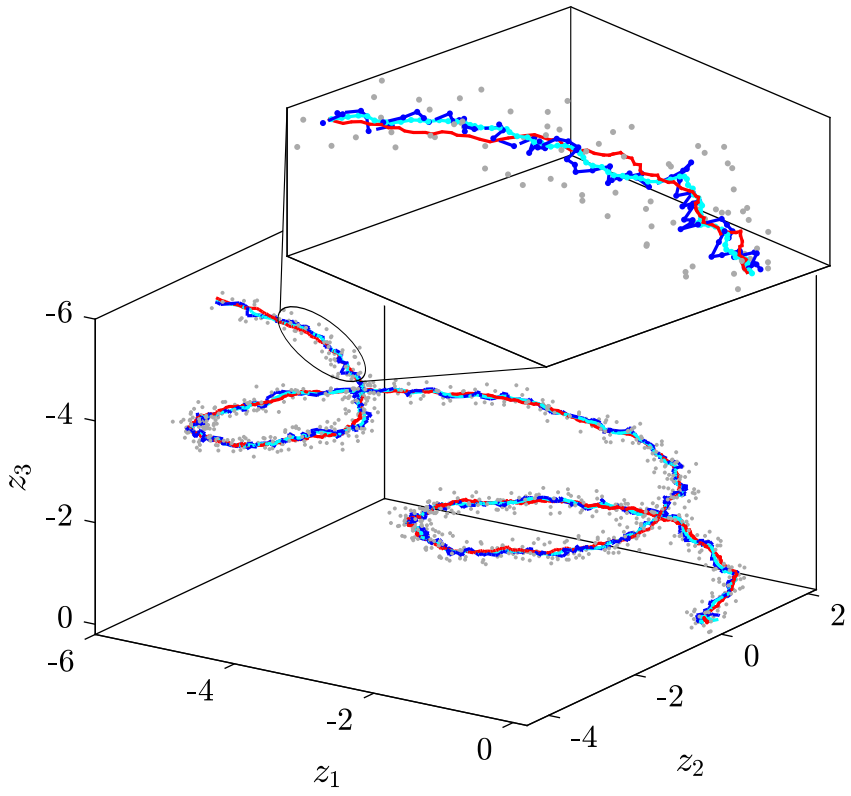

Figure 6.8. Quadrotor: Exemplary 3D trajectory for one specific disturbance realization; comparison of the true trajectory (red), measurements (gray dots), MHE with filtering prior (blue), and δMHE for $\delta = N/2 = 15$ (cyan).

approximately 10 % for $\delta = 1$, of 25 % for $\delta = 3$, and of by 50 % for $\delta = N/2$, which is also close the SSE of the IHE.

To conclude, this example illustrates that the developed theory is also applicable to more complex and realistic systems from the literature. In particular, it again shows that using the proposed δMHE scheme with a small delay δ can already significantly improve the estimation performance in practice.

6.5. Summary

In this chapter, we investigated the turnpike phenomenon in optimal state estimation problems and developed novel accuracy and performance guarantees for optimization-based state estimation techniques, in particular MHE.

First, we showed that the solution of the (acausal) infinite-horizon optimal estimation problem involving all past and future data serves as a turnpike for finite-horizon problems that form the core of MHE and FIE. We considered different mathematical characterizations of this phenomenon and provided sufficient conditions that involve strict dissipativity and decaying sensitivity. Moreover, for the linear quadratic setting, we showed that decaying sensitivity is naturally present under controllability

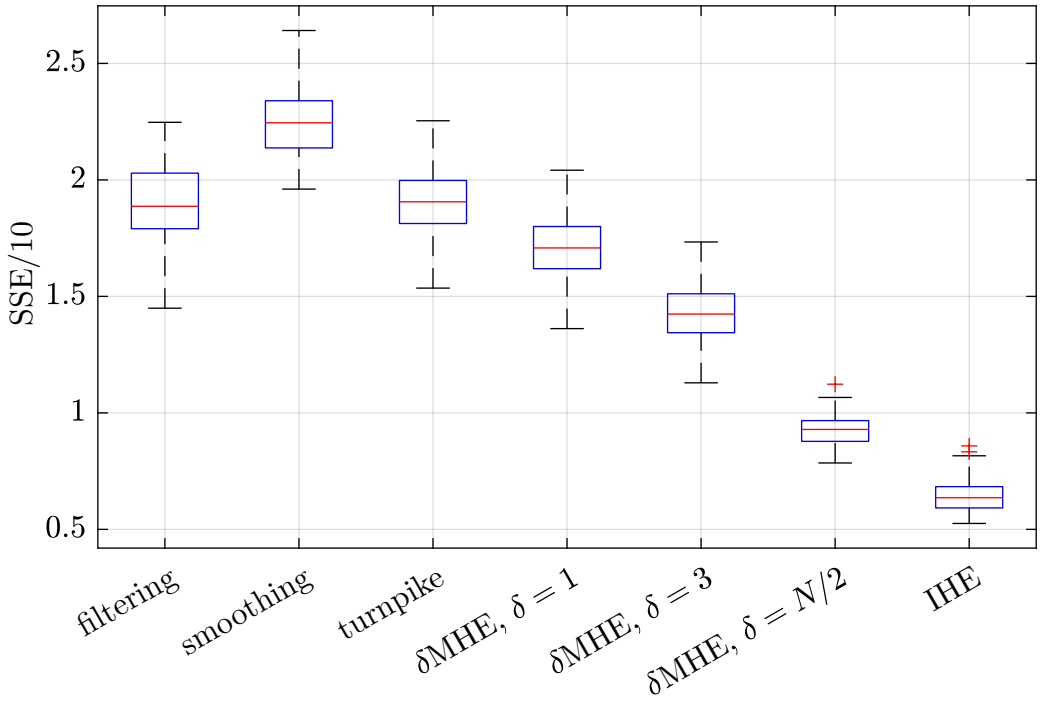

Figure 6.9. Quadrotor: Boxplot of the SSE for MHE using the filtering prior, the smoothing prior, and the turnpike prior, δMHE using the turnpike prior for $\delta = 1$, $\delta = 3$, and $\delta = N/2 = 15$, and the IHE over 100 different simulations with random disturbance/noise and randomly selected initial priors.

and observability using standard arguments from optimal control theory.

From our turnpike analysis, we found that MHE problems generally exhibit both a leaving and an approaching arc that can in fact have a potentially strong negative impact on the overall estimation accuracy. To counteract the leaving arc, we suggested using an artificial delay in the MHE scheme, and we showed that the resulting performance (both averaged and non-averaged) is approximately optimal and yields bounded regret with respect to the infinite-horizon solution, with error terms that can be made arbitrarily small by an appropriate choice of the delay. Regardless of using a delay in the estimation, we proposed a novel turnpike prior for MHE formulations with prior weighting, effectively counteracting the approaching arc and proven to be a valid alternative to the classical options (such as the filtering or smoothing prior) with superior theoretical properties. An interesting topic for future work is to analyze the turnpike prior with respect to the gradient condition proposed in [BZD20] to better understand and, if possible, further reduce the influence of the approaching arc.

In our simulations, we found that MHE with the proposed turnpike prior performs comparably well to MHE with filtering or smoothing priors, while the delay resulted in a significant improvement of the estimation results. In particular, considering a continuously stirred tank reactor example and a highly nonlinear quadrotor model from the literature, we observed the turnpike phenomenon and found that a delay of one to three steps improved the overall estimation error by 20-25 % compared to

standard MHE (without delay). For offline estimation, the proposed delayed MHE scheme has proven to be a useful alternative to established iterative filtering and smoothing methods, significantly outperforming them especially in the presence of non-normally distributed noise.

Our performance results are particularly relevant for applications where a small delay in the online estimation can be tolerated, which is especially the case for system monitoring, fault detection or parameter estimation. An interesting topic for future work is the combination of the delayed MHE scheme with state feedback control, and in particular the investigation of whether the delay in the closed loop is worthwhile for significantly better estimation results, see also Chapter 8 for further details.

7. Verification methods

In this chapter, we focus on the numerical verification of detectability (in terms of i-IOSS) and PE properties for general nonlinear systems. Here, we rely on various tools to reformulate the corresponding mathematical conditions in the form of LMIs that can be efficiently solved using SDP. This is an important contribution in itself, since such properties play a central role in any estimator or observer design in the respective stability and robustness analysis, but practical tools to actually verify them are lacking. In the context of the MHE schemes developed and analyzed in this thesis, however, this becomes even more important, as the detectability and excitation properties need to be known beforehand (or verified online) in order to design and implement the corresponding MHE cost functions in the first place. In Section 7.1, we focus on the computation of i-IOSS and i-iIOSS Lyapunov functions, while in Section 7.2 we show how certain PE conditions can be verified by evaluating a suitably constructed observability metrics.

Disclosure: The following chapter is based upon and in parts literally taken from our previous publications [Sch+23, Sec. IV] and [SM24b; SM23b; SM23a]. A detailed description of the contributions of each author is given in Appendix A.

7.1. Nonlinear detectability

In the following section, we provide a constructive and systematic approach to compute i-IOSS and i-iIOSS Lyapunov functions for discrete- and continuous-time systems, respectively. We again want to emphasize that the lack of such a method in the literature was generally considered a major problem in [AR21], as i-IOSS became a standard detectability assumption in the recent nonlinear MHE literature, see, e.g., [Mül17; AR19b; RMD20; Hu24; KM23; AR21; Ale25] and compare also Section 3.3. Here, we address this problem and provide practical tools to actually verify this crucial property in practice. To this end, we employ the differential dynamics, which results in simple LMI conditions involving the Jacobians of the system that can be efficiently verified using standard tools such as SOS optimization, LPV embeddings, or gridding techniques.

In general, the differential analysis of nonlinear systems plays an important role, as simple and intuitive tools from linear control theory become applicable; for example, by shifting the analysis of convergence between arbitrary system trajectories to the study of the linearizations along each trajectory, see, e.g., [LS98]. Global properties can then be inferred by using tools from differential geometry—typically based on a suitable Riemannian (or Finsler) metric under which the differential displacements

decrease with the flow of the system. This universal concept offers wide applicability in the analysis [MS14; FS13; FS14; TRK19] and control [MS18; MS17; KTW21] of nonlinear systems. In addition, as pointed out in [LS98], it is also naturally suitable for characterizing the convergence of observers (see, for example, [YWM22; SP12; SP16]), and consequently, also for i-IOSS and i-iIOSS. In Section 7.1.1, we address the discrete-time case and i-IOSS, whereas the continuous-time case and i-iIOSS is dealt with in Section 7.1.2.

7.1.1. i-IOSS Lyapunov functions for discrete-time systems

We consider the system description from (3.1), that is, the nonlinear discrete-time state-space model

$$x(t+1) = f(x(t), u(t), w(t)),\ x(0) = \chi, \tag{7.1a}$$
$$y(t) = h(x(t), u(t), w(t)) \tag{7.1b}$$

with discrete time $t \in \mathbb{I}_{\geq 0}$, state $x(t) \in \mathbb{R}^n$, initial condition $\chi \in \mathbb{R}^n$, control input $u(t) \in \mathbb{R}^m$, (generalized) disturbance input $w(t) \in \mathbb{R}^q$, output $y(t) \in \mathbb{R}^p$, and functions $f : \mathbb{R}^n \times \mathbb{R}^m \times \mathbb{R}^q \to \mathbb{R}^n$ and $h : \mathbb{R}^n \times \mathbb{R}^m \times \mathbb{R}^q \to \mathbb{R}^p$. Let $\mathcal{Z} := \mathcal{X} \times \mathcal{U} \times \mathcal{W}$ for some $\mathcal{X} \subseteq \mathbb{R}^n$, $\mathcal{U} \subseteq \mathbb{R}^m$, and $\mathcal{W} \subseteq \mathbb{R}^q$ be such that $f(x, u, w) \in \mathcal{X}$ and $h(x, u, w) \in \mathcal{Y}$ for all $(x, u, w) \in \mathcal{Z}$. In the context of state estimation, this forward-invariance property allows to incorporate *a priori* knowledge of the physical domain of the system, compare Section 3.1. Here, it is merely required for technical reasons in the proof of Theorem 7.1 below.

We are interested in verifying the following exponential detectability property of the system in (7.1).

Definition 7.1 (Quadratically bounded i-IOSS Lyapunov function)**.** *A continuous function $U : \mathcal{X} \times \mathcal{X} \to \mathbb{R}_{\geq 0}$ is a quadratically bounded i-IOSS Lyapunov function on $\mathcal{Z}$ if there exist matrices $\underline{P}, \overline{P}, Q, R \succ 0$ and a constant $\eta \in (0, 1)$ such that*

$$|x_1 - x_2|_{\underline{P}}^2 \leq U(x_1, x_2) \leq |x_1 - x_2|_{\overline{P}}^2, \tag{7.2a}$$

$$\begin{aligned} &U(f(x_1, u, w_2), f(x_2, u, w_2)) \\ &\leq \eta U(x_1, x_2) + |w_1 - w_2|_Q^2 + |h(x_1, u, w_1) - h(x_2, u, w_2)|_R^2 \end{aligned} \tag{7.2b}$$

for all $(x_1, u, w_1), (x_2, u, w_2) \in \mathcal{Z}$.

Note that by a straightforward adaption of the converse Lyapunov theorem from [ART21], one can easily show that the existence of a quadratically bounded i-IOSS Lyapunov function in the sense of Definition 7.1 is equivalent to the system (7.1) being exponentially i-IOSS (and hence exponentially detectable).

We make the following assumption on the regularity of the system (7.1).

Assumption 7.1 (Differentiability)**.** *The functions f and h are continuously differentiable on $\mathcal{Z}$.*

Under Assumption 7.1, we can evaluate the linearizations of f and h at a given point $(x, u, w) \in \mathcal{Z}$ as

$$\begin{aligned} A(x,u,w) &= \frac{\partial f}{\partial x}(x,u,w), \quad B(x,u,w) = \frac{\partial f}{\partial w}(x,u,w), \\ C(x,u,w) &= \frac{\partial h}{\partial x}(x,u,w), \quad D(x,u,w) = \frac{\partial h}{\partial w}(x,u,w), \end{aligned} \tag{7.3}$$

where we omit the dependency of A, B, D, C on (x, u, w) whenever it is clear from the context.

Now consider an arbitrary change of coordinates $\bar{x} = \phi(x)$ with $\phi : \mathbb{R}^n \to \mathbb{R}^n$, which results in the equivalent system dynamics

$$\bar{f}(\bar{x}, u, w) := \phi(f(\phi^{-1}(\bar{x}), u, w)), \tag{7.4a}$$

$$\bar{h}(\bar{x}, u, w) := h(\phi^{-1}(\bar{x}), u, w). \tag{7.4b}$$

Assumption 7.2 (Coordinate transformation)**.** *There exists a diffeomorphism $\phi : \mathbb{R}^n \to \mathbb{R}^n$ such that the function $\bar{h}$ in* (7.4b) *is affine in $(\bar{x}, w)$, and $\partial \bar{h}/\partial \bar{x}_i = 0$ for all $i = 1, \dots n - p$.*

Provided that Assumption 7.2 holds, the transformed dynamics (7.4) are such that the transformed output $\bar{h}$ in (7.4b) depends affinely on a subset of the system state $\bar{x}$, which is similar to the class of systems considered in [YWM22]. Note that this is a fairly general setup covering several observability normal forms and therefore many physical models that admit a corresponding transformation, compare [YWM22, Rem. 1] and see also [NS90, Sec. 5.1] for further details. Moreover, as we show in the following remark, the design of ϕ is particularly simple when a linear combination of the state is measured, which is the case in many practical applications, compare the example systems in Section 3.4.

Remark 7.1 (Coordinate transformation)**.** *In case the output function in* (7.1b) *is linear, i.e., satisfies $h(x, \cdot, \cdot) = Cx$ for some appropriate matrix $C \in \mathbb{R}^{p \times n}$ (neglecting the inputs u and w for clarity), Assumption 7.2 can be trivially fulfilled using a linear change of coordinates $\bar{x} = \phi(x) = Tx$ with T being a suitable non-singular transformation matrix. Indeed, for any $C \in \mathbb{R}^{p \times n}$, one can find a non-singular $T \in \mathbb{R}^{n \times n}$ such that $h(x, \cdot, \cdot) = Cx = CT^{-1}\bar{x} = [0_{p \times (n-p)}, \bar{C}]\bar{x} =: \bar{h}(\bar{x}, \cdot, \cdot)$ holds for some matrix $\bar{C} \in \mathbb{R}^{p \times p}$. This immediately implies that $\bar{h}$ is linear (and thus affine) in $\bar{x}$ and $\partial \bar{h}/\partial \bar{x}_i = 0$ for all $i = 1, \dots, n-p$. In fact, the condition $CT^{-1} = [0_{p \times (n-p)}, \bar{C}]$ represents an underdetermined system of linear equations that has infinitely many solutions, which can therefore also be used as an additional tuning knob (e.g., for normalization).*

We partition the state $\bar{x}$ into two parts

$$\bar{x} = \begin{bmatrix} \bar{x}_x \\ \bar{x}_y \end{bmatrix}$$

with $\bar{x}_x \in \mathbb{R}^{n-p}$ and $\bar{x}_y \in \mathbb{R}^p$. Then, the following Theorem yields a quadratically bounded i-IOSS Lyapunov function according to Definition 7.1.

Theorem 7.1. *Let Assumptions 7.1 and 7.2 hold and $P : \mathbb{R}^n \to \mathbb{R}^{n\times n}$ be such that*

$$P(x) = \frac{\partial \phi}{\partial x}(x)^\top \bar{P}(\phi(x)) \frac{\partial \phi}{\partial x}(x) \tag{7.5}$$

with

$$\bar{P}(\bar{x}) = \begin{bmatrix} \bar{P}_x(\bar{x}_x) & 0 \\ 0 & \bar{P}_y \end{bmatrix} \tag{7.6}$$

for some $\bar{P}_x : \mathbb{R}^{n-p} \to \mathbb{R}^{(n-p)\times(n-p)}$ and $\bar{P}_y \in \mathbb{R}^{p\times p}$. Let $\mathcal{X}$ be weakly geodesically convex[1], and $\mathcal{W}$ be convex. If there exist $\eta \in (0,1)$ and symmetric matrices $\underline{P}, \overline{P} \succ 0$ and $Q, R \succeq 0$ such that

$$\begin{bmatrix} A^\top P_+ A - \eta P - C^\top R C & A^\top P_+ B - C^\top R D \\ B^\top P_+ A - D^\top R C & B^\top P_+ B - Q - D^\top R D \end{bmatrix} \preceq 0 \tag{7.7}$$

and

$$\underline{P} \preceq P(x) \preceq \overline{P} \tag{7.8}$$

hold for all $(x, u, w) \in \mathcal{Z}$ with $P_+ = P(f(x, u, w))$, then there exists a quadratically bounded i-IOSS Lyapunov function U that satisfies Definition 7.1.

The proof of Theorem 7.1 employs several properties and arguments from Riemannian geometry. For the sake of notation, we use $x^+ = f(x, u, w)$ to denote the successor state of x under the dynamics f given the inputs u and w.

Proof of Theorem 7.1. The proof consists of three parts. First, we establish the dissipation inequality (7.2b); second, we derive the bounds (7.2a), where we initially assume that the conditions (7.7)–(7.8) hold globally on $\mathbb{R}^n \times \mathbb{R}^m \times \mathbb{R}^q$. Finally, we show that the corresponding results also hold if the conditions are enforced on the subset $\mathcal{Z} = \mathcal{X} \times \mathcal{U} \times \mathcal{W}$ only.

Part I: Consider two arbitrary points (x_1, u, w_1) and (x_2, u, w_2) that are element of $\mathbb{R}^n \times \mathbb{R}^m \times \mathbb{R}^q$ with their corresponding outputs $y_1 = h(x_1, u, w_1)$ and $y_2 = h(x_2, u, w_2)$. Define a smooth path $c : [0, 1] \to \mathbb{R}^n$ parameterized by s joining x_1 to x_2 with $c(0) = x_1$ and $c(1) = x_2$. Define the smooth path of disturbances $\omega(s)$ joining $\omega(0) = w_1$ and $\omega(1) = w_2$ by the straight line

$$\omega(s) = w_1 + s(w_2 - w_1), \quad s \in [0, 1]. \tag{7.9}$$

Note that this particular choice is valid since the disturbance can generally be treated as an external variable that does not depend on any dynamics; therefore, the path connecting w_1 and w_2 can be of arbitrary form. Given the tuple $(c(s), u, \omega(s))$, we can apply the dynamics (7.1) and obtain

$$c^+(s) = f(c(s), u, \omega(s)), \tag{7.10a}$$
$$\zeta(s) = h(c(s), u, \omega(s)), \tag{7.10b}$$

[1]Geodesic convexity is a natural generalization of convexity for sets to Riemannian manifolds, which reduces to convexity for the special case of constant metrics. For a formal definition, see, e.g., [SP12, Def. 2.6].

where the corresponding output ζ yields a smooth path joining $\zeta(0) = y_1$ and $\zeta(1) = y_2$. By differentiating (7.10) with respect to $s \in [0, 1]$, from the chain rule and the linearizations (7.3) we obtain the differential dynamics

$$\delta_x^+ = A(c(s), u, \omega(s))\delta_x + B(c(s), u, \omega(s))\delta_w, \tag{7.11a}$$
$$\delta_y = C(c(s), u, \omega(s))\delta_x + D(c(s), u, \omega(s))\delta_w, \tag{7.11b}$$

where the path derivatives are defined as $\delta_x^+ := dc^+/ds(s)$, $\delta_x := dc/ds(s)$, $\delta_w := d\omega/ds(s)$, and $\delta_y := d\zeta/ds(s)$. Formally, each δ_i with $i \in \{x, w, y\}$ denotes a vector on the tangent space of the domain of i at i, compare [MS17; MS18]. We make the following claim.

Claim 7.1. *Let* (7.7) *hold for some* $(x, u, w) \in \mathbb{R}^n \times \mathbb{R}^m \times \mathbb{R}^q$. *Then,* $V(x, \delta_x) = \delta_x^\top P(x)\delta_x$ *satisfies*

$$V(x^+, \delta_x^+) \leq \eta V(x, \delta_x) + |\delta_w|_Q^2 + |\delta_y|_R^2. \tag{7.12}$$

Proof. By applying the definition of V together with the differential dynamics (7.11a)-(7.11b) to (7.12), we obtain

$$\begin{bmatrix}\delta_x \\ \delta_w\end{bmatrix}^\top \begin{bmatrix}A^\top P_+ A - \eta P & A^\top P_+ B \\ B^\top P_+ A & B^\top P_+ B\end{bmatrix} \begin{bmatrix}\delta_x \\ \delta_w\end{bmatrix} \preceq \begin{bmatrix}\delta_x \\ \delta_w\end{bmatrix}^\top \begin{bmatrix}C^\top RC & C^\top RD \\ D^\top RC & Q + D^\top RD\end{bmatrix} \begin{bmatrix}\delta_x \\ \delta_w\end{bmatrix},$$

which clearly is equivalent to (7.7). □

Consequently, by definition of V and the path derivatives $(\delta_x, \delta_w, \delta_y)$, from (7.12) it follows that

$$\left|\frac{dc^+}{ds}(s)\right|_{P_+}^2 \leq \eta \left|\frac{dc}{ds}(s)\right|_P^2 + \left|\frac{d\omega}{ds}(s)\right|_Q^2 + \left|\frac{d\zeta}{ds}(s)\right|_R^2. \tag{7.13}$$

This differential property can now be transformed into an incremental property by integration over $s \in [0, 1]$ and utilizing tools from Riemannian geometry. In particular, we treat P as a Riemannian[2] metric with which the manifold $\mathbb{R}^n$ is endowed. Let

$$E(c) := \int_0^1 \frac{dc}{ds}(s)^\top P(c(s)) \frac{dc}{ds}(s) ds \tag{7.14}$$

denote the Riemannian energy associated with the path c. The minimizer of $E(c)$ over all possible smooth paths joining $c(0)$ to $c(1)$ is given by a (possibly non-unique) *geodesic* γ, existence of which is ensured by the uniformly boundedness of P in (7.8), compare [MS17, Lem. 1] and see also [SP12, Lem. A.1].

Now, consider (7.13) and choose $c = \gamma$; it hence follows that $c^+(s) = f(\gamma(s), u, \omega(s))$ by (7.10a). Let γ^+ denote the geodesic at the subsequent time instant joining the successor states $x_1^+ = f(x_1, u, w_1)$ and $x_2^+ = f(x_2, u, w_2)$, where we point out that in

[2] A Riemannian metric $P : \mathbb{R}^n \to \mathbb{R}^{n \times n}$ is a symmetric covariant 2-tensor with positive definite values that defines local notions of length, angle, and orthogonality by the inner product $\langle \delta_1, \delta_2 \rangle_x = \delta_1^\top P(x)\delta_2$ for any two tangent vectors δ_1, δ_2, compare [SP12; MS17], and see also [GHL04] for further details.

general $c^+ \neq \gamma^+$. However, by integration of (7.13) over $s \in [0,1]$ and the definition of the Riemannian energy (7.14), we obtain

$$E(\gamma^+) \leq E(c^+) \leq \eta E(\gamma) + \int_0^1 \left| \frac{d\omega}{ds}(s) \right|_Q^2 ds + \int_0^1 \left| \frac{d\zeta}{ds}(s) \right|_R^2 ds, \tag{7.15}$$

where the first inequality used the fact that c^+ is a feasible candidate curve providing an upper bound for the (minimal) energy $E(\gamma^+)$. In the following, we show that $U(x_1, x_2) = E(\gamma)$ satisfies the dissipation inequality (7.2b). First, exploiting our particular choice of ω in (7.9) yields

$$\int_0^1 \left| \frac{d\omega}{ds}(s) \right|_Q^2 ds = \int_0^1 |w_1 - w_2|_Q^2 \, ds = |w_1 - w_2|_Q^2 \,. \tag{7.16}$$

Now we focus on the output term in (7.15) and make the following claim.

Claim 7.2. *The derivative $d\zeta/ds(s)$ is constant in $s \in [0,1]$.*

Proof. Given γ and ϕ, we can define the geodesic in transformed coordinates $\bar{\gamma} := \phi(\gamma)$. From (7.10b) and (7.4b), we have that

$$\zeta(s) = h(\phi^{-1}(\bar{\gamma}(s)), u, \omega(s)) = \bar{h}(\bar{\gamma}(s), u, \omega(s)) \tag{7.17}$$

for all $s \in [0,1]$. Taking the derivative of (7.17) with respect to $s \in [0,1]$ using the chain rule yields

$$\frac{d\zeta}{ds}(s) = \frac{d\bar{h}}{ds}(\bar{\gamma}(s), u, \omega(s)) = \frac{\partial \bar{h}}{\partial \bar{x}}(\bar{\gamma}(s), u, \omega(s)) \frac{d\bar{\gamma}}{ds}(s) + \frac{\partial \bar{h}}{\partial w}(\bar{\gamma}(s), u, \omega(s)) \frac{d\omega}{ds}(s).$$

Assumption 7.2 ensures that $\bar{h}$ is affine in $\bar{x}, w$, and consequently, the partial derivatives $\partial \bar{h}/\partial \bar{x}(\bar{\gamma}(s), u, \omega(s))$ and $\partial \bar{h}/\partial w(\bar{\gamma}(s), u, \omega(s))$ do not depend on s; furthermore, $\partial \bar{h}/\partial \bar{x}_i(\bar{\gamma}(s), u, \omega(s)) = 0$ for all $i = 1, \ldots, n-p$. Since, in addition, $d\omega/ds(s)$ is constant in $s \in [0,1]$ due to (7.9), it remains to show that this is also the case for $d\bar{\gamma}_i/ds(s)$ for all $i = n-p+1, \ldots, n$.

To this end, recall that $\bar{\gamma} = \phi(\gamma)$. Hence, by the chain rule,

$$\frac{d\bar{\gamma}}{ds}(s) = \frac{\partial \phi}{\partial x}(\gamma(s)) \frac{d\gamma}{ds}(s).$$

Due to our choice of P in (7.5), it therefore holds that

$$\begin{aligned}
\bar{E}(\bar{\gamma}) &:= \int_0^1 \frac{d\bar{\gamma}}{ds}(s)^\top \bar{P}(\bar{\gamma}(s)) \frac{d\bar{\gamma}}{ds}(s) ds \\
&= \int_0^1 \frac{d\gamma}{ds}(s)^\top \frac{\partial \phi}{\partial x}(\gamma(s))^\top \bar{P}(\phi(\gamma(s))) \frac{\partial \phi}{\partial x}(\gamma(s)) \frac{d\gamma}{ds}(s) ds \\
&= \int_0^1 \frac{d\gamma}{ds}(s)^\top P(\gamma(s)) \frac{d\gamma}{ds}(s) ds \\
&= E(\gamma).
\end{aligned}$$

Thus, given a minimizing geodesic γ for $E(\gamma)$, the curve $\bar{\gamma}$ is a minimizing geodesic for $\bar{E}(\bar{\gamma})$ (by contradiction). Consequently, we have that $\bar{\gamma}(s) = \phi(\gamma(s))$ is a solution to the geodesic equation [GHL04, Def. 2.77], i.e., to the differential system

$$\frac{d^2\bar{\gamma}_k}{ds^2}(s) - \sum_{i,j} \bar{\Gamma}^k_{i,j}(\bar{\gamma}(s))\frac{d\bar{\gamma}_i}{ds}(s)\frac{d\bar{\gamma}_j}{ds}(s) = 0, \quad k = 1, \dots, n. \tag{7.18}$$

The objects $\bar{\Gamma}^k_{i,j}$ represent the Christoffel symbols associated with the metric $\bar{P}$ which are, following [GHL04, Prop 2.54] and Appendix A1.1 in the report (arXiv) version of the article [SP24], defined by

$$\bar{\Gamma}^k_{i,j}(\bar{x}) = \frac{1}{2}\sum_{a=1}^{n} \bar{Y}_{k,a}(\bar{x}) \left(\frac{\partial \bar{P}_{a,i}}{\partial \bar{x}_j}(\bar{x}) + \frac{\partial \bar{P}_{a,j}}{\partial \bar{x}_i}(\bar{x}) - \frac{\partial \bar{P}_{i,j}}{\partial \bar{x}_a}(\bar{x}) \right) \tag{7.19}$$

with the shorthand notation $\bar{Y}(\bar{x}) = \bar{P}(\bar{x})^{-1}$ and $\bar{Y}_{k,a}$ the (k,a)-element of $\bar{Y}$. Note that in (7.18), we are only interested in the states of the geodesic $\bar{\gamma}$ that appear in the output (7.17), i.e., $\bar{\gamma}_k$ for all $k = n - p + 1, \dots, n$. For ease of notation, let us define $r := n - p + 1$ for the remainder of this proof. Calculating the respective Christoffel symbols reveals that

$$\bar{\Gamma}^k_{ij} = 0, \quad k = r, \dots, n, \tag{7.20}$$

which is a direct consequence of the proposed block-diagonal structure of $\bar{P}$ in (7.6); to see this, note the following: First, the fact that $\bar{P}$ is block-diagonal implies that also $\bar{Y} = \bar{P}^{-1}$ is block-diagonal, and thus $\bar{Y}_{i,j} = \bar{P}_{i,j} = 0$ for $i < r$ and $j \geq r$ (and *vice versa*); second, each derivative $\partial \bar{P}_{i,j}/\partial \bar{x}_a = 0$ if $a \geq r$ since $\bar{P}$ is independent of $\bar{x}_y$; third, each derivative $\partial \bar{P}_{a,i}/\partial \bar{x}_j = 0$ if $a, i \geq r$, and $j < r$ since $\bar{P}_y$ is constant.

Consequently, from (7.20), we have that all the Christoffel symbols affecting the states $\bar{\gamma}_i$, $i = r, \dots, n$ vanish, and hence our special choice of $\bar{P}$ leads to a decoupling of the geodesic equation (7.18); in particular, we obtain the simple second-order homogeneous differential equation

$$\frac{d^2\bar{\gamma}_k}{ds^2}(s) = 0, \quad k = r, \dots, n,$$

which directly implies that $d\bar{\gamma}_i/ds(s)$ is constant in $s \in [0,1]$ for all $i = r, \dots, n$ and hence yields the desired result. □

Consequently, the output term in (7.15) consists only of terms constant in $s \in [0,1]$. Hence, by the Fundamental Theorem of Calculus, we obtain

$$\int_0^1 \left| \frac{d\zeta}{ds}(s) \right|_R^2 ds = (\zeta(1) - \zeta(0))^\top R(\zeta(1) - \zeta(0)) = |y_1 - y_2|_R^2 . \tag{7.21}$$

Applying (7.16) and (7.21) to (7.15) then yields

$$E(\gamma^+) \leq \eta E(\gamma) + |w_1 - w_2|_Q^2 + |y_1 - y_2|_R^2, \tag{7.22}$$

which establishes the dissipation inequality (7.2b) with $U(x_1, x_2) = E(\gamma)$.

Part II: We now show satisfaction of (7.2a) and start with the upper bound. Note that since γ is the path of minimum energy joining x_1 to x_2, every other path yields a higher amount of energy, which clearly also applies to the straight line $l(s) = x_1 + s(x_2 - x_1)$. Therefore,

$$E(\gamma) \leq E(l) = \int_0^1 (x_1 - x_2)^\top P(l(s))(x_1 - x_2) ds \leq |x_1 - x_2|_{\overline{P}}^2, \tag{7.23}$$

where the last step follows from uniform boundedness of P in (7.8). For the lower bound, again by uniform boundedness of P, we have

$$E(\gamma) \geq \int_0^1 \frac{\partial \gamma}{ds}(s)^\top \underline{P} \frac{\partial \gamma}{ds}(s) ds \tag{7.24}$$

$$\geq \int_0^1 \frac{\partial l}{ds}(s)^\top \underline{P} \frac{\partial l}{ds}(s) ds = |x_1 - x_2|_{\underline{P}}^2, \tag{7.25}$$

where for the second inequality we exploited the fact that the minimizer of the expression on the right hand side of (7.24) is given by the straight line l since $\underline{P}$ is constant. To verify this, recall that each minimizer of the Riemannian energy E solves the geodesic equation (7.18); now observe that all the Christoffel symbols (7.19) vanish if the underlying metric is constant. Therefore, (7.23) and (7.25) establish (7.2a). Together with the first part of this proof, we can thus conclude that $U(x_1, x_2) = E(\gamma)$ is an i-IOSS Lyapunov function satisfying (7.2a) and (7.2b) for all $(x_1, u, w_1), (x_2, u, w_2) \in \mathbb{R}^n \times \mathbb{R}^m \times \mathbb{R}^q$.

Part III: Finally, we note that the results from Part I and Part II, (including the Claims 7.1 and 7.2) can be easily restricted to any subset $\mathcal{X} \times \mathcal{U} \times \mathcal{W}$ if it is ensured that the minimizing geodesic connecting any two points on each of the subsets $\mathcal{X}$ and $\mathcal{W}$ stays in the respective subset for all $s \in [0, 1]$. This is indeed the case for $\mathcal{X}$ being weakly geodesically convex [SP12, Def. 2.6] and $\mathcal{W}$ being convex (as long as ω is chosen according to (7.9)). Provided that this applies, if conditions (7.7)-(7.8) are enforced on the subset $\mathcal{Z} = \mathcal{X} \times \mathcal{U} \times \mathcal{W}$, we have that $U(x_1, x_2) = E(\gamma)$ is a quadratically bounded i-IOSS Lyapunov function satisfying Definition 7.1 for all $(x_1, u, w_1), (x_2, u, w_2) \in \mathcal{Z}$, which completes this proof. □

We point out that for a fixed transformation ϕ and a constant $\eta \in (0, 1)$, conditions (7.7)-(7.8) reduce to linear constraints that need to be verified over the full domain $\mathcal{Z} = \mathcal{X} \times \mathcal{U} \times \mathcal{W}$. Computationally tractable sufficient conditions in terms of LMIs can then be obtained by using, for example, LPV embeddings [KT21], SOS relaxations [Par03; WMB22], or simple gridding methods. In case ϕ is treated as a decision variable (which may be less restrictive due to this additional degree of freedom), the conditions of Theorem 7.1 can be reformulated as a convex optimization problem in a similar manner as in [YWM22].

The following corollary of Theorem 7.1 provides even simpler conditions for the case where h in (7.1b) is affine in (x, w) and we restrict ourselves to a quadratic (instead of quadratically bounded) i-IOSS Lyapunov function.

Corollary 7.1. *Let Assumption 7.1 hold, the output function h in* (7.1b) *be affine in (x, w), and $\mathcal{X}$ and $\mathcal{W}$ be convex. If there exist $\eta \in (0, 1)$ and symmetric matrices $P \succ 0$ and $Q, R \succeq 0$ such that*

$$\begin{bmatrix} A^\top PA - \eta P - C^\top RC & A^\top PB - C^\top RD \\ B^\top PA - D^\top RC & B^\top PB - Q - D^\top RD \end{bmatrix} \preceq 0 \tag{7.26}$$

holds for all $(x, u, w) \in \mathcal{Z}$, then $U(x_1, x_2) = |x_1 - x_2|_P^2$ is an i-IOSS Lyapunov function on $\mathcal{Z}$ and satisfies Definition 7.1 with $\underline{P} = \overline{P} = P$.

Proof. The result follows immediately by setting $\bar{x}_y = \bar{x} = \phi(x) = x$ in the proof of Theorem 7.1, which can then be significantly streamlined (without the need for Assumption 7.2), compare also the proof of Theorem 7.2 for the continuous-time case below. As a direct consequence, we obtain (7.22) with $E(\gamma) = |x_1 - x_2|_P^2$ and $E(\gamma^+) = |x_1^+ - x_2^+|_P^2$ since P is constant (resulting in the geodesics being straight lines), which lets us conclude that $U(x_1, x_2) = |x_1 - x_2|_P^2$ is a quadratic i-IOSS Lyapunov function that satisfies Definition 7.1 with $\underline{P} = \overline{P} = P$ for all $(x_1, u, w_1), (x_2, u, w_2) \in \mathcal{Z}$. □

Some remarks are in order.

Remark 7.2 (Relation to dissipativity)**.** *The proof of Theorem 7.1 introduces a differential version of IOSS (see Claim 7.1). This characterization is equivalent to the notion of differential (Q,S,R)-dissipativity [Ver+23, Def. 3] with $S = 0$, compare also [KT21; FS13]. However, as pointed out in [Ver+23, Rem. 7], the corresponding works crucially rely on $R \preceq 0$ in order to derive incremental results by simply exhausting the Cauchy-Schwartz inequality, see [KT21, Lem. 16] and compare also [MS18, Thm. 1] and [WMB22, Thm. 2.4]. Note that in our case, this would restrict the results to open-loop stable systems (since* (7.2b) *would need to hold with $R = 0$, which directly implies i-ISS of system* (7.1)*). Moreover, this would result in the cost function* (3.6) *not being positive definite, which generally can lead to an ill-defined optimization problem* (3.4)*. In contrast, we circumvent this technical condition by suitably relating the state and output manifolds as it was similarly done in [SP24; YWM22] for observer design. More specifically, from Assumption 7.2, i.e., by imposing the existence of coordinates $\bar{x}$ in which the output function $\bar{h}$ is affine (which directly implies that $\bar{h}$ is totally geodesic by assumption, compare [Vil70]), and due to our choice of the metric $\bar{P}(\bar{x})$ according to Theorem 7.1 (or Corollary 7.1), we immediately obtain an equality relation between the integral of the differential supply rates and the incremental supply rates, see* (7.16) *and* (7.21) *for details. Consequently, as a side result, we note that Theorem 7.1 (and Corollary 7.1) with $\eta = 1$ can be used to verify incremental dissipativity of system* (7.1) *subject to a positive definite supply rate, relaxing [Ver+23, Rem. 7].*

Remark 7.3 (Extensions)**.** *To further generalize the parametrization of $\bar{P}(\bar{x})$ with respect to $\bar{x}$, we note that the following minor extension of Theorem 7.1 is possible if, e.g., $\bar{h}(\bar{x}) = \bar{x}_y$ (neglecting u and w for ease of presentation). We could choose*

$$\bar{P}(\bar{x}) = \begin{bmatrix} \bar{P}_x(\bar{x}_x) & 0 \\ 0 & \bar{P}_y(\bar{x}_y) \end{bmatrix} \tag{7.27}$$

with $\bar{P}_{y,1} \preceq \bar{P}_y(\bar{x}_y) \preceq \bar{P}_{y,2}$ uniformly for all possible $\bar{x}_y$ and some constant matrices $\bar{P}_{y,1}, \bar{P}_{y,2} \succ 0$; that is, $\bar{P}$ in (7.6) *with an additional dependency of $\bar{P}_y$ on $\bar{x}_y$. Then, the geodesic $\bar{\gamma}$ minimizes the two independent functionals*

$$\bar{E}(\bar{\gamma}) = \int_0^1 \frac{d\bar{\gamma}_x}{ds}(s)^\top \bar{P}_x(\bar{\gamma}_x(s)) \frac{d\bar{\gamma}_x}{ds}(s) ds + \int_0^1 \frac{d\bar{\gamma}_y}{ds}(s)^\top \bar{P}_y(\bar{\gamma}_y(s)) \frac{d\bar{\gamma}_y}{ds}(s) ds. \tag{7.28}$$

Note that a direct consequence of $\bar{P}_y(\bar{x}_y)$ not being constant is that Claim 7.2 does not hold in this case. However, by additionally imposing that $R \preceq \bar{P}_y(\bar{x}_y)$ in (7.7)*, the output functional in* (7.13) *can be bounded by*

$$\int_0^1 \left| \frac{d\zeta}{ds}(s) \right|_R^2 ds \leq \int_0^1 \frac{d\bar{\gamma}_y}{ds}(s)^\top \bar{P}_y(\bar{\gamma}_y(s)) \frac{d\bar{\gamma}_y}{ds}(s) ds, \tag{7.29}$$

i.e., the same functional that also appears in (7.28) *and hence is minimized by $\bar{\gamma}$. Then, by following similar arguments as in the second part of the proof of Theorem 7.1 (in particular, exploiting* (7.29) *and uniform boundedness of $\bar{P}_y$), one can show that*

$$\int_0^1 \left| \frac{d\zeta}{ds}(s) \right|_R^2 ds \leq |y_1 - y_2|^2_{\bar{P}_{y,2}}$$

and subsequently derive a similar i-IOSS Lyapunov function as in Theorem 7.1 that satisfies Definition 7.1. Finally, we note that one may relax Assumption 7.2, i.e., affinity of $\bar{h}$, by imposing that $\bar{h}$ is a Riemannian submersion, compare [SP24].

Remark 7.4 (Closed-form expression)**.** *Note that Theorem 7.1 yields only an implicit i-IOSS Lyapunov function U, which is due to the fact that we have no analytical closed-form expression for the Riemannian energy of the minimizing geodesic. However, note also that this is not needed for the design of Lyapunov-based MHE (or FIE) schemes, since we only require knowledge of the discount factor η and the matrices $\overline{P}, Q, R$ to design the MHE cost function (and additionally $\underline{P}$ to compute the minimal horizon length for guaranteed RGES of MHE, see [Sch+23, Sec. III] for further details). Similar considerations apply if Theorem 7.1 is used to compute the $\mathcal{KL}$-functions of the standard i-IOSS bound. Again, one only needs to know the matrices $\underline{P}, \overline{P}, Q, R$ and use* (7.2a) *after repeated application of the dissipation inequality* (7.2b) *to obtain the desired result. If nevertheless an analytical expression for the i-IOSS Lyapunov function U is desired, Corollary 7.1 can be used to obtain a quadratic function.*

Remark 7.5 (Alternative derivation)**.** *An alternative way to compute a quadratic i-IOSS Lyapunov function is to first design an RGES observer based on, e.g., [SP16; YWM22; Ast+21]. Then, under certain conditions, one can show that the corresponding Lyapunov function also serves as an i-IOSS Lyapunov function, see [KMA21, Prop. 4] and compare also [SM23d, Sec. VII]. However, these sufficient conditions are crucially limited to quadratic Lyapunov functions and additive disturbances in the dynamics* (7.1a)*, and hence are only applicable to a smaller class of detectable systems (in comparison to Theorem 7.1).*

7.1.2. i-iIOSS Lyapunov functions for continuous-time systems

We consider the continuous-time, nonlinear perturbed system from (3.7), that is,

$$\dot{x}(t) = f(x(t), u(t), w(t)), \quad x(0) = \chi, \tag{7.30a}$$
$$y(t) = h(x(t), u(t), w(t)), \tag{7.30b}$$

with continuous time $t \geq 0$, state $x(t) \in \mathcal{X} \subseteq \mathbb{R}^n$, initial condition $\chi \in \mathcal{X}$, control input $u(t) \in \mathcal{U} \subseteq \mathbb{R}^m$, (generalized) disturbance input $w(t) \in \mathcal{W} \subseteq \mathbb{R}^q$, and output $y(t) \in \mathcal{Y} \subseteq \mathbb{R}^p$. Throughout the following, for simplicity we assume that for any $\chi \in \mathcal{X}$, and functions $u \in \mathcal{M}_\mathcal{U}$ and $w \in \mathcal{M}_\mathcal{W}$ (where we recall that $\mathcal{M}_\mathcal{U}$ and $\mathcal{M}_\mathcal{W}$ contain all measurable, locally essentially bounded functions defined on $\mathbb{R}_{\geq 0}$ and taking values in $\mathcal{U}$ and $\mathcal{W}$, respectively), the solution $x(t, \chi, u, w)$ is unique, exists globally on $\mathbb{R}_{\geq 0}$, and satisfies $x(t, \chi, u, w) \in \mathcal{X}$ and $y(t, \chi, u, w) = h(x(t, \chi, u, w), u(t), w(t)) \in \mathcal{Y}$ for all $t \geq 0$, see also Section 3.2.1 for more details regarding the setup. Furthermore, we define $\mathcal{Z} := \mathcal{X} \times \mathcal{U} \times \mathcal{W}$.

We impose the following regularity properties on the system and its input signals.

Assumption 7.3 (Regularity conditions)**.** *The function f is continuously differentiable in all of its arguments, h is affine in (x, w), and the sets $\mathcal{X}$ and $\mathcal{W}$ are convex. Furthermore, the input signals u and w are piecewise[3] right-continuous.*

We comment on Assumption 7.3 below Remark 7.6. In the remainder of this section, we focus on the construction of smooth, quadratically bounded i-iIOSS Lyapunov functions.

Definition 7.2 (Quadratically bounded i-iIOSS Lyapunov function)**.** *A smooth function $U : \mathcal{X} \times \mathcal{X} \to \mathbb{R}_{\geq 0}$ is a quadratically bounded i-iIOSS Lyapunov function on $\mathcal{Z}$ if it is continuous and there exist matrices $\underline{P}, \overline{P}, Q, R \succ 0$ and a constant $\kappa > 0$ such that*

$$|x_1 - x_2|_{\underline{P}}^2 \leq U(x_1, x_2) \leq |x_1 - x_2|_{\overline{P}}^2, \tag{7.31a}$$
$$\dot{U}(x_1, x_2) \leq -\kappa U(x_1, x_2) + |w_1 - w_2|_Q^2 + |h(x_1, u, w_1) - h(x_2, u, w_2)|_R^2 \tag{7.31b}$$

for all $(x_1, u, w_1), (x_2, u, w_2) \in \mathcal{Z}$.

Remark 7.6 (Integral form)**.** *An i-iIOSS Lyapunov function satisfying Definition 7.2 is also an i-iIOSS Lyapunov function in the sense of Definition 2.3 using a dissipation inequality in integral form, compare also Assumption 3.1). To see this, consider any $\chi_1, \chi_2 \in \mathcal{X}$, $u \in \mathcal{M}_\mathcal{U}$, and $w_1, w_2 \in \mathcal{M}_\mathcal{W}$ satisfying Assumption 7.3 and define the corresponding trajectories $x_i(t) = x(t, \chi_i, u, w_i)$ and output signals*

[3] If the results contained in this section are to be applied to the methods presented in Section 3.2, it must be ensured that the estimated disturbance $\bar{w}_{t_i}$ in the MHE problem in (3.12) is also piecewise right-continuous. In practice, this is immediately the case when standard discretization methods are used to solve (3.12).

$y_i(t) = y(t, \chi_i, u, w_i)$, $t \geq 0$, $i = 1, 2$. *Now, let* $v : \mathbb{R}_{\geq 0} \to \mathbb{R}_{\geq 0}$ *be the solution of the initial value problem*

$$\dot{v}(t) = -\kappa v(t) + |w_1(t) - w_2(t)|_Q^2 + |y_1(t) - y_2(t)|_R^2, \quad v(0) = U(\chi_1, \chi_2).$$

Solving for v *yields*

$$v(t) = e^{-\kappa t} v(0) + \int_0^t e^{-\kappa(t-\tau)} \left(|w_1(t) - w_2(t)|_Q^2 + |y_1(t) - y_2(t)|_R^2 \right) d\tau.$$

Since the property in (7.31b) *applies, from the standard comparison principle we know that* $U(x_1(t), x_2(t)) \leq v(t)$ *for all* $t \geq 0$. *Recalling that* $v(0) = U(\chi_1, \chi_2)$ *establishes* (2.19b)*, where* $\eta = e^{-\kappa}$.

The construction of i-iIOSS Lyapunov functions satisfying Definition 7.2 can conceptually be performed similarly to the discrete-time case in Section 7.1.1—namely, by applying arguments from contraction theory and Riemannian geometry. For clarity of presentation, however, in the following we restrict ourselves to systems where the output equation (7.30b) is already affine in (x, w) as stated in Assumption 7.3, without considering a state-space transformation and partitioning as in Section 7.1.1, compare also Remark 7.7 below. This corresponds to the condition of Corollary 7.1 for the discrete-time case and allows us to easily transfer a differential property to an incremental one (it basically ensures that the output h evaluated along the shortest path between any two points $x_1, x_2 \in \mathcal{X}$ is a linear combination of the respective outputs y_1, y_2 for any point of that path). Note again that this is directly satisfied if a subset (or linear combination) of the system state is measured, which is the case for many practical applications, compare the examples in Section 3.4. Furthermore, it is still quite general in the sense that it covers several observable canonical forms, see [YWM22, Rem. 1].

We define the linearizations of (7.30) at a given point $(x, u, w) \in \mathcal{Z}$ as

$$\begin{aligned} A(x,u,w) &= \frac{\partial f}{\partial x}(x,u,w), \quad B(x,u,w) = \frac{\partial f}{\partial w}(x,u,w), \\ C(x,u,w) &= \frac{\partial h}{\partial x}(x,u,w), \quad D(x,u,w) = \frac{\partial h}{\partial w}(x,u,w), \end{aligned} \tag{7.32}$$

where we omit the dependency of A, B, D, C on (x, u, w) whenever it is clear from the context. The following result provides LMI conditions for the construction of quadratic Lyapunov functions.

Theorem 7.2. *Let Assumption 7.3 be satisfied. If there exist matrices* $P, Q, R \succ 0$ *and a constant* $\kappa > 0$ *such that*

$$\begin{bmatrix} PA + A^\top P + \kappa P - C^\top R C & PB - C^\top R D \\ B^\top P - D^\top R C & -D^\top R D - Q \end{bmatrix} \preceq 0 \tag{7.33}$$

holds for all $(x, u, w) \in \mathcal{Z}$, *then* $U(x_1, x_2) = |x_1 - x_2|_P^2$ *is a smooth i-iIOSS Lyapunov function on* $\mathcal{Z}$ *and satisfies Definition 7.2 with* $\underline{P} = \overline{P} = P$.

The proof follows similar lines as the proofs of, e.g., [MS18, Th. 1] and Theorem 7.1 above (with technical differences resulting from the continuous-time setup), compare also [MS17; Sin+17].

Proof of Theorem 7.2. For any pair of points $x_1, x_2 \in \mathcal{X}$, let $\Xi(x_1, x_2)$ denote the set of piecewise smooth curves $[0,1] \to \mathcal{X}$ connecting x_1 and x_2 such that $c \in \Xi(x_1, x_2)$ satisfies $c(0) = x_1$ and $c(1) = x_2$.

Given any $\chi_1, \chi_2 \in \mathcal{X}$, $u \in \mathcal{M}_{\mathcal{U}}$, and $w_1, w_2 \in \mathcal{M}_{\mathcal{W}}$ satisfying Assumption 7.3, we consider the trajectories $x_i(t) = x(t, \chi_i, u, w_i)$ and their output signals $y_i(t) = y(t, \chi_i, u, w_i)$, $t \geq 0$, $i = 1, 2$.

At any fixed time $t = t^\star \geq 0$, let us consider the following smoothly parameterized paths for $s \in [0,1]$: the path of states $c(t,s) \in \Xi(x_1(t), x_2(t))$ and the paths of disturbances $\omega(t,s) = w_1(t) + s(w_2(t) - w_1(t))$. For $t \in [t^\star, t^\star + \epsilon)$ (with $\epsilon > 0$ arbitrarily small to guarantee local existence of solutions and continuity of u, w over $t \in [t^\star, t^\star + \epsilon)$) and each fixed $s \in [0,1]$, the path $c(t,s)$ evolves according to (7.30) such that

$$\dot{c}(t,s) = f(c(t,s), u(t), \omega(t,s)), \tag{7.34a}$$
$$\zeta(t,s) = h(c(t,s), u(t), \omega(t,s)), \tag{7.34b}$$

where $\zeta(t,s)$ satisfies $y_1(t) = \zeta(t,0)$ and $y_2(t) = \zeta(t,1)$ for each $t \in [t^\star, t^\star + \epsilon)$. Differentiating (7.34) with respect to $s \in [0,1]$ yields (after interchanging the order of differentiation of t and s)

$$\dot{\delta}_x = A\delta_x + B\delta_w, \tag{7.35a}$$
$$\delta_y = C\delta_x + D\delta_w \tag{7.35b}$$

for all $t \in [t^\star, t^\star + \epsilon)$ using the substitutions $\delta_x := dc/ds(t,s)$, $\delta_w := d\omega/ds(t,s)$, and $\delta_y := d\zeta/ds(t,s)$, and where the matrices A, B, C, D are the linearizations of f and h as in (7.32) evaluated at $(c(t,s), u(t), \omega(t,s))$. Assuming that $(c(t,s), u(t), \omega(t,s)) \in \mathcal{X} \times \mathcal{U} \times \mathcal{W}$ for all $t \in [t^\star, t^\star + \epsilon)$, one can easily verify (by exploiting (7.35)) that satisfaction of the pointwise LMI condition (7.33) implies that

$$\frac{d}{dt}|\delta_x|_P^2 \leq -\kappa|\delta_x|_P^2 + |\delta_w|_Q^2 + |\delta_y|_R^2 \tag{7.36}$$

for all $t \in [t^\star, t^\star + \epsilon)$. By integrating (7.36) over $s \in [0,1]$, interchanging integration and differentiation, and defining $E(c(t,s)) := \int_0^1 |dc/ds(t,s)|_P^2 ds$, we obtain

$$\dot{E}(c(t,s)) \leq -\kappa E(c(t,s)) + \int_0^1 \left|\frac{d\omega}{ds}(t,s)\right|_Q^2 ds + \int_0^1 \left|\frac{d\zeta}{ds}(t,s)\right|_R^2 ds$$

for $t \in [t^\star, t^\star + \epsilon)$. The integration over $t \in [t^\star, t^\star + \epsilon)$ yields

$$\begin{aligned} &E(c(t^\star + \epsilon, s)) - E(c(t^\star, s)) \\ &\leq \int_{t^\star}^{t^\star + \epsilon} \left(-\kappa E(c(t,s)) + \int_0^1 \left|\frac{d\omega}{ds}(t,s)\right|_Q^2 ds + \int_0^1 \left|\frac{d\zeta}{ds}(t,s)\right|_R^2 ds \right) dt. \end{aligned} \tag{7.37}$$

Note that $E(c(t,s))$ can be interpreted as the Riemannian energy of the path $c(t,s)$. Since P is constant and $\mathcal{X}$ is convex, the shortest path $\gamma(t,s)$ (with the minimum energy $E(\gamma(t,s))$ over all possible curves $c(t,s) \in \Xi(x_1(t), x_2(t))$) is, at each fixed $t \geq 0$, always given by the straight line connecting $x_1(t)$ and $x_2(t)$, i.e., $\gamma(t,s) = x_1(t)+s(x_2(t)-x_1(t))$. Now let $c(t^\star, s) = \gamma(t^\star, s)$ in (7.37) and note that $E(\gamma(t,s)) \leq E(c(t,s))$ for all $t \in [t^\star, t^\star + \epsilon)$. Therefore, by taking $\epsilon \to 0$, we have that

$$\dot{E}(\gamma(t^\star,s)) \leq -\kappa E(\gamma(t^\star,s)) + \int_0^1 \left|\frac{d\omega}{ds}(t^\star,s)\right|_Q^2 ds + \int_0^1 \left|\frac{d\zeta}{ds}(t^\star,s)\right|_R^2 ds.$$

By construction of γ and ω (in particular, the fact that their derivatives with respect to $s \in [0,1]$ are constant in $s \in [0,1]$), it follows that

$$E(\gamma(t^\star,s)) = \int_0^1 \left|\frac{d\gamma}{ds}(t^\star,s)\right|_P^2 ds = |x_1(t^\star) - x_2(t^\star)|_P^2 \,,$$

and similarly,

$$\int_0^1 \left|\frac{d\omega}{ds}(t^\star,s)\right|_Q^2 ds = |w_1(t^\star) - w_2(t^\star)|_Q^2 \,.$$

Using the fact that h is affine in (x,w) by Assumption 7.3 (which implies that C and D are constant in s), we also obtain

$$\int_0^1 \left|\frac{d\zeta}{ds}(t^\star,s)\right|_R^2 ds = |y_1(t^\star) - y_2(t^\star)|_R^2 \,.$$

Since $t^\star \geq 0$ was arbitrary, using the definition $U(x_1,x_2) := |x_1 - x_2|_P^2$ we can infer that

$$\dot{U}(x_1(t),x_2(t)) \leq -\kappa U(x_1(t),x_2(t)) + |w_1(t) - w_2(t)|_Q^2 + |y_1(t) - y_2(t)|_R^2$$

for each $t \geq 0$. Since $x_i(t)$ and $y_i(t)$, $i = 1,2$ correspond to solutions of (7.30) for arbitrary $\chi_1, \chi_2 \in \mathcal{X}$, $u \in \mathcal{M}_\mathcal{U}$, and $w_1, w_2 \in \mathcal{M}_\mathcal{W}$ satisfying Assumption 7.3, we can conclude that U satisfies (7.31a)-(7.31b) for all $(x_1,u,w_1),(x_2,u,w_2) \in \mathcal{Z}$ with $\underline{P} = \overline{P} = P$, which establishes the statement and finishes this proof. □

For a fixed value of $\kappa > 0$, condition (7.33) represents an infinite set of LMIs (note that (7.33) is linear in the remaining decision variables P, Q, R). These may be solved using a finite set of LMIs and standard convex analysis tools based on semidefinite programming (SDP), e.g., by applying SOS relaxations [Par03], by embedding the nonlinear behavior in an LPV model [ST23], or by suitably gridding the state space and verifying (7.33) on the grid points.

Remark 7.7 (Generalizations)**.** *The requirement in Theorem 7.2 for P to be constant can be relaxed to a (block diagonal) state-dependent matrix $P(x)$ similar to Theorem 7.1 in discrete time if the system* (7.30) *is in some observer canonical form (or admits an appropriate state-space transformation), see Section 7.1.1 for more details. In this case, the LMI condition* (7.33) *can be accordingly modified to account for a state-dependent matrix $P(x)$, similar to, e.g., [MS18, Prop. 1].*

Remark 7.8 (Dissipativity)**.** *The LMI condition* (7.33) *can be modified to verify more general notions such as differential and incremental dissipativity (see, e.g., [Ver+23, Def. 2, Def. 3]). Here, we note that Theorem 7.2 is a generalization of established results in the sense that the LMI condition* (7.33) *is not restricted to certain supply rates with $R \preceq 0$ (which is a technical requirement in [Ver+23] to deduce incremental from differential properties [Ver+23, Rem. 7]), compare also Remark 7.2.*

7.2. Persistence of excitation

In this section, we focus on general nonlinear discrete-time systems that are subject to an additional unknown parameter. Identifying unknown parameters is a fundamental problem in control and signal processing, and various different approaches exist, see, e.g., the book [Lju99] for an introduction and overview of this topic. The ability to uniquely identify the system parameters requires that the measured (input-output) data is informative enough, which is usually achieved by ensuring that the input injected to the system is sufficiently exciting. In this context, PE is an important technical concept to formalize this condition and is usually the basis for the technical convergence analysis of corresponding identification or estimation algorithms, see, e.g., [Bit84; GM86; LG90; LB24], and compare also [Lju99, Ch. 13] and [Bes07, Ch. 1, Ch. 7]. While an *a priori* verification of PE is easily possible for LTV systems and can be ensured by a suitable choice of the input signal, this is generally impossible in the presence of nonlinear systems. For this reason, such rather abstract PE conditions are usually replaced in practice by considering suitable heuristics that are evaluated online, for example based on a sensitivity analysis as in [Liu+21], albeit at the price of losing formal guarantees.

In this section, we propose a method to online verify PE that is applicable to general nonlinear systems, which is a major relaxation in this context. We construct and evaluate a certain matrix recursion, which can be interpreted as the filtered linearized regressor information that is visible at the output. These results are applicable for the MHE schemes presented in Chapter 5 for joint state and parameter estimation, but also generally useful to verify PE of nonlinear systems online. We treat the case of constant parameters in Section 7.2.1 and the more general case of time-varying parameters in Section 7.2.2.

7.2.1. Constant parameters

We consider nonlinear discrete-time system in the form of (5.1) for the special case of constant parameters:

$$x(t+1) = f(x(t), u(t), w(t), p), \quad x(0) = \chi, \tag{7.38a}$$

$$y(t) = h(x(t), u(t), w(t), p). \tag{7.38b}$$

Here, we recall that $t \in \mathbb{I}_{\geq 0}$ is the discrete time, $x(t) \in \mathbb{R}^n$ is the state, $\chi \in \mathbb{R}^n$ is the initial condition, $u(t) \in \mathbb{R}^m$ is the control input, $w(t) \in \mathbb{R}^q$ is the disturbance

input, $y(t) \in \mathbb{R}^p$ is the output, and $p \in \mathbb{R}^o$ is a constant parameter. Let[4] $\mathcal{Z} := \{(x, u, w, p) \in \mathcal{X} \times \mathcal{U} \times \mathcal{W} \times \mathcal{P}\}$ for some sets $\mathcal{X} \subseteq \mathbb{R}^n$, $\mathcal{U} \subseteq \mathbb{R}^m$, $\mathcal{W} \subseteq \mathbb{R}^q$, $\mathcal{P} \subseteq \mathbb{R}^o$. We impose the following regularity condition on the system.

Assumption 7.4 (Differentiability)**.** *The functions f and h are continuously differentiable on $\mathcal{Z}$.*

Assumption 7.4 essentially allows us to apply the mean-value theorem. To this end, for any $z_1, z_2 \in \mathcal{Z}$, let $z_s(s) := z_1 + s(z_2 - z_1)$ for $s \in [0, 1]$ and define

$$\begin{aligned} A(z_1, z_2) &:= \int_0^1 \frac{\partial f}{\partial x}(z_s(s))ds, \quad C(z_1, z_2) := \int_0^1 \frac{\partial h}{\partial x}(z_s(s))ds, \\ B(z_1, z_2) &:= \int_0^1 \frac{\partial f}{\partial w}(z_s(s))ds, \quad D(z_1, z_2) := \int_0^1 \frac{\partial h}{\partial w}(z_s(s))ds, \\ E(z_1, z_2) &:= \int_0^1 \frac{\partial f}{\partial p}(z_s(s))ds, \quad F(z_1, z_2) := \int_0^1 \frac{\partial h}{\partial p}(z_s(s))ds. \end{aligned} \tag{7.39}$$

We require some boundedness properties of the terms in (7.39).

Assumption 7.5 (Bounded linearizations)**.** *There exist constants $\bar{B}, \bar{C}, \bar{D} \geq 0$ such that $|B(z_1, z_2)| \leq \bar{B}$, $|C(z_1, z_2)| \leq \bar{C}$, $|D(z_1, z_2)| \leq \bar{D}$ for all $z_1, z_2 \in \mathcal{Z}$.*

Note that Assumption 7.5 is naturally satisfied for special classes of systems (e.g., for systems with additive disturbances w in (7.38) and where the output equation h in (7.38b) is linear in x, which renders B, C, D constant) or generally if $\mathcal{Z}$ is compact.

Assumption 7.6 (State detectability)**.** *There exists a mapping $L : \mathcal{Z} \times \mathcal{Z} \to \mathbb{R}^{n \times p}$, a symmetric matrix $P \succ 0$, and a constant $\eta \in (0, 1)$ such that the matrix*

$$\Phi(z_1, z_2) := A(z_1, z_2) + L(z_1, z_2)C(z_1, z_2) \tag{7.40}$$

satisfies

$$\Phi(z_1, z_2)^\top P \Phi(z_1, z_2) \preceq \eta P \tag{7.41}$$

for all $z_1, z_2 \in \mathcal{Z}$. Furthermore, there exists $\bar{L} > 0$ such that $|L(z_1, z_2)| \leq \bar{L}$ for all $z_1, z_2 \in \mathcal{Z}$.

Remark 7.9 (State detectability)**.** *Assumption 7.6 is motivated by linear systems theory, where detectability is equivalent to the existence of an output injection term which renders the error system asymptotically stable. For any fixed constant $\eta \in (0, 1)$, by using the Schur complement and the definition $Y(z_1, z_2) := PL(z_1, z_2)$, condition* (7.41) *can be transformed into an infinite set of LMIs (linear in the decision variables P and Y). Then, these may be solved under a suitable parameterization of Y (e.g., polynomial in z_1, z_2) using a finite set of LMIs and standard convex analysis tools based on SDP, e.g., by applying SOS relaxations [Par03], by embedding*

[4] In contrast to Chapter 5, we do not require $\mathcal{Z}$ to possess a forward invariance property here, as we restrict our analysis to system trajectories satisfying (7.42).

the nonlinear behavior in an LPV model [ST23], or by suitably gridding the state space and verifying (7.41) *on the grid points (assuming compactness of $\mathcal{Z}$). We also want to emphasize that L does* not *need to be constant as it is usually required in the context of (adaptive) observer design, where this is crucial to be able to perform the observer update recursions online, compare, for example, [Ibr18]. Instead, the additional degree of freedom resulting from the fact that L may depend on both z_1 and z_2 can be used, e.g., to compensate for nonlinear terms in $A(z_1, z_2)$ or $C(z_1, z_2)$ from* (7.39)*. Furthermore, if $L(z_1, z_2)$ can be chosen such that $\Phi(z_1, z_2)$ in* (7.40) *becomes constant, the condition* (7.41) *can be drastically simplified (to one single LMI), compare the simulation example in Section 5.2.4. Finally, we note that the additional uniform bound on $L(z_1, z_2)$ is not restrictive under compactness of $\mathcal{Z}$.*

Remark 7.10 (Relation to i-IOSS in the sense of Assumption 5.1)**.** *In case the system equations f and h are differentiable (Assumption 7.4) and admit bounded linearizations (Assumption 7.5), Assumption 7.6 implies the i-IOSS property from Assumption 5.1 used in the context of MHE for joint state and parameter estimation (see Chapter 5). This can be shown by applying similar arguments as in the proof of Proposition 7.1 below. However, the resulting i-IOSS gains Q and R in* (5.4) *might be overly conservative compared to a direct verification of Assumption 5.1 using the methods from Section 7.1.1, compare also the examples in Sections 5.2.4 and 5.3.3.*

Now, consider an arbitrary trajectory pair

$$\left(\{(x_1(t), u(t), w_1(t), p_1)\}_{t=0}^{T-1}, \{(x_2(t), u(t), w_2(t), p_2)\}_{t=0}^{T-1}\right) \in \mathcal{Z}^T \times \mathcal{Z}^T \tag{7.42}$$

for some $T \in \mathbb{I}_{\geq 0}$, where $x_i(t+1) = f(x_i(t), u(t), w_i(t), p_i)$, $i = 1, 2$, $t \in \mathbb{I}_{[0,T-1]}$. For the sake of brevity, we define $z_i(t) := (x_i(t), u(t), w_i(t), p_i)$, $i = 1, 2$, $t \in \mathbb{I}_{[0,T-1]}$, and

$$Z_i := \left(x_i(0), p_i, \{u(t)\}_{t=0}^{T-1}, \{w_i(t)\}_{t=0}^{T-1}\right), \ i = 1, 2. \tag{7.43}$$

Here, we note that each Z_i (involving the initial condition $x_i(0)$) uniquely defines the sequence $\{z_i(t)\}_{t=0}^{T-1}$ (involving the states $x_i(t)$, $t \in \mathbb{I}_{[0,T-1]}$) for $i = 1, 2$ using the system dynamics (7.38a).

The following result provides a sufficient condition for the trajectory pair (7.42) to be persistently excited, in the sense that the PE condition characterizing the set $\mathbb{E}_T$ in Definition 5.1 holds.

Proposition 7.1. *Let Assumptions 7.4, 7.5, and 7.6 hold. Consider some $\alpha > 0$. There exist matrices $S_\mathrm{p}, P_\mathrm{p}, Q_\mathrm{p}, R_\mathrm{p} \succ 0$ and a constant $\eta_\mathrm{p} \in (0, 1)$ such that the following implication holds. If a trajectory pair as in* (7.42) *satisfies*

$$\mathcal{C}_T(Z_1, Z_2) := \sum_{t=0}^{T-1} \mu^{T-1-t} \overline{Y}(t, z_1(t), z_2(t))^\top \overline{Y}(t, z_1(t), z_2(t)) \succ \alpha I_o \tag{7.44}$$

for any $T \in \mathbb{I}_{\geq 0}$, where $\overline{Y}(t, z_1, z_2) := C(z_1, z_2)Y(t) + F(z_1, z_2)$ and

$$Y(t+1) = \Phi(z_1(t), z_2(t))Y(t) + E(z_1(t), z_2(t)) + L(z_1(t), z_2(t))F(z_1(t), z_2(t)) \tag{7.45}$$

for $t \in \mathbb{I}_{[0,T-1]}$ with $Y(0) = 0_{n\times o}$, then the trajectory pair (7.42) also satisfies

$$|p_1 - p_2|_{S_\mathrm{p}}^2 \leq \eta_\mathrm{p}^T |x_1(0) - x_2(0)|_{P_\mathrm{p}}^2 + \sum_{j=0}^{T-1} \eta_\mathrm{p}^{T-j-1} \left(|w_1(j) - w_2(j)|_{Q_\mathrm{p}}^2 + |y_1(j) - y_2(j)|_{R_\mathrm{p}}^2 \right). \tag{7.46}$$

Proof. Consider the trajectory pair (7.42) and the corresponding outputs $y_i(t) = h(x_i(t), u(t), w_i(t), p_i)$, $i = 1, 2$, $t \in \mathbb{I}_{[0,T-1]}$. Define $\Delta q(t) := q_1(t) - q_2(t)$ for $q \in \{x, w, y\}$, $t \in \mathbb{I}_{[0,T-1]}$ and $\Delta p := p_1 - p_2$. In the following, we will omit the dependency of terms on $(z_1(t), z_2(t))$, $z_i(t) = (x_i(t), u(t), w_i(t), p_i)$, $i = 1, 2$ for the sake of brevity. Using the mean-value theorem and the definitions from (7.39), we obtain the incremental system

$$\Delta x(t+1) = A\Delta x(t) + B\Delta w(t) + E\Delta p, \tag{7.47a}$$
$$\Delta y(t) = C\Delta x(t) + D\Delta w(t) + F\Delta p \tag{7.47b}$$

for $t \in \mathbb{I}_{[0,T-1]}$. Now consider the transformed coordinates $\zeta_i(t) := x_i(t) - Y(t)p_i$, $i = 1, 2$, $t \in \mathbb{I}_{[0,T-1]}$, where $Y(t)$ is from (7.45). Define $\Delta\zeta_i(t) = \zeta_1(t) - \zeta_2(t)$, $t \in \mathbb{I}_{[0,T]}$ and note that

$$\Delta\zeta(t) = \Delta x(t) - Y(t)\Delta p. \tag{7.48}$$

The difference $\Delta\zeta(t)$ in (7.48) evolves according to

$$\begin{aligned}\Delta\zeta(t+1) &= \Delta x(t+1) - Y(t+1)\Delta p \\ &= A\Delta x(t) + B\Delta w(t) + E\Delta p - (\Phi Y(t) + E + LF)\Delta p.\end{aligned} \tag{7.49}$$

To the right-hand side of the previous equation, we add

$$0 = L(\Delta y(t) - \Delta y(t)) = L(C\Delta x(t) + D\Delta w(t) + F\Delta p) - L\Delta y(t),$$

where L is from Assumption 7.6 and the latter equality follows by the incremental output (7.47b). Hence, from (7.49) together with the definitions of Φ from (7.40) and $\Delta\zeta(t)$ from (7.48), we get

$$\Delta\zeta(t+1) = \Phi\Delta\zeta(t) + (B + LD)\Delta w(t) - L\Delta y(t). \tag{7.50}$$

Applying the norm $|\cdot|_P = \sqrt{|\cdot|_P^2}$ to both sides and using the triangle inequality leads to

$$|\Delta\zeta(t+1)|_P \leq |\Phi\Delta\zeta(t)|_P + |(B + LD)\Delta w(t)|_P + |L\Delta y(t)|_P.$$

We square both sides, use the fact that for any $\epsilon > 0$, $(a+b)^2 \leq (1+\epsilon)a^2 + \frac{1+\epsilon}{\epsilon}b^2$ for all $a, b \geq 0$ by Young's inequality, apply Assumption 7.6, and exploit that $(\sum_{i=1}^n a_i)^2 \leq n\sum_{i=1}^n a_i^2$ for any $n \in \mathbb{I}_{\geq 0}$ and $a_i \geq 0$, $i \in \mathbb{I}_{[1,n]}$ by Jensen's inequality, which results in

$$|\Delta\zeta(t+1)|_P^2 \leq (1+\epsilon)\eta|\Delta\zeta(t)|_P^2 + \frac{2(1+\epsilon)}{\epsilon}\left(|(B + LD)\Delta w(t)|_P^2 + |L\Delta y(t)|_P^2\right). \tag{7.51}$$

Now, consider the recursion

$$S(t+1) = \mu S(t) + \overline{Y}(t, z_1(t), z_2(t))^\top \overline{Y}(t, z_1(t), z_2(t)),\ t \in \mathbb{I}_{[0,T-1]} \tag{7.52}$$

with $S(0) = 0_{o\times o}$, $\overline{Y}$ from (7.44), and some $\mu \in (0,1)$ that will be specified below. Using (7.52), we can write that

$$|\Delta p|^2_{S(t+1)} = \mu |\Delta p|^2_{S(t)} + |\overline{Y}(t, z_1(t), z_2(t))\Delta p|^2. \tag{7.53}$$

Furthermore, by the definition of $\overline{Y}$, the transformation (7.48), and the incremental output (7.47b), it follows that

$$\begin{aligned} |\overline{Y}(t, z_1(t), z_2(t))\Delta p|^2 &= |\Delta y(t) - D\Delta w(t) - C\Delta\zeta(t)|^2 \\ &\leq 3|\Delta y(t)|^2 + 3|D\Delta w(t)|^2 + 3\frac{\bar{C}^2}{\lambda_{\min}(P)}|\Delta\zeta(t)|^2_P, \end{aligned} \tag{7.54}$$

where the last step followed by applying Jensen's inequality, Assumption 7.5, and P from Assumption 7.6.

Now consider the function $W(t, \zeta_1, \zeta_2, p_1, p_2) := |\zeta_1 - \zeta_2|^2_P + \gamma |p_1 - p_2|^2_{S(t)}$, $t \in \mathbb{I}_{[0,T]}$ for some $\gamma > 0$. We choose the constants μ, ϵ, γ introduced above such that

$$\mu = (1+\epsilon)\eta + 3\gamma\bar{C}^2/\lambda_{\min}(P) < 1. \tag{7.55}$$

Using (7.51), (7.52), (7.54), and (7.55), we obtain that

$$\begin{aligned} &W(t+1, \zeta_1(t+1), \zeta_2(t+1), p_1, p_2) \\ &= |\Delta\zeta(t+1)|^2_P + \gamma|\Delta p|^2_{S(t+1)} \\ &\leq \mu(|\Delta\zeta(t)|^2_P + \gamma|\Delta p|^2_{S(t)}) + c_\epsilon|(B+LD)\Delta w(t)|^2_P + 3\gamma|D\Delta w(t)|^2 \\ &\quad + c_\epsilon|L\Delta y(t)|^2_P + 3\gamma|\Delta y(t)|^2 \end{aligned}$$

for all $t \in \mathbb{I}_{[0,T-1]}$, where $c_\epsilon := 2(1+\epsilon)/\epsilon$. Due to satisfaction of Assumptions 7.5 and 7.6, we can find uniform $Q, R \succ 0$ such that

$$|\bar{w}|^2_Q \geq c_\epsilon|(B+LD)\bar{w}|^2_P + 3\gamma|D\bar{w}|^2, \tag{7.56}$$

$$|\bar{y}|^2_R \geq c_\epsilon|L\bar{y}|^2_P + 3\gamma|\bar{y}|^2 \tag{7.57}$$

for all $z_1, z_2 \in \mathcal{Z}$ and all $\bar{w} \in \mathbb{R}^q$, $\bar{y} \in \mathbb{R}^p$. Consequently, we can infer that

$$\begin{aligned} &W(t+1, \zeta_1(t+1), \zeta_2(t+1), p_1, p_2) \\ &\leq \mu W(t, \zeta_1(t), \zeta_2(t), p_1, p_2) + |\Delta w(t)|^2_Q + |\Delta y(t)|^2_R \end{aligned} \tag{7.58}$$

for all $t \in \mathbb{I}_{[0,T-1]}$. The recursive application of (7.58) yields

$$\begin{aligned} &W(T, \zeta_1(T), \zeta_2(T), p_1, p_2) \\ &\leq \mu^T W(0, \zeta_1(0), \zeta_2(0), p_1, p_2) + \sum_{j=1}^{T} \mu^{j-1}\left(|\Delta w(T-j)|^2_Q + |\Delta y(T-j)|^2_R\right). \end{aligned} \tag{7.59}$$

By the definition of W, the recursion (7.52) with $S(0) = 0$, and the definition of $\mathcal{C}_T$ in (7.44), we obtain

$$W(T, \zeta_1(T), \zeta_2(T), p_1, p_2) \geq \gamma \Delta p(T)^\top \mathcal{C}_T(Z, \tilde{Z}) \Delta p(T) \geq \gamma\alpha |\Delta p(T)|^2. \tag{7.60}$$

Furthermore, since $Y(0) = 0$, we also have that

$$W(0, \zeta_1(0), \zeta_2(0), p_1, p_2) = |\Delta x(0) - Y(0)\Delta p|_P^2 + \gamma |\Delta p|_{S(0)}^2 = |\Delta x(0)|_P^2. \tag{7.61}$$

From (7.59) and the bounds (7.60) and (7.61), it hence follows that

$$\alpha\gamma |\Delta p|^2 \leq \mu^T |\Delta x(0)|_P^2 + \sum_{j=1}^{T} \mu^{j-1} \left(|\Delta w(T-j)|_Q^2 + |\Delta y(T-j)|_R^2 \right),$$

which is equivalent to (7.46) with $\eta_\mathrm{p} = \mu$, $P_\mathrm{p} = P$, $S_\mathrm{p} = \alpha\gamma I_o$, $Q_\mathrm{p} = Q$, $R_\mathrm{p} = R$. Noting that these choices are independent of the trajectories (7.42) and the value of T concludes this proof. □

The numerical verification of (7.44) requires the knowledge of both trajectories in (7.42). This is not the case when applied to the estimation problem presented in Section 5.2, since the true trajectory is generally unknown. However, we can make local statements based on data from only one of the trajectories that are valid in a surrounding neighborhood. To this end, we define the closed ball centered at some $Z \in \mathcal{X} \times \mathcal{P} \times \mathcal{U}^T \times \mathcal{W}^T$ of radius $r > 0$ by $\mathcal{B}(Z, r) := \{\tilde{Z} \in \mathcal{X} \times \mathcal{P} \times \mathcal{U}^T \times \mathcal{W}^T : |Z - \tilde{Z}| \leq r\}$. Then, we can evaluate (7.44) at (Z, Z) and define

$$\mathcal{O}_T(Z) := \mathcal{C}_T(Z, Z). \tag{7.62}$$

Proposition 7.2. *Let f and h in (7.38) be twice continuously differentiable on $\mathcal{Z}$. If $|\mathcal{O}_T(Z)| \geq \alpha'$ for some $\alpha' > 0$, then for any $\alpha \in (0, \alpha')$ there exists $r > 0$ small enough such that $|\mathcal{C}_T(Z, \tilde{Z})| \geq \alpha$ for all $\tilde{Z} \in \mathcal{B}(Z, r)$.*

Proof. The proof follows similar lines as the proof of [FS23, Lemma 4.14]. For $Z \in \mathcal{X} \times \mathcal{P} \times \mathcal{U}^T \times \mathcal{W}^T$, $T \in \mathbb{I}_{\geq 1}$, let

$$M(Z, r) := \max_{\tilde{Z} \in \mathcal{B}(Z,r)} \left| \frac{\partial \mathcal{C}_T}{\partial (Z, \tilde{Z})}(Z, \tilde{Z}) \right|.$$

Note that for each $Z \in \mathcal{X} \times \mathcal{P} \times \mathcal{U}^T \times \mathcal{W}^T$ and $r > 0$, $M(Z, r)$ exists since every function involved is sufficiently smooth and $\mathcal{B}(Z, r)$ is compact. By the mean-value theorem and the definition of $M(Z, r)$, we can infer that

$$|\mathcal{O}_T(Z) - \mathcal{C}_T(Z, \tilde{Z})| \leq M(Z, r) r. \tag{7.63}$$

From the triangle inequality, it further follows that

$$|\mathcal{O}_T(Z) - \mathcal{C}_T(Z, \tilde{Z})| \geq |\mathcal{O}_T(Z)| - |\mathcal{C}_T(Z, \tilde{Z})|. \tag{7.64}$$

Combining (7.63) and (7.64), we obtain

$$|\mathcal{C}_T(Z, \tilde{Z})| \geq |\mathcal{O}_T(Z)| - |\mathcal{O}_T(Z) - \mathcal{C}_T(Z, \tilde{Z})| \geq \alpha' - M(Z, r) r.$$

Now, for any $\alpha \in (0, \alpha')$, there exists $r > 0$ small enough such that $\alpha' - M(Z, r) r = \alpha$, which implies that $|\mathcal{C}_T(Z, \tilde{Z})| \geq \alpha$ and hence concludes this proof. □

To summarize, for the trajectory pair (7.42) and Z_1 and Z_2 from (7.43), we can make the following conclusion: if $Z_2 \in \mathcal{B}(Z_1, r)$ with r small enough, then

$$\mathcal{O}_T(Z_1) \geq \alpha' > 0 \quad \Rightarrow \quad \mathcal{C}_T(Z_1, Z_2) > \alpha > 0$$

by Proposition 7.2, which implies that the trajectory pair (7.42) satisfies the PE condition in (7.46) by Proposition 7.1 and hence is an element of the set $\mathbb{E}_T$ as characterized in Definition 5.1. This is particularly important in the context of MHE for joint state and parameter estimation (Chapter 5), as the excitation condition in (5.17) used in the MHE algorithm to update the parameter prior can now be checked based on the estimated trajectory only—without knowing the (unknown) true one.

Remark 7.11 (Local nature of Proposition 7.2)**.** *Proposition 7.2 provides a local result. Applied to the MHE scheme from Section 5.2, it requires small disturbances w and a proper guess of the initial condition χ and the parameter p. Note, however, that this is a standard condition for testing observability properties in the presence of general nonlinear systems, compare, e.g., [SJ11] and [FS23]. Although the condition on r is not explicitly verifiable in the context of state estimation for general nonlinear systems (due to the fact that r is unknown), checking $\mathcal{O}_T(Z) \geq \alpha'$ for some $\alpha' > 0$ yields a reliable heuristic to test in practice if a trajectory pair is PE and satisfies* (7.46) *or not, which is also evident in the simulation example in Section 5.2.4. The construction of α in the proof of Proposition 7.2 also shows that larger values of α' should be chosen if the estimates are more uncertain and therefore r is expected to be large, which is consistent with intuition.*

The main advantage of the proposed method for online PE verification is that it can be applied to general nonlinear systems and requires only a few and relatively mild assumptions, which is a major relaxation compared to most of the related literature; its only limitation lies in its local nature. In the following section, we show how global statements about PE of trajectories can be made by restricting the class of systems under consideration.

Special case: linearly parameterized systems

In this section, we consider the special case where the system (7.38) is linearly parameterized, subject to additive disturbances, and possesses a linear output equation; more precisely, we assume that

$$f(x, u, w, p) = f_{\mathrm{s}}(x, u) + G(x, u)p + Bw, \tag{7.65a}$$
$$h(x, u, w, p) = Cx + Dw \tag{7.65b}$$

for some constant matrices B, C, D of appropriate dimensions. Note that this corresponds to a class of systems that is often considered in the adaptive observer literature, see, for example, [Fra+20; Ekr+13], and it particularly covers the adaptive observer canonical form used in the works [TM23; EEZ16; MST01; MT92; BG88] as special case.

In the following, we show how for such systems the proof of Proposition 7.1 can be modified to construct a mapping $\mathcal{C}_T$ similar to (7.44) that satisfies the identity $\mathcal{C}_T(Z_1, Z_2) = \mathcal{C}_T(Z_1, Z_1) = \mathcal{O}_T(Z_1)$ for any Z_1, Z_2 and thus enables global statements about PE of a trajectory pair based on data of only one of the trajectories.

To this end, note that under Assumption 7.4, the definition $G'(x, u, p) := G(x, u)p$ represents a continuously differentiable function $G' : \mathbb{R}^n \times \mathbb{R}^m \times \mathbb{R}^o \to \mathbb{R}^n$. Therefore, by applying the mean-value theorem, we can write that

$$\Delta_G(x_1, x_2, u, p) := G(x_1, u)p - G(x_2, u)p = \mathcal{G}(x_1, x_2, u, p)(x_1 - x_2), \tag{7.66}$$

where

$$\mathcal{G}(x_1, x_2, u, p) := \int_0^1 \frac{\partial G'}{\partial x}(x_1 + s(x_2 - x_1), u, p)ds \tag{7.67}$$

for all $x_1, x_2 \in \mathcal{X}$ and $u \in \mathcal{U}$.

Assumption 7.7 (Regressor observability)**.** *There exists a constant matrix H such that*

$$\mathcal{G}(x_1, x_2, u, p)^\top P \mathcal{G}(x_1, x_2, u, p) \preceq C^\top H C \tag{7.68}$$

uniformly for all $x_1, x_2 \in \mathcal{X}$, $u \in \mathcal{U}$, and $p \in \mathcal{P}$ with $P \succ 0$ from Assumption 7.6.

Remark 7.12 (Conditions on G)**.** *Assumption 7.7 essentially requires that changes in the regressor $G(x, u)$ are directly visible in the output, which is related to a matching condition used in [Tyu+13; CR97; MT92]. Note that condition* (7.68) *is linear in H and thus can be easily verified using standard LMI methods under compactness of $\mathcal{X}$, $\mathcal{U}$, and $\mathcal{P}$. For compact $\mathcal{P}$, such H always exists for the special case where $G(x, u) = G(Cx, u)$, which includes the important classes of nonlinear adaptive observer canonical forms that are often considered in the adaptive observer literature, compare, e.g., [TM23; MST01; MT92; BG88].*

Corollary 7.2. *Consider the system* (7.38) *with f and h satisfying* (7.65)*. Let Assumptions 7.4, 7.5, 7.6, and 7.7 hold and assume that Φ in* (7.40) *is constant. Then, the conclusion from Proposition 7.1 remains valid if in the definition of $\mathcal{C}_T$ in* (7.44) *we replace $\overline{Y}$ by $CY(t)$, where $Y(t)$ is the matrix recursion*

$$Y(t+1) = \Phi Y(t) + G(x_1(t), u(t)), \ t \in \mathbb{I}_{[0,T-1]} \tag{7.69}$$

with $Y(0) = 0_{n \times o}$. Furthermore, we have the identity $\mathcal{C}_T(Z_1, Z_2) = \mathcal{C}_T(Z_1, Z_1)$.

Corollary 7.2 requires finding a map L in Assumption 7.6 such that Φ in (7.40) becomes constant. This might be achieved by exploiting the fact that L can depend on both z_1 and z_2, compare Remark 7.9 and see the simulation example in Section 5.2.4.

Proof of Corollary 7.2. We start by performing the same steps that were applied in the proof of Proposition 7.1 to derive (7.51), which yields

$$\begin{aligned} |\Delta\zeta(t+1)|_P^2 \leq (1+\epsilon)\eta|\Delta\zeta(t)|_P^2 + \frac{3(1+\epsilon)}{\epsilon}\left(|(B+LD)\Delta w(t)|_P^2 + |L\Delta y(t)|_P^2\right) \\ + \frac{3(1+\epsilon)}{\epsilon}|\Delta_G(x_1(t), x_2(t), u(t), p_2)|_P^2, \end{aligned} \tag{7.70}$$

where $\Delta_G(x_1(t), x_2(t), u(t), p_2)$ is from (7.66). Note that the only difference to (7.51) is the presence of the additional term $\Delta_G(x_1(t), x_2(t), u(t), p_2)$ and the resulting factor 3 (instead of 2). By application of (7.66), Assumption 7.7, the output function (7.65b), and Jensen's inequality, we obtain

$$\begin{aligned}|\Delta_G(x_1(t), x_2(t), u(t), p_2)|_P^2 &= |\mathcal{G}(x_1(t), x_2(t), u(t), p_2)\Delta x(t)|_P^2 \\ &\leq |C\Delta x(t)|_H^2 = |\Delta y(t) - D\Delta w(t)|_H^2 \\ &\leq 2|\Delta y(t)|_H^2 + 2|D\Delta w(t)|_H^2. \end{aligned} \tag{7.71}$$

The combination of (7.70) and (7.71) then yields

$$\begin{aligned}|\Delta\zeta(t+1)|_P^2 \leq (1+\epsilon_1)\mu|\Delta\zeta(t)|_P^2 &+ \frac{3(1+\epsilon_1)}{\epsilon_1}\left(|(B+LD)\Delta w(t)|_P^2 + 2|D\Delta w(t)|_H^2\right) \\ &+ \frac{3(1+\epsilon_1)}{\epsilon_1}\left(|L\Delta y(t)|_P^2 + 2|\Delta y(t)|_H^2\right). \end{aligned} \tag{7.72}$$

Note that (7.72) is again very similar to (7.51), with additional terms involving $|\cdot|_H^2$. From here, we apply the same steps that followed after (7.51) to derive (7.46).

It remains to show that $\mathcal{C}_T(Z_1, Z_2) = \mathcal{C}_T(Z_1, Z_1) = \mathcal{O}_T(Z_1)$. However, this immediately follows by noting that the recursion in (7.69) solely depends on the sequences $\{x_1(t)\}_{t=0}^{T-1}$ and $\{u(t)\}_{t=0}^{T-1}$ (i.e., Z_1), which concludes this proof. □

7.2.2. Time-varying parameters

In this section, we extend Proposition 7.1 to the case of time-varying parameters. In particular, we consider the system description from (5.1) for the important special case of parameter dynamics described by (5.2). The overall state-space model reads

$$x(t+1) = f(x(t), u(t), w(t), p(t)), \quad x(0) = \chi, \tag{7.73a}$$
$$p(t+1) = p(t) + B_{\mathrm{p}} w(t), \quad p(0) = \xi, \tag{7.73b}$$
$$y(t) = h(x(t), u(t), w(t), p(t)) \tag{7.73c}$$

with states $x(t) \in \mathbb{R}^n$, time-varying parameters $p(t) \in \mathbb{R}^o$, initial conditions $\chi \in \mathbb{R}^n$ and $\xi \in \mathbb{R}^o$, control input $u(t) \in \mathbb{R}^m$, disturbance input $w(t) \in \mathbb{R}^q$, output $y(t) \in \mathbb{R}^p$, and discrete time $t \in \mathbb{I}_{\geq 0}$. We define $\mathcal{Z} = \{(x, u, w, p) \in \mathcal{X} \times \mathcal{U} \times \mathcal{W} \times \mathcal{P}\}$ for some sets $\mathcal{X} \subseteq \mathbb{R}^n$, $\mathcal{U} \subseteq \mathbb{R}^m$, $\mathcal{W} \subseteq \mathbb{R}^q$, $\mathcal{P} \subseteq \mathbb{R}^o$.

In the following, we make use of the setup from Section 7.2.1. In particular, we consider Assumption 7.4 (i.e., differentiability of f and h), which lets us construct the matrices A, B, C, D, E, F in (7.39) that involve the Jacobians of f and h with respect to x, w, and p. Moreover, we require Assumption 7.5 (i.e., uniform bounds on B, C, D) and Assumption 7.6 (state detectability in terms of the existence of a suitable output injection term); in the case of time-varying parameters, however, we additionally require boundedness of the terms in (7.39) involving the partial derivatives of f and h with respect to the parameters (i.e., E and F).

Assumption 7.8 (Bounded linearizations with respect to the parameter)**.** *There exist constants $\bar{E}, \bar{F} \geq 0$ such that $|E(z_1, z_2)| \leq \bar{E}$ and $|F(z_1, z_2)| \leq \bar{F}$ for all $z_1, z_2 \in \mathcal{Z}$, where $E(z_1, z_2)$ and $F(z_1, z_2)$ are defined in* (7.39)*.*

Now, consider an arbitrary trajectory pair

$$\left(\{(x_1(t), u(t), w_1(t), p_1(t))\}_{t=0}^{T-1}, \{(x_2(t), u(t), w_2(t), p_2(t))\}_{t=0}^{T-1}\right) \in \mathcal{Z}^T \times \mathcal{Z}^T \quad (7.74)$$

for some $T \in \mathbb{I}_{\geq 0}$, where $x_i(t+1) = f(x_i(t), u(t), w_i(t), p_i(t))$, $i = 1, 2$, $t \in \mathbb{I}_{[0,T-1]}$. For the sake of brevity, we define $z_i(t) := (x_i(t), u(t), w_i(t), p_i(t))$, $i = 1, 2$, $t \in \mathbb{I}_{[0,T-1]}$, and $Z_i := \left(x_i(0), p_i(0), \{u(t)\}_{t=0}^{T-1}, \{w_i(t)\}_{t=0}^{T-1}\right)$, $i = 1, 2$. Note again that each Z_i (involving the initial conditions $x_i(0)$ and $p_i(0)$) uniquely defines the sequence $\{z_i(t)\}_{t=0}^{T-1}$ (involving the states $x_i(t)$ and parameters $p_i(t)$, $t \in \mathbb{I}_{[0,T-1]}$) for $i = 1, 2$ using the dynamics in (7.73a) and in (7.73b).

The following result provides a sufficient condition for the trajectory pair (7.74) to be persistently excited, in the sense that the PE condition characterizing the set $\mathbb{E}_T$ in Definition 5.2 holds.

Proposition 7.3. *Let Assumptions 7.4, 7.5, 7.6, and 7.8 hold. Consider some $\alpha > 0$. There exist matrices $S_\mathrm{p}, P_\mathrm{p}, Q_\mathrm{p}, R_\mathrm{p} \succ 0$ and a constant $\eta_\mathrm{p} \in (0, 1)$ such that the following implication holds. If a trajectory pair as in* (7.74) *satisfies*

$$\mathcal{C}_T(Z_1, Z_2) := \sum_{t=0}^{T-1} \mu^{T-1-t} \overline{Y}(t, z_1(t), z_2(t))^\top \overline{Y}(t, z_1(t), z_2(t)) \succ \alpha I_o \quad (7.75)$$

for some $T \in \mathbb{I}_{\geq 0}$, where $\overline{Y}(t, z_1, z_2) := C(z_1, z_2)Y(t) + F(z_1, z_2)$ and

$$Y(t+1) = \Phi(z_1(t), z_2(t))Y(t) + E(z_1(t), z_2(t)) + L(z_1(t), z_2(t))F(z_1(t), z_2(t)) \quad (7.76)$$

for $t \in \mathbb{I}_{[0,T-1]}$ with $Y(0) = 0_{n \times o}$, then the trajectory pair (7.74) *also satisfies*

$$|p_1(0) - p_2(0)|_{S_\mathrm{p}}^2 \leq \eta_\mathrm{p}^T |x_1(0) - x_2(0)|_{P_\mathrm{p}}^2 + \sum_{j=0}^{T-1} |w_1(j) - w_2(j)|_{Q_\mathrm{p}}^2 + |y_1(j) - y_2(j)|_{R_\mathrm{p}}^2. \quad (7.77)$$

The proof of Proposition 7.3 is an extension of the proof of Proposition 7.1, where we first require uniform boundedness of the recursion in (7.76).

Lemma 7.1. *Let Assumptions 7.4, 7.5, 7.6, and 7.8 hold. Then, there exists a constant $Y_\mathrm{max} > 0$ such that $Y(t)$ in* (7.76) *satisfies $|Y(t)| \leq Y_\mathrm{max}$ uniformly for all possible $t \in \mathbb{I}_{\geq 0}$. Here, a particular choice is*

$$Y_\mathrm{max} = \frac{1 + \epsilon_3}{(1 - \eta)\epsilon_3 - \eta\epsilon_3^2} \frac{\lambda_\mathrm{max}(P)}{\lambda_\mathrm{min}(P)} (\bar{E} + \bar{L}\bar{F})^2 \quad (7.78)$$

for any value of $\epsilon_3 \in (0, \eta^{-1} - 1)$ with $\bar{C}$ from Assumption 7.5, $\eta, P, \bar{L}$ from Assumption 7.6, and $\bar{E}$,$\bar{F}$ from Assumption 7.8.

Proof. Consider the trajectories (7.74) with $T \in \mathbb{I}_{\geq 0}$. In the following, we will omit the dependency of terms depending on $(z_1(t), z_2(t))$, $z_i(t) = (x_i(t), u_i(t), w_i(t), p_i(t))$, $i = 1, 2$ for brevity. Consider some constant vector $v \in \mathbb{R}^o$ with $v \neq 0$ and define $\nu(t) := Y(t)v \in \mathbb{R}^n$. By performing the recursion (7.76), we obtain

$$\nu(t+1) = Y(t+1)v = \Phi Y(t)v + Ev + LFv = \Phi\nu(t) + (E + LF)v.$$

Applying the norm $|\cdot|_P = \sqrt{|\cdot|_P^2}$ (with P from Assumption 7.6) to both sides and using the triangle inequality and (7.41) leads to

$$|\nu(t+1)|_P \leq |\Phi\nu(t)|_P + |(E + LF)v|_P \leq \sqrt{\eta}|\nu(t)|_P + |(E + LF)v|_P.$$

By squaring both sides and using the fact that for any $\epsilon_3 > 0$, $(a+b)^2 \leq (1+\epsilon_3)a^2 + \frac{1+\epsilon_3}{\epsilon_3}b$ for any $a, b > 0$, it follows that

$$|\nu(t+1)|_P^2 \leq (1+\epsilon_3)\eta|\nu(t)|_P^2 + \frac{1+\epsilon_3}{\epsilon_3}|(E + LF)v|_P^2. \tag{7.79}$$

Now consider ϵ_3 small enough such that $\tilde{\eta} := (1+\epsilon_3)\eta < 1$ (this requires $\epsilon_3 \in (0, \eta^{-1} - 1)$). Since E and F are bounded by Assumption 7.8, we have

$$|(E + LF)v|_P^2 = v^\top (E + LF)^\top P(E + LF)v \leq c_1|v|^2 \tag{7.80}$$

uniformly for all $z_1, z_2 \in \mathcal{Z}$, where

$$c_1 := \lambda_{\max}(P)|E + LF|^2 \leq \lambda_{\max}(P)(|E| + |L||F|)^2 \leq \lambda_{\max}(P)(\bar{E} + \bar{L}\bar{F})^2 =: c_2.$$

Define $\bar{c} := \frac{1+\epsilon_3}{\epsilon_3}c_2$. In combination, (7.79) yields

$$|\nu(t)|_P^2 \leq \tilde{\eta}^t|\nu(0)|_P^2 + \bar{c}\sum_{j=1}^{t}\tilde{\eta}^{j-1}|v|^2.$$

By the definition of ν, it hence follows that

$$v^\top Y(t)^\top PY(t)v \leq \tilde{\eta}^t v^\top Y(0)^\top PY(0)v + \sum_{j=1}^{t}\tilde{\eta}^{j-1}\bar{c}|v|^2 \leq \frac{\bar{c}}{1-\tilde{\eta}}|v|^2,$$

where in the latter inequality we have used that $Y(0) = 0$ and the geometric series. This leads to the implication

$$v^\top \left(Y(t)^\top PY(t) - \frac{\bar{c}}{1-\tilde{\eta}}I_o\right)v \leq 0 \quad \overset{v\neq 0}{\Rightarrow} \quad Y(t)^\top PY(t) \preceq \frac{\bar{c}}{1-\tilde{\eta}}I_o,$$

which lets us conclude that

$$Y(t)^\top Y(t) \preceq \frac{\bar{c}}{\lambda_{\min}(P)(1-\tilde{\eta})}I_o.$$

Hence, all eigenvalues of the symmetric positive semidefinite matrix $Y(t)^\top Y(t)$ are uniformly bounded for all times $t \in \mathbb{I}_{\geq 0}$ by the constant $\bar{c}(\lambda_{\min}(P)(1-\tilde{\eta}))^{-1}$. Since $|Y(t)| = \sqrt{\lambda_{\max}(Y(t)^\top Y(t))}$ by definition of the spectral norm, we have that

$$|Y(t)|^2 \leq \frac{\bar{c}}{\lambda_{\min}(P)(1-\tilde{\eta})} = Y_{\max},$$

where the last equality follows by simple algebraic manipulations using the definitions of c_2 and $\tilde{\eta}$ from above and $Y_{\max}$ from (7.78), which concludes this proof. □

Proof of Proposition 7.3. We apply similar arguments as in the proof of Proposition 7.1, with differences resulting from the parameter dynamics (7.73b). Consider the trajectory pair (7.74) and their outputs $y_i(t) = h(x_i(t), u(t), w_i(t), p_i(t))$, $i = 1, 2$, $t \in \mathbb{I}_{[0,T-1]}$. Define $\Delta q(t) := q_1(t) - q_2(t)$ for $q \in \{x, w, p, y\}$, $t \in \mathbb{I}_{[0,T-1]}$. In the following, we will omit the dependency of terms on $(z_1(t), z_2(t))$, $z_i(t) = (x_i(t), u(t), w_i(t), p_i(t))$, $i = 1, 2$ for the sake of brevity. Using the mean-value theorem, the definitions from (7.39), and the parameter dynamics (7.73b), we obtain the incremental system

$$\Delta x(t+1) = A\Delta x(t) + B\Delta w(t) + E\Delta p(t), \tag{7.81a}$$
$$\Delta p(t+1) = \Delta p(t) + B_{\mathrm{p}}\Delta w(t), \tag{7.81b}$$
$$\Delta y(t) = C\Delta x(t) + D\Delta w(t) + F\Delta p(t) \tag{7.81c}$$

for $t \in \mathbb{I}_{[0,T-1]}$. Now consider the transformed coordinates $\zeta_i(t) := x_i(t) - Y(t)p_i(t)$, $i = 1, 2$, $t \in \mathbb{I}_{[0,T-1]}$, where $Y(t)$ is from (7.76). Define $\Delta\zeta_i(t) = \zeta_1(t) - \zeta_2(t)$, $t \in \mathbb{I}_{[0,T]}$ and note that

$$\Delta\zeta(t) = \Delta x(t) - Y(t)\Delta p(t). \tag{7.82}$$

Performing the same steps that we applied to derive (7.51), we obtain

$$\begin{aligned}|\Delta\zeta(t+1)|_P^2 \leq{}& (1+\epsilon)\eta|\Delta\zeta(t)|_P^2 \\ &+ \frac{2(1+\epsilon)}{\epsilon}\left(|(B + LD - Y(t+1)B_{\mathrm{p}})\Delta w(t)|_P^2 + |L\Delta y(t)|_P^2\right),\end{aligned} \tag{7.83}$$

where the only difference to (7.51) is the additional term $Y(t+1)B_{\mathrm{p}}$ that originates from the parameter dynamics (7.73b) applied in (7.82).

Now, consider the recursion (7.52), i.e.,

$$S(t+1) = \mu S(t) + \overline{Y}(t, z_1(t), z_2(t))^\top \overline{Y}(t, z_1(t), z_2(t)),\ t \in \mathbb{I}_{[0,T-1]} \tag{7.84}$$

with $S(0) = 0_{o\times o}$, $\overline{Y}$ from (7.75), and some $\mu \in (0, 1)$ that will be specified below. By Lemma 7.1 and Assumption 7.5, note that

$$|S(t)| \leq \mu|S(t-1)| + |CY(t-1) + F|^2 \leq \mu^t|S(0)| + \sum_{j=1}^{t} \mu^{j-1}(\bar{C}Y_{\max} + \bar{F})^2,$$

which by application of the geometric series and $S(0) = 0$ implies that

$$|S(t)| \leq \frac{(\bar{C}Y_{\max} + \bar{F})^2}{1-\mu} =: S_{\max} \tag{7.85}$$

uniformly for all $t \in \mathbb{I}_{[0,T]}$ (where $S_{\max}$ is independent of T). For any $t \in \mathbb{I}_{[0,T-1]}$, consider $|\Delta p(t+1)|_{S(t+1)}$ and note that by the parameter dynamics 7.73b and the triangle inequality,

$$|\Delta p(t+1)|_{S(t+1)} \leq |\Delta p(t)|_{S(t+1)} + |B_{\mathrm{p}}\Delta w(t)|_{S(t+1)}.$$

By squaring both sides, using the fact that for any $\epsilon_2 > 0$, $(a+b)^2 \leq (1+\epsilon_2)a^2 + \frac{1+\epsilon_2}{\epsilon_2}b^2$ for any $a, b > 0$, and employing the recursion (7.84), we obtain

$$\begin{aligned}
&|\Delta p(t+1)|^2_{S(t+1)} \\
&\leq (1+\epsilon_2)|\Delta p(t)|^2_{S(t+1)} + \frac{1+\epsilon_2}{\epsilon_2}|B_{\mathrm{p}}\Delta w(t)|^2_{S(t+1)} \\
&= (1+\epsilon_2)\mu|\Delta p(t)|^2_{S(t)} + (1+\epsilon_2)|\overline{Y}(t, z_1(t), z_2(t))\Delta p(t)|^2 + \frac{1+\epsilon_2}{\epsilon_2}|B_{\mathrm{p}}\Delta w(t)|^2_{S(t+1)}.
\end{aligned} \tag{7.86}$$

Furthermore, by the definition of $\overline{Y}$, the transformation (7.82), and the incremental output (7.81c), it follows that

$$\begin{aligned}
|\overline{Y}(t, z_1(t), z_2(t))(\Delta p(t))|^2 &= |\Delta y(t) - D\Delta w(t) - C\Delta\zeta(t)|^2 \\
&\leq 3|\Delta y(t)|^2 + 3|D\Delta w(t)|^2 + 3\frac{\bar{C}^2}{\lambda_{\min}(P)}|\Delta\zeta(t)|^2_P,
\end{aligned} \tag{7.87}$$

where the last step followed by applying Jensen's inequality, Assumption 7.5, and P from Assumption 7.6.

Now consider the function $W(t, \zeta_1, \zeta_2, p_1, p_2) := |\zeta_1 - \zeta_2|^2_P + \gamma|p_1 - p_2|^2_{S(t)}$, $t \in \mathbb{I}_{[0,T]}$ for some $\gamma > 0$. We choose the constants μ, ϵ, γ introduced above such that

$$\tilde{\mu} := (1+\epsilon_2)\mu = (1+\epsilon)\eta + \gamma(1+\epsilon_2)\frac{3\bar{C}^2}{\lambda_{\min}(P)} < 1. \tag{7.88}$$

Using (7.83), (7.84), (7.87), and (7.88), we obtain that

$$\begin{aligned}
&W(t+1, \zeta_1(t+1), \zeta_2(t+1), p_1(t+1), p_2(t+1)) \\
&\leq \tilde{\mu}W(t, \zeta_1(t), \zeta_2(t), p_1(t), p_2(t)) + \gamma\frac{1+\epsilon_2}{\epsilon_2}|B_{\mathrm{p}}\Delta w(t)|^2_{S(t+1)} \\
&\quad + \frac{2(1+\epsilon)}{\epsilon}|(B + LD - Y(t+1))\Delta w(t)|^2_P + 3\gamma(1+\epsilon_2)|D\Delta w(t)|^2 \\
&\quad + \frac{2(1+\epsilon)}{\epsilon}|L\Delta y(t)|^2_P + \gamma(1+\epsilon_2)3|\Delta y(t)|^2
\end{aligned}$$

for all $t \in \mathbb{I}_{[0,T-1]}$. Here, we note that

$$|B_{\mathrm{p}}\Delta w(t)|^2_{S(t+1)} \leq |B_{\mathrm{p}}|^2 S_{\max}|\Delta w(t)|^2$$

with $S_{\max}$ from (7.85). Similarly, due to Assumptions 7.5 and 7.6, we have that

$$|(B + LD - Y(t+1))\Delta w(t)|^2_P \leq (\bar{B} + \bar{L}\bar{D} + Y_{\max})^2|P||\Delta w(t)|^2$$

with $Y_{\max}$ from Lemma 7.1. Hence, we can select $Q, R \succ 0$ such that

$$\begin{aligned}
|\bar{w}|^2_Q &\geq \gamma\frac{1+\epsilon_2}{\epsilon_2}|B_{\mathrm{p}}\bar{w}|^2_{S(t+1)} + \frac{2(1+\epsilon)}{\epsilon}|(B + LD - Y(t+1))\bar{w}|^2_P + 3\gamma(1+\epsilon_2)|D\bar{w}|^2, \\
|\bar{y}|^2_R &\geq \frac{2(1+\epsilon)}{\epsilon}|L\bar{y}|^2_P + \gamma(1+\epsilon_2)3|\bar{y}|^2
\end{aligned}$$

for all $z_1, z_2 \in \mathcal{Z}$ and all $\bar{w} \in \mathbb{R}^q$, $\bar{y} \in \mathbb{R}^p$. Consequently, we can infer that

$$\begin{aligned} &W(t+1, \zeta_1(t+1), \zeta_2(t+1), p_1(t+1), p_2(t+1)) \\ &\leq \tilde{\mu} W(t, \zeta_1(t), \zeta_2(t), p_1(t), p_2(t)) + |\Delta w(t)|_Q^2 + |\Delta y(t)|_R^2 \end{aligned} \tag{7.89}$$

for all $t \in \mathbb{I}_{[0,T-1]}$. Recursive application of (7.89) yields

$$\begin{aligned} &W(T, \zeta_1(T), \zeta_2(T), p_1(T), p_2(T)) \\ &\leq \tilde{\mu}^T W(0, \zeta_1(0), \zeta_2(0), p_1(0), p_2(0)) + \sum_{j=1}^{T} \tilde{\mu}^{j-1} \left(|\Delta w(T-j)|_Q^2 + |\Delta y(T-j)|_R^2 \right). \end{aligned} \tag{7.90}$$

By the definition of W, the recursion (7.84) with $S(0) = 0$, and the definition of $\mathcal{C}_T$ in (7.75), we obtain

$$W(T, \zeta_1(T), \zeta_2(T), p_1(T), p_2(T)) \geq \gamma \Delta p(T)^\top \mathcal{C}_T(Z, \tilde{Z}) \Delta p(T) \geq \gamma \alpha |\Delta p(T)|^2. \tag{7.91}$$

Furthermore, since $Y(0) = 0$ and $S(0) = 0$ we also have that

$$W(0, \zeta_1(0), \zeta_2(0), p_1(0), p_2(0)) = |\Delta x(0) - Y(0)\Delta p(0)|_P^2 + \gamma |\Delta p(0)|_{S(0)}^2 = |\Delta x(0)|_P^2. \tag{7.92}$$

From (7.90) and the bounds (7.91) and (7.92), it hence follows that

$$\alpha\gamma |\Delta p(T)|^2 \leq \tilde{\mu}^T |\Delta x(0)|_P^2 + \sum_{j=1}^{T} \tilde{\mu}^{j-1} \left(|\Delta w(T-j)|_Q^2 + |\Delta y(T-j)|_R^2 \right).$$

Thus, we derived a bound on $|\Delta p(T)|^2$; to infer a bound on the difference in the initial parameters $|\Delta p(0)|^2$ as required, we note that by the dynamics (7.81b) and the triangle inequality, it holds that

$$\Delta p(T) = \Delta p(0) + \sum_{j=0}^{T-1} B_{\mathrm{p}} \Delta w(j) \quad \Rightarrow \quad |\Delta p(0)| \leq |\Delta p(T)| + \sum_{j=0}^{T-1} |\Delta w(j)|_{B_{\mathrm{p}}^\top B_{\mathrm{p}}}.$$

In combination, we obtain

$$\begin{aligned} \alpha\gamma |\Delta p(0)|^2 &\leq \alpha\gamma |\Delta p(T)| + \alpha\gamma \sum_{j=1}^{T-j} |\Delta w(j)|_{B_{\mathrm{p}}^\top B_{\mathrm{p}}} \\ &\leq \tilde{\mu}^T |\Delta x(0)|_P^2 + \sum_{j=0}^{T-1} |\Delta w(j)|_Q^2 + |\Delta y(j)|_R^2 \end{aligned}$$

with $\bar{Q} = Q + \alpha\gamma B_{\mathrm{p}}^\top B_{\mathrm{p}}$, which is equivalent to (7.77) with $\eta_{\mathrm{p}} = \tilde{\mu}$, $S_{\mathrm{p}} = \alpha\gamma I_o$, $Q_{\mathrm{p}} = \bar{Q}$, $R_{\mathrm{p}} = R$. Noting that these choices are independent of the trajectories (7.42) and the value of T concludes this proof. □

As in Proposition 7.1, the numerical verification of (7.75) requires the knowledge of both trajectories in (7.74), which is not the case when applied to the estimation problem presented in Section 5.3. However, we can again derive local statements

based on data from only one of the trajectories that are valid in a surrounding neighborhood by defining

$$\mathcal{O}_T(Z) := \mathcal{C}_T(Z, Z) \tag{7.93}$$

with $\mathcal{C}_T$ from (7.75). By invoking Proposition 7.2, for the pair (Z_1, Z_2) defined by the trajectories in (7.74), we know that there exists a neighborhood of Z_1 such that if $\mathcal{O}(Z_1) > \alpha'$ for some $\alpha' > 0$ and Z_2 is in the neighborhood of Z_1, there exists $\alpha > 0$ such that $\mathcal{C}(Z_1, Z_2) > \alpha$. Hence, this method allows us to verify if a given trajectory pair is (locally) PE or not, compare also Remark 7.11. Again, note that this is of particular importance in the context of MHE for joint state and parameter estimation (Chapter 5), as the excitation condition used in (5.80) can thus be checked based on the estimated trajectory only, without knowing the (unknown) true one. We conclude this section by noting that global PE statements can be derived for the special case of linearly parameterized dynamics and linear outputs (7.65) by suitable modifying Corollary 7.2.

7.3. Summary

In this chapter, we focused on the numerical verification of detectability and PE properties for general nonlinear systems. These are fundamental concepts in control and signal processing and play an important role in observer design and system identification; however, practical tools to actually verify them are lacking.

To this end, we developed several methods to certify detectability (in terms of i-IOSS for discrete-time systems and i-iIOSS for continuous-time systems) and check if a given trajectory pair satisfies a PE property or not. The verification methods rely on arguments from contraction theory involving the differential dynamics, Riemannian geometry, and the mean-value theorem in order to reformulate the underlying and rather abstract mathematical conditions in the form of simple LMIs. These can be numerically solved using standard methods such as SDP in combination with LPV embeddings, SOS relaxations, or simple gridding techniques.

Our results are suitable in the context of the MHE schemes presented and analyzed in Chapters 3–6 to provide robustness guarantees for MHE under practical conditions. Moreover, they generally provide useful tools to actually verify detectability and PE of nonlinear systems in practice, where such properties are generally often assumed, but could not be certified due to a lack of methods.

8. Conclusions

We now summarize the main results obtained within this thesis and discuss possible topics for future work.

8.1. Summary

In this thesis, we obtained various new results in the field of nonlinear MHE theory. In particular, we established robust stability and performance guarantees under practically relevant conditions and developed MHE algorithms for real-time applications and joint state and parameter estimation problems with rigorous theoretical guarantees.

In Chapter 2, we focused on the notion of i-IOSS as a characterization of detectability for nonlinear systems. We discussed the classical asymptotic-gain formulation of i-IOSS and two modern time-discounted variants, which became standard detectability concepts in the context of MHE in the recent years. While these properties coincide for discrete-time systems, this is generally not the case in continuous time, and we must carefully distinguish between them. We proposed the notion of i-iIOSS for continuous-time systems, which essentially constitutes a time-discounted integral variant of i-IOSS, and provided equivalent Lyapunov function characterizations. Moreover, we showed that i-iIOSS is in fact necessary for the existence of state observers that exhibit a certain robust stability property with respect to the unknown disturbances and measurement noise, which turned out to be very desirable as it combines the advantages of classical ISS and iISS characteristics. Overall, we provided a general Lyapunov framework for the robust stability analysis of state observers in continuous time, which forms the basis for the Lyapunov-based MHE schemes analyzed in this thesis.

In Chapter 3, we focused on robust stability guarantees of MHE for detectable nonlinear systems under process disturbances and measurement noise. We briefly introduced the Lyapunov-based MHE scheme from [Sch+23, Sec. III], which employs a least squares objective under additional discounting and enjoys many beneficial theoretical properties, provided that the cost function is selected in accordance with a known i-IOSS Lyapunov function. Then, we presented a Lyapunov-based MHE scheme for general nonlinear continuous-time systems. Assuming that the system is detectable (i-iIOSS) and admits a corresponding i-iIOSS Lyapunov function, we showed that there exists a sufficiently long estimation horizon that guarantees robust global exponential stability of the estimation error. The continuous-time MHE scheme has the decisive advantage that the sampling times at which the underly-

ing optimization problem is solved can be chosen arbitrarily. This allows the MHE scheme to be tailored to the problem at hand, which can yield more accurate results with less computational effort compared to standard equidistant sampling used in discrete-time MHE approaches. Moreover, we showed that Lyapunov-based MHE generally allows for significantly less conservative (i.e., smaller) estimates of the minimum required horizon length compared to the literature. The applicability of Lyapunov-based MHE for discrete- and continuous-time systems was illustrated using a nonlinear chemical reaction and a quadrotor model from the literature. Here, we certified detectability by computing i-IOSS and i-iIOSS Lyapunov functions using our methods from Section 7.1 and successfully applied the Lyapunov-based MHE schemes. This illustrates that the combination of Lyapunov-based MHE and the verification methods from Section 7.1 allow for guaranteed robustly stable state estimation under practically relevant conditions, for both discrete- and continuous-time systems.

In Chapter 4, we presented two suboptimal MHE schemes and established global robust stability guarantees with respect to unknown process disturbances and measurement noise. This is crucial in order to ensure real-time applicability of MHE in cases where the optimization problem cannot be solved to optimality within one fixed sampling interval. The suboptimal schemes rely on an *a priori* known, robustly stable auxiliary observer, which is used to construct a suitable candidate solution to the respective MHE problems. By imposing that any suboptimal solution to the MHE problem achieves at most the same cost, the proposed suboptimal estimators inherit the stability properties of the auxiliary observer while benefiting from the performance of the numerical optimizers. Here, we considered two conceptually different MHE formulations: first, a rather classical one that optimizes over trajectories of the system, and second, a modified version that optimizes directly over trajectories of the auxiliary observer. While the first one allows the user to employ a standard least squares cost function, the second one enables better theoretical guarantees and can improve the convergence speed of MHE in case the auxiliary observer is rather aggressive. In contrast to most of the related literature, the corresponding robustness guarantees are valid independent of the chosen optimization algorithm and the number of solver iterations performed at each time step (including zero). The simulation examples showed that both MHE formulations are very effective, especially in the case of poor transient behavior of the auxiliary observer. Moreover, with only a few iterations of the optimizer, we were able to significantly improve the estimates of the auxiliary observer and achieve an overall estimation performance close to that obtained with standard (optimal) MHE, while significantly reducing the required computation times.

In Chapter 5, we proposed MHE schemes for joint state and parameter estimation, particularly tailored for parameters that may suffer from insufficient excitation. Specifically, the cost function involves an adaptive regularization term that is adjusted according to real-time excitation information, where we rely on the excitation monitoring techniques developed in Section 7.2. We considered the case of constant and time-varying parameters and derived a bound for the state and parameter estimation error that is valid regardless of the excitation of the parameter

and in particular also applies if the parameter is never or only rarely excited during operation. The bound improves with respect to the initial estimates the more often the parameter is detected to be sufficiently excited. Moreover, if the time between two PE intervals occurred during online operation can be uniformly bounded (which may be the case in practice for periodic operations), our result specializes to RGES, i.e., it implies exponential convergence of the state and parameter estimation error to a neighborhood around the origin defined by the true disturbances. The numerical examples illustrated that the proposed MHE schemes in combination with the PE monitoring techniques from Section 7.2 are able to efficiently compensate for phases of weak excitation. For both constant and time-varying parameters, we obtained reliable estimation results for all times, which in particular were prevented from deteriorating arbitrarily in phases without excitation, while being accurate in phases with sufficient excitation.

In Chapter 6, we studied the turnpike phenomenon in optimal state estimation problems and developed novel accuracy and performance guarantees for MHE. We showed that the solution to the (acausal) infinite-horizon optimal estimation problem involving all past and future data serves as a turnpike for finite horizon problems, which are the core of MHE and FIE. We investigated different mathematical characterizations of this phenomenon and established sufficient conditions involving strict dissipativity and decaying sensitivity. For linear systems and quadratic cost functions, we showed that decaying sensitivity is naturally present under controllability and observability using standard arguments from optimal control theory. From our turnpike analysis, we found that MHE problems generally exhibit both an approaching and a leaving arc, which may in fact have a potentially strong negative impact on the overall estimation accuracy. To counteract the leaving arc, we suggested using an artificial delay in the MHE scheme, and we showed that the resulting performance (both averaged and non-averaged) is approximately optimal and yields bounded dynamic regret with respect to the infinite-horizon benchmark solution, with error terms that can be rendered arbitrarily small by an appropriate choice of delay. We proposed a novel turnpike prior for MHE formulations with prior weighting, effectively counteracting the approaching arc and proven to be a valid alternative to the classical options (such as the filtering or smoothing prior) with superior theoretical properties. In our simulations, we found that MHE with the proposed turnpike prior performs comparably well to MHE with filtering or smoothing priors, while the delay resulted in a significant improvement of the estimation results. In particular, considering a continuously stirred tank reactor example and a highly nonlinear quadrotor model from the literature, we observed the turnpike phenomenon and found that a delay of one to three steps improved the overall estimation error by 20-25 % compared to standard MHE (without delay). For offline estimation, the proposed delayed MHE scheme has proven to be a useful alternative to established iterative filtering and smoothing methods, significantly outperforming them especially in the presence of non-normally distributed noise.

In Chapter 7, we focused on the numerical verification of detectability and PE properties for general nonlinear systems. These are fundamental concepts in control and signal processing and play an important role in observer design and system identifi-

cation. We developed several methods to certify detectability (in terms of i-IOSS for discrete-time systems and i-iIOSS for continuous-time systems) and check if a given trajectory pair satisfies a certain PE property or not. The verification methods rely on arguments from contraction theory involving the differential dynamics, Riemannian geometry, and the mean-value theorem in order to reformulate the underlying and rather abstract mathematical conditions in the form of simple LMIs. These can be numerically solved using standard methods such as SDP in combination with LPV embeddings, SOS relaxations, or simple gridding techniques. The proposed verification methods are essential to provide robustness guarantees for MHE under practical conditions in Chapters 3–6. However, they also represent useful tools beyond the field of MHE to verify important properties such as detectability, incremental dissipativity, and PE of nonlinear systems in practice, where such properties are generally often assumed but could not be certified due to a lack of methods.

In summary, this thesis successfully extends the systems-theoretic understanding of MHE and contributes to the overall goal of supporting the great success of MHE in practical applications with appropriate theory. In particular, we were finally able to provide robustness guarantees for MHE under practically relevant conditions, mainly by combining Lyapunov-based MHE schemes with our numerical methods to verify the required detectability condition. Furthermore, we established global robustness properties for real-time capable MHE schemes that allow for a completely free choice of the optimization algorithm and the corresponding termination criterion. In addition, we developed MHE schemes for joint state and parameter estimation, particularly tailored to applications in which weak excitation occurs frequently and unpredictably. Finally, we established a theoretical link between MHE and the acausal infinite-horizon solution involving all past and future data using turnpike arguments, leading to a new perspective on MHE and ultimately to novel performance estimates and regret guarantees.

8.2. Outlook

The results obtained in this thesis considerably extend the theory of nonlinear MHE, while at the same time opening the field for many further investigations. In the following, we outline some interesting areas for possible future work.

In Chapter 2, we discussed three technically different characterizations of i-IOSS, including the original asymptotic-gain formulation and time-discounted (integral or max-based) variants. While these could be shown to be completely equivalent in the context of discrete-time systems, their formal relations are far less clear for continuous-time systems. Notice that this even applies to the (non-discounted) stability notions without outputs, i.e., i-ISS and[1] (non-discounted) i-iISS. An interesting theory-oriented topic for future work is therefore proving (or disproving) some open relations between i-iI(O)SS and i-I(O)SS (without discounting), e.g., by

[1]The work [Ang09] establishes the implication i-iISS $\Rightarrow$ i-ISS; however, [Ang09, Thm. 3] relies on the converse Lyapunov result [Ang09, Thm. 1], the proof of which, however, seems to be erroneous (this applies to the first inequality above (23)) and yet requires a suitable fix.

constructing suitable counterexamples. Another interesting future direction concerns the converse Lyapunov theorem presented in Chapter 2 (Theorem 2.1), where the fact that the Lyapunov function is necessarily continuous could only be shown for the weaker notion of i-iIOSS with nominal outputs (Definition 2.2). However, in the context of MHE, we are actually interested in i-iIOSS with disturbed outputs (Definition 2.1), as this allows to develop suitable estimation schemes with strong robustness guarantees for systems where the measurement noise enters the output equation nonlinearly. So far, however, it is unknown if considering a continuous i-iIOSS Lyapunov function as detectability property (Assumption 3.1) is more restrictive than i-iIOSS with disturbed outputs (Definition 2.1), unless we restrict ourselves to additive measurement noise, see Proposition 2.2. Intuitively, these characterizations should be equivalent, but a formal proof is yet missing.

In Chapter 3, we focused on Lyapunov-based MHE frameworks for general detectable nonlinear systems. These facilitate establishing RGES of MHE, that is, a strong and desirable robust stability property of the estimation error, see Definition 3.1 for details. In some applications, however, the provided robustness guarantees might be in fact stronger than required. Here, it seems interesting to investigate conditions under which MHE exhibits only weaker forms of robust stability, for example in a practical sense or with asymptotic (rather than exponential) convergence rates. This might further increase the practical relevance of nonlinear MHE theory, especially in applications where the system is not uniformly exponentially detectable. Some first steps in this direction are taken in, e.g., [MKZ23b] in the context of MHE under parametric uncertainties, or in [KM23] by establishing RGAS of MHE through a nonlinear contraction. Another interesting future direction is the extension of Lyapunov-based MHE to the case of standard least squares cost functions, particularly without discounting. This is covered in, e.g., [AR21; Mül17], but the results are either conservative or require restrictive and impractical conditions on the horizon length, compare the discussion in Section 3.3. As the lack of discounting prevents applying the theory from Chapter 3, a new proof technique would need to be derived. Here, a promising approach is to address this problem using our turnpike results from Chapter 6 and trying to infer robust stability of MHE by exploiting the turnpike property with respect to the infinite-horizon solution.

Regarding the suboptimal MHE schemes proposed in Chapter 4, the established estimation error bounds are quite conservative, in the sense that they cannot be better than those provided by the auxiliary observer. This is a natural consequence of our approach, since we aim to preserve stability of MHE even in the case where no optimization is performed (i.e., without applying any iteration of the optimization algorithm). This has the particular advantage that our results are completely independent of the optimization algorithm; however, the downside is that (i) the stability properties of the auxiliary observer cannot be improved and (ii) the guarantees for suboptimal MHE do not capture the interplay between the number of solver iterations performed and the accuracy of the estimation results. Addressing these two problems is an interesting topic for future work; especially the second one is of interest for practical applications, as it would provide an estimate on the trade-off between estimation accuracy and computational requirements which would be useful

in the MHE design. This could be achieved by combining the guarantees developed in Chapter 4 with a specific optimization algorithm (or a class of algorithms), such as gradient or Newton methods, compare, e.g., [WVD14; AG17; GGE22; Ale25]. The key challenge here is that the results should not lose their global character, which is usually the case in the convergence analysis of such optimization algorithms.

In Chapter 5, we proposed MHE schemes specifically tailored to joint state and parameter estimation, despite potentially weak or missing excitation. Here, the key ingredient was using an adaptive regularization term in the cost function, incorporating online information about the current excitation. However, the excitation-dependent update rules proposed in (5.17) and (5.80) for the prior parameter estimate involve a binary decision, relying on a PE condition that considers the whole parameter vector. In particular, only if the whole parameter vector is sufficiently excited, the prior estimate is updated; in case at least one single element is not sufficiently excited, however, the PE condition cannot be satisfied and the prior estimate is not updated. An interesting (and practically relevant) topic for future work is therefore the investigation of directional excitation properties, considering the case where some parameters may be sufficiently excited for estimation and others not. To this end, a promising approach might be to combine the developed MHE scheme with directional PE metrics as used in, e.g., [SJ11; BRD22], in order to extend the MHE framework to parameter-individual excitation monitoring and regularization.

Our findings from Chapter 6 represent a new approach and perspective in the MHE literature; therefore, many interesting topics for future work arise. The first one concerns the turnpike property from Definition 6.1, where we essentially require an explicit time-dependent bound on the difference between optimal solutions and the turnpike. Here, a thorough turnpike analysis for nonlinear systems and general cost functions is yet to be done, particularly focusing on sufficient conditions that are of global nature. An important question here is whether turnpike behavior in the sense of the Definition 6.1 can be established using a global dissipativity concept. To this end, one could first investigate how the framework and arguments used [Dam+14] can be extended to the more general case of a time-varying turnpike. Another interesting problem is the extension of the developed theory to the case of discounted cost functions, which are in fact crucial in our robust stability analysis in Chapter 3. This, however, requires a careful investigation of a suitable benchmark solution and corresponding turnpike properties. Here, some insights obtained in the field of discounted optimal control could be useful, e.g., [Gai+18; GSS15; Pos+17]. This might also require investigating and extending discounted dissipativity concepts that are proposed in [Grü+21; ZG22].

Our performance results presented in Chapter 6 are particularly relevant for applications where a small delay in the online estimation can be tolerated, which is especially the case for system monitoring, fault detection or parameter estimation. However, if the estimates are to be used for state feedback control, the picture is not as clear. Indeed, the additional delay in the closed loop requires careful design of the control algorithm to ensure its stability. Hence, an interesting future direction is the investigation of suitable controllers, focusing on the trade-off between improved

estimates and a more involved control technique. Here, we note that improved estimates may be particularly beneficial for robust output feedback tube-based MPC approaches, as such designs are often overly conservative and result in a small region of attraction, compare, for example, [GK07; LSG08; May+09; DA21]. In this context, it would be interesting to investigate whether the proposed δMHE scheme can be used to reduce some conservatism in the overall scheme, exploiting the fact that the obtained state estimates are close to the turnpike.

In conclusion, the results presented in this thesis open up various research directions, ranging from a further theoretical analysis of suitable detectability notions, robust stability properties, and turnpike behavior of MHE problems, to further development of the proposed MHE schemes for real-time applications and joint state and parameter estimation problems.

Bibliography

[AA16] Angelo Alessandri and Moath Awawdeh. "Moving-horizon estimation with guaranteed robustness for discrete-time linear systems and measurements subject to outliers". In: *Automatica* 67 (2016), pp. 85–93. DOI: 10.1016/j.automatica.2016.01.015.

[ABB08] Angelo Alessandri, Marco Baglietto, and Giorgio Battistelli. "Moving-horizon state estimation for nonlinear discrete-time systems: new stability results and approximation schemes". In: *Automatica* 44.7 (2008), pp. 1753–1765. DOI: 10.1016/j.automatica.2007.11.020.

[ABB12] Angelo Alessandri, Marco Baglietto, and Giorgio Battistelli. "Min-max moving-horizon estimation for uncertain discrete-time linear systems". In: *SIAM J. Control Optim.* 50.3 (2012), pp. 1439–1465. DOI: 10.1137/090762798.

[ABN16] Mark Asch, Marc Bocquet, and Maëlle Nodet. *Data Assimilation: Methods, Algorithms, and Applications*. Philadelphia, PA, USA: SIAM, 2016. DOI: 10.1137/1.9781611974546.

[ACJ21] Priyank Agrawal, Jinglin Chen, and Nan Jiang. "Improved worst-case regret bounds for randomized least-squares value iteration". In: *Proc. AAAI Conf. Artif. Intell.* 35.8 (2021), pp. 6566–6573. DOI: 10.1609/aaai.v35i8.16813.

[AG17] Angelo Alessandri and Mauro Gaggero. "Fast moving horizon state estimation for discrete-time systems using single and multi iteration descent methods". In: *IEEE Trans. Autom. Control* 62.9 (2017), pp. 4499–4511. DOI: 10.1109/TAC.2017.2660438.

[Aga+19] Naman Agarwal, Brian Bullins, Elad Hazan, Sham Kakade, and Karan Singh. "Online control with adversarial disturbances". In: *Proc. Int. Conf. Mach. Learn. (ICML)*. Vol. 97. 2019, pp. 111–119. URL: https://proceedings.mlr.press/v97/agarwal19c.html.

[Ale+10] Angelo Alessandri, Marco Baglietto, Giorgio Battistelli, and Victor M. Zavala. "Advances in moving horizon estimation for nonlinear systems". In: *Proc. IEEE Conf. Decis. Control (CDC)*. 2010, pp. 5681–5688. DOI: 10.1109/cdc.2010.5718126.

[Ale25] Angelo Alessandri. "Robust moving-horizon estimation for nonlinear systems: From perfect to imperfect optimization". In: *Automatica* 175 (2025), p. 112187. DOI: 10.1016/j.automatica.2025.112187.

[All+17] Douglas A. Allan, Cuyler N. Bates, Michael J. Risbeck, and James B. Rawlings. "On the inherent robustness of optimal and suboptimal

nonlinear MPC". In: *Syst. Control Lett.* 106 (2017), pp. 68–78. DOI: 10.1016/j.sysconle.2017.03.005.

[All20] Douglas A. Allan. "A Lyapunov-like function for analysis of model predictive control and moving horizon estimation". PhD thesis. Univ. Wisconsin-Madison, 2020. URL: https://digital.library.wisc.edu/1711.dl/S23IGECST72G48H.

[And+18] Joel A. E. Andersson, Joris Gillis, Greg Horn, James B. Rawlings, and Moritz Diehl. "CasADi: a software framework for nonlinear optimization and optimal control". In: *Math. Program. Comput.* 11.1 (2018), pp. 1–36. DOI: 10.1007/s12532-018-0139-4.

[Ang+04] David Angeli, Brian Ingalls, Eduardo D. Sontag, and Yuan Wang. "Separation principles for input-output and integral-input-to-state stability". In: *SIAM J. Control Optim.* 43.1 (2004), pp. 256–276. DOI: 10.1137/s0363012902419047.

[Ang02] David Angeli. "A Lyapunov approach to incremental stability properties". In: *IEEE Trans. Autom. Control* 47.3 (2002), pp. 410–421. DOI: 10.1109/9.989067.

[Ang09] David Angeli. "Further results on incremental input-to-state stability". In: *IEEE Trans. Autom. Control* 54.6 (2009), pp. 1386–1391. DOI: 10.1109/tac.2009.2015561.

[AR19a] Douglas A. Allan and James B. Rawlings. "A Lyapunov-like function for full information estimation". In: *Proc. Am. Control Conf. (ACC)*. 2019, pp. 4497–4502. DOI: 10.23919/ACC.2019.8814807.

[AR19b] Douglas A. Allan and James B. Rawlings. "Moving horizon estimation". In: *Handbook of Model Predictive Control*. Ed. by Saša V. Raković and William S. Levine. Basel, Switzerland: Birkhäuser, 2019, pp. 99–124. DOI: 10.1007/978-3-319-77489-3_5.

[AR21] Douglas A. Allan and James B. Rawlings. "Robust stability of full information estimation". In: *SIAM J. Control Optim.* 59.5 (2021), pp. 3472–3497. DOI: 10.1137/20m1329135.

[ART20] Douglas A. Allan, James B. Rawlings, and Andrew R. Teel. *Nonlinear detectability and incremental input/output-to-state stability*. Tech. rep. 01. TWCCC, 2020. URL: https://sites.engineering.ucsb.edu/~jbraw/jbrweb-archives/tech-reports/twccc-2020-01.pdf.

[ART21] Douglas A. Allan, James B. Rawlings, and Andrew R. Teel. "Nonlinear detectability and incremental input/output-to-state stability". In: *SIAM J. Control Optim.* 59.4 (2021), pp. 3017–3039. DOI: 10.1137/20m135039x.

[Ast+21] Daniele Astolfi, Pauline Bernard, Romain Postoyan, and Lorenzo Marconi. "Constrained state estimation for nonlinear systems: a redesign approach based on convexity". In: *IEEE Trans. Autom. Control* 67.2 (2021), pp. 824–839. DOI: 10.1109/tac.2021.3064537.

[ASW00a] David Angeli, Eduardo D. Sontag, and Yuan Wang. "A characterization of integral input-to-state stability". In: *IEEE Trans. Autom. Control* 45.6 (2000), pp. 1082–1097. DOI: 10.1109/9.863594.

[ASW00b] David Angeli, Eduardo D. Sontag, and Yuang Wang. "Further equivalences and semiglobal versions of integral input to state stability". In: *Dyn. Control* 10.2 (2000), pp. 127–149. DOI: 10.1023/a:1008356223747.

[BAA22] Pauline Bernard, Vincent Andrieu, and Daniele Astolfi. "Observer design for continuous-time dynamical systems". In: *Annu. Rev. Control* 53 (2022), pp. 224–248. DOI: 10.1016/j.arcontrol.2021.11.002.

[Bau+21] Katrin Baumgärtner, Jonathan Frey, Reza Hashemi, and Moritz Diehl. "Zero-order moving horizon estimation for large-scale nonlinear processes". In: *Comput. Chem. Eng.* 154 (2021), p. 107433. DOI: 10.1016/j.compchemeng.2021.107433.

[BC85] Stephen Boyd and Leon O. Chua. "Fading memory and the problem of approximating nonlinear operators with Volterra series". In: *IEEE Trans. Circuits Syst.* 32.11 (1985), pp. 1150–1161. DOI: 10.1109/tcs.1985.1085649.

[BDF23] Jean-Sébastien Brouillon, Florian Dörfler, and Giancarlo Ferrari-Trecate. "Minimal regret state estimation of time-varying systems". In: *IFAC-PapersOnLine* 56.2 (2023), pp. 2595–2600. DOI: 10.1016/j.ifacol.2023.10.1345.

[Bes07] Gildas Besançon. *Nonlinear Observers and Applications*. Berlin, Heidelberg, Germany: Springer, 2007. DOI: 10.1007/978-3-540-73503-8.

[Bes16] Gildas Besançon. "A link between output time derivatives and persistent excitation for nonlinear observers". In: *IFAC-PapersOnLine* 49.18 (2016), pp. 493–498. DOI: 10.1016/j.ifacol.2016.10.213.

[BG88] Georges Bastin and Michel R. Gevers. "Stable adaptive observers for nonlinear time-varying systems". In: *IEEE Trans. Autom. Control* 33.7 (1988), pp. 650–658. DOI: 10.1109/9.1273.

[BH75] Arthur E. Bryson and Yu-Chi Ho. *Applied Optimal Control. Optimization, Estimation and Control*. Rev. printing. New York, NY, USA: Taylor & Francis, 1975.

[Bih56] Imre Bihari. "A generalization of a lemma of Bellman and its application to uniqueness problems of differential equations". In: *Acta Math. Acad. Sci. Hungaricae* 7.1 (1956), pp. 81–94. DOI: 10.1007/bf02022967.

[Bit84] Robert Bitmead. "Persistence of excitation conditions and the convergence of adaptive schemes". In: *IEEE Trans. Inf. Theory* 30.2 (1984), pp. 183–191. DOI: 10.1109/tit.1984.1056898.

[BM21] Michelangelo Bin and Lorenzo Marconi. "Model identification and adaptive state observation for a class of nonlinear systems". In:

IEEE Trans. Autom. Control 66.12 (2021), pp. 5621–5636. DOI: 10.1109/tac.2020.3041238.

[BRD22] Katrin Baumgärtner, Rudolf Reiter, and Moritz Diehl. "Moving horizon estimation with adaptive regularization for ill-posed state and parameter estimation problems". In: *Proc. 61st IEEE Conf. Decis. Control (CDC)*. 2022, pp. 2165–2171. DOI: 10.1109/cdc51059.2022.9993416.

[Bre19] Jonathan Brembeck. "Nonlinear constrained moving horizon estimation applied to vehicle position estimation". In: *Sensors* 19.10 (2019), p. 2276. DOI: 10.3390/s19102276.

[BŢ07] Gildas Besançon and Alexandru Ţiclea. "An immersion-based observer design for rank-observable nonlinear systems". In: *IEEE Trans. Autom. Control* 52.1 (2007), pp. 83–88. DOI: 10.1109/tac.2006.889867.

[BZD19] Katrin Baumgärtner, Andrea Zanelli, and Moritz Diehl. "Zero-order moving horizon estimation". In: *Proc. IEEE 58th Conf. Decis. Control (CDC)*. 2019, pp. 4140–4146. DOI: 10.1109/cdc40024.2019.9029525.

[BZD20] Katrin Baumgärtner, Andrea Zanelli, and Moritz Diehl. "A gradient condition for the arrival cost in moving horizon estimation". In: *Proc. Eur. Control Conf. (ECC)*. 2020, pp. 1286–1291. DOI: 10.23919/ecc51009.2020.9143653.

[Car+18] Alberto Carrassi, Marc Bocquet, Laurent Bertino, and Geir Evensen. "Data assimilation in the geosciences: An overview of methods, issues, and perspectives". In: *WIREs Climate Change* 9.5 (2018). DOI: 10.1002/wcc.535.

[CHL91] Dean A. Carlson, Alain B. Haurie, and Arie Leizarowitz. *Infinite Horizon Optimal Control*. Berlin, Heidelberg, Germany: Springer, 1991. DOI: 10.1007/978-3-642-76755-5.

[CJ11] John L. Crassidis and John L. Junkins. *Optimal Estimation of Dynamic Systems*. 2nd ed. Boca Raton, FL, USA: Chapman and Hall/CRC, 2011. DOI: 10.1201/b11154.

[CL55] Earl A. Coddington and Norman Levinson. *Theory of Ordinary Differential Equations*. New York, NY, USA: McGraw Hill, 1955.

[CLH22] Yuchi Cao, Tieshan Li, and Liying Hao. "Nonlinear model predictive control of shipboard boom cranes based on moving horizon state estimation". In: *J. Mar. Sci. Eng.* 11.1 (2022), p. 4. DOI: 10.3390/jmse11010004.

[Con95] Adrian Constantin. "Global existence of solutions for perturbed differential equations". In: *Ann. di Mat. Pura ed Appl.* 168.1 (1995), pp. 237–299. DOI: 10.1007/bf01759263.

[CR97] Young Man Cho and Rajesh Rajamani. "A systematic approach to adaptive observer synthesis for nonlinear systems". In: *IEEE Trans. Autom. Control* 42.4 (1997), pp. 534–537. DOI: 10.1109/9.566664.

[CT08] Chaohong Cai and Andrew R. Teel. “Input–output-to-state stability for discrete-time systems”. In: *Automatica* 44.2 (2008), pp. 326–336. DOI: 10.1016/j.automatica.2007.05.022.

[DA21] Zihang Dong and David Angeli. “Homothetic tube-based robust economic MPC with integrated moving horizon estimation”. In: *IEEE Trans. Autom. Control* 66.1 (2021), pp. 64–75. DOI: 10.1109/tac.2020.2973606.

[Dam+14] Tobias Damm, Lars Grüne, Marleen Stieler, and Karl Worthmann. “An exponential turnpike theorem for dissipative discrete time optimal control problems”. In: *SIAM J. Control Optim.* 52.3 (2014), pp. 1935–1957. DOI: 10.1137/120888934.

[DSZ22] Alexandre Didier, Jerome Sieber, and Melanie N. Zeilinger. “A system level approach to regret optimal control”. In: *IEEE Control Syst. Lett.* 6 (2022), pp. 2792–2797. DOI: 10.1109/lcsys.2022.3177780.

[EBO19] Denis Efimov, Nikita Barabanov, and Romeo Ortega. “Robustness of linear time-varying systems with relaxed excitation”. In: *Int. J. Adapt. Control Signal Process.* 33.12 (2019), pp. 1885–1900. DOI: 10.1002/acs.2997.

[EEZ16] Denis Efimov, Christopher Edwards, and Ali Zolghadri. “Enhancement of adaptive observer robustness applying sliding mode techniques”. In: *Automatica* 72 (2016), pp. 53–56. DOI: 10.1016/j.automatica.2016.05.029.

[Ekr+13] Mohsen Ekramian, Farid Sheikholeslam, Saeed Hosseinnia, and Mohammad J. Yazdanpanah. “Adaptive state observer for Lipschitz nonlinear systems”. In: *Syst. Control Lett.* 62.4 (2013), pp. 319–323. DOI: 10.1016/j.sysconle.2013.01.002.

[Els+21] Mohamed Elsheikh, Rubin Hille, Alexandru Tatulea-Codrean, and Stefan Krämer. “A comparative review of multi-rate moving horizon estimation schemes for bioprocess applications”. In: *Comput. Chem. Eng.* 146 (2021), p. 107219. DOI: 10.1016/j.compchemeng.2020.107219.

[Far+09] Mondher Farza, Mohammed M’Saad, Tarek Maatoug, and Mohammed Kamoun. “Adaptive observers for nonlinearly parameterized class of nonlinear systems”. In: *Automatica* 45.10 (2009), pp. 2292–2299. DOI: 10.1016/j.automatica.2009.06.008.

[Fau+22] Timm Faulwasser, Lars Grüne, Jukka-Pekka Humaloja, and Manuel Schaller. “The interval turnpike property for adjoints”. In: *Pure Appl. Funct. Anal.* 7.4 (2022), pp. 1187–1207. DOI: 10.48550/arXiv.2005.12120.

[FG22] Timm Faulwasser and Lars Grüne. “Turnpike properties in optimal control”. In: *Handbook of Numerical Analysis*. Ed. by Emmanuel Trélat and Enrique Zuazua. Vol. 23. Amsterdam, The Netherlands: Elsevier, 2022, pp. 367–400. DOI: 10.1016/bs.hna.2021.12.011.

[FGM18] Timm Faulwasser, Lars Grüne, and Matthias A. Müller. "Economic nonlinear model predictive control". In: *Found. Trends Syst. Control* 5.1 (2018), pp. 1–98. DOI: 10.1561/2600000014.

[Fit71] Robert J. Fitzgerald. "Divergence of the Kalman filter". In: *IEEE Trans. Autom. Control* 16.6 (1971), pp. 736–747. DOI: 10.1109/tac.1971.1099836.

[FN05] Augusto Ferrante and Lorenzo Ntogramatzidis. "Employing the algebraic Riccati equation for a parametrization of the solutions of the finite-horizon LQ problem: the discrete-time case". In: *Syst. Control Lett.* 54.7 (2005), pp. 693–703. DOI: 10.1016/j.sysconle.2004.11.008.

[FN07] Augusto Ferrante and Lorenzo Ntogramatzidis. "A unified approach to finite-horizon generalized LQ optimal control problems for discrete-time systems". In: *Linear Algebra Appl.* 425.2–3 (2007), pp. 242–260. DOI: 10.1016/j.laa.2007.01.026.

[Fra+20] Roberto Franco, Héctor Ríos, Denis Efimov, and Wilfrid Perruquetti. "Adaptive estimation for uncertain nonlinear systems with measurement noise: A sliding-mode observer approach". In: *Int. J. Robust Nonlinear Control* 31.9 (2020), pp. 3809–3826. DOI: 10.1002/rnc.5220.

[FS13] Fulvio Forni and Rodolphe Sepulchre. "On differentially dissipative dynamical systems". In: *IFAC Proceedings Volumes* 46.23 (2013), pp. 15–20. DOI: 10.3182/20130904-3-fr-2041.00038.

[FS14] Fulvio Forni and Rodolphe Sepulchre. "A differential Lyapunov framework for contraction analysis". In: *IEEE Trans. Autom. Control* 59.3 (2014), pp. 614–628. DOI: 10.1109/tac.2013.2285771.

[FS23] Emilien Flayac and Iman Shames. "Nonuniform observability for moving horizon estimation and stability with respect to additive perturbation". In: *SIAM J. Control Optim.* 61.5 (2023), pp. 3018–3050. DOI: 10.1137/22m1475132.

[FTK13] Mohammad Mehdi Fateh, Hojjat Ahsani Tehrani, and Seyed Mehdi Karbassi. "Repetitive control of electrically driven robot manipulators". In: *Int. J. Syst. Sci.* 44.4 (2013), pp. 775–785. DOI: 10.1080/00207721.2011.625478.

[Gai+18] Vladimir Gaitsgory, Lars Grüne, Matthias Höger, Christopher M. Kellett, and Steven R. Weller. "Stabilization of strictly dissipative discrete time systems with discounted optimal control". In: *Automatica* 93 (2018), pp. 311–320. DOI: 10.1016/j.automatica.2018.03.076.

[GBE21] Meriem Gharbi, Fabia Bayer, and Christian Ebenbauer. "Proximity moving horizon estimation for discrete-time nonlinear systems". In: *IEEE Contr. Syst. Lett.* 5.6 (2021), pp. 2090–2095. DOI: 10.1109/lcsys.2020.3046377.

[GGE21] Meriem Gharbi, Bahman Gharesifard, and Christian Ebenbauer. "Anytime proximity moving horizon estimation: stability and regret for non-

linear systems". In: *Proc. 60th IEEE Conf. Decision Control (CDC)*. 2021, pp. 728–735. DOI: 10.1109/cdc45484.2021.9683122.

[GGE22] Meriem Gharbi, Bahman Gharesifard, and Christian Ebenbauer. "Anytime proximity moving horizon estimation: stability and regret". In: *IEEE Trans. Autom. Control* 68.6 (2022), pp. 3393–3408. DOI: 10.1109/tac.2022.3190044.

[GH23] Gautam Goel and Babak Hassibi. "Regret-optimal estimation and control". In: *IEEE Trans. Autom. Control* 68.5 (2023), pp. 3041–3053. DOI: 10.1109/tac.2023.3253304.

[GHL04] Sylvestre Gallot, Dominique Hulin, and Jacques Lafontaine. *Riemannian Geometry*. Berlin, Heidelberg, Germany: Springer, 2004. DOI: 10.1007/978-3-642-18855-8.

[GHO92] Jean-Paul Gauthier, Hassan Hammouri, and Sami Othman. "A simple observer for nonlinear systems applications to bioreactors". In: *IEEE Trans. Autom. Control* 37.6 (1992), pp. 875–880. DOI: 10.1109/9.256352.

[GK07] Paul J. Goulart and Eric C. Kerrigan. "Output feedback receding horizon control of constrained systems". In: *Int. J. Control* 80.1 (2007), pp. 8–20. DOI: 10.1080/00207170600892949.

[GK94] Jean-Paul Gauthier and Ivan A. K. Kupka. "Observability and observers for nonlinear systems". In: *SIAM J. Control Optim.* 32.4 (1994), pp. 975–994. DOI: 10.1137/s0363012991221791.

[GKW16] Lars Grüne, Christopher M. Kellett, and Steven R. Weller. "On a discounted notion of strict dissipativity". In: *IFAC-PapersOnLine* 49.18 (2016), pp. 247–252. DOI: 10.1016/j.ifacol.2016.10.171.

[GM16] Lars Grüne and Matthias A. Müller. "On the relation between strict dissipativity and turnpike properties". In: *Syst. Control Lett.* 90 (2016), pp. 45–53. DOI: 10.1016/j.sysconle.2016.01.003.

[GM86] Michael Green and John B. Moore. "Persistence of excitation in linear systems". In: *Syst. Control Lett.* 7.5 (1986), pp. 351–360. DOI: 10.1016/0167-6911(86)90052-6.

[GP15] Lars Grüne and Anastasia Panin. "On non-averaged performance of economic MPC with terminal conditions". In: *Proc. IEEE Conf. Decis. Control (CDC)*. 2015, pp. 4332–4337. DOI: 10.1109/cdc.2015.7402895.

[GP19] Lars Grüne and Simon Pirkelmann. "Economic model predictive control for time-varying system: Performance and stability results". In: *Optim. Control Appl. Methods* 41.1 (2019), pp. 42–64. DOI: 10.1002/oca.2492.

[GPS18] Lars Grüne, Simon Pirkelmann, and Marleen Stieler. "Strict dissipativity implies turnpike behavior for time-varying discrete time optimal control problems". In: *Control Systems and Mathematical Methods in Economics*. Ed. by G. Feichtinger, R. Kovacevic, and G. Tragler. Cham,

Germany: Springer, 2018, pp. 195–218. DOI: 10.1007/978-3-319-75169-6_10.

[Grü+21] Lars Grüne, Matthias A. Müller, Christopher M. Kellett, and Steven R. Weller. "Strict dissipativity for discrete time discounted optimal control problems". In: *Math. Control Relat. Fields* 11.4 (2021), p. 771. DOI: 10.3934/mcrf.2020046.

[Grü16] Lars Grüne. "Approximation properties of receding horizon optimal control". In: *Jahresber. Dtsch. Math. Ver.* 118.1 (2016), pp. 3–37. DOI: 10.1365/s13291-016-0134-5.

[GSS15] Lars Grüne, Willi Semmler, and Marleen Stieler. "Using nonlinear model predictive control for dynamic decision problems in economics". In: *J. Econ. Dyn. Control* 60 (2015), pp. 112–133. DOI: 10.1016/j.jedc.2015.08.010.

[GSS20] Lars Grüne, Manuel Schaller, and Anton Schiela. "Exponential sensitivity and turnpike analysis for linear quadratic optimal control of general evolution equations". In: *J. Differ. Equ.* 268.12 (2020), pp. 7311–7341. DOI: 10.1016/j.jde.2019.11.064.

[HCE18] Xiaosong Hu, Dongpu Cao, and Bo Egardt. "Condition monitoring in advanced battery management systems: Moving horizon estimation using a reduced electrochemical model". In: *IEEE ASME Trans. Mechatron.* 23.1 (2018), pp. 167–178. DOI: 10.1109/tmech.2017.2675920.

[HL93] Jean-Baptiste Hiriart-Urruty and Claude Lemaréchal. *Convex Analysis and Minimization Algorithms I*. Berlin, Heidelberg, Germany: Springer, 1993. DOI: 10.1007/978-3-662-02796-7.

[HM20] Hernan Haimovich and José Luis Mancilla-Aguilar. "Strong ISS implies strong iISS for time-varying impulsive systems". In: *Automatica* 122 (2020), p. 109224. DOI: 10.1016/j.automatica.2020.109224.

[Hu17] Wuhua Hu. "Robust stability of optimization-based state estimation". In: *arXiv:1702.01903v3* (2017). DOI: 10.48550/arXiv.1702.01903.

[Hu24] Wuhua Hu. "Generic stability implication from full information estimation to moving-horizon estimation". In: *IEEE Trans. Autom. Control* 69.2 (2024), pp. 1164–1170. DOI: 10.1109/tac.2023.3277315.

[HZ22] Zhong-Jie Han and Enrique Zuazua. "Slow decay and turnpike for infinite-horizon hyperbolic linear quadratic problems". In: *SIAM J. Control Optim.* 60.4 (2022), pp. 2440–2468. DOI: 10.1137/21m1441985.

[Ibr18] Salim Ibrir. "Joint state and parameter estimation of non-linearly parameterized discrete-time nonlinear systems". In: *Automatica* 97 (2018), pp. 226–233. DOI: 10.1016/j.automatica.2018.06.027.

[Ing01a] Brian Ingalls. "Comparisons of notions of stability for nonlinear control systems with outputs". PhD thesis. New Brunswick, NJ, USA: Rutgers School of Graduate Studies, 2001. URL: https://www.proquest.com/dissertations-theses/comparisons-notions-stability-nonlinear-control/docview/276307727/se-2.

[Ing01b] Brian Ingalls. "Integral-input-output to state stability". In: *arXiv:-math/0106138* (2001). DOI: 10.48550/arXiv.math/0106138.

[Ion96] Vlad Ionescu. "Reverse discrete-time Riccati equation and extended Nehari's problem". In: *Linear Algebra Appl.* 236 (1996), pp. 59–94. DOI: 10.1016/0024-3795(94)00129-4.

[IOW99] Vlad Ionescu, Cristian Oară, and Martin Weiss. *Generalized Riccati Theory and Robust Control. A Popov Function Approach*. Chichester, England: John Wiley & Sons, 1999.

[IS12] Petros Ioannou and Jing Sun. *Robust Adaptive Control*. Mineola, NY, USA: Dover Publications, Inc., 2012.

[Jat00] Ravindra V. Jategaonkar. "Bounded-variable Gauss-Newton algorithm for aircraft parameter estimation". In: *J. Aircr.* 37.4 (2000), pp. 742–744. DOI: 10.2514/2.2666.

[Ji+16] Luo Ji, James B. Rawlings, Wuhua Hu, Andrew Wynn, and Moritz Diehl. "Robust stability of moving horizon estimation under bounded disturbances". In: *IEEE Trans. Autom. Control* 61.11 (2016), pp. 3509–3514. DOI: 10.1109/TAC.2015.2513364.

[JOA10] Thomas Jaksch, Ronald Ortner, and Peter Auer. "Near-optimal regret bounds for reinforcement learning". In: *J. Mach. Learn. Res.* 11.51 (2010), pp. 1563–1600. URL: http://jmlr.org/papers/v11/jaksch10a.html.

[JRB05] Chandrasekar Jaganath, Aaron Ridley, and Dennis. S. Bernstein. "A SDRE-based asymptotic observer for nonlinear discrete-time systems". In: *Proc. Am. Control Conf. (ACC)*. 2005, pp. 3630–3635. DOI: 10.1109/acc.2005.1470537.

[JW01] Zhong-Ping Jiang and Yuan Wang. "Input-to-state stability for discrete-time nonlinear systems". In: *Automatica* 37.6 (2001), pp. 857–869. DOI: 10.1016/s0005-1098(01)00028-0.

[Kai+17] Jean-Marie Kai, Guillaume Allibert, Minh-Duc Hua, and Tarek Hamel. "Nonlinear feedback control of quadrotors exploiting first-order drag effects". In: *IFAC-PapersOnLine* 50.1 (2017), pp. 8189–8195. DOI: 10.1016/j.ifacol.2017.08.1267.

[Kel14] Christopher M. Kellett. "A compendium of comparison function results". In: *Math. Control Signals Syst.* 26.3 (2014), pp. 339–374. DOI: 10.1007/s00498-014-0128-8.

[Kim13] Pyung Soo Kim. "A computationally efficient fixed-lag smoother using recent finite measurements". In: *Measurement* 46.1 (2013), pp. 846–850. DOI: 10.1016/j.measurement.2012.09.021.

[KK22] Bokyu Kwon and Pyung Soo Kim. "Novel unbiased optimal receding-horizon fixed-lag smoothers for linear discrete time-varying systems". In: *Appl. Sci.* 12.15 (2022), p. 7832. DOI: 10.3390/app12157832.

[Kle+23] Viktoria Kleyman, Manuel Schaller, Mario Mordmüller, Mitsuru Wilson, Ralf Brinkmann, Karl Worthmann, and Matthias A. Müller. "State and parameter estimation for retinal laser treatment". In: *IEEE Trans. Control Syst. Technol.* 31.3 (2023), pp. 1366–1378. DOI: 10.1109/tcst.2022.3228442.

[KM18] Sven Knüfer and Matthias A. Müller. "Robust global exponential stability for moving horizon estimation". In: *Proc. IEEE Conf. Decis. Control (CDC)*. 2018, pp. 3477–3482. DOI: 10.1109/CDC.2018.8619617.

[KM20] Sven Knüfer and Matthias A. Müller. "Time-discounted incremental input/output-to-state stability". In: *Proc. IEEE Conf. Decis. Control (CDC)*. 2020, pp. 5394–5400. DOI: 10.1109/cdc42340.2020.9304034.

[KM23] Sven Knüfer and Matthias A. Müller. "Nonlinear full information and moving horizon estimation: Robust global asymptotic stability". In: *Automatica* 150 (2023), p. 110603. DOI: 10.1016/j.automatica.2022.110603.

[KMA19] Johannes Köhler, Matthias A. Müller, and Frank Allgöwer. "Nonlinear reference tracking: An economic model predictive control perspective". In: *IEEE Trans. Autom. Control* 64.1 (2019), pp. 254–269. DOI: 10.1109/tac.2018.2800789.

[KMA21] Johannes Köhler, Matthias A. Müller, and Frank Allgöwer. "Robust output feedback model predictive control using online estimation bounds". In: *arXiv:2105.03427* (2021). DOI: 10.48550/arXiv.2105.03427.

[KN99] Hiroyuki Kano and Toshimitsu Nishimura. "Existence conditions of stabilizing and anti-stabilizing solutions of discrete-time algebraic matrix Riccati equations". In: *Trans. Soc. Instrum. Control Eng.* 35.7 (1999), pp. 886–895. DOI: 10.9746/sicetr1965.35.886.

[Kor+22] Marina M. Korotina, José G. Romero, Stanislav V. Aranovskiy, Alexey A. Bobtsov, and Romeo Ortega. "A new on-line exponential parameter estimator without persistent excitation". In: *Syst. Control Lett.* 159 (2022), p. 105079. DOI: 10.1016/j.sysconle.2021.105079.

[KP13] Hassan K. Khalil and Laurent Praly. "High-gain observers in nonlinear feedback control". In: *Int. J. Robust Nonlinear Control* 24.6 (2013), pp. 993–1015. DOI: 10.1002/rnc.3051.

[Kre77] Gerhard Kreisselmeier. "Adaptive observers with exponential rate of convergence". In: *IEEE Trans. Autom. Control* 22.1 (1977), pp. 2–8. DOI: 10.1109/tac.1977.1101401.

[KSW01] Mikhail Krichman, Eduardo D. Sontag, and Yuan Wang. "Input-output-to-state stability". In: *SIAM J. Control Optim.* 39.6 (2001), pp. 1874–1928. DOI: 10.1137/s0363012999365352.

[KT21] Patrick J. W. Koelewijn and Roland Tóth. "Incremental stability and performance analysis of discrete-time nonlinear systems using the LPV

framework". In: *IFAC-PapersOnLine* 54.8 (2021), pp. 75–82. DOI: 10.1016/j.ifacol.2021.08.584.

[KTW21] Patrick J. W. Koelewijn, Roland Tóth, and Siep Weiland. "Incremental dissipativity based control of discrete-time nonlinear systems via the LPV framework". In: *Proc. IEEE Conf. Decis. Control (CDC)*. 2021. DOI: 10.1109/cdc45484.2021.9682893.

[Kuč72] Vladimír Kučera. "The discrete Riccati equation of optimal control". In: *Kybernetika* 8.5 (1972), pp. 430–447. URL: https://dml.cz/handle/10338.dmlcz/125696.

[Küh+11] Peter Kühl, Moritz Diehl, Tom Kraus, Johannes P. Schlöder, and Hans Georg Bock. "A real-time algorithm for moving horizon state and parameter estimation". In: *Comput. Chem. Eng.* 35.1 (2011), pp. 71–83. DOI: 10.1016/j.compchemeng.2010.07.012.

[LB24] Brian Lai and Dennis S. Bernstein. "Generalized forgetting recursive least squares: Stability and robustness guarantees". In: *IEEE Trans. Autom. Control* 69.11 (2024), pp. 7646–7661. DOI: 10.1109/TAC.2024.3394351.

[LCL19] Yingying Li, Xin Chen, and Na Li. "Online optimal control with linear dynamics and predictions: Algorithms and regret analysis". In: *Adv. Neural Inf. Process. Syst. (NeurIPS)*. Vol. 32. 2019. URL: https://proceedings.neurips.cc/paper/2019/hash/6d1e481bdcf159961818823e652a7725-Abstract.html.

[LG90] Lennart Ljung and Svante Gunnarsson. "Adaptation and tracking in system identification—A survey". In: *Automatica* 26.1 (1990), pp. 7–21. DOI: 10.1016/0005-1098(90)90154-a.

[Lip00] Olivia Lipovan. "A retarded Gronwall-like inequality and its applications". In: *J. Math. Anal. Appl.* 252.1 (2000), pp. 389–401. DOI: 10.1006/jmaa.2000.7085.

[Liu+17] Andong Liu, Wen-An Zhang, Michael Z. Q. Chen, and Li Yu. "Moving horizon estimation for mobile robots with multirate sampling". In: *IEEE Trans. Ind. Electron.* 64.2 (2017), pp. 1457–1467. DOI: 10.1109/tie.2016.2611458.

[Liu+21] Jianbang Liu, Aristarchus Gnanasekar, Yi Zhang, Song Bo, Jinfeng Liu, Jingtao Hu, and Tao Zou. "Simultaneous state and parameter estimation: The role of sensitivity analysis". In: *Ind. Eng. Chem. Res.* 60.7 (2021), pp. 2971–2982. DOI: 10.1021/acs.iecr.0c03793.

[Liu+22] Shenyu Liu, Antonio Russo, Daniel Liberzon, and Alberto Cavallo. "Integral-input-to-state stability of switched nonlinear systems under slow switching". In: *IEEE Trans. Autom. Control* 67.11 (2022), pp. 5841–5855. DOI: 10.1109/tac.2021.3124189.

[Liu13] Jinfeng Liu. "Moving horizon state estimation for nonlinear systems with bounded uncertainties". In: *Chem. Eng. Sci.* 93 (2013), pp. 376–386. DOI: 10.1016/j.ces.2013.02.030.

[Lju99] Lennart Ljung. *System Identification: Theory for the User*. 2nd ed. 14th printing. Upper Saddle River, NJ, USA: Prentice Hall, 1999.

[Löf04] Johan Löfberg. "YALMIP: a toolbox for modeling and optimization in MATLAB". In: *Proc. IEEE Int. Conf. Robot. Autom. (ICRA)*. 2004, pp. 284–289. DOI: 10.1109/CACSD.2004.1393890.

[Löf09] Johan Löfberg. "Pre- and post-processing sum-of-squares programs in practice". In: *IEEE Trans. Autom. Control* 54.5 (2009), pp. 1007–1011. DOI: 10.1109/tac.2009.2017144.

[LS98] Winfried Lohmiller and Jean-Jacques E. Slotine. "On contraction analysis for non-linear systems". In: *Automatica* 34.6 (1998), pp. 683–696. DOI: 10.1016/s0005-1098(98)00019-3.

[LSG08] Christian Løvaas, María M. Seron, and Graham C. Goodwin. "Robust output-feedback model predictive control for systems with unstructured uncertainty". In: *Automatica* 44.8 (2008), pp. 1933–1943. DOI: 10.1016/j.automatica.2007.10.003.

[LSW96] Yuandan Lin, Eduardo D. Sontag, and Yuan Wang. "A smooth converse Lyapunov theorem for robust stability". In: *SIAM J. Control Optim.* 34.1 (1996), pp. 124–160. DOI: 10.1137/s0363012993259981.

[LT01] Craig T. Lawrence and André L. Tits. "A computationally efficient feasible sequential quadratic programming algorithm". In: *SIAM J. Optim.* 11.4 (2001), pp. 1092–1118. DOI: 10.1137/s1052623498344562.

[Mar+22] Vicent Rodrigo Marco, Jens C. Kalkkuhl, Jörg Raisch, and Thomas Seel. "Regularized adaptive Kalman filter for non-persistently excited systems". In: *Automatica* 138 (2022), pp. 110–147. DOI: 10.1016/j.automatica.2021.110147.

[Mar+24a] Andrea Martin, Luca Furieri, Florian Dörfler, John Lygeros, and Giancarlo Ferrari-Trecate. "On the guarantees of minimizing regret in receding horizon". In: *IEEE Trans. Autom. Control* (2024). Early Access. DOI: 10.1109/tac.2024.3464013.

[Mar+24b] Andrea Martin, Luca Furieri, Florian Dörfler, John Lygeros, and Giancarlo Ferrari-Trecate. "Regret optimal control for uncertain stochastic systems". In: *Eur. J. Control* 80, Part A (2024), p. 101051. DOI: 10.1016/j.ejcon.2024.101051.

[May+09] David Q. Mayne, Saša V. Raković, Rolf Findeisen, and Frank Allgöwer. "Robust output feedback model predictive control of constrained linear systems: Time varying case". In: *Automatica* 45.9 (2009), pp. 2082–2087. DOI: 10.1016/j.automatica.2009.05.009.

[McK86] Lionel W. McKenzie. "Optimal economic growth, turnpike theorems and comparative dynamics". In: *Handbook of Mathematical Economics*. Ed. by Kenneth J. Arrow and Michael D. Intriligator. Vol. 3. Amsterdam, The Netherlands: Elsevier, 1986, pp. 1281–1355. DOI: 10.1016/s1573-4382(86)03008-4.

[Mir23] Andrii Mironchenko. *Input-to-State Stability: Theory and Applications*. Cham, Switzerland: Springer, 2023. DOI: 10.1007/978-3-031-14674-9.

[MK17] Peyman Mohajerin Esfahani and Daniel Kuhn. "Data-driven distributionally robust optimization using the Wasserstein metric: performance guarantees and tractable reformulations". In: *Math. Program.* 171.1–2 (2017), pp. 115–166. DOI: 10.1007/s10107-017-1172-1.

[MKZ23a] Simon Muntwiler, Johannes Köhler, and Melanie N. Zeilinger. "MHE under parametric uncertainty – Robust state estimation without informative data". In: *arXiv:2312.14049* (2023). DOI: 10.48550/arxiv.2312.14049.

[MKZ23b] Simon Muntwiler, Johannes Köhler, and Melanie N. Zeilinger. "Nonlinear functional estimation: Functional detectability and full information estimation". In: *Automatica* 171 (2023), p. 111945. DOI: 10.1016/j.automatica.2024.111945.

[MM95] Hannah Michalska and David Q. Mayne. "Moving horizon observers and observer-based control". In: *IEEE Trans. Autom. Control* 40.6 (1995), pp. 995–1006. DOI: 10.1109/9.388677.

[Moh+18] Peyman Mohajerin Esfahani, Tobias Sutter, Daniel Kuhn, and John Lygeros. "From infinite to finite programs: explicit error bounds with applications to approximate dynamic programming". In: *SIAM J. Optim.* 28.3 (2018), pp. 1968–1998. DOI: 10.1137/17m1133087.

[Moo73] John B. Moore. "Discrete-time fixed-lag smoothing algorithms". In: *Automatica* 9.2 (1973), pp. 163–173. DOI: 10.1016/0005-1098(73)90071-x.

[MOS24] MOSEK ApS. *The MOSEK optimization toolbox for MATLAB manual. version 10.2.* 2024. URL: https://docs.mosek.com/10.2/toolbox/index.html.

[MR95] Kenneth R. Muske and James B. Rawlings. "Nonlinear moving horizon state estimation". In: *Methods of Model Based Process Control*. Ed. by Ridvan Berber. Dordrecht, The Netherlands: Springer, 1995, pp. 349–365. DOI: 10.1007/978-94-011-0135-6_14.

[MS00] Wolfgang Maass and Eduardo D. Sontag. "Neural systems as nonlinear filters". In: *Neural Comput.* 12.8 (2000), pp. 1743–1772. DOI: 10.1162/089976600300015123.

[MS14] Ian R. Manchester and Jean-Jacques E. Slotine. "Transverse contraction criteria for existence, stability, and robustness of a limit cycle". In: *Syst. Contr. Lett.* 63 (2014), pp. 32–38. DOI: 10.1016/j.sysconle.2013.10.005.

[MS17] Ian R. Manchester and Jean-Jacques E. Slotine. "Control contraction metrics: convex and intrinsic criteria for nonlinear feedback design". In: *IEEE Trans. Autom. Control* 62.6 (2017), pp. 3046–3053. DOI: 10.1109/tac.2017.2668380.

[MS18] Ian R. Manchester and Jean-Jacques E. Slotine. "Robust control contraction metrics: a convex approach to nonlinear state-feedback H^∞ control". In: *IEEE Control Syst. Lett.* 2.3 (2018), pp. 333–338. DOI: 10.1109/lcsys.2018.2836355.

[MST01] Riccardo Marino, Giovanni L. Santosuosso, and Patrizio Tomei. "Robust adaptive observers for nonlinear systems with bounded disturbances". In: *IEEE Trans. Autom. Control* 45.6 (2001), pp. 967–972. DOI: 10.1109/9.928609.

[MT92] Riccardo Marino and Patrizio Tomei. "Global adaptive observers for nonlinear systems via filtered transformations". In: *IEEE Trans. Autom. Control* 37.8 (1992), pp. 1239–1245. DOI: 10.1109/9.151117.

[Mül17] Matthias A. Müller. "Nonlinear moving horizon estimation in the presence of bounded disturbances". In: *Automatica* 79 (2017), pp. 306–314. DOI: 10.1016/j.automatica.2017.01.033.

[Mun24] Simon Muntwiler. "Optimization-based estimation and control under uncertainty". PhD thesis. ETH Zurich, 2024. DOI: 10.3929/ETHZ-B-000706773.

[NA20] Sen Na and Mihai Anitescu. "Exponential decay in the sensitivity analysis of nonlinear dynamic programming". In: *SIAM J. Optim.* 30.2 (2020), pp. 1527–1554. DOI: 10.1137/19m1265065.

[NM05] Lorenzo Ntogramatzidis and Giovanni Marro. "A parametrization of the solutions of the Hamiltonian system for stabilizable pairs". In: *Int. J. Control* 78.7 (2005), pp. 530–533. DOI: 10.1080/00207170500075348.

[NM22] Marko Nonhoff and Matthias A. Müller. "Online convex optimization for data-driven control of dynamical systems". In: *IEEE Open J. Control Syst.* 1 (2022), pp. 180–193. DOI: 10.1109/ojcsys.2022.3200021.

[NM23] Marko Nonhoff and Matthias A. Müller. "On the relation between dynamic regret and closed-loop stability". In: *Syst. Control Lett.* 177 (2023), p. 105532. DOI: 10.1016/j.sysconle.2023.105532.

[NS19] Tiago P. Nascimento and Martin Saska. "Position and attitude control of multi-rotor aerial vehicles: A survey". In: *Annu. Rev. Control* 48 (2019), pp. 129–146. DOI: 10.1016/j.arcontrol.2019.08.004.

[NS90] Henk Nijmeijer and Arjan van der Schaft. *Nonlinear Dynamical Control Systems*. New York, NY, USA: Springer, 1990. DOI: 10.1007/978-1-4757-2101-0.

[ORA22] Romeo Ortega, José G. Romero, and Stanislav V. Aranovskiy. "A new least squares parameter estimator for nonlinear regression equations with relaxed excitation conditions and forgetting factor". In: *Syst. Control Lett.* 169 (2022), p. 105377. DOI: 10.1016/j.sysconle.2022.105377.

[Osg98] William F. Osgood. "Beweis der Existenz einer Lösung der Differentialgleichung $\frac{dy}{dx} = f(x, y)$ ohne Hinzunahme der Cauchy-Lipschitz'schen

Bedingung". In: *Monatsh. Math. Phys.* 9.1 (1898), pp. 331–345. DOI: 10.1007/bf01707876.

[Par03] Pablo A. Parrilo. "Semidefinite programming relaxations for semialgebraic problems". In: *Math. Program.* 96.2 (2003), pp. 293–320. DOI: 10.1007/s10107-003-0387-5.

[Per01] Lawrence Perko. *Differential Equations and Dynamical Systems*. New York, NY, USA: Springer, 2001. DOI: 10.1007/978-1-4613-0003-8.

[PLT01] Elena Panteley, Antonio Loría, and Andrew R. Teel. "Relaxed persistency of excitation for uniform asymptotic stability". In: *IEEE Trans. Autom. Control* 46.12 (2001), pp. 1874–1886. DOI: 10.1109/9.975471.

[Pos+17] Romain Postoyan, Lucian Buşoniu, Dragan Nešić, and Jamal Daafouz. "Stability analysis of discrete-time infinite-horizon optimal control with discounted cost". In: *IEEE Trans. Autom. Control* 62.6 (2017), pp. 2736–2749. DOI: 10.1109/tac.2016.2616644.

[PR03] Gabriele Pannocchia and James B. Rawlings. "Disturbance models for offset-free model-predictive control". In: *AIChE Journal* 49.2 (2003), pp. 426–437. DOI: 10.1002/aic.690490213.

[PRW11] Gabriele Pannocchia, James B. Rawlings, and Stephen J. Wright. "Inherently robust suboptimal nonlinear MPC: Theory and application". In: *Proc. 50th IEEE Conf. Decision Control (CDC), Eur. Control Conf. (ECC)*. 2011, pp. 3398–3403. DOI: 10.1109/cdc.2011.6161240.

[PW96] Laurent Praly and Yuan Wang. "Stabilization in spite of matched unmodeled dynamics and an equivalent definition of input-to-state stability". In: *Math. Control Signals Syst.* 9.1 (1996), pp. 1–33. DOI: 10.1007/bf01211516.

[QH09] Cheryl C. Qu and Juergen Hahn. "Computation of arrival cost for moving horizon estimation via unscented Kalman filtering". In: *J. Process Control* 19.2 (2009), pp. 358–363. DOI: 10.1016/j.jprocont.2008.04.005.

[Rao00] Christopher V. Rao. "Moving horizon strategies for the constrained monitoring and control of nonlinear discrete-time systems". PhD thesis. Univ. Wisconsin-Madison, 2000. URL: https://www.proquest.com/dissertations-theses/moving-horizon-strategies-constrained-monitoring/docview/304638563/se-2.

[Rib+20] Antônio H. Ribeiro, Koen Tiels, Jack Umenberger, Thomas B. Schön, and Luis A. Aguirre. "On the smoothness of nonlinear system identification". In: *Automatica* 121 (2020), p. 109158. DOI: 10.1016/j.automatica.2020.109158.

[RJ12] James B. Rawlings and Luo Ji. "Optimization-based state estimation: Current status and some new results". In: *J. Process Control* 22.8 (2012), pp. 1439–1444. DOI: 10.1016/j.jprocont.2012.03.001.

[RMD20] James B. Rawlings, David Q. Mayne, and Moritz Diehl. *Model Predictive Control: Theory, Computation, and Design*. 2nd ed. 3rd printing.

Santa Barbara, CA, USA: Nob Hill Publish., LLC, 2020. URL: https://sites.engineering.ucsb.edu/~jbraw/mpc/.

[Rom+22] Angel Romero, Sihao Sun, Philipp Foehn, and Davide Scaramuzza. "Model predictive contouring control for time-optimal quadrotor flight". In: *IEEE Trans. Robot.* 38.6 (2022), pp. 3340–3356. DOI: 10.1109/tro.2022.3173711.

[RP15] Obaid Ur Rehman and Ian R. Petersen. "A robust continuous-time fixed-lag smoother for nonlinear uncertain systems". In: *Int. J. Robust Nonlinear Control* 26.2 (2015), pp. 345–364. DOI: 10.1002/rnc.3318.

[RRM03] Christopher V. Rao, James B. Rawlings, and David Q. Mayne. "Constrained state estimation for nonlinear discrete-time systems: stability and moving horizon approximations". In: *IEEE Trans. Autom. Control* 48.2 (2003), pp. 246–258. DOI: 10.1109/tac.2002.808470.

[RS12] Luis Miguel Rios and Nikolaos V. Sahinidis. "Derivative-free optimization: a review of algorithms and comparison of software implementations". In: *J. Glob. Optim.* 56.3 (2012), pp. 1247–1293. DOI: 10.1007/s10898-012-9951-y.

[RU99] Konrad Reif and Rolf Unbehauen. "The extended Kalman filter as an exponential observer for nonlinear systems". In: *IEEE Trans. Signal Process.* 47.8 (1999), pp. 2324–2328. DOI: 10.1109/78.774779.

[Sab+21] Oron Sabag, Gautam Goel, Sahin Lale, and Babak Hassibi. "Regret-optimal controller for the full-information problem". In: *Proc. Am. Control Conf. (ACC)*. 2021, pp. 4777–4782. DOI: 10.23919/acc50511.2021.9483023.

[SAZ22] Sungho Shin, Mihai Anitescu, and Victor M. Zavala. "Exponential decay of sensitivity in graph-structured nonlinear programs". In: *SIAM J. Optim.* 32.2 (2022), pp. 1156–1183. DOI: 10.1137/21m1391079.

[Sch+23] Julian D. Schiller, Simon Muntwiler, Johannes Köhler, Melanie N. Zeilinger, and Matthias A. Müller. "A Lyapunov function for robust stability of moving horizon estimation". In: *IEEE Trans. Autom. Control* 68.12 (2023), pp. 7466–7481. DOI: 10.1109/tac.2023.3280344. arXiv: 2202.12744.

[SGM24] Julian D. Schiller, Lars Grüne, and Matthias A. Müller. "Optimal state estimation: turnpike analysis and performance results". In: *arXiv:2409.14873* (2024). Accepted for presentation at the European Control Conference (ECC2025). DOI: 10.48550/arxiv.2409.14873.

[SGM25] Julian D. Schiller, Lars Grüne, and Matthias A. Müller. "Performance guarantees for optimization-based state estimation using turnpike properties". In: *arXiv:2501.18385* (2025). Submitted to IEEE Trans. Autom. Control. DOI: 10.48550/arXiv.2501.18385.

[SH22] Oron Sabag and Babak Hassibi. "Regret-optimal filtering for prediction and estimation". In: *IEEE Trans. Signal Process.* 70 (2022), pp. 5012–5024. DOI: 10.1109/tsp.2022.3212153.

[Shi+23] Sungho Shin, Yiheng Lin, Guannan Qu, Adam Wierman, and Mihai Anitescu. "Near-optimal distributed linear-quadratic regulator for networked systems". In: *SIAM J. Control Optim.* 61.3 (2023), pp. 1113–1135. DOI: 10.1137/22m1489836.

[Sin+17] Sumeet Singh, Anirudha Majumdar, Jean-Jacques Slotine, and Marco Pavone. "Robust online motion planning via contraction theory and convex optimization". In: *Proc. IEEE Int. Conf. Robot. Autom. (ICRA)*. 2017, pp. 5883–5890. DOI: 10.1109/icra.2017.7989693.

[SJ11] Dan Sui and Tor A. Johansen. "Moving horizon observer with regularisation for detectable systems without persistence of excitation". In: *Int. J. Control* 84.6 (2011), pp. 1041–1054. DOI: 10.1080/00207179.2011.589081.

[SJ14] Dan Sui and Tor A. Johansen. "Linear constrained moving horizon estimator with pre-estimating observer". In: *Syst. Control Lett.* 67 (2014), pp. 40–45. DOI: 10.1016/j.sysconle.2014.02.003.

[SJF10] Dan Sui, Tor A. Johansen, and Le Feng. "Linear moving horizon estimation with pre-estimating observer". In: *IEEE Trans. Autom. Control* 55.10 (2010), pp. 2363–2368. DOI: 10.1109/tac.2010.2053060.

[SKM21] Julian D. Schiller, Sven Knüfer, and Matthias A. Müller. "Robust stability of suboptimal moving horizon estimation using an observer-based candidate solution". In: *IFAC-PapersOnLine* 54.6 (2021), pp. 226–231. DOI: 10.1016/j.ifacol.2021.08.549. arXiv: 2011.08723.

[SM23a] Julian D. Schiller and Matthias A. Müller. "A moving horizon state and parameter estimation scheme with guaranteed robust convergence". In: *IFAC-PapersOnLine* 56.2 (2023), pp. 6759–6764. DOI: 10.1016/j.ifacol.2023.10.382. arXiv: 2211.09053.

[SM23b] Julian D. Schiller and Matthias A. Müller. "Nonlinear moving horizon estimation for robust state and parameter estimation – extended version". In: *arXiv:2312.13175v2* (2023). Submitted to Automatica. DOI: 10.48550/arxiv.2312.13175.

[SM23c] Julian D. Schiller and Matthias A. Müller. "On an integral variant of incremental input/output-to-state stability and its use as a notion of nonlinear detectability". In: *IEEE Control Syst. Lett.* 7 (2023), pp. 2341–2346. DOI: 10.1109/LCSYS.2023.3286174. arXiv: 2305.05442.

[SM23d] Julian D. Schiller and Matthias A. Müller. "Suboptimal nonlinear moving horizon estimation". In: *IEEE Trans. Autom. Control* 68.4 (2023), pp. 2199–2214. DOI: 10.1109/tac.2022.3173937. arXiv: 2108.13750.

[SM24a] Julian D. Schiller and Matthias A. Müller. "Moving horizon estimation for nonlinear systems with time-varying parameters". In: *IFAC-PapersOnLine* 58.18 (2024), pp. 341–348. DOI: 10.1016/j.ifacol.2024.09.053. arXiv: 2404.09566.

[SM24b] Julian D. Schiller and Matthias A. Müller. "Robust stability of moving horizon estimation for continuous-time systems". In: *at – Automati-*

sierungstechnik 72.2 (2024), pp. 120–133. DOI: 10.1515/auto-2023-0087. arXiv: 2305.06614.

[SMR99] Pierre O. M. Scokaert, David Q. Mayne, and James B. Rawlings. "Suboptimal model predictive control (feasibility implies stability)". In: *IEEE Trans. Autom. Control* 44.3 (1999), pp. 648–654. DOI: 10.1109/9.751369.

[Son90] Eduardo D. Sontag. *Mathematical Control Theory: Deterministic Finite Dimensional Systems*. 2nd ed. New York, NY, USA: Springer, 1990. DOI: 10.1007/978-1-4612-0577-7.

[Son98] Eduardo D. Sontag. "Comments on integral variants of ISS". In: *Syst. Control Lett.* 34.1-2 (1998), pp. 93–100. DOI: 10.1016/s0167-6911(98)00003-6.

[SP12] Ricardo G. Sanfelice and Laurent Praly. "Convergence of nonlinear observers on $\mathbb{R}^n$ with a Riemannian metric (Part I)". In: *IEEE Trans. Autom. Control* 57.7 (2012), pp. 1709–1722. DOI: 10.1109/tac.2011.2179873.

[SP16] Ricardo G. Sanfelice and Laurent Praly. "Convergence of nonlinear observers on $\mathbb{R}^n$ with a Riemannian metric (Part II)". In: *IEEE Trans. Autom. Control* 61.10 (2016), pp. 2848–2860. DOI: 10.1109/tac.2015.2504483.

[SP24] Ricardo G. Sanfelice and Laurent Praly. "Convergence of nonlinear observers on $\mathbb{R}^n$ with a Riemannian metric (Part III)". In: *IEEE Trans. Autom. Control* 69.3 (2024), pp. 1432–1447. DOI: 10.1109/TAC.2023.3321236. arXiv: 2102.08340.

[SS13] Dan Simon and Yuriy S. Shmaliy. "Unified forms for Kalman and finite impulse response filtering and smoothing". In: *Automatica* 49.6 (2013), pp. 1892–1899. DOI: 10.1016/j.automatica.2013.02.026.

[SS71] Harold W. Sorenson and Jerome E. Sacks. "Recursive fading memory filtering". In: *Inf. Sci.* 3.2 (1971), pp. 101–119. DOI: 10.1016/s0020-0255(71)80001-4.

[ST23] Arash Sadeghzadeh and Roland Tóth. "Improved embedding of nonlinear systems in linear parameter-varying models with polynomial dependence". In: *IEEE Trans. Control Syst. Technol.* 31.1 (2023), pp. 70–82. DOI: 10.1109/tcst.2022.3173891.

[Suw+14] Rata Suwantong, Sylvain Bertrand, Didier Dumur, and Dominique Beauvois. "Stability of a nonlinear moving horizon estimator with pre-estimation". In: *Proc. Am. Control Conf. (ACC)*. 2014, pp. 5688–5693. DOI: 10.1109/acc.2014.6859072.

[SW95] Eduardo D. Sontag and Yuan Wang. "On characterizations of the input-to-state stability property". In: *Syst. Control Lett.* 24.5 (1995), pp. 351–359. DOI: 10.1016/0167-6911(94)00050-6.

[SW97] Eduardo D. Sontag and Yuan Wang. "Output-to-state stability and detectability of nonlinear systems". In: *Syst. Control Lett.* 29 (1997), pp. 279–290. DOI: 10.1016/S0167-6911(97)90013-X.

[SWM23] Julian D. Schiller, Boyang Wu, and Matthias A. Müller. "A simple suboptimal moving horizon estimation scheme with guaranteed robust stability". In: *IEEE Control Syst. Lett.* 7 (2023), pp. 19–24. DOI: 10.1109/LCSYS.2022.3186236. arXiv: 2203.16090.

[SZ21] Sungho Shin and Victor M. Zavala. "Controllability and observability imply exponential decay of sensitivity in dynamic optimization". In: *IFAC-PapersOnLine* 54.6 (2021), pp. 179–184. DOI: 10.1016/j.ifacol.2021.08.542.

[ŢB16] Alexandru Ţiclea and Gildas Besançon. "Adaptive observer design for discrete time LTV systems". In: *Int. J. Control* 89.12 (2016), pp. 2385–2395. DOI: 10.1080/00207179.2016.1157901.

[TM23] Patrizio Tomei and Riccardo Marino. "An enhanced feedback adaptive observer for nonlinear systems with lack of persistency of excitation". In: *IEEE Trans. Autom. Control* 68.8 (2023), pp. 5067–5072. DOI: 10.1109/tac.2022.3214798.

[TR02] Matthew J. Tenny and James B. Rawlings. "Efficient moving horizon estimation and nonlinear model predictive control". In: *Proc. Am. Control Conf.* 2002, pp. 4475–4480. DOI: 10.1109/acc.2002.1025355.

[Tré23] Emmanuel Trélat. "Linear turnpike theorem". In: *Math. Control Signals Syst.* 35.3 (2023), pp. 685–739. DOI: 10.1007/s00498-023-00354-5.

[TRK16] Duc N. Tran, Björn S. Rüffer, and Christopher M. Kellett. "Incremental stability properties for discrete-time systems". In: *Proc. 55th IEEE Conf. Decis. Control (CDC)*. 2016. DOI: 10.1109/cdc.2016.7798314.

[TRK19] Duc N. Tran, Björn S. Rüffer, and Christopher M. Kellett. "Convergence properties for discrete-time nonlinear systems". In: *IEEE Trans. Autom. Control* 64.8 (2019), pp. 3415–3422. DOI: 10.1109/tac.2018.2879951.

[Tyu+13] Ivan Y. Tyukin, Erik Steur, Henk Nijmeijer, and Cees van Leeuwen. "Adaptive observers and parameter estimation for a class of systems nonlinear in the parameters". In: *Automatica* 49.8 (2013), pp. 2409–2423. DOI: 10.1016/j.automatica.2013.05.008.

[TZ15] Emmanuel Trélat and Enrique Zuazua. "The turnpike property in finite-dimensional nonlinear optimal control". In: *J. Differ. Equ.* 258.1 (2015), pp. 81–114. DOI: 10.1016/j.jde.2014.09.005.

[Vau70] David R. Vaughan. "A nonrecursive algebraic solution for the discrete Riccati equation". In: *IEEE Trans. Autom. Control* 15.5 (1970), pp. 597–599. DOI: 10.1109/tac.1970.1099549.

[Ver+21] Robin Verschueren, Gianluca Frison, Dimitris Kouzoupis, Jonathan Frey, Niels van Duijkeren, Andrea Zanelli, Branimir Novoselnik, Thiva-

haran Albin, Rien Quirynen, and Moritz Diehl. “acados—a modular open-source framework for fast embedded optimal control”. In: *Math. Program. Comput.* 14.1 (2021), pp. 147–183. DOI: 10.1007/s12532-021-00208-8.

[Ver+23] Chris Verhoek, Patrick J. W. Koelewijn, Sofie Haesaert, and Roland Tóth. “Convex incremental dissipativity analysis of nonlinear systems”. In: *Automatica* 150 (2023), p. 110859. DOI: 10.1016/j.automatica.2023.110859.

[Vil70] Jaak Vilms. “Totally geodesic maps”. In: *J. Differ. Geom.* 4.1 (1970). DOI: 10.4310/jdg/1214429276.

[WB05] Andreas Wächter and Lorenz T. Biegler. “On the implementation of an interior-point filter line-search algorithm for large-scale nonlinear programming”. In: *Math. Program.* 106.1 (2005), pp. 25–57. DOI: 10.1007/s10107-004-0559-y.

[WK17] Yiming Wan and Tamás Keviczky. “Real-time nonlinear moving horizon observer with pre-estimation for aircraft sensor fault detection and estimation”. In: *Int. J. Robust Nonlinear Control* 29.16 (2017), pp. 5394–5411. DOI: 10.1002/rnc.4011.

[WK72] R. Wilde and P. Kokotovic. “A dichotomy in linear control theory”. In: *IEEE Trans. Autom. Control* 17.3 (1972), pp. 382–383. DOI: 10.1109/tac.1972.1099976.

[WMB22] Lai Wei, Ryan McCloy, and Jie Bao. “Contraction analysis and control synthesis for discrete-time nonlinear processes”. In: *J. Process Control* 115 (2022), pp. 58–66. DOI: 10.1016/j.jprocont.2022.04.016.

[WVD14] Andrew Wynn, Milan Vukov, and Moritz Diehl. “Convergence guarantees for moving horizon estimation based on the real-time iteration scheme”. In: *IEEE Trans. Autom. Control* 59.8 (2014), pp. 2215–2221. DOI: 10.1109/TAC.2014.2298984.

[YWM22] Bowen Yi, Ruigang Wang, and Ian R. Manchester. “Reduced-order nonlinear observers via contraction analysis and convex optimization”. In: *IEEE Trans. Autom. Control* 67.8 (2022), pp. 4045–4060. DOI: 10.1109/tac.2021.3115887.

[YZ15] Jihua Yang and Liqin Zhao. “Bifurcation analysis and chaos control of the modified chua’s circuit system”. In: *Chaos Solit. Fractals* 77 (2015), pp. 332–339. DOI: 10.1016/j.chaos.2015.05.028.

[YZ23] Shenglun Yi and Mattia Zorzi. “Robust fixed-lag smoothing under model perturbations”. In: *J. Franklin Inst.* 360.1 (2023), pp. 458–483. DOI: 10.1016/j.jfranklin.2022.10.050.

[ZB13] Ali Zemouche and Mohamed Boutayeb. “On LMI conditions to design observers for Lipschitz nonlinear systems”. In: *Automatica* 49.2 (2013), pp. 585–591. DOI: 10.1016/j.automatica.2012.11.029.

[ZG22] Mario Zanon and Sébastien Gros. "A new dissipativity condition for asymptotic stability of discounted economic MPC". In: *Automatica* 141 (2022), p. 110287. DOI: 10.1016/j.automatica.2022.110287.

[Zha+19] Wei Zhang, Younan Zhao, Masoud Abbaszadeh, Mingming Ji, and Xiushan Cai. "Exponential observers for discrete-time nonlinear systems with incremental quadratic constraints". In: *Proc. Am. Control Conf. (ACC)*. 2019, pp. 477–482. DOI: 10.23919/acc.2019.8814484.

A. Publications of the author and CRediT author statement

This thesis comprises the results of five years of research in the field of MHE. Therefore, significant parts have already been published in scientific journals and presented at conferences (or have been submitted for peer review). In the following, we list all publications in reverse chronological order that are included in this thesis, with additional information such as special honors or awards a publication has received.

The author of this thesis is listed as first author in all publications involved; nevertheless, the intellectual property is indeed shared by several co-authors. Here, we emphasize that all parts taken verbatim from previous works were also originally written by the author of this thesis. To ensure full transparency in accordance with good research practice, we describe the contributions of all co-authors using the Contributor Role Taxonomy (CRediT). In particular, this shows that the author of this thesis, Julian D. Schiller, was primarily responsible for the conceptualization, methodological development, formal analysis, software, visualization, and original writing of the publications involved.

[SGM25] Julian D. Schiller, Lars Grüne, and Matthias A. Müller. "Performance guarantees for optimization-based state estimation using turnpike properties". In: *arXiv:2501.18385* (2025). Submitted to IEEE Trans. Autom. Control. DOI: 10.48550/arXiv.2501.18385.

Julian D. Schiller: Conceptualization, Methodology, Formal analysis, Software, Visualization, Writing – original draft. **Lars Grüne:** Conceptualization, Methodology, Validation, Writing – Review & Editing. **Matthias A. Müller:** Conceptualization, Funding acquisition, Methodology, Project administration, Resources, Supervision, Validation, Writing – Review & Editing.

[SGM24] Julian D. Schiller, Lars Grüne, and Matthias A. Müller. "Optimal state estimation: turnpike analysis and performance results". In: *arXiv:2409.14873* (2024). Accepted for presentation at the European Control Conference (ECC2025). DOI: 10.48550/arxiv.2409.14873.

Julian D. Schiller: Conceptualization, Methodology, Formal analysis, Software, Visualization, Writing – original draft. **Lars Grüne:** Conceptualization, Methodology, Validation, Writing – Review & Editing. **Matthias A. Müller:** Conceptualization, Funding acquisition,

Methodology, Project administration, Resources, Supervision, Validation, Writing – Review & Editing.

[SM24a] Julian D. Schiller and Matthias A. Müller. "Moving horizon estimation for nonlinear systems with time-varying parameters". In: *IFAC-PapersOnLine* 58.18 (2024), pp. 341–348. DOI: 10.1016/j.ifacol.2024.09.053. arXiv: 2404.09566. © 2024 The Authors. CC BY-NC-ND. *Selected as finalist for the Young Author Award at the 8th IFAC Conference on Nonlinear Model Predictive Control (NMPC2024).*

Julian D. Schiller: Conceptualization, Methodology, Formal analysis, Software, Visualization, Writing – original draft. **Matthias A. Müller:** Conceptualization, Funding acquisition, Methodology, Project administration, Resources, Supervision, Validation, Writing – Review & Editing.

[SM24b] Julian D. Schiller and Matthias A. Müller. "Robust stability of moving horizon estimation for continuous-time systems". In: *at – Automatisierungstechnik* 72.2 (2024), pp. 120–133. DOI: 10.1515/auto-2023-0087. arXiv: 2305.06614. © 2024 De Gruyter.

Julian D. Schiller: Conceptualization, Methodology, Formal analysis, Software, Visualization, Writing – original draft. **Matthias A. Müller:** Conceptualization, Funding acquisition, Methodology, Project administration, Resources, Supervision, Validation, Writing – Review & Editing.

[SM23b] Julian D. Schiller and Matthias A. Müller. "Nonlinear moving horizon estimation for robust state and parameter estimation – extended version". In: *arXiv:2312.13175v2* (2023). Submitted to Automatica. DOI: 10.48550/arxiv.2312.13175. © 2023 The Authors.

Julian D. Schiller: Conceptualization, Methodology, Formal analysis, Software, Visualization, Writing – original draft. **Matthias A. Müller:** Conceptualization, Funding acquisition, Methodology, Project administration, Resources, Supervision, Validation, Writing – Review & Editing.

[SM23c] Julian D. Schiller and Matthias A. Müller. "On an integral variant of incremental input/output-to-state stability and its use as a notion of nonlinear detectability". In: *IEEE Control Syst. Lett.* 7 (2023), pp. 2341–2346. DOI: 10.1109/LCSYS.2023.3286174. arXiv: 2305.05442. © 2023 IEEE.

Julian D. Schiller: Conceptualization, Methodology, Formal analysis, Writing – original draft. **Matthias A. Müller:** Conceptualization, Funding acquisition, Methodology, Project administration, Resources, Supervision, Validation, Writing – Review & Editing.

[SM23a] Julian D. Schiller and Matthias A. Müller. "A moving horizon state and parameter estimation scheme with guaranteed robust convergence". In: *IFAC-PapersOnLine* 56.2 (2023), pp. 6759–6764. DOI: 10.1016/j.ifacol.2023.10.382. arXiv: 2211.09053. © 2023 The Authors. CC BY-NC-ND.

Julian D. Schiller: Conceptualization, Methodology, Formal analysis, Software, Visualization, Writing – original draft. **Matthias A. Müller:** Conceptualization, Funding acquisition, Methodology, Project administration, Resources, Supervision, Validation, Writing – Review & Editing.

[SWM23] Julian D. Schiller, Boyang Wu, and Matthias A. Müller. "A simple suboptimal moving horizon estimation scheme with guaranteed robust stability". In: *IEEE Control Syst. Lett.* 7 (2023), pp. 19–24. DOI: 10.1109/LCSYS.2022.3186236. arXiv: 2203.16090. © 2023 IEEE. *Awarded the 2023 IEEE Process Control TC Outstanding Student Paper Prize.*

Julian D. Schiller: Conceptualization, Methodology, Formal analysis, Software, Visualization, Writing – original draft. **Boyang Wu:** Formal analysis. **Matthias A. Müller:** Conceptualization, Funding acquisition, Methodology, Project administration, Resources, Supervision, Validation, Writing – Review & Editing.

[Sch+23] Julian D. Schiller, Simon Muntwiler, Johannes Köhler, Melanie N. Zeilinger, and Matthias A. Müller. "A Lyapunov function for robust stability of moving horizon estimation". In: *IEEE Trans. Autom. Control* 68.12 (2023), pp. 7466–7481. DOI: 10.1109/tac.2023.3280344. arXiv: 2202.12744. © 2023 IEEE.

Julian D. Schiller: Conceptualization, Methodology, Formal analysis, Software, Visualization, Writing – original draft (Sections III-D – VI). **Simon Muntwiler:** Conceptualization, Methodology, Formal analysis, Writing – original draft (Sections I – III-C). **Johannes Köhler:** Conceptualization, Methodology, Formal analysis, Writing – Review & Editing. **Melanie N. Zeilinger:** Conceptualization, Funding acquisition, Project administration, Resources, Supervision, Validation, Writing – Review & Editing. **Matthias A. Müller:** Conceptualization, Funding acquisition, Methodology, Project administration, Resources, Supervision, Validation, Writing – Review & Editing.

[SM23d] Julian D. Schiller and Matthias A. Müller. "Suboptimal nonlinear moving horizon estimation". In: *IEEE Trans. Autom. Control* 68.4 (2023), pp. 2199–2214. DOI: 10.1109/tac.2022.3173937. arXiv: 2108.13750. © 2023 IEEE.

Julian D. Schiller: Conceptualization, Methodology, Formal analysis, Software, Visualization, Writing – original draft. **Matthias A. Müller:** Conceptualization, Funding acquisition, Methodology, Project administration, Resources, Supervision, Validation, Writing – Review & Editing.

[SKM21] Julian D. Schiller, Sven Knüfer, and Matthias A. Müller. "Robust stability of suboptimal moving horizon estimation using an observer-based candidate solution". In: *IFAC-PapersOnLine* 54.6 (2021), pp. 226–231. DOI: 10.1016/j.ifacol.2021.08.549. arXiv: 2011.08723.

 Selected as keynote presentation at the 7th IFAC Conference on Nonlinear Model Predictive Control (NMPC2021).

Julian D. Schiller: Conceptualization, Methodology, Formal analysis, Software, Visualization, Writing – original draft. **Sven Knüfer:** Conceptualization, Methodology, Validation, Writing – Review & Editing. **Matthias A. Müller:** Conceptualization, Funding acquisition, Methodology, Project administration, Resources, Supervision, Validation, Writing – Review & Editing.

Having access to the internal state of a dynamical system is of crucial importance for many control applications. In most practical cases, however, the state cannot be completely measured for various reasons, demanding the use of appropriate reconstruction methods. This represents a challenging problem, especially in the presence of nonlinear systems and when robustness to model errors and measurement noise must be ensured. Moving horizon estimation (MHE) is a modern optimization-based state estimation strategy that is naturally suitable for this purpose.

In this thesis, we develop various new results in the field of nonlinear MHE. We establish desired robust stability guarantees under realistic conditions, propose MHE schemes for real-time applications, and investigate methods for joint state and parameter estimation – particularly tailored to applications in which weak excitation occurs frequently and unpredictably. Moreover, we draw connections to optimal control and turnpike theory, leading to a new perspective on MHE and ultimately to novel performance estimates and regret guarantees. We illustrate our theoretical results with various numerical examples from the literature, which highlight the applicability and practical relevance of the developed theory.

Logos Verlag Berlin

ISBN 978-3-8325-5963-2

https://www.logos-verlag.de/oekobuch